



HIGHLY MODULAR P -OP LIGANDS FOR RHODIUM- AND IRIIDIUM-MEDIATED ASYMMETRIC HYDROGENATIONS

José Luis Núñez Rico

Dipòsit Legal: T.994-2013

ADVERTIMENT. L'accés als continguts d'aquesta tesi doctoral i la seva utilització ha de respectar els drets de la persona autora. Pot ser utilitzada per a consulta o estudi personal, així com en activitats o materials d'investigació i docència en els termes establerts a l'art. 32 del Text Refós de la Llei de Propietat Intel·lectual (RDL 1/1996). Per altres utilitzacions es requereix l'autorització prèvia i expressa de la persona autora. En qualsevol cas, en la utilització dels seus continguts caldrà indicar de forma clara el nom i cognoms de la persona autora i el títol de la tesi doctoral. No s'autoritza la seva reproducció o altres formes d'explotació efectuades amb finalitats de lucre ni la seva comunicació pública des d'un lloc aliè al servei TDX. Tampoc s'autoritza la presentació del seu contingut en una finestra o marc aliè a TDX (framing). Aquesta reserva de drets afecta tant als continguts de la tesi com als seus resums i índexs.

ADVERTENCIA. El acceso a los contenidos de esta tesis doctoral y su utilización debe respetar los derechos de la persona autora. Puede ser utilizada para consulta o estudio personal, así como en actividades o materiales de investigación y docencia en los términos establecidos en el art. 32 del Texto Refundido de la Ley de Propiedad Intelectual (RDL 1/1996). Para otros usos se requiere la autorización previa y expresa de la persona autora. En cualquier caso, en la utilización de sus contenidos se deberá indicar de forma clara el nombre y apellidos de la persona autora y el título de la tesis doctoral. No se autoriza su reproducción u otras formas de explotación efectuadas con fines lucrativos ni su comunicación pública desde un sitio ajeno al servicio TDR. Tampoco se autoriza la presentación de su contenido en una ventana o marco ajeno a TDR (framing). Esta reserva de derechos afecta tanto al contenido de la tesis como a sus resúmenes e índices.

WARNING. Access to the contents of this doctoral thesis and its use must respect the rights of the author. It can be used for reference or private study, as well as research and learning activities or materials in the terms established by the 32nd article of the Spanish Consolidated Copyright Act (RDL 1/1996). Express and previous authorization of the author is required for any other uses. In any case, when using its content, full name of the author and title of the thesis must be clearly indicated. Reproduction or other forms of for profit use or public communication from outside TDX service is not allowed. Presentation of its content in a window or frame external to TDX (framing) is not authorized either. These rights affect both the content of the thesis and its abstracts and indexes.

José Luis Núñez Rico

**HIGHLY MODULAR P-OP LIGANDS FOR RHODIUM-
AND IRIIDIUM-MEDIATED ASYMMETRIC
HYDROGENATIONS**

PhD Thesis

Supervised by Prof. Dr. Anton Vidal i Ferran
Institut Català d'Investigació Química (ICIQ)

Tarragona
2013



UNIVERSITAT ROVIRA I VIRGILI

UNIVERSITAT ROVIRA I VIRGILI
HIGHLY MODULAR P -OP LIGANDS FOR RHODIUM- AND IRIIDIUM-MEDIATED ASYMMETRIC HYDROGENATIONS
José Luis Núñez Rico
DL: T.994-2013



UNIVERSITAT
ROVIRA I VIRGILI

DEPARTAMENT DE QUÍMICA ANALÍTICA
I QUÍMICA ORGÀNICA

C/ Marcel·lí Domingo s/n
Campus Sescelades
43007 Tarragona
Tel. 34 977 55 97 69
Fax 34 977 55 84 46
e-mail: secqaqo@urv.net

Prof. Dr. Anton Vidal Ferran, Group Leader of the Institute of Chemical Research of Catalonia (ICIQ) and Research Professor of the Catalan Institution for Research and Advanced Studies (ICREA),

CERTIFY that the present Doctoral Thesis entitled: “Highly modular P-OP ligands for rhodium- and iridium-mediated asymmetric hydrogenations”, presented by José Luis Núñez Rico to receive the PhD degree in Chemistry, has been carried out under my supervision, in the Institute of Chemical Research of Catalonia (ICIQ).

Tarragona, 09 May 2013

PhD Thesis supervisor

Prof. Dr. Anton Vidal Ferran

UNIVERSITAT ROVIRA I VIRGILI
HIGHLY MODULAR P -OP LIGANDS FOR RHODIUM- AND IRIIDIUM-MEDIATED ASYMMETRIC HYDROGENATIONS
José Luis Núñez Rico
DL: T.994-2013

*“Dans les champs de l'observation le hasard
ne favorise que les esprits préparés”*

*“In the fields of observation chance favors
the prepared mind”*

Louis Pasteur, 1854

*“Ah, not in knowledge is happiness, but in
the acquisition of knowledge!”*

*The power of words, Edgar Allan Poe,
1845*

UNIVERSITAT ROVIRA I VIRGILI
HIGHLY MODULAR P -OP LIGANDS FOR RHODIUM- AND IRIIDIUM-MEDIATED ASYMMETRIC HYDROGENATIONS
José Luis Núñez Rico
DL: T.994-2013

AGRADECIMIENTOS

Señores, esto que sostenéis en vuestras manos no es tan solo un conjunto ordenado de palabras, se trata también de la culminación de una etapa, de un sueño. Y esto no se construye de la noche a la mañana, se ha tratado de un proceso largo, apasionado, como todo proceso científico y creativo, por el cual me encuentro tremendamente agradecido a todos aquellos que han hecho posible, aportando cada uno su granito de arena, que os pueda presentar la tesis que tenéis hoy en las manos.

A la primera persona que quiero agradecer es a Anton, mi director de tesis. Él fue quien me dio la oportunidad, hace ya unos años, de hacer la tesis en su grupo. Eran momentos complicados para mí, y no solo me brindó la oportunidad de hacer la tesis con él, sino que no cejó en su apuesta por mí y es el principal causante de poder cerrar de esta forma este capítulo. De entre todas las cosas que desconozco, hoy desconozco muchas menos, y en parte es por él. Moltes gràcies Anton.

También he de agradecer a todos los compañeros del grupo, presentes y pasados porque todos han contribuido a su manera a la consecución de esta tesis y a la evolución tanto científica como personalmente que ella ha supuesto. A Xavi, Juan, Dana, Amilan, Helmut, a los nuevos lechacitos Joan, Bala y Laura, y a todos los demás, gracias. No es mi intención hacerme pesado, pero hay personas que no puedo pasar la oportunidad de agradecer. A Elisenda por inculcarme el sentido por la seguridad, a los franceses, Armen y Anne Sophie, con los que vivimos la época dorada multicultural del grupo, a Nacho, con quien desahogaba mis cabreos cuando la química no hacía lo que yo quería, sino lo que ella prefería. A Pablo, nuestro pequeño libro con patas, por su apoyo científico, que tantas búsquedas me ha aborrido. Y como no, dejo para el final a Héctor, y a M^a Ángeles por extensión, porque no sólo son artífices de que hiciera la tesis sino que hicieron mi adaptación a Tarragona mucho más agradable y que a día de hoy sigo viendo casi a diario, fuera y dentro del laboratorio.

A las unidades de soporte a la investigación, es increíble lo que se puede hacer en un centro como el ICIQ con el equipamiento y personal que tiene. A casi todas las unidades he

tenido que acudir, alicaído, con problemas de química y con prisas y de todas ellas he salido con los problemas encauzados. Es de especial agradecer el apoyo del personal de RMN, rayos X, cromatografía y muy especialmente a las chicas de CRTU por todas las horas en alta presión que he pasado con ellas y con mil reacciones... poco amigables.

Todo esto no surgió de la nada, he comentado, fueron muchos, muchos años desde que descubrí mi temprana vocación por la química y en los que he tenido el apoyo incondicional de mis padres y mi hermano. Sin el cual, si no hubieran aguantado tanto, hoy me dedicaría a otras tareas igualmente loables, pero más apartadas de mi vocación química. De mi madre aprendí que si eres feliz en lo que haces, vives dos veces, y de mi padre que las cosas bien hechas, bien parecen. Y esto señores, conforman unos excelentes pilares para la investigación.

A esto me viene a la mente la persona a la que agradezco que me introdujera el gusanillo por la investigación, a la Dra. Purificación Cuadrado Curto, Puri, con quien como alumno me hizo apreciar las técnicas de resonancia magnética, y que más tarde hizo que amara la investigación. Si no hubiera pasado por su grupo, mini de tamaño pero grande en corazón, no hubiera encontrado el camino hacia la tesis doctoral. Y esto se extiende también a con los que allí compartí laboratorio, Blanca, Patri, Amaya y el resto, siempre recordaré esa época.

Y como no, mi más profundo agradecimiento para quien me ha estado apoyando y sufriendo mis ausencias a diario, para Gema. Cuando llegaba tarde, o cuando llegaba cabreado por las cosas de la química, ella siempre estaba allí para hacerme cargar las pilas, para renovarme, todos y cada uno de los días. Con esta tesis cierro una etapa de mi vida, y comienzo otra, a tu lado.

Espero que la disfrutéis leyendo tanto como yo disfruté haciéndola.

El trabajo desarrollado en esta tesis doctoral ha sido posible gracias a la financiación de L'Institut Català d'Investigació Química (ICIQ) y se ha desarrollado dentro del marco de los proyectos CTQ-2008-00950/BQU, CTQ2011-28512 del MICINN, Consolider Ingenio 2010 (CSD2006-0003) y al DURSI (2009SGR623) de la Generalitat de Catalunya.



UNIVERSITAT ROVIRA I VIRGILI
HIGHLY MODULAR P -OP LIGANDS FOR RHODIUM- AND IRIIDIUM-MEDIATED ASYMMETRIC HYDROGENATIONS
José Luis Núñez Rico
DL: T.994-2013

*A mis padres,
y a Gemma*

UNIVERSITAT ROVIRA I VIRGILI
HIGHLY MODULAR P -OP LIGANDS FOR RHODIUM- AND IRIIDIUM-MEDIATED ASYMMETRIC HYDROGENATIONS
José Luis Núñez Rico
DL: T.994-2013

At the submission of this thesis, the results contained therein have so far resulted in the following publications:

[Ir(P-OP)]-Catalyzed Asymmetric Hydrogenation of Diversely Substituted C=N-Containing Heterocycles. Núñez-Rico, J. L.; Vidal-Ferran, A. *Org. Lett.* **2013**, *15*, 2066.

Modular P-OP Ligands in Rhodium-Mediated Asymmetric Hydrogenation: A Comparative Catalysis Study. Núñez-Rico, J. L.; Etayo, P.; Fernández-Pérez, H.; Vidal-Ferran, A. *Adv. Synth. Catal.* **2012**, *354*, 3025.

Enantioselective Access to Chiral Drugs by using Asymmetric Hydrogenation Catalyzed by Rh (P-OP) Complexes. Etayo, P.; Núñez-Rico, J. L.; Fernández-Pérez, H.; Vidal-Ferran, A. *Chem. Eur. J.* **2011**, *17*, 13978.

Chiral Rhodium Complexes Derived From Electron-Rich Phosphine-Phosphites as Asymmetric Hydrogenation Catalysts. Etayo, P.; Núñez-Rico, J. L.; Vidal-Ferran, A. *Organometallics* **2011**, *30*, 6718.

Asymmetric Hydrogenation of Heteroaromatic Compounds Mediated by Iridium-(P-OP) Complexes. Núñez-Rico, J. L.; Fernández-Pérez, H.; Benet-Buchholz, J.; Vidal-Ferran, A. *Organometallics* **2010**, *29*, 6627.

P-OP-Mediated Asymmetric Hydrogenation of Functionalised Alkenes. Fernández-Pérez, H.; Etayo, P.; Núñez-Rico, J. L.; Vidal-Ferran, A. *Chim. Oggi* **2010**, *28*, XXVI.

UNIVERSITAT ROVIRA I VIRGILI
HIGHLY MODULAR P -OP LIGANDS FOR RHODIUM- AND IRIIDIUM-MEDIATED ASYMMETRIC HYDROGENATIONS
José Luis Núñez Rico
DL: T.994-2013

TABLE OF CONTENTS

Table of Contents	i
Acronyms and Abbreviations	v
Prólogo	ix
Resumen	xiii

INTRODUCTION	1
---------------------------	----------

CHAPTER I – Asymmetric Hydrogenation Catalyzed by Rhodium-(*P-OP*) Complexes

29

1.1 Antecedents	31
1.1.1 Background.....	31
1.1.2 Synthetic Strategies towards Modular Phosphine-Phosphinites and Phosphine-Phosphites.....	48
1.1.3 Mechanism	55
1.1.4 Rhodium-mediated Asymmetric Hydrogenation in the Preparation of API Intermediates.....	65
1.2 Asymmetric Hydrogenations Catalyzed by Rhodium-(<i>P-OP</i>) Complexes	79
1.2.1 Synthesis of Phosphine-Phosphinite and Phosphine-Phosphite (<i>P-OP</i>) Ligands and their Derived Rhodium Complexes.....	79
1.2.1.1 <i>P-OP Ligand Synthesis</i>	79
1.2.1.2 <i>Preparation of Rhodium Complexes Derived from P-OP Ligands</i>	86
1.2.2 <i>P-OP Ligands in Asymmetric Hydrogenation</i>	88
1.2.2.1 <i>TOF & TON Determination in Asymmetric Hydrogenations Mediated by Rhodium Complexes Derived from P-OP Ligands</i>	89
1.2.3 Hydrogenation of functionalized alkenes.....	95

1.2.3.1 Hydrogenation of β -substituted α -(acylamino) acrylates	96
1.2.3.2 Hydrogenation of α -substituted enamides	101
1.2.3.3 Hydrogenation of α -substituted enol esters.....	105
1.2.3.4 Hydrogenation of itaconate derivatives and analogs	111
1.2.4 Enantioselective Access to Chiral Drugs	116
1.2.4.1 Access to Chiral Drug Precursors from β -Aryl- and β -Alkyl-Substituted α -(Acylamino)acrylates	116
1.2.4.2 Access to Chiral Drug Precursors from α -Arylenamides and α -Arylenol Acetates	126
1.2.4.3 Access to Chiral Drug Precursors of Lacosamide by Hydrogenation of β -Alkoxy-substituted α -(Acylamino)-acrylates	131
1.2.5 Rationalization of the Stereochemical Outcome of the Reaction	136
1.3 Experimental Section.....	140
1.3.1 General Remarks	140
1.3.2 Synthesis of Ligands	141
1.3.2.1 Synthesis of Rhodium Complexes.....	144
1.3.3 Preparation and Characterization of Substrates	145
1.3.4 General Procedure for the Rh-Mediated Asymmetric Hydrogenation.....	151
1.3.4.1 General Procedure for Monitoring the Hydrogenation Reactions by Gas Uptake Measurements	152
1.3.4.2 General Procedure for Hydrogenations Using S/C ratios > 1,000:1	152
1.3.5 Characterization of Hydrogenation Products and Determination of the Enantiomeric Excesses.....	153

CHAPTER II – Asymmetric Hydrogenation Catalyzed by Iridium-(P-OP) Complexes 165

2.1 Antecedents.....	167
2.1.1 Background	167
2.1.2 Importance of Chiral <i>N</i> -containing Heterocycles	173
2.1.3 Strategies for Catalyst and Substrate Activation: the Role of the Additives.....	184
2.1.4 Mechanistic Proposals	189
2.2 P-OP Ligands in Iridium-Mediated Asymmetric Hydrogenations ..	197
2.2.1 Studies on Iridium- <i>P-OP</i> Coordination.....	197
2.2.1.1 Iridium Complexes from phosphine-phosphinites .	199
2.2.1.2 Iridium Complexes from phosphine-phosphites	203
2.2.1.3 $^{31}\text{P}\{^1\text{H}\}$ NMR Titrations of <i>P-OP</i> ligands with iridium precursors.....	213
2.2.2 Hydrogenation of <i>N</i> -Containing Structures	220
2.2.2.1 Hydrogenation of Ketimines.....	220
2.2.2.2 Hydrogenation of Quinolines and Quinoxalines ...	228
2.2.2.3 Hydrogenation of Unprotected Indoles	245
2.2.2.4 Hydrogenation of Benzoxazines.....	259
2.2.2.5 Hydrogenation of Benzoxazinones.....	266
2.2.2.6 Hydrogenation of Benzothiazinones.....	272
2.2.2.7 Hydrogenation of Quinoxalinones	276
2.2.3 Deuteration and Mechanistic Studies on the Hydrogenation of Heterocycles	281
2.3 Experimental Section	292
2.3.1 General Remarks	292
2.3.2 General Synthetic Procedures for the Preparation of Iridium Complexes.....	294
2.3.2.1 Cationic Iridium Complexes Derived from Phosphine-Phosphinite Ligands.....	294

2.3.2.2 Neutral Iridium Complexes Derived from Phosphine-Phosphite Ligands	297
2.3.2.3 Cationic Iridium Complexes Derived from Phosphine-Phosphite Ligands	298
2.3.2.4 Iridium Complexes 227 and 228	300
2.3.3 Preparation and Characterization of Substrates	302
2.3.4 General Procedure for the Ir-Mediated Asymmetric Hydrogenation.....	309
2.3.5 Characterization of Hydrogenation Products and Determination of the Enantiomeric Excesses.....	311
2.3.6 Deuterium Labeling Experiments.....	323
<hr/>	
Conclusions	341
<hr/>	
Appendix	Attached CD
<hr/>	
NMR spectra of new compounds and X-Ray structures	
<hr/>	

ACRONYMS AND ABBREVIATIONS

Reference guide of all the employed abbreviations

ACRONYMS AND ABBREVIATIONS

In the present document, and additionally to the recommendations of ACS “Guidelines for authors”, other acronyms and abbreviations have been used and listed below:

Ac	acetyl
API	active pharmaceutical ingredient
BArF	tetrakis[(3,5-trifluoromethyl)phenyl]borate
Bn	benzyl
BNP	4-hydroxydinaphtho[2,1-d:1',2'- f][1,3,2]dioxaphosphepine 4-oxide
Boc	(<i>tert</i> -butoxy)carbonyl
Bz	benzoyl
Cbz	benzyloxycarbonyl
Cod	1,5-cyclooctadiene
Conv.	conversion
CSA	camphorsulfonic acid
DABCO	1,4-diazabicyclo[2.2.2]octane
DCM	dichloromethane
DIPE	diisopropyl ether
DMAP	4-(dimethylamino)pyridine
DMC	dimethyl carbonate
DMI	dimethyl itaconate
DME	1,2-dimethoxyethane
DMF	<i>N,N</i> -dimethylformamide
DMS	dimethylsulfane
DPP	diphenylphosphoric acid
ESI	Electrospray Ionization
Ee	enantiomeric excess
FID	Flame Ionization Detector
Fmoc	9-fluorenylmethoxycarbonyl
GABA	γ -Aminobutyric acid
GC	Gas Chromatography
HPLC	High Performance Liquid Chromatography
IPA	isopropanol

IR	Infrared
L-DOPA	(<i>S</i>)-3',4'-dihydroxyphenylalanine
MAA	methyl (<i>N</i>)-(acetylamino)acrylate
MeTHF	2-methyltetrahydrofuran
MOM	methoxymethyl
MsOH	methanesulfonic acid
Nbd	1,5-norbornadiene
<i>n</i> -BuLi	<i>n</i> -butyllithium
NMR	Nuclear Magnetic Resonance
ORTEP	Oak Ridge Thermal Ellipsoid Plot Program
RT	Room Temperature
SPS	Solvent Purification System
Tfb	tetrafluorobarrelene
TFA	trifluoroacetic acid
THF	tetrahydrofuran
TOF	turnover frequency
TON	turnover number
Tr	trityl
t_R	retention time
UV	Ultraviolet
TsOH	<i>p</i> -toluenesulfonic acid
Z-MAC	methyl (<i>Z</i>)-(<i>N</i>)-acetylaminocinnamate
2M2B	2-methyl-2-butanol

PRÓLOGO

Comentarios iniciales y distribución de contenidos

PRÓLOGO

El grado de doctor se trata del más alto grado académico concedido por una universidad. Etimológicamente, el grado de doctor se nombra muchas veces como PhD, Philosophiae Doctor, o doctor en filosofía por el grado de implicación y compromiso en la persona que lo posee por la sabiduría y el conocimiento. Un doctorado en investigación es un proceso que culmina con la presentación de un trabajo original de investigación y defensa del mismo ante las alegaciones de un tribunal compuesto asimismo por doctores, de forma que dado el caso, el aspirante es declarado por aquellos como un igual.

Para ello presento a valoración el siguiente monográfico. Esta tesis doctoral se compone de una introducción general en la que se sentarán las bases de conocimiento que inspiraron este trabajo, con las principales aportaciones que permitan tener una visión del estado del área de conocimiento, centrándolo en el campo de la asimetría, la catálisis y la hidrogenación enantioselectiva. Al final de la introducción se encuentran los objetivos que, a la vista de lo expuesto en la introducción, se tratarán de conseguir en el resto del trabajo.

El cuerpo principal del presente trabajo se encuentra dividido en dos capítulos. En el primero de ellos se describirá la coordinación de ligandos P-OP altamente modulares a rodio, su posterior evaluación como catalizadores eficientes para la hidrogenación asimétrica de alquenos funcionalizados de muy diversa naturaleza, así como su aplicación posterior en la síntesis de ingredientes farmacéuticos activos.

El segundo capítulo está dedicado al estudio de la coordinación de estos ligandos a iridio, los cuales permitirán acceder a otros modos de acción que posibiliten la hidrogenación de enlaces C=N. Esto se evaluará a través de la hidrogenación principalmente de compuestos heterocíclicos y heteroaromáticos, que nos permitirán obtener aminas quirales como valiosos intermedios sintéticos. El capítulo culminará con un estudio del mecanismo de hidrogenación de una quinoleína sustituida a través de una aproximación con experimentos de marcaje isotópico.

Al final de cada uno de los dos capítulos y después de la discusión de resultados, se encuentra la correspondiente sección experimental, donde se podrá buscar información acerca de los métodos de síntesis, caracterización de nuevos compuestos, separación de enantiómeros así como todo tipo de detalles experimentales empleados en la elaboración de los correspondientes capítulos.

Finalmente se encuentra el apartado de las conclusiones, en donde se relacionarán los hitos conseguidos en la presente tesis, y la evaluación de la consecución de los objetivos marcados al inicio de la tesis.

RESUMEN

Visión general y resumida de la tesis

RESUMEN

La hidrogenación asimétrica catalítica de sustratos proquirales posee una gran importancia como herramienta para la obtención de compuestos enantioenriquecidos debido a su versatilidad y atractivo perfil industrial. En el seno de nuestro grupo de investigación se sentaron las bases y la estrategia sintética necesaria que permitió la síntesis de una librería de ligandos *P-OP* altamente modulares (Figura 1). Esta estrategia posibilita optimizar independientemente cada uno de los módulos para conseguir una óptima transferencia de quiralidad hacia el sustrato.

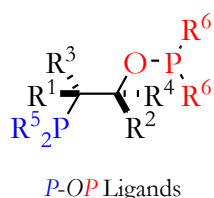


Figura 1. El diseño altamente modular de nuestros ligandos permite incorporar hasta seis módulos diferentes.

Los estudios de coordinación con precursores de rodio y una exploración de su capacidad como catalizadores en la hidrogenación asimétrica de alquenos funcionalizados llevados a cabo previamente en el grupo nos llevaron a plantear para el desarrollo de la presente tesis doctoral la expansión del alcance de la reacción hacia otras familias de alquenos funcionalizados. Asimismo, se creyó altamente interesante explorar la coordinación de los ligandos *P-OP* con precursores de iridio y evaluar el uso de los complejos resultantes en la hidrogenación de otros tipos de sustratos.

Por lo que se refiere a los estudios realizados en el campo de la hidrogenación asimétrica catalizada por complejos de rodio enantioméricamente puros, se han desarrollado en primer lugar nuevos ligandos con sustituyentes más voluminosos en el grupo CH_2OR . Se ha determinado la eficiencia catalítica de los catalizadores de rodio derivados de los mejores ligandos de la librería, observándose una muy alta eficacia en la hidrogenación de alquenos funcionalizados, con cargas de catalizador de hasta 0.01 mol% así como unos perfiles de velocidad en la hidrogenación de cuatro

alquenos modelo con valores de TOF mayores de 49000 h⁻¹ para el mejor de los casos (véase la Figura 2).

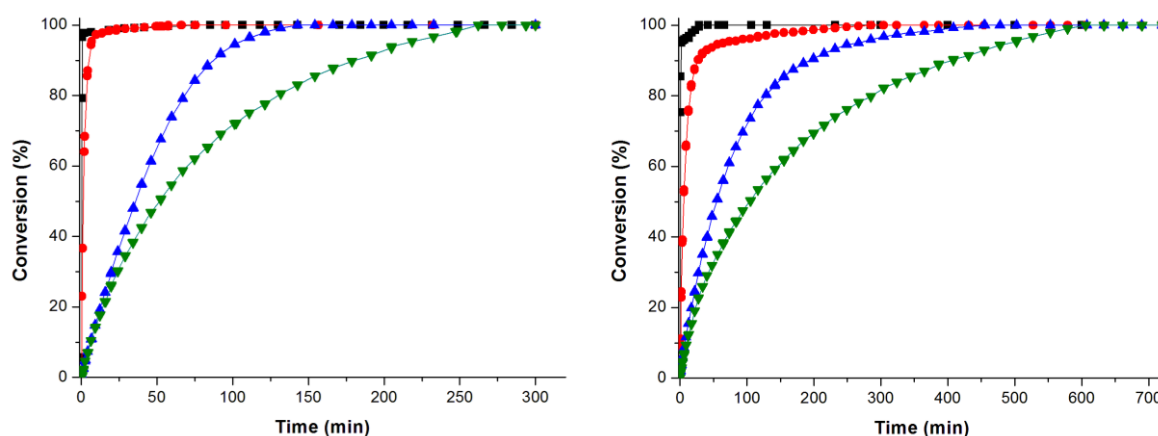
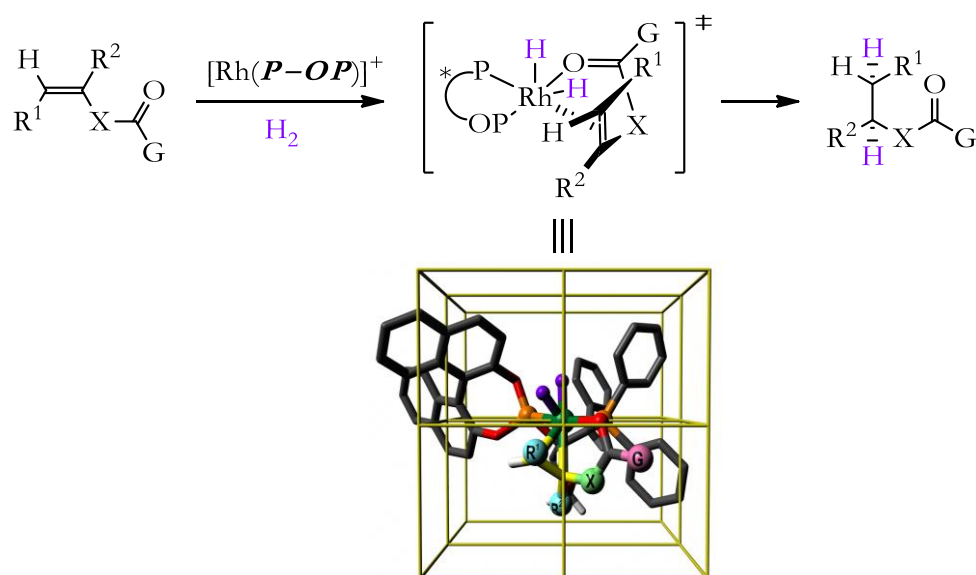


Figura 2. Curvas de absorción de hidrógeno para la determinación para 2-acetamidoacrilato de metilo (negro), itaconato de dimetilo (rojo), acetato de 1-fenilvinilo (azul) y *N*-(1-fenilvinil)acetamida (verde).

Dada la alta reactividad de estos catalizadores se evaluó la hidrogenación asimétrica sobre treinta y cinco sustratos diferentes, pertenecientes a familias de α -(acilamino)acrilatos β -sustituídos, enamidas α -sustituídas, ésteres de enol α -sustituídos, así como derivados del ácido itacónico y análogos (Esquema 1).



Esquema 1. Hidrogenación de alquenos funcionalizados y diagrama de cuadrantes del estado de transición más favorable para el alqueno funcionalizado con la fórmula general indicada en la parte superior de la figura.

Los altos valores de conversión y enantioselectividad obtenidos en la práctica totalidad de los casos nos condujo a sintetizar e hidrogenar una serie de sustratos estratégicamente concebidos (13 ejemplos), cuyos productos de hidrogenación fueran directamente principios activos farmacéuticos (APIs), o intermedios avanzados en su síntesis, incorporando de esta forma centros estereogénicos clave en su estructura. De esta forma se consiguieron encontrar las condiciones catalíticas adecuadas para la preparación enantioselectiva de intermedios sintéticos de compuestos bioactivos tales como el levetiracetam, la lacosamida, la rivastigmina o el aprepitant, entre otros (Figura 3).

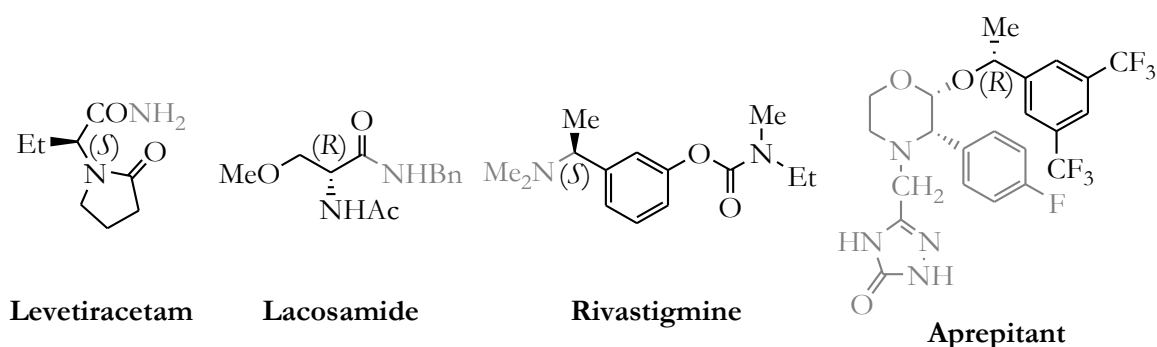


Figura 3. Ejemplos de APIs quirales accesibles con nuestra metodología.

Se exploró entonces la coordinación de los ligandos *P-OP* a precursores de iridio, obteniéndose tanto complejos neutros como catiónicos derivados de fosfina-fosfinitos y fosfina-fosfitos, generando especies catalíticamente activas para hidrogenación. Su evaluación en la hidrogenación de seis iminas acíclicas condujo a bajos niveles de enantioselección. No obstante en la exploración de otras iminas cíclicas, como son benzoxazinas, benzoxazinonas, benzotiazinonas o quinoxalinonas se obtuvieron altos niveles de conversión y enantioselectividad, con cargas de catalizador de hasta 0.05 mol% y enantioselectividades típicamente superiores al 90% ee. Se obtuvieron de esta forma cuarenta y cuatro heterociclos quirales parcialmente reducidos, para los cuales su acceso *vía* hidrogenación asimétrica, o bien no había sido descrito en la bibliografía con anterioridad, o bien existían muy pocos precedentes.

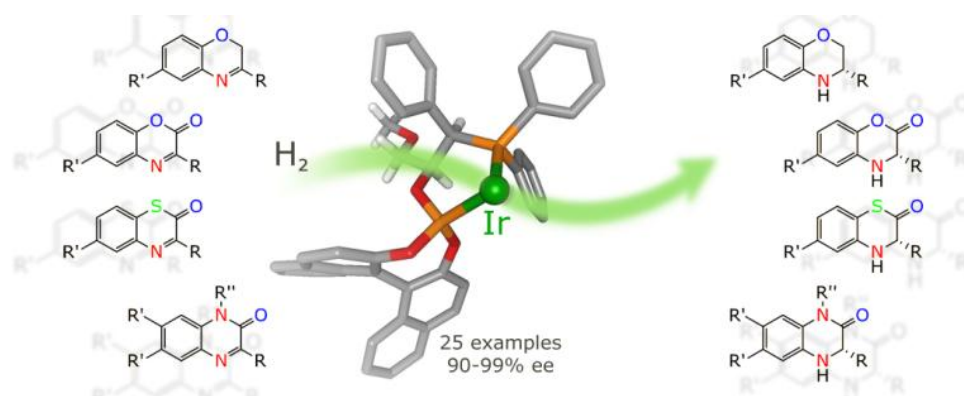
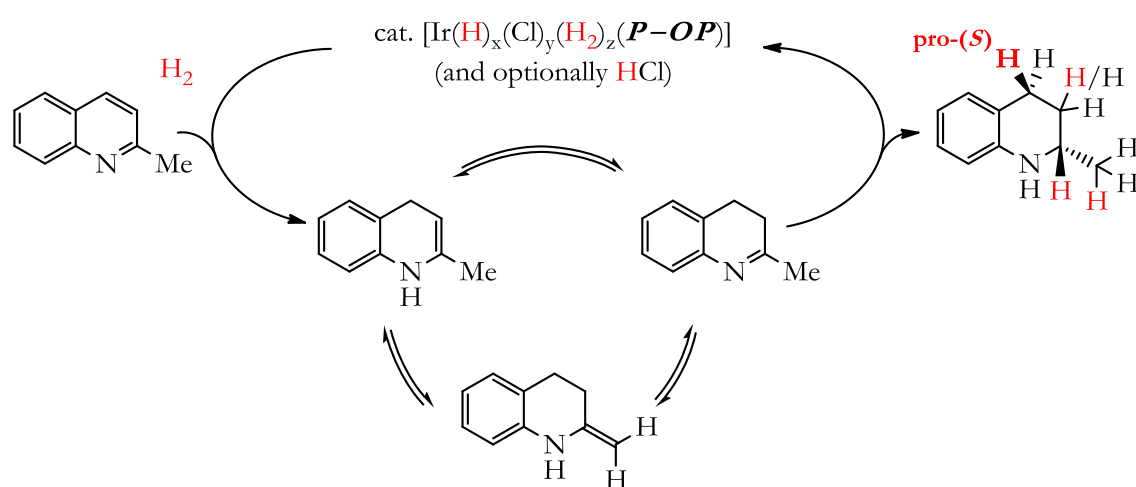


Figura 4. Hidrogenación enantioselectiva de una amplia variedad de heterociclos proquirales catalizada por $[\text{Ir}(\text{P-OP})]^+$.

Para la exploración de la hidrogenación asimétrica de sustratos heteroaromáticos como quinoleínas, quinoxalinas e indoles con los catalizadores $[\text{Ir}(\text{P-OP})]^+$, se desarrollaron estrategias de activación de sustrato basadas en la adición de cantidades catalíticas o estequiométricas de ácidos de Brønsted, tales como HCl, ácido canforsulfónico (CSA) o resinas ácidas de intercambio catiónico.

Finalmente se han estudiado los caminos de hidrogenación de una benzoxazina y quinoleína modelo mediante marcaje isotópico con especies deuteradas (posibles combinaciones de H_2/D_2 y HCl/DCl). El tautómero C=C exocíclico se ha detectado en el crudo de hidrogenación de la 2-metilquinoleína, lo que amplía y complementa los posibles caminos de hidrogenación que se habían propuesto con anterioridad en la literatura para ese compuesto.



Esquema 2. Estudios en el mecanismo de hidrogenación asimétrica de quinoleínas mediada por catalizadores $[\text{Ir}(\text{P-OP})]^+$.

INTRODUCTION

Where we are, where we will go

UNIVERSITAT ROVIRA I VIRGILI
HIGHLY MODULAR P -OP LIGANDS FOR RHODIUM- AND IRIIDIUM-MEDIATED ASYMMETRIC HYDROGENATIONS
José Luis Núñez Rico
DL: T.994-2013

INTRODUCTION

Asymmetry is everywhere. Just taking a quick look reveals that our world is full of examples of asymmetry in such varied fields as nature, art, photography and of course, chemistry. We are ourselves, in fact, asymmetric beings. One of the first discoveries that every young scientist makes is the empirical verification of the dissimilarity on his hands (or feet). They seem identical, but are non-superimposable mirror images of one another. These kinds of objects, which are non-superimposable onto their mirror image are said to be chiral. In fact, the origin of the word chiral can be found in the Greek word “ $\chi\epsilon\rho$ ”, meaning hand. Any pair of chiral objects are said to be enantiomorphous.¹ This topic has interested for decades not only scientists, but also artists such as Escher, mathematicians such as Möbius and philosophers such as Kant.²

Lord Kelvin, in his contribution to the 1884 Baltimore Lectures, was the first to introduce the concept of chirality to science, and gave his definition as

¹ Eliel, E. E.; Wilen, S. H. *Stereochemistry of Organic Compounds*; John Wiley & Sons, Inc.: New York, 1994.

² Cintas, P. *Angew. Chem., Int. Ed.* **2007**, *46*, 4016.

follows:³ “I call any geometrical figure, or group of points, chiral, and say that it has chirality, if its image in a plane mirror, ideally realized, cannot be brought to coincide with itself”. When we adapt this concept to the molecular level, we call *molecules that are non-superimposable mirror images of each other* enantiomers. Enantiomers have exactly the same properties in an achiral environment, but show a different response to chemical or physical asymmetric stimuli.

In a chiral environment, the plane of polarization of polarized light gets rotated, a phenomenon known as optical rotation or optical activity. The specific rotation⁴ is a property of a material (a solution of a chiral molecule, a chiral liquid or a chiral solid or object) and is exactly opposite for both

“Je regarde comme extrêmement probable que la disposition mystérieuse, inconnue, des molécules physiques, dans un cristal entier et fini de quartz, se retrouve dans les corps actifs, mais, cette fois, dans chaque molécule prise en particulier.”

“I consider as extremely probable that the mysterious, unknown disposition of physical molecules in a whole and finite quartz crystal is found in (optically) active bodies, but, this time, in each molecule taken in particular.”

Figure 1. Pasteur’s correlation of macroscale properties and molecular structure.

³ Kelvin, W. T. *The Baltimore Lectures*, 1884; later published in Kelvin, W. T. *Baltimore Lectures on Molecular Dynamics and the Wave Theory of Light*, C.J. Clay: London, 1904.

⁴ The specific rotation (denoted as $[\alpha]_D^{25}$) depends on wavelength and temperature, usually indicated as subscript and superscript (wavelength of the sodium D-line (589 nm) at 25 °C). Specific rotation is calculated for solutions of chiral compounds with the following formula:

$$[\alpha]_D^{25} = \frac{\alpha \text{ (observed angle)}}{l \text{ (length of the cell in dm)} \cdot c \text{ (concentration in g} \cdot \text{ mL}^{-1}\text{)}}$$

Specific rotation also depends on the solvent and to some extent on the concentration, which must be specified. This is done by giving this information in parentheses with the following format (concentration expressed as grams of substrate in 100 mL of solvent, solvent used for the measurement).

enantiomers or enantiomorphous objects under the same conditions. This fact was discovered in the first quarter of the 19th century by François Arago,⁵ irradiating slabs of a perpendicularly cut quartz crystal. The phenomenon is a property of some crystals and Jean-Baptiste Biot extended it to naturally occurring liquids such as lemon oil, turpentine and sugar solutions.⁶

Since the fundamental discoveries of Arago and Biot, many efforts were dedicated to the study of the optical properties of matter. In 1848, Louis Pasteur was working with non-optically active solutions of sodium ammonium tartrate. He realized that when letting these solutions crystallize, they did so as either right- or left-handed hemihedral crystals. After dissolving these pure form crystals, the solution rotated polarized light to the right or the left. Pasteur had performed the first known physical separation of enantiomers.⁷ Moreover, he hypothesized the relationship between the hemihedric crystal faces (at the macroscale) and the constituting molecules as described in Figure 1. He called this phenomenon molecular dissymmetry,⁸ which is an obsolete synonym of chirality. It should also be noted that the first experimentally studied asymmetric reaction is attributable to Pasteur, when he observed that the organism *Penicillium glauca* in a racemic solution of ammonium tartrate destroyed one of the enantiomers faster than the other. The observed asymmetric reaction can be named in modern organic chemistry as a decarboxylative kinetic resolution.⁹ As a consequence of the chiral elements of which a biological system (*i.e.* living organisms, enzymes, biological receptors and so on) is composed, there can be a different response from these systems

⁵ Arago's work was published posthumously as: *Oeuvres de François Arago*; Barral, J. A., Ed.; Gide et J. Baudry: Paris, 1854.

⁶ Biot, J. B. *Mélanges Scientifiques et Littéraires*, Michel Lévi Frères: Paris, 1858.

⁷ Pasteur, L. *Compt. Rend. Acad. Sci.* **1858**, *46*, 15.

⁸ Pasteur, L. *Œuvres de Pasteur, Vol 1*, Masson: Paris, 1922, p. 21 (La dissymétrie moléculaire).

⁹ Kagan, H. B. In *Comprehensive Asymmetric Catalysis*; Jacobsen, E. N.; Pfaltz A.; Yamamoto H., Eds.; Springer-Verlag: Berlin, 1999; Vol 1, p. 101.

to both enantiomers of a given substance (for instance, the two enantiomers of the tartaric acid derivative previously mentioned).

Biological odorant receptors constitute another example of different responses of biological receptors to chiral molecules, as perfumers often experience. As an example, (+)-(*R*)-limonene smells like orange, while the (–)-(*S*)-enantiomer smells like lemon; the enantiomer (–)-(*R*)-carvone smells like peppermint, while the (+)-(*S*)-form smells like caraway (see Figure 2).

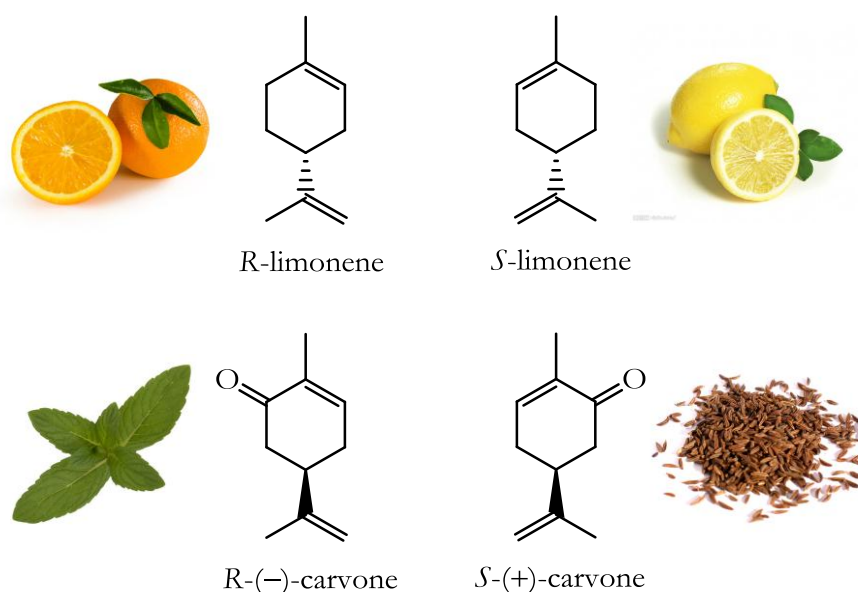


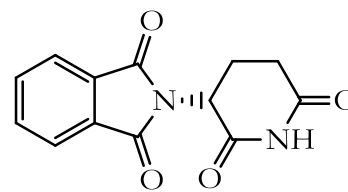
Figure 2. Differences in odor in enantiomeric pairs.

Racemic mixtures of biologically active compounds used to be given to subjects with the assumption of the same activity for both enantiomers, or in the hope that the subject would be able to differentiate and choose the “adequate” one, leaving the other enantiomer untransformed or ignored completely. Sometimes, it was found that enantiomers had radically different physiological effects such as in the case of the thalidomide controversy in the 1960’s. It was discovered that this drug, administered for several years in a racemic form to prevent “morning sickness” (nausea) during pregnancy,

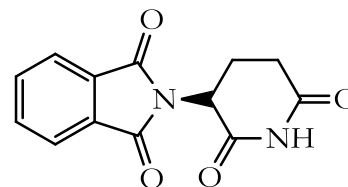
showed different activities depending on the enantiomer. While the (*R*)-configured enantiomer is a sedative with anti-inflammatory activity, the (*S*)-enantiomer of thalidomide is teratogenic, which can seriously damage human embryos (Figure 3).¹⁰ To aggravate the situation, it was discovered that human liver contains an enzyme capable of transforming (*R*)-thalidomide into its (*S*)-enantiomer.¹¹ This situation, with more than 10,000 estimated children born with defects,

forced the U.S. Food and Drug Administration (FDA) to order the testing of the pharmacological activities of both enantiomers of any drug in its racemic form before being authorized.¹² As a consequence of the FDA's 1992 policy announcement on stereoisomers, attention was focused on synthetic chemists to develop new and efficient methods for obtaining enantiomerically pure compounds.

Furthermore, the additional efforts and cost of producing a new single enantiomerically pure drug, compared with the cost of producing the corresponding racemate, is in many cases even lower as extra efforts are



(*R*)-Thalidomide: Calm nauseas



(*S*)-Thalidomide: Teratogenic

Figure 3. Thalidomide enantiomers.

¹⁰ McCredie, J. J. *Med. Imaging Radiat. Oncol.* **2009**, *53*, 433.

¹¹ Stephens, T. *Chem. Br.* **2001**, *37*, 38.

¹² For example see: a) Investigation of Chiral Active Substance: http://www.ema.europa.eu/docs/en_GB/document_library/Scientific_guideline/2009/09/WC500002816.pdf. b) FDA Policy Statement for the Development of New Stereoisomeric Drugs, Washington DC, 1992: <http://www.fda.gov/Drugs/GuidanceCompliance-RegulatoryInformation/Guidances/ucm122883.htm>.

required to elucidate the toxicological and pharmacokinetic profile of the distomer¹³ when racemates are employed.

As a result of the 1992 legislation, the trend in the number of launched chiral drugs on the market in the following ten year period (1993-2003) decreased dramatically for racemic mixture drugs, whereas it increased slightly for new single enantiomer drugs (Figure 4).¹⁴

Along these lines, 94% of the approved chiral drugs by the FDA in 2006 were commercialized in enantiomerically pure form.¹⁵ It should also be mentioned that seven of the ten top-selling drugs in the US for the year 2010 were all single enantiomers.¹⁶ According to the Global Industry Analysts Inc. report, the global market for Chiral Technology products is forecast to reach \$4.9 billion by the year 2015.¹⁷ Apart from pharmaceutical products, agrochemicals are another class of compounds that will probably have to meet increasing demands regarding enantiopurity in the near future.¹⁸

¹³ A distomer is the enantiomer with the lesser activity or affinity for a given receptor; one receptor's distomer can be another receptor's eutomer.

¹⁴ Farina, V.; Reeves, J. T.; Senanayake, C. H.; Song, J. J. *Chem. Rev.* **2006**, *106*, 2734.

¹⁵ a) Thayer, A. M. *Chem. Eng. News* **2007**, *85*, 11. b) Thayer, A. M. *Chem. Eng. News* **2008**, *86*, 12.

¹⁶ These drugs are Lipitor[®], Nexium[®], Plavix[®], Advair[®], Singulair[®], Crestor[®] and Actos[®] representing \$35.8 billion in sales in 2010. Source IMS Health, Pharmacy Times: <http://www.pharmacytimes.com/publications/issue/2011/May2011/Top-200-Drugs-of-2010>.

¹⁷ Global Industry Analysts, Inc. (GIA) is a publisher of off-the-shelf market research. An abstract of the chiral technology report can be found in: http://www.prweb.com/releases/chiral_technology/separation_stereogenic/prweb8145406.htm

¹⁸ See for example Sekhon, B. S. J. *J. Pestic. Sci.* **2009**, *34*, 1 and the references cited therein.

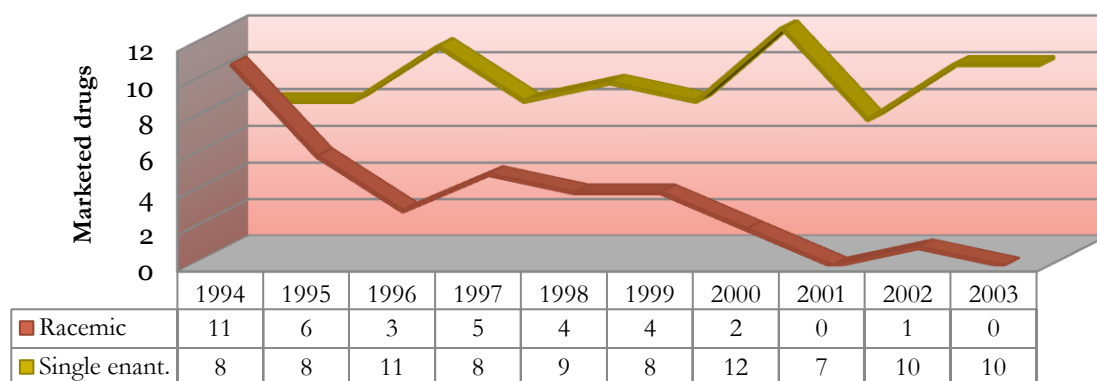


Figure 4. Marketed chiral drugs: comparison between racemic *vs.* single enantiomer.¹⁹

In principle, two general strategies for obtaining single enantiomers or enantioenriched mixtures, apart from synthesizing them up from a starting material from the natural chiral pool, can be considered:

1.- Separation of a racemic mixture into isolated enantiomers. The resolution of racemates into their enantiomers by preferential or diastereomer crystallization²⁰ was one of the first methods to be used and it still is the most important method for the industrial preparation of enantiomers. Theoretical yields of 100% of the pure enantiomer are achievable for both crystallization types under certain conditions, like spontaneous *in situ* racemization (for preferential crystallization) and spontaneous diastereomer interconversion (for diastereomer crystallization). However, the more common cases result in theoretical yields of 50%, which represents a drawback unless the undesired enantiomers can be racemized and recycled, or there is a demand for each of the enantiomers.

¹⁹ Other types of marketed drugs (non-chiral molecules, natural products and derivatives, proteins and related compounds and inorganic derivatives) have been omitted for clarity. See ref 14 for the complete information.

²⁰ Sheldon, R. A. *Chirotechnology: Industrial Synthesis of Optically Active Compounds*; Marcel Dekker: New York, 1993.

Large-scale chromatographic separation techniques (*i.e. simulated moving bed* (SMB) chromatography²¹) are emerging and are becoming important preparation methods for APIs, especially at the early phases of product development or even for the whole production.

Kinetic resolution^{20,22} allows for the differentiation of two enantiomers in a racemate, when the enantiomers of a given starting material react at different rates with a chiral reagent, or interact differently with a chiral catalyst. In these cases, kinetic resolution results in an enantioenriched sample of the less reactive enantiomer of the starting material and an enantioenriched product derived from the most reactive substrate's enantiomer. Unless the two enantiomers of the starting material are capable of interconverting (dynamic kinetic resolution),²² overall theoretical yields of 50% for unreacted starting material and product are achievable.

2.- Asymmetric chemical reactions. Organic synthesis that creates in a controlled manner one or more new stereogenic elements in a molecule is referred to as stereoselective synthesis,²³ which implies either transformation of a certain substrate's pro-stereogenic element into a stereogenic element (center, plane or axis) in the product, or removal of elements of symmetry in the starting material (desymmetrization).

The use of chiral reagents or chiral auxiliaries²⁴ allowed the preparation of complex enantiopure organic molecules.²⁰ However, both approaches (the use of chiral reagents and chiral auxiliaries) have substantial drawbacks. Chiral

²¹ *Chiral Separation Techniques: A Practical Approach*; Subramanian, G., Ed.; Wiley-VCH: Weinheim, 2001; 2nd Ed.

²² Pellissier, H. *Chirality from Dynamic Kinetic Resolution*; RSC: Cambridge, 2011.

²³ *Comprehensive Chirality*; Carreira, E. M.; Yamamoto, H. Eds.; Elsevier Science: Oxford, 2012; Vols. 1-9.

²⁴ A chiral auxiliary is a chemical compound that is reversibly incorporated into an organic substrate so that the required reaction can be carried out asymmetrically under selective formation of one diastereoisomer.

reagents must be applied in stoichiometric amounts, whilst chiral auxiliaries require additional synthesis steps (attachment, removal and recycling of the chiral auxiliary).

Asymmetric catalysis, in which each molecule of chiral catalyst, by virtue of its continuous regeneration, mediates the formation of a large number of molecules of enantiomerically pure product, is *a priori* the more elegant approach in stereoselective synthesis.²⁵

Asymmetric catalysis had attracted a lot of interest from the scientific community since its inception, as most *in vivo* biological reactions are catalyzed by biochemical, hence chiral, catalysts.

A chiral catalyst, either organic or organometallic, provides to reactants a low energy pathway to the final products and mediates the preferential formation of one of the possible stereoisomers. Furthermore, the option of using a chiral catalyst as a source of chirality may have several advantages compared with stoichiometric asymmetric synthesis, such as atom economy, simplicity for scaling up, energy-saving, minimum waste generation, minimum by-product formation, and due to the generally low catalyst loadings, lower cost. The great importance of asymmetric catalysis is reflected in the ever increasing number of publications in this field as well as in the award of the Nobel Prize in 2001 to W. S. Knowles and R. Noyori “for their work on chirally

8	9	10	11
26 Fe	27 Co	28 Ni	29 Cu
44 Ru	45 Rh	46 Pd	47 Ag
76 Os	77 Ir	78 Pt	79 Au

Figure 5. Some transition metals involved in pivotal transformations in organometallic chemistry, including hydrogenation.

²⁵ Noyori, R. *Chem. Soc. Rev.* **1989**, *18*, 187.

catalysed hydrogenation reactions” and K. B. Sharpless for “*his work on chirally catalysed oxidation reactions*”.²⁶

Asymmetric catalysis was originally divided into two branches: enzymatic catalysis and non-enzymatic catalysis (metal catalysis), but since the blossoming in the past decade of catalysis mediated by relatively small, low molecular weight organic molecules, a new branch referred to as organocatalysis²⁷ has emerged and it is now commonly accepted that the three main categories are enzymatic catalysis, metal catalysis and organocatalysis.

Many achievements have been made in the three fields of asymmetric catalysis making possible the synthesis of a myriad of chiral compounds in enantiomerically pure or highly enantioenriched form.

The main topic of this thesis, asymmetric homogeneous hydrogenation, has interested many scientific groups, motivated by an expanding universe of interesting prochiral substrates capable of being asymmetrically hydrogenated to highly valuable chiral products. Asymmetric hydrogenation is attractive due to its operational simplicity and sustainable conditions. Starting from the earliest days of asymmetric catalysis, there has been ever increasing research efforts in asymmetric hydrogenation within academia and industry. This work has provided a deep mechanistic understanding of the chemistry and enabled the development of a myriad of chiral Ru-, Rh-, and Ir-coordination compounds (mostly phosphorus-containing derivatives) that can mediate the addition of hydrogen to prochiral C=C, C=N, and C=O double bonds with

²⁶ a) Knowles, W. S. *Angew. Chem., Int. Ed.* **2002**, *41*, 1998. b) Noyori, R. *Angew. Chem., Int. Ed.* **2002**, *41*, 2008. c) Sharpless, K. B. *Angew. Chem., Int. Ed.* **2002**, *41*, 2024.

²⁷ For example, see: (a) *Enantioselective Organocatalysis*; Dalko, P. I., Ed.; Wiley-VCH: Weinheim, 2007. (b) *Asymmetric Organocatalysis*, List, B., Ed.; Springer: Berlin, 2010. (c) *Comprehensive Chirality*; Carreira, E. M.; Yamamoto, H. Eds.; Elsevier Science: Oxford, 2012; Vol. 6.

very high enantioselectivities. As a consequence, transition metal-mediated^{28, 29} asymmetric hydrogenation of prochiral unsaturated substrates is now amongst the most efficient³⁰ and reliable methodologies in asymmetric catalysis. From a practical perspective, enantioselective hydrogenation offers several advantages for the synthesis of valuable chiral products (optimal atom economy, broad substrate scope, high reactivity and selectivity, as well as operational simplicity). For all of these reasons, many industrial methods for the synthesis of optically active products for the pharmaceutical, agrochemical, advanced material, and fragrance sectors rely on catalytic asymmetric hydrogenation reactions.³¹

²⁸ Asymmetric hydrogenation by using enzymatic methods has experienced limited advances in the last few years. See for example: (a) Wada, M.; Yoshizumi, A.; Noda, Y.; Kataoka, M.; Shimizu, S.; Takagi, H.; Nakamori, S. *Appl Environ Microbiol* **2003**, *69*, 933. (b) Wei, L.; Makowski, T.; Martinez, C.; Ghosh, A. *Tetrahedron: Asymmetry* **2008**, *19*, 2648. (c) Glueck, D. S. *Chem.-Eur. J.* **2008**, *14*, 7108.

²⁹ To the best of this thesis' author knowledge, reports on organocatalytic direct hydrogenation are scarce (see, for example Liu, Y.; Du, H. *J. Am. Chem. Soc.* **2013**, *135*, 6810). Organocatalyzed asymmetric transfer hydrogenation (ATH) constitutes an efficient alternative strategy that does not involve the use of metals and hydrogen and mostly relies on mimicking the way in which Nature conducts hydrogenation reactions. NADH, NADPH or FADH₂ are cofactors in enzyme-catalyzed hydride reductions, and biomimetic reductions are possible with Hantzsch esters as structural analogues of the aforementioned cofactors. For recent reviews on the field, see: (a) Kagan, H. B. Organocatalytic Enantioselective Reduction of Olefins, Ketones, and Imines. In *Enantioselective Organocatalysis*; Dalko, P. I., Ed.; Wiley-VCH: Weinheim, 2007. (b) Rueping, M.; Sugiono, E.; Schoepke, F. R. *Synlett* **2010**, 852. (c) de Vries, J. G.; Mrcic, N. *Catal. Sci. Technol.* **2011**, *1*, 51. (d) Zheng, C.; You, S.-L. Reduction: Asymmetric Transfer Hydrogenation with Hantzsch Esters. In *Comprehensive Chirality*; Carreira, E. M., Yamamoto, H., Eds.; Elsevier: Oxford, 2012; Vol. 6, p. 586.

³⁰ Despite the usually very low metal concentrations employed, a lot of strategies have been developed for the efficient removal of metal residues from valuable products obtained by asymmetric hydrogenation (see for example: Bien, J. T.; Lane, G. C.; Oberholzer, M. R. Removal of Metals from Process Streams: Methodologies and Applications. In *Organometallics in Process Chemistry*; Larsen, R. D., Ed.; Springer-Verlag: Berlin, 2004; Top. Organomet. Chem. Vol 6, p. 263). Hydrogenation products must be delivered within the allowed concentration limits for platinoid metals (the European Agency for the Evaluation of Medicinal Products (EMA) proposes 5-50 ppm as concentration limit values; see: The European Agency for the Evaluation of Medicinal Products: Note for guidance on specification limits for residues of metal catalysts, December 2002.).

³¹ (a) Saudan, L. A. *Acc. Chem. Res.* **2007**, *40*, 1309. (b) Shultz, C. S.; Krska, S. W. *Acc. Chem. Res.* **2007**, *40*, 1320. (c) Klingler, F. D. *Acc. Chem. Res.* **2007**, *40*, 1367. (d) Shimizu, H.;

The key step in most catalytic asymmetric processes involves the assembly at the supramolecular level of the substrate and reagent(s), usually around a chiral organometallic complex (ligand accelerated catalysis, LAC³²), or purely around an enantiopure chiral molecule (organocatalysis). As in every supramolecular process, non-covalent interactions (mainly hydrogen bonding, π - π stacking or metal-ligand bonding) are responsible for the reversible assembly of substrates and reagents around the chiral catalyst. The nature and strength of the binding forces by which the reagents assemble around the catalyst are highly dependent on the nature of the catalyst, the chemical transformation and the mechanism of stereinduction. In such catalytic systems, the organometallic complex (or the enantiomerically pure organic molecule alone) provides a low energy reaction pathway to the products. Furthermore, the enantiomerically pure ligand is responsible for enantioselection as it creates a chiral environment around the active site which ultimately allows the preferential recognition of an enantiotopic atom, group or face from the substrate. With the aim of developing improved asymmetric catalysts, many classes of chiral ligands (both from the “chiral pool” and “non-natural” sources) have been designed, synthesized and tested in almost every synthetic transformation amenable to catalysis. Significant effort in the field has focused on ligand design and trial-and-error optimization cycles, but at times serendipity has also played a role. Two main factors have contributed, in the opinion of this author, to the remarkable progress in the field. First and foremost, the use of ligands derived from enantiopure non-natural starting materials has broadened the structural diversity of available catalysts. Secondly, the modular nature of the ligands has facilitated the tuning of their

Nagasaki, I.; Matsumura, K.; Sayo, N.; Saito, T. *Acc. Chem. Res.* **2007**, *40*, 1385. (e) Etayo, P.; Vidal-Ferran, A. *Chem. Soc. Rev.* **2013**, *42*, 728.

³² Berrisford, D. J.; Bolm, C.; Sharpless, K. B. *Angew. Chem., Int. Ed. Engl.* **1995**, *34*, 1059.

performance by modifying the stereoelectronic properties of the different molecular fragments (modules).³³

When developing or improving a catalytic process *via* catalyst tuning, catalyst design is crucial. Ideally, ligand design should incorporate several independent modules or molecular fragments arranged around a chiral skeleton. If these modules are designed such that they can influence the catalytic site, then modification of their steric and electronic properties should provide a higher performing catalytic system (*i.e.* one that offers higher conversion, regio- and/or enantio-selectivity). Indeed, the sterics and electronics factors of the constituent modules/molecular fragments can be considered the *input parameters* in the optimization process. Many research groups,³⁴ including ours³⁵, have been attracted by the design and development of modular ligands for asymmetric catalysis of transformations of interest.

³³ The modular nature of a ligand normally allows accommodation of the chiral catalysts to the practical necessities of the system under investigation (*e.g.* immobilization onto a solid support).

³⁴ See for example: (a) Trost, B. M.; Van Vranken, D. L.; Bingel, C. J. *Am. Chem. Soc.* **1992**, *114*, 9327. (b) Rajanbabu, T. V.; Casalnuovo, A. L.; Ayers, T. A. *Adv. Catal. Processes* **1997**, *2*, 1. (c) Kranich, R.; Eis, K.; Geis, O.; Mühle, S.; Bats, J. W.; Schmalz, H.-G. *Chem.-Eur. J.* **2000**, *6*, 2874. (d) Degrado, S. J.; Mizutani, H.; Hoveyda, A. H. *J. Am. Chem. Soc.* **2001**, *123*, 755. (e) Hamashima, Y.; Kanai, M.; Shibasaki, M. *Tetrahedron Lett.* **2001**, *42*, 691. (f) Pàmies, O.; van Strijdonck, G. P. F.; Diéguez, M.; Deerenberg, S.; Net, G.; Ruiz, A.; Claver, C.; Kamer, P. C. J.; van Leeuwen, P. W. N. M. *J. Org. Chem.* **2001**, *66*, 8867. (g) Dalko, P. I.; Moisan, L.; Cossy, J. *Angew. Chem., Int. Ed.* **2002**, *41*, 625. (h) Diéguez, M.; Ruiz, A.; Claver, C. *J. Org. Chem.* **2002**, *67*, 3796. (i) Locatelli, M.; Cozzi, P. G. *Angew. Chem., Int. Ed.* **2003**, *42*, 4928. (j) Jensen, J. F.; Søtofte, I.; Sørensen, H. O.; Johannsen, M. *J. Org. Chem.* **2003**, *68*, 1258. (k) Jeulin, S.; De Paule, S. D.; Ratovelomanana-Vidal, V.; Genêt, J.-P.; Champion, N.; Dellis, P. *Proc. Natl. Acad. Sci. U. S. A.* **2004**, *101*, 5799. (l) Goldfuss, B.; Löschmann, T.; Rominger, F. *Chem.-Eur. J.* **2004**, *10*, 5422. (m) Knöpfel, T. F.; Zarotti, P.; Ichikawa, T.; Carreira, E. M. *J. Am. Chem. Soc.* **2005**, *127*, 9682. (n) Liu, Y.; Ding, K. *J. Am. Chem. Soc.* **2005**, *127*, 10488. (o) Leroux, F. R.; Mettler, H. *Adv. Synth. Catal.* **2007**, *349*, 323. (p) Miller, J. J.; Sigman, M. S. *J. Am. Chem. Soc.* **2007**, *129*, 2752. (q) Wang, Y.; Sturm, T.; Steurer, M.; Arion, V. B.; Mereiter, K.; Spindler, F.; Weissensteiner, W. *Organometallics* **2008**, *27*, 1119. (r) Goudriaan, P. E.; van Leeuwen, P. W. N. M.; Birkholz, M.-N.; Reek, J. N. H. *Eur. J. Inorg. Chem.* **2008**, 2939. (s) Meeuwissen, J.; Kuil, M.; van der Burg, A. M.; Sandee, A. J.; Reek, J. N. H. *Chem.-Eur. J.* **2009**, *15*, 10272. (t) Caldentey, X.; Pericàs, M. A. *J. Org. Chem.* **2010**, *75*, 2628. (u) Loelsberg, W.; Ye, S.; Schmalz, H.-G. *Adv. Synth. Catal.* **2010**, *352*, 2023. (v) Robert, T.; Abiri, Z.; Wassenaar, J.; Sandee, A. J.; Romanski, S.; Neudörfl, J.-M.; Schmalz,

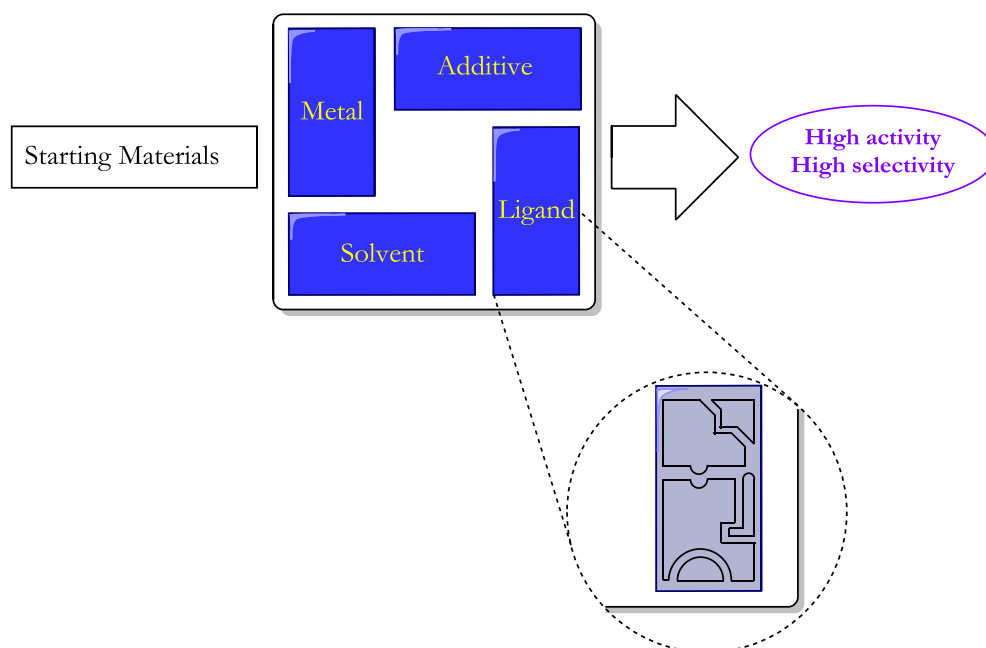


Figure 6. Catalytic system: from the proper combination of elements to success.

Although the ligand plays a key role in the catalytic performance of a catalyst, there are other important factors to consider. In fact, there must be the right combination between metal, ligand, additives and solvents, *i.e.* catalytic system (Figure 6), to achieve high chemo- and stereoselectivity in a given transformation.

Knowles accomplished in 1968 the first homogeneous asymmetric hydrogenation of a C=C bond by using a modified version of Wilkinson's catalyst ($[\text{Rh}(\text{Cl})(\text{PPh}_3)_3]$; see Figure 7 for its structure), in which

H.-G.; Reek, J. N. H. *Organometallics* **2010**, *29*, 478. (w) Chávez, M. A.; Vargas, S.; Suárez, A.; Álvarez, E.; Pizzano, A. *Adv. Synth. Catal.* **2011**, *353*, 2775. (x) Mazuela, J.; Norrby, P.-O.; Andersson, P. G.; Pamies, O.; Dieguez, M. *J. Am. Chem. Soc.* **2011**, *133*, 13634. (y) Kluwer, A. M.; Detz, R. J.; Abiri, Z.; van der Burg, A. M.; Reek, J. N. H. *Adv. Synth. Catal.* **2012**, *354*, 89.

³⁵ (a) Fernández-Pérez, H.; Pericàs, M. A.; Vidal-Ferran, A. *Adv. Synth. Catal.* **2008**, *350*, 1984. (b) Donald, S. M. A.; Vidal-Ferran, A.; Maseras, F. *Can. J. Chem.* **2009**, *87*, 1273. (c) Fernández-Pérez, H.; Donald, S. M. A.; Munslow, I. J.; Benet-Buchholz, J.; Maseras, F.; Vidal-Ferran, A. *Chem.-Eur. J.* **2010**, *16*, 6495. (d) Panossian, A.; Fernández-Pérez, H.; Popa, D.; Vidal-Ferran, A. *Tetrahedron: Asymmetry* **2010**, *21*, 2281.

triphenylphosphine ligands were replaced by monodentate chiral phosphines (CAMP ligand, see Figure 8).³⁶ Mislow³⁷ and Horner³⁸

set the foundations for this important achievement, as they previously developed practical synthetic methodologies for

preparing chiral phosphines with P-stereogenic centers. They also showed that phosphines are stable to pyramidal inversion well above room temperature.

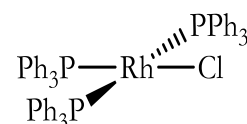
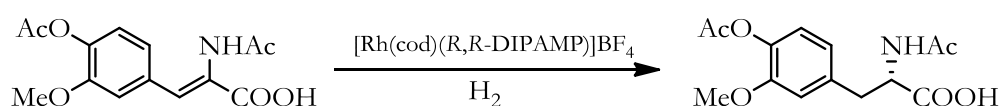


Figure 7. Wilkinson's catalyst.

Later on, Kagan *et al.* developed the DIOP ligand (see Figure 8),³⁹ a C₂-symmetric ligand capable of coordinating the Rh center in a bidentate mode. C₂-symmetry reduces the number of possible catalyst-substrate combinations, thus reducing the number of alternative and competing possible reaction pathways.

Knowles combined Kagan's idea of C₂-symmetric bidentate ligands with stereogenic phosphorus binding groups to prepare DIPAMP, an evolution of their previously prepared monophosphine CAMP ligands (Figure 8).⁴⁰



Scheme 1. Monsanto's L-DOPA process hydrogenation step.

³⁶ Knowles, W. S.; Sabacky, M. J. *J. Chem. Soc., Chem. Commun.* **1968**, 1445.

³⁷ (a) Korpiun, O.; Lewis, R. A.; Chickos, J.; Mislow, K. *J. Am. Chem. Soc.* **1968**, *90*, 4842. (b) Naumann, K.; Zon, G.; Mislow, K. *J. Am. Chem. Soc.* **1969**, *91*, 7012.

³⁸ Horner, L.; Siegel, H.; Bueche, H. *Angew. Chem., Int. Ed. Engl.* **1968**, *7*, 942.

³⁹ (a) Kagan, H. B.; Dang, T. P. *J. Chem. Soc., Chem. Commun.* **1971**, 481. (b) Kagan, H. B.; Dang, T.-P. *J. Am. Chem. Soc.* **1972**, *94*, 6429.

⁴⁰ (a) Vineyard, B. D.; Knowles, W. S.; Sabacky, M. J.; Bachman, G. L.; Weinkauff, D. J. *J. Am. Chem. Soc.* **1977**, *99*, 5946. (b) Knowles, W. S. *Acc. Chem. Res.* **1983**, *16*, 106.

Rh-mediated asymmetric hydrogenation with the catalytic system derived from DIPAMP afforded L-DOPA with an initial 95% ee value (Scheme 1), and further optimization of this chemistry for the industrial scale production of L-DOPA led to the “Monsanto L-DOPA process”.⁴¹

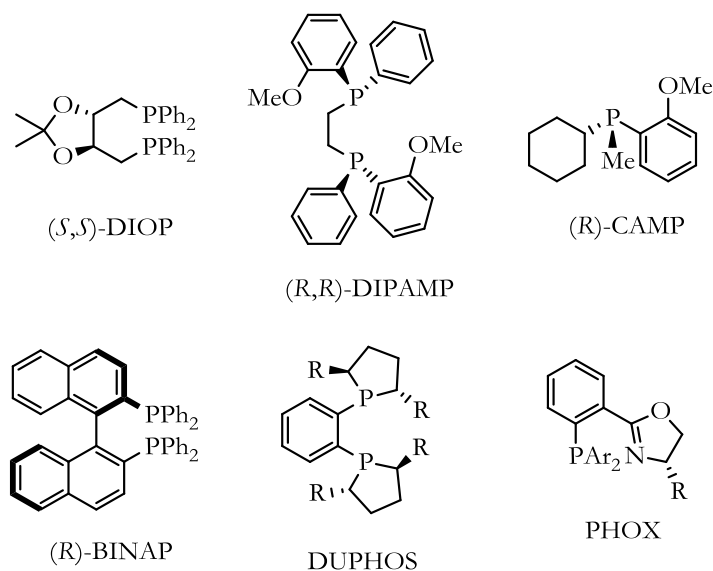


Figure 8. Selected chiral ligands for asymmetric hydrogenation.

The next milestone in asymmetric hydrogenation was achieved by Noyori, who incorporated the concept of axial chirality into the development of a new ligand, the C_2 -axially chiral diphosphine BINAP (Figure 8).⁴² BINAP is a conformationally stable biaryl derivative which incorporates two phosphorus binding groups. Rhodium⁴³ and ruthenium⁴⁴ complexes derived from BINAP proved to have very attractive catalytic profiles in asymmetric hydrogenation (see Scheme 2 as an example of BINAP-rhodium complexes in

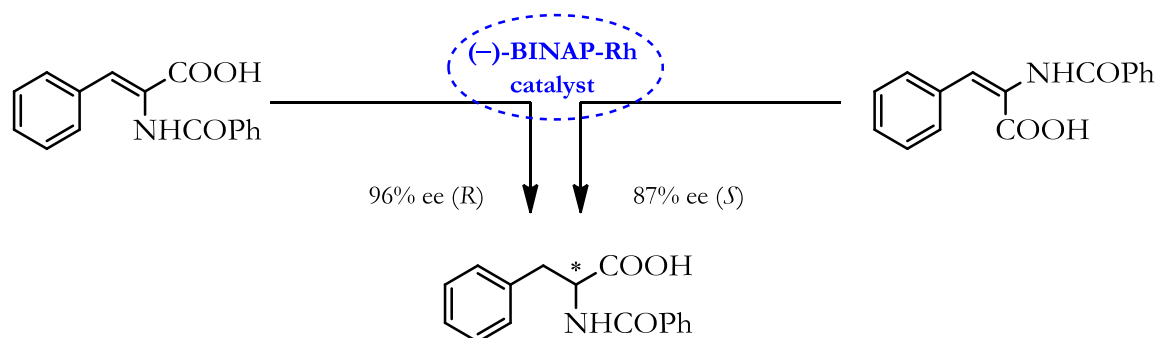
⁴¹ (a) Knowles, W. S.; Sabacky, M. J.; Vineyard, B. D. *J. Chem. Soc., Chem. Commun.* **1972**, 10. (b) *Asymmetric Catalysis on Industrial Scale: Challenges, Approaches and Solutions*; Blaser, H. U., Schmidt, E., Eds; Wiley-VCH: Weinheim, 2004.

⁴² Miyashita, A.; Yasuda, A.; Takaya, H.; Toriumi, K.; Ito, T.; Souchi, T.; Noyori, R. *J. Am. Chem. Soc.* **1980**, *102*, 7932.

⁴³ Miyashita, A.; Takaya, H.; Souchi, T.; Noyori, R. *Tetrahedron* **1984**, *40*, 1245.

⁴⁴ Ikariya, T.; Ishii, Y.; Kawano, H.; Arai, T.; Saburi, M.; Yoshikawa, S.; Akutagawa, S. *J. Chem. Soc., Chem. Commun.* **1985**, 922.

asymmetric hydrogenation), and BINAP-rhodium complexes have not only been efficiently used in the asymmetric hydrogenation of C=C double bonds, but also in the isomerization of allylic amines towards a key intermediate of (-)-menthol.⁴⁵



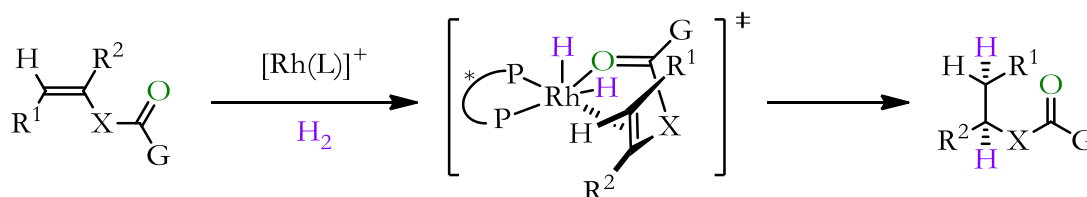
Scheme 2. Seminal examples of BINAP-rhodium complexes in asymmetric hydrogenation.

After these first successes, the palette of available chiral ligands grew, exponentially expanding the scope and applicability of this chemistry. One of the ligands discovered at this stage was DUPHOS (Figure 8), first reported by Burk, which in combination with rhodium reached enantioselectivities of up to 99% ee for asymmetric hydrogenation of functionalized alkenes.⁴⁶ The successful application of enantiomerically pure rhodium complexes in asymmetric hydrogenation relies on the ability of the substrate to form a rhodium chelate involving the C=C double bond and a donor atom, which is generally placed in the γ -position of a substituent attached to the C=C double bond. Chelating assistance of an *N*-acyl group is the classical paradigm for

⁴⁵ (a) Tani, K.; Yamagata, T.; Otsuka, S.; Akutagawa, S.; Kumobayashi, H.; Taketomi, T.; Takaya, H.; Miyashita, A.; Noyori, R. *J. Chem. Soc., Chem. Commun.* **1982**, 600. (b) Tani, K.; Yamagata, T.; Akutagawa, S.; Kumobayashi, H.; Taketomi, T.; Takaya, H.; Miyashita, A.; Noyori, R.; Otsuka, S. *J. Am. Chem. Soc.* **1984**, *106*, 5208.

⁴⁶ (a) Burk, M. J. *J. Am. Chem. Soc.* **1991**, *113*, 8518. (b) Burk, M. J.; Feaster, J. E.; Nugent, W. A.; Harlow, R. L. *J. Am. Chem. Soc.* **1993**, *115*, 10125. (c) Burk, M. J.; Gross, M. F.; Martinez, J. P. *J. Am. Chem. Soc.* **1995**, *117*, 9375. (d) Burk, M. J. *Acc. Chem. Res.* **2000**, *33*, 363.

achieving high reactivity and enantioselectivity in this transformation (see Scheme 3).⁴⁷



Scheme 3. Chelating assistance of a binding group situated in the γ -position of a substituent in the C=C bond.

In the early stages of hydrogenation studies, iridium was also considered a catalytic metal together with rhodium, but the lack of reactivity of the iridium analog of Wilkinson's catalyst ($[\text{Ir}(\text{Cl})(\text{PPh}_3)_3]$) in hydrogenations, shifted the attention to rhodium chemistry.

Vaska's work in the late 1960's,⁴⁸ led to a better understanding of the lack of reactivity for the iridium analog of Wilkinson catalyst: increased stability of its hydrogen oxidative addition product (*i.e.* $[\text{Ir}(\text{Cl})(\text{H})_2(\text{PPh}_3)_3]$) made dissociation of a PPh_3 ligand difficult. Thus, a vacant coordination site for binding the substrate was not provided.

Schrock and Osborn transferred their previously described work in rhodium chemistry to iridium complexes. When the iridium analogs to their rhodium complexes (*i.e.* $[\text{Ir}(\text{cod})(\text{L})_2]^+$) were allowed to react with hydrogen, a moderately stable oxidative addition product, $[\text{Ir}(\text{H})_2(\text{S})_2(\text{L})_2]^+$ ($\text{L} = \text{PPh}_3$, $\text{S} = \text{acetone}$) was formed, which gave moderate rates of hydrogenation.⁴⁹

⁴⁷ (a) Brown, J. M.; Chaloner, P. A. *J. Am. Chem. Soc.* **1980**, *102*, 3040. (b) Chan, A. S. C.; Pluth, J. J.; Halpern, J. *J. Am. Chem. Soc.* **1980**, *102*, 5952. (c) Landis, C. R.; Halpern, J. *J. Am. Chem. Soc.* **1987**, *109*, 1746.

⁴⁸ Vaska, L. *Acc. Chem. Res.* **1968**, *1*, 335.

⁴⁹ (a) Shapley, J. R.; Schrock, R. R.; Osborn, J. A. *J. Am. Chem. Soc.* **1969**, *91*, 2816. (b) Osborn, J. A.; Schrock, R. R. *J. Am. Chem. Soc.* **1971**, *93*, 3089.

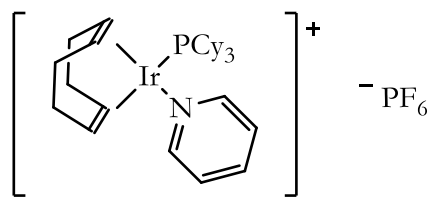
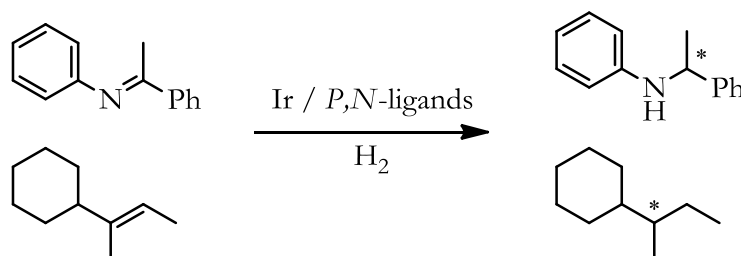


Figure 9. Crabtree's catalyst.

The discovery of the subsequently known Crabtree catalyst, $[\text{Ir}(\text{cod})(\text{py})(\text{PCy}_3)]\text{PF}_6$ (Figure 9),⁵⁰ opened a new type of *P,N*-iridium complex for asymmetric hydrogenation, which attracted the attention of organic chemists.⁵¹

After Crabtree's finding, the next breakthrough in chiral iridium chemistry was made by Pfaltz, who designed a chiral version of Crabtree's catalyst. Pfaltz combined a new chiral mixed *P,N*-donor ligand (named phosshinoxazolines, PHOX, see Figure 8),⁵² with an iridium(I) center, and the large, non-coordinating counteranion tetrakis[3,5-bis(trifluoromethyl)phenyl]borate (BArF). On using this class of iridium(I) complexes, Pfaltz and coworkers successfully hydrogenated an array of unfunctionalized alkenes and imines (Scheme 4).⁵³



Scheme 4. Hydrogenation of unfunctionalized alkenes and imines by iridium complexes of *P,N*-ligands.

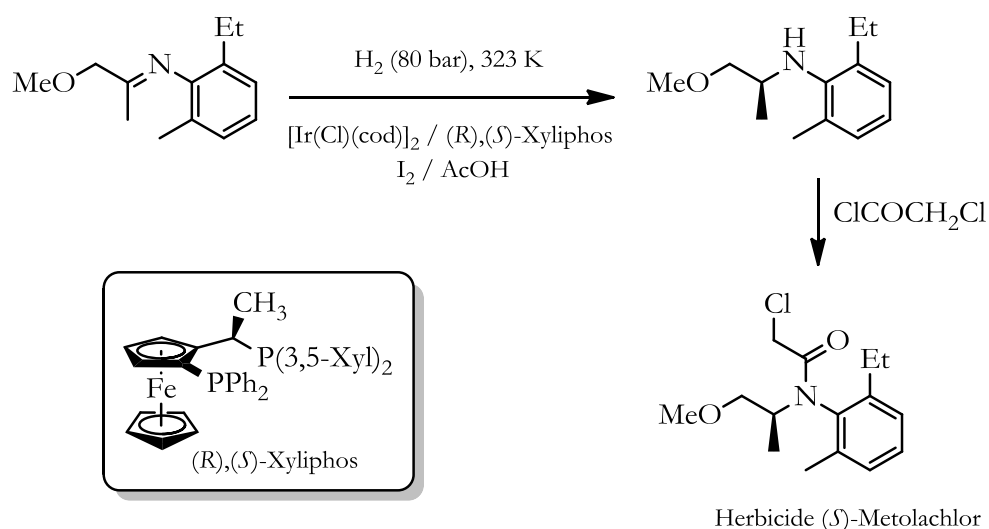
⁵⁰ Crabtree, R. *Acc. Chem. Res.* **1979**, *12*, 331.

⁵¹ (a) Suggs, J. W.; Cox, S. D.; Crabtree, R. H.; Quirk, J. M. *Tetrahedron Lett.* **1981**, *22*, 303. (b) Stork, G.; Kahne, D. E. *J. Am. Chem. Soc.* **1983**, *105*, 1072. (c) Schultz, A. G.; McCloskey, P. J.; Court, J. J. *J. Am. Chem. Soc.* **1987**, *109*, 6493.

⁵² PHOX was initially designed as ligand for Pd-catalyzed allylic substitution, see: von Matt, P.; Pfaltz, A. *Angew. Chem., Int. Ed.* **1993**, *32*, 566.

⁵³ See, for example: (a) Helmchen, G.; Pfaltz, A. *Acc. Chem. Res.* **2000**, *33*, 336. (b) Bell, S.; Wuestenberg, B.; Kaiser, S.; Menges, F.; Netscher, T.; Pfaltz, A. *Science* **2006**, *311*, 642. (c) Roseblade, S. J.; Pfaltz, A. *C. R. Chim.* **2007**, *10*, 178. (d) Woodmansee, D. H.; Pfaltz, A. *Chem. Commun.* **2011**, *47*, 7912.

Iridium-mediated asymmetric hydrogenation also proved to be an efficient tool in industrial applications. In 1999, Blaser *et al.* reported the production of the herbicide (*S*)-metolachlor (Scheme 5), whose trade name is Dual Magnum[®] (Novartis), by using an iridium ferrocenyl bisphosphine type catalyst in the asymmetric hydrogenation of a C=N double bond as the key step. High enantioselectivity and impressive catalytic activity (turnover number (TON) >1,000,000 and initial turnover frequency (TOF) > 1,800,000 h⁻¹) were observed.⁵⁴



Scheme 5. (*S*)-Metolachlor hydrogenation step.

Owing to the special metal-ligand binding properties of phosphorus ligands, trivalent phosphorus derivatives have played and still play an important role as metal binders in asymmetric homogeneous organometallic catalysis. Trivalent phosphorus derivatives form stable complexes⁵⁵ with catalytically active metals in pivotal transformations. Furthermore, P-compounds have a greater potential for steric and electronic modifications than other binding groups. The electronic character of trivalent phosphorus

⁵⁴ Blaser, H.-U.; Buser, H.-P.; Coers, K.; Hanreich, R.; Jalett, H.-P.; Jelsch, E.; Pugin, B.; Schneider, H.-D.; Spindler, F.; Wegmann, A. *Chimia* **1999**, *53*, 275.

⁵⁵ Ligands and metal cations tend to follow hard soft acid base theory (HSAB) trends. Soft binding atoms like phosphorus tend to form stable complexes with soft metals.

derivatives (*i.e.* their π -accepting ability) can be modified by recursively changing the P–C bonds in the basic structure by P–O bonds (Figure 10), leading from phosphines to phosphinites, phosphonites and phosphites.

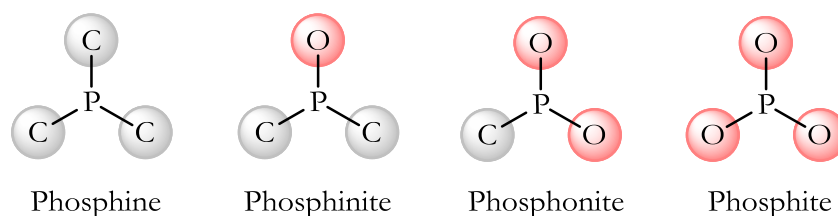


Figure 10. *P,O*-substituted trivalent phosphorus derivatives.

Later advancements in the field of asymmetric catalysis demonstrated that, regarding enantioselectivities, C_2 -symmetric ligands are not necessarily intrinsically better than their analogs lacking any symmetry element (*i.e.* C_1 -ligands).⁵⁶ In certain situations, ligands with two different coordinating groups should allow for a better stereocontrol. This has led to growing interest in the design, preparation and study of the catalytic properties of C_1 -symmetric bidentate ligands. Phosphine-phosphinites and phosphine-phosphites are examples of non-symmetric ligands that differ in the electronic and the steric nature of their respective binding groups. Since the reports of the seminal phosphine-phosphites designed by the groups of Pringle and Takaya,^{57b,c} and the phosphine-phosphinites developed by Brunner,^{57a} several other related ligands have been described. These *P-OP* ligands include diverse carbon backbones and stereogenic elements as well as different distances between the

⁵⁶ (a) Pavlov, V. A. *Russ. Chem. Rev.* **2004**, *73*, 1173. (b) Grushin, V. V. *Chem. Rev.* **2004**, *104*, 1629. (c) Pavlov, V. A. *Tetrahedron* **2008**, *64*, 1147. (d) Moberg, C. *Isr. J. Chem.* **2012**, *52*, 653.

⁵⁷ (a) Brunner, H.; Pieronczyk, W. *J. Chem. Res., Synop.* **1980**, 74. (b) Baker, M. J.; Pringle, P. G. *J. Chem. Soc., Chem. Commun.* **1993**, 314. (c) Sakai, N.; Mano, S.; Nozaki, K.; Takaya, H. *J. Am. Chem. Soc.* **1993**, *115*, 7033.

two phosphorus functionalities.⁵⁸ These compounds have been widely studied in enantioselective catalysis, for which they have afforded excellent results in various asymmetric transformations.

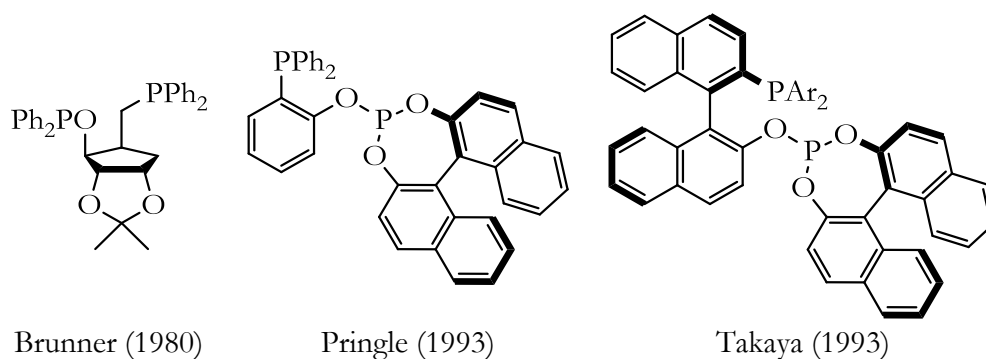


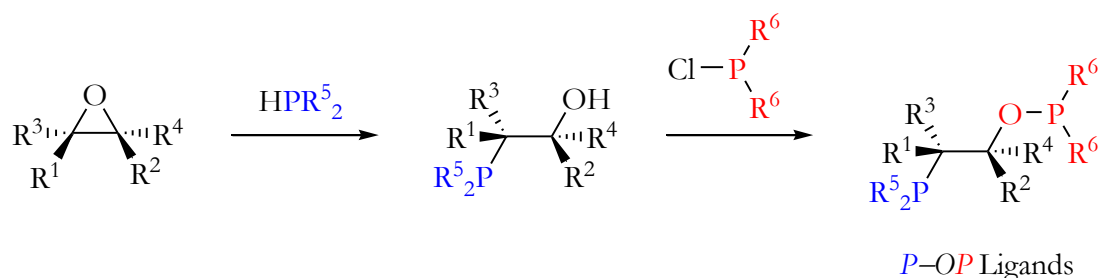
Figure 11. First reported *P-OP* ligands.

Our research group became interested in designing and developing a library of highly modular and enantiopure *P-OP* ligands derived from chiral epoxides. Although *P-OP* ligands encompassing diverse carbon backbones and stereogenic elements had been reported in the literature,⁵⁸ our ligand design (Scheme 6) incorporated an understudied structural motif: two consecutive stereogenic centres between the two phosphorus functionalities. In accordance with a goal of a highly modular synthetic methodology, Dr. Héctor Fernández-Pérez described within his PhD Thesis a wide variety of chiral *P-OP* (phosphine-phosphinite or phosphine-phosphite) ligands.⁵⁹ His synthetic strategy was based on the use of enantiomerically pure epoxides as starting materials, from which the target ligands were available in two steps: ring-opening of an epoxide with nucleophilic trivalent phosphorus derivatives

⁵⁸ Fernández-Pérez, H.; Etayo, P.; Panossian, A.; Vidal-Ferran, A. *Chem. Rev.* **2011**, *111*, 2119.

⁵⁹ H. Fernández-Pérez, Doctoral Thesis, Universitat Rovira i Virgili, Tarragona, 2009.

followed by *O*-phosphorylation of the intermediate phosphino alcohols with trivalent phosphorus electrophiles.^{35a,c}



Scheme 6. Synthetic strategy towards *P-OP* ligands developed in our group.

Rhodium complexes of these ligands proved to be highly efficient in the Rh-catalysed asymmetric hydrogenation of model functionalised alkenes (α -(acylamino)acrylate derivatives, α -arylenamides and itaconic acid derivatives and analogs). The best ligand for rhodium-mediated hydrogenation of functionalized alkenes derived from Sharpless epoxy ethers incorporating the diphenylphosphino group and the phosphite fragment derived from (*S*_a)-BINOL (Figure 12).

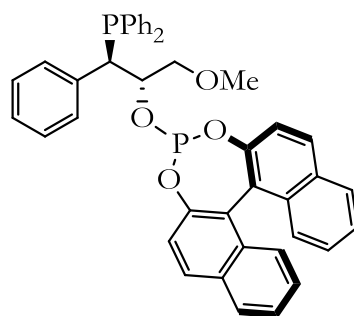


Figure 12. Highest performing ligand derived from Sharpless epoxy ethers for rhodium-mediated asymmetric hydrogenation of alkenes.

Encouraged by the good results obtained in the previous work, the first general aim of the present thesis involves extension of the substrate scope and utilization of rhodium complexes derived from our *P-OP* ligands in

asymmetric hydrogenation of strategically devised substrates leading to active pharmaceutical ingredients (API).

A second general aim will be the assessment of the coordination properties of these *P-OP* ligands with iridium precursors and their further evaluation in the Ir-mediated asymmetric hydrogenation of C=N bonds.

Thus, the objectives of the present thesis are as follows:

- ❖ Assessment and optimization of the catalytic performance of our $[\text{Rh}(P\text{-}OP)]^+$ complexes in the Rh-mediated asymmetric hydrogenation of new functionalized alkenes.
- ❖ Application of our $[\text{Rh}(P\text{-}OP)]^+$ catalysts in the hydrogenation of strategically devised substrates leading to API intermediates or other biologically active compounds.
- ❖ Exploration of the coordination properties of our $P\text{-}OP$ ligands with diverse iridium precursors.
- ❖ Evaluation of the catalytic activity of $[\text{Ir}(P\text{-}OP)]^+$ complexes in the asymmetric hydrogenation of imines and other C=N-containing derivatives.

CHAPTER I

Rhodium-mediated asymmetric hydrogenations

UNIVERSITAT ROVIRA I VIRGILI
HIGHLY MODULAR P -OP LIGANDS FOR RHODIUM- AND IRIIDIUM-MEDIATED ASYMMETRIC HYDROGENATIONS
José Luis Núñez Rico
DL: T.994-2013

CHAPTER I

ASYMMETRIC HYDROGENATION CATALYZED BY RHODIUM-(*P-OP*) COMPLEXES

1.1 ANTECEDENTS

1.1.1 Background

Asymmetric hydrogenation has been used for decades as a simple and cost effective way to introduce chirality into molecules of interest and production processes. In fact, homogeneous hydrogenation is one of the most extensively studied transformations of homogeneous catalysis. The ability of many metal complexes to accomplish this transformation under very mild conditions has attracted the interest of an ever increasing number of chemists and has led to the development of efficient methodologies for the asymmetric reduction of C=C, C=O and C=N bonds. Such complexes are usually derived from transition metals with unfilled *d* orbitals, as they possess the ability to bind ligands, reagents and reactants. Late transition metals, especially some of those lying in the *d*-block (groups 8, 9, and 10, periods 5 and 6) have been

extensively used in asymmetric hydrogenation in combination with phosphorus ligands.

Rhodium complexes were the first, and for many years, the most abundant catalysts used for homogeneous asymmetric hydrogenation, due to the excellent rates, activity and selectivity reached.

As has already been mentioned in the introduction, Kagan devised in the early 1970s the C_2 -symmetric chelating diphosphine DIOP (Figure 13)⁶⁰ and demonstrated that rhodium complexes of bidentate diphosphines catalyzed the asymmetric hydrogenation of C=C bonds with higher enantioselectivities than those obtained with monodentate analogs. The topology of DIOP (chelating coordination and C_2 -symmetry) strongly influenced the design of future ligands. It was believed that C_2 -symmetry ligands were advantageous with respect to unsymmetrical ones, as they simplified the number of possible reaction pathways. Knowles's bidentate ligand DIPAMP with stereogenic phosphorous centers constituted a milestone in the field of rhodium-mediated asymmetric hydrogenation (Figure 13).⁶¹

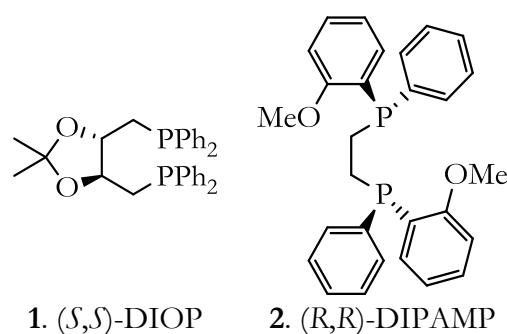


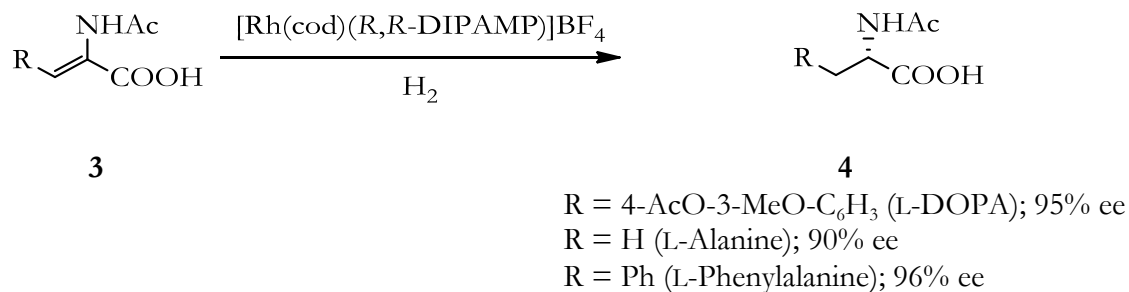
Figure 13. Seminal C_2 -symmetric ligands for rhodium-mediated asymmetric hydrogenation.

Rh-mediated asymmetric hydrogenation using the catalytic system derived from DIPAMP allowed industrial production of L-DOPA with 95%

⁶⁰ (a) Kagan, H. B.; Dang, T. P. *J. Chem. Soc., Chem. Commun.* **1971**, 481. (b) Kagan, H. B.; Dang, T.-P. *J. Am. Chem. Soc.* **1972**, *94*, 6429.

⁶¹ (a) Vineyard, B. D.; Knowles, W. S.; Sabacky, M. J.; Bachman, G. L.; Weinkauff, D. J. *J. Am. Chem. Soc.* **1977**, *99*, 5946. (b) Knowles, W. S. *Acc. Chem. Res.* **1983**, *16*, 106.

ee (Scheme 7).⁶² The same catalyst was used to prepare other α -amino acids such as L-alanine or L-phenylalanine with high enantioselectivities (90% ee or 96% ee, respectively).⁶³



Scheme 7. Synthesis of amino acids by asymmetric hydrogenation.

Researchers soon realized that because of the limited structural diversity of those two ligands, it was unlikely that they could provide a satisfactory response in terms of selectivity to all conceivable situations in catalysis (metals, substrates, etc.). Thus, asymmetric synthesis was harnessed to broaden the repertoire of available ligand scaffolds, to incorporate every conceivable type of molecular chirality, and to functionalize ligands with binding groups for the metals, which are suitable for asymmetric hydrogenation. Amongst the hundreds of known ligands for rhodium-mediated asymmetric hydrogenation,⁶⁴ 1,2-Bis((2*R*,5*R*)- or (2*S*,5*S*)-2,5-dialkylphospholano)benzene (DUPHOS),⁶⁵ (*R*)- or (*S*)-(*tert*-butylmethylphosphino)(di-*tert*-butylphosphino)-methane (Trichickenfootphos),⁶⁶ and (*R,R*)- or (*S,S*)-2,3-bis(*tert*-butylmethyl-

⁶² Knowles, W. S.; Sabacky, M. J.; Vineyard, B. D. *J. Chem. Soc., Chem. Commun.* **1972**, 10.

⁶³ See the following reference and those cited therein: Koenig, K. E. *Asymmetric Synthesis*. In *Chiral Catalysis*; Morrison J. D., Ed.; Academic Press: New York, 1985; Vol. 5, Chap. 3: The Applicability of Asymmetric Homogeneous Catalytic Hydrogenation.

⁶⁴ *Phosphorus Ligands in Asymmetric Catalysis*; Börner, A., Ed.; Wiley-VCH: Weinheim, 2008; Vols. I-III.

⁶⁵ (a) Burk, M. J. *J. Am. Chem. Soc.* **1991**, *113*, 8518. (b) Burk, M. J.; Feaster, J. E.; Nugent, W. A.; Harlow, R. L. *J. Am. Chem. Soc.* **1993**, *115*, 10125. (c) Burk, M. J.; Gross, M. F.; Martinez, J. P. *J. Am. Chem. Soc.* **1995**, *117*, 9375. (d) Burk, M. J. *Acc. Chem. Res.* **2000**, *33*, 363.

⁶⁶ Gridnev, I. D.; Imamoto, T.; Hoge, G.; Kouchi, M.; Takahashi, H. *J. Am. Chem. Soc.* **2008**, *130*, 2560.

phosphino)quinoxaline (QuinoxP*)⁶⁷ deserve, in this author's opinion, mention as outstanding ligands in rhodium-mediated asymmetric hydrogenation (Figure 14). Assessment of the catalytic properties of C₁-symmetric diphosphines, like "Trichickenfootphos (TCFP)" and many other examples,⁶⁴ demonstrated that, regarding enantioselectivities, C₂-symmetric ligands are not necessarily intrinsically better than their analogs lacking symmetry elements.

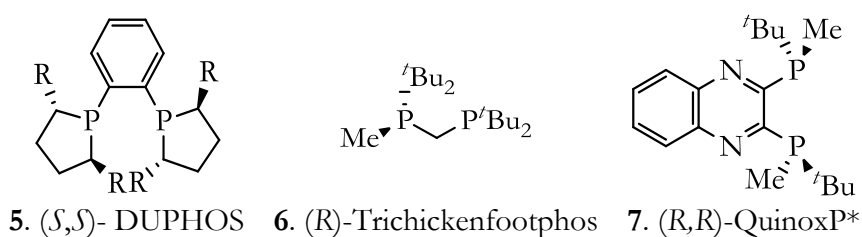


Figure 14. Selected diphosphines for rhodium-mediated asymmetric hydrogenation.

The quest towards catalyst diversity for rhodium-mediated asymmetric hydrogenation also led the development of hybrid bidentate ligands with electronic dissimilarity in their ligating groups: the use of two coordinating functions of different nature in a chiral ligand constitutes a very powerful approach in the field of asymmetric hydrogenation (and also in general in asymmetric catalysis). To this aim, many variations on the diphosphino scaffold have been devised. A full description of all P-containing hybrid bidentate ligands is beyond the scope of this section, and only those arising from the replacement of the P–C bonds in one of the phosphino groups with P–O bonds will be briefly discussed. Phosphine-phosphinites, phosphine-phosponites and phosphine-phosphites (Figure 15) derive formally from diphosphines by stepwise P–C/P–O bond replacement. All of these hybrid

⁶⁷ Imamoto, T.; Tamura, K.; Zhang, Z.; Horiuchi, Y.; Sugiya, M.; Yoshida, K.; Yanagisawa, A.; Gridnev, I. D. *J. Am. Chem. Soc.* **2012**, *134*, 1754.

ligands present electronic dissimilarity in their coordination functions: whilst the phosphino group is a good σ -donor group, phosphinite, phosphonite and phosphite moieties have diminished σ -donor capabilities and enhanced abilities as π -acceptors.⁶⁸

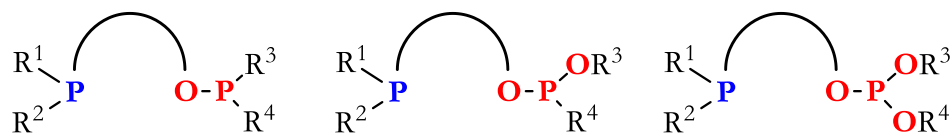


Figure 15. Phosphine-phosphinite, phosphine-phosphonite and phosphine-phosphite ligands.

Enantiopure phosphine-phosphinites were first developed in 1980 by Brunner from a sugar derived chiral skeleton.^{69a} Enantiopure phosphine-phosphites were developed later, in 1993, and simultaneously reported by the groups of Takaya and Pringle^{69b,c} (Figure 16).

⁶⁸ *The Organometallic Chemistry of the Transition Metals*; Crabtree, R.H., Ed.; John Wiley & Sons: New York, 1988.

⁶⁹ (a) Brunner, H.; Pieronczyk, W. *J. Chem. Res., Synop.* **1980**, 74. (b) Baker, M. J.; Pringle, P. G. *J. Chem. Soc., Chem. Commun.* **1993**, 314. (c) Sakai, N.; Mano, S.; Nozaki, K.; Takaya, H. *J. Am. Chem. Soc.* **1993**, *115*, 7033.

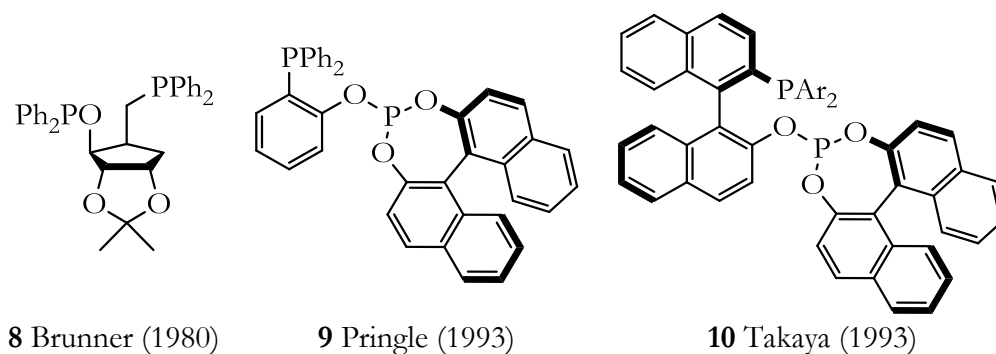


Figure 16. The first reported phosphine-phosphinite and phosphine-phosphite ligands.

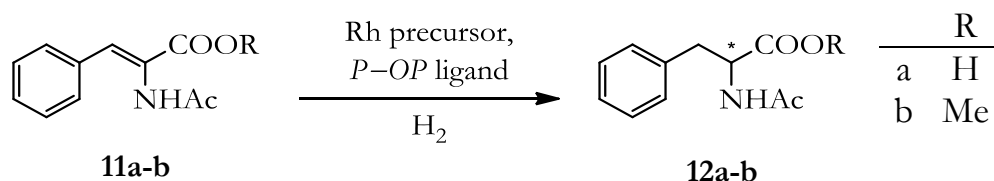
Since the appearance of these seminal *P-OP* derivatives, several other ligands of this type have been reported encompassing diverse carbon backbones and stereogenic elements, as well as distances between the two phosphorus functionalities.⁷⁰

Phosphine-phosphinite and phosphine-phosphonite ligands have been used in the rhodium-mediated asymmetric hydrogenation (AH) of 2-acetamido-3-arylacrylates **11a-b** (Figure 17, Figure 18 and Scheme 8).⁷¹ Acetamidoacrylates usually serve as benchmark substrates for this kind of transformation. Asymmetric hydrogenations of other kinds of olefins using catalysts derived from phosphine-phosphinites are scarce in the literature. As a general trend, very high activity values can be observed, but enantioselectivity varies largely. Binaphthyl- and ferrocene-based ligands **13**^{71a} and **14**^{71b} respectively give the highest values of enantioselectivity for the hydrogenation of the benchmark substrates **11a-b** (Scheme 8). It is noteworthy to mention the additional tolerance of ligand **13** to the free carboxylic acid. None of the other phosphine-phosphinites reported achieved such high

⁷⁰ Fernández-Pérez, H.; Etayo, P.; Panossian, A.; Vidal-Ferran, A. *Chem. Rev.* **2011**, *111*, 2119.

⁷¹ (a) Yan, Y.; Chi, Y.; Zhang, X. *Tetrahedron: Asymmetry* **2004**, *15*, 2173. (b) Jia, X.; Li, X.; Lam, W. S.; Kok, S. H. L.; Xu, L.; Lu, G.; Yeung, C.-H.; Chan, A. S. C. *Tetrahedron: Asymmetry* **2004**, *15*, 2273.

enantioselectivities.⁷² Our group also reported the synthesis of phosphine-phosphinite **21**⁷³ from a Sharpless epoxy ether, giving only moderate results in the hydrogenation of **11b**.



Scheme 8. Asymmetric hydrogenation of α -(acylamino)acrylates.

Phosphine-phosphonites have been rarely tested in asymmetric hydrogenation. Reetz *et al.* reported the ligands **22-24** (Figure 18) and their evaluation in the asymmetric hydrogenation of dimethyl itaconate **38a** with moderate enantioselectivities.⁷⁴

⁷² (a) Yamashita, M.; Hiramatsu, K.; Yamada, M.; Suzuki, N.; Inokawa, S. *Bull. Chem. Soc. Jpn.* **1982**, *55*, 2917. (b) Ohe, K.; Morioka, K.; Yonehara, K.; Uemura, S. *Tetrahedron: Asymmetry* **2002**, *13*, 2155. (c) Monsees, A.; Laschat, S. *Synlett* **2002**, 1011. (d) Bosch, B. E.; Monsees, A.; Dingerdissen, U.; Knochel, P.; Hupe, E., 014330, 2002. (e) Boyer, N.; Léautey, M.; Jubault, P.; Pannecoucke, X.; Quirion, J.-C. *Tetrahedron: Asymmetry* **2005**, *16*, 2455. (f) Jiang, R.; He, W.; Wang, P.-a.; Li, X.-y.; Zhang, S.-y. *Fenzji Cuibua* **2006**, *20*, 207.

⁷³ Fernández-Pérez, H.; Pericàs, M. A.; Vidal-Ferran, A. *Adv. Synth. Catal.* **2008**, *350*, 1984.

⁷⁴ Reetz, M. T.; Gosberg, A. *Tetrahedron: Asymmetry* **1999**, *10*, 2129.

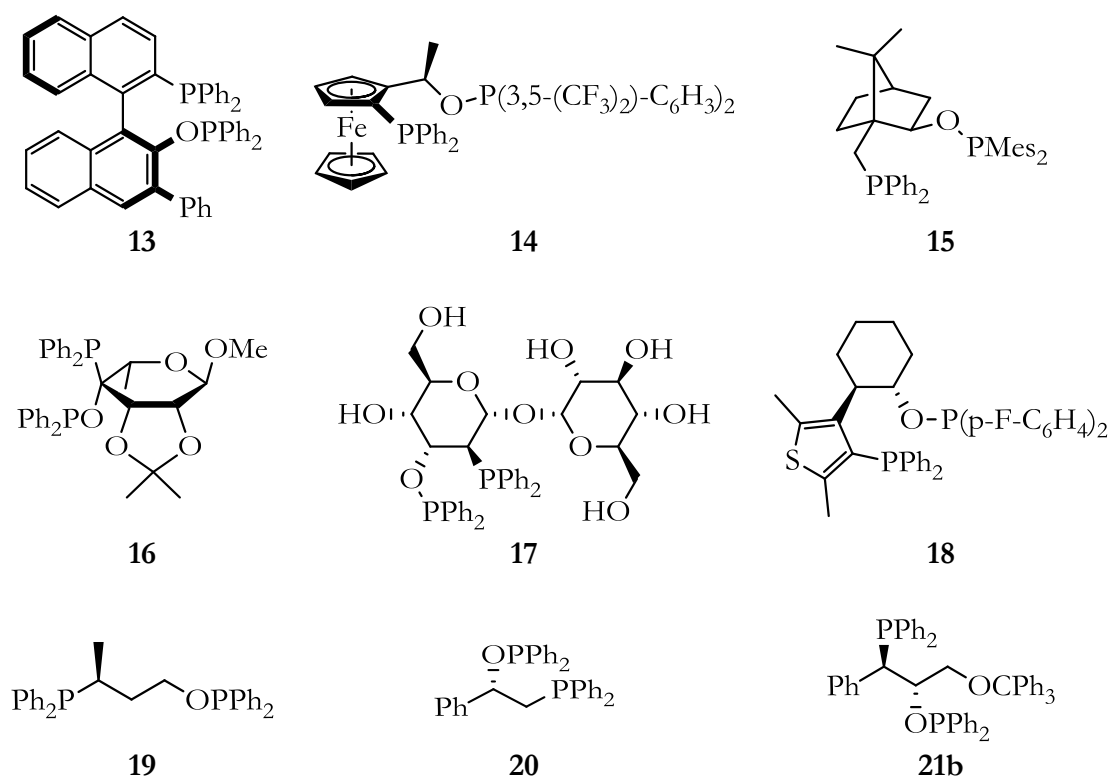


Figure 17. Phosphine-phosphinites used in Rh-mediated AH of alkenes.

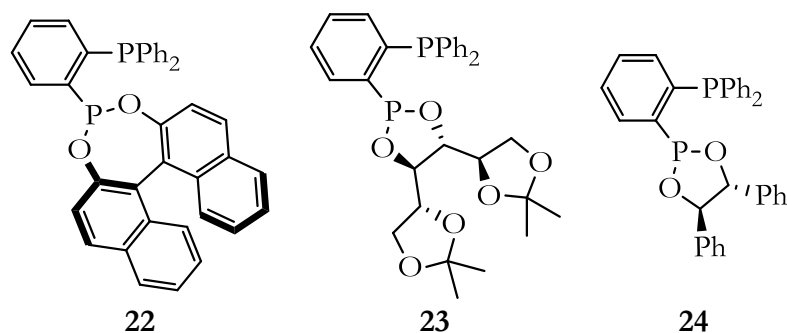


Figure 18. Phosphine-phosphonites used in Rh-mediated AH of alkenes.

As opposed to phosphine-phosphinites and phosphine-phosphonites, phosphine-phosphites have been more widely explored as ligands for the enantioselective hydrogenation of alkenes. Due to the relative success of this transformation using phosphine-phosphites as ligands, the process has been expanded to a wider variety of functionalized olefins beyond benchmark substrates.

A wide array of phosphine-phosphite ligands have provided excellent conversions and enantioselectivities when the benchmark substrates mentioned above are used (Figure 19). Ligands **25** (Zhang *et al.*),^{71a} **26-27** (Ruiz, Claver and co-workers),⁷⁵ **28-29** (van Leeuwen *et al.*),⁷⁶ **32-33** (Pizzano *et al.*),⁷⁷ and also ligand **30a**,⁷³ developed in our group all exhibited high enantioselectivity (>95% ee) in the hydrogenation of 2-acetamido-3-phenylacrylate **11b**. On the other hand, ligands **31**,^{78a} **34**,^{78b} **35**^{71b} and **36**^{78c, d} led only to moderate enantioselectivity in the hydrogenation of **11b**. Ligand **25** has been successfully tested in the hydrogenation of several β -aryl-dehydro- α -amino acids, exhibiting a good tolerance to free carboxylic acids.^{71a}

⁷⁵ Pàmies, O.; Diéguez, M.; Net, G.; Ruiz, A.; Claver, C. *Chem. Commun.* **2000**, 2383.

⁷⁶ Deerenberg, S.; Pàmies, O.; Diéguez, M.; Claver, C.; Kamer, P. C. J.; van Leeuwen, P. W. N. M. *J. Org. Chem.* **2001**, *66*, 7626.

⁷⁷ Suárez, A.; Méndez-Rojas, M. A.; Pizzano, A. *Organometallics* **2002**, *21*, 4611.

⁷⁸ (a) Müller, C.; Lopez, L. G.; Kooijman, H.; Spek, A. L.; Vogt, D. *Tetrahedron Lett.* **2006**, *47*, 2017. (b) Breit, B.; Fuchs, E. *Synthesis* **2006**, 2121. (c) Hattori, G.; Hori, T.; Miyake, Y.; Nishibayashi, Y. *J. Am. Chem. Soc.* **2007**, *129*, 12930. (d) Li, Y.; Feng, Y.; He, Y.-M.; Chen, F.; Pan, J.; Fan, Q.-H. *Tetrahedron Lett.* **2008**, *49*, 2878.

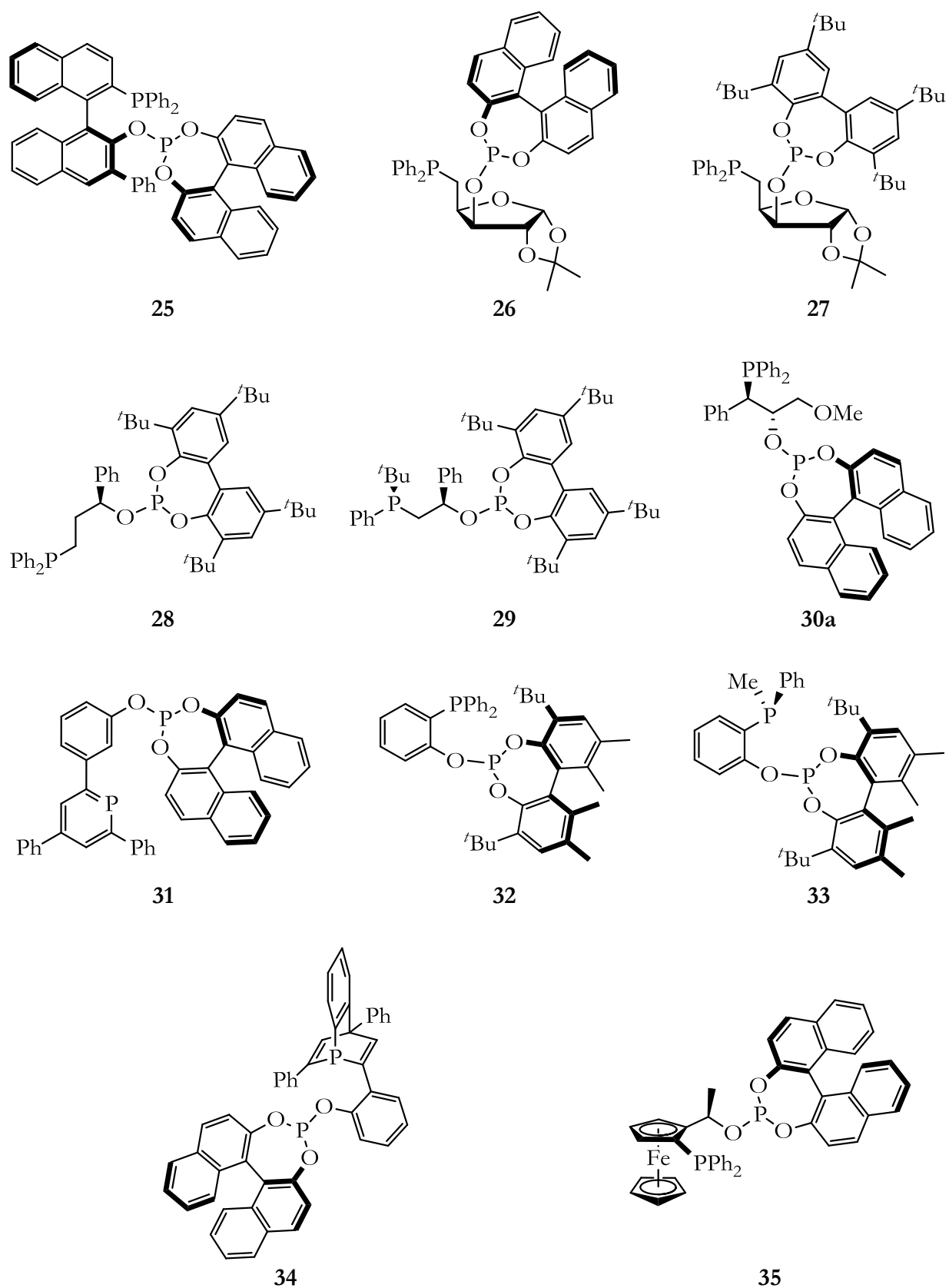


Figure 19. Selected phosphine-phosphites used in Rh-mediated asymmetric hydrogenation.

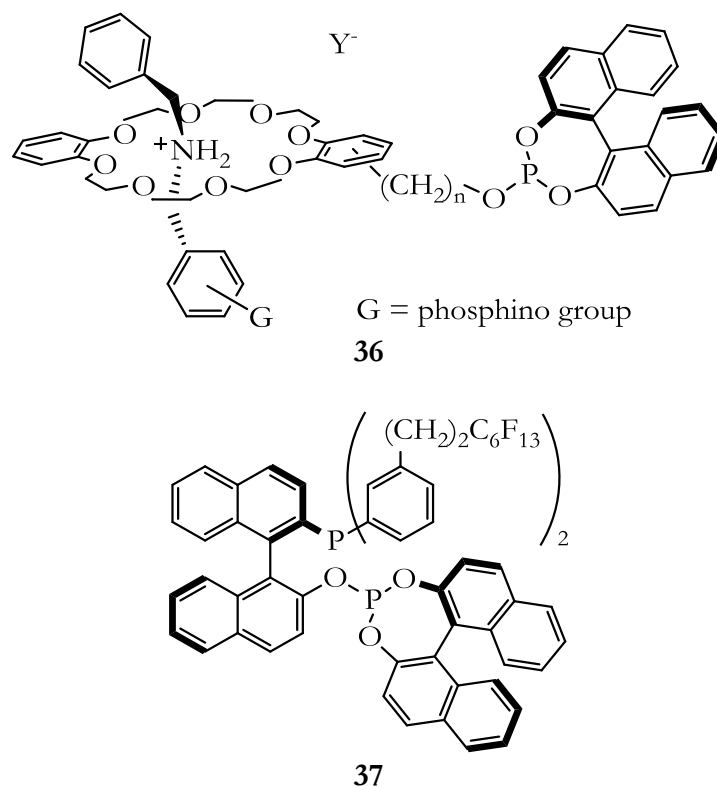
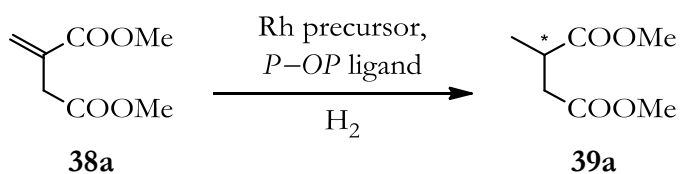


Figure 19 cont. Selected phosphine-phosphites used in Rh-mediated asymmetric hydrogenation.

Rhodium complexes derived from ligand **32** efficiently mediated the hydrogenation of dimethyl itaconate **38a** with excellent enantioselectivity (Scheme 9).⁷⁹

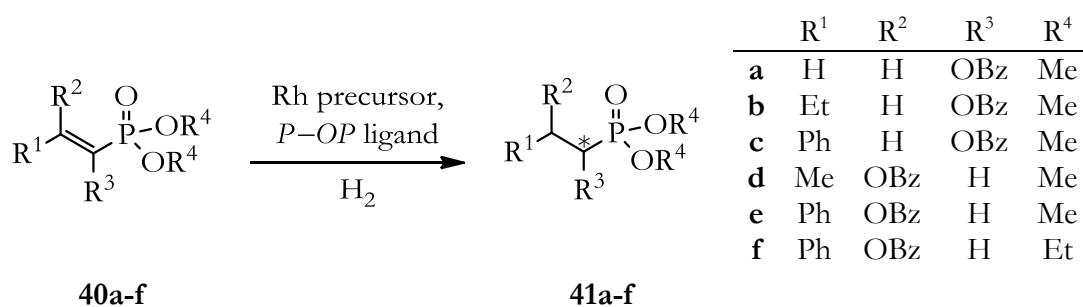


Scheme 9. Asymmetric hydrogenation of dimethyl itaconate.

Derivatives of ligand **32**, developed by Pizzano *et al.* also mediated the asymmetric hydrogenation of a wide array of functionalized unsaturated

⁷⁹ Suárez, A.; Pizzano, A. *Tetrahedron: Asymmetry* **2001**, *12*, 2501.

phosphonates **40** (Scheme 10).⁸⁰ The enantioselectivities achieved in this work vary largely with the tested phosphonate in question.



Scheme 10. Asymmetric hydrogenation of unsaturated phosphonates.

With respect to the phosphine-phosphite ligands already prepared in our research group,^{73, 81, 82} the best catalyst of the series for rhodium-mediated asymmetric hydrogenation is derived from ligand **30a**, which incorporates a diphenylphosphino moiety, an (*S*)-BINOL fragment and a methyl group in the phosphino, phosphite and R-oxy groups, respectively. Catalytic screenings showed a top level stereoselectivity and performance in the hydrogenation of a diverse array of functionalized alkenes.

The catalyst based on **30a** provided excellent conversions (70 – 99%) and very high enantioselectivities (92 – 99% ee) in the hydrogenation of (*Z*)-configured α -(acylamino)acrylates **11a-p** (see Figure 20) leading to β -unsubstituted, β -alkyl and β -aryl substituted α -amino acid derivatives. It should be also mentioned that a broad palette of solvents can be used (methanol, dichloromethane, tetrahydrofuran and toluene) without appreciable loss in

⁸⁰ (a) Rubio, M.; Suárez, A.; Álvarez, E.; Pizzano, A. *Chem. Commun.* **2005**, 628. (b) Rubio, M.; Vargas, S.; Suárez, A.; Álvarez, E.; Pizzano, A. *Chem.–Eur. J.* **2007**, *13*, 1821. (c) Vargas, S.; Suárez, A.; Álvarez, E.; Pizzano, A. *Chem.–Eur. J.* **2008**, *14*, 9856. (d) Vargas, S.; Suarez, A.; Alvarez, E.; Pizzano, A. *Chem.–Eur. J.* **2010**, *16*, 9937. (e) Chávez, M. A.; Vargas, S.; Suárez, A.; Álvarez, E.; Pizzano, A. *Adv. Synth. Catal.* **2011**, *353*, 2775.

⁸¹ H. Fernández-Pérez, Doctoral Thesis, Universitat Rovira i Virgili, Tarragona, 2009.

⁸² Fernández-Pérez, H.; Donald, S. M. A.; Munslow, I. J.; Benet-Buchholz, J.; Maseras, F.; Vidal-Ferran, A. *Chem.–Eur. J.* **2010**, *16*, 6495.

catalytic activity (conversion and enantioselectivity). In all cases, cationic Rh(I) complexes derived from **30a** led to (*R*)-configured hydrogenation products. In general, regardless of the alkylic or aromatic nature of the substituent on the double bond, or the electronic and positional nature of the substituents on the aromatic ring, or whether the substrates contained an ester or an acid group, substrates were hydrogenated with high enantioselectivity. The excellent enantioselectivities achieved upon hydrogenation of the α -(acylamino)acrylates **11j-l** to give the corresponding α -amino acid derivatives illustrate the tolerance of the catalytic system derived from **30a** to a broad variety of carbamate-type amino protecting groups (Boc, Cbz and Fmoc groups). With regard to the catalytic activity of the rhodium complexes derived from **30a**, the *in situ* formed complex **135** (see page 85 for its structure) sufficed to fully hydrogenate (*Z*)-MAC (**11b**) with a substrate to catalyst ratio (S/C) of 2,500:1 in tetrahydrofuran.

For β -substituted dehydroamino acid **11q**, which constituted a mixture of *E/Z* isomers, the use of [Rh(nbd)(**30a**)]BF₄ only provided moderate enantioselectivity for the (*Z*)-isomer (56% ee for the (*R*)-configured hydrogenation product) and was inactive for the (*E*)-isomer. Dr. Fernández-Pérez also observed a total lack of catalytic activity with the *E*-isomers of the Fmoc and Boc protected dehydroalanines **11r-t**. Likewise, no activity was observed for alkenes **11u-v**.

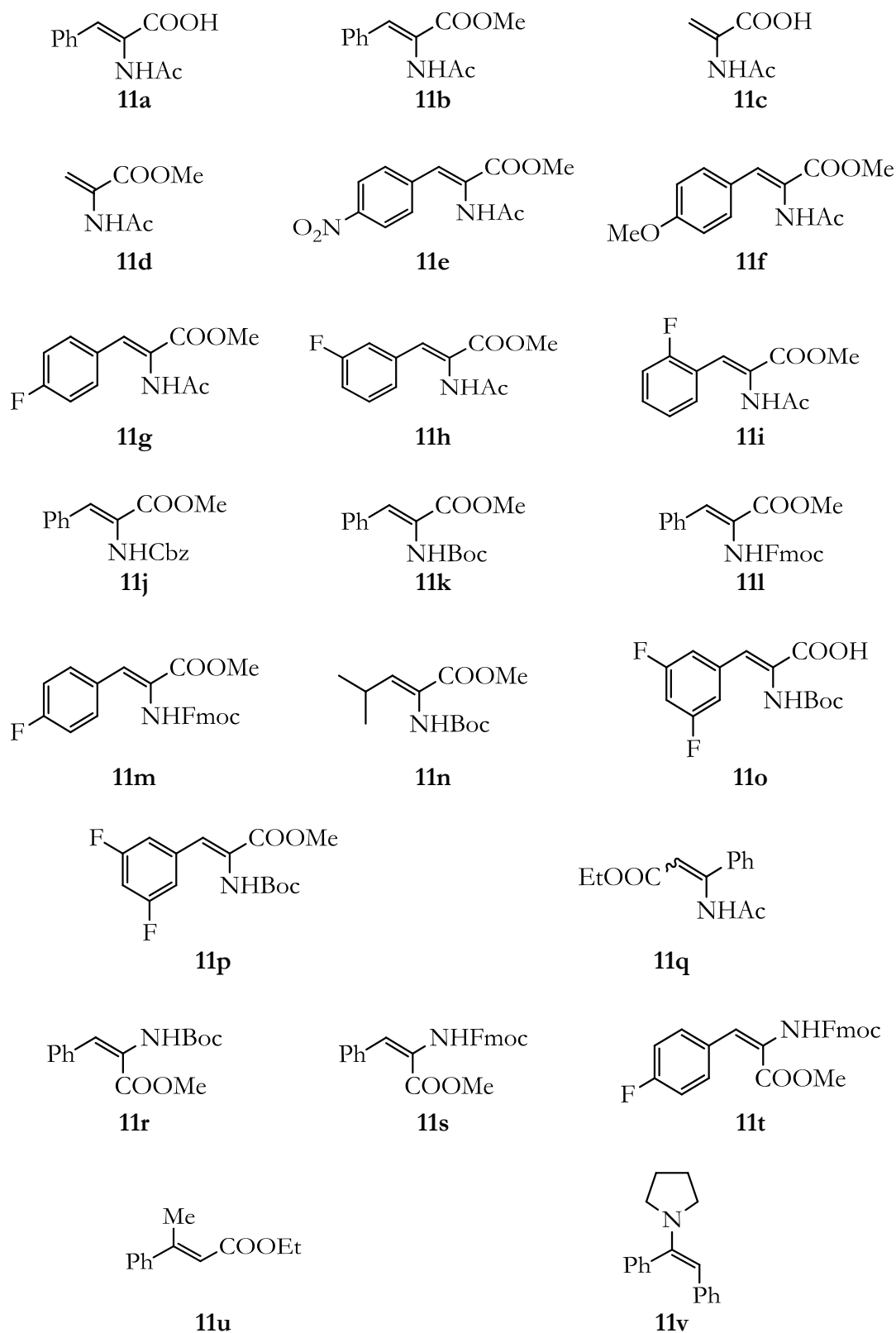


Figure 20. Tested substrates in asymmetric hydrogenations mediated by $[\text{Rh}(\text{nbd})(\mathbf{30a})]\text{BF}_4$.

Itaconate derivatives are another class of compounds that yield interesting enantiopure derivatives upon asymmetric hydrogenation. Dr. Fernández-Pérez tested the catalytic system derived from $[\text{Rh}(\text{nbd})(\mathbf{30a})]\text{BF}_4$ in the hydrogenation of dimethyl itaconate **38a** and the related Roche ester precursor (**38e**) and compound **38f**. Excellent enantioselectivities were observed for **38a** (99% ee, (*S*)-configured hydrogenation product) and **38e** (90% ee, (*S*)-configured hydrogenation product). On the contrary, however, hydrogenation of substrate **38f** proceeded with poor enantioselectivity (15% ee).

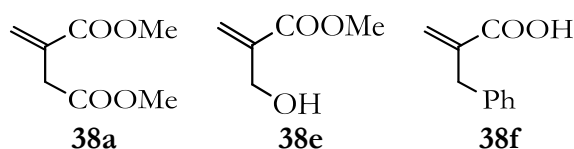
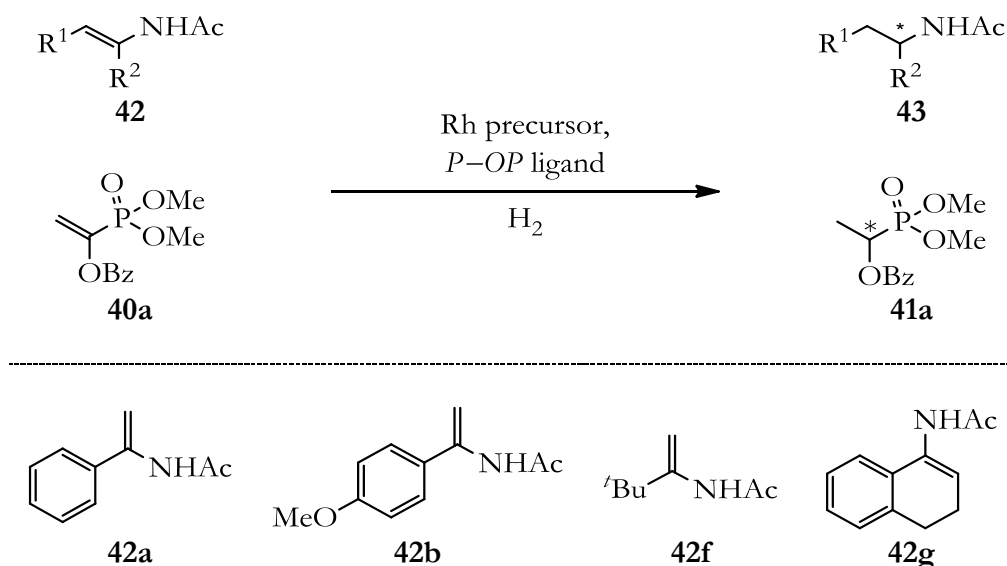


Figure 21. Itaconic acid derivatives and analogs tested in asymmetric hydrogenations mediated by $[\text{Rh}(\text{nbd})(\mathbf{30a})]\text{BF}_4$.

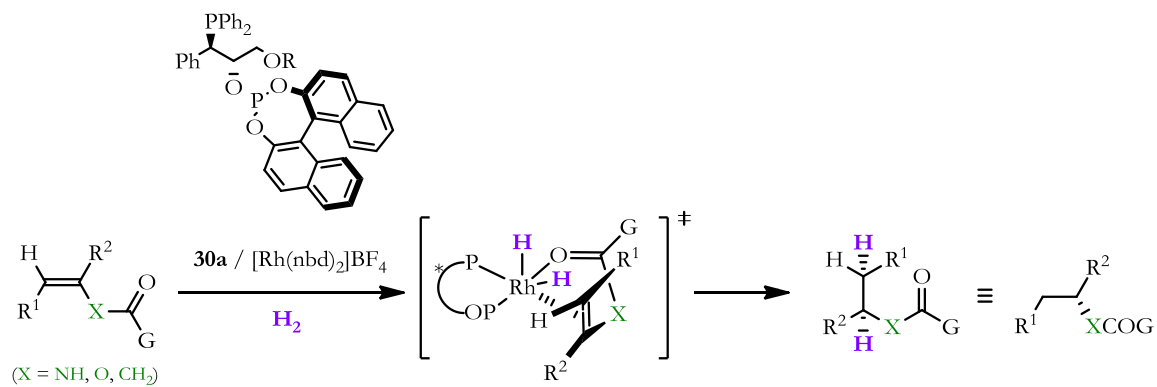
Evaluation of the catalytic performance of $[\text{Rh}(\text{nbd})(\mathbf{30a})]\text{BF}_4$ using enamides **42** and an enol ester phosphonate **40a** (Scheme 11) was also carried out by Dr. Fernández-Pérez in his seminal investigations. With regard to α -arylenamides **42a-b**, enantioselectivities were very high (98% and 97% ee, respectively, (*R*)-configured hydrogenation products), whereas moderate enantioselectivities were observed for the alkyl-substituted and cyclic enamides **42f** (23% ee) and **42g** (58% ee), respectively. Hydrogenation of **40a** using the rhodium complex derived from ligand **30a** led to the functionalized product **41a** with 92% ee.



Scheme 11. Asymmetric hydrogenation of α -substituted enamides and an enol ester phosphonate.

In conclusion, our group had developed the highly enantioselective hydrogenation of a structurally diverse array of substrates mediated by cationic rhodium complexes of the ligand **30a**. α -(Acylamino)acrylates, itaconic acid derivatives and analogs, α -substituted enamides, and one enol benzoate were hydrogenated using $[\text{Rh}(\mathbf{30a})]^+$ complexes as precatalysts with high enantioselectivities (up to 99% ee). The stereochemical outcome of all of these hydrogenations can be predicted with the model indicated in Scheme 12.

The successful application of enantiomerically pure rhodium complexes in asymmetric hydrogenation relies on the ability of the substrate to form a rhodium chelate involving the C=C double bond and a donor atom, which is generally placed in the γ -position of a substituent attached to the C=C double bond. Chelating assistance of an *N*-acyl group is the classical paradigm for achieving high reactivity and enantioselectivity in this transformation. Not surprisingly, substrates **11u**, **11v** and **38f**, which lack such a binding group in the γ -position, were not hydrogenated with our catalytic system.



α -(acylamino)acrylates (XC(O)G = NHAc, NHBoc, NHCbz, NHFmoc; R¹ = H, alkyl, aryl; R² = CO₂H, CO₂Me)

itaconic acid derivatives (XC(O)G = CH₂CO₂Me, CH₂OH; R¹ = H; R² = CO₂Me)

α -substituted enamides (XC(O)G = NHAc; R¹ = H; R² = alkyl, aryl)

α -substituted enol esters (XC(O)G = OBz; R¹ = H; R² = PO(OMe)₂)

Scheme 12. Asymmetric hydrogenation of functionalized alkenes catalyzed by [Rh(P-OP)]⁺ complexes.

1.1.2 Synthetic Strategies towards Modular Phosphine-Phosphinites and Phosphine-Phosphites

Ligand tuning in asymmetric catalysis has facilitated rapid development of efficient catalytic systems.⁸³ The concept of modularity has an outstanding significance within ligand (or catalyst) tuning. When a catalytic process is developed or optimized with this strategy, it is crucial to progressively move to more efficient catalytic systems according to mechanistic and molecular interaction principles. Ligand (or catalyst) design is crucial and it is advantageous to design a ligand in such a way that incorporates several independent modules or molecular fragments arranged around a chiral skeleton. Modification of the steric and electronic properties of these modules (or molecular fragments) generally allows for achieving higher performing catalytic systems (*i.e.* one that offers higher conversion, regio- and/or enantioselectivity). The steric and electronic factors of the constituent modules/molecular fragments can be considered the *input parameters* in the optimization process.

Phosphine-phosphite or phosphine-phosphinite ligands (*P-OP* ligands) are intrinsically modular ligands, as the two phosphorus functionalities are attached to a central backbone in a step-wise manner (Figure 22).

Typically, the phosphinite or phosphite groups in *P-OP* ligands are introduced by *O*-phosphorylation of phosphino alcohols (or their phenolic analogs) with electrophilic phosphorus reagents (chlorophosphines or chlorophosphites, respectively).⁸⁴

⁸³ See footnotes 31 and 32 in the introduction for leading references in the field.

⁸⁴ For a recent and comprehensive review on the field, see reference 70.

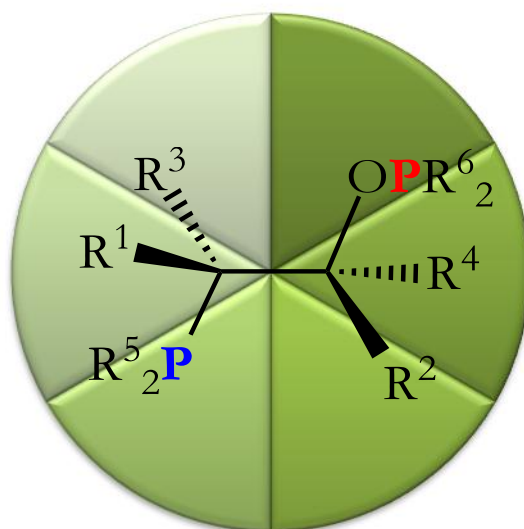


Figure 22. General structure of a modular *P-OP* ligand, which incorporates up to six different molecular fragments or modules.

Synthetic methodologies to introduce the phosphino group are more varied and encompass nucleophilic displacement using phosphorus nucleophilic reagents, addition of *P*-nucleophiles onto C=O groups, epoxide ring-opening and *C*-phosphorylation with a chlorophosphine, amongst others. Representative examples of the introduction of the phosphino group on a carbon scaffold, both from the chiral pool or synthetic origin, have been summarized in Scheme 13 and are summarized herein:

1) In the synthesis of the phosphine-phosphinite ligand **8**, Brunner *et al.*^{69a} introduced the phosphino moiety by nucleophilic displacement of a tosyl group by diphenylphosphide. Ruiz, Claver and co-workers⁷⁵ also used this chemistry on other sugar derivatives and Laschat *et al.*⁸⁵ and Bakos *et al.*⁸⁶ have performed this transformation on halo derivatives to access diversely substituted phosphino alcohols.

⁸⁵ Sell, T.; Laschat, S.; Dix, I.; Jones, P. G. *Eur. J. Org. Chem.* **2000**, 4119.

⁸⁶ (a) Gulyas, H.; Arva, P.; Bakos, J. *Chem. Commun.* **1997**, 2385. (b) Farkas, G.; Balogh, S.; Madarasz, J.; Szoellosy, A.; Darvas, F.; Uerge, L.; Gouygou, M.; Bakos, J. *Dalton Trans.* **2012**, 41, 9493.

2) Yamashita *et al.*^{72a} generated a sugar-derived phosphino alcohol by diastereoselective addition of diphenylphosphine onto a carbonyl group in their synthesis of ligand **16**.

3) Schmaltz *et al.*⁸⁷ reported the introduction of the phosphino group through rearrangement of an *ortho*-lithiated borane-protected phosphinite to the borane complex of an *ortho*-(diphenylphosphino)phenol.

4) Bakos *et al.*^{86, 89} has used ring-opening of cyclic sulfates or cyclic ethers as an elegant strategy to introduce the phosphine moiety.

5) Uemura *et al.*^{72b} directly prepared the phosphino alcohol intermediate through epoxide ring-opening using a phosphide reagent. Epoxide ring-opening by alkali metal phosphide derivatives has been used by the groups of Jiang,^{72f} van Leeuwen,⁸⁸ Bakos,⁸⁹ Pizzano⁹⁰ and by our group.⁷³ In some of these cases, the use of enantiomerically pure *P*-stereogenic nucleophilic phosphorus reagents provided extra elements of chirality in the final ligand.^{77, 79, 88} The ring-opening of stereochemically well-defined polysubstituted epoxides provides phosphino alcohols in a stereo controlled manner. For instance, *trans*-disubstituted epoxides lead to *anti*-phosphino alcohols after ring-opening, since this transformation proceeds via a S_N2

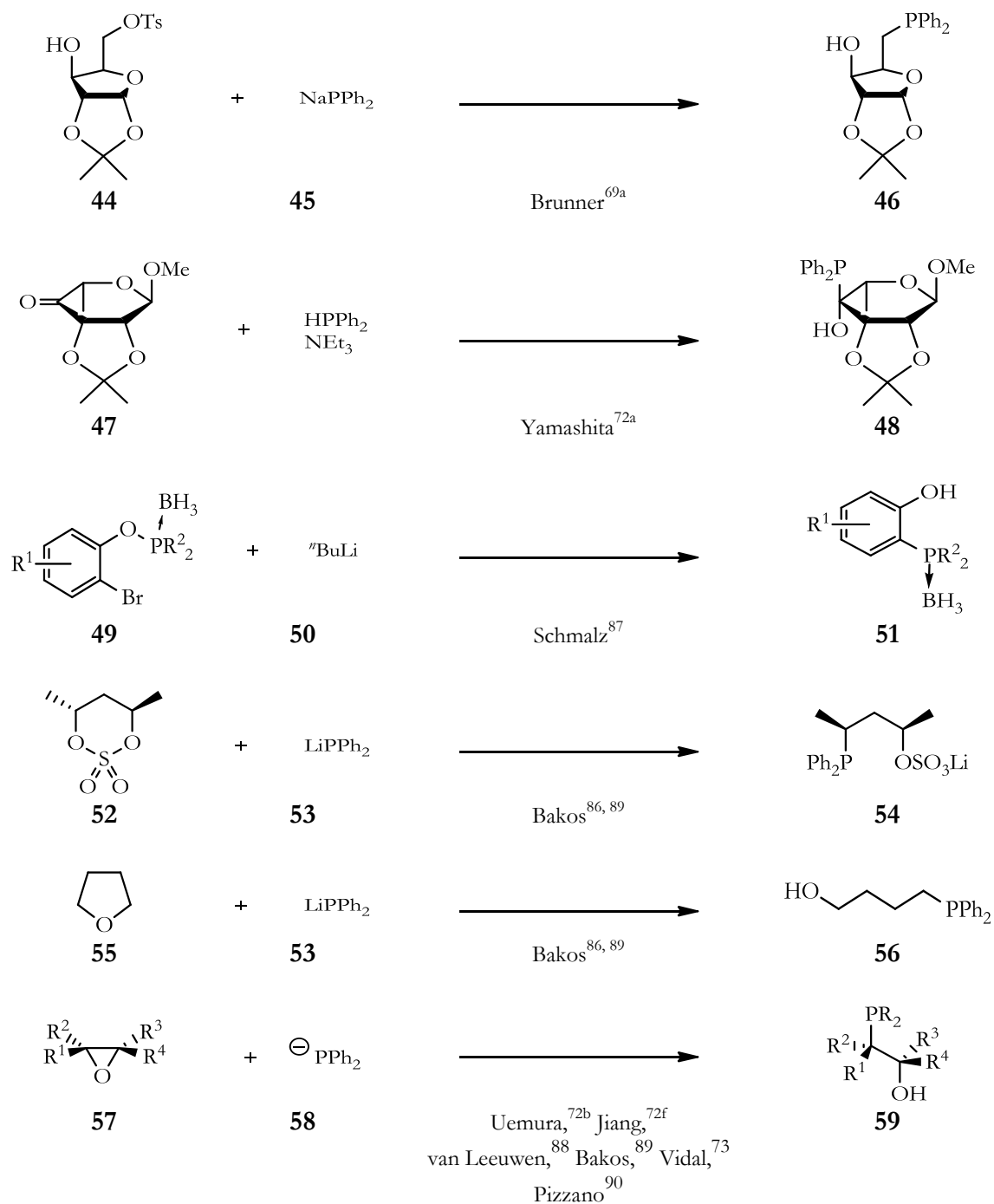
⁸⁷ (a) Velder, J.; Robert, T.; Weidner, I.; Neudörfl, J.-M.; Lex, J.; Schmalz, H.-G. *Adv. Synth. Catal.* **2008**, *350*, 1309. (b) Robert, T.; Abiri, Z.; Wassenaar, J.; Sandee, A. J.; Romanski, S.; Neudörfl, J.-M.; Schmalz, H.-G.; Reek, J. N. H. *Organometallics* **2010**, *29*, 478. (c) Dindaroglu, M.; Falk, A.; Schmalz, H.-G. *Synthesis* **2013**, *45*, 527.

⁸⁸ (a) Deerenberg, S.; Kamer, P. C. J.; van Leeuwen, P. W. N. M. *Organometallics* **2000**, *19*, 2065. (b) Deerenberg, S.; Schrekker, H. S.; van Strijdonck, G. P. F.; Kamer, P. C. J.; van Leeuwen, P. W. N. M.; Fraanje, J.; Goubitz, K. J. *Org. Chem.* **2000**, *65*, 4810.

⁸⁹ (a) Hegedüs, C.; Gulyás, H.; Szöllosy, A.; Bakos, J. *Inorg. Chim. Acta* **2009**, *362*, 1650. (b) Farkas, G.; Balogh, S.; Szoellosy, A.; Uerge, L.; Darvas, F.; Bakos, J. *Tetrahedron: Asymmetry* **2011**, *22*, 2104.

⁹⁰ Arribas, I.; Vargas, S.; Rubio, M.; Suárez, A.; Domene, C.; Álvarez, E.; Pizzano, A. *Organometallics* **2010**, *29*, 5791.

mechanism⁹¹ with inversion of configuration at the attacked carbon and retention of configuration at the other.



Scheme 13. Most relevant strategies developed for introducing the phosphino group.

⁹¹ See (a) Brunner, H.; Sicheneder, A. *Angew. Chem., Int. Ed. Engl.* **1988**, *100*, 718. (b) Gorla, F.; Togni, A.; Venanzi, L. M.; Albinati, A.; Lianza, F. *Organometallics* **1994**, *13*, 1607., and references cited therein.

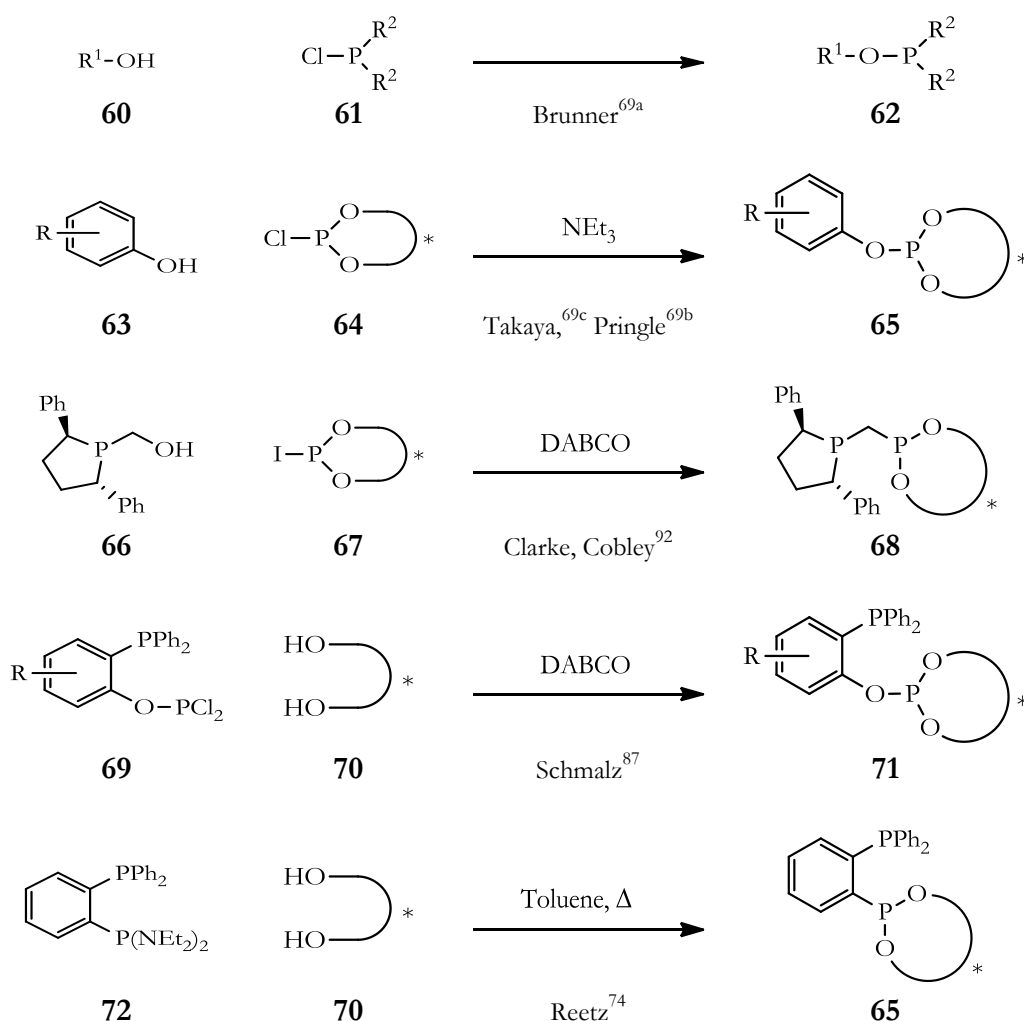
As has already been mentioned, the most usual strategy to introduce the phosphinite or phosphite groups into the ligand structure is the O-phosphorylation of the intermediate phosphino alcohol or phenolic analog with a trivalent phosphorus electrophile (chlorophosphines for a phosphinite or chlorophosphites for a phosphite) in the presence of a base. This strategy was already used in the seminal work of Brunner *et al.*,^{69a} Takaya *et al.*,^{69c} and Pringle *et al.*^{69b}

Clarke and Copley and co-workers have recently reported an elegant strategy to overcome the lack of reactivity of sterically hindered chlorophosphites, whose reactivity towards hydroxyl groups under basic conditions is greatly enhanced by transforming them into the corresponding iodo derivatives.⁹²

Schmalz *et al.* has used an interesting alternative for introducing a phosphite moiety, which consists of the reaction of the corresponding diol with a dichlorophosphine that also contains the final phosphino group of the *P-OP* ligand.⁸⁷ Reetz *et al.* followed a similar strategy to generate a phosphonite group by reaction of a bis(dialkylamino)phosphino group with the corresponding diol.⁷⁴

Strategies to introduce the phosphinite, phosphonite or phosphite group have been schematized in Scheme 14. As recently reviewed by our group,⁷⁰ a diverse array of phosphinite and phosphite groups have been incorporated to *P-OP* ligands using the transformations previously indicated.

⁹² Noonan, G. M.; Fuentes, J. A.; Copley, C. J.; Clarke, M. L. *Angew. Chem., Int. Ed.* **2012**, *51*, 2477.



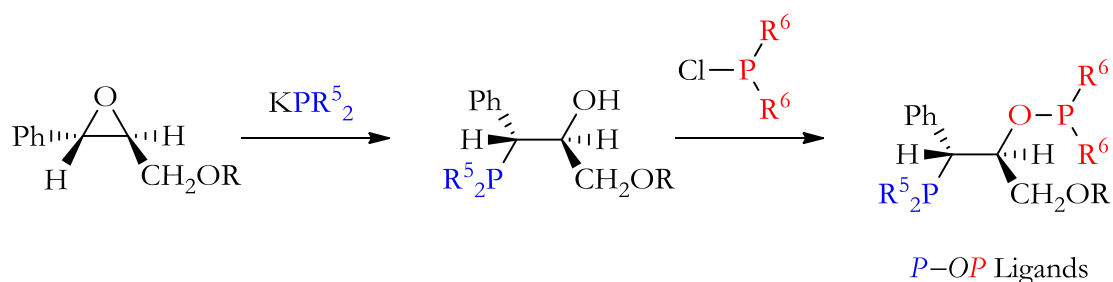
Scheme 14. Most relevant strategies for introducing phosphinite, phosphonite and phosphite groups.

Specifically, the synthetic strategy developed by H. Fernández-Pérez during his PhD combined several of the aforementioned transformations for the preparation of our *P-OP* ligands, mainly phosphine-phosphites.^{73, 81, 82} Dr. Fernández-Pérez's design (Scheme 15) incorporated an understudied structural motif: two consecutive stereogenic centers between the two phosphorus functionalities. In accordance with a general goal of high modularity, Dr. Héctor Fernández-Pérez prepared a wide variety of chiral phosphine-phosphinite or phosphine-phosphite ligands. His synthetic strategy was based

on the use of enantiomerically pure Sharpless epoxy ethers as starting materials, from which the target ligands were available in two steps (Scheme 15):

1.- Ring-opening of a Sharpless epoxy ether with a trivalent phosphorus nucleophilic derivative to introduce the phosphino functionality. The isolated phosphino-alcohols were rather prone to oxidation, and subsequent protection as the corresponding borane adducts allowed for more convenient handling and storage.

2.- Base-mediated *O*-phosphorylation of the resulting phosphino alcohol, after base-mediated borane decomplexation, with a trivalent phosphorus electrophilic derivative allowed for the introduction of the phosphinite or phosphite functionality.



Scheme 15. Synthetic route to *P-OP* ligands derived from Sharpless epoxides.

1.1.3 Mechanism

The rhodium-mediated hydrogenation of alkenes under homogeneous conditions is one of the mechanistically best understood transformations in organometallic chemistry. In principle, different types of catalysts can be considered depending on the number of hydrido-ligands bound to the metal center. Monohydrido catalysts can directly react with alkenes to form a metal-alkyl intermediate, which is susceptible to further reaction with molecular hydrogen to give the corresponding hydrogenated product, regenerating the initial monohydrido catalyst. Few catalytic systems follow this path, which can be exemplified by the rhodium complex $[\text{Rh}(\text{H})(\text{CO})(\text{PPh}_3)_3]$.⁹³

Other catalytic cycles in homogeneous hydrogenation start from metal complexes bearing no hydrido ligands, which evolve to metal dihydrido intermediates by reaction with molecular hydrogen. Previous or subsequent substrate coordination to the metal center with respect to the molecular hydrogen activation step leads to $[\text{M}(\text{H})_2(\text{alkene})]^{n+}$ complexes, which are key intermediate complexes in the whole catalytic process. Thus, two different types of catalytic cycles are possible depending on whether activation of molecular hydrogen takes place prior to substrate coordination (*dihydride route*) or the substrate coordinates to the metal center as the first step (*unsaturated or alkene route*, see Figure 23). Wilkinson's catalyst ($[\text{Rh}(\text{Cl})(\text{PPh}_3)_3]$) and $[\text{Rh}(\text{nbd})(\text{dppe})]^+$ constitute two homogeneous hydrogenation catalysts, each of which follow one of the two aforementioned mechanistic possibilities: whilst hydrogenations mediated by Wilkinson's catalyst ($[\text{Rh}(\text{Cl})(\text{PPh}_3)_3]$) evolve first to a dihydrido complex with uncoordinated substrate (*dihydride route*), $[\text{Rh}(\text{nbd})(\text{dppe})]^+$ evolves first to a substrate-bound complex with no hydrido ligands (*unsaturated or alkene route*).

⁹³ Carmona, D.; Oro, L. A. Hydrogenation—Homogeneous. In *Encyclopedia of Catalysis*; Horváth, I. T., Ed.; John Wiley & Sons: New York, 2010.

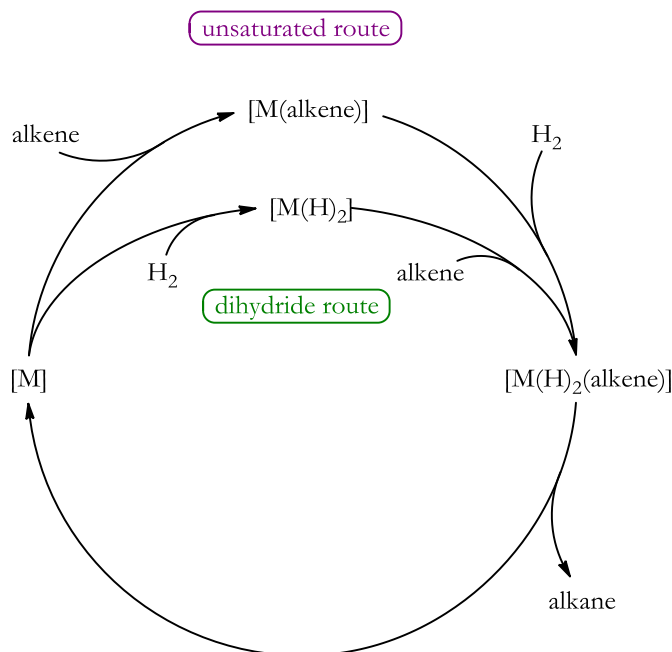


Figure 23. Dihydride or unsaturated routes in hydrogenation reactions.

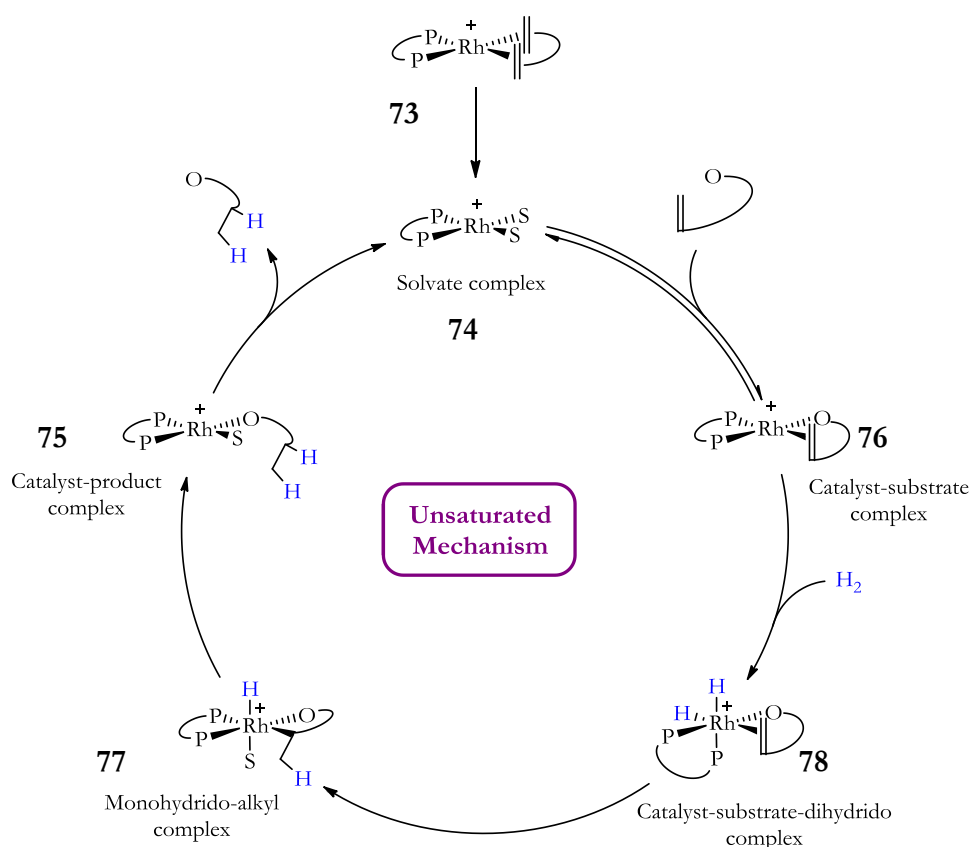
The mechanism of rhodium-catalyzed asymmetric hydrogenation of functionalized alkenes mediated by rhodium(I) complexes of chelating diphosphines like DIPAMP is one of the most investigated and best understood processes. The reaction pathways were initially studied by Halpern⁹⁴ and Brown.⁹⁵ In their studies, they proposed the mechanism depicted in Scheme 16 for the asymmetric hydrogenation of an α -(acylamino)acrylate promoted by a diphosphine-rhodium(I) complex.

In this catalytic cycle, known as the “*unsaturated* or *Halpern-Brown mechanism*”, the active species is formed after hydrogenation of the sacrificial diene (*i.e.* cyclooctadiene (cod), norbornadiene (nbd), or tetrafluorobarrelene

⁹⁴ (a) Halpern, J.; Riley, D. P.; Chan, A. S. C.; Pluth, J. J. *J. Am. Chem. Soc.* **1977**, *99*, 8055. (b) Halpern, J. *Science* **1982**, *217*, 401. (c) Landis, C. R.; Halpern, J. *J. Am. Chem. Soc.* **1987**, *109*, 1746.

⁹⁵ (a) Brown, J. M.; Chaloner, P. A. *J. Chem. Soc., Chem. Commun.* **1980**, 344. (b) Brown, J. M. *Chem. Soc. Rev.* **1993**, *22*, 25. (c) Brown, J. M. in *Comprehensive Asymmetric Catalysis*; Jacobsen, E. N., Pfaltz, A., Yamamoto, H. Eds.; Springer: Berlin, Germany, 1999; Vol. 1, pp 121-182.

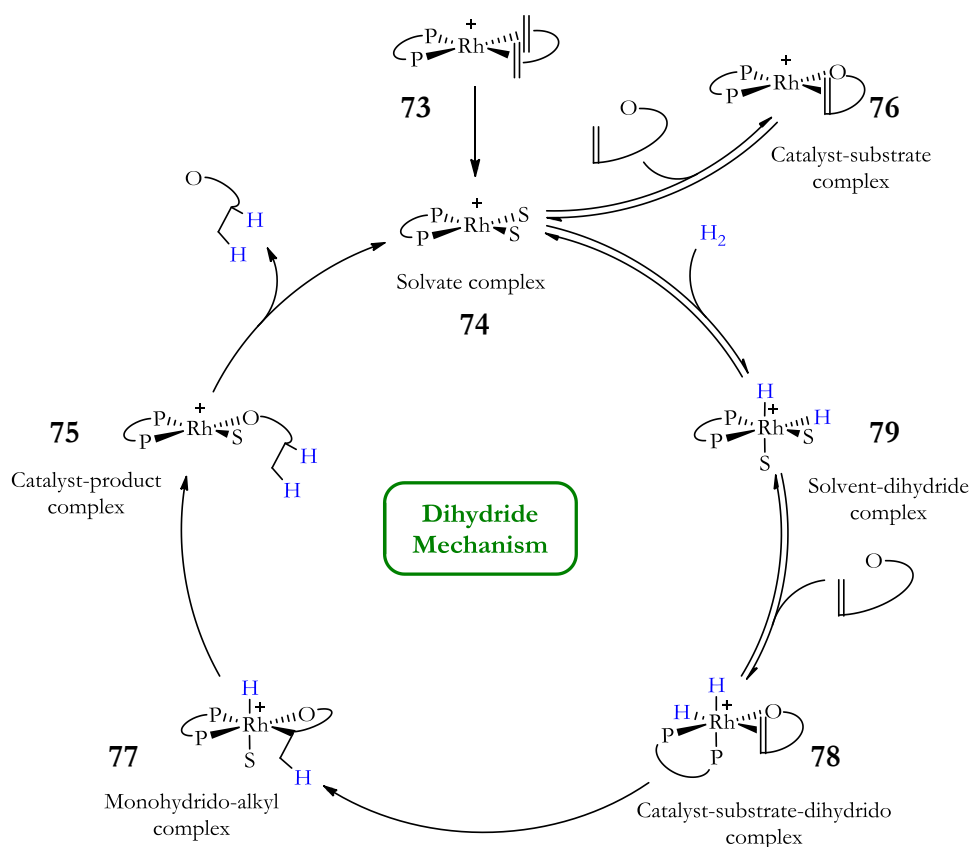
(tfb)) coordinated to the precatalytic complex (**73**).⁹⁶ The vacant coordination sites after hydrogenation of the sacrificial diene are filled by solvent molecules (**74**). A molecule of substrate displaces those solvent molecules to form the catalyst-substrate complex (**76**), as indicated in Scheme 16, which undergoes an irreversible oxidative addition of molecular hydrogen to form a catalyst-substrate-dihydrido complex (**78**). This irreversible step is the rate- and stereodetermining step: upon substrate coordination and dihydrogen oxidative addition, the two new carbon-hydrogen bonds are formed from the side of the metal during the stereospecific catalytic process.



Scheme 16. Unsaturated mechanism for the asymmetric hydrogenation of alkenes.

⁹⁶ Esteruelas, M. A.; Oro, L. A. *Coord. Chem. Rev.* **1999**, 193-195, 557.

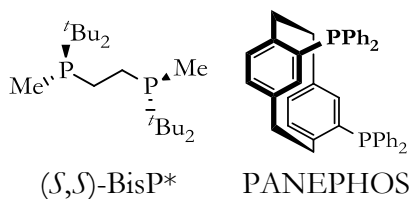
Further research from Gridnev and Imamoto⁹⁷ revealed that on using more electron rich ligands such as BisP* in polar solvents,⁹⁸ the catalytic cycle proceeds through the dihydride mechanism (See Scheme 17), which was also noted by Brown *et al.* for Rh-PANEPHOS⁹⁸ derived catalytic systems.⁹⁹



Scheme 17. Dihydride mechanism for the asymmetric hydrogenation of alkenes.

⁹⁷ (a) Gridnev, I. D.; Higashi, N.; Asakura, K.; Imamoto, T. *J. Am. Chem. Soc.* **2000**, *122*, 7183. (b) Gridnev, I. D.; Higashi, N.; Imamoto, T. *Organometallics* **2001**, *20*, 4542. (c) Gridnev, I. D.; Imamoto, T. *Acc. Chem. Res.* **2004**, *37*, 633.

⁹⁸



⁹⁹ (a) Giernoth, R.; Heinrich, H.; Adams, N. J.; Deeth, R. J.; Bargon, J.; Brown, J. M. *J. Am. Chem. Soc.* **2000**, *122*, 12381. (b) Heinrich, H.; Giernoth, R.; Bargon, J.; Brown, J. M. *J. Chem. Soc., Chem. Commun.* **2001**, 1296.

The formation of the catalyst-substrate complex (76) from the solvate complex (74) can be a reversible process in this case. The solvate complex (74) can subsequently undergo oxidative addition with molecular hydrogen to form the solvate-dihydride complex (79) also in a reversible way.^{97a} The solvate-dihydride complex can further react with substrate molecules to form the catalyst-substrate-dihydrido intermediate (78). This complex is common with the unsaturated catalytic cycle and, as in the previous case, it has never been observed, the monohydride-alkyl complex (77) being the first observable species. It has been observed that the rate- and stereo-determining step for the hydrogenations following the dihydride mechanism depend on the exact nature of the catalytic system. Whilst Imamoto, Gridnev and co-workers have suggested that migratory insertion is the rate- and stereo-determining step when (*S,S*)-1,2-bis(*tert*-butylmethylphosphino)ethane (BisP*) is used as the ligand,^{97a} the same authors indicate that in Trichickenfootphos-mediated hydrogenations, stereoselection originates prior to the irreversible migratory insertion step, by a reversible solvent insertion into the catalyst-substrate complex with alkene decoordination.¹⁰⁰

¹⁰⁰ Gridnev, I. D.; Imamoto, T.; Hoge, G.; Kouchi, M.; Takahashi, H. *J. Am. Chem. Soc.* **2008**, *130*, 2560.

In order to shed light on the correlation between enantioselection and the features of *P-OP* ligands, theoretical studies at the DFT level on the hydrogenation of methyl 2-acetamidoacrylate (**11d**) mediated by the rhodium complex derived from ligand **30a** were carried out by Maseras *et al.*^{82b} The “*unsaturated*” mechanism¹⁰¹ has been systematically explored at the theoretical level by a number of research groups.¹⁰² These theoretical studies observed competition between oxidative addition and migratory insertion as possible rate-determining steps. For hydrogenations mediated by our $[\text{Rh}(\text{P-OP})]^+$ complexes, Maseras *et al.* observed that the highest energy corresponds to the transition state for oxidative addition, followed by that for migratory insertion ($\Delta G^\ddagger_{\text{OA}} > \Delta G^\ddagger_{\text{MI}}$ by *ca.* 1 kcal/mol for phosphine-phosphite ligands, Figure 24).¹⁰³

¹⁰¹ The “dihydride” mechanism, in which dihydrogen oxidative addition occurs prior to substrate coordination, is limited to those cases involving highly electron-rich alkyl phosphines in polar solvents, and thus is not related to the current case.

¹⁰² See for example references 94a, 94c, 95b, 107b and the following: (a) Wilczynski, R.; Fordyce, W. A.; Halpern, J. *J. Am. Chem. Soc.* **1983**, *105*, 2066. (b) Landis, C. R.; Hilfenhaus, P.; Feldgus, S. *J. Am. Chem. Soc.* **1999**, *121*, 8741. (c) Feldgus, S.; Landis, C. R. *J. Am. Chem. Soc.* **2000**, *122*, 12714. (d) Landis, C. R.; Feldgus, S. *Angew. Chem., Int. Ed.* **2000**, *39*, 2863. (e) Feldgus, S.; Landis, C. R. *Organometallics* **2001**, *20*, 2374.

¹⁰³ It is generally accepted that dihydrogen oxidative addition starts from a 5-coordinate dihydrogen intermediate (**RMolH₂**) *via* the corresponding transition state **RMolH₂-TS** to the rhodium dihydrido complex **RDIHY**. Migratory insertion of the β carbon of the olefin in **RDIHY** into a Rh-H bond follows to give an alkyl hydride complex with a C-H \cdots Rh agostic interaction **RALHY_{ag}** *via* the corresponding transition state **RDIHY-TS**. The previous abbreviations are widely used in the original theoretical studies¹⁰³⁻¹⁰⁴ and for this reason we have maintained this nomenclature.

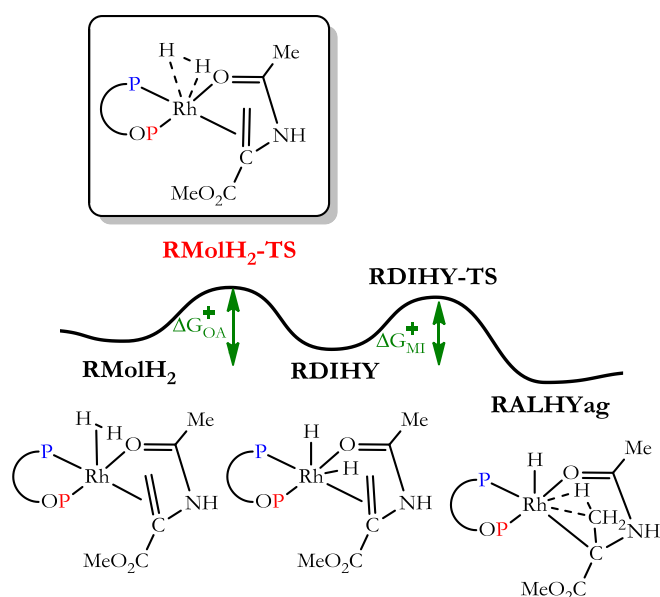


Figure 24. Highest-lying transition states in the *P-OP* mediated asymmetric hydrogenation (unsaturated mechanism).¹⁰³

In systems that involve the use of C_2 symmetric ligands, there are only two possible substrate-catalyst adducts which arise from coordination of the two possible enantiotopic olefin faces to any of the two equivalent binding sites in the metal center. For C_1 symmetric ligands such as the *P-OP* ones that are central to the present Thesis, the equivalence between the two available rhodium binding sites is lost, and thus there are four possible binding modes that arise from coordination of the two enantiotopic faces of the olefin to each of the two rhodium binding sites (coordination *cis*- and *trans*- to the phosphino group). Thus, four catalyst-substrate adducts are possible, as shown in Figure 25.

The geometries and energies were optimized for intermediates **RMolH₂**, **RDIHY** and **RALHY_{ag}** and for transition state structures **RMolH₂-TS** and **RDIHY-TS** for the four possible reaction manifolds. The corresponding migratory insertion transition states were found to be lower in

energy by *ca.* 1 kcal/mol to those associated to dihydrogen oxidative addition.^{82b}

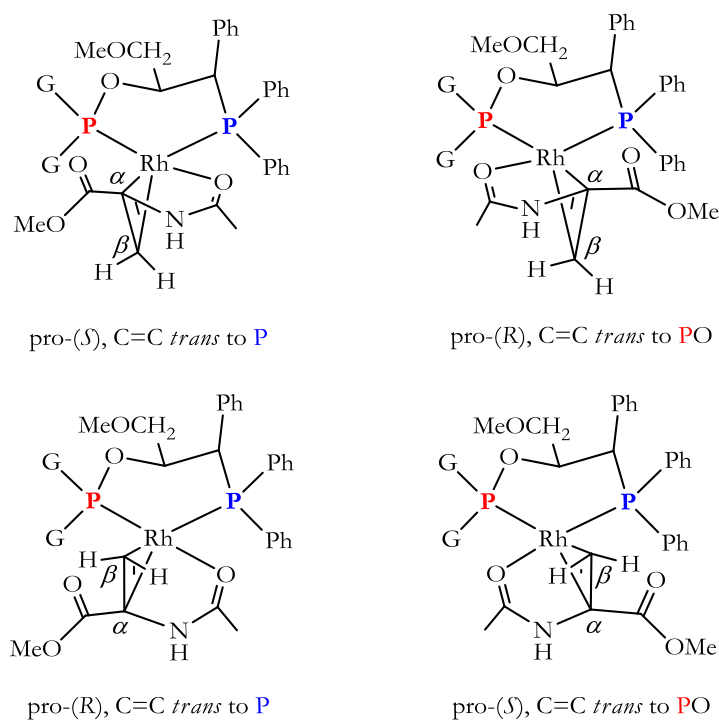


Figure 25. The four possible binding modes for the substrate with $[\text{Rh}(\text{P}-\text{OP})]^+$ catalysts.

Figure 26 shows the optimized structures and computed relative energies of the dihydrogen oxidative addition transition states (OATS) for the four possible reaction manifolds in the hydrogenation of methyl 2-acetamidoacrylate (**11d**) mediated by the highest performing phosphine-phosphite ligand **30a**. In calculating the enantiomeric excess obtained for the catalyst derived from ligand **30a**, Maseras *et al.* considered the $\Delta G_{\text{OA}}^\ddagger$ values for the four reaction manifolds and predicted an ee value of 90% in favor of the (*R*)-configured hydrogenation product (*cf.* 99% ee (*R*) experimental result^{82b}). The experimental behavior was thus reproduced.

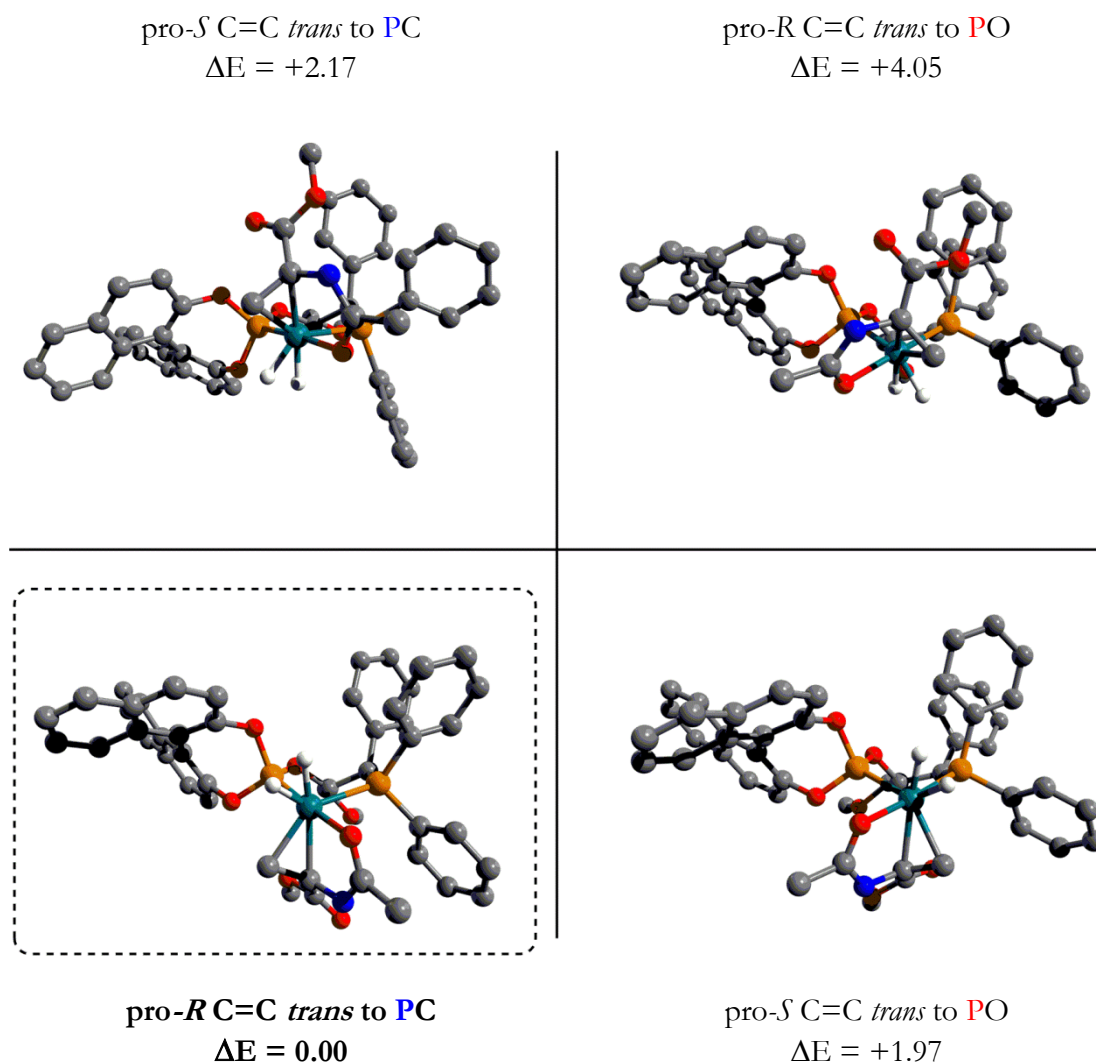


Figure 26. Optimized structures and computed relative energies of the OATS for the four possible reaction manifolds in the hydrogenation of methyl 2-acetamidoacrylate mediated by the highest performing ligand **30a** (relative free energies in kcal mol⁻¹).

The studies from Maseras *et al.* showed that enantioselection in the *P-OP* mediated catalysis is a fine balance of electronic and steric effects. Primarily, the strong electronic effect of the phosphite donor group results in blocking of product formation through the two manifolds with the olefin *trans* to phosphite. Moreover, the phenyl group in the backbone provides additional steric blocking of the pro-*R* C=C *trans* to the *PO* manifold. Finally, the principal steric director in our *P-OP* mediated catalysis is clearly the BINOL scaffold, whose steric hindrance is associated with the manifold in which the

binaphthyl group points towards the substrate (pro-*S* C=C *trans* to PC manifold).

This can be visualized in a quadrant diagram (Figure 27) by saying that the two right-hand sites are electronically disfavored with respect to the placement of the C_α and C_β olefin carbon atoms of the substrate and that the two upper sites are blocked by the steric effects of the BINOL scaffold and backbone Ph groups. Ultimately, steric and electronic factors leave the lower-left quadrant as the lowest energy direction of approach for the substrate, since it is well established in this chemistry that steric hindrance in the transition state of the rate- and stereo-determining step (OA) is developed in the quadrant initially occupied by the C_α olefin atom.¹⁰²

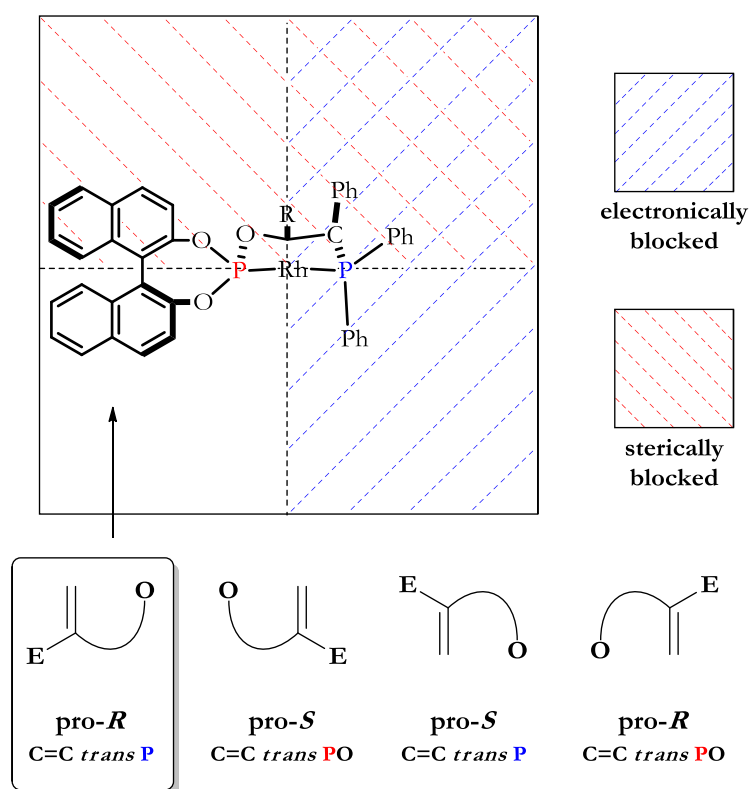


Figure 27. Quadrant representation for possible substrate orientations in the OATS with ligand 30a.

1.1.4 Rhodium-mediated Asymmetric Hydrogenation in the Preparation of API Intermediates

The ultimate goal in any synthetic methodology should be give access to a variety of new products or strategic compounds in an efficient way and with a high degree of enantiopurity. Where enantiomerically pure (or highly enriched) products are concerned, asymmetric hydrogenation is considered one of the methods of choice for their preparation.¹⁰⁴ Asymmetric hydrogenation's operational simplicity, selectivity, wide scope in substrates, atom economy and operational costs have attracted great attention from industry making it one of the most effective and trustworthy methodologies in asymmetric catalysis.¹⁰⁵ Thus, industry relies on this methodology for the production of enantiopure or highly enantioenriched products as the key step in the production of active pharmaceutical ingredients (APIs), agrochemicals, fragrance compounds and advanced materials.^{105a,e, 106}

Chiral rhodium catalysts are amongst the most used in industrial asymmetric hydrogenation of functionalized C=C bonds.^{105e} The successful application of enantiomerically pure rhodium complexes in asymmetric

¹⁰⁴ *Asymmetric Catalysis on Industrial Scale: Challenges, Approaches and Solutions*, 2nd edn.; Blaser, H.-U., Federsel, H.-J., Eds.; Wiley-VCH: Weinheim, 2010.

¹⁰⁵ (a) Palmer, A. M.; Zanotti-Gerosa, A. *Curr. Opin. Drug Discovery Dev.* **2010**, *13*, 698. (b) Xie, J.-H.; Zhu, S.-F.; Zhou, Q.-L. *Chem. Rev.* **2011**, *111*, 1713. (c) Wang, D.-S.; Chen, Q.-A.; Lu, S.-M.; Zhou, Y.-G. *Chem. Rev.* **2012**, *112*, 2557. (d) Xie, J.-H.; Zhu, S.-F.; Zhou, Q.-L. *Chem. Soc. Rev.* **2012**, *41*, 4126. (e) Ager, D. J.; de Vries, A. H. M.; de Vries, J. G. *Chem. Soc. Rev.* **2012**, *41*, 3340. (f) Arai, N.; Ohkuma, T. *Chem. Rec.* **2012**, *12*, 284.

¹⁰⁶ (a) Lida, T.; Mase, T. *Curr. Opin. Drug Discovery Dev.* **2002**, *5*, 834. (b) Blaser, H.-U.; Malan, C.; Pugin, B.; Spindler, F.; Steiner, H.; Studer, M. *Adv. Synth. Catal.* **2003**, *345*, 103. (c) Lennon, I. C.; Pilkington, C. J. *Synthesis* **2003**, 1639. (d) Blaser, H.-U.; Pugin, B.; Spindler, F. *J. Mol. Catal. A: Chem.* **2005**, *231*, 1. (e) Farina, V.; Reeves, J. T.; Senanayake, C. H.; Song, J. *J. Chem. Rev.* **2006**, *106*, 2734. (f) Blaser, H.-U.; Pugin, B.; Spindler, F.; Thommen, M. *Acc. Chem. Res.* **2007**, *40*, 1240. (g) Johnson, N. B.; Lennon, I. C.; Moran, P. H.; Ramsden, J. A. *Acc. Chem. Res.* **2007**, *40*, 1291. (h) Saudan, L. A. *Acc. Chem. Res.* **2007**, *40*, 1309. (i) Shimizu, H.; Nagasaki, I.; Matsumura, K.; Sayo, N.; Saito, T. *Acc. Chem. Res.* **2007**, *40*, 1385. (j) *Green Chemistry in the Pharmaceutical Industry*; Dunn, P. J., Wells, A. S., Williams, M. T., Eds.; Wiley-VCH: Weinheim, 2010; 1st edn. (k) Busacca, C. A.; Fandrick, D. R.; Song, J. J.; Senanayake, C. H. *Adv. Synth. Catal.* **2011**, *353*, 1825. (l) Etayo, P.; Vidal-Ferran, A. *Chem. Soc. Rev.* **2013**, *42*, 728.

hydrogenation relies on the ability of the substrate to form a rhodium chelate involving the C=C double bond and a donor atom (generally provided by a C=O binding group situated at the γ position respect to the C=C bond).^{94c, 107} This fact accounts for the excellent results in terms of reaction rate and enantioselectivity obtained for Rh-mediated asymmetric hydrogenation of several functionalized alkene classes: α -(acylamino)acrylates, α -substituted enamides, α -arylenol esters, itaconate derivatives and other minimally functionalized olefins. This section is intended to provide a summary of the most relevant contributions in this field, organized according to the aforementioned substrate classes.

1.1.4.1 Acrylate Derivatives

The anti-Parkinson drug L-DOPA ((*S*)-3',4'-dihydroxyphenylalanine, **82**; Scheme 18 (a)) was the first industrial application of rhodium-mediated asymmetric hydrogenation applied to the synthesis of an active pharmaceutical ingredient (API). This chiral drug was synthesized by Knowles *et al.*, while working at Monsanto, with a Rh-(*R,R*)-DIPAMP complex.¹⁰⁸ After this successful example, rhodium-mediated asymmetric hydrogenation of key α -(acylamino)acrylates attracted the interest of several pharmaceutical companies. These efforts culminated in the synthesis of various non-natural α -amino acids and APIs.¹⁰⁹ Selected examples of this chemistry have been summarized in Scheme 18.

Scientists at Abbot Laboratories developed a procedure for the asymmetric hydrogenation of the β -aryl-substituted α -(acylamino)acrylate **83**,

¹⁰⁷ (a) Brown, J. M.; Chaloner, P. A. *J. Am. Chem. Soc.* **1980**, *102*, 3040. (b) Chan, A. S. C.; Pluth, J. J.; Halpern, J. *J. Am. Chem. Soc.* **1980**, *102*, 5952.

¹⁰⁸ (a) Knowles, W. S. *Angew. Chem., Int. Ed.* **2002**, *41*, 1998. (b) Knowles, W. S. *Adv. Synth. Catal.* **2003**, *345*, 3.

¹⁰⁹ Beck, G. *Synlett* **2002**, 837.

mediated by the Rh complex derived from (*R,R*)-Et-DUPHOS (Scheme 18 (b)), to give a precursor in the synthesis of the antitumor agent L-azatyrosine **85** with an initial 83% ee (further increased up to 96% ee by recrystallization).¹¹⁰

Researchers at Johnson & Johnson synthesized an advanced intermediate in the synthesis of a dual CCK1/CCK2 receptor antagonist **88**¹¹¹ which is currently in human clinical trials for the treatment of various gastrointestinal diseases. The (*R,S*)-Me-BoPhoz ligand (Scheme 18 (c)) was the ligand of choice for performing the enantioselective hydrogenation of β -arylacrylate **86**. The enantioselectivity achieved initially was 94% ee and it could be further increased to >99% ee upon recrystallization.¹¹²

Researchers at UCB Pharma devised a methodology for the synthesis of the anti-epileptic drug levetiracetam **90**.¹¹³ Enantioselective hydrogenation of the acrylamide **89** with (*S,S*)-Et-DUPHOS afforded the final chiral drug with 98% ee (upgraded to >99% ee by recrystallization; Scheme 18 (d)).¹¹⁴

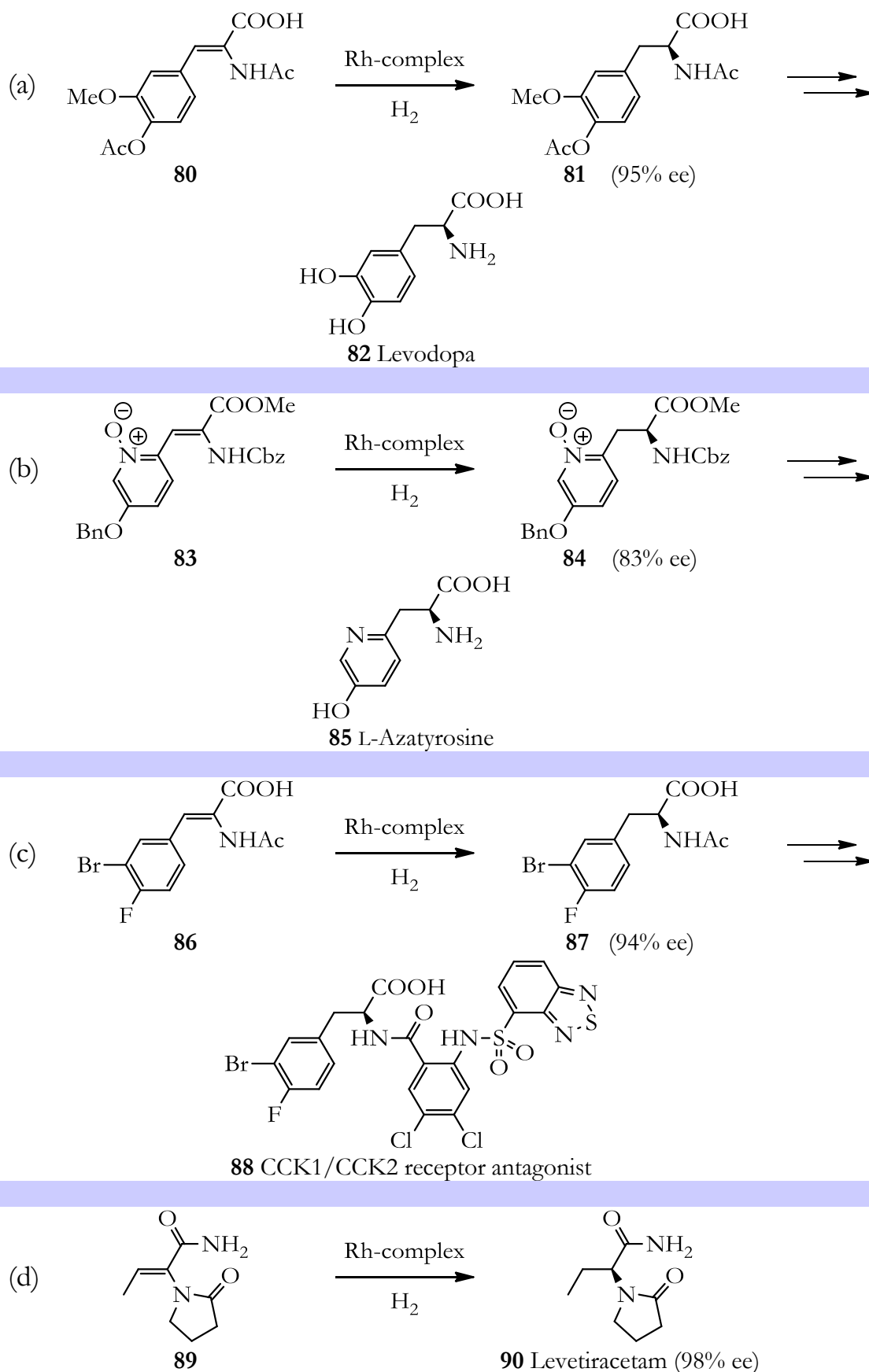
¹¹⁰ Adamczyk, M.; Akireddy, S. R.; Reddy, R. E. *Org. Lett.* **2001**, *3*, 3157.

¹¹¹ Pippel, M.; Boyce, K.; Venkatesan, H.; Phuong, V. K.; Yan, W.; Barrett, T. D.; Lagaud, G.; Li, L.; Morton, M. F.; Prendergast, C.; Wu, X.; Shankley, N. P.; Rabinowitz, M. H. *Bioorg. Med. Chem. Lett.* **2009**, *19*, 6376.

¹¹² Liu, J.; Deng, X.; Fitzgerald, A. E.; Sales, Z. S.; Venkatesan, H.; Mani, N. S. *Org. Biomol. Chem.* **2011**, *9*, 2654.

¹¹³ Kenda, B. M.; Matagne, A. C.; Talaga, P. E.; Pasau, P. M.; Differding, E.; Lallemand, B. I.; Frycia, A. M.; Moureau, F. G.; Klitgaard, H. V.; Gillard, M. R.; Fuks, B.; Michel, P. J. *Med. Chem.* **2004**, *47*, 530.

¹¹⁴ Surtees, J.; Marmon, V.; Differding, E.; Zimmermann, V. (UCB Pharma). Int. Patent WO 01/64637, 2001.



Scheme 18. Rhodium-mediated asymmetric hydrogenation of α -(acylamino)acrylates.

The rhodium-mediated asymmetric hydrogenation of other types of acrylic acid derivatives has also been studied to prepare precursors of biologically relevant compounds or API precursors. These acrylic acid derivatives vary greatly in terms of structure and include, amongst others, β -(amino)acrylates, and α -(alkyl)acrylates.

Researchers at Merck and Solvias developed a hydrogenation-based synthetic route to sitagliptin **92**, in the so-called 2nd generation process.¹¹⁵ The β -(amino)acrylate, dehydro-sitagliptin **91**, was subjected to hydrogenation with a rhodium complex derived from (*S,R*)-^tBu-JOSIPHOS, yielding the compound sitagliptin **92** as a free base with an enantioselectivity of 95% ee (further increased to >99% ee by recrystallization, Scheme 19 (a)).¹¹⁶ Sitagliptin **92** is a DPP IV inhibitor used for the treatment of type 2 diabetes mellitus.¹¹⁷

Imagabalin hydrochloride **95** is a drug candidate for the treatment of anxiety and insomnia. Its precursor **94** has been accessed by enantioselective hydrogenation of a *Z/E* mixture of β -(amino)acrylate **93** using a rhodium complex derived from (*S*)-Trichickenfootphos (TCFP) with a diastereomeric excess (de) >95% (Scheme 19 (b)).¹¹⁸

Aliskiren **98** is an important drug marketed by Novartis for the treatment of hypertension.¹¹⁹ Several groups attempted the enantioselective hydrogenation of α -alkylacrylate **96** (Scheme 19 (c)),¹²⁰ by using rhodium com-

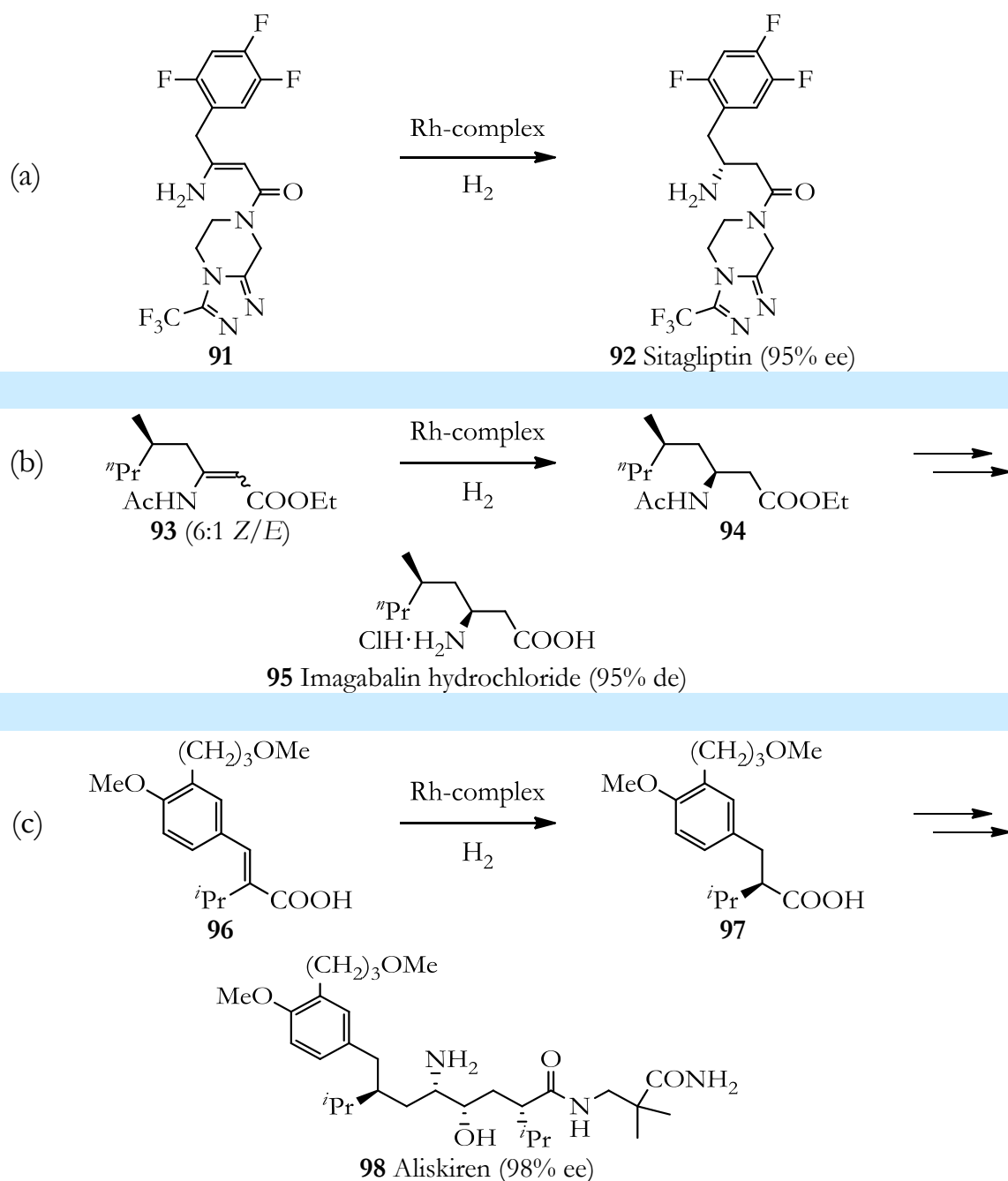
¹¹⁵ Desai, A. A. *Angew. Chem., Int. Ed.* **2011**, *50*, 1974.

¹¹⁶ Hansen, K. B.; Hsiao, Y.; Xu, F.; Rivera, N.; Clausen, A.; Kubryk, M.; Krska, S.; Rosner, T.; Simmons, B.; Balsells, J.; Ikemoto, N.; Sun, Y.; Spindler, F.; Malan, C.; Grabowski, E. J. J.; Armstrong, J. D. *J. Am. Chem. Soc.* **2009**, *131*, 8798.

¹¹⁷ Drucker, D.; Easley, C.; Kirkpatrick, P. *Nat. Rev. Drug Discovery* **2007**, *6*, 109.

¹¹⁸ (a) Magano, J.; Conway, B.; Bowles, D.; Nelson, J.; Nanninga, T. N.; Winkle, D. D.; Wu, H.; Chen, M. H. *Tetrahedron Lett.* **2009**, *50*, 6329. (b) Birch, M.; Challenger, S.; Crochard, J.-P.; Fradet, D.; Jackman, H.; Luan, A.; Madigan, E.; McDowall, N.; Meldrum, K.; Gordon, C. M.; Widegren, M.; Yeo, S. *Org. Process Res. Dev.* **2011**, *15*, 1172.

¹¹⁹ Frampton, J. E.; Curran, M. P. *Drugs* **2007**, *67*, 1767.



Scheme 19. Rhodium-mediated asymmetric hydrogenation of other acrylate derivatives.

¹²⁰ (a) Sturm, T.; Weissensteiner, W.; Spindler, F. *Adv. Synth. Catal.* **2003**, *345*, 160. (b) Lefort, L.; Boogers, J. A. F.; de Vries, A. H. M.; de Vries, J. G. *Top. Catal.* **2006**, *40*, 185. (c) Boogers, J. A. F.; Felfer, U.; Kotthaus, M.; Lefort, L.; Steinbauer, G.; De Vries, A. H. M.; De Vries, J. G. *Org. Process Res. Dev.* **2007**, *11*, 585. (d) Chen, W.; McCormack, P. J.; Mohammed, K.; Mbafor, W.; Roberts, S. M.; Whittall, J. *Angew. Chem., Int. Ed.* **2007**, *46*, 4141. (e) Andrushko, N.; Andrushko, V.; Thyraan, T.; Koenig, G.; Boerner, A. *Tetrahedron Lett.* **2008**, *49*, 5980.

plexes derived from the PipPhos,^{120b, c} Walphos-based^{120a} and TriFer ligands.^{120d} Hydrogenation of compound **96**, which is an intermediate in the synthetic route towards aliskiren **98**, was excellent, but the TriFer ligand provided the highest enantioselectivity (98% ee), whereas PipPhos- and Walphos-based systems exhibited better industrial profiles with increased TONs (>5,000) and TOFs (up to 1,800 h⁻¹).

1.1.4.2 α -Substituted Enamides

Due to the ubiquity of chiral *N*-acylamino motifs in pharmacologically active compounds, the hydrogenation products of α -substituted enamides are a very important class of precursors of key biologically active compounds. Enantioselective hydrogenation is a core methodology that efficiently delivers chiral α -substituted *N*-acylamines with excellent enantioselectivities. Selected examples of the preparation of API precursors by hydrogenation of α -substituted enamides have been summarized in Scheme 20.

Imamoto, Gridnev *et al.*¹²¹ reported the hydrogenation of some α -arylenamides by using rhodium complexes derived from *P*-stereogenic ligands QuinoxP*, BenzP* or DioxyBenzP* to achieve valuable synthetic intermediates (Scheme 20 (a-c)).

The hydrogenation of α -arylenamide **99** afforded compound **100** with >99% ee regardless of the ligand employed ((*R,R*)-QuinoxP* or (*R,R*)-BenzP*).¹²¹ Compound **100** is an important synthon in the synthesis of casopitant **101** (Scheme 20 (a)), which is a potent NK₁ receptor antagonist useful in chemotherapy-induced nausea and vomiting treatment.¹²²

¹²¹ Imamoto, T.; Tamura, K.; Zhang, Z.; Horiuchi, Y.; Sugiya, M.; Yoshida, K.; Yanagisawa, A.; Gridnev, I. D. *J. Am. Chem. Soc.* **2012**, *134*, 1754.

¹²² Cimaresti, Z.; Bravo, F.; Castoldi, D.; Tinazzi, F.; Provera, S.; Perboni, A.; Papini, D.; Westerduin, P. *Org. Process Res. Dev.* **2010**, *14*, 805.

Regarding the hydrogenation of α -arylenamide **102**, the catalytic system derived from (R,R)-DioxyBenzP* provided 97% ee in the resulting product **103** (Scheme 20 (b)).¹²¹ Zhang *et al.* had previously reported this transformation with 94% ee.¹²³ The hydrogenated product is an advanced intermediate in the synthesis of cinacalcet hydrochloride **104**, which is used for the treatment of secondary hyperparathyroidism and hypercalcemia.¹²⁴

Imamoto, Gridnev *et al.* also improved the hydrogenation of **105**,¹²¹ which was previously reported by Merck,¹²⁵ with the catalytic system derived from (S,S)-QuinoxP* to afford **106** with 98% ee (Scheme 20 (c)). This compound is a precursor in the synthesis of the Novartis potential anti-epileptic drug CGP-55845 (**107**).¹²⁶ Recently, Stephan *et al.* have reported the hydrogenation of the same substrate under very mild conditions (1 bar H₂) and low catalyst loadings (S/C ratio equals to 10,000) with very high enantioselectivity (> 99 ee) using a DIPAMP analog.¹²⁷

The known psychostimulant agent (S)-amphetamine **110** can also be synthesized by using Rh-catalyzed asymmetric hydrogenation as the key step. Lei, Zhang *et al.* reported the hydrogenation of the α -alkylenamide **108** by using (S,S,R,R)-TangPhos as ligand to obtain **109** with an enantioselectivity of 99% ee (Scheme 20 (d)).¹²⁸ The chiral amine **109** can be transformed into (S)-amphetamine **110** by simple hydrolysis of the acetyl group in **109**.

¹²³ Zhang, W.; Zhang, X. *Angew. Chem., Int. Ed.* **2006**, *45*, 5515.

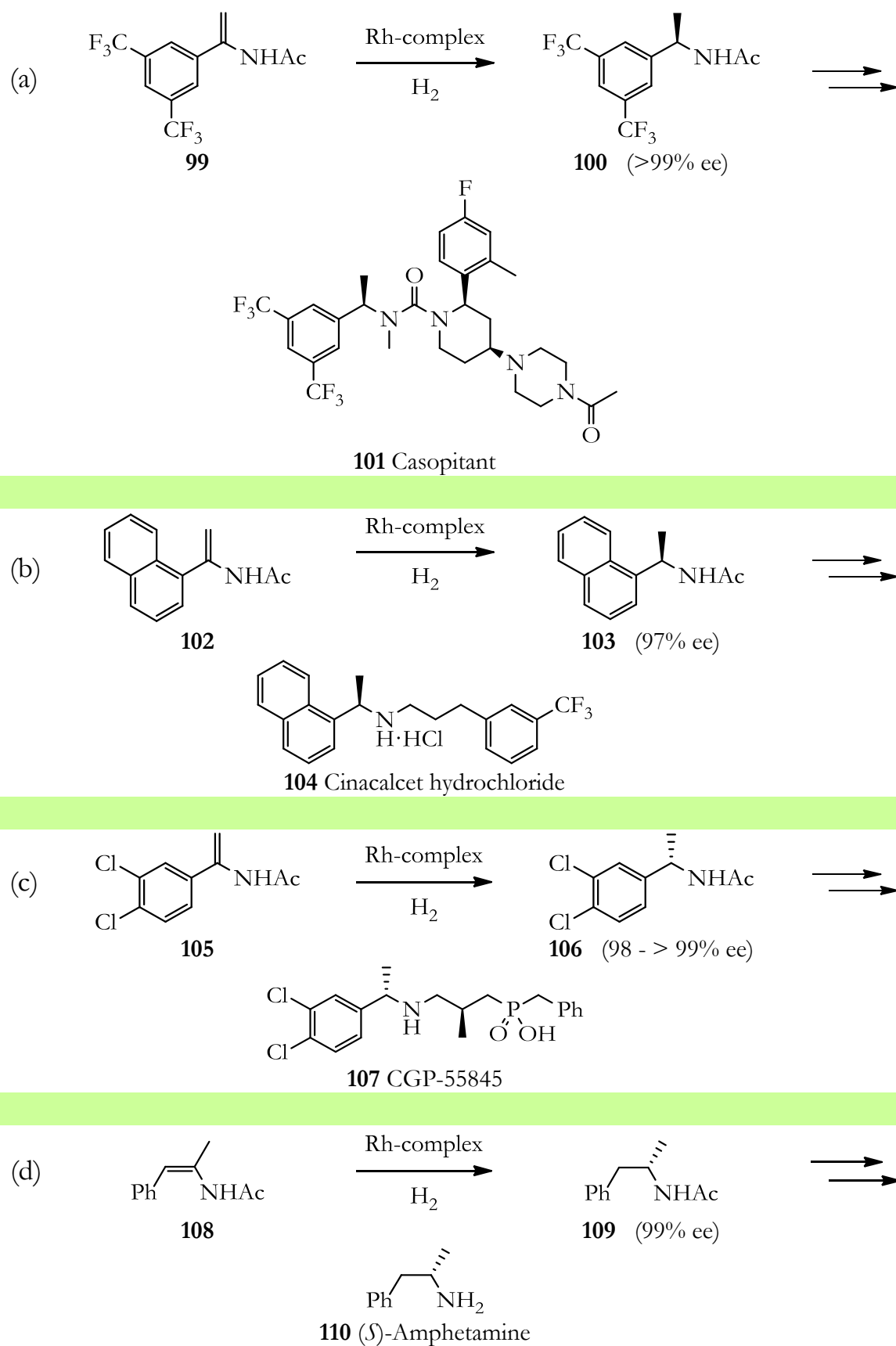
¹²⁴ Franceschini, N.; Joy, M. S.; Kshirsagar, A. *Expert Opin. Invest. Drugs* **2003**, *12*, 1413.

¹²⁵ Harrison, P.; Meek, G. *Tetrahedron Lett.* **2004**, *45*, 9277.

¹²⁶ Mickel, S. J. E.P. Patent 543,780, 1993.

¹²⁷ Mohar, B.; Stephan, M. *Adv. Synth. Catal.* **2013**, *355*, 594.

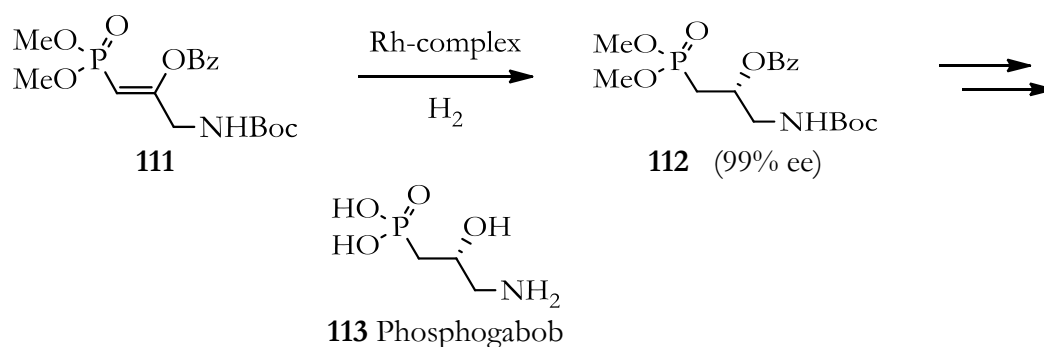
¹²⁸ Chen, J.; Zhang, W.; Geng, H.; Li, W.; Hou, G.; Lei, A.; Zhang, X. *Angew. Chem., Int. Ed.* **2009**, *48*, 800.



Scheme 20. Rhodium-mediated asymmetric hydrogenation of α -substituted enamides.

1.1.4.3 α -Substituted Enol Esters

Despite the structural similarity between α -substituted enol esters and α -substituted enamides, little progress has been made in the development of synthetic methodologies towards API precursors that rely on Rh-mediated asymmetric hydrogenation as the key step. The Pizzano group is one of the groups that explored this class of substrates,^{80c, e} and they devised the enantioselective hydrogenation of the enol ester phosphonate **111** leading to the synthetic intermediate **112** with 99% ee, which is a direct precursor in the synthesis of the phosphonate analog of GABA **113** (Scheme 21).¹²⁹



Scheme 21. Rhodium-mediated asymmetric hydrogenation of an enol ester phosphonate.

¹²⁹ Wroblewski, A. E.; Halajewska-Wosik, A. *Tetrahedron: Asymmetry* **2003**, *14*, 3359.

1.1.4.4 Itaconate Derivatives

Whilst β -unsubstituted acid derivatives have been widely explored in Rh-catalyzed asymmetric hydrogenations, hydrogenation studies on their β -substituted parent derivatives are scarce in the literature, despite having broad applicability in the pharmaceutical, agrochemical and fragrance sectors.^{106a-e, 109} The few known hydrogenation examples of itaconate derivatives leading to API precursors are summarized in Scheme 22.

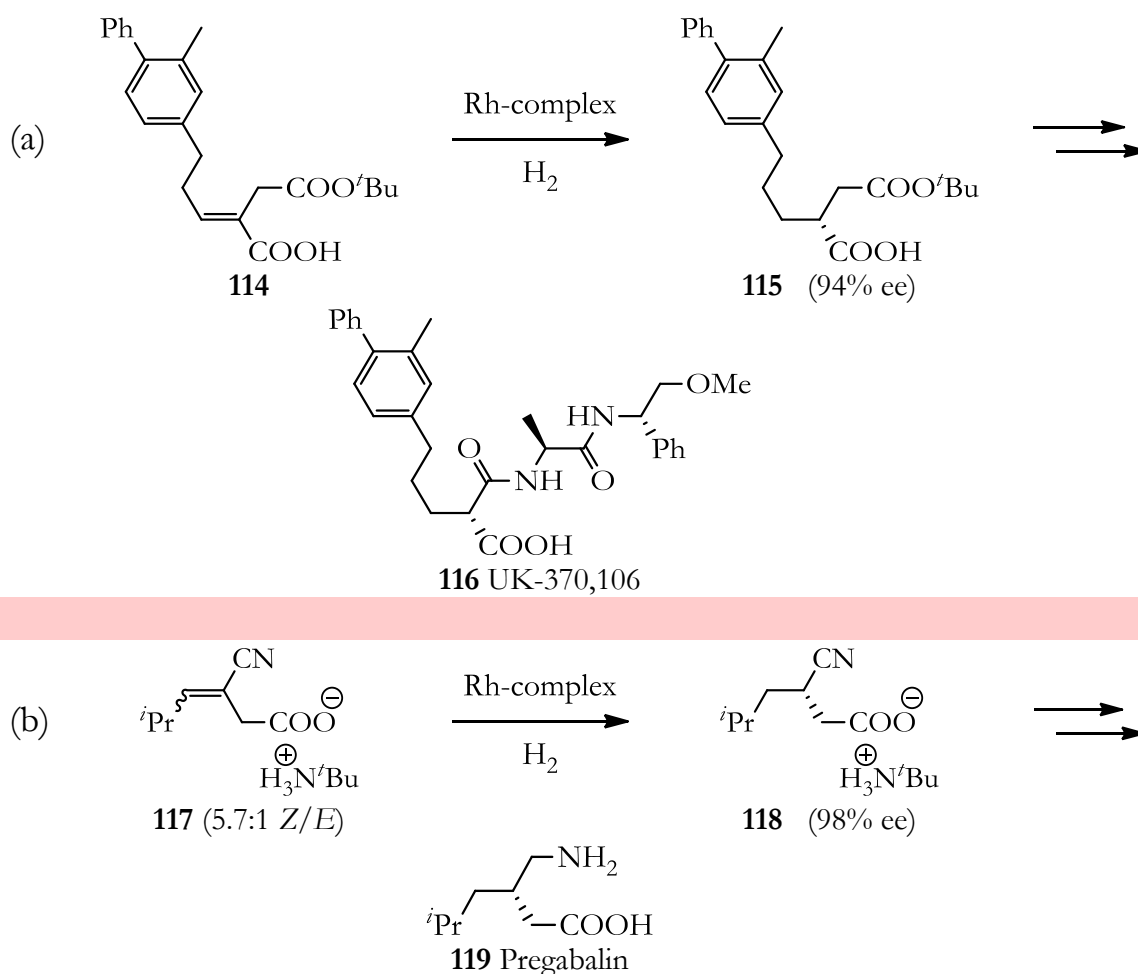
The Pfizer drug candidate UK-370,106 (**116**) has the potential to cure tissue destruction, for which Thomson *et al.* reported the enantioselective hydrogenation of itaconate derivative **114** leading to intermediate **115** (Scheme 22 (a)).¹³⁰ When using (*S,S*)-Et-FerroTANE, the hydrogenation proceeded with 94% ee under mild conditions.

Researchers at Pfizer also reported the hydrogenation of a *Z/E* mixture of substrate **117** with the *P*-stereogenic ligand (*S*)-Trichickenfootphos as chiral inducer. As a result, they were able to synthesize carboxylate derivative **118** in 98% ee with TON > 27,000 under mild conditions (Scheme 22 (b)).¹³¹ Compound **118** is a direct precursor of the drug pregabalin **119**, used as an anticonvulsive agent and in the treatment of neuropathic pain, anxiety and social phobia.¹³²

¹³⁰ Ashcroft, C. P.; Challenger, S.; Derrick, A. M.; Storey, R.; Thomson, N. M. *Org. Process Res. Dev.* **2003**, *7*, 362.

¹³¹ Hoge, G.; Wu, H.-P.; Kissel, W. S.; Pflum, D. A.; Greene, D. J.; Bao, J. J. *Am. Chem. Soc.* **2004**, *126*, 5966.

¹³² Yuen, P. W.; Kanter, G. D.; Taylor, C. P.; Vartanian, M. G. *Bioorg. Med. Chem. Lett.* **1994**, *4*, 823.



Scheme 22. Rhodium-mediated asymmetric hydrogenation of itaconic acid derivatives.

1.1.4.5 Minimally Functionalized Olefins

Minimally functionalized olefins are a challenging substrate class for rhodium catalysts, as they possess unusual coordination groups next to the C=C double bond. Asymmetric hydrogenation of this class of substrate has been mostly studied using iridium catalysts derived from *P,N*-ligands. Nevertheless, some recent reports deal with the use of rhodium complexes in enantioselective hydrogenation of minimally functionalized olefins with good results. This chemistry provides a synthetic alternative for those biologically active compounds that can derive from compounds with this structural motif. Most representative examples have been summarized in Scheme 23.

In this way, (*R*)-tolterodine **121** can be directly accessed by asymmetric hydrogenation of its precursor **120** with 99% ee using a rhodium complex derived from (*S,S*)-BPE ligand in the presence of a stoichiometric amount of lithium *tert*-butoxide (Scheme 23 (a)).¹³³ The success in this transformation relies on the coordinating abilities of the deprotonated phenol moiety. Tolterodine **121** is a chiral drug used in the treatment of urinary bladder disorders.¹³⁴

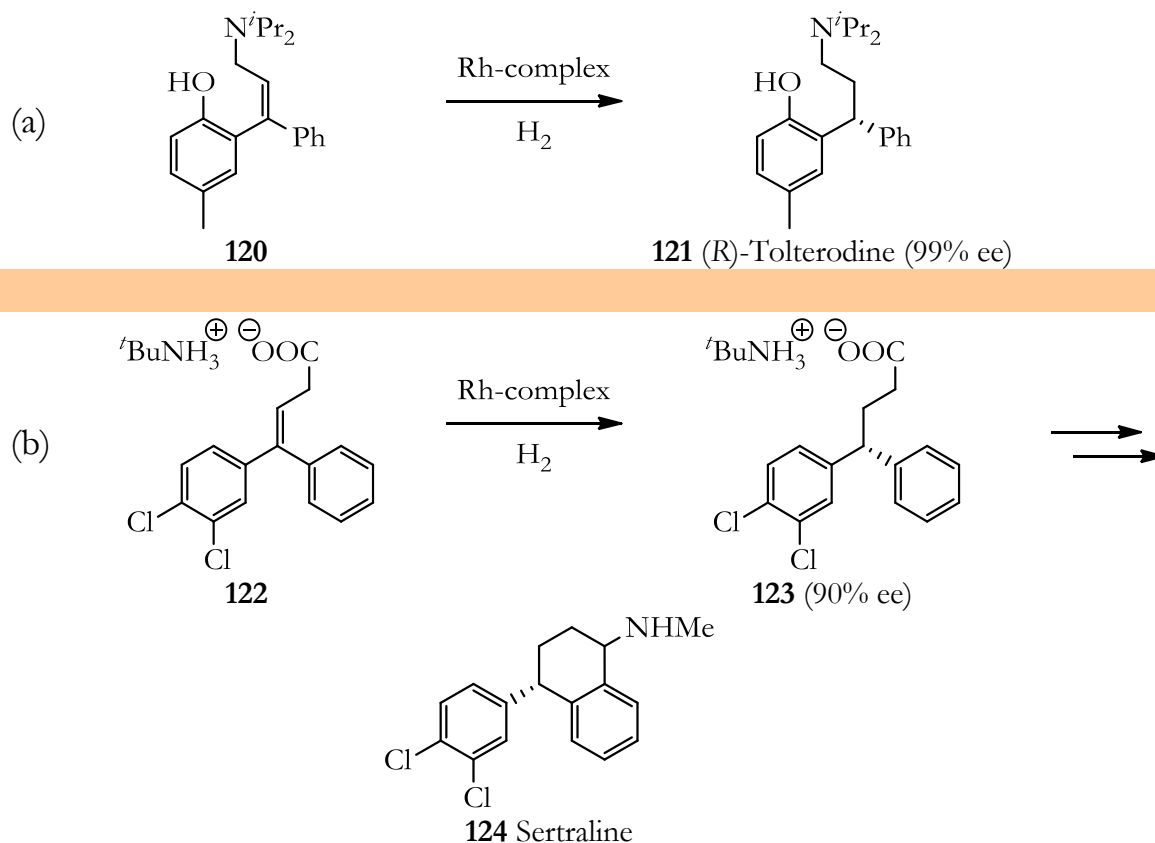
Minimally functionalized olefin **122** has been hydrogenated in 90% ee to yield compound **123** with the complex derived from (*S*)-PhanePhos (Scheme 23 (b)).¹³⁵ In this case, the carboxylate group has a stronger binding ability than the corresponding carboxylic acid. The hydrogenated compound **123** is an intermediate in the synthesis of the widely used antidepressant agent sertraline **124**.¹³⁶

¹³³ Wang, X.; Guram, A.; Caille, S.; Hu, J.; Preston, J. P.; Ronk, M.; Walker, S. *Org. Lett.* **2011**, *13*, 1881.

¹³⁴ Appell, R. A. *Urology* **1997**, *50*, 90.

¹³⁵ Boulton, L. T.; Lennon, I. C.; McCague, R. *Org. Biomol. Chem.* **2003**, *1*, 1094.

¹³⁶ Welch, W. M.; Kraska, A. R.; Sarges, R.; Koe, B. K. *J. Med. Chem.* **1984**, *27*, 1508.



Scheme 23. Rhodium-mediated asymmetric hydrogenation of minimally functionalized olefins.

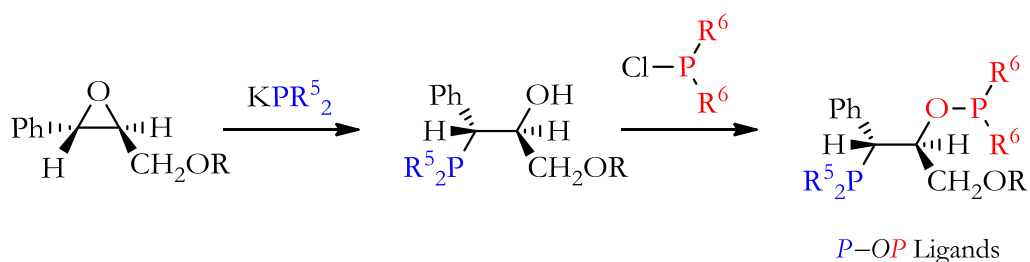
1.2 ASYMMETRIC HYDROGENATION CATALYZED BY RHODIUM- (*P-OP*) COMPLEXES

1.2.1 Synthesis of Phosphine-Phosphinite and Phosphine- Phosphite (*P-OP*) Ligands and their Derived Rhodium Complexes

1.2.1.1 *P-OP* Ligand Synthesis

The synthetic methodology followed for the preparation of *P-OP* ligands was previously developed in our group during the PhD thesis of Dr. H. Fernández-Pérez.^{73, 81, 82} Enantiomerically pure Sharpless epoxy ethers were converted into *P-OP* ligands in two steps (Scheme 24):

- 1.- Ring-opening of a Sharpless epoxy ether with a trivalent phosphorus nucleophilic derivative to introduce the phosphino group.
- 2.- *O*-phosphorylation of the resulting phosphino group with a trivalent phosphorus electrophilic derivative to introduce the phosphinite or phosphite functionality.



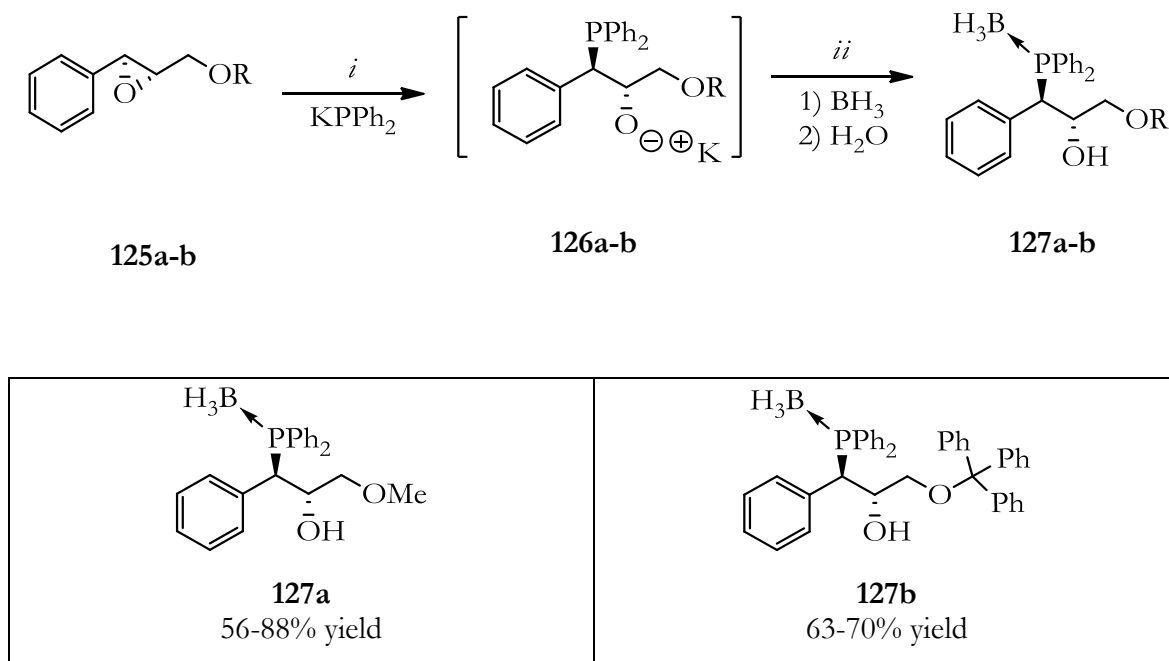
Scheme 24. Synthetic route to *P-OP* ligands derived from Sharpless epoxides.

The use of these epoxy alcohols allowed for the introduction of a supplementary CH₂OR group into the final chiral ligands. The steric environment at this position has proven to be important for the catalytic activity of other chiral ligands derived from Sharpless epoxy alcohols in several enantioselective transformations.¹³⁷ Two different Sharpless epoxy ethers bearing groups of varying sterical bulk at the OR position (OMe or OTr) were synthesized within this PhD thesis.

Epoxy ethers **125** were allowed to react with a stoichiometric amount of potassium diphenylphosphide (-30 °C → rt) to afford the corresponding phosphino alkoxides **126**, which were rather prone to oxidation. Thus, subsequent *in situ* protection as the corresponding borane adducts **127**, using either BH₃·DMS complex or a BH₃·THF solution in THF, allowed for more convenient handling during aqueous workup and chromatography over SiO₂ (Scheme 25).¹³⁸ The results obtained in Dr. Fernández-Pérez thesis could be reproduced within the present work.

¹³⁷ (a) Vidal-Ferran, A.; Moyano, A.; Pericàs, M. A.; Riera, A. *J. Org. Chem.* **1997**, *62*, 4970. (b) Vidal-Ferran, A.; Moyano, A.; Pericàs, M. A.; Riera, A. *Tetrahedron Lett.* **1997**, *38*, 8773. (c) Vidal-Ferran, A.; Bampos, N.; Moyano, A.; Pericàs, M. A.; Riera, A.; Sanders, J. K. M. *J. Org. Chem.* **1998**, *63*, 6309. (d) Puigjaner, C.; Vidal-Ferran, A.; Moyano, A.; Pericàs, M. A.; Riera, A. *J. Org. Chem.* **1999**, *64*, 7902. (e) Jimeno, C.; Pasto, M.; Riera, A.; Pericàs, M. A. *J. Org. Chem.* **2003**, *68*, 3130. (f) Rodríguez, B.; Pasto, M.; Jimeno, C.; Pericàs, M. A. *Tetrahedron: Asymmetry* **2006**, *17*, 151. (g) Jimeno, C.; Vidal-Ferran, A.; Pericàs, M. A. *Org. Lett.* **2006**, *8*, 3895.

¹³⁸ Pellon, P. *Tetrahedron Lett.* **1992**, *33*, 4451.



i: THF, KPPH₂ (0.98 equiv.), -30 °C to -10 °C, 2 h (R = Me) or 4 h (R = Tr); *ii*: BH₃·DMS (3 equiv.), -10 °C to RT, 2 h.

Scheme 25. Introduction of the phosphino group.

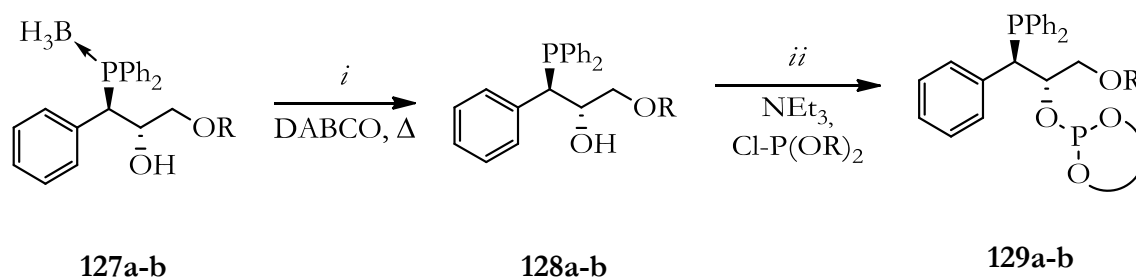
The ring-opening of the Sharpless epoxides with trivalent phosphorus nucleophiles occurs in a regioselective way, with nucleophilic attack taking place at the benzylic carbon (C3).¹³⁹ As expected, a stereospecific S_N2-like oxirane ring opening took place (inversion of configuration at the attacked carbon (C3) and retention of configuration at the other one) and, as a consequence, *anti*-phosphino alcohols were obtained from *trans*-disubstituted epoxides.

In the original experimental procedure developed by Dr. Fernández-Pérez (Scheme 26), the phosphine-borane complexes **127a-b** were cleaved prior to *O*-phosphorylation. This step was easily and quantitatively done by

¹³⁹ Whilst the regioisomers arising from attack of the nucleophile at the non-benzylic position C2 have been isolated (yield < 5%) from ring-opening reaction mixtures on epoxyethers **125a-b** using dicyclohexylphosphide (Etayo, P.; Núñez-Rico, J. L.; Vidal-Ferran, A. *Organometallics* **2011**, *30*, 6718), such regioisomers have never been unequivocally identified by NMR in the numerous reaction mixtures leading to **127a-b** that have been analyzed during the experimental studies of this PhD thesis.

heating for two hours the desired phosphine-borane complex at 60 °C in the presence of 1,4-diazabicyclo[2.2.2]octane (DABCO).¹⁴⁰ After a short chromatographic filtration to remove unreacted DABCO and DABCO-borane complexes, free phosphino alcohols **128a-b** were subjected to O-phosphorylation with the required chlorophosphites (1.1 equiv.) as the electrophilic trivalent phosphorus reagent in the presence of an excess of base (2 equiv. triethylamine) at room temperature (Scheme 26). The desired phosphine-phosphite ligands of general structure **129a-b** were then obtained in yields ranging from 64% to 71% when chlorophosphites **130-132** were used.⁸¹

With regard to the required chlorophosphites **130-132**, these electrophilic phosphorus reagents were purchased from ordinary suppliers or readily prepared by reacting the corresponding diaryl diols with PCl₃ in the presence of a base (NEt₃).¹⁴¹



i: Toluene, DABCO (2.2 equiv.), 60 °C, 2 h; *ii*: Toluene, NEt₃ (2 equiv.), ClP(OR)₂ (1.1 equiv.), RT, 16 h.

Scheme 26. Previously reported methodology to access phosphine-phosphites.

¹⁴⁰ (a) Ohff, M.; Holz, J.; Quirnbach, M.; Börner, A. *Synthesis* **1998**, 1391. (b) Brisset, H.; Gourdel, Y.; Pellon, P.; Le, C. M. *Tetrahedron Lett.* **1993**, *34*, 4523.

¹⁴¹ (a) Scherer, J.; Huttner, G.; Buechner, M.; Bakos, J. J. *Organomet. Chem.* **1996**, *520*, 45. (b) Lot, O.; Suisse, I.; Mortreux, A.; Agbossou, F. J. *Mol. Catal. A: Chem.* **2000**, *164*, 125.

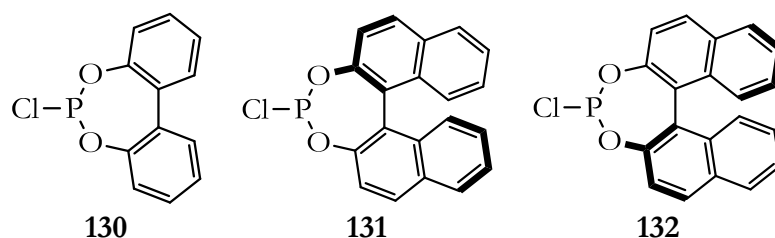


Figure 28. Chlorophosphites derived from bis(aryl) diols originally used in the group.

As both the deprotection of the borane complexes and the *O*-phosphorylation synthetic steps required using a base (DABCO and triethylamine, respectively), we wondered whether a one-pot methodology involving a common base for both transformations would be efficient. After the borane cleavage step following the established methodology (2.2 equiv. DABCO, 60 °C, 2 h), the corresponding chlorophosphite (1.1 equiv.) was directly added to the reaction mixture without purification of the phosphine-alcohol and without adding more base. Most gratifyingly, we observed that *O*-phosphorylation proceeded to completion under the new reaction conditions. Furthermore, phosphine-phosphites **133**, **30** and **134** were isolated at the end of the deprotection and phosphorylation steps in high purities with good overall yields for these two steps (Figure 29).

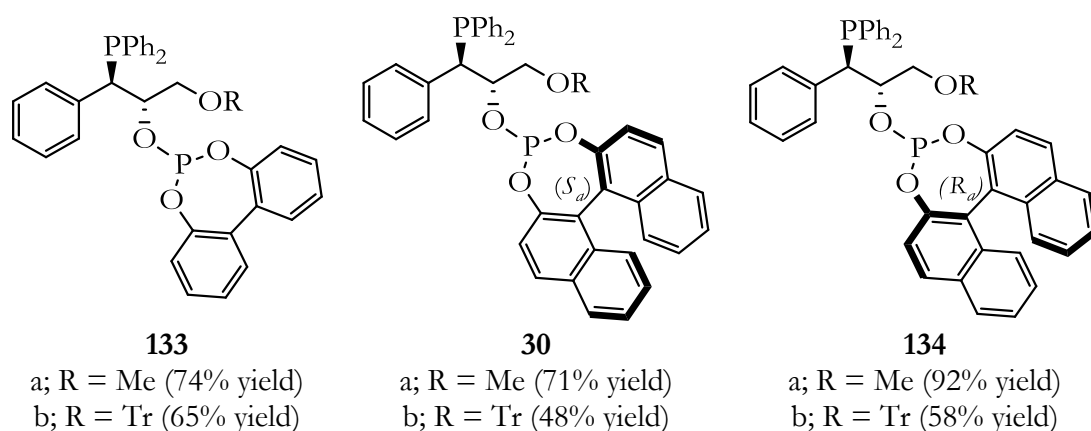


Figure 29. Synthesized phosphine-phosphite ligands.

Monocrystals of phosphine-phosphite derivative **30b** were grown and then analyzed by X-Ray diffraction (Figure 30), which confirmed the structure of the ligand and also the absolute stereochemistry.

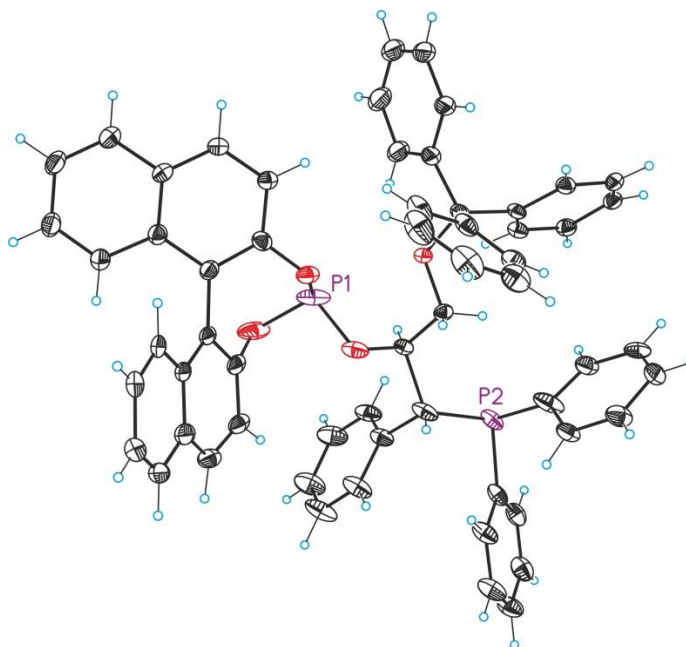


Figure 30. Crystal structure of **30b**.

In addition to these ligands that derive from (*S,S*)-configured Sharpless epoxy ether, we also synthesized the enantiomer of ligand **30b** (*ent-30b*) following the aforementioned one-pot synthetic procedure and starting from *ent-125b* ((2*R*,3*R*)-2-phenyl-3-((trityloxy)methyl)oxirane). Ligand *ent-30b* was isolated in 66% overall yield (Figure 31).

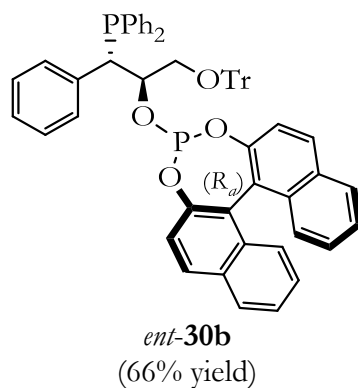
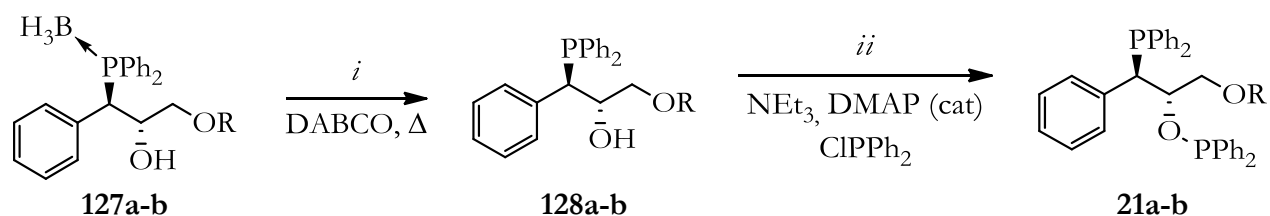


Figure 31. Synthesized phosphine-phosphite ligands from the opposite enantiomeric series.

Phosphine-phosphinites **21a-b** (Figure 32) were prepared following the procedure reported by Dr. Fernández-Pérez in his thesis.⁸¹ This synthetic methodology involved a two-step sequence similar to the one previously described for phosphine-phosphites (borane deprotection followed by *O*-phosphorylation), but using chlorodiphenylphosphine (ClPPh₂) as the electrophilic phosphorus reagent in the presence of an excess of triethylamine and catalytic *N,N*-dimethylaminopyridine (DMAP) as bases (Scheme 27). Yields were around 75% for the two assayed cases, and were similar to the ones obtained in the seminal work of Dr. Fernández-Pérez.



i: Toluene, DABCO (2.2 equiv.), 60 °C, 2 h; *ii*: THF, NEt₃ (1.1 equiv.), DMAP (0.16 equiv.), ClPPh₂ (1.1 equiv.), 0 °C, 1 h.

Scheme 27. Synthetic strategy towards phosphine-phosphinites.

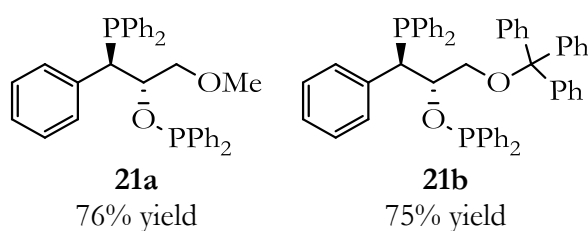


Figure 32. Prepared phosphine-phosphinite ligands.

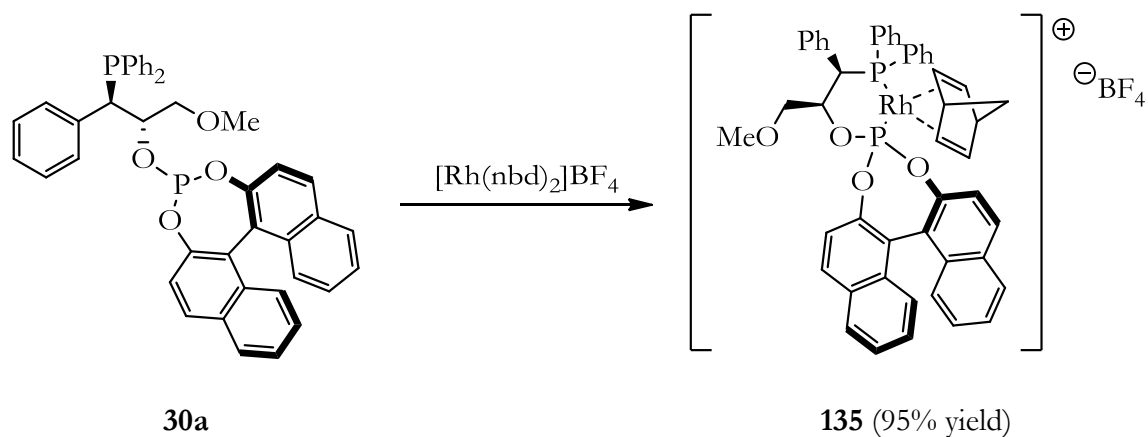
1.2.1.2 Preparation of Rhodium Complexes Derived from *P-OP* Ligands

The general ability of bidentate *P-OP* ligands to form stable, well-defined complexes with transition metals is well-known.⁷⁰ In particular, Dr. Fernández-Pérez demonstrated that enantiomerically pure *P-OP* ligands react with stoichiometric amounts of $[\text{Rh}(\text{nbd})_2]\text{BF}_4$ (nbd = norbornadiene) to provide in a quantitative way the corresponding cationic complexes $[\text{Rh}(\text{nbd})(\text{P-OP})]\text{BF}_4$.⁸¹ As these rhodium complexes are generally prepared to be used as precatalysts in asymmetric hydrogenation reactions, they are not isolated and are directly used from the solutions in which they are prepared. However, $[\text{Rh}(\text{nbd})(\text{P-OP})]\text{BF}_4$ complexes can be easily isolated by crystallization.^{76, 81, 82} Thus, rhodium complexes derived from ligands **30a** and **134a** were quantitatively prepared by reacting stoichiometric amounts of the chiral phosphine-phosphite ligands **30a** or **134a** and $[\text{Rh}(\text{nbd})_2]\text{BF}_4$ in dichloromethane. Further crystallization by layered addition of Et_2O onto the solution of the complex in dichloromethane furnished the corresponding complexes $[\text{Rh}(\text{nbd})(\text{30a})]\text{BF}_4$ (**135**), and $[\text{Rh}(\text{nbd})(\text{134a})]\text{BF}_4$ (**136**) as orange solids in very high yields (Scheme 28).

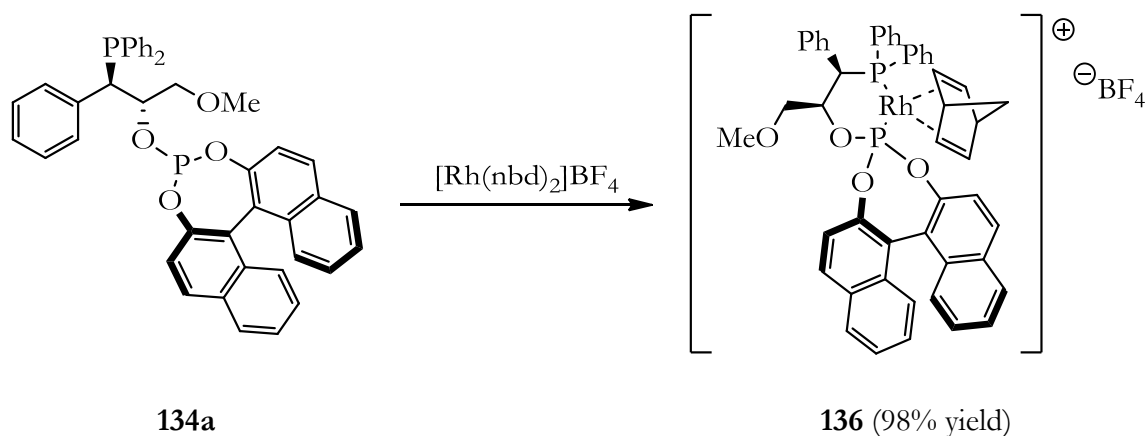
Their spectrometric data (ESI mass spectra) were in agreement with a cationic 1:1 complex between the rhodium precursor and the *P-OP* ligand.¹⁴² The $^{31}\text{P}\{^1\text{H}\}$ NMR spectra for both complexes showed two sharp doublets of doublets, arising from the $^{31}\text{P}-^{103}\text{Rh}$ and $^{31}\text{P}-^{31}\text{P}$ couplings. All of these results are in agreement with the presence of a six-membered chelate ring in the $[\text{Rh}(\text{nbd})(\text{P-OP})]\text{BF}_4$ complexes (Table 1).

¹⁴² Spectroscopic data for compound **135** were in agreement with those previously reported by Dr. Fernández-Pérez.

(*S*)-BINOL-derived Rh-complex



(*R*)-BINOL-derived Rh-complex



Scheme 28. Synthesis of $[\text{Rh}(\text{nbd})(P\text{-}OP)]\text{BF}_4$ complexes.

Table 1. $^{31}\text{P}\{^1\text{H}\}$ NMR data of $[\text{Rh}(\text{nbd})(P\text{-}OP)]\text{BF}_4$ complexes.

Complex	Phosphite group			Phosphino group		
	δ (ppm)	$J_{\text{P-Rh}}$ (Hz)	$J_{\text{P-P}}$ (Hz)	δ (ppm)	$J_{\text{P-Rh}}$ (Hz)	$J_{\text{P-P}}$ (Hz)
135	138.9	268	65	35.2	144	65
136	137.3	268	67	26.0	146	67

1.2.2 P-OP Ligands in Asymmetric Hydrogenation

As a continuation of Dr. Pérez-Fernández's work, and with the aim to investigate in more detail the catalytic performance of ligands **30a-b**, we explored the $[\text{Rh}(\mathbf{30a-b})]^+$ catalyzed asymmetric hydrogenation of representative examples of four different substrate classes: MAA (methyl 2-acetamidoacrylate, **11d**), DMI (dimethyl itaconate, **38a**), the α -arylenamide *N*-(1-phenylvinyl)acetamide (**42a**) and the enol acetate 1-phenylvinyl acetate (**137a**), see Figure 33.

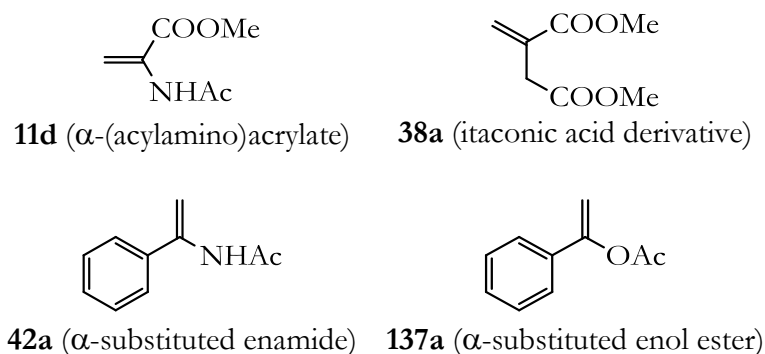


Figure 33. Representative examples of the different substrate classes studied.

The main parameters related with the performance of such a catalytic system are turnover number (TON) and turnover frequency (TOF).¹⁴³ These parameters provide a comprehensive way to make catalyst comparisons. TON is defined as the number of substrate molecules converted per molecule of catalyst, and thus is a unitless magnitude which determines the maximum substrate/catalyst ratio for such a catalytic system. An ideal catalyst would have an infinite turnover number, in the sense that it would never become

¹⁴³ Rothenberg, G. *Catalysis: Concepts and Green Applications*; Wiley-VCH: Weinheim, 2008.

deactivated. On the other hand, TOF is defined as the number of substrate molecules converted per unit of time, *i.e.* TON per time unit. The higher the TOF number, the more active a catalyst is. For most relevant industrial applications based on non-natural catalysts, the turnover frequency is in the range of 10^{-2} - 10^2 s⁻¹, whilst for enzymes it ranges from 10^3 to 10^7 s⁻¹.¹⁴⁴ In the context of a catalytic reaction, TOF is the number of catalytic cycles that occur in a specific time period. As the conversion rate varies with time according to the corresponding rate law, TOF values differ with conversion. TOF values not labeled with any suffix, have been measured at >99% conversion, whereas TOF_{1/2} is measured at 50% of conversion.

1.2.2.1 TOF & TON Determination in Asymmetric Hydrogenations Catalyzed by Rhodium Complexes Derived from P-OP Ligands

An accurate determination of the TOF values for the hydrogenation of model substrates **11d**, **38a**, **42a** and **137a** were performed in a SPR-16 AMTEC parallel autoclave reactor, as it allows recording the gas uptake. The system is equipped with pressure probes and a mass-flow controller that enable accurate monitoring of the absorbed amount of gas. We then recorded the gas uptake profiles throughout the hydrogenation reactions on using either **30a** or **30b** as ligands with the four substrates previously indicated. The reactions were adjusted to a substrate to catalyst ratio of 1,000:1 in THF and 20 bar of H₂ pressure. Full conversion was confirmed in all cases by ¹H NMR at the end of the reaction. Enantioselectivities of the different hydrogenation reactions were also determined and coincided with the ones obtained under the usual reaction set-up for catalyst screening.

¹⁴⁴ Hagen, J. *Industrial Catalysis: A Practical Approach*; Wiley-VCH: Weinheim, Germany, 2006.

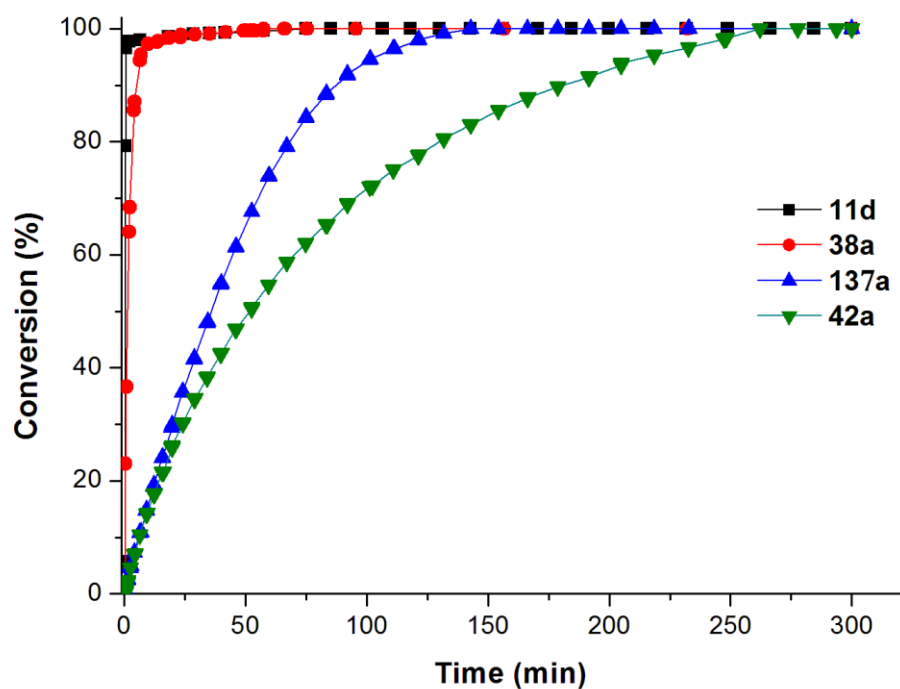


Figure 34. Asymmetric hydrogenation profiles of the representative model substrates with **30a** as ligand.

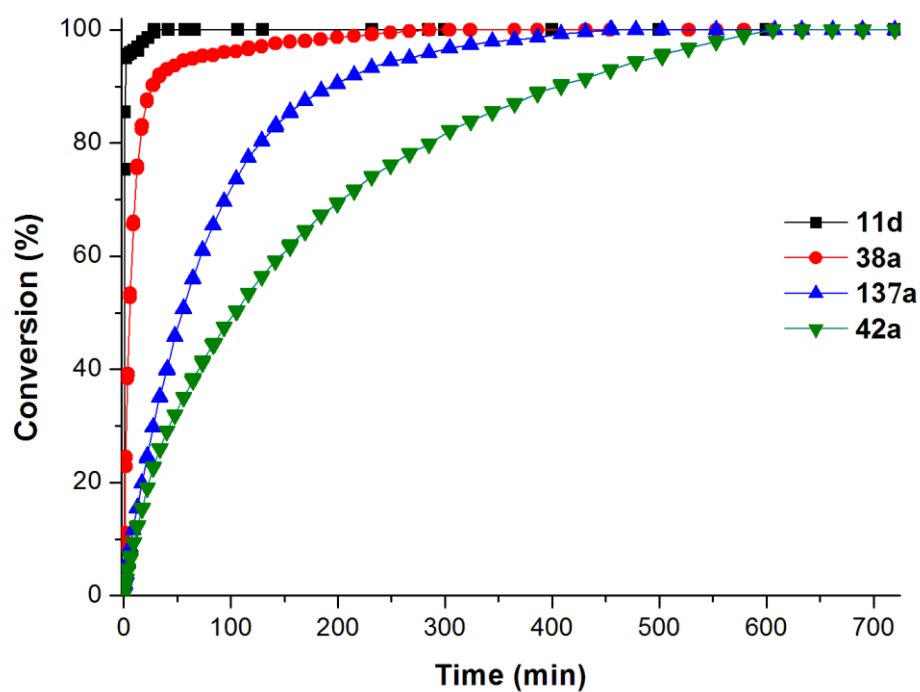


Figure 35. Asymmetric hydrogenation profiles of the representative model substrates with **30b** as ligand.

The different reaction profiles are shown in Figure 34 for ligand **30a** and in Figure 35 for the ligand **30b**. In both cases, and using an S/C ratio of 1,000:1 from *in situ* formed precatalysts, performing the hydrogenation in THF at room temperature in a 2 mmol substrate scale revealed very high activity for the rhodium complexes derived from ligands **30a** or **30b**. The gas up-take curves indicated in Figure 34 and Figure 35 were used to calculate TOF values at 50% conversion ($\text{TOF}_{1/2}$) using the formula indicated below:

$$\text{TOF}_{1/2} = \frac{50}{\text{load} \cdot t_{1/2}}$$

Where *load* refers to the catalyst loading, expressed in percentage, and $t_{1/2}$ the time required to reach 50% conversion.¹⁴⁵

TOF values are summarized in Table 2 and were found to be very high in some cases ($>49,000 \text{ h}^{-1}$ for α -(acylamino)acrylate **11d** using ligand **30a**).

It can be clearly observed from Figure 34, Figure 35 and Table 2 that the rhodium complex derived from the sterically congested triphenylmethoxy-substituted ligand **30b** requires longer reaction times for all studied substrates than does its methoxy-substituted analog **30a**. The $\text{TOF}_{1/2}$ values of any given substrate are consistently lower when **30b** is used as ligand than those corresponding to **30a**. The increased steric congestion correlates with slower hydrogenation rates.

¹⁴⁵ Caldentey, X.; Cambeiro, X. C.; Pericàs, M. A. *Tetrahedron* **2011**, *67*, 4161.

Table 2. Comparison of the catalytic activity exhibited by rhodium complexes of ligands **30a** and **30b** in the enantioselective hydrogenation of model substrates.^[a]

Entry	Substrate	TOF _{1/2} (h ⁻¹)	
		Ligand 30a	Ligand 30b
1	11d (methyl 2-acetamidoacrylate)	>49,000	>40,000
2	38a (dimethyl itaconate)	>14,000	>5,000
3	137a (1-phenylvinyl acetate)	>850	>500
4	42a (<i>N</i> -(1-phenylvinyl)acetamide)	>550	>250

^[a] Reaction conditions: [Rh(nbd)₂]BF₄/*P-OP* ligand/substrate molar ratio = 0.10 : 0.11 : 100, room temperature, 20 bar H₂, 2.0 mmol of substrate in 2.5 mL of THF (0.8 M).

Another important conclusion that can be drawn from the TOF values indicated in Table 2 is that the reaction rate of the four model substrates studied follows the same trend, independently of the ligand. The reactivity orders are illustrated in the graphic below:

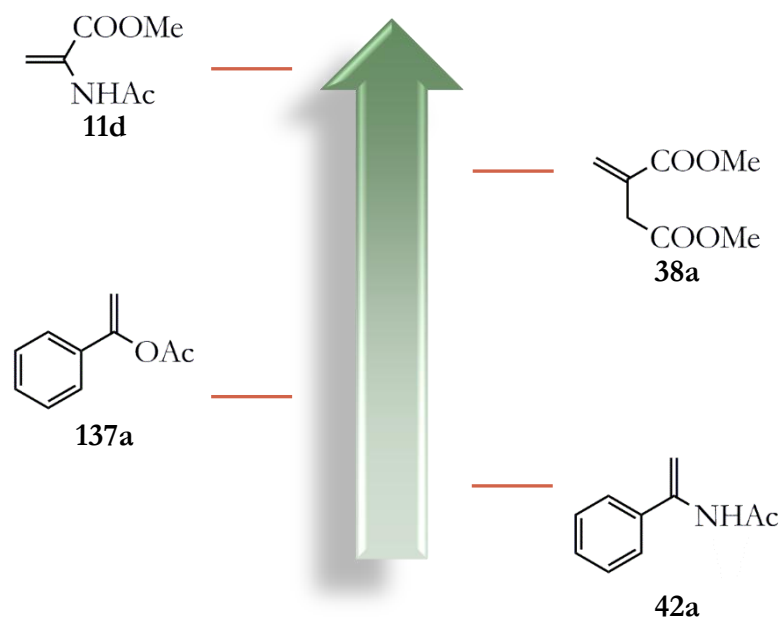


Figure 36. Trend in the hydrogenation rates of model substrates with ligands **30a-b**.

In order to study the minimum catalyst loading which is required to achieve full conversion, and therefore to determine accurate TON values, several experiments were carried out using dimethyl itaconate **38a** as a model substrate of intermediate reactivity, with increasing substrate to catalyst ratios.

The reaction conditions used in the optimization studies towards the determination of S/C values (room temperature, 20 bar H₂) are summarized in Table 3. Full conversion is observed under the hydrogenation conditions normally used for catalyst screening, which imply a S/C = 100 (see entry 1 in Table 3). The catalyst amount could be further reduced by a factor of 10 without any loss in catalytic activity (see entry 2 in Table 3). However, when we intended to further reduce the catalyst amount to a S/C ratio = 10,000, incomplete conversion was observed (see entry 3 in Table 3). In these comparative experiments the amount of substrate was kept constant, and an increase of the S/C value obviously led to handle amounts of precatalyst that became smaller as S/C increased. A very small amount of precatalyst (only 0.2 mg) was required in this case for hydrogenating 320 mg of substrate **38a**. When the required amounts of catalyst become too small, deactivation or poisoning of the catalyst may easily occur due to the presence of trace amounts of oxygen, water or other unknown chemicals inside the autoclave.¹⁴⁶

Thus, further optimization studies on the catalyst loading were performed using fixed amounts of preformed catalyst (*ca.* 8 mg of [Rh(nbd)(**30a**)]BF₄) independently of the scale of the reaction. This constraint forced us to work with higher amounts of substrate at higher concentrations, as the autoclave volume could not be further increased. Under these conditions, dimethyl itaconate **38a** was hydrogenated at >10 g scale and S/C = 10,000 with no differences in terms of conversion or enantioselectivity with

¹⁴⁶ *Asymmetric Catalysis on Industrial Scale: Challenges, Approaches and Solutions*, 1st edn.; Blaser, H. U., Schmidt, E., Eds.; Wiley-VCH: Weinheim, 2004; p 45.

respect to the ones done at a substrate to catalyst ratio of 100:1 (compare entries 1 and 4 in Table 3).

Table 3. Catalyst loading optimization studies in the hydrogenation of dimethyl itaconate **38a** mediated by [Rh(nbd)(**30a**)]BF₄ (**135**).^[a]

Entry	S/C	Reaction conditions	Conv. [%] ^[b]	ee [%] ^[c] (config.) ^[d]
1	100	25 mg 38a (0.16 mmol), 0.2 M in THF, 1.5 mg (<i>in situ</i> , 1.6 μmol precatalyst 135)	>99	99 (<i>S</i>)
2	1,000	0.32 g 38a (2.0 mmol), 0.8 M in THF, 1.9 mg (<i>in situ</i> , 2.0 μmol precatalyst 135)	>99	99 (<i>S</i>)
3	10,000	0.32 g 38a (2.0 mmol), 0.8 M in THF, 0.2 mg (0.2 μmol precatalyst 135)	46	99 (<i>S</i>)
4	10,000	13.6 g 38a (85.7 mmol), <i>ca.</i> 5.0 M in THF, 8.1 mg (8.6 μmol precatalyst 135)	>99	99 (<i>S</i>)

^[a] Reaction conditions: room temperature, 20 bar H₂, 24 h.

^[b] Conversions were determined by ¹H NMR.

^[c] Enantiomeric excesses were determined by GC using chiral stationary phases.

^[d] Absolute configurations were assigned by comparison with reported data.

1.2.3 Hydrogenation of functionalized alkenes

Initial results in the asymmetric hydrogenation of diversely substituted functionalized alkenes, exploring up to 29 substrates, were summarized in the introductory section to this chapter.^{73, 81, 82}

Following these initial studies, we assessed the rhodium complexes derived from ligand **30a** to investigate less explored kinds of substrates, such as β -alkyl-substituted acrylates, α -substituted enamides, α -arylenol esters and other itaconate derivatives.

We also became interested in comparing the catalytic activity of **30a** with the one provided by its trityl-substituted analog **30b**, which was not studied by Dr. Fernández-Pérez in his PhD thesis.

All of these results will be summarized in the next sections.

1.2.3.1 Hydrogenation of β -Substituted α -(Acylamino)acrylates

β -Alkyl or β -heteroatom-substituted α -(acylamino)acrylates are less explored in the literature than their β -aryl-substituted analogs. In order to have a general and comprehensive overview of the catalytic activity of the rhodium complexes derived from our *P-OP* ligands, ten new substrates of this kind were synthesized (or purchased).¹⁴⁷ Most of the non-commercially available starting α -(acylamino)-acrylates could be easily prepared by following a Wadsworth-Emmons olefination protocol¹⁴⁸ from the corresponding carbonyl compound (**11x**, **11y**, **11z**, **11a'**, **11b'**, **11c'** and **11i'**). Some other substrates required specific preparation methods (**11d'**, **11e'** and **11f'**).¹⁴⁹

These substrates include the β -unsubstituted acrylic acid derivative **11w**, six β -alkyl α -(acylamino)acrylates (**11x-c'**), the β -heteroatom-substituted α -(acylamino)acrylate **11d'**, the β -alkoxy-substituted α -(acylamino)acrylate **11e'**, and the Weinreb amide **11f'** (see Scheme 29).

The activity of the substrates **11w-f'** was tested in asymmetric hydrogenation mediated by the *in situ* formed complex **135** derived from the corresponding ligand **30a**. The standard screening hydrogenation conditions used in this study were 1.0 mol % of precatalyst formed *in situ*, 20 bar of H₂, THF as solvent, room temperature and 18 h reaction time, unless otherwise stated.

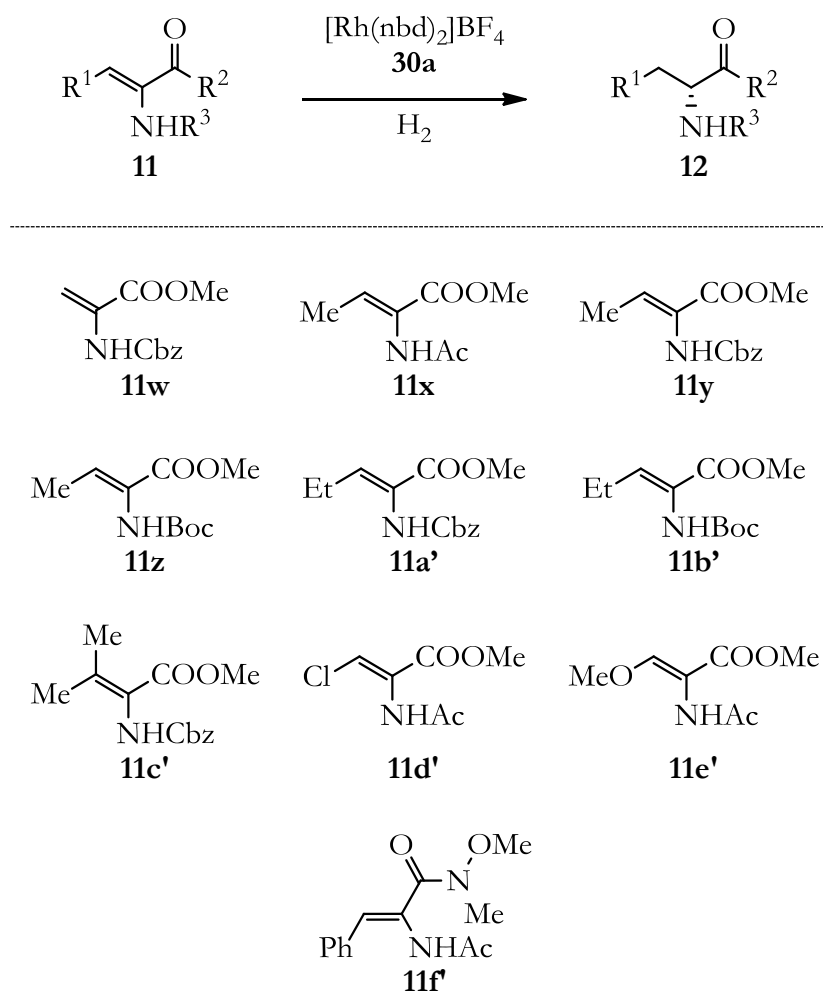
The results of the screening experiments have been summarized in Table 4.

¹⁴⁷ I gratefully acknowledge Dr. H. Fernández-Pérez and Dr. P. Etayo for the loan of some substrates for catalytic purposes and for sharing the analytical methods.

¹⁴⁸ Schmidt, U.; Lieberknecht, A.; Wild, J. *Synthesis* **1984**, 53.

¹⁴⁹ See experimental section, 1.3.3, for further details on synthetic methods and characterization of substrates.

In the majority of cases, conversion was complete and enantioselectivity was excellent (94% to 99% ee), except in the case of the challenging tetrasubstituted acrylate **11c'**, for which full conversion was not observed even at 80 bar H₂, and in the case of the β-chloro derivative **11d'**, which was not hydrogenated at all, even at higher H₂ pressures. The excellent enantioselectivities achieved upon hydrogenation of the α-(acylamino)acrylates **11** to give the corresponding α-amino acid derivatives **12** illustrate the tolerance of the catalytic system derived from ligand **30a** to a broad variety of carbamate-type amino protecting groups.



Scheme 29. Rhodium-mediated asymmetric hydrogenation of α-(acylamino)acrylates mediated by [Rh(nbd)(**30a**)]BF₄.

Table 4. Rhodium-mediated asymmetric hydrogenation of α -(acylamino)acrylates **11** using *P-OP* ligand **30a**.^[a]

Entry	Substrate	Observations	[Rh(nbd)(30a)]BF ₄	
			Conv. [%] ^[b]	ee [%] ^[c] (config.) ^[d]
1	11w	-	>99	98 (R)
2	11x	-	>99	99 (R)
3	11y	-	>99	98 (R)
4	11z	-	>99	98 (R)
5	11a'	80 bar H ₂	>99	99 (R)
6	11b'	80 bar H ₂	>99	96 (R)
7	11c'	80 bar H ₂	57	54 (R) ^[e]
8	11d'	80 bar H ₂	0	-
9	11e'	DCM	>99 ^[f]	97 (R)
10	11f'	DCM	>99	94 (R) ^[e]

^[a] Reaction conditions: [Rh(nbd)₂]BF₄/*P-OP* ligand/substrate molar ratio = 1.0 : 1.1 : 100, room temperature, 20 bar H₂, 18 h, 0.2 M in THF, unless otherwise indicated.

^[b] Conversions were determined by ¹H NMR.

^[c] Enantiomeric excesses were determined by GC or HPLC using chiral stationary phases.

^[d] Absolute configurations were assigned by comparison with reported data.

^[e] Absolute configuration was tentatively assigned by analogy based on the stereochemical outcome for analogous substrates.

^[f] The amount of the hydrogenated MeOH-elimination product (methyl 2-acetamidopropanoate) observed was 4 mol %.

Several of these α -(acylamino)acrylates were also hydrogenated using the rhodium complexes derived from the trityl-substituted ligand **30b** (**11f** and **11w**, β -alkyl-substituted derivatives **11a'-b'**, β -aryl-substituted compounds **11d**

and **11f** and β -alkoxy-substituted alkene **11e'**; see Scheme 29 for the structures).

The results of this comparative catalytic study using rhodium complexes derived from **30a** and **30b** for the hydrogenation of the previously mentioned substrates have been summarized in Table 5.

Table 5. Rhodium-mediated asymmetric hydrogenation of α -(acylamino)acrylates using *P-OP* ligands **30a** or **30b**.^[a]

Entry	Substrate	Observations	Results with 30a		Results with 30b	
			Conv. [%] ^[b]	ee [%] ^[c] (config.) ^[d]	Conv. [%] ^[b]	ee [%] ^[c] (config.) ^[d]
1	11f	-	>99	99 (R) ^[f]	>99	99 (R)
2	11w	-	>99	98 (R)	>99	98 (R)
3	11a'	80 bar H ₂	>99	99 (R)	>99	99 (R)
4	11b'	80 bar H ₂	>99	96 (R)	>99	97 (R)
5	11d	-	>99	99 (R) ^[f]	>99	99 (R)
6	11f'	DCM	>99	94 (R) ^[e]	92	95 (R) ^[e]
7	11e'	DCM	>99 ^[g]	97 (R)	>99 ^[g]	97 (R)

^[a] Reaction conditions: [Rh(nbd)₂]BF₄/*P-OP* ligand/substrate molar ratio = 1.0 : 1.1 : 100, room temperature, 20 bar H₂, 18 h, 0.2 M in THF, unless otherwise indicated.

^[b] Conversions were determined by ¹H NMR.

^[c] Enantiomeric excesses were determined by GC or HPLC using chiral stationary phases.

^[d] Absolute configurations were assigned by comparison with reported data.

^[e] Absolute configuration was tentatively assigned by analogy based on the stereochemical outcome for analogous substrates.

^[f] Results previously reported by our group.^{73, 81, 82}

^[g] The observed amount of the hydrogenated MeOH-elimination product (methyl 2-acetamidopropanoate) was 4 mol %.

In almost all cases conversion was complete and enantioselectivity was excellent (94% to 99% ee). Phosphine-phosphite **30b** performed slightly better

(compare entries 4 and 6 in Table 5) or equal than **30a**. Furthermore, excellent results were obtained for the understudied *N*-Boc- or *N*-Cbz-protected, β -ethyl-substituted, α -amino acid precursors **11a'** and **11b'** (Table 5, entries 3 and 4). In this case, 80 bar of H₂ was required, as hydrogenations which ran at hydrogen pressures below 80 bar of H₂ led to incomplete conversion, regardless of the ligand employed. Preparation of compound **12a'** by enantioselective hydrogenation had been previously reported only once,^{65b} with comparable enantioselectivity. To the best of our knowledge, there are no known examples of the preparation of its Boc-substituted analog **12b'** by asymmetric hydrogenation.

The *N*-methoxy-*N'*-methylcarbamoyl group (also known as the Weinreb amide group) is a highly versatile synthetic group that can act as an antecedent of numerous functional groups.¹⁵⁰ Thus, we became interested in preparing the corresponding α -(acylamino)acrylates with a Weinreb amide group attached to the double bond (**11f**) to study its behavior in asymmetric hydrogenation mediated by rhodium complexes of our *P-OP* ligands. Phosphine-phosphite ligands **30a** and **30b** mediated the hydrogenation reaction leading to product **12f** with very high enantioselectivity (94 – 95% ee; Table 5, entry 6).

The hydrogenation product **12e'** is a direct precursor of the antiepileptic drug lacosamide.^{151, 152} The β -alkoxy-substituted amino acid derivative **12e'** was

¹⁵⁰ See, for instance: (a) Balasubramaniam, S.; Aidhen, I. S. *Synthesis* **2008**, 3707. (b) Shang, J.; Han, Z.; Li, Y.; Wang, Z.; Ding, K. *Chem. Commun.* **2012**, 48, 5172., and references cited therein.

¹⁵¹ For total syntheses of (*R*)-lacosamide, see: (a) Choi, D.; Stables, J. P.; Kohn, H. *J. Med. Chem.* **1996**, 39, 1907. (b) Andurkar, S. V.; Stables, J. P.; Kohn, H. *Tetrahedron: Asymmetry* **1998**, 9, 3841. (c) Morieux, P.; Stables, J. P.; Kohn, H. *Bioorg. Med. Chem.* **2008**, 16, 8968. (d) Salomé, C.; Salomé-Grosjean, E.; Park, K.-D.; Morieux, P.; Swendiman, R.; De Marco, E.; Stables, J. P.; Kohn, H. *J. Med. Chem.* **2010**, 53, 1288. (e) Muthukrishnan, M.; Mujahid, M.; Sasikumar, M.; Mujumdar, P. *Tetrahedron: Asymmetry* **2011**, 22, 1353. (f) Bernaz-Vazquez, P. M.; Lazcano-Seres, J. M.; Contreras-Martinez, Y. M.-A.; Juarez-Lagunas, J. A.; Sanchez-Mereles, D.; Vazquez-Miranda, J. R.; Zambrano-Huerta, A. (Signa S. A. de C. V.). Patent

accessed by enantioselective hydrogenation using the rhodium complex of **30a** or **30b**. The results were excellent in terms of enantioselectivity, (97% ee; Table 5, entry 7), albeit the selectivity towards the desired product was not complete, and small amounts of the hydrogenated MeOH-elimination product were found (4% of methyl 2-acetamidopropanoate; Table 5, entry 7). The selectivity of the hydrogenation (*i.e.* formation of the desired hydrogenation product with respect to conversion) was strongly influenced by the solvent used, dichloromethane being the solvent in which elimination took place to a lower extent (see section 1.2.4.3 for extended information).

1.2.3.2 Hydrogenation of α -Substituted Enamides

Rhodium complexes derived from ligand **30a** efficiently mediated the asymmetric hydrogenation of *N*-acyl α -aryl enamides **42a**, **42b**, **42f** and **42g** (Figure 37).^{73,81,82} Due to the importance of the chiral amines **43** as chiral building blocks for the preparation of life-science products, we decided to expand the substrate scope to an array of diversely substituted α -substituted enamides **42**¹⁵³ (Scheme 30). Most of the non-commercially available starting α -arylenamides could be easily prepared by following Burk's¹⁵⁴ method involving reduction of ketone oximes followed by acetylation (**42c**, **42e**, **42h** and **42i**). Substrate **42d** required a specific preparation method.¹⁴⁹

WO2013030654A1, 2013. (g) Raman, J. V.; Pillai, B. G.; Hamirani, B. (Alembic Pharmaceuticals Limited). Patent WO2013024383A1, 2013.

¹⁵² Perucca, E.; Yasothan, U.; Clincke, G.; Kirkpatrick, P. *Nat. Rev. Drug Discovery* **2008**, *7*, 973.

¹⁵³ I gratefully acknowledge Dr. H. Fernández-Pérez and Dr. P. Etayo for the loan of some substrates for catalytic purposes and for sharing the analytical methods.

¹⁵⁴ Burk, M. J.; Casy, G.; Johnson, N. B. *J. Org. Chem.* **1998**, *63*, 6084.

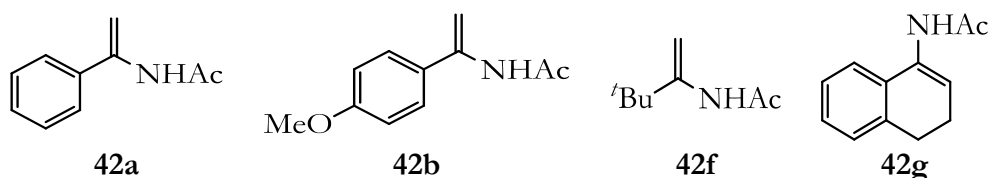
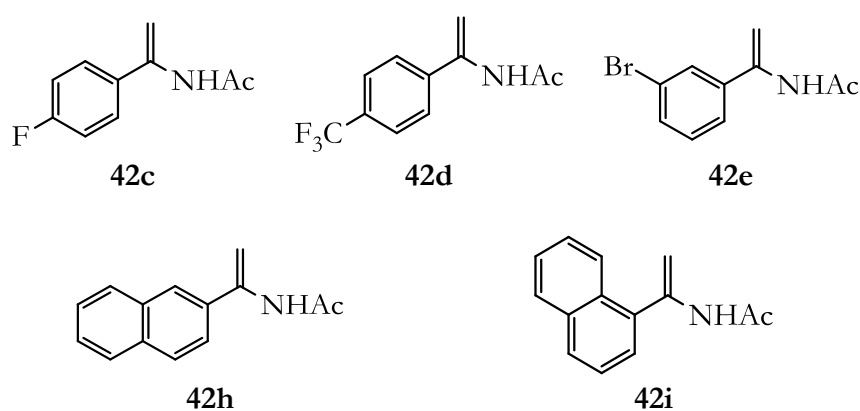
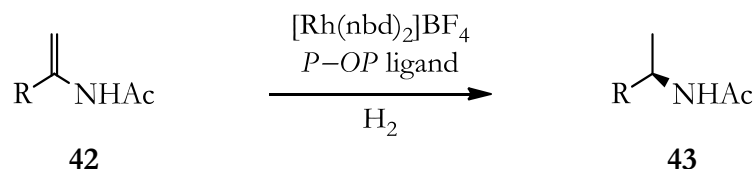


Figure 37. Previously hydrogenated α -substituted enamides using ligand **30a**.



Scheme 30. Rhodium-mediated asymmetric hydrogenation of an array of diversely substituted α -arylenamides mediated by $[\text{Rh}(\text{nbd})(\mathbf{30a})]\text{BF}_4$.

These new substrates encompassed aryl-substituted enamides with electronically diverse groups in the aryl ring as well as the more sterically hindered naphthyl derivatives **42h** and **42i** (Scheme 30).

Substrates **42** were assessed in asymmetric hydrogenations using the rhodium complex **135**, which derives from ligand **30a**. The standard screening hydrogenation conditions used were 1.0 mol % of *in situ* prepared precatalyst, 20 bar of H_2 , THF as solvent, room temperature and 18 h reaction time, unless otherwise stated. The results obtained for this screening were summarized in Table 6.

Table 6. Rhodium-mediated asymmetric hydrogenation of α -substituted enamides **42** using *P-OP* ligand **30a**.^[a]

Entry	Substrate	Observations	[Rh(nbd)(30a)]BF ₄	
			Conv. [%] ^[b]	ee [%] ^[c] (config.) ^[d]
1	42c	-	>99	98 (R)
2	42d	-	>99	98 (R)
3	42e	-	>99	97 (R)
4	42h	-	>99	99 (R)
5	42i	40 bar H ₂	90	83 (R)

^[a] Reaction conditions: [Rh(nbd)₂]BF₄/*P-OP* ligand/substrate molar ratio = 1.0 : 1.1 : 100, room temperature, 20 bar H₂, 18 h, 0.2 M in THF, unless otherwise indicated.

^[b] Conversions were determined by ¹H NMR.

^[c] Enantiomeric excesses were determined by GC or HPLC using chiral stationary phases.

^[d] Absolute configurations were assigned by comparison with reported data.

In general, high enantioselectivities (up to 99% ee) were observed for α -aryl-substituted enamides. We had previously learnt that enamide **42b**, which bears an electron rich aryl moiety, was efficiently hydrogenated to afford **43b** with 97% ee.⁸² The results obtained in the present PhD thesis for aryl-substituted enamides with electron withdrawing groups on the aryl ring (substrates **42c-e**) were also good and rhodium complexes derived from ligand **30a** provided excellent enantioselectivities (97-98% ee, Table 6, entries 1-3). When the 2-naphthyl derivative **42h** was hydrogenated, high levels of activity and excellent enantioselectivities for the hydrogenated product **43h** were observed, whilst the hydrogenation of its more sterically hindered 1-naphthyl analog **42i** only proceeded at higher H₂ pressure (40 bar). Enantioselectivity was lower for the 1-naphthyl-substituted enamide (83 % ee) with respect to its 2-naphthyl-substituted analog (compare entries 4 and 5 in Table 6).

The catalytic activity of rhodium complexes incorporating the trityl substituted ligand **30b** was compared with that obtained for ligand **30a**. The results of this comparative study have been summarized in Table 7.

Table 7. Comparative study on the rhodium-mediated asymmetric hydrogenation of α -arylenamides using *P-OP* ligands **30a** and **30b**.^[a]

Entry	Substrate	Observations	Results with 30a		Results with 30b	
			Conv. [%] ^[b]	ee [%] ^[c] (config.) ^[d]	Conv. [%] ^[b]	ee [%] ^[c] (config.) ^[d]
1	42a	-	>99	98 (R) ^[e]	>99	98 (R)
2	42h	-	>99	99 (R)	>99	99 (R)
3	42i	40 bar H ₂	90	83 (R)	>99	83 (R)

^[a] Reaction conditions: [Rh(nbd)₂]BF₄/*P-OP* ligand/substrate molar ratio = 1.0 : 1.1 : 100, room temperature, 20 bar H₂, 18 h, 0.2 M in THF, unless otherwise indicated.

^[b] Conversions were determined by ¹H NMR.

^[c] Enantiomeric excesses were determined by GC or HPLC using chiral stationary phases.

^[d] Absolute configurations were assigned by comparison with reported data.

^[e] Results previously reported by our group.^{81, 82}

As can be observed by comparing entries 1-3 in Table 7, enantioselectivity remained constant regardless of the ligand used for all of the enamides tested. However, an increased activity was observed in the case of 1-naphthylenamide **42i** when **30b** was used as ligand. Rh-mediated asymmetric hydrogenation of this substrate is a challenging process, both in terms of conversion and enantioselectivity, as rhodium complexes of many ligands fail to provide satisfactory results.¹⁵⁵ Ligand **30b** led to full conversion in the same conditions in which ligand **30a** only provided 90% conversion (40 bar of H₂). The hydrogenated product **43i** is an intermediate in the synthesis of cinacalcet

¹⁵⁵ See for example Zhang, W.; Zhang, X. *Angew. Chem., Int. Ed.* **2006**, *45*, 5515., and references cited therein.

hydrochloride,¹⁵⁶ a calcimimetic agent used for secondary hyperparathyroidism therapy.

1.2.3.3 Hydrogenation of α -Substituted Enol Esters

The structural resemblance between α -substituted enol esters **137** and α -arylenamides **42** led us to assess the application of our enantiopure *P-OP* ligands in the enantioselective hydrogenation of α -arylenol esters **137**. This kind of derivative appears *a priori* to be suitable as a substrate for Rh-mediated asymmetric hydrogenation as the chelating assistance of the *O*-acyl binding group should allow the formation of the required five-membered chelate *via* coordination of the rhodium center to the C=C double bond and the C=O group, both of which are present in enol ester derivatives.^{94c, 107}

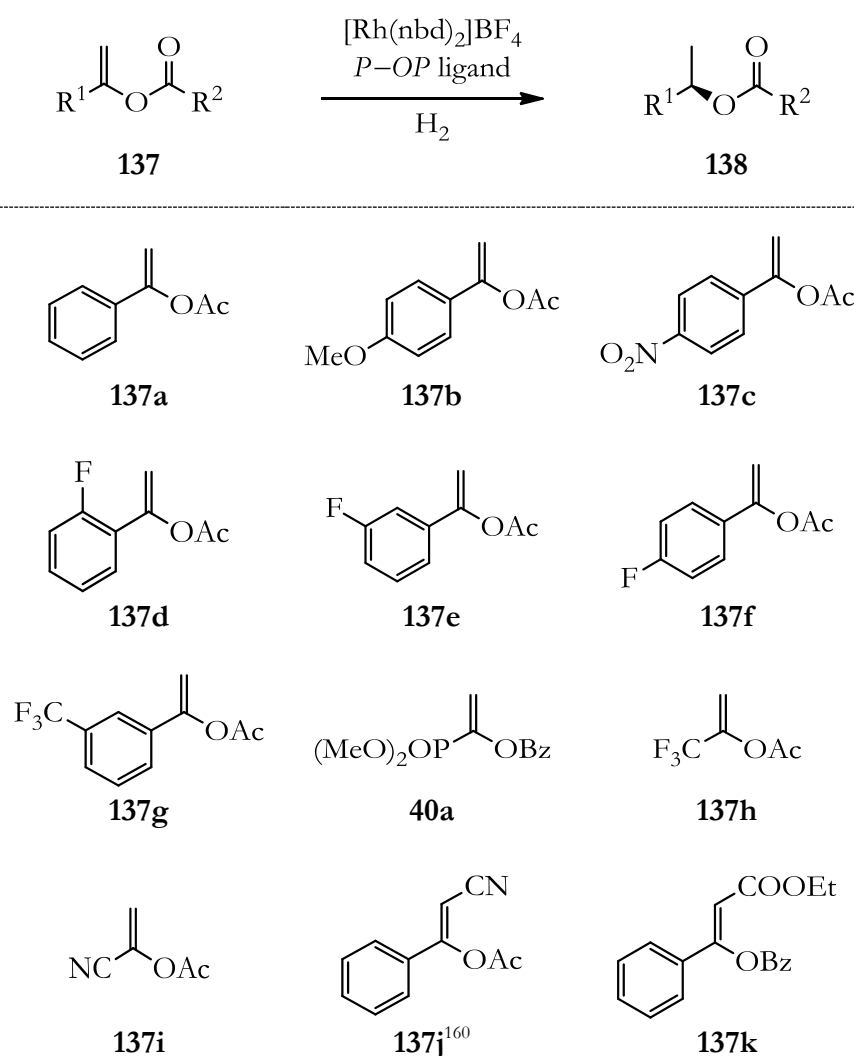
Despite this inherent suitability, the Rh-mediated asymmetric hydrogenation of this kind of functionalized alkene remains an underexplored area in the literature, particularly in a systematic manner.^{65a, 157}

Furthermore, the enantioselective hydrogenation of α -arylenol esters paves the way to an alternative route to chiral benzylic alcohols, which are valuable intermediates that are widely used in asymmetric organic synthesis.

¹⁵⁶ For recent synthetic routes towards cinacalcet, see Shinde, G. B.; Niphade, N. C.; Deshmukh, S. P.; Toche, R. B.; Mathad, V. T. *Org. Process Res. Dev.* **2011**, *15*, 455., and references cited therein.

¹⁵⁷ (a) Koenig, K. E.; Bachman, G. L.; Vineyard, B. D. *J. Org. Chem.* **1980**, *45*, 2362. (b) Burk, M. J. (du Pont de Nemours, E. I., and Co.), U.S. Patent 5,171,892, 1992. (c) Jiang, Q.; Xiao, D.; Zhang, Z.; Chao, P.; Zhang, X. *Angew. Chem., Int. Ed.* **1999**, *38*, 516. (d) Tang, W.; Liu, D.; Zhang, X. *Org. Lett.* **2003**, *5*, 205. (e) Liu, D.; Zhang, X. *Eur. J. Org. Chem.* **2005**, 646. (f) Panella, L.; Feringa, B. L.; de Vries, J. G.; Minnaard, A. J. *Org. Lett.* **2005**, *7*, 4177. (g) Stephan, M.; Sterk, D.; Mohar, B. *Adv. Synth. Catal.* **2009**, *351*, 2779. (h) Zhang, X.; Huang, K.; Hou, G.; Cao, B.; Zhang, X. *Angew. Chem., Int. Ed.* **2010**, *49*, 6421. (i) Zupančič, B.; Mohar, B.; Stephan, M. *Org. Lett.* **2010**, *12*, 1296. (j) Zupančič, B.; Mohar, B.; Stephan, M. *Org. Lett.* **2010**, *12*, 3022. (k) Zhang, J.; Dong, K.; Wang, Z.; Ding, K. *Org. Biomol. Chem.* **2012**, *10*, 1598. (l) Liu, Y.; Wang, Z.; Ding, K. *Tetrahedron* **2012**, *68*, 7581.

We synthesized (or purchased) an array of diversely α -substituted enol esters **137** (see Scheme 31).¹⁵⁸ Most of the non-commercially available starting α -arylenol acetates could be easily prepared by following Berkessel's procedure¹⁵⁹ involving condensation of the corresponding acetophenone and isopropenyl acetate under *p*-toluenesulfonic acid catalysis (**137a**, **137b**, **137c**, **137d**, **137e**, **137f** and **137g**). Some other substrates required specific preparation methods (**137j** and **137k**).¹⁴⁹



Scheme 31. Rhodium-mediated asymmetric hydrogenation of α -substituted enol esters mediated by $[\text{Rh}(\text{nbd})(\mathbf{30a})]\text{BF}_4$ or $[\text{Rh}(\text{nbd})(\mathbf{30b})]\text{BF}_4$ complexes.

¹⁵⁸ I gratefully acknowledge Dr. H. Fernández-Pérez and Dr. P. Etayo for the loan of some substrates for catalytic purposes and for sharing the analytical methods.

¹⁵⁹ Berkessel, A.; Sebastian-Ibarz, M. L.; Mueller, T. N. *Angew. Chem., Int. Ed.* **2006**, *45*, 6567.

¹⁶⁰ This substrate was prepared as a 13:1 *Z/E* mixture.

Our set of selected substrates included seven α -aryl-substituted enol esters with electron-donating and electron-withdrawing groups on the aryl ring (**137a-g**), the previously studied α -phosphonate enol ester (**40a**),¹⁶¹ α -CF₃- and α -cyano-substituted enol acetates (**137h** and **137i**, respectively), and two β -substituted enol esters (**137j** and **137k**).

The results of the comparative study on asymmetric hydrogenation of these substrates mediated by rhodium complexes derived from ligands **30a**, **30b** or *ent*-**30b** have been summarized in Table 8.

Rhodium catalysts derived from ligands **30a** and **30b** (or *ent*-**30b**) proved to be good catalysts in the Rh-mediated asymmetric hydrogenation of α -arylenol acetates **137a-g**; full conversions and enantioselectivities ranging from 90% to 99% ee were achieved. In general, regardless of the electronic nature or position of the substituents on the aromatic ring, asymmetric hydrogenation proceeded with excellent enantioselectivities. Although rhodium complexes of ligands **30b** (or *ent*-**30b**) mediated the hydrogenation of **137a**, **137c**, and **137e-g** with comparable enantioselectivities (difference of $\pm 1\%$ ee; see entries 1, 3 and 5–7 in Table 8), ligand **30b** provided higher enantiomeric excesses in the hydrogenation of **137b** and **137d** (see entries 2 and 4 in Table 8). Analogously, the Rh complex of ligand **30b** led to significantly higher enantioselectivities in the hydrogenations of α -substituted enol esters **40a** and **137i** (see entries 8 and 10 in Table 8). These results suggest that the steric bulkiness of the R-oxy substituent in the *P-OP* ligand plays a role in the enantioselectivity.

¹⁶¹ Hydrogenation of **40a** under different conditions had been studied previously (see ref 73, 81 and 82).

Table 8. Comparative rhodium-mediated asymmetric hydrogenation of α -substituted enol esters using *P-OP* ligands **30a** or **30b**.^[a]

Entry	Substrate	Observations	Results with 30a		Results with 30b	
			Conv. [%] ^[b]	ee [%] ^[c] (config.) ^[d]	Conv. [%] ^[b]	ee [%] ^[c] (config.) ^[d]
1	137a	-	>99	96 (R)	>99	97 (R)
2	137b	-	>99	91 (R)	>99	95 (R)
3	137c	-	>99	99 (R)	>99	98 (R)
4	137d	-	>99	90 (R) ^[e]	>99	94 (R) ^[e]
5	137e	-	>99	97 (R) ^[e]	>99	98 (R) ^[e]
6	137f	-	>99	97 (R)	>99	96 (R)
7	137g	-	>99	97 (R)	>99	98 (S) ^[f]
8	40a	-	>99	90 (S)	>99	95 (S)
9	137h	-	>99 ^[g]	99 (R)	-	-
10	137i	2.0 mol % cat.	>99	87 (R)	>99	97 (R)
11	137j	-	6	n.d.	-	-
12	137j	3.0 mol % cat., 80 bar H ₂ , 65 h	30	n.d.	-	-
13	137k	-	4	n.d.	-	-
14	137k	80 bar H ₂ , 65h	18	n.d.	-	-

^[a] Reaction conditions: [Rh(nbd)₂]BF₄/*P-OP* ligand/substrate molar ratio = 1.0 : 1.1 : 100, room temperature, 20 bar H₂, 18 h, 0.2 M in THF, unless otherwise indicated.

^[b] Conversions were determined by ¹H NMR.

^[c] Enantiomeric excesses were determined by GC or HPLC using chiral stationary phases.

^[d] Absolute configurations were assigned by comparison with reported data.

^[e] Absolute configuration was tentatively assigned by analogy based on the stereochemical outcome for analogous substrates.

^[f] Ligand *ent*-**30b** was used in this case in order to obtain the desired (S)-configured product.

^[g] Conversion was determined by ¹⁹F NMR.

The present work represents the first preparation of enantiomerically enriched products **138d** and *ent*-**138g** by hydrogenation. With regard to product **138e**, we found only one example of it being prepared by rhodium-mediated asymmetric hydrogenation by Burk *et al.*,^{157b} who obtained this product in 89% ee using Et-DUPHOS as the chiral ligand. Gratifyingly, ligand **30b** provided a significantly superior enantioselectivity (98% ee). In addition, **30a** and **30b** afforded products **138a-c** and **138f** with levels of enantioselectivity comparable to the best ones reported for the Rh-mediated asymmetric hydrogenation of such α -arylenol acetates.^{157d-j} Interestingly, the chiral fluorinated products **138d-f** are valuable synthetic precursors to numerous pharmaceutically active compounds.¹⁶² The (*S*)-configured hydrogenation product *ent*-**138g** constitutes a key chiral precursor for the preparation of Mitsubishi's compound (*S*)-MA20565, a broad-spectrum agrochemical agent showing potent fungicidal activity against various crop diseases.¹⁶³

The asymmetric hydrogenation of 1-(trifluoromethyl)vinyl acetate **137h** and 1-cyanovinyl acetate **137i** are challenging transformations. To the best of our knowledge, there were no reports on preparing **138i** by asymmetric hydrogenation, and only a few possibilities for **138h**.^{65, 157a,g,i, 164} These

¹⁶² For some leading examples, see: (a) Mastalerz, H.; Chang, M.; Chen, P.; Dextraze, P.; Fink, B. E.; Gavai, A.; Goyal, B.; Han, W.-C.; Johnson, W.; Langley, D.; Lee, F. Y.; Marathe, P.; Mathur, A.; Oppenheimer, S.; Ruediger, E.; Tarrant, J.; Tokarski, J. S.; Vite, G. D.; Vyas, D. M.; Wong, H.; Wong, T. W.; Zhang, H.; Zhang, G. *Bioorg. Med. Chem. Lett.* **2007**, *17*, 2036. (b) Singer, J. M.; Wilson, M. W.; Johnson, P. D.; Graham, S. R.; Cooke, L. W.; Roof, R. L.; Boxer, P. A.; Gold, L. H.; Meltzer, L. T.; Janssen, A.; Roush, N.; Campbell, J. E.; Su, T.-Z.; Hurst, S. I.; Stoner, C. L.; Schwarz, J. B. *Bioorg. Med. Chem. Lett.* **2009**, *19*, 2409. (c) Jiang, X.; Prasad, K.; Repic, O. *Synth. Commun.* **2009**, *39*, 2640. (d) Huang, X.; Aslanian, R.; Zhou, W.; Zhu, X.; Qin, J.; Greenlee, W.; Zhu, Z.; Zhang, L.; Hyde, L.; Chu, I.; Cohen-Williams, M.; Palani, A. *ACS Med. Chem. Lett.* **2010**, *1*, 184.

¹⁶³ Tanaka, K.; Katsurada, M.; Ohno, F.; Shiga, Y.; Oda, M.; Miyagi, M.; Takehara, J.; Okano, K. *J. Org. Chem.* **2000**, *65*, 432.

¹⁶⁴ (a) Pullmann, T.; Engendahl, B.; Zhang, Z.; Hoelscher, M.; Zanotti-Gerosa, A.; Dyke, A.; Francio, G.; Leitner, W. *Chem.-Eur. J.* **2010**, *16*, 7517. (b) Hammerer, T.; Weisgerber, L.;

substrates, together with the enol ester phosphonate **40a**,^{157i-k} were all hydrogenated in very high enantioselectivities (95% to 99% ee) using *P-OP* ligands **30a** or **30b** (see entries 8-10 in Table 8).

Whereas the catalyst derived from **30b** was required to achieve enantioselectivities of at least 95% ee in other substrates, rhodium complexes of **30a** already gave the hydrogenated product **138h** in 99% ee (Table 8, entry 9), which matches the highest value in the literature reported by Stephan *et al.*¹⁵⁷ⁱ

In the case of the hydrogenation of the 1-cyanovinyl acetate **137i**, full conversion required an increased catalyst loading of 2.0 mol %; interestingly, with this substrate, ligand **30b** gave a ten percent higher enantiomeric excess than did **30a** in the same conditions (see entry 10 in Table 8). To the best of our knowledge, the aforementioned results represent the highest enantioselectivity ever achieved in the synthesis of (*R*)-*O*-acetyl-1-cyanoethanol **138i**. The only previously reported route to this compound is based on the enzyme-mediated enantioselective hydrolysis of racemic mixtures of 1-cyanoethyl acetate, which gives poor yield and only moderate enantiomeric excess.¹⁶⁵ Furthermore, the asymmetric hydrogenation approach is synthetically advantageous, because the hydrolysis product derived from the chiral **138i** product (*i.e.*, (*R*)-1-cyanoethanol) is a valuable chiral synthon for which only two enantioselective methods were found in the literature, both of which gave only moderate enantiomeric excesses.¹⁶⁶

On the other hand, the hydrogenation products of the β -substituted enol esters **137j** and **137k**, or their hydrolyzed products, are known

Schenk, S.; Stelzer, O.; Englert, U.; Leitner, W.; Francio, G. *Tetrahedron: Asymmetry* **2012**, *23*, 53.

¹⁶⁵ Ohta, H.; Hiraga, S.; Miyamoto, K.; Tsuchihashi, G. *Agric. Biol. Chem.* **1988**, *52*, 3023.

¹⁶⁶ (a) Matthews, B. R.; Jackson, W. R.; Jayatilake, G. S.; Wilshire, C.; Jacobs, H. A. *Aust. J. Chem.* **1988**, *41*, 1697. (b) Aspinall, H. C.; Greeves, N.; Smith, P. M. *Tetrahedron Lett.* **1999**, *40*, 1763.

intermediates¹⁶⁷ in the synthesis of the widely used anti-depressants fluoxetine¹⁶⁸ and tomoxetine.¹⁶⁹ Sadly, ligand **30a** failed in the asymmetric hydrogenation of these β -substituted enol esters, leading to low conversion in the reduction of **137j** and **137k**, even with increased catalyst loading, H₂ pressure and reaction time (compare entries 11 and 12, and 13 and 14 in Table 8).

1.2.3.4 Hydrogenation of Itaconate Derivatives and Analogs

Ligand **30a** has demonstrated a high activity and enantioselectivity profile for the asymmetric hydrogenation of the previously reported itaconate derivative **38a** (already described in section 1.2.2.1) and *Roche ester* precursor **38e**.^{73, 81, 82} Thus, we decided to expand the substrate scope for this kind of functionalized alkene (Scheme 32).

The structural diversity of the new substrates to be studied encompassed itaconic acid (**38b**) and its dimethyl ester (**38a**),¹⁷⁰ succinamic acid derivative (**38d**) and its methyl ester (**38c**). Additionally, we also decided to explore three itaconic acid analogs **38e-g**, in which the aliphatic carboxylic acid group has been replaced by a hydroxyl or a bromo substituent. Succinamic derivatives **38c** and **38d** could be easily prepared by following described procedures.¹⁴⁹ Asymmetric hydrogenation of all these compounds

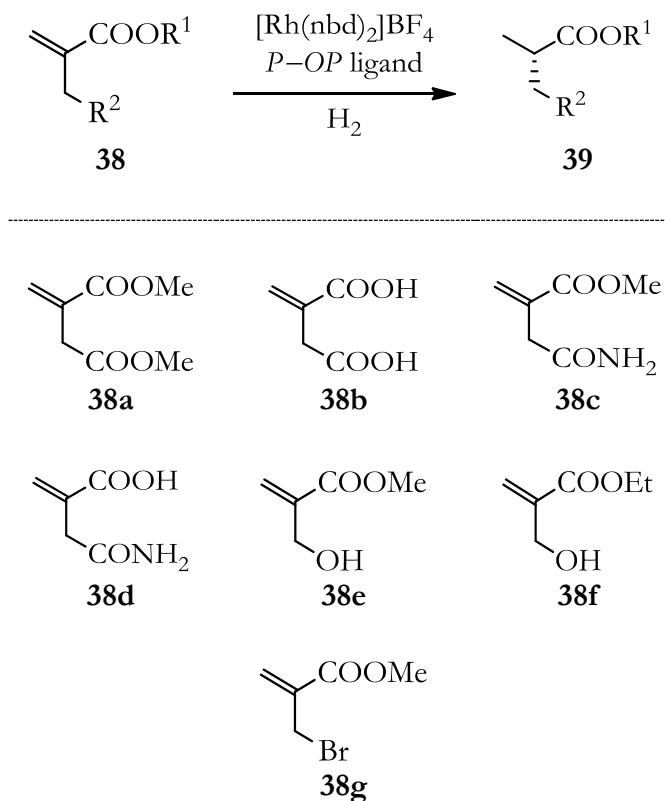
¹⁶⁷ (a) Kamal, A.; Khanna, G. B. R.; Ramu, R. *Tetrahedron: Asymmetry* **2002**, *13*, 2039. (b) Xu, C.-F.; Yuan, C.-Y. *Chin. J. Chem.* **2004**, *22*, 775. (c) Xu, C.; Yuan, C. *Tetrahedron* **2005**, *61*, 2169.

¹⁶⁸ (a) Klieser, E.; Lehmann, E.; Heinrich, K. *Pharmacopsychiatry* **1995**, *28*, 14. (b) Wong, D. T.; Bymaster, F. P.; Engleman, E. A. *Life Sci.* **1995**, *57*, 411.

¹⁶⁹ (a) Chouinard, G.; Annable, L.; Bradwejn, J. *Psychopharmacology* **1984**, *83*, 126. (b) Chouinard, G.; Annable, L.; Bradwejn, J.; Labonte, A.; Jones, B.; Mercier, P.; Belanger, M. C. *Psychopharmacol. Bull.* **1985**, *21*, 73.

¹⁷⁰ Hydrogenation of **38a** under different conditions had been studied previously (see ref 73, 81 and 82).

was studied using the rhodium complexes derived from ligands **30a** and **30b**, under standard screening conditions, unless otherwise stated (Table 9).



Scheme 32. Rhodium-mediated asymmetric hydrogenation of itaconic acid derivatives and analogs mediated by $[\text{Rh}(\text{nbd})(\mathbf{30a})]\text{BF}_4$ or $[\text{Rh}(\text{nbd})(\mathbf{30b})]\text{BF}_4$ complexes.

Table 9. Comparative study of the rhodium-mediated asymmetric hydrogenation of itaconic acid derivatives and analogs using *P-OP* ligands **30a** or **30b**.^[a]

Entry	Substrate	Observations	Results with 30a		Results with 30b	
			Conv. [%] ^[b]	ee [%] ^[c] (config.) ^[d]	Conv. [%] ^[b]	ee [%] ^[c] (config.) ^[d]
1	38a	-	>99	99 (<i>S</i>) ^[e]	>99	98 (<i>S</i>)
2	38b	-	>99	95 (<i>S</i>)	>99	99 (<i>S</i>)
3	38c	-	>99	99 (<i>S</i>)	-	-
4	38d	-	>99	95 (<i>S</i>)	>99	93 (<i>S</i>)
5	38e	-	>99	90 (<i>S</i>) ^[e]	>99	95 (<i>S</i>)
6	38e	0 °C, 0.5 mol % cat	>99	95 (<i>S</i>) ^[e]	>99	97 (<i>S</i>)
7	38f	0 °C, 0.5 mol % cat	>99	94 (<i>S</i>)	>99	98 (<i>S</i>)
8	38g	-	-	-	0	n.d.

^[a] Reaction conditions: [Rh(nbd)₂]BF₄/*P-OP* ligand/substrate molar ratio = 1.0 : 1.1 : 100, room temperature, 20 bar H₂, 18 h, 0.2 M in THF, unless otherwise indicated.

^[b] Conversions were determined by ¹H NMR.

^[c] Enantiomeric excesses were determined by GC using chiral stationary phases.

^[d] Absolute configurations were assigned by comparison with reported data.

^[e] Results previously reported by our group.^{73, 81, 82}

Excellent enantioselectivities were achieved in the asymmetric hydrogenations of dimethyl itaconate **38a** and itaconic acid **38b** (up to 99% ee; Table 9, entries 1 and 2). Enantioselective hydrogenation of methyl 2-methylenesuccinamate **38c** took place with excellent enantioselectivities (Table 9, entry 3), whereas the hydrogenations of its carboxylic acid parent compound **38d**¹⁵⁷ⁱ furnished lower enantiomeric excess (up to 95% ee; Table 9, entry 4). Rhodium complexes derived from **30a** already gave the hydrogenated product **39c** in 99% ee (Table 9, entry 3). The resultant enantioenriched hydrogenated products **39a-d** all showed an (*S*) absolute configuration. Whilst in the

hydrogenation of α -(acylamino)acrylates or α -substituted enol esters enantioselectivity was consistently better with **30b**, with itaconic acid derivatives **38a-d**, enantioselectivity ultimately depended on the combination of substrate and ligand: for **38a** and **38d**, ligand **30a** was a better choice; whereas for **38b**, ligand **30b** was better (see Table 9, entries 1, 2 and 4). These results clearly illustrate that the stereoselectivity of this chemistry can be fine-tuned according to the size of the substituents in the pendant ether functionality of the ligand.

(*S*)-Methyl 3-hydroxy-2-methylpropanoate **39e**, also known as Roche ester, is an industrially relevant chiral building block.¹⁷¹ It is used in the total synthesis of several anti-tumor agents.¹⁷² Its enantiomeric purity cannot be upgraded by crystallization because **39e** is liquid at room temperature; thus, only those synthetic procedures that provide it with an enantioselectivity of at least 95% ee are useful.^{171a} Such a degree of enantiopurity was achieved at room temperature by using 1.0 mol % of the rhodium complex derived from ligand **30b** (Table 9, entry 5), and we were able to further increase the ee to 97% by slightly decreasing the reaction temperature to 0 °C, which worked even at a lower catalyst loading of 0.50 mol % (Table 9, entry 6). These hydrogenation conditions are, to the best of our knowledge, the most attractive ones reported for the preparation of enantiomerically enriched Roche ester. Reek *et al.* have previously reported hydrogenation conditions for the Roche ester precursor that also reach the same high level of

¹⁷¹ See, for example: (a) Wassenaar, J.; Kuil, M.; Reek, J. N. H. *Adv. Synth. Catal.* **2008**, *350*, 1610. (b) Pautigny, C.; Jeulin, S.; Ayad, T.; Zhang, Z.; Genêt, J.-P.; Ratovelomanana-Vidal, V. *Adv. Synth. Catal.* **2008**, *350*, 2525. (c) Holz, J.; Schaeffner, B.; Zayas, O.; Spannenberg, A.; Börner, A. *Adv. Synth. Catal.* **2008**, *350*, 2533. (d) Robert, T.; Abiri, Z.; Sandee, A. J.; Schmalz, H.-G.; Reek, J. N. H. *Tetrahedron: Asymmetry* **2010**, *21*, 2671.

¹⁷² (a) Barrow, R. A.; Hemscheidt, T.; Liang, J.; Paik, S.; Moore, R. E.; Tius, M. A. *J. Am. Chem. Soc.* **1995**, *117*, 2479. (b) Smith, A. B., III; Adams, C. M.; Barbosa Lodise, S. A.; Degnan, A. P. *Proc. Natl. Acad. Sci. U. S. A.* **2004**, *101*, 12042. (c) Shin, Y.; Fournier, J.-H.; Fukui, Y.; Brueckner, A. M.; Curran, D. P. *Angew. Chem., Int. Ed.* **2004**, *43*, 4634. (d) Paterson, I.; Delgado, O.; Florence, G. J.; Lyothier, I.; O'Brien, M.; Scott, J. P.; Sereinig, N. *J. Org. Chem.* **2005**, *70*, 150.

enantioselectivity (98% ee), but they required lower temperatures (-40 °C instead of 0 °C) and higher catalyst loadings (1.0 mol % instead of 0.50 mol %).^{171a} Even a better enantioselectivity (98% ee, Table 9, entry 7) was observed in the hydrogenation leading to the ethyl ester analog **39f**,^{157j} under the same reaction conditions (0 °C, 0.50 mol % of Rh complex derived from the ligand **30b**).

Lastly, our system failed in the hydrogenation of the Roche ester precursor's analog **38g**. This compound has a bromo group replacing the hydroxyl group present in the Roche ester precursor. The absence of this chelation assisting group led to zero conversion (Table 9, entry 8), thus reaffirming the importance of the coordinating group that assists in the substrate binding to the catalyst.

1.2.4 Enantioselective Access to Chiral Drugs

Given the outstanding performance of the rhodium complexes derived from our *P-OP* ligands, we envisioned that they should efficiently enable the asymmetric synthesis of precursors of pharmaceutical targets by asymmetric hydrogenation of functionalized alkenes as the key step.

In this section, we have summarized the efforts in the asymmetric hydrogenation of strategically devised β -aryl-substituted and β -alkyl-substituted α -(acylamino)acrylates, α -arylenamides and α -arylenol acetates, whose hydrogenation products are valuable precursors to pharmaceutically relevant chiral building blocks.

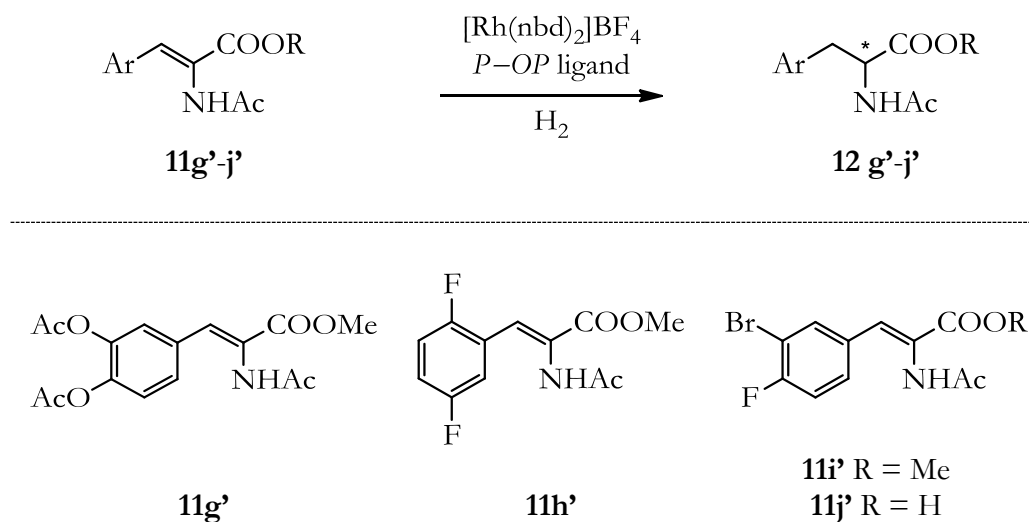
1.2.4.1 Access to Chiral Drug Precursors from β -Aryl- and β -Alkyl-Substituted α -(Acylamino)acrylates

The required substrates were synthesized using well-established synthetic methodologies¹⁷³ (or purchased, subjected to commercial availability) and then tested under the standard hydrogenation screening conditions (1 mol % precatalyst, THF, room temperature and overnight stirring), prior to further optimization of the hydrogenation conditions. The optimization process was made considering the use of ligands **30a**, **30b** or *ent*-**30b**, which enables access to both enantiomeric series of the hydrogenation products.

The first *sub*-family of chiral drug precursors corresponds to β -aryl substituted α -(acylamino)acrylates (Scheme 33), and we were in all cases

¹⁷³ The general synthetic procedure for α -(acylamino)acrylates has been described in Section 1.2.3.1. I gratefully acknowledge Dr. H. Fernández-Pérez and Dr. P. Etayo for the loan of some substrates for catalytic purposes and for sharing the analytical methods.

capable of finding conditions to fully hydrogenate substrates **11g'-j'** with excellent enantioselectivities.



Scheme 33. β -Aryl substituted α -(acylamino)acrylates **11g'-j'** hydrogenated by $[\text{Rh}(\text{nbd})(\mathbf{30a})]\text{BF}_4$ or $[\text{Rh}(\text{nbd})(\mathbf{30b})]\text{BF}_4$ complexes.

The hydrogenation product of **11g'** is a key substrate in the synthesis of biologically active compounds, and whilst the (*R*)-configured hydrogenation product **12g'** constitutes a valuable chiral precursor for the synthesis of rosmarinic acid analogs,¹⁷⁴ its enantiomer (*S*)-**12g'** is a fully protected derivative of levodopa, a very useful chiral drug for the treatment of Parkinson's disease (Scheme 33).^{108a} To the best to this author's knowledge, there is no precedent for the enantioselective hydrogenation of alkene **11g'**. Our approach enables access to both enantiomers of the chiral product **12g'**: Very high enantioselectivity (99% ee) was obtained under standard hydrogenation conditions with **30a** or *ent*-**30b** as ligands (entries 1 and 2 in Table 10). An increased pressure of 40 bar allow us to increase the substrate to catalyst ratio

¹⁷⁴ (a) Park, S.-H.; Kang, S.-H.; Lim, S.-H.; Oh, H.-S.; Lee, K.-H. *Bioorg. Med. Chem. Lett.* **2003**, *13*, 3455. (b) Park, S.-H.; Oh, H.-S.; Kang, M.-A.; Cho, H.; Prasad, J. B.; Won, J.; Lee, K.-H. *Bioorg. Med. Chem.* **2007**, *15*, 3938.

up to 1,000 with full conversion and 98% ee. The hydrogenation could also be done in MeOH in 99% ee with no reduction in conversion (compare entries 3 and 4 in Table 10).

Table 10. Rhodium-mediated asymmetric hydrogenation of α -acetamido β -aryl acrylates **11g'-j'** using *P-OP* ligands **30**.^[a]

Entry	Substrate	Ligand	Observations	Conv. [%] ^[b]	ee [%] ^[c] (config.) ^[d]
1	11g'	30a	-	>99	99 (R)
2	11g'	<i>ent</i> - 30b	-	>99	99 (S)
3	11g'	<i>ent</i> - 30b	40 bar H ₂ , 0.1 mol % cat	>99	98 (S)
4	11g'	<i>ent</i> - 30b	40 bar H ₂ , 0.1 mol % cat, MeOH	>99	99 (S)
5	11h'	30a	-	>99	99 (R) ^[e]
6	11h'	30a	0.1 mol % cat	>99	98 (R) ^[e]
7	11h'	30a	0.1 mol % cat, MeOH	>99	96 (R) ^[e]
8	11i'	<i>ent</i> - 30b	-	>99	99 (S)
9	11j'	<i>ent</i> - 30b	-	0	n.d.
10	11j'	<i>ent</i> - 30b	MeOH	>99	98 (S)
11	11j'	<i>ent</i> - 30b	0.25 mol % cat, MeOH	>99	96 (S)

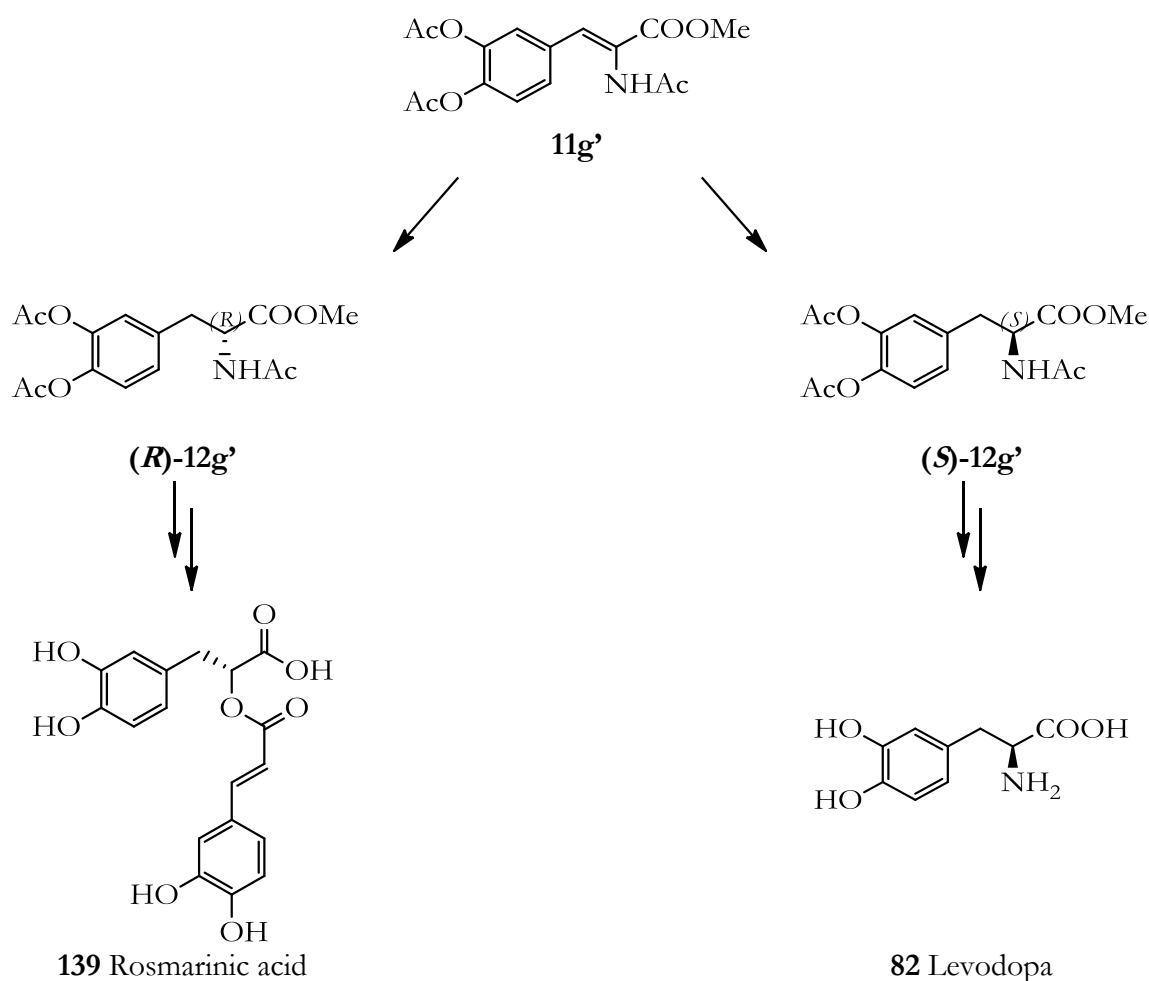
^[a] Reaction conditions: [Rh(nbd)₂]BF₄/*P-OP* ligand/substrate molar ratio = 1.0 : 1.1 : 100, room temperature, 20 bar H₂, 18 h, 0.2 M in THF, unless otherwise indicated.

^[b] Conversions were determined by ¹H NMR.

^[c] Enantiomeric excesses were determined by HPLC using chiral stationary phases.

^[d] Absolute configurations were assigned by comparison with reported data.

^[e] Absolute configuration was tentatively assigned by analogy based on the stereochemical outcome for analogous substrates.

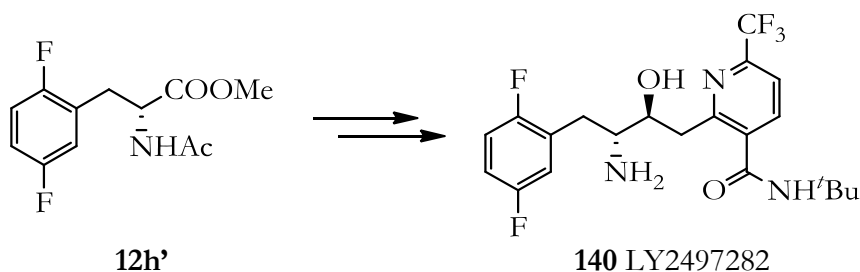


Scheme 34. Compound **11g'** as precursor of biologically active compounds.

Substrate **11h'** was fully hydrogenated under screening conditions with ligand **30a** affording **12h'** with 99% ee. Catalyst loading could be reduced by a factor of 10 to get the totally reduced product **12h'** with 98% ee (see entries 5 and 6 in Table 10). Use of MeOH as solvent did not improve the enantioselectivity but still afforded an excellent value of 96% ee (entry 7 in Table 10). Product **12h'** is a key intermediate in the synthesis of LY2497282 (**140**) (Scheme 35) a promising pro-drug for the treatment of type 2 diabetes.¹⁷⁵ Despite the pharmacological relevance of **12h'**, to the best of the author's

¹⁷⁵ Blaszczyk, L. C.; Mathes, B. M.; Pulley, S. R.; Robertson, M. A.; Sheehan, S. M.; Shi, Q.; Watson, B. M.; Wiley, M. R. (Elly Lilly and Company), Patent 015767, 2007.

knowledge, the results disclosed here constitute the first enantioselective synthesis of **12h'** by asymmetric hydrogenation.

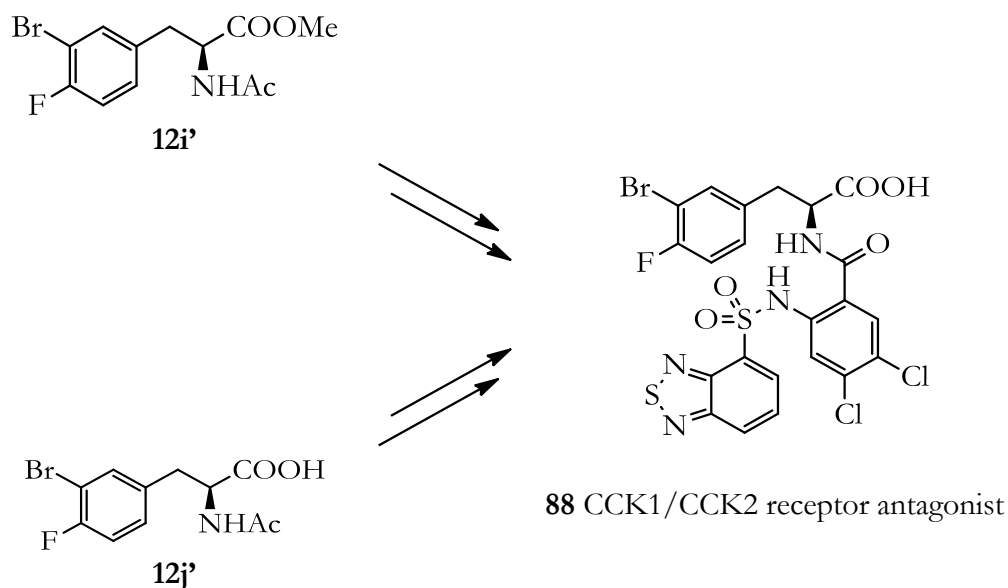


Scheme 35. Hydrogenation product **12h'** is an intermediate in the synthesis of LY2497282.

Whilst substrate **11i'** was fully hydrogenated under screening conditions using tetrahydrofuran as the solvent with excellent enantioselectivity, its acidic analog **11j'** gave zero conversion (compare entries 8 and 9 in Table 10). To settle this matter, the hydrogenation was carried out in MeOH as solvent, which afforded the totally reduced product **12j'** with excellent enantioselectivity (98% ee). Further attempts to reduce the catalyst loading to 0.25% led to a slight decrease in enantioselectivity with conversion remaining unaltered (see entries 10 and 11 in Table 10). The present approach constitutes an efficient enantioselective entry into (*S*)-*N*-acetyl-3-bromo-4-fluorophenylalanine (**12j'**), a key pharmaceutical building block used for the preparation of dual CCK1/CCK2 receptor antagonist^{176, 112} (Scheme 36), which has recently been developed for the treatment of various gastrointestinal diseases.¹¹¹ A precedent for the asymmetric hydrogenation of alkene **11i'** was not found in the literature, but the high level of enantioselectivity achieved for its analog **11j'** (96–98% ee) represents an improvement on the enantiomeric

¹⁷⁶ Allison, B.; Phuong, V. K.; Pippel, M. C. W.; Rabinowitz, M. H.; Venkatesan, H. (Janssen Pharmaceutica N. V.), U.S. Patent 0,069,286, 2006.

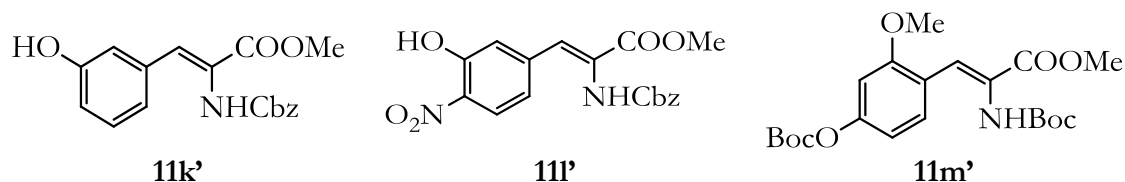
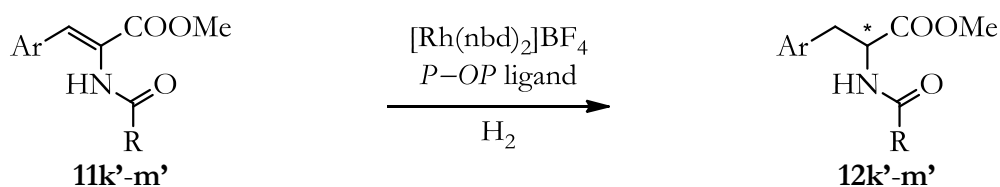
excess previously obtained for this type of alkene upon using a Rh complex derived from Me-BoPhoz¹⁷⁷, which gave the product with 94% ee.^{176, 112}



Scheme 36. CCK1/CCK2 receptor antagonist **88** derived from the hydrogenation products **12i'** and **12j'**.

The asymmetric hydrogenation of other α -(acylamino)acrylates leading to precursors of other pharmaceutically relevant compounds was also studied. The structures of the selected α -(acylamino)acrylates are indicated in Scheme 37 and the results on the asymmetric hydrogenation using rhodium complexes derived from *P-OP* ligands are summarized in Table 11.

¹⁷⁷ *N*-methyl-*N*-di-phenylphosphino-1-[2-(diphenylphosphino)ferrocenyl]ethyl-amine.



Scheme 37. Hydrogenation of β -aryl-substituted α -(acylamino)acrylates **11k'-m'** mediated by $[\text{Rh}(\text{nbd})(\text{P-OP})]\text{BF}_4$ complexes.

Table 11. Rhodium-mediated asymmetric hydrogenation of β -aryl-substituted α -(acylamino)acrylates **11k'-m'** using P-OP ligands **30**.^[a]

Entry	Substrate	Ligand	Observations	Conv. [%] ^[b]	ee [%] ^[c] (config.) ^[d]
1	11k'	<i>ent</i> - 30b	-	>99	98 (<i>S</i>) ^[e]
2	11k'	<i>ent</i> - 30b	60 bar H ₂ , 0.3 mol % cat	97	98 (<i>S</i>) ^[e]
3	11l'	30a	-	>99	98 (<i>R</i>) ^[e]
4	11l'	30a	0.5 mol % cat	>99	98 (<i>R</i>) ^[e]
5	11l'	30a	0.5 mol % cat, MeOH	>99	96 (<i>R</i>) ^[e]
6	11m'	<i>ent</i> - 30b	-	>99	98 (<i>S</i>)
7	11m'	<i>ent</i> - 30b	0.5 mol % cat	>99	98 (<i>S</i>)
8	11m'	<i>ent</i> - 30b	0.5 mol % cat, MeOH	>99	98 (<i>S</i>)

^[a] Reaction conditions: $[\text{Rh}(\text{nbd})_2]\text{BF}_4/\text{P-OP}$ ligand/substrate molar ratio = 1.0 : 1.1 : 100, room temperature, 20 bar H₂, 18 h, 0.2 M in THF, unless otherwise indicated.

^[b] Conversions were determined by ¹H NMR.

^[c] Enantiomeric excesses were determined by HPLC using chiral stationary phases.

^[d] Absolute configurations were assigned by comparison with reported data.

^[e] Absolute configuration was tentatively assigned by analogy based on the stereochemical outcome for analogous substrates.

β -aryl substituted *N*-benzyloxycarbonyl (Cbz)-protected acrylate **11k'** was tested in asymmetric hydrogenation with ligand *ent*-**30b** in order to obtain the desired (*S*)-configured product. Reaction under screening conditions proceeded smoothly with 98% ee and total conversion. Reaction also proceeded in the same terms of conversion and enantioselectivity using 0.3 mol % of catalyst loading by using a higher H₂ pressure (60 bar instead of 20 bar; see entries 1 and 2 in Table 11). The hydrogenated product, (*S*)-*m*-tyrosine methyl ester derivative **12k'**, as well as other *L*-*m*-tyrosine derivatives, has pharmaceutical applicability. Product **12k'** has been used as a synthetic intermediate in the preparation of HCV NS3 protease inhibitors¹⁷⁸ and in the total synthesis of the immunosuppressant sanglifehrin A.¹⁷⁹

Cbz-protected phenylalanine **12l'** was obtained by reduction of **11l'** using screening conditions or by halving the catalyst loading with excellent enantioselectivity (compare entries 3 and 4 in Table 11), or with only a slight decrease in enantioselectivity when MeOH was used as solvent (see entry 5 in Table 11). The aforementioned compound **12j'** is a building block in the preparation of antimigraine compounds.¹⁸⁰

tert-Butoxycarbonyl-protected acrylate **11m'** was also successfully reduced with the complexes derived from our *P-OP* ligands. Product **12m'** was obtained with full conversion and 98% ee by using ligand *ent*-**30b**, under the usual screening conditions or under optimized ones (*S/C* = 200, MeOH as solvent) (compare entries 6 and 8 in Table 11). Product **12m'** constitutes a

¹⁷⁸ Burger, M. T.; Bussiere, D.; Murray, J.; Ng, S.; Ni, Z.-J.; Pfister, K. B.; Wagman, A. S.; Zhou, Y. (Chiron Corporation). Patent WO 001406, 2007.

¹⁷⁹ (a) Nicolaou, K. C.; Ohshima, T.; Murphy, F.; Barluenga, S.; Xu, J.; Winssinger, N. *Chem. Commun.* **1999**, 809. (b) Nicolaou, K. C.; Murphy, F.; Barluenga, S.; Ohshima, T.; Wei, H.; Xu, J.; Gray, D. L. F.; Baudoïn, O. *J. Am. Chem. Soc.* **2000**, *122*, 3830.

¹⁸⁰ (a) Chaturvedula, P. V.; Chen, L.; Civiello, R.; Degnan, A. P.; Dubowchik, G. M.; Han, X.; Jiang, X. J. J.; Macor, J. E.; Poindexter, G. S.; Tora, G. O.; Luo, G. U. S. Patent 0149503, 2007. (b) Han, X.; Civiello, R. L.; Fang, H.; Wu, D.; Gao, Q.; Chaturvedula, P. V.; Macor, J. E.; Dubowchik, G. M. *J. Org. Chem.* **2008**, *73*, 8502.

valuable intermediate in the synthesis of non-natural analogs of the N-SMases inhibitor scyphostatin.¹⁸¹

Researchers at UCB-Pharma have reported the preparation of the antiseizure agent levetiracetam **90**^{114, 182} by rhodium-mediated asymmetric hydrogenation as key the step in its synthesis. We describe herein another alternative synthetic entry to this interesting compound by using *P-OP* ligands **30** in the asymmetric hydrogenation step. The structure of levetiracetam and the results obtained in this chemistry are shown in Table 12 and Scheme 38.

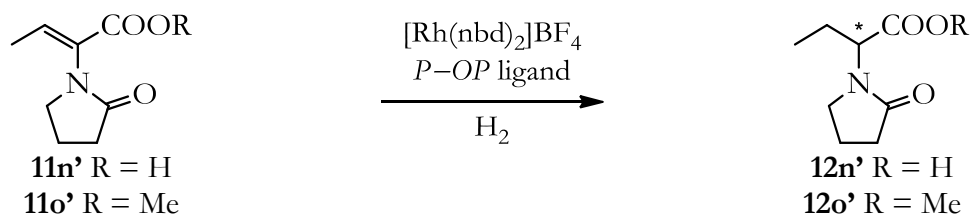
Alkene **11o'** has recently proven to be a challenging substrate in rhodium-mediated asymmetric hydrogenation, as only moderate enantioselectivities were achieved even under optimized conditions.¹⁸³ Total enantioselectivity for both enantiomers of **12n'** were achieved by using ligands **30a** or *ent*-**30b** under screening conditions (see entries 1 and 2 in Table 12). Excellent enantioselectivities were also obtained when substrate **11o'** was hydrogenated in methanol as solvent and a catalyst loading of 0.5 mol % (97% ee; compare entry 6 with 3-5 in Table 12). It has been reported that Levetiracetam **90** can be straightforwardly obtained from the hydrogenated product **12o'** (or **12n'** after sterification) by treatment with NH₃ (Scheme 38).^{114, 182a}

¹⁸¹ Cha, J. Y.; Burnett, G. L.; Huang, Y.; Davidson, J. B.; Pettus, T. R. R. *J. Org. Chem.* **2011**, *76*, 1361.

¹⁸² (a) Ates, C.; Surtees, J.; Burteau, A.-C.; Marmon, V.; Cavoy, E. (UCB, S. A.). Patent WO 014080, 2003. (b) Kenda, B. M.; Matagne, A. C.; Talaga, P. E.; Pasau, P. M.; Differding, E.; Lallemand, B. I.; Frycia, A. M.; Moureau, F. G.; Klitgaard, H. V.; Gillard, M. R.; Fuks, B.; Michel, P. *J. Med. Chem.* **2004**, *47*, 530. (c) Surtees, J.; Lurquin, F.; Diouf, O. (UCB, S. A.). Patent WO 028435, 2005.

¹⁸³ Khiri, N.; Bertrand, E.; Ondel-Eymin, M.-J.; Rousselin, Y.; Bayardon, J.; Harvey, P. D.; Jugé, S. *Organometallics* **2010**, *29*, 3622.

Table 12. Rhodium-mediated asymmetric hydrogenation of levetiracetam precursors **11n'** and **11o'** using *P-OP* ligands **30**.^[a]



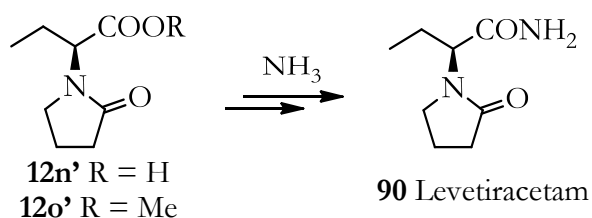
Entry	Substrate	Ligand	Observations	Conv. [%] ^[b]	ee [%] ^[c] (config.) ^[d]
1	11n'	30a	-	>99	99 (R)
2	11n'	<i>ent</i> - 30b	-	>99	99 (S)
3	11o'	30a	-	>99	98 (R)
4	11o'	<i>ent</i> - 30b	-	>99	98 (S)
5	11o'	<i>ent</i> - 30b	40 bar H ₂ , 0.5 mol % cat	>99	98 (S)
6	11o'	<i>ent</i> - 30b	0.5 mol % cat, MeOH	>99	97 (S)

^[a] Reaction conditions: [Rh(nbd)₂]BF₄/*P-OP* ligand/substrate molar ratio = 1.0 : 1.1 : 100, room temperature, 20 bar H₂, 18 h, 0.2 M in THF, unless otherwise indicated.

^[b] Conversions were determined by ¹H NMR.

^[c] Enantiomeric excesses were determined by HPLC using chiral stationary phases.

^[d] Absolute configurations were assigned by comparison with reported data.



Scheme 38. Synthesis of levetiracetam from precursors **12n'** and **12o'**.

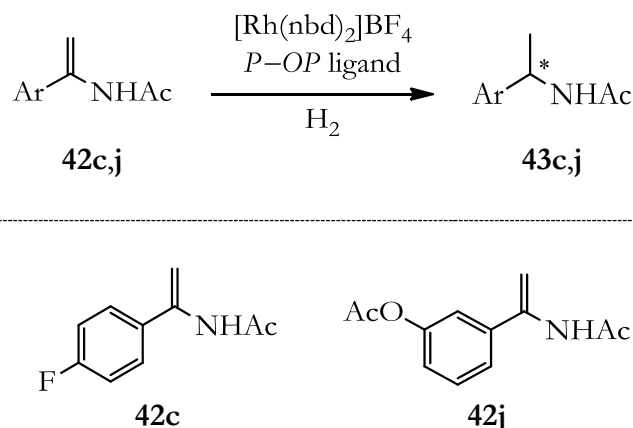
1.2.4.2 Access to Chiral Drug Precursors from α -Arylenamides and α -Arylenol Acetates

Following our studies on the preparation of valuable precursors of biologically active compounds by hydrogenation of α -(acylamino)acrylates, we also studied the asymmetric hydrogenation of α -arylenamides¹⁸⁴ towards valuable precursors of several chiral drugs (Scheme 39). Alkene **42i**, which product (*S*)-**43i** is a valuable intermediate in the synthesis of the calcimimetic agent cinacalcet hydrochloride,¹⁵⁶ was tested in our comparative ligand study (see section 1.2.3.2), affording (*S*)-**43i** with 83% ee (see entry 3 in Table 7). Alkene **42c** was successfully hydrogenated using *P-OP* ligand *ent*-**30b**, which enabled access to the (*S*)-configured product **43c** (98% ee, see entry 2 in Table 13). (*S*)-**43c** is a useful synthetic precursor of the compound denoted as AZ960¹⁸⁵ and related JAK2 kinase inhibitors¹⁸⁶ currently in clinical development for cancer therapy.

¹⁸⁴ The general synthetic procedures for α -arylenamides and α -arylenol acetates have been described in Section 1.2.3.2 and 1.2.3.3, respectively. I gratefully acknowledge Dr. H. Fernández-Pérez and Dr. P. Etayo for the loan of some substrates for catalytic purposes and for sharing the analytical methods.

¹⁸⁵ (a) Davies, A.; Lamb, M.; Lyne, P.; Mohr, P.; Wang, B.; Wang, T.; Yu, D. (Astrazeneca). Patent WO 082392, 2006. (b) Gozgit, J. M.; Bebernitz, G.; Patil, P.; Ye, M.; Parmentier, J.; Wu, J.; Su, N.; Wang, T.; Ioannidis, S.; Davies, A.; Huszar, D.; Zinda, M. *J. Biol. Chem.* **2008**, *283*, 32334.

¹⁸⁶ Wang, T.; Ioannidis, S.; Almeida, L.; Block, M. H.; Davies, A. M.; Lamb, M. L.; Scott, D. A.; Su, M.; Zhang, H.-J.; Alimzhanov, M.; Bebernitz, G.; Bell, K.; Zinda, M. *Bioorg. Med. Chem. Lett.* **2011**, *21*, 2958.



Scheme 39. Hydrogenation of α -arylenamides **42c,j** mediated by $[\text{Rh}(\text{nbd})(P-OP)]\text{BF}_4$ complexes.

The hydrogenation of 3-acetoxyphenyl-substituted enamide **42j** using the rhodium complex derived from *ent*-**30b** enabled access to the (*S*)-configured product **43j** with 98% ee under screening conditions (see entry 3 in Table 13). This substrate is a synthetic precursor of rivastigmine (**141**), a well-known chiral drug that has been used to treat dementia associated with Alzheimer's disease.¹⁸⁷ The present result represents a slight improvement in enantioselectivity with respect to the sole precedent found in the literature for the hydrogenation of the enamide **42j** described by Gridnev *et al.*¹⁸⁸

However, a more elegant access to rivastigmine (**141**) was devised by hydrogenation of the α -arylenol acetate **137i** (Scheme 40).

¹⁸⁷ For examples of routes to the asymmetric total syntheses of rivastigmine, see: (a) Han, K.; Kim, C.; Park, J.; Kim, M.-J. *J. Org. Chem.* **2010**, *75*, 3105. (b) Arunkumar, K.; Appi Reddy, M.; Sravan Kumar, T.; Vijaya Kumar, B.; Chandrasekhar, K. B.; Rajender Kumar, P.; Pal, M. *Beilstein J. Org. Chem.* **2010**, *6*, 1174., and references cited therein.

¹⁸⁸ See Ref 222 for complete information.

Table 13. Rhodium-mediated asymmetric hydrogenation of α -arylenamides **42c, j** using *P-OP* ligands **30**.^[a]

Entry	Substrate	Ligand	Observations	Conv. [%] ^[b]	ee [%] ^[c] (config.) ^[d]
1	42c ^[e]	30a	-	>99	98 (<i>R</i>)
2	42c	<i>ent</i> - 30b	-	>99	98 (<i>S</i>)
3	42j	<i>ent</i> - 30b	-	>99	98 (<i>S</i>)

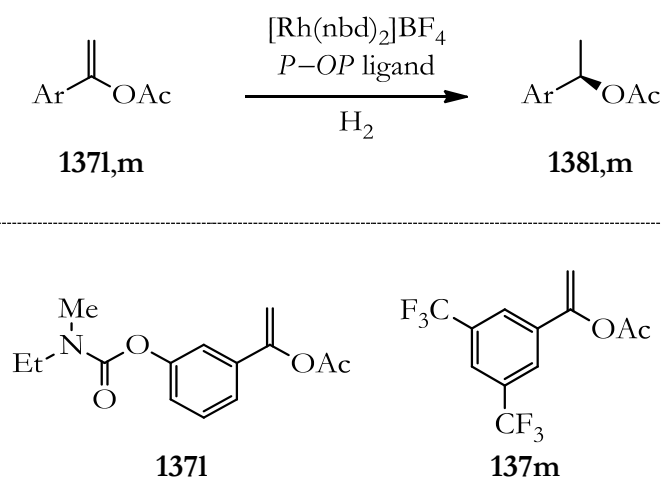
^[a] Reaction conditions: [Rh(nbd)₂]BF₄/*P-OP* ligand/substrate molar ratio = 1.0 : 1.1 : 100, room temperature, 20 bar H₂, 18 h, 0.2 M in THF, unless otherwise indicated.

^[b] Conversions were determined by ¹H NMR.

^[c] Enantiomeric excesses were determined by HPLC using chiral stationary phases.

^[d] Absolute configurations were assigned by comparison with reported data.

^[e] Results already described in Section 2.2.3.2.



Scheme 40. α -Arylenol acetates **137l,m** hydrogenated by [Rh(nbd)(**30b**)]BF₄ complex as access points to chiral drugs.

The asymmetric hydrogenation of this substrate proceeded smoothly with full conversion and in 97% ee using 0.5 mol % of catalyst (entry 1, Table 14). The resulting hydrogenation product has been recently used as a direct precursor to the pharmaceutical drug rivastigmine, which can be readily prepared by an S_N2 reaction with dimethylamine directly from the benzylic acetate **138l** (Scheme 41).^{187b} The advantage of our synthetic approach relies in

the exploitation of the acetate group, both for the creation of the stereocenter (chelation-assisting group during hydrogenation) and for the further transformations required to obtain the target molecule (nucleophilic substitution on the acetoxy-substituted carbon). Enantioselective approaches to the benzylic acetate **138l** are scarce in the literature and reported methodologies rely on lipase-mediated acetylations.^{187a, b}

In the case of the hydrogenation of the fluorinated enol acetate **137m**, the reaction proceeded also with total conversion and enantioselectivity to the desired (*R*)-configured product even with catalyst loadings of 0.5 mol % (see entries 2 and 3 in Table 14). The transformation of the hydrogenated product (*R*)-**138m** into the antiemetic drug aprepitant (**142**, Figure 38) has been described in the literature.^{189, 190} All reported enantioselective syntheses for **138m** rely on lipase-catalyzed acetylations¹⁹¹ and our asymmetric hydrogenation methodology represents an alternative synthetically useful access to **138m**.

¹⁸⁹ Vankawala, P. J.; Kolla, N.; Elati, C. R.; Sreenivasulu, M.; Kumar, K. A.; Anjaneyulu, Y.; Venkatraman, S.; Bhattacharya, A.; Mathad, V. T. *Synth. Commun.* **2007**, *37*, 3439.

¹⁹⁰ (a) Brands, K. M. J.; Payack, J. F.; Rosen, J. D.; Nelson, T. D.; Candelario, A.; Huffman, M. A.; Zhao, M. M.; Li, J.; Craig, B.; Song, Z. J.; Tschaen, D. M.; Hansen, K.; Devine, P. N.; Pye, P. J.; Rossen, K.; Dormer, P. G.; Reamer, R. A.; Welch, C. J.; Mathre, D. J.; Tsou, N. N.; McNamara, J. M.; Reider, P. J. *J. Am. Chem. Soc.* **2003**, *125*, 2129. (b) Brands, K. M. J.; Krska, S. W.; Rosner, T.; Conrad, K. M.; Corley, E. G.; Kaba, M.; Larsen, R. D.; Reamer, R. A.; Sun, Y.; Tsay, F.-R. *Org. Process Res. Dev.* **2006**, *10*, 109.

¹⁹¹ (a) Matsuda, T.; Tsuji, K.; Kamitanaka, T.; Harada, T.; Nakamura, K.; Ikariya, T. *Chem. Lett.* **2005**, *34*, 1102. (b) Bogar, K.; Bäckvall, J.-E. *Tetrahedron Lett.* **2007**, *48*, 5471.

Table 14. Rhodium-mediated asymmetric hydrogenation of α -aryl enol acetates **137l,m** using **30b**.^[a]

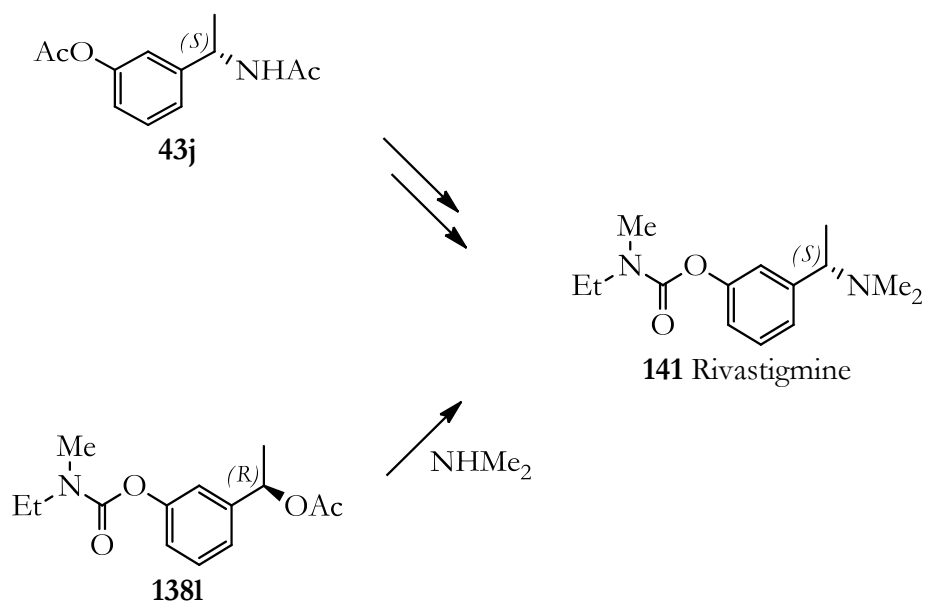
Entry	Substrate	Ligand	Observations	Conv. [%] ^[b]	ee [%] ^[c] (config.) ^[d]
1	137l	30b	0.5 mol % cat	>99	97 (R)
2	137m	30b	-	>99	99 (R)
3	137m	30b	0.5 mol % cat	>99	99 (R)

^[a] Reaction conditions: [Rh(nbd)₂]BF₄/P-OP ligand/substrate molar ratio = 1.0 : 1.1 : 100, room temperature, 20 bar H₂, 18 h, 0.2 M in THF, unless otherwise indicated.

^[b] Conversions were determined by ¹H NMR.

^[c] Enantiomeric excesses determined by GC or HPLC using chiral stationary phases.

^[d] Absolute configurations were assigned by comparison with reported data.



Scheme 41. Synthetic routes to access rivastigmine **141** from **43j** or **138l**.

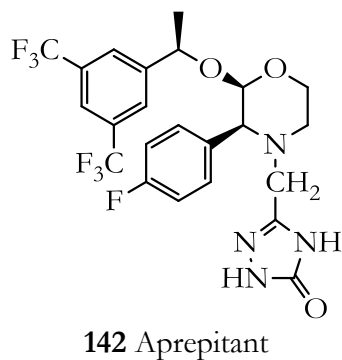


Figure 38. Aprepitant **142** (drug against chemotherapy induced side-effects).

1.2.4.3 Access to Chiral Drug Precursors of Lacosamide by Hydrogenation of β -Alkoxy-substituted α -(Acylamino)acrylates

Epilepsy is a complex neurological disorder which affects individuals regardless of age, gender or socioeconomic status. This disorder affects nearly 50 million people worldwide,¹⁹² and more than 2 million people suffer from epilepsy and its consequences in the United States alone.¹⁹³ The life-time prevalence of this disease is approximately 1% and epilepsy requires prolonged or life-long drug therapy with the administration of anticonvulsant drugs.¹⁹⁴

Lacosamide (**143**, Figure 39),^{151,152} (Trade Name: Vimpat[®], owned by UCB Pharma) is the (*R*)-enantiomer of *N*-benzyl-2-acetamido-3-methoxypropionamide, which was approved by the FDA in 2008 as an add-on therapy for partial-onset seizures in adults with epilepsy. It is believed that lacosamide enhances the slow inactivation of voltage-gated Na⁺ channels and binds to dihydropyrimidinase-related protein 2 (CRMP 2), and thus controls the seizures.¹⁹⁵

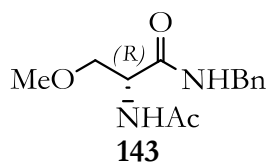


Figure 39. (*R*)-Lacosamide.

The (*R*)-stereoisomer of lacosamide (**143**) was approximately 10 times more potent in the control of Maximal Electroshock Seizure (MES)-induced

¹⁹² Duncan, J. S.; Sander, J. W.; Sisodiya, S. M.; Walker, M. C. *Lancet* **2006**, *367*, 1087.

¹⁹³ See, for example: (a) Begley, C. E.; Annegers, J. F.; Lairson, D. R.; Reynolds, T. F.; Hauser, W. A. *Epilepsia* **1994**, *35*, 1230. (b) Begley, C. E.; Lairson, D. R.; Reynolds, T. F.; Coan, S. *Epilepsy Res.* **2001**, *47*, 205.

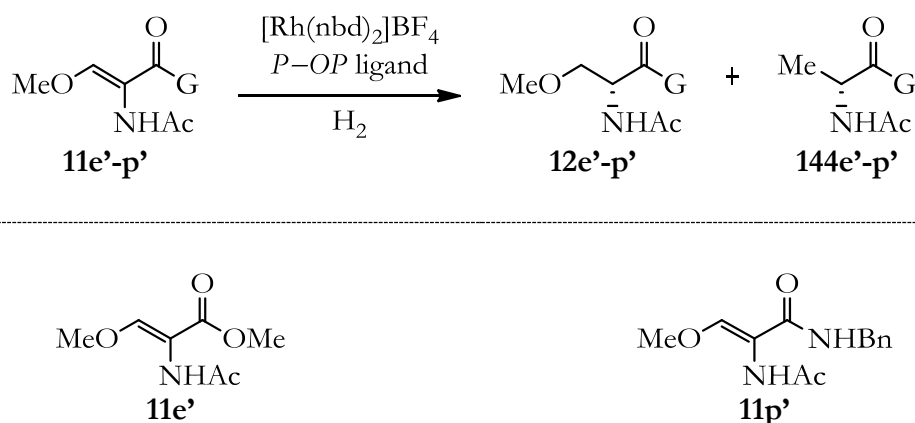
¹⁹⁴ (a) Dichter, M. A.; Brodie, M. J. *N. Engl. J. Med.* **1996**, *334*, 1583. (b) Aiken, S. P.; Brown, W. M. *Front. Biosci.* **2000**, *5*, E124.

¹⁹⁵ Bialer, M.; White, H. S. *Nat. Rev. Drug Discovery* **2010**, *9*, 68.

seizure test,¹⁹⁶ than the (*S*)-enantiomer. This difference in activity is amongst the highest eudismic ratio¹⁹⁷ reported for MES-selective anticonvulsants.

Commercially, lacosamide is prepared using a chiral pool approach starting from unnatural amino acid D-serine and its derivatives.¹⁵¹ To the best of this author's knowledge and at the time the experimental work of this PhD thesis was being carried out, there was only one reported asymmetric synthesis of this molecule, which relied on a hydrolytic kinetic resolution strategy.^{151e} Herein is described an alternative route to lacosamide by enantioselective hydrogenation catalyzed by chiral rhodium complexes of a β -alkoxy-substituted α -(acylamino)acrylate to introduce the only stereocenter present in the molecule.

For this purpose, we synthesized β -alkoxy-substituted α -(acylamino)acrylates **11e'**, and **11p'** and tested them in asymmetric hydrogenation using our *P-OP* ligands. It should be recalled at this point that **11p'** is the direct precursor of lacosamide.

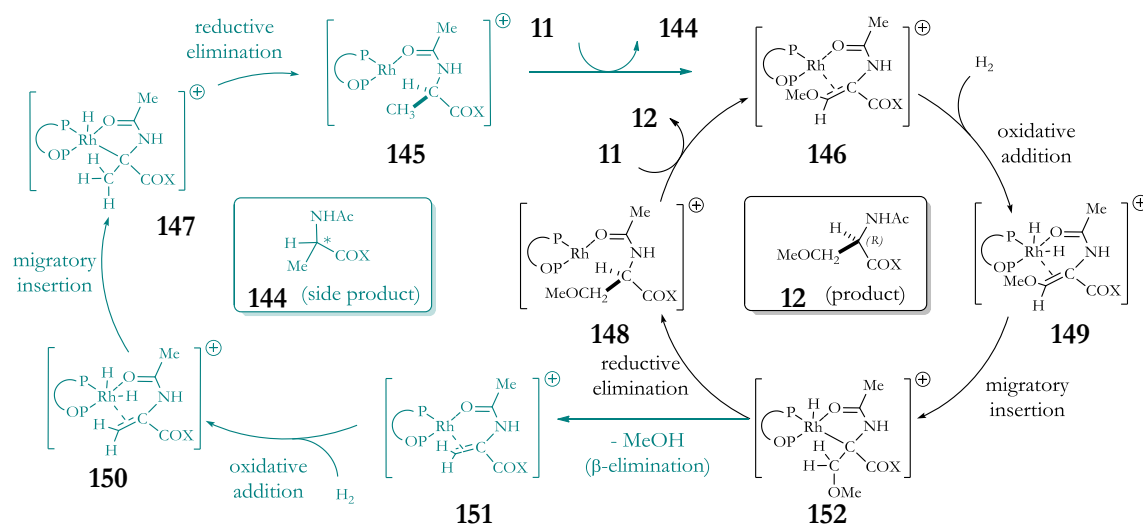


Scheme 42. Lacosamide precursors hydrogenated by $[\text{Rh}(\text{nbd})(\text{P-OP})]\text{BF}_4$ complexes.

¹⁹⁶ CasteI-Branco, M. M.; Alves, G. L.; Figueiredo, I. V.; Falcao, A. C.; Caramona, M. M. *Methods Find. Exp. Clin. Pharmacol.* **2009**, *31*, 101.

¹⁹⁷ The eudismic ratio indicates the ratio of activities of the two enantiomers. See Lehmann, F. P. A. *Trends Pharmacol. Sci.* **1982**, *3*, 103.

The hydrogenation of substrate **11e'** as model substrate with the Rh complex derived from **30a** afforded full conversion and an excellent enantioselectivity of 97% ee towards the desired (*R*)-configured product under standard screening conditions (1.0 mol % cat., THF, room temperature, 20 bar H₂). However, although the conversion of the starting alkene **11e'** was complete, the selectivity of the reaction was only 85% as the hydrogenated MeOH-elimination product **144e'** was also obtained in 15% amount (see Scheme 42 and entry 1 in Table 15). According to related examples in the literature,¹⁹⁸ the formation of the hydrogenated MeOH-elimination **144** may be rationalized as a side reaction of the hydride intermediates **152** involved in the hydrogenation catalytic cycle of alkenes **11** (see Scheme 43). Elimination from hydride intermediates¹⁹⁹ **152** releases MeOH along with the rhodium complex of 2-acetamidoacrylic acid derivatives **151**, which further evolves to **144** by hydrogenation.



Scheme 43. Formation of hydrogenated MeOH-elimination products **144** under hydrogenation conditions.

¹⁹⁸ For a closely related precedent of such a side reaction, see Ramer, S. E.; Moore, R. N.; Vederas, J. C. *Can. J. Chem.* **1986**, *64*, 706.

¹⁹⁹ For related transformations, see: Matsuda, T.; Shiose, S.; Suda, Y. *Adv. Synth. Catal.* **2011**, *353*, 1923, and references cited therein.

The formation of undesired hydrogenated MeOH-elimination product **144** could not be circumvented by using the rhodium complex derived from trityl-substituted ligand **30b** instead. Complete conversion was observed, although the selectivity achieved in this case was only 67% (compare entries 1 and 2 in Table 15). Catalysis experiments were then done using other solvents. When MeOH was used, only 10% of the desired hydrogenation product was found in the final mixture. Most gratifyingly, when DCM was employed, the selectivity of the reaction increased to 96% without erosion of the enantioselectivity (see entries 3 and 4 in Table 15).

The rhodium complex derived from *P-OP* ligand **153**, analogous to **30a** and developed by Dr. Etayo,²⁰⁰ mediated the hydrogenation of substrate **11e'** in dichloromethane with almost no methanol elimination (99% selectivity) and in very high enantioselectivity (96% ee, entry 5 in Table 15). The first reported enantioselective total synthesis of lacosamide **143** was developed by Dr. Etayo by hydrogenating Lacosamide precursor **11p'** with the rhodium complex derived from ligand **153** in DCM, affording Lacosamide **143** with perfect selectivity and excellent enantioselectivity (99% ee, entry 6 in Table 15). The measured specific rotation for **143** was in perfect agreement with the reported value (**143** $[\alpha]_D^{26} = +16.7$ (*c* 0.74, MeOH); lit.^{151c} $[\alpha]_D^{25} = +16.1$ (*c* 0.9, MeOH)), definitely confirming the absolute configuration of the hydrogenation product.

After publication of the results described in this section in 2011,^{200, 201} a patent describing the synthesis of Lacosamide by asymmetric hydrogenation using (*S,S*)-Ph-BPE or (*R,R*)-DIPAMP as chiral ligands was published.²⁰²

²⁰⁰ Etayo, P.; Núñez-Rico, J. L.; Vidal-Ferran, A. *Organometallics* **2011**, *30*, 6718.

²⁰¹ Etayo, P.; Núñez-Rico, J. L.; Fernández-Pérez, H.; Vidal-Ferran, A. *Chem.-Eur. J.* **2011**, *17*, 13978.

²⁰² Merschaert, A.; Bouvy, D.; Vasselin, D.; Carly, N. (UCB Pharma, S. A.). Patent WO2012041986A1, 2012.

Table 15. Rhodium-mediated asymmetric hydrogenation of β -methoxy substituted α -(acylamino)acrylates **11c'**, **p'** using *P-OP* ligands.^[a]

Entry	Subst.	Ligand	Observations	Conv. [%] ^[b]	Select. [%] ^[b]	ee [%] ^[c] (config.) _[c]
1	11e'	30a	-	>99	85	97 (R)
2	11e'	30b	-	>99	67	96 (R)
3	11e'	30a	MeOH	>99	10	90 (R)
4	11e'	30a	DCM	>99	96	97 (R)
5 ^[e]	11e'	153 ^[f]	2.0 mol % cat., DCM	>99	99	96 (R)
6 ^[e]	11p'	153 ^[f]	2.0 mol % cat., DCM	>99	>99	99 (R)

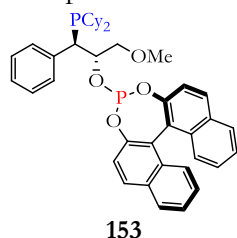
^[a] Reaction conditions: [Rh(nbd)₂]BF₄/*P-OP* ligand/substrate molar ratio = 1.0 : 1.1 : 100, room temperature, 20 bar H₂, 18 h, 0.2 M in THF, unless otherwise indicated.

^[b] Conversions and selectivities were determined by ¹H NMR.

^[c] Enantiomeric excesses were determined by GC using chiral stationary phases.

^[d] Absolute configurations were assigned by comparison with reported data.

^[e] Experiment carried out by Dr. P. Etayo, using the following *P-OP* ligand:

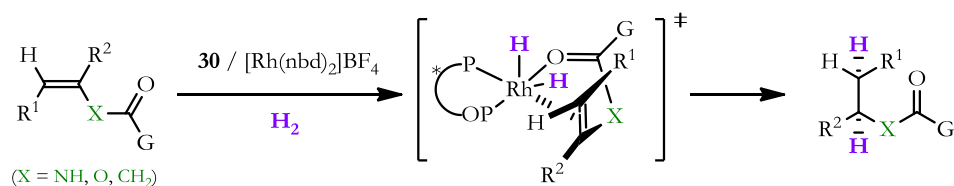


^[f] Preformed complex, [Rh(nbd)(**153**)]BF₄.

1.2.5 Rationalization of the Stereochemical Outcome of the Reaction

As it has been previously indicated in the previous sections, cationic rhodium(I) complexes of ligands **30a,b** catalyze hydrogenations leading to (*R*)-configured products derived from α -(acylamino)acrylates, α -arylenamides and α -arylenol esters (with the exception of enol ester phosphonate **40a**, whose hydrogenation product has the (*S*)-configuration), whilst those derived from itaconic acid derivatives and analogs present the (*S*)-configuration. It is worth mentioning at this point, that the change to the (*S*)-configuration in the hydrogenation products of itaconic acid derivatives and analogs (**39**), as well as for the product derived from enol ester phosphonate **40a**, is due to an inversion in the CIP priority rules. Thus, regarding the stereochemical outcome of the $[\text{Rh}(\mathbf{30})]^+$ -catalyzed asymmetric hydrogenations for all reported substrates, ligands **30** consistently mediate the coordination of the functionalized alkenes around the rhodium center in an analogous way. A schematic view of the hydrogenation reaction mediated by rhodium complexes derived from ligand **30** is presented in Scheme 44, in which the two new carbon-hydrogen bonds are formed from the side of the double bond of the metal during the catalytic process.¹⁰²

Computational studies on the origin of enantioselection in the asymmetric hydrogenation of methyl 2-acetamidoacrylate **11d** catalyzed by rhodium complexes of **30** have provided the basis for the simple analyses of quadrant diagrams.⁸² As indicated in Section 1.1.3, page 61, the two right-hand quadrants are disfavoured by the electronic effects of the BINOL-derived phosphite group, whereas the upper-left quadrant is blocked by the steric effects of the binaphthyl unit, which points towards the substrate for (*S_a*)-con-



α -(acylamino)acrylates (20 examples)
 itaconic acid derivatives (7 examples)
 α -substituted enamides (14 examples)
 α -substituted enol esters (7 examples)

Scheme 44. Schematic view of the hydrogenation reaction of a functionalized alkene catalyzed by rhodium complexes derived from **30**.

figured BINOL scaffold. This spatial arrangement can be visualized in the quadrant diagrams of a generic substrate showed in Figure 40 by considering that the two right-hand sites are electronically disfavoured with respect to the placement of the C_α and C_β olefin carbon atoms (represented in yellow in Figure 40). The difference with the placement of C_α in the two left-hand quadrants is associated with steric effects. Since steric hindrance in the transition state of the rate- and stereo-determining step (oxidative addition) is developed in the quadrant originally occupied by the C_α olefin carbon,¹⁰² its placement in the lower-left quadrant, far from the steric congestion of the binaphthyl group, is strongly favoured.

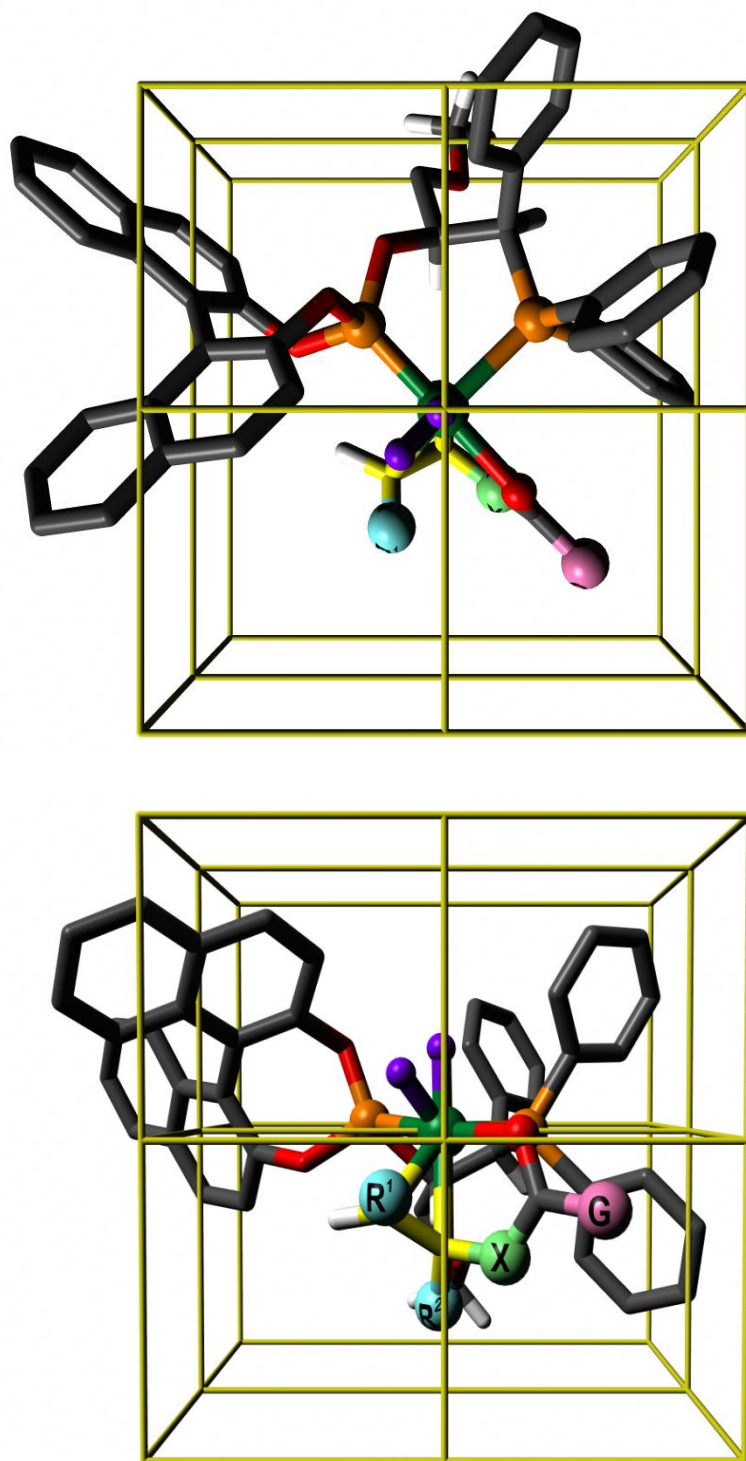
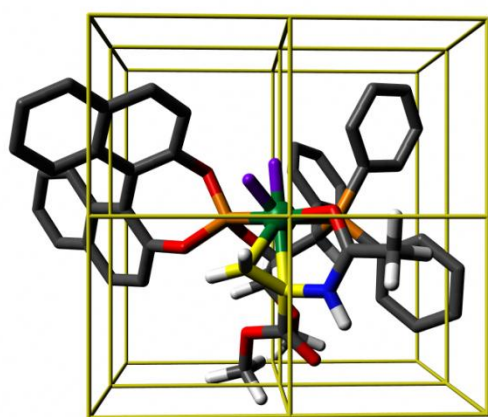
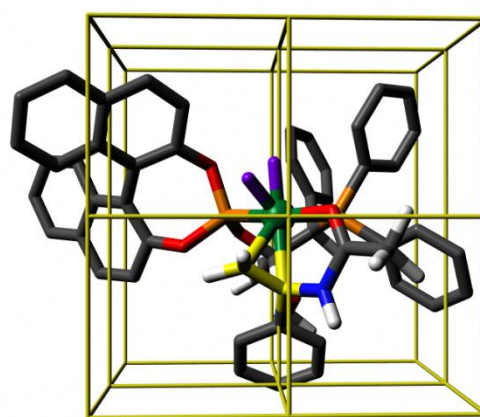


Figure 40. Top: Overhead view, Bottom: Frontal view. Quadrant diagram for a 3D model of the favorable transition state of the enantioselective hydrogenations catalyzed by the rhodium complex of ligand **30a**, for a general structure of a functionalised alkene. (Color key: green = rhodium; orange = phosphorus; red = oxygen; purple = hydrido ligand; yellow = C_{α} and C_{β} carbon atoms; white = hydrogen; pale blue, green and pink = alkene substituents.)

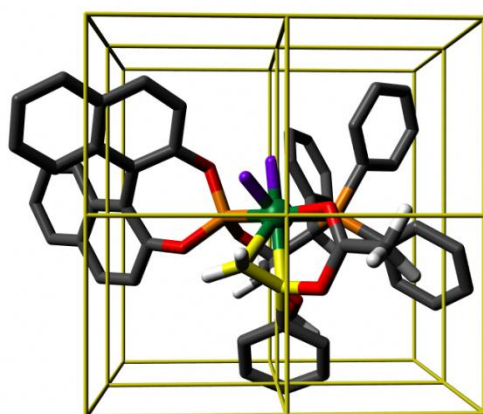
To conclude, three quadrants are blocked in the case of $[\text{Rh}(\mathbf{30})]^+$ catalysts, and this leaves the olefin with only one low-energy direction of approach: the C=C bond is placed in the lower left quadrant and is coordinated *trans*- to the phosphino group (frontal views of the CAChe minimized 3D models for the four types of substrates are depicted in Figure 41). Dihydrogen will then be added across the olefin, thus forming two new carbon-hydrogen bonds from the double bond side towards the metal during the catalytic process. Therefore, (*R*)-, (*S*)-, (*R*)- and (*R*)-configured hydrogenation products are obtained from α -(acylamino)acrylate derivatives, itaconic acid derivatives and analogs, α -arylenamides, and α -substituted enol esters, respectively.



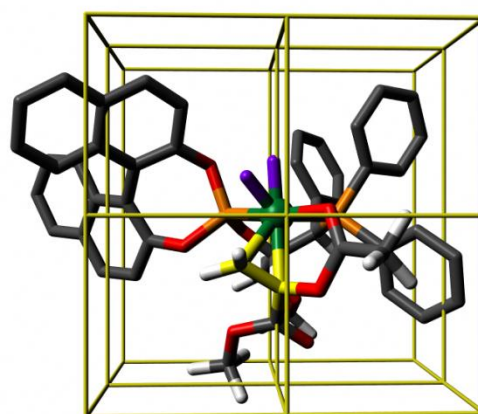
Methyl 2-acetamidoacrylate, **11d**



N-(1-phenylvinyl)acetamide, **42a**



1-Phenylvinyl acetate, **137a**



Dimethyl itaconate, **38a**

Figure 41. Frontal views of the OATS 3D structures for the four types of substrates (Figure 40 for color codes).

1.3 EXPERIMENTAL SECTION

1.3.1 General Remarks

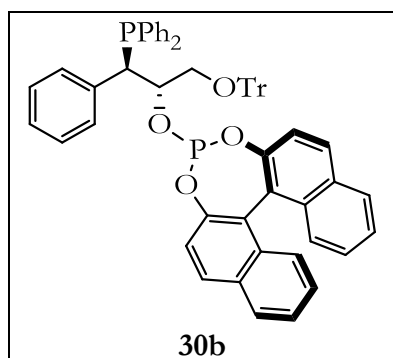
All syntheses were carried out on chemicals purchased from commercial sources unless otherwise stated. All manipulations and reactions were run under inert atmosphere using anhydrous solvents, in either a Braun glove box or with standard Schlenk-type techniques. Glassware was dried under vacuum and heated with a hot air gun before use. All solvents were dried by using a Solvent Purification System (SPS). Silica gel 60 (230–400 mesh) was used for column chromatography. NMR spectra were recorded in CDCl_3 unless otherwise stated, on a Bruker Avance 400 MHz or 500 MHz Ultrashield spectrometer. ^1H NMR and ^{13}C NMR chemical shifts are quoted in ppm relative to residual solvent peaks, whereas $^{31}\text{P}\{^1\text{H}\}$ NMR chemical shifts are quoted in ppm relative to 85% phosphoric acid in water. $^{11}\text{B}\{^1\text{H}\}$ NMR chemical shifts are quoted in ppm relative to $\text{BF}_3\cdot\text{OEt}_2$ in CDCl_3 . $^{19}\text{F}\{^1\text{H}\}$ NMR chemical shifts are quoted in ppm relative to $\text{BF}_3\cdot\text{OEt}_2$ in CDCl_3 . High resolution mass spectra (HRMS) were recorded by using ESI or APCI ionization methods in positive mode. Optical rotations were measured on a Jasco P-1030 polarimeter. Melting points were measured in open capillaries on a Büchi B-540 instrument and are uncorrected. Enantiomeric excesses were determined by GC or HPLC on using chiral stationary phases. GC analyses were performed on an Agilent 6890N chromatograph equipped with a FID detector. HPLC analyses were performed on an Agilent 1200 Series chromatograph equipped with a diode array UV detector.

Crystal structure determination was carried out using a Bruker-Nonius diffractometer equipped with APPEX 2 4K CCD area detector, a FR591 rotating anode with $\text{Mo}_{\text{K}\alpha}$ radiation, Montel mirrors as monochromator and a Kryoflex low temperature device ($T = 100\text{K}$). Fullsphere data was collected using omega and phi scans. Apex2 V. 1.0-22 (Bruker-Nonius 2004) for the data reduction and SADABS V. 2.10 (2003) for the absorption correction. Crystal structure was achieved using direct methods as implemented in SHELXTL Version 6.10 (Sheldrick, Universität Göttingen (Germany), 2000). Least-squares refinement on F2 using all measured intensities was carried out using the program SHELXTL Version 6.10 (Sheldrick, Universität Göttingen (Germany), 2000). All non-hydrogen atoms were refined including anisotropic displacement parameters.

1.3.2 Synthesis of Ligands

The preparation and full characterization of phosphine-phosphinite ligands **21a** and **21b**, and phosphine-phosphite ligands **133a**, **133b**, **30a** and **134a** have previously been reported by our group,^{73, 81, 82} and the physical and spectroscopic data obtained from their syntheses were found to be identical to those previously reported.

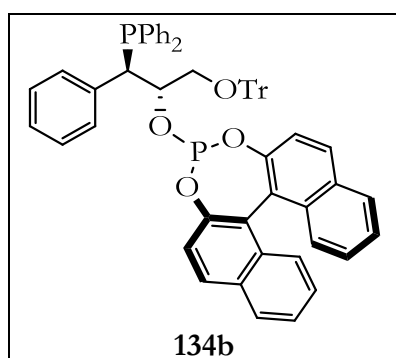
Phosphine-phosphite ligands **30b** and **134b** were synthesized *via* a simplified experimental procedure with respect to that previously reported: The phosphine-borane complex **127b** (1.0 mmol) and 1,4-diazabicyclo[2.2.2]octane (2.2 mmol) were loaded into a dried Schlenk flask, which was quickly purged by doing four fast vacuum/argon cycles. Toluene (15.0 mL) was added and the flask was dipped into a 60 °C oil bath. After 2h, it was allowed to cool down to r.t. Then, a solution of the adequate chlorophosphite (1.1 mmol) in toluene (5.0 mL) was added dropwise *via* cannula onto the reaction mixture. The resulting mixture was stirred overnight at room temperature. The reaction mixture was introduced into the glove box and filtered through a very short pad of previously dried and deoxygenated silica gel. The pad was washed with 10.0 mL of toluene. The filtrate was concentrated *in vacuo* and then purified by a short silica gel chromatography using hexanes/Et₂O as eluent in the glove box to give the corresponding phosphine-phosphites **30b** and **134b** as white solids.



Phosphine-phosphite **30b** was synthesized following the general procedure, starting from the corresponding phosphine-borane adduct **127b** (0.600 g, 1.01 mmol), DABCO (0.255 g, 2.23 mmol), and (*S*)-(binaphthalene-2,2'-diyl)chlorophosphite (0.391 g, 1.11 mmol). The product was obtained as a white solid (0.434 g, 48% yield) after chromatography with silica gel (hexanes/Et₂O 67:33). M.p.

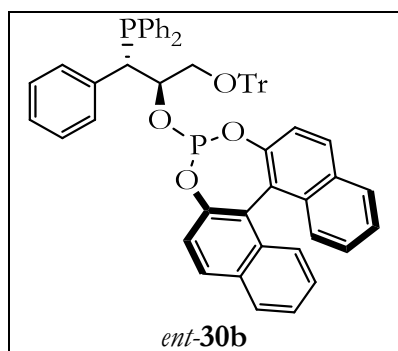
111.8–120.6 °C; $[\alpha]_D^{25} = +95.0$ ($c = 0.40$, THF); ¹H NMR (400 MHz, CDCl₃) δ 7.95-7.90 (m, 2H), 7.84-7.82 (m, 1H), 7.67-7.63 (m, 2H), 7.52-7.16 (m, 29H), 7.08-6.94 (m, 7H), 6.77-6.74 (m, 1H), 4.77-4.70 (m, 1H), 3.82 (dd, $J = 4.6$ Hz, $J = 4.6$ Hz, 1H), 3.14 (dd, $J = 9.9$ Hz, $J = 5.3$ Hz, 1H), 3.07 (dd, $J = 9.9$ Hz, $J = 7.0$ Hz, 1H); DEPTQ 135 (100 MHz, CDCl₃) δ 148.04 (C), 148.00 (C), 147.7 (C), 143.6 (C), 136.5 (C), 136.4 (C), 136.3 (C), 136.2 (C), 134.7 (CH), 134.4 (CH), 133.4 (CH), 133.2 (CH), 132.8 (C), 132.5 (C), 131.4 (C), 131.0 (C), 130.8 (CH), 130.7 (CH), 130.0 (CH), 129.6 (CH), 129.2 (CH), 128.74 (CH), 128.67 (CH), 128.3

(CH), 128.2 (CH), 128.1 (CH), 127.84 (CH), 127.81 (CH), 127.73 (CH), 127.66 (CH), 127.1 (CH), 127.0 (CH), 126.5 (CH), 126.0 (CH), 125.8 (CH), 124.8 (CH), 124.6 (CH), 124.44 (CH), 124.39 (C), 122.8 (C), 122.3 (CH), 122.1 (CH), 87.4 (C), 76.0 (dd, $J = 18.2$ Hz, $J = 18.2$ Hz, CH), 65.8 (CH₂), 48.3 (dd, $J = 15.8$ Hz, $J = 4.3$ Hz, CH); ³¹P{¹H} NMR (162 MHz, CDCl₃) δ 156.2 (d, $J = 18.2$ Hz, P-O), -7.1 (d, $J = 18.2$ Hz, P-C); HRMS (ESI) calcd for C₆₀H₄₇O₄P₂ [(M+H)⁺] 893.2950, found 893.2954.



Phosphine-phosphite **134b** was synthesized following the general procedure, starting from the corresponding phosphine-borane adduct **127b** (0.800 g, 1.35 mmol), DABCO (0.340 g, 2.97 mmol), and (*R*)-(binaphthalene-2,2'-diyl)chlorophosphite (0.537 g, 1.49 mmol). The product was obtained as a white solid (0.697 g, 58% yield) after chromatography with silica gel (hexanes/Et₂O 75:25). M.p.

171.4–176.7 °C; [α]_D²⁵ = -275.3 ($c = 1.30$, THF); ¹H NMR (400 MHz, CDCl₃) δ 7.91-7.82 (m, 4H), 7.68-7.64 (m, 2H), 7.42-7.02 (m, 36H), 4.77-4.70 (m, 1H), 3.73 (dd, $J = 4.9$ Hz, $J = 4.9$ Hz, 1H), 3.06 (dd, $J = 9.9$ Hz, $J = 4.4$ Hz, 1H), 2.92 (dd, $J = 9.9$ Hz, $J = 8.4$ Hz, 1H); ¹³C{¹H} NMR (100 MHz, CDCl₃) δ 148.45 (C), 148.41 (C), 147.77 (C), 147.75 (C), 143.8 (C), 136.9 (C), 136.8 (C), 136.5 (C), 136.4 (C), 135.9 (C), 135.8 (C), 134.7 (CH), 134.5 (CH), 133.4 (C), 133.2 (C), 131.4 (C), 131.2 (C), 130.5 (CH), 130.4 (CH), 129.9 (CH), 129.7 (CH), 129.3 (CH), 128.80 (CH), 128.75 (CH), 128.2 (CH), 128.0 (CH), 127.81 (CH), 127.77 (CH), 127.7 (CH), 127.1 (CH), 127.0 (CH), 126.9 (CH), 126.6 (CH), 126.0 (CH), 125.8 (CH), 124.8 (CH), 124.6 (CH), 124.4 (C), 124.3 (C), 123.0 (CH), 122.9 (CH), 122.81 (C), 122.80 (C), 122.0 (CH), 87.6 (C), 76.4 (dd, $J = 20.3$ Hz, $J = 20.3$ Hz, CH), 66.2 (d, $J = 2.6$ Hz, CH₂), 48.3 (dd, $J = 16.4$ Hz, $J = 5.7$ Hz, CH); ³¹P{¹H} NMR (162 MHz, CDCl₃) δ 157.1 (d, $J = 3.1$ Hz, P-O), -7.1 (bs, P-C); HRMS (ESI) calcd for C₆₀H₄₇O₄P₂ [(M+H)⁺] 893.2950, found 893.2936.



Enantiomerically pure *P-OP* ligand *ent-30b*, the enantiomer of phosphine-phosphite **30b**, has been prepared by following the same experimental procedures that were previously used for the synthesis of ligand **30b**. The synthetic route towards the newly designed phosphine-phosphite *ent-30b* started from commercially available (2*R*,3*R*)-2,3-epoxy-3-phenyl-1-propanol,²⁰³ which was protected as the corresponding triphenylmethyl ether derivative *ent-126b* on using standard reaction conditions.¹³⁷ Enantiopure epoxy ether *ent-126b* was a known compound and physical and spectroscopic data obtained for this compound were perfectly in agreement with those previously reported in the literature.²⁰⁴ The ring-opening of epoxide *ent-126b* with potassium diphenylphosphide as the nucleophile proceeded smoothly at -30 °C to room temperature and took place in a regioselective and stereospecific manner, accordingly to the ring-opening of its enantiomer **126b** under the same reaction conditions. After in situ protection of the phosphino alcohol intermediate as borane adduct, the resulting phosphine-borane *ent-127b* was isolated in 78% overall yield from epoxy ether *ent-126b*. Physical and spectroscopic data of compound *ent-127b* were identical to the reported data for its enantiomer **127b**. The specific rotation measured for phosphine-borane *ent-127b* ($[\alpha]_D^{26} = +89.6$ (c 1.03, CHCl_3)) matched with the described value for its enantiomer ($[\alpha]_D^{25} = -83.7$ (c 1.00, CHCl_3)),⁷³ finding an opposite sign of the optical rotation. The preparation of phosphine-phosphite *ent-30b* was further accomplished by following the above mentioned one-pot procedure. This one-pot protocol involved DABCO-mediated deprotection of borane adduct *ent-127b* and subsequent *O*-phosphorylation reaction by treatment with commercially available chlorophosphite derived from (*R_a*)-BINOL (**132**). After column chromatography purification, the desired ligand *ent-30b* was isolated in 66% overall yield from phosphine-borane *ent-127b*. Physical and spectroscopic data obtained for *P-OP* ligand *ent-30b* were identical to the data reported for its enantiomer **30b**. The specific rotation measured for phosphine-phosphite *ent-30b* ($[\alpha]_D^{28} = -101.0$ (c 0.40, THF)) matched

²⁰³ The enantiomeric purity of epoxy alcohol **1**, as received from Aldrich® supplier, was determined to be greater than 99% *ee* by HPLC analysis [Daicel Chiralcel® OD-H (25 cm x 0.46 cm), 95:5 *n*-hexane/2-propanol, 1.0 mL/min, 216 nm, $t_R(S,S) = 21.2$ min, $t_R(R,R) = 24.0$ min].

²⁰⁴ Wang, Z.-X.; Tu, Y.; Frohn, M.; Zhang, J.-R.; Shi, Y. *J. Am. Chem. Soc.* **1997**, *119*, 11224.

with the value for its enantiomer **30b** ($[\alpha]_D^{25} = +95.0$ (c 0.40, THF)), finding an opposite sign of the optical rotation.

1.3.2.1 Synthesis of Rhodium Complexes

Rhodium complexes **135** and **136** were prepared following the described procedures.⁸² The corresponding phosphine-phosphite **30a** or **134a** (1.0 mmol) and $[\text{Rh}(\text{nbd})_2]\text{BF}_4$ (0.98 mmol) were loaded into a flame-dried Schlenk flask to which DCM (6.0 mL) was added. The reaction mixture was stirred at room temperature for 4h, after which the DCM was evaporated off until the mixture had one fourth of its original volume. Diethyl ether (15.0 mL) was added, and a precipitate was formed. The mother liquor was extracted and the orange solid washed with a small quantity of diethyl ether (2 x 5.0 mL) to give the desired rhodium complexes as orange powders.

$[\text{Rh}(\text{nbd})(\mathbf{30a})]\text{BF}_4$ (**135**)

Rhodium complex **135** was prepared following the general procedure starting from $[\text{Rh}(\text{nbd})_2]\text{BF}_4$ (0.097 g, 0.242 mmol). It was obtained as an orange powder (0.217 g, 0.229 mmol, 95% yield). Physical and spectroscopic data obtained were in perfect agreement with the reported.⁸²

$[\text{Rh}(\text{nbd})(\mathbf{134a})]\text{BF}_4$ (**136**)

Rhodium complex **136** was prepared following the general procedure starting from $[\text{Rh}(\text{nbd})_2]\text{BF}_4$ (0.067 g, 0.178 mmol) and ligand **134a**. It was obtained as an orange powder (0.165 g, 0.174 mmol, 98% yield). ^1H NMR (500 MHz, CD_2Cl_2) δ 8.39 (d, $J = 8.5$ Hz, 1H), 8.32-8.25 (m, 2H), 8.14 (d, $J = 8.5$ Hz, 1H), 8.50-7.15 (m, 21H), 6.59-6.51 (m, 2H), 5.87 (bs, 1H), 5.65 (bs, 1H), 5.11 (bs, 1H), 4.59 (bs, 1H), 4.42-4.34 (m, 1H), 4.22-4.10 (m, 3H), 3.07-3.01 (m, 1H), 2.99 (s, 3H), 2.95-2.90 (m, 1H), 1.66 (bs, 2H); $^{13}\text{C}\{^1\text{H}\}$ NMR (125 MHz, CD_2Cl_2) δ 147.2 (d, $J = 13.0$ Hz, C), 146.0 (d, $J = 7.1$ Hz, C), 135.5 (d, $J = 13.4$ Hz, CH), 133.6 (CH), 132.6 (C), 132.1 (C), 131.9 (C), 131.8 (CH), 131.7 (CH), 131.6 (C), 131.1 (CH), 130.7 (CH), 130.3 (CH), 129.4 (CH), 129.19 (CH), 129.22 (CH), 128.9 (CH), 128.8 (CH), 128.5 (CH), 127.7 (C), 127.4 (C), 127.2 (CH), 127.0 (CH), 126.9 (CH), 126.6 (CH), 126.3 (CH), 125.9 (CH), 123.0 (C), 121.8 (C), 120.6 (CH), 101.4 (CH), 100.2 (CH), 89.7 (CH), 88.6 (CH), 74.8 (d, $J = 6.3$ Hz, CH), 72.1 (CH_2), 70.8 (dd, $J = 8.1$ Hz, $J = 8.1$ Hz, CH_2), 58.9

(CH₃), 55.8 (CH), 55.0 (CH), 42.5 (d, $J = 29.7$ Hz, CH); ³¹P{¹H} NMR (202 MHz, CD₂Cl₂) δ 137.3 (dd, $J = 267.7$ Hz, $J = 67.0$ Hz, P-O), 26.0 (dd, $J = 146.4$ Hz, $J = 67.0$ Hz, P-C); ¹¹B{¹H} NMR (128.4 MHz, CD₂Cl₂) δ -1.1; ¹⁹F{¹H} NMR (376 MHz, CD₂Cl₂) δ -153.2; HRMS (ESI) calcd for C₄₉H₄₂O₄P₂Rh [(M-BF₄)⁺] 859.1608, found 859.1626.

1.3.3 Preparation and Characterization of Substrates

Methyl 2-((benzyloxycarbonyl)amino)acrylate **11w** (Aldrich[®]), 1-(Trifluoromethyl)vinyl acetate **137h** (Acros Organics[®]), 1-cyanovinyl acetate **137i** (Aldrich[®]), dimethyl itaconate **38a** (Aldrich[®]), itaconic acid **38b** (Aldrich[®]), and ethyl 2-(hydroxymethyl)acrylate **38f** (TCI[®]), methyl 2-(bromomethyl)acrylate **38g** (Aldrich[®]), (*Z*)-Methyl 2-acetamido-3-(3,4-diacetoxyphenyl)acrylate **11g'** (Toronto Research Chemicals[®]) and (*Z*)-methyl 2-acetamido-3-(2,5-difluorophenyl)acrylate **11h'** (Gencore BioPharma[®]) are all commercially available substrates which were used as received from the chemical supplier cited in brackets.

(*Z*)-methyl 2-acetamido-2-butenolate **11x**,²⁰⁵ (*Z*)-methyl 2-((*tert*-butoxycarbonyl)amino)-2-butenolate **11z**,²⁰⁶ and (*Z*)-methyl 2-((benzyloxycarbonyl)amino)-2-butenolate **11y**,²⁰⁷ (*Z*)-Methyl 2-((benzyloxycarbonyl)amino)-2-pentenoate **11a'**,²⁰⁸ (*Z*)-methyl 2-((*tert*-butoxycarbonyl)amino)-2-pentenoate **11b'**,²⁰⁵ and methyl 2-(((benzyloxy)carbonyl)amino)-3-methylbut-2-enoate **11c'**²⁰⁹ are all known compounds which were prepared by following Schmidt's olefination procedure¹⁴⁸ starting from the corresponding carbonyl compound and commercially available (*R/S*)-methyl 2-((*tert*-butoxycarbonyl)amino)-2-(dimethoxyphosphoryl)acetate (for **11z** and **11b'**) or (*R/S*)-methyl 2-((benzyloxycarbonyl)amino)-2-(dimethoxyphosphoryl)acetate (for **11y** and **11a'**), or either (*R/S*)-methyl 2-acetamido-2-(dimethoxyphosphoryl)acetate¹⁴⁸ (for **11x**).

²⁰⁵ Kometani, M.; Ihara, K.; Kimura, R.; Kinoshita, H. *Bull. Chem. Soc. Jpn.* **2009**, *82*, 364.

²⁰⁶ Nugent, W. A.; Feaster, J. E. *Synth. Commun.* **1998**, *28*, 1617.

²⁰⁷ Ramesh, R.; De, K.; Chandrasekaran, S. *Tetrahedron* **2007**, *63*, 10534.

²⁰⁸ Mazurkiewicz, R.; Kuznik, A. *Tetrahedron Lett.* **2006**, *47*, 3439.

²⁰⁹ Jiang, X.-b.; van, d. B. M.; Minnaard, A. J.; Feringa, B. L.; de, V. J. G. *Tetrahedron: Asymmetry* **2004**, *15*, 2223.

(*Z*)-methyl 2-acetamido-3-chloroacrylate¹⁹⁸ **11d'**, (*Z*)-methyl 2-acetamido-3-methoxyacrylate¹⁹⁸ **11e'**, (*Z*)-2-Acetamido-*N*-methoxy-*N*-methyl-3-phenylacrylamide **11f'**:²⁰⁰ were all prepared according to the cited literature procedures. Physical and spectroscopic data obtained for these substrates were in perfect agreement with the data reported in the references indicated for each case.

N-(1-(4-fluorophenyl)vinyl)acetamide²¹⁰ **42c**, *N*-(1-(3-bromophenyl)vinyl)acetamide²¹⁰ **42e**, *N*-(1-(naphthalen-2-yl)vinyl)acetamide²¹¹ **42h**, and *N*-(1-(naphthalen-1-yl)vinyl)acetamide²¹² **42i** are all known compounds which were all prepared by following Burk's two-step procedure for α -arylenamide synthesis¹⁵⁴ starting from the corresponding commercially available aryl methyl ketone.

N-(1-(4-(Trifluoromethyl)phenyl)vinyl)acetamide **42d** is a known compound²¹¹ which was prepared by following Beller's general procedure for α -arylenamide synthesis²¹³ starting from commercially available 4-(trifluoromethyl)benzotrile.

1-Phenylvinyl acetate¹⁵⁹ **137a**, 1-(4'-methoxyphenyl)vinyl acetate²¹⁴ **137b**, 1-(4'-nitrophenyl)vinyl acetate^{157f} **137c**, 1-(2'-fluorophenyl)vinyl acetate **137d**, 1-(3'-fluorophenyl)vinyl acetate **137e**, 1-(4'-fluorophenyl)vinyl acetate²¹⁵ **137f**, and 1-(3'-(trifluoromethyl)phenyl)vinyl acetate **137g** were all prepared by following Berkessel's general procedure¹⁵⁹ for α -arylenol acetate synthesis starting from the corresponding commercially available acetophenone and working under reflux conditions of neat 2-propenyl acetate in combination with catalytic amounts of *p*-toluenesulfonic acid.

2-cyano-1-phenylvinyl acetate **137j**²¹⁶ and (*Z*)-3-ethoxy-3-oxo-1-phenylprop-1-en-1-yl benzoate **137k**²¹⁷ were prepared according to the cited literature procedures. Physical and

²¹⁰ Burk, M. J.; Wang, Y. M.; Lee, J. R. *J. Am. Chem. Soc.* **1996**, *118*, 5142.

²¹¹ Tang, W.; Capacci, A.; Sarvestani, M.; Wei, X.; Yee, N. K.; Senanayake, C. H. *J. Org. Chem.* **2009**, *74*, 9528.

²¹² For a full characterization of alkene **42i**, see: Liu, Z.; Xu, D.; Tang, W.; Xu, L.; Mo, J.; Xiao, J. *Tetrahedron Lett.* **2008**, *49*, 2756.

²¹³ Enthaler, S.; Hagemann, B.; Junge, K.; Erre, G.; Beller, M. *Eur. J. Org. Chem.* **2006**, 2912.

²¹⁴ Song, C.-X.; Cai, G.-X.; Farrell, T. R.; Jiang, Z.-P.; Li, H.; Gan, L.-B.; Shi, Z.-J. *Chem. Commun.* **2009**, 6002.

²¹⁵ Chen, Q.; Yuan, C. *Tetrahedron* **2010**, *66*, 3707.

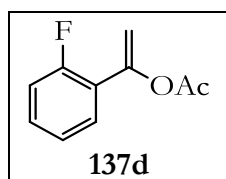
²¹⁶ Mansour, T. S. *Tetrahedron Lett.* **1988**, *29*, 3437.

²¹⁷ Yoo, W.-J.; Li, C.-J. *J. Org. Chem.* **2006**, *71*, 6266.

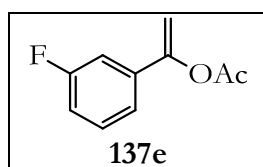
spectroscopic data obtained for these substrates were in perfect agreement with the data reported in the references indicated for each case.

Substrates **137a-137c** and **137f** are all known compounds. Physical and spectroscopic data obtained for these alkenes were in perfect agreement with the data reported in the references above-indicated for each case.

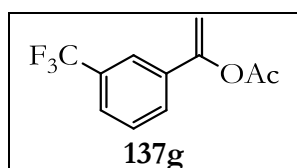
Substrates **137d**, **137e**, and **137g** are all new compounds. The full characterization for each one of these substrates is provided in the next lines.



1-(2'-Fluorophenyl)vinyl acetate (**137d**): Yellowish oil; IR absorption (neat) ν 1760, 1643, 1194, 1158 cm^{-1} ; ^1H NMR (400 MHz, CDCl_3) δ 7.41-7.34 (m, 1H), 7.33-7.24 (m, 1H), 7.16-7.04 (m, 2H), 5.57 (dd, $J = 2.0$ and 0.4 Hz, 1H), 5.23 (dd, $J = 2.0$ and 1.9 Hz, 1H), 2.24 (s, 3H); $^{13}\text{C}\{^1\text{H}\}$ NMR (100 MHz, CDCl_3) δ 168.9 (C), 159.8 (d, $J = 252.1$ Hz, C), 147.9 (d, $J = 3.3$ Hz, C), 130.2 (d, $J = 8.7$ Hz, CH), 128.0 (d, $J = 2.3$ Hz, CH), 124.0 (d, $J = 3.6$ Hz, CH), 122.4 (d, $J = 11.1$ Hz, C), 116.3 (d, $J = 22.7$ Hz, CH), 107.3 (d, $J = 8.4$ Hz, CH_2), 20.9 (CH_3); $^{19}\text{F}\{^1\text{H}\}$ NMR (376 MHz, CDCl_3) δ -113.1; HRMS (APCI $^+$) calcd for $\text{C}_{10}\text{H}_9\text{FO}_2\text{Na}$ [(M+Na) $^+$] 203.0484, found 203.0484.



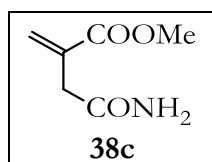
1-(3'-Fluorophenyl)vinyl acetate (**137e**): Yellowish liquid; IR absorption (neat) ν 1761, 1644, 1208, 1183, 1159 cm^{-1} ; ^1H NMR (400 MHz, CDCl_3) δ 7.37-7.25 (m, 2H), 7.22-7.14 (m, 1H), 7.08-6.99 (m, 1H), 5.52 (d, $J = 2.4$ Hz, 1H), 5.10 (d, $J = 2.4$ Hz, 1H), 2.28 (s, 3H); $^{13}\text{C}\{^1\text{H}\}$ NMR (100 MHz, CDCl_3) δ 168.7 (C), 162.7 (d, $J = 245.6$ Hz, C), 151.6 (d, $J = 2.8$ Hz, C), 136.5 (d, $J = 7.8$ Hz, CH), 130.0 (d, $J = 8.4$ Hz, CH), 120.4 (d, $J = 2.9$ Hz, C), 115.6 (d, $J = 21.3$ Hz, CH), 111.8 (d, $J = 23.4$ Hz, CH), 103.1 (CH_2), 20.7 (CH_3); $^{19}\text{F}\{^1\text{H}\}$ NMR (376 MHz, CDCl_3) δ -112.5; HRMS (APCI $^+$) calcd for $\text{C}_{10}\text{H}_9\text{FO}_2\text{Na}$ [(M+Na) $^+$] 203.0484, found 203.0485.



1-(3'-(Trifluoromethyl)phenyl)vinyl acetate (**137g**): Colourless oil; IR absorption (neat) ν 1763, 1645, 1259, 1195, 1121 cm^{-1} ; ^1H NMR

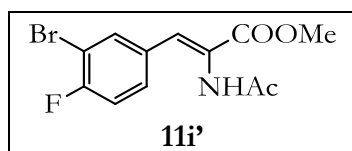
(400 MHz, CDCl₃) δ 7.74-7.69 (m, 1H), 7.64 (bd, $J = 7.8$ Hz, 1H), 7.58 (bd, $J = 7.8$ Hz, 1H), 7.47 (bdd, $J = 7.8$ and 7.8 Hz, 1H), 5.55 (d, $J = 2.5$ Hz, 1H), 5.14 (d, $J = 2.5$ Hz, 1H), 2.29 (s, 3H); ¹³C{¹H} NMR (100 MHz, CDCl₃) δ 168.8 (C), 151.6 (C), 135.2 (C), 131.0 (q, $J = 32.5$ Hz, C), 129.1 (CH), 128.1 (q, $J = 1.0$ Hz, CH), 125.5 (q, $J = 3.7$ Hz, CH), 123.9 (q, $J = 272.3$ Hz, C), 121.7 (q, $J = 3.9$ Hz, CH), 103.7 (CH₂), 20.8 (CH₃); ¹⁹F{¹H} NMR (376 MHz, CDCl₃) δ -63.0; HRMS (APCI⁺) calcd for C₁₁H₈F₃O₂ [(M-H⁺)] 229.0476, found 229.0480.

2-methylenesuccinamic acid²¹⁸ **38d**, methyl 2-(hydroxymethyl)acrylate²¹⁹ **38e** were prepared according to the cited literature procedures. Physical and spectroscopic data obtained for these substrates were in perfect agreement with the data reported in the references indicated for each case.



Methyl 2-methylenesuccinamate **38c** is a new compound which was readily prepared by esterification reaction of 2-methylenesuccinamic acid²¹⁸ with TMSCHN₂ on following the experimental procedure employed for the

synthesis of (*Z*)-methyl 2-acetamido-3-phenylacrylate from (*Z*)-2-acetamido-3-phenylacrylic acid.²²⁰ Characterization data for **38c**: Crystalline white solid; M.p. = 96.4-98.1 °C; IR absorption (neat) ν 3375, 3169, 1704, 1651, 1632; ¹H NMR (400 MHz, CDCl₃) δ 6.34 (d, $J = 0.92$ Hz, 1H, C=CHH), 5.99 (bs, CONHH), 5.85 (d, $J = 0.92$ Hz, 1H, C=CHH), 5.69 (bs, CONHH), 3.78 (s, 3H, OMe), 3.27-3.22 (m, 2H, CH₂CONH₂); ¹³C{¹H} NMR (100 MHz, CDCl₃) δ 172.2 (C), 171.4 (C), 134.1 (C), 129.3 (CH₂), 52.3 (CH₃), 39.8 (CH₂); HRMS (ESI⁺) calcd for C₆H₉NO₃Na [(M+Na)⁺] 166.0480, found 166.0480.



(*Z*)-Methyl 2-acetamido-3-(3-bromo-4-fluorophenyl)acrylate **11i'** is a new compound which was prepared by the following experimental procedure.¹⁴⁸ DBU (0.51 mL, 3.39 mmol) was

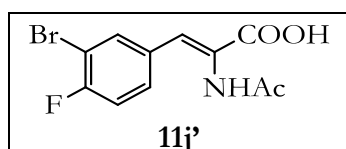
added dropwise to a solution of (*R/S*)-methyl 2-acetamido-2-(dimethoxyphosphoryl)acetate

²¹⁸ C. J. Cogley, I. C. Lennon, C. Praquin, A. Zanotti-Gerosa, R. B. Appell, C. T. Goralski, A. C. Sutterer, *Org. Process Res. Dev.* **2003**, 7, 407.

²¹⁹ Sawamura, K.; Yoshida, K.; Suzuki, A.; Motozaki, T.; Kozawa, I.; Hayamizu, T.; Munakata, R.; Takao, K.-I.; Tadano, K.-I. *J. Org. Chem.* **2007**, 72, 6143.

²²⁰ Lee, J.; Bernard, S.; Liu, X.-C. *React. Funct. Polym.* **2009**, 69, 650.

(0.88 g, 3.69 mmol) in CH_2Cl_2 (7.5 mL) at room temperature. The reaction mixture was further stirred for 15 min. A solution of 3-bromo-4-fluorobenzaldehyde (0.63 g, 3.08 mmol) in CH_2Cl_2 (7.5 mL) was added via cannula to the initial mixture. The resulting solution was subsequently stirred at room temperature overnight. The reaction mixture was concentrated under vacuum and the resulting residue was dissolved in EtOAc (50 mL) and washed with 1.0 M H_2SO_4 (1 x 15 mL) and brine solution (1 x 15 mL). The organic phase was dried over anhydrous MgSO_4 and concentrated under vacuum. A 95:5 *Z/E* ratio for the resulting isomeric olefins was determined by ^1H NMR analysis of the crude product. Purification by silica gel column chromatography (1st eluent: hexanes, 2nd eluent: 30:70 EtOAc/hexanes) allowed for the isolation of 0.62 g (64% yield) of pure *Z* isomer **11i'** as a white solid; M.p. 174.6-176.4 °C; IR absorption (neat) ν 3238, 1716, 1657, 1650, 1641, 1518 cm^{-1} ; ^1H NMR (400 MHz, CDCl_3) δ 7.65 (d, $J = 5.4$ Hz, 1H), 7.35 (bs, 1H), 7.30 (s, 1H), 7.19 (s, 1H), 7.09 (t, $J = 8.4$ Hz, 1H), 3.85 (s, 3H), 2.13 (s, 3H); $^{13}\text{C}\{^1\text{H}\}$ NMR (100 MHz, CDCl_3) δ 168.4 (C), 165.5 (C), 159.1 (d, $J = 251.0$ Hz, C), 134.6 (C), 131.8 (CH), 130.3 (d, $J = 7.3$ Hz, CH), 129.3 (CH), 124.1 (C), 116.5 (d, $J = 22.2$ Hz, CH), 109.2 (d, $J = 21.7$ Hz, C), 52.9 (CH_3), 23.6 (CH_3); $^{19}\text{F}\{^1\text{H}\}$ NMR (376 MHz, CDCl_3) δ -104.6; HRMS (ESI⁺) calcd for $\text{C}_{12}\text{H}_{11}\text{BrFNO}_3\text{Na}$ [(M+Na)⁺] 337.9804, found 337.9814.



(*Z*)-2-Acetamido-3-(3-bromo-4-fluorophenyl)acrylic acid **11j'** is a known compound which was prepared by following the next experimental procedure. To a solution of **11i'** (0.25 g, 0.79

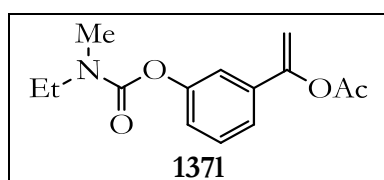
mmol) in 2:1 MeOH/dioxane (3.0 mL) was added 2.0 M KOH (1.27 mL, 2.53 mmol) and the reaction mixture was stirred at room temperature overnight. After acidification with 1.0 M KHSO_4 (2.5 mL) to pH 2-3, a white solid precipitated which was filtered and washed with H_2O (2 x 3.0 mL). Subsequent washing with acetonitrile (2 x 3.0 mL) afforded 0.17 g (72% yield) of pure *Z* isomer **11j'**. Substrate **11j'** was very recently prepared by following a different procedure.¹¹² Physical and spectroscopic data obtained for this alkene were found to be identical to those previously reported.¹¹²

(*Z*)-Methyl 2-((benzyloxycarbonyl)amino)-3-(3-hydroxyphenyl)acrylate^{179b} **11k'**, (*Z*)-methyl 2-((benzyloxycarbonyl)amino)-3-(3-hydroxy-4-nitrophenyl)acrylate^{180b} **11l'**, (*Z*)-methyl 2-

((*tert*-butoxycarbonyl)amino)-3-(4-((*tert*-butoxycarbonyl)oxy)-2-methoxyphenyl)acrylate²²¹ **11m'**, (*Z*)-methyl 2-(2-oxopyrrolidin-1-yl)-2-butenolate¹¹⁴ **11n'**, (*Z*)-2-(2-oxopyrrolidin-1-yl)-2-butenic acid¹¹⁴ **11o'**, and *N*-(1-(4-fluorophenyl)vinyl)acetamide²¹⁰ **42b** were all prepared according to the cited literature procedures. Physical and spectroscopic data obtained for these substrates were in perfect agreement with the data reported in the references indicated for each case.

N-(1-(3-Acetoxyphenyl)vinyl)acetamide **42j** is a known compound²²² which was prepared by following Burk's two-step procedure for α -arylenamide synthesis¹⁵⁴ starting from the corresponding commercially available aryl methyl ketone.

1-(3-((Ethyl(methyl)carbamoyl)oxy)phenyl)vinyl acetate **137l** and 1-(3,5-bis(trifluoromethyl)phenyl)vinyl acetate **137m** are both new compounds which were prepared by following Berkessel's general procedure¹⁵⁹ as previously mentioned for the rest of α -arylenol acetates. Substrate **137l** was prepared from 3'-(ethyl(methyl)carbamoyl)oxyacetophenone obtained by *O*-carbamoylation reaction from commercially available 3'-hydroxyacetophenone according to the literature procedure.^{187a} Substrate **137m** was straightforwardly accessible from commercially available 3',5'-bis(trifluoromethyl)acetophenone.



1-(3-((Ethyl(methyl)carbamoyl)oxy)phenyl)vinyl acetate

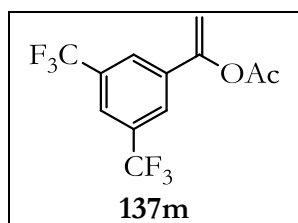
(137l): Yellowish liquid; IR absorption (neat) ν 1762, 1715,

1642, 1582 cm^{-1} ; ^1H NMR (500 MHz, CDCl_3 , mixture of

rotamers) δ 7.35-7.26 (m, 2H), 7.23-7.19 (m, 1H), 7.12-7.06 (m, 1H), 5.48 (d, $J = 2.3$ Hz, 1H), 5.05 (d, $J = 2.3$ Hz, 1H), 3.47 and 3.41 (q, $J = 7.0$ Hz, 2H), 3.06 and 2.99 (s, 3H), 2.27 (s, 3H), 1.23 and 1.19 (t, $J = 7.0$ Hz, 3H); $^{13}\text{C}\{^1\text{H}\}$ NMR (125 MHz, CDCl_3 , mixture of rotamers) δ 169.0 (C), 154.3 and 154.1 (C), 152.0 (CH), 151.6 (C), 135.7 and 135.6 (CH), 129.3 and 129.2 (C), 122.4 and 122.4 (CH), 121.6 and 121.6 (CH), 118.3 (CH_2), 102.8 and 102.8 (C), 44.1 (CH_3), 34.2 and 33.8 (CH_2), 21.0 (CH_3), 13.2 and 12.4 (CH_3); HRMS (ESI⁺) calcd for $\text{C}_{14}\text{H}_{17}\text{NO}_4\text{Na}$ [$\text{M}+\text{Na}$]⁺ 286.1055, found 286.1054.

²²¹ J. Y. Cha, Y. Huang, T. R. R. Pettus, *Angew. Chem. Int. Ed.* **2009**, *48*, 9519.

²²² Gridnev, I. D.; Yasutake, M.; Higashi, N.; Imamoto, T. *J. Am. Chem. Soc.* **2001**, *123*, 5268.



1-(3,5-Bis(trifluoromethyl)phenyl)vinyl acetate (**137m**): Colourless oil; IR absorption (neat) ν 1768, 1645, 1276, 1174, 1125 cm^{-1} ; ^1H NMR (500 MHz, CDCl_3) δ 7.92-7.85 (m, 2H), 7.85-7.78 (m, 1H), 5.63 (d, $J = 2.8$ Hz, 1H), 5.27 (d, $J = 2.8$ Hz, 1H), 2.32 (s, 3H); $^{13}\text{C}\{^1\text{H}\}$ NMR (125 MHz, CDCl_3) δ 168.7 (C), 150.3 (C), 136.8 (C), 132.1 (q, $J_{\text{C-F}} = 33.5$ Hz, 2C), 125.0 (q, $J_{\text{C-F}} = 3.2$ Hz, 2CH), 123.1 (q, $J_{\text{C-F}} = 272.8$ Hz, 2C), 122.5 (sp, $J_{\text{C-F}} = 3.8$ Hz, CH), 105.5 (CH_2), 20.9 (CH_3); $^{19}\text{F}\{^1\text{H}\}$ NMR (376 MHz, CDCl_3) δ -62.8; HRMS (APCI $^+$) calcd for $\text{C}_{12}\text{H}_7\text{F}_6\text{O}_2$ [(M-H) $^+$] 297.0350, found 297.0346.

1.3.4 General Procedure for the Rh-Mediated Asymmetric Hydrogenation

A solution of the required amount of $[\text{Rh}(\text{nbd})_2]\text{BF}_4$, the *P-OP* ligand **30a**, **30b** or *ent-30b* (10% molar excess with respect to the rhodium precursor) and the corresponding functionalized alkene (0.10 mmol) in anhydrous and degassed solvent (0.50 mL) was prepared inside a glass vessel under N_2 atmosphere in a glove box. In all cases the molar concentration of the substrate in the reaction medium was adjusted to 0.20 M.

Once the reaction mixture had been loaded, the glass vessel was then placed into one of the holes of a steel autoclave reactor (HEL Cat-24 parallel pressure multireactor). The autoclave was purged three times with H_2 gas (at a pressure not higher than the chosen one). Finally, the autoclave was pressurized under the required pressure of H_2 gas. The mixture was stirred at the desired temperature (in a thermostatic bath) for the stated reaction time (overnight reaction). The autoclave was then depressurized slowly, at which point the reaction mixture was filtered through a short pad of SiO_2 and subsequently eluted with EtOAc (1.0 mL). The resulting solution was concentrated under vacuum. The conversion was determined by ^1H NMR (^{19}F NMR in the case of substrate **137h**) and the enantiomeric excess was determined by GC or HPLC analysis on chiral stationary phases.

1.3.4.1 General Procedure for Monitoring the Hydrogenation Reactions by Gas Uptake Measurements

The gas uptake measurement experiments were performed in an SPR-16 AMTEC parallel autoclave reactor equipped with pressure probes and a mass-flow controller that enabled monitoring and recording of gas uptake profiles throughout the hydrogenation reactions. The required amount of $[\text{Rh}(\text{nbd})_2]\text{BF}_4$ (0.90 mg, 2.40 μmol) and ligand **30a** or **30b** (10% molar excess with respect to the rhodium precursor) were dissolved in anhydrous and degassed THF (1.2 mL) under N_2 atmosphere inside a glove box. This solution was stirred at room temperature for 30 min in order to form the desired precatalyst. Separately, another solution (1.7 mL) of the corresponding model substrate, **11d**, **38a**, **42a** or **137a**, (2.27 mmol) in anhydrous and degassed THF was prepared under N_2 atmosphere inside a glove box.

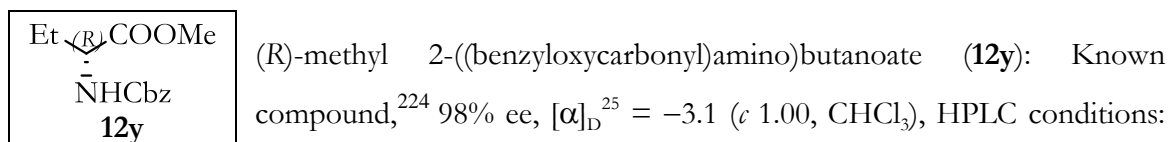
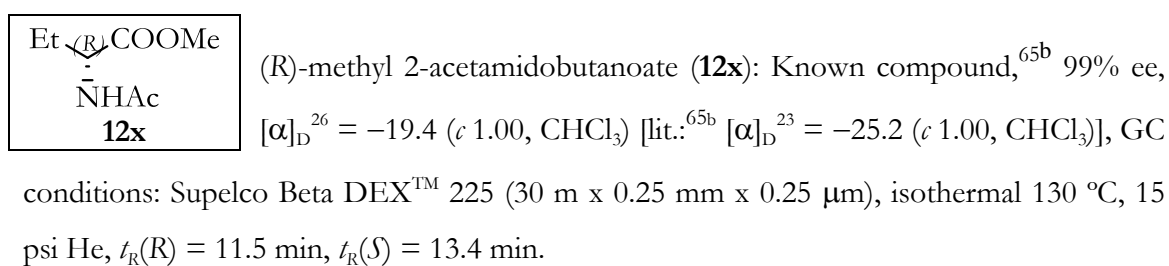
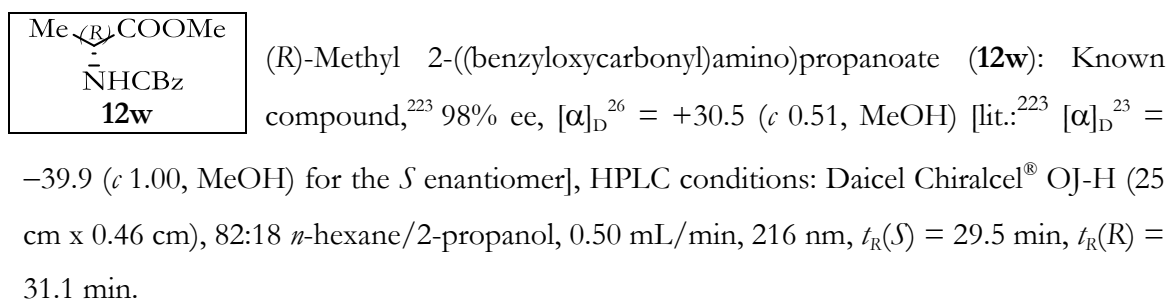
The stainless steel SPR-16 AMTEC reactor was warmed up to 110 $^\circ\text{C}$ and pressurized with N_2 to 50 bar, vented (five cycles) and finally, cooled down to room temperature. Afterwards, the solutions of the precatalyst (1.0 mL, 2.0 μmol ; 0.1 mol %) and the substrate (1.5 mL, 2.0 mmol) were subsequently added (*via* syringe) into the reactor, which was further flushed with H_2 and then pressurized to 20 bar. The stirring rate was adjusted to 1000 rpm and the hydrogen gas uptake was monitored and recorded automatically. Once steady hydrogen consumption had indicated that the reaction had reached completion, the reactor was further depressurized slowly. The reaction mixture was filtered through a short pad of SiO_2 and eluted with EtOAc (20.0 mL). The resulting solution was concentrated under vacuum. Full conversion was confirmed by ^1H NMR and enantioselectivity was determined by GC or HPLC analysis on chiral stationary phases.

1.3.4.2 General Procedure for Hydrogenations Using S/C ratios > 1,000 : 1

Working inside a glove box, a solution of the required amount of dimethyl itaconate (**38a**) in anhydrous and deoxygenated THF (ca. 75% w/w) was added (*via* syringe) into a steel liner, followed by the addition of a solution of ca. 8 mg of $[\text{Rh}(\text{nbd})(\text{30a})]\text{BF}_4$ (**135**) (8.6 μmol) in 2 mL of THF. The steel liner was closed, and then removed from the glove box. The final molar concentration of the substrate was ca. 5.0 M.

The steel liner was then attached to the liquid filling port of an adequately sized and dried autoclave (previously heated overnight at 110 °C under 30 bar of N₂). Once the reactor had reached 25 °C and the liner had been attached to the autoclave, the reaction mixture was loaded into the reactor by pressurizing the liner with N₂. The reactor was then purged three times with H₂ gas (5 bar) and subsequently pressurized to 20 bar with H₂. The reaction mixture was stirred at room temperature for 24 h. The autoclave was subsequently depressurized and purged with N₂. The resulting solution was concentrated under vacuum. Full conversion was confirmed by ¹H NMR analysis and enantioselectivity was determined by GC analysis on chiral stationary phases.

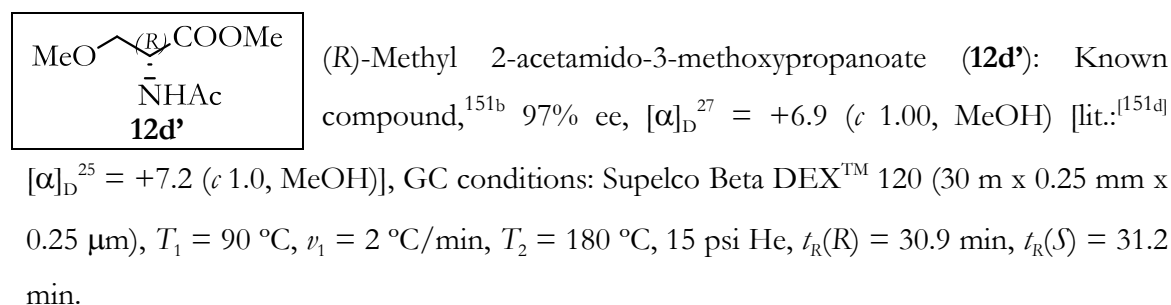
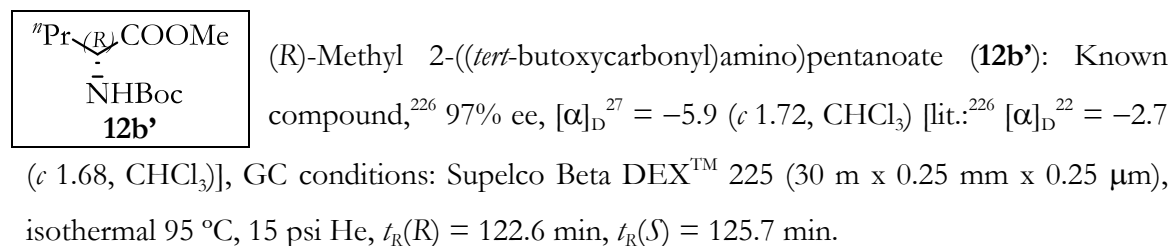
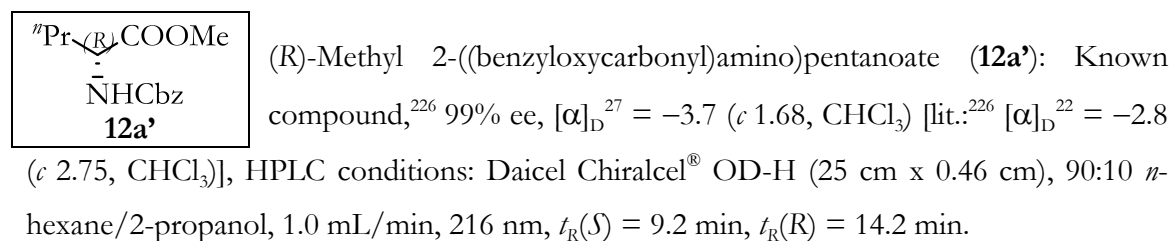
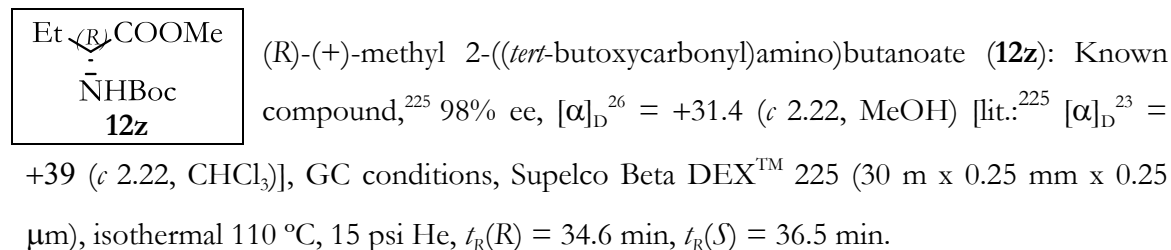
1.3.5 Characterization of Hydrogenation Products and Determination of the Enantiomeric Excesses



²²³ Wakasugi, K.; Iida, A.; Misaki, T.; Nishii, Y.; Tanabe, Y. *Adv. Synth. Catal.* **2003**, *345*, 1209.

²²⁴ Itaya, T.; Shimizu, S.; Nakagawa, S.; Morisue, M. *Chem. Pharm. Bull.* **1994**, *42*, 1927.

Daicel Chiralcel[®] OD-H (25 cm x 0.46 cm), 90:10 *n*-hexane/2-propanol, 1.0 mL/min, 216 nm, $t_R(+)$ = 9.3 min, $t_R(-)$ = 16.0 min (major enantiomer).



²²⁵ Agosta, E.; Caligiuri, A.; D'Arrigo, P.; Servi, S.; Tessaro, D.; Canevotti, R. *Tetrahedron: Asymmetry* **2006**, *17*, 1995.

²²⁶ Fraser, B. H.; Mulder, R. J.; Perlmutter, P. *Tetrahedron* **2006**, *62*, 2857.

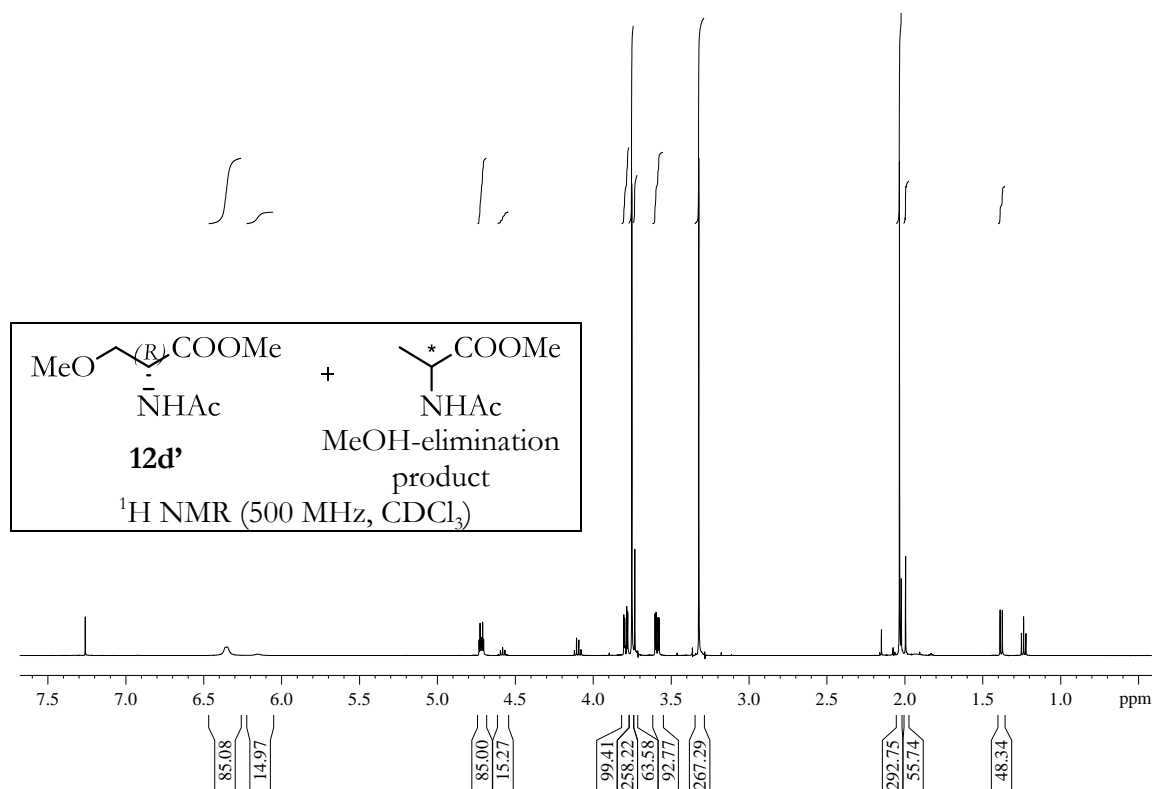
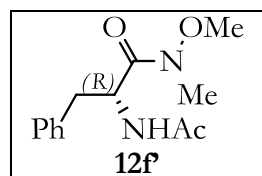
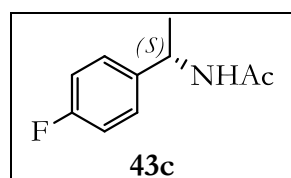


Figure 42. ¹H NMR spectrum for the hydrogenation product **12d'** along with 15 mol % of the MeOH-elimination product methyl 2-acetamidopropanoate.



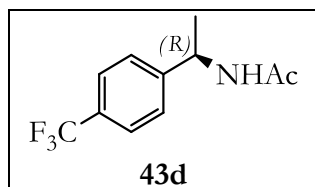
(*R*)-2-Acetamido-*N*-methoxy-*N*-methyl-3-phenylpropanamide (**12f**):
 Known compound,²⁰⁰ 95% ee, $[\alpha]_D^{26} = -29.5$ (c 1.18, CHCl₃) [lit.:²⁰⁰
 $[\alpha]_D^{26} = -29.5$ (c 1.18, CHCl₃)], HPLC conditions: Daicel Chiralcel[®]

OD-H (25 cm x 0.46 cm), 85:15 *n*-hexane/2-propanol, 1.0 mL/min, 216 nm, $t_R(-) = 16.9$ min (major enantiomer), $t_R(+)$ = 27.1 min, $t_R(\mathbf{11f}) = 28.3$ min.

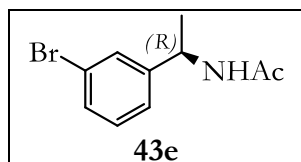


(*S*)-*N*-Acetyl-1-(4-fluorophenyl)ethylamine (**43c**): Known
 compound,²¹⁰ 98% ee, $[\alpha]_D^{25} = +104.8$ (c 0.28, CHCl₃) [lit.:²¹⁰ $[\alpha]_D^{20} =$
 -119 (c 0.28, CHCl₃) for the *R* enantiomer], HPLC conditions:

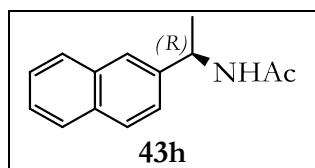
Daicel Chiralpak[®] AD-H (25 cm x 0.46 cm), 95:5 *n*-hexane/2-propanol, 1.0 mL/min, 216 nm, $t_R(R) = 10.0$ min, $t_R(S) = 12.5$ min.



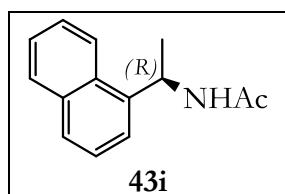
(R)-N-acetyl-1-(4-(trifluoromethyl)phenyl)ethylamine (**43d**):
Known compound,²²⁷ 98% ee, $[\alpha]_{\text{D}}^{25} = +94.7$ (c 1.00, CHCl_3)
[lit.:²²⁷ $[\alpha]_{\text{D}} = +89.1$ (c 1.0, CHCl_3)], HPLC conditions: Daicel
Chiralpak[®] AD-H (25 cm x 0.46 cm), 95:5 *n*-hexane/2-propanol,
1.0 mL/min, 216 nm, $t_{\text{R}}(\text{R}) = 8.8$ min, $t_{\text{R}}(\text{S}) = 12.4$ min.



(R)-N-(1-(3-bromophenyl)ethyl)acetamide (**43e**): Known
compound,²²⁸ 97% ee, $[\alpha]_{\text{D}}^{25} = +84.3$ (c 1.00, CHCl_3) [lit.:²¹⁰ $[\alpha]_{\text{D}} =$
 -106 (c 1.0, CHCl_3) for the *S* enantiomer], HPLC conditions: Daicel
Chiralpak[®] AD-H (25 cm x 0.46 cm), 95:5 *n*-hexane/2-propanol, 1.0 mL/min, 216 nm,
 $t_{\text{R}}(\text{R}) = 10.0$ min, $t_{\text{R}}(\text{S}) = 12.9$ min.



(R)-N-Acetyl-1-(naphthalen-2-yl)ethylamine (**43h**): Known
compound,²¹⁰ 99% ee, $[\alpha]_{\text{D}}^{25} = +149.9$ (c 1.00, CH_2Cl_2) [lit.:²²⁹ $[\alpha]_{\text{D}}$
 $= +115.6$ (c 1.0, CH_2Cl_2)], HPLC conditions: Daicel Chiralpak[®]
AD-H (25 cm x 0.46 cm), 95:5 *n*-hexane/2-propanol, 1.0 mL/min, 216 nm, $t_{\text{R}}(\text{R}) = 12.9$
min, $t_{\text{R}}(\text{S}) = 19.5$ min.



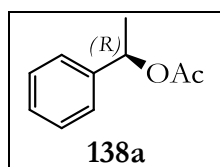
(R)-N-Acetyl-1-(naphthalen-1-yl)ethylamine (**43i**): Known
compound,²³⁰ 83% ee, $[\alpha]_{\text{D}}^{27} = +52.8$ (c 0.82, EtOH) [lit.:²³⁰ $[\alpha]_{\text{D}}^{20} =$
 -47.9 (c 0.82, EtOH) for the *S* enantiomer], GC conditions: Supelco
Beta DEXTM 120 (30 m x 0.25 mm x 0.25 μm), isothermal 170 °C, 15 psi He, $t_{\text{R}}(\text{S}) = 140.3$
min, $t_{\text{R}}(\text{R}) = 143.3$ min.

²²⁷ Kim, M.-J.; Kim, W.-H.; Han, K.; Choi, Y. K.; Park, J. *Org. Lett.* **2007**, *9*, 1157.

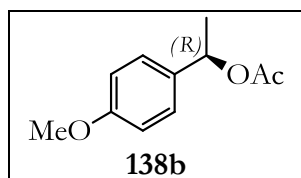
²²⁸ Andrade, L. H.; Barcellos, T.; Santiago, C. G. *Tetrahedron: Asymmetry* **2010**, *21*, 2419.

²²⁹ Paetzold, J.; Bäckvall, J. E. *J. Am. Chem. Soc.* **2005**, *127*, 17620.

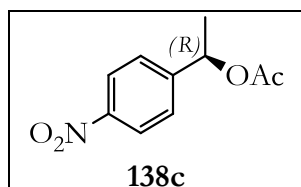
²³⁰ Li, G.; Antilla, J. C. *Org. Lett.* **2009**, *11*, 1075.



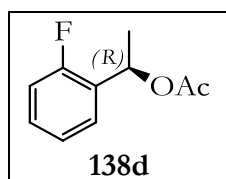
(*R*)-*O*-Acetyl-1-phenylethanol (**138a**): Known compound,²³¹ 97% ee, $[\alpha]_{\text{D}}^{28} = +82.2$ (c 0.86, CHCl_3) [lit.:²³¹ $[\alpha]_{\text{D}}^{22} = +106$ (c 1, CHCl_3)], HPLC conditions: Daicel Chiralcel[®] OD-H (25 cm x 0.46 cm), 99:1 *n*-hexane/2-propanol, 0.30 mL/min, 216 nm, $t_{\text{R}}(\text{R}) = 19.5$ min, $t_{\text{R}}(\text{S}) = 21.3$ min.



(*R*)-*O*-Acetyl-1-(4'-methoxyphenyl)ethanol (**138b**): Known compound,²³¹ 95% ee, $[\alpha]_{\text{D}}^{28} = +115.3$ (c 1.00, CHCl_3) [lit.:²³¹ $[\alpha]_{\text{D}}^{22} = +129$ (c 1, CHCl_3)], HPLC conditions: Daicel Chiralcel[®] OB-H (25 cm x 0.46 cm), 99.2:0.8 *n*-hexane/2-propanol, 1.0 mL/min, 225 nm, $t_{\text{R}}(\text{S}) = 22.3$ min, $t_{\text{R}}(\text{R}) = 26.1$ min.



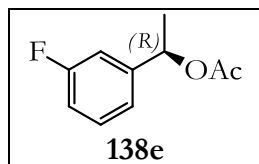
(*R*)-*O*-Acetyl-1-(4'-nitrophenyl)ethanol (**138c**): Known compound,²³¹ 98% ee, $[\alpha]_{\text{D}}^{28} = +98.3$ (c 1.00, CHCl_3) [lit.:²³¹ $[\alpha]_{\text{D}}^{22} = +95$ (c 1, CHCl_3)], HPLC conditions: Daicel Chiralcel[®] OJ-H (25 cm x 0.46 cm), 95:5 *n*-hexane/2-propanol, 0.50 mL/min, 254 nm, $t_{\text{R}}(\text{S}) = 31.4$ min, $t_{\text{R}}(\text{R}) = 33.6$ min.



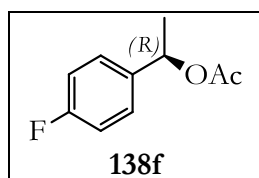
(*R*)-*O*-Acetyl-1-(2'-fluorophenyl)ethanol (**138d**): Yellowish liquid, 94% ee, IR absorption (neat) ν 1737, 1227 cm^{-1} ; $[\alpha]_{\text{D}}^{28} = +73.9$ (c 1.20, CHCl_3); ^1H NMR (500 MHz, CDCl_3) δ 7.39 (ddd, 1H, $J = 7.5, 7.5$ and 1.8 Hz, 1H), 7.29-7.24 (m, 1H), 7.14 (ddd, 1H, $J = 7.5, 7.5$ and 1.1 Hz, 1H), 7.04 (ddd, $J = 10.3, 8.3$ and 1.1 Hz, 1H), 6.14 (q, $J = 6.6$ Hz, 1H), 2.09 (s, 3H), 1.55 (d, $J = 6.6$ Hz, 3H); $^{13}\text{C}\{^1\text{H}\}$ NMR (125 MHz, CDCl_3) δ 170.0 (C), 159.6 (d, $J = 247.3$ Hz, C), 129.3 (d, $J = 8.2$ Hz, CH), 128.9 (d, $J = 13.5$ Hz, C), 127.1 (d, $J = 4.3$ Hz, CH), 124.2 (d, $J = 3.6$ Hz, CH), 115.5 (d, $J = 21.7$ Hz, CH), 66.6 (d, $J = 2.8$ Hz, CH), 21.2 (2 CH_3); $^{19}\text{F}\{^1\text{H}\}$ NMR (376 MHz, CDCl_3) δ -118.1; MS (EI^+): m/z 182 (M^+ , 14%), 140 (38%), 122 (100%), 103 (22%), 96 (19%); HRMS (APCI^+) calcd for $\text{C}_8\text{H}_8\text{F}$ [$(\text{M}-\text{OAc})^+$] 123.0610, found 123.0603; HPLC conditions: Daicel

²³¹ Paeivioe, M.; Mavrynsky, D.; Leino, R.; Kanerva, L. T. *Eur. J. Org. Chem.* **2011**, 1452.

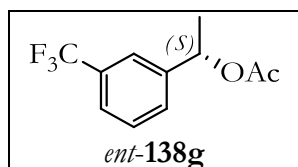
Chiralpak[®] IA (25 cm x 0.46 cm), 99:1 *n*-hexane/2-propanol, 0.30 mL/min, 210 nm, $t_R(+)$ = 15.0 min (major enantiomer), $t_R(-)$ = 15.9 min.



(*R*)-*O*-Acetyl-1-(3'-fluorophenyl)ethanol (**138e**): Yellowish liquid, 98% ee, IR absorption (neat) ν 1734, 1229 cm^{-1} ; $[\alpha]_D^{27} = +67.2$ (c 1.22, CHCl_3); ^1H NMR (400 MHz, CDCl_3) δ 7.34-7.27 (m, 1H), 7.13-7.09 (m, 1H), 7.08-7.03 (m, 1H), 6.96 (dddd, $J = 8.5, 8.5, 2.6$ and 0.9 Hz, 1H), 5.86 (q, $J = 6.6$ Hz, 1H), 2.09 (s, 3H), 1.52 (d, $J = 6.6$ Hz, 3H); $^{13}\text{C}\{^1\text{H}\}$ NMR (100 MHz, CDCl_3) δ 170.2 (C), 162.9 (d, $J = 246.0$ Hz, C), 144.3 (d, $J = 7.2$ Hz, C), 130.0 (d, $J = 8.2$ Hz, CH), 121.6 (d, $J = 2.9$ Hz, CH), 114.7 (d, $J = 21.1$ Hz, CH), 112.9 (d, $J = 22.0$ Hz, CH), 71.5 (d, $J = 2.3$ Hz, CH), 22.2 (CH_3), 21.2 (CH_3); $^{19}\text{F}\{^1\text{H}\}$ NMR (376 MHz, CDCl_3) δ -112.5; MS (EI^+): 182 (M^+ , 12%), 140 (100%), 122 (93%), 103 (25%), 96 (31%); HRMS (APCI^+) calcd for $\text{C}_8\text{H}_8\text{F}$ [$\text{M}-\text{OAc}$] $^+$ 123.0610, found 123.0606; HPLC conditions: Daicel Chiralcel[®] OJ-H (25 cm x 0.46 cm), 99:1 *n*-hexane/2-propanol, 0.30 mL/min, 210 nm, $t_R(-)$ = 30.3 min, $t_R(+)$ = 32.1 min (major enantiomer).



(*R*)-*O*-Acetyl-1-(4'-fluorophenyl)ethanol (**138f**): Known compound,²³¹ 96% ee, $[\alpha]_D^{25} = +87.2$ (c 1.26, CHCl_3) [lit.:²¹⁵ $[\alpha]_D^{26} = +89$ (c 0.98, CHCl_3)], HPLC conditions: Daicel Chiralcel[®] OJ-H (25 cm x 0.46 cm), 97:3 *n*-hexane/2-propanol, 0.50 mL/min, 254 nm, $t_R(R)$ = 16.2 min, $t_R(S)$ = 18.4 min.

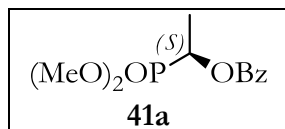


(*S*)-*O*-Acetyl-1-(3'-(trifluoromethyl)phenyl)ethanol (*ent*-**138g**): Known compound,²³² 98% ee, $[\alpha]_D^{25} = -62.8$ (c 0.95, CHCl_3) [lit.:²³³ $[\alpha]_D^{25} = +70.7$ (c 2.63, CHCl_3) for the *R* enantiomer], GC

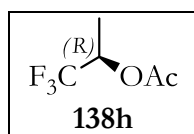
²³² Rodriguez, C.; de, G. G.; Rioz-Martínez, A.; Torres, P. D. E.; Fraaije, M. W.; Gotor, V. *Org. Biomol. Chem.* **2010**, *8*, 1121.

²³³ Naemura, K.; Murata, M.; Tanaka, R.; Yano, M.; Hirose, K.; Tobe, Y. *Tetrahedron: Asymmetry* **1996**, *7*, 3285.

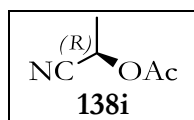
conditions: Supelco Beta DEXTM 120 (30 m x 0.25 mm x 0.25 μ m), $T_1 = 70$ °C, $t_1 = 10$ min, $\nu_1 = 2$ °C/min, 15 psi He, $T_2 = 180$ °C, $t_R(S) = 33.9$ min, $t_R(R) = 35.2$ min.



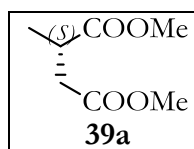
(*S*)-*O*-Benzoyl-1-(dimethoxyphosphoryl)ethanol (**41a**): Known compound,²³⁴ 95% ee, $[\alpha]_D^{28} = -9.0$ (c 1.26, CHCl₃) [lit.:²³⁴ $[\alpha]_D^{25} = -23.0$ (c 0.172, CHCl₃)], HPLC conditions: Daicel Chiralcel[®] OJ-H (25 cm x 0.46 cm), 98:2 *n*-hexane/2-propanol, 1.0 mL/min, 216 nm, $t_R(S) = 28.5$ min, $t_R(R) = 32.1$ min.



(*R*)-*O*-Acetyl-1-(trifluoromethyl)ethanol (**138h**): Known compound,¹⁵⁷ⁱ 99% ee, $[\alpha]_D^{27} = -11.3$ (c 1.77, THF) [lit.:^{157b} $[\alpha]_D^{23} = +18.7$ (neat) for the *S* enantiomer], GC-MS conditions: Agilent J&W HP-Chiral 20BTM (30 m x 0.25 mm x 0.25 μ m), $T_1 = 40$ °C, $t_1 = 10$ min, $\nu_1 = 25$ °C/min, $T_2 = 150$ °C, 0.50 mL/min He, $t_R(S) = 8.5$ min, $t_R(R) = 9.1$ min.



(*R*)-*O*-Acetyl-1-cyanoethanol (**138i**): Known compound,²³⁵ 97% ee, $[\alpha]_D^{28} = +78.5$ (c 2.00, C₆H₆) [lit.:¹⁶⁵ $[\alpha]_D^{RT} = +72$ (c 2, C₆H₆)], GC conditions: Supelco Beta DEXTM 120 (30 m x 0.25 mm x 0.25 μ m), isothermal 70 °C, 15 psi He, $t_R(R) = 13.6$ min, $t_R(S) = 17.8$ min.



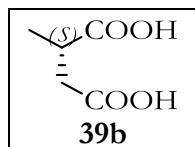
(*S*)-Dimethyl 2-methylsuccinate (**39a**): Known compound,²³⁶ 99% ee, $[\alpha]_D^{27} = -3.3$ (c 1.00, CHCl₃) [lit.:²³⁶ $[\alpha]_D^{20} = -3.0$ (c 1.0, CHCl₃)], GC conditions:

²³⁴ Wang, D.-Y.; Huang, J.-D.; Hu, X.-P.; Deng, J.; Yu, S.-B.; Duan, Z.-C.; Zheng, Z. *J. Org. Chem.* **2008**, *73*, 2011.

²³⁵ Hoffmann, H. M. R.; Ismail, Z. M.; Hollweg, R.; Zein, A. R. *Bull. Chem. Soc. Jpn.* **1990**, *63*, 1807.

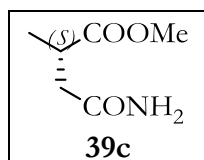
²³⁶ Yu, L.; Wang, Z.; Wu, J.; Tu, S.; Ding, K. *Angew. Chem., Int. Ed.* **2010**, *49*, 3627.

Supelco Beta DEX™ 225 (30 m x 0.25 mm x 0.25 μm), isothermal 70 °C, 15 psi He, $t_R(S) = 46.4$ min, $t_R(R) = 53.4$ min.



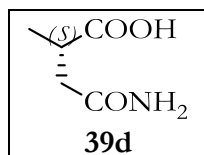
(*S*)-2-Methylsuccinic acid²³⁷ (**39b**): Known compound,²³⁸ 99% ee. Prior to analysis of the enantiomeric excess both carboxylic acid groups of the hydrogenation product **39b** were quantitatively esterified with TMSCHN₂.

For GC analysis conditions after derivatisation with TMSCHN₂ see the above-described data for **39a**.



(*S*)-methyl 2-methylsuccinamate (**39c**): Known compound,²³⁹ 99% ee, $[\alpha]_D^{27} = -4.1$ (c 0.66, MeOH) [lit.:²³⁹ $[\alpha]_D^{22} = -4.5$ (c 1.0, MeOH) for the R enantiomer] GC conditions, Supelco Beta DEX™ 120 (30 m x 0.25 mm x

0.25 μm), $T_1 = 105$ °C, $t_1 = 5$ min, $v_1 = 5$ °C/min, $T_2 = 150$ °C, $t_2 = 45$ min, 20 psi He, $t_R(R) = 25.1$ min, $t_R(S) = 25.8$ min.



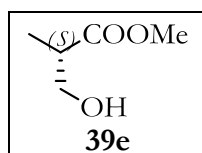
(*S*)-2-Methylsuccinamic acid (**39d**): Known compound,^{157g} 95% ee, $[\alpha]_D^{27} = -8.0$ (c 0.66, MeOH) [lit.:²³⁹ $[\alpha]_D^{22} = +17.7$ (c 2.0, MeOH)], GC conditions:

Supelco Beta DEX™ 120 (30 m x 0.25 mm x 0.25 μm), isothermal 90 °C, 15 psi He, $t_R(R) = 44.9$ min, $t_R(S) = 45.8$ min.

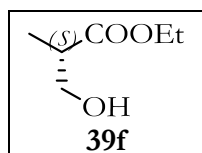
²³⁷ The absolute configuration for the hydrogenation product was unequivocally assigned by comparison of the specific rotation of (*S*)-dimethyl 2-methylsuccinate with the data reported for this compound, which was quantitatively prepared by esterification reaction with TMSCHN₂.

²³⁸ Bajwa, J. S.; Miller, M. J. *J. Org. Chem.* **1983**, *48*, 1114.

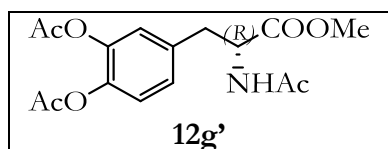
²³⁹ Takeda, H.; Tachinami, T.; Hosokawa, S.; Aburatani, M.; Inoguchi, K.; Achiwa, K. *Chem. Pharm. Bull.* **1991**, *39*, 2706.



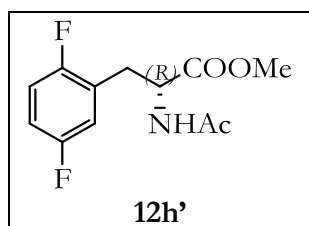
(*S*)-Methyl 3-hydroxy-2-methylpropanoate (**39e**): Known compound,^{171a} 97% ee, $[\alpha]_{\text{D}}^{27} = +56.1$ (c 1.34, CHCl_3) [lit.:^{171a} $[\alpha]_{\text{D}}^{20} = +15.4$ (c 3.1, CHCl_3)], GC conditions: Supelco Beta DEXTM 225 (30 m x 0.25 mm x 0.25 μm), isothermal 90 °C, 15 psi He, $t_{\text{R}}(\text{S}) = 14.9$ min, $t_{\text{R}}(\text{R}) = 16.9$ min.



(*S*)-Ethyl 3-hydroxy-2-methylpropanoate (**39f**): Known compound,²⁴⁰ 98% ee, $[\alpha]_{\text{D}}^{27} = +18.5$ (c 0.51, MeOH) [lit.:²⁴⁰ $[\alpha]_{\text{D}}^{20} = -15.8$ (c 1.04, MeOH) for the R enantiomer], GC conditions: Supelco Beta DEXTM 120 (30 m x 0.25 mm x 0.25 μm), isothermal 85 °C, 15 psi He, $t_{\text{R}}(\text{R}) = 23.8$ min, $t_{\text{R}}(\text{S}) = 25.0$ min.



(*R*)-Methyl 2-acetamido-3-(3,4-diacetoxyphenyl)propanoate ((*R*)- **12g'**): Known compound,²⁴¹ 99% ee, $[\alpha]_{\text{D}}^{26} = -26.1$ (c 1.00, MeOH) [lit.:²⁴¹ $[\alpha]_{\text{D}}^{20} = +21.0$ (c 1.0, MeOH) for the *S* enantiomer], HPLC conditions: Daicel Chiralcel[®] OJ-H (25 cm x 0.46 cm), 80:20 *n*-hexane/2-propanol, 0.90 mL/min, 216 nm, $t_{\text{R}}(\text{R}) = 33.0$ min, $t_{\text{R}}(\text{S}) = 57.0$ min.

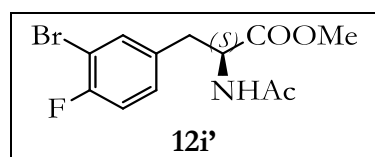


(*R*)-Methyl 2-acetamido-3-(2,5-difluorophenyl)propanoate (**12h'**): Crystalline white solid, 99% ee, M.p. = 76.5-77.8 °C; IR absorption (neat) ν 3310, 1737, 1654, 1541, 1220, 1174 cm^{-1} ; $[\alpha]_{\text{D}}^{25} = -73.7$ (c 0.94, CHCl_3); ^1H NMR (400 MHz, CDCl_3) δ 6.98 (ddd, $J = 9.0, 9.0$ and 4.6 Hz, 1H), 6.95-6.87 (m, 1H), 6.83 (ddd, $J = 8.7, 5.7$ and 3.1 Hz, 1H), 6.06 (bd, $J = 7.7$ Hz, 1H), 4.86 (ddd, $J = 7.7, 6.0$ and 5.8 Hz, 1H), 3.74 (s, 3H), 3.20 (ddd, $J = 13.9, 5.8$ and 0.9 Hz, 1H), 3.08 (ddd, $J = 13.9, 6.0$ and 0.8 Hz, 1H), 1.98 (s, 3H); $^{13}\text{C}\{^1\text{H}\}$ NMR (100 MHz, CDCl_3) δ 171.7 (C), 169.6 (C), 158.4 (dd, $J = 242.7$ and 2.3 Hz, C), 157.3 (dd, $J = 241.0$ and 2.5 Hz, C), 124.7 (dd, $J = 18.8$ and 7.9 Hz, C), 117.9 (dd, $J = 23.9$ and 4.9 Hz,

²⁴⁰ Jeulin, S.; Ayad, T.; Ratovelomanana-Vidal, V.; Genet, J.-P. *Adv. Synth. Catal.* **2007**, *349*, 1592.

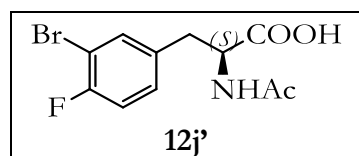
²⁴¹ Ishida, A.; Fujii, H.; Nakamura, T.; Oh-Ishi, T.; Aoe, K.; Nishibata, Y.; Kinumaki, A. *Chem. Pharm. Bull.* **1986**, *34*, 1994.

CH), 116.3 (dd, $J = 25.5$ and 8.8 Hz, CH), 115.3 (dd, $J = 24.0$ and 8.6 Hz, CH), 52.5 (CH), 52.3 (CH₂), 31.5 (CH₃), 23.0 (CH₃); ¹⁹F{¹H} NMR (376 MHz, CDCl₃) δ -123.6 (d, $J = 17.8$ Hz, 1F), -118.6 (d, $J = 17.8$ Hz, 1F); HRMS (ESI⁺) calcd for C₁₂H₁₃F₂NO₃Na [(M+Na)⁺] 280.0761, found 280.0753; HPLC conditions: Daicel Chiralcel[®] OJ-H (25 cm x 0.46 cm), 90:10 *n*-hexane/2-propanol, 1.0 mL/min, 216 nm, $t_{R(-)}$ = 11.9 min (major enantiomer), $t_{R(+)}$ = 15.8 min.



(*S*)-Methyl 2-acetamido-3-(3-bromo-4-fluorophenyl)propanoate²⁴² (**12i'**): White solid, 99% ee, M.p. = 110.4-111.6 °C; IR absorption (neat) ν 3283, 1731, 1654,

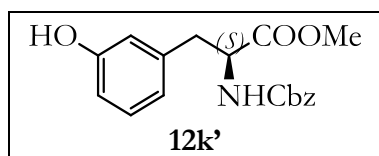
1545 cm⁻¹; [α]_D²⁶ = +56.5 (c 0.46, CHCl₃); ¹H NMR (500 MHz, CDCl₃) δ 7.30-7.28 (m, 1H), 7.05-6.99 (m, 2H), 5.97 (bd, $J = 7.4$ Hz, 1H), 4.84 (ddd, $J = 7.4, 5.8$ and 5.8 Hz, 1H), 3.74 (s, 3H), 3.12 (dd, $J = 14.0$ and 5.8 Hz, 1H), 3.04 (dd, $J = 14.0$ and 5.8 Hz, 1H), 2.01 (s, 3H); ¹³C{¹H} NMR (125 MHz, CDCl₃) δ 171.7 (C), 169.6 (C), 158.3 (d, $J = 245.7$ Hz, C), 134.2 (C), 133.4 (d, $J = 3.8$ Hz, CH), 129.7 (d, $J = 7.2$ Hz, CH), 116.5 (d, $J = 22.1$ Hz, CH), 109.0 (d, $J = 21.0$ Hz, C), 53.1 (CH), 52.5 (CH₂), 36.9 (CH₃), 23.2 (CH₃); ¹⁹F{¹H} NMR (376 MHz, CDCl₃) δ -109.4; HRMS (ESI⁺) calcd for C₁₂H₁₃BrFNO₃Na [(M+Na)⁺] 339.9961, found 339.9952; HPLC conditions: Daicel Chiralcel[®] OJ-H (25 cm x 0.46 cm), 90:10 *n*-hexane/2-propanol, 1.0 mL/min, 216 nm, $t_{R(R)}$ = 15.7 min, $t_{R(S)}$ = 18.7 min.



(*S*)-2-Acetamido-3-(3-bromo-4-fluorophenyl)propanoic acid (**12j'**): Known compound,¹¹² 98% ee, [α]_D²⁵ = +37.0 (c 1.00, MeOH) [lit.¹¹² [α]_D²⁰ = +35.1 (c 1.37, MeOH)]. Prior to

analysis of the enantiomeric excess the carboxylic acid group of the hydrogenation product **12j'** was quantitatively esterified with TMSCHN₂. The resulting derivatized product, (*S*)-methyl 2-acetamido-3-(3-bromo-4-fluorophenyl)propanoate (**12i'**), was analyzed on using the HPLC conditions above-indicated for **12i'**.

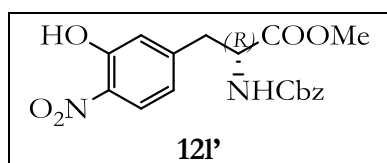
²⁴² The absolute configuration for this new compound was unequivocally assigned by comparison of the specific rotation of the carboxylic acid **12j'** with the data reported for this known compound, which was quantitatively derivatised to the methyl ester **12i'** by esterification reaction with TMSCHN₂.



(*S*)-Methyl 2-((benzyloxycarbonyl)amino)-3-(3-hydroxyphenyl)propanoate (**12k'**): Known compound,^{179b}

98% ee, $[\alpha]_D^{26} = +40.0$ (*c* 1.24, CHCl₃), HPLC conditions:

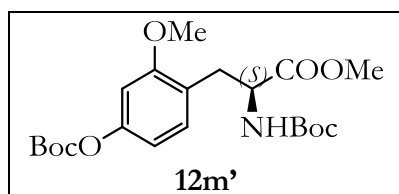
Daicel Chiralcel[®] OJ-H (25 cm x 0.46 cm), 80:20 *n*-hexane/2-propanol, 0.90 mL/min, 216 nm, $t_R(+)$ = 30.4 min (major enantiomer), $t_R(-)$ = 44.2 min.



(*R*)-Methyl 2-((benzyloxycarbonyl)amino)-3-(3-hydroxy-4-nitrophenyl)propanoate (**12l'**): Known compound,^{180b} 98%

ee, $[\alpha]_D^{28} = -62.8$ (*c* 1.10, CHCl₃), HPLC conditions: Daicel

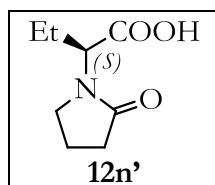
Chiralpak[®] AD-H (25 cm x 0.46 cm), 80:20 *n*-hexane/2-propanol, 1.0 mL/min, 216 nm, $t_R(+)$ = 17.6 min, $t_R(-)$ = 21.3 min (major enantiomer).



(*S*)-Methyl 2-((*tert*-butoxycarbonyl)amino)-3-(4-((*tert*-butoxycarbonyl)oxy)-2-methoxyphenyl)propanoate (**12m'**):

Known compound,²²¹ 98% ee, $[\alpha]_D^{28} = +17.0$ (*c* 0.87,

CHCl₃) [lit.:¹⁸¹ $[\alpha]_D^{20} = +16.2$ (*c* 1.0, CHCl₃)], HPLC conditions: Daicel Chiralcel[®] OJ-H (25 cm x 0.46 cm), 90:10 *n*-hexane/2-propanol, 0.50 mL/min, 216 nm, $t_R(R)$ = 22.7 min, $t_R(S)$ = 28.4 min.

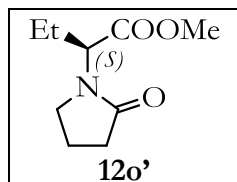


(*S*)-2-(2-Oxopyrrolidin-1-yl)-2-butanoic acid ²⁴³ (**12n'**): Known compound,²⁴⁴ 99% ee. Prior to analysis of the enantiomeric excess the carboxylic acid group of the hydrogenation product **12n'** was

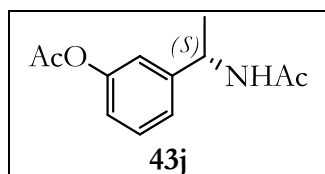
²⁴³ The absolute configuration for the hydrogenation product **12n'** was unequivocally assigned by comparison of the specific rotation of the methyl ester **12o'** with the data reported for this compound, which was quantitatively prepared by esterification reaction of **12o'** with TMSCHN₂.

²⁴⁴ Imahori, T.; Omoto, K.; Hirose, Y.; Takahata, H. *Heterocycles* **2008**, *76*, 1627.

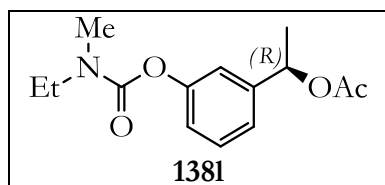
quantitatively esterified with TMSCHN₂. The resulting derivatized product, (*S*)-methyl 2-(2-oxopyrrolidin-1-yl)-2-butanoate (**12o'**), was analyzed on using the HPLC conditions next indicated for **12o'**.



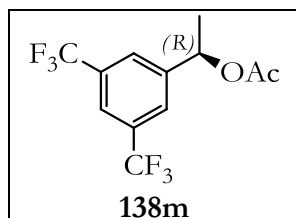
(*S*)-Methyl 2-(2-oxopyrrolidin-1-yl)-2-butanoate (**12o'**): Known compound,²⁴⁵ 99% ee, $[\alpha]_D^{28} = -47.7$ (*c* 1.00, MeOH) [lit.:²⁴⁵ $[\alpha]_D^{20} = -52.2$ (*c* 1, MeOH)], HPLC conditions: Daicel Chiralcel[®] OD-H (25 cm x 0.46 cm), 95:5 *n*-hexane/2-propanol, 1.0 mL/min, 210 nm, $t_R(S) = 14.7$ min, $t_R(R) = 17.3$ min.



(*S*)-*N*-Acetyl-1-(3-acetoxyphenyl)ethylamine (**43j**): Known compound,²²² 98% ee, $[\alpha]_D^{26} = -100.3$ (*c* 0.39, CHCl₃) [lit.:²²² $[\alpha]_D^{21} = -82.2$ (*c* 0.39, CHCl₃)], HPLC conditions: Daicel Chiralpak[®] AD-H (25 cm x 0.46 cm), 90:10 *n*-hexane/2-propanol, 1.0 mL/min, 216 nm, $t_R(R) = 6.9$ min, $t_R(S) = 8.4$ min.



(*R*)-*O*-Acetyl-1-(3-((ethyl(methyl)carbamoyl)oxy)ethyl)phenyl)ethanol (**138l**): Known compound,^{187a} 97% ee, $[\alpha]_D^{26} = +75.8$ (*c* 1.56, CHCl₃) [lit.:^{187a} $[\alpha]_D^{25} = +68.2$ (*c* 1.1, CHCl₃)], HPLC conditions: Daicel Chiralcel[®] OD-H (25 cm x 0.46 cm), 95:5 *n*-hexane/2-propanol, 1.0 mL/min, 217 nm, $t_R(R) = 9.4$ min, $t_R(S) = 11.3$ min.



(*R*)-*O*-Acetyl-1-(3,5-bis(trifluoromethyl)phenyl)ethanol (**138m**): Known compound,¹⁸⁹ 99% ee, $[\alpha]_D^{28} = +52.9$ (*c* 1.00, MeOH) [lit.:¹⁸⁹ $[\alpha]_D^{20} = +57$ (*c* 1, MeOH)], GC conditions: Supelco Beta DEX[™] 225 (30 m x 0.25 mm x 0.25 μm), isothermal 100 °C, 16 psi He, $t_R(R) = 12.8$ min, $t_R(S) = 13.6$ min.

²⁴⁵ Das Sarma, K.; Zhang, J.; Huang, Y.; Davidson, J. G. *Eur. J. Org. Chem.* **2006**, 3730.

CHAPTER II

Iridium-mediated asymmetric hydrogenations

UNIVERSITAT ROVIRA I VIRGILI
HIGHLY MODULAR P -OP LIGANDS FOR RHODIUM- AND IRIIDIUM-MEDIATED ASYMMETRIC HYDROGENATIONS
José Luis Núñez Rico
DL: T.994-2013

CHAPTER II

ASYMMETRIC HYDROGENATION CATALYZED BY IRIIDIUM-(P-OP) COMPLEXES

2.1 ANTECEDENTS

2.1.1 Background

In an analogous way to rhodium-mediated enantioselective hydrogenation, the same chemistry using iridium catalysts has proved to be an efficient tool in industrial applications. One of the first and still major advances in the field is the example of the metolachlor synthetic process. In 1999, Blaser *et al.* reported asymmetric hydrogenation as the key step in the production of the herbicide (*S*)-metolachlor whose trade name is Dual Magnum[®] (Novartis), using an iridium ferrocenyl bisphosphine type catalyst, where the C=N double bond of an imine intermediate was hydrogenated with

high enantioselectivity resulting in an impressive turnover number (TON) >1,000,000 and an initial turnover frequency (TOF) > 1,800,000 h⁻¹.²⁴⁶

Intense efforts have been made during the past few decades in the study of the asymmetric hydrogenation of C=N double bonds, since it has been difficult to achieve improved enantioselectivities, high rates, and broad substrate scope at the same time. Therefore, this transformation remains challenging compared to the well-established and efficient methodology for the catalytic asymmetric hydrogenation of C=C and C=O bonds.

Intensive research in asymmetric imine hydrogenation has led to the discovery of new and efficient catalysts in hydrogenation (and also transfer hydrogenation) mainly based on chiral iridium, palladium, rhodium and ruthenium complexes, with which the number of hydrogenated substrates has grown exponentially.^{247, 248} Asymmetric imine hydrogenation has now reached a level of maturity that should make this reaction useful in organic synthesis. However, despite this progress there are still important challenges that need to be addressed (*e.g.* discovery of catalyst providing high enantioselectivities in the hydrogenation of dialkylsubstituted imines, development of robust supported catalysts, etc.).

²⁴⁶ Blaser, H.-U.; Buser, H.-P.; Coers, K.; Hanreich, R.; Jalett, H.-P.; Jelsch, E.; Pugin, B.; Schneider, H.-D.; Spindler, F.; Wegmann, A. *Chimia* **1999**, *53*, 275.

²⁴⁷ For metal-mediated transformations, see for example: (a) *Comprehensive Asymmetric Catalysis*; Jacobsen, E. N., Pfaltz, A., Yamamoto, H., Eds.; Springer: Berlin, 1999; Vol. 1. (b) Tang, W.; Zhang, X. *Chem. Rev.* **2003**, *103*, 3029. (c) Blaser, H.-U.; Malan, C.; Pugin, B.; Spindler, F.; Steiner, H.; Studer, M. *Adv. Synth. Catal.* **2003**, *345*, 103. (d) Zhang, J. F.; Yang, D. Q.; Long, Y. H. *Chin. J. Org. Chem.* **2009**, *29*, 835. (e) Fleury-Brégeot, N.; de la Fuente, V.; Castellón, S.; Claver, C. *ChemCatChem* **2010**, *2*, 1346. (f) Palmer, A. M.; Zanotti-Gerosa, A. *Curr. Opin. Drug Discovery Dev.* **2010**, *13*, 698. (g) *Catalytic Asymmetric Synthesis*; Ojima, I. Ed.; John Wiley & Sons: Hoboken, New Jersey, 2010. (h) Xie, J.-H.; Zhu, S.-F.; Zhou, Q.-L. *Chem. Rev.* **2011**, *111*, 1713. (i) Yu, Z.; Jin, W.; Jiang, Q. *Angew. Chem., Int. Ed.* **2012**, *51*, 6060. (j) *Comprehensive Chirality*; Carreira, E. M.; Yamamoto, H. Eds.; Elsevier Science: Oxford, 2012; Vol. 5. (k) Chen, Q.-A.; Ye, Z.-S.; Duan, Y.; Zhou, Y.-G. *Chem. Soc. Rev.* **2013**, *42*, 497. (l) Bartoszewicz, A.; Ahlsten, N.; Martín-Matute, B. *Chem.-Eur. J.* **2013**, DOI: 10.1002/chem.201202836.

²⁴⁸ For organocatalyzed C=N reductions, see ref 247l and: (a) de Vries, J. G.; Mrcic, N. *Catal. Sci. Technol.* **2011**, *1*, 51. (b) Zheng, C.; You, S.-L. *Chem. Soc. Rev.* **2012**, *41*, 2498.

There are only two examples in the literature involving the use of iridium-*P-OP* complexes in the asymmetric hydrogenation of imines.²⁴⁹ Iridium complexes of the phosphine-phosphite ligands **154** and **155**, developed by Pizzano *et al.* afforded high enantioselectivities in the reduction of cyclic and acyclic imines (up to 85% ee for ligands **155**).

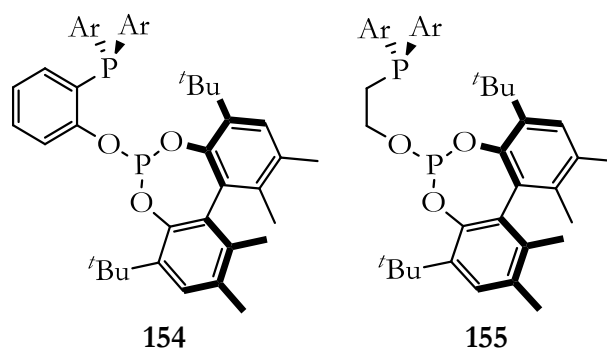


Figure 43. Pizzano's phosphine-phosphite ligands for the reduction of imines.

Asymmetric hydrogenation²⁵⁰ (or transfer hydrogenation) of C=N-containing heterocyclic compounds have been less explored than acyclic imines. Heterocyclic compounds such as benzodiazepines and benzodiazepinones,^{251 a,c} benzoxazepines and benzothiazepines²⁵² or benzoxazines,^{253a,b} have been recently hydrogenated with iridium catalysts with

²⁴⁹ (a) Vargas, S.; Rubio, M.; Suárez, A.; Pizzano, A. *Tetrahedron Lett.* **2005**, *46*, 2049. (b) Vargas, S.; Rubio, M.; Suárez, A.; del Río, D.; Álvarez, E.; Pizzano, A. *Organometallics* **2006**, *25*, 961.

²⁵⁰ The reviews indicated in reference 247d, e, f, h and k and reference 248 contain sections on the hydrogenation or transfer hydrogenation of C=N-containing heterocycles.

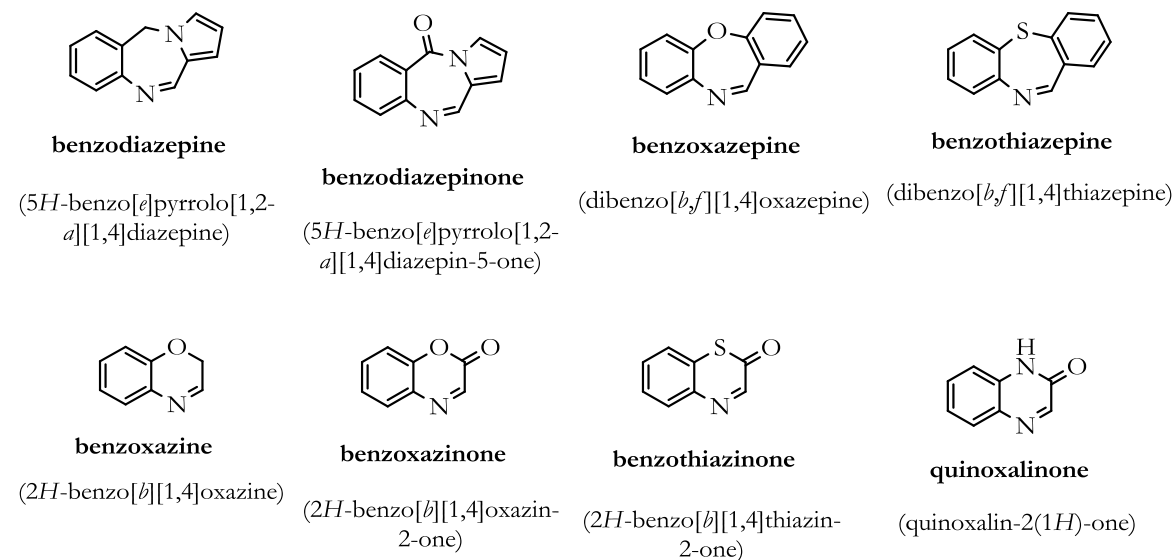
²⁵¹ (a) Gao, K.; Wu, B.; Yu, C.-B.; Chen, Q.-A.; Ye, Z.-S.; Zhou, Y.-G. *Org. Lett.* **2012**, *14*, 3890. (b) Ding, Z.-Y.; Chen, F.; Qin, J.; He, Y.-M.; Fan, Q.-H. *Angew. Chem., Int. Ed.* **2012**, *51*, 5706. (c) Ma, B.; Ding, Z.; Liu, J.; He, Y.; Fan, Q.-H. *Chem.-Asian J* **2013**, DOI: 10.1002/asia.201300150.

²⁵² (a) Gao, K.; Yu, C.-B.; Li, W.; Zhou, Y.-G.; Zhang, X.-M. *Chem. Commun.* **2011**, *47*, 7845. (b) Guo, R.-N.; Gao, K.; Ye, Z.-S.; Shi, L.; Li, Y.; Zhou, Y.-G. *Pure Appl. Chem.* **2013**, *85*, 843.

²⁵³ (a) Gao, K.; Yu, C.-B.; Wang, D.-S.; Zhou, Y.-G. *Adv. Synth. Catal.* **2012**, *354*, 483. (b) Hu, J.; Wang, D.; Zheng, Z.; Hu, X. *Chin. J. Chem.* **2012**, *30*, 2664. (c) Fleischer, S.; Zhou, S.; Werkmeister, S.; Junge, K.; Beller, M. *Chem.-Eur. J.* **2013**, *19*, 4997.

relative success and scope (see Scheme 45 - Scheme 47).²⁵⁴ Benzodiazepines and benzoxazines have also been hydrogenated using ruthenium-^{251b} and iron-based catalysts,^{253c} respectively. Benzoxacines,²⁵⁵ benzoxazinones^{255a} and quinoxalinones²⁵⁶ have been reduced by organocatalyzed asymmetric transfer hydrogenation reactions, whilst benzoxacines and benzoxazinones have also been asymmetrically reduced by relay-catalyzed organocatalytic methods.^{257, 258}

²⁵⁴ The nomenclature used throughout the text for these heterocyclic compounds correspond to abbreviations that will be used for the sake of simplicity. General structures and systematic and abbreviated names for the C=N-containing heterocyclic compounds indicated in the text are as follows:



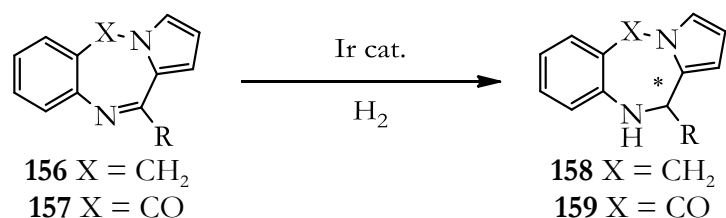
²⁵⁵ (a) Rueping, M.; Antonchik, A. P.; Theissmann, T. *Angew. Chem., Int. Ed.* **2006**, *45*, 6751. (b) Rueping, M.; Stoeckel, M.; Sugiono, E.; Theissmann, T. *Tetrahedron* **2010**, *66*, 6565. (c) Rueping, M.; Sugiono, E.; Steck, A.; Theissmann, T. *Adv. Synth. Catal.* **2010**, *352*, 281. (d) Rueping, M.; Theissmann, T. *Chem. Sci.* **2010**, *1*, 473. (e) Bleschke, C.; Schmidt, J.; Kundu, D. S.; Blechert, S.; Thomas, A. *Adv. Synth. Catal.* **2011**, *353*, 3101. (f) Kundu, D. S.; Schmidt, J.; Bleschke, C.; Thomas, A.; Blechert, S. *Angew. Chem., Int. Ed.* **2012**, *51*, 5456.

²⁵⁶ Rueping, M.; Tato, F.; Schoepke, F. R. *Chem.-Eur. J.* **2010**, *16*, 2688.

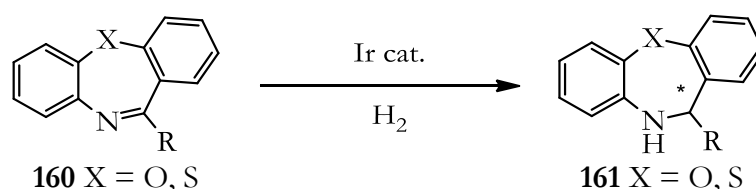
²⁵⁷ Relay catalysis indicates that hydrogen gas acts in the presence of a metal-catalyst as the terminal reducing agent in the catalytic asymmetric transfer hydrogenation of C=N-containing heterocycles, by regenerating the organic compound that delivers a hydride to the substrate (for instance a Hantzsch ester). For a full description of the concept, see: Shi, F.; Gong, L.-Z. *Angew. Chem., Int. Ed.* **2012**, *51*, 11423.

²⁵⁸ (a) Chen, Q.-A.; Chen, M.-W.; Yu, C.-B.; Shi, L.; Wang, D.-S.; Yang, Y.; Zhou, Y.-G. *J. Am. Chem. Soc.* **2011**, *133*, 16432. (b) Chen, Q.-A.; Gao, K.; Duan, Y.; Ye, Z.-S.; Shi, L.; Yang, Y.; Zhou, Y.-G. *J. Am. Chem. Soc.* **2012**, *134*, 2442. (c) Du, W.; Yu, Z. *Synlett* **2012**, *23*, 1300. (d) Du, Z.; Shao, Z. *Chem. Soc. Rev.* **2013**, *42*, 1337.

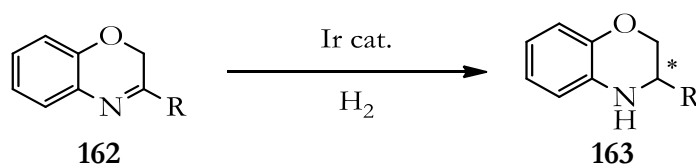
It should be recalled at this point that, to the best of this author's knowledge, benzoxazinones and quinoxalinones have not been enantioselectively hydrogenated and benzothiazinones have neither been enantioselectively hydrogenated nor reduced.



Scheme 45. Asymmetric hydrogenation of benzodiazepines **156** and benzodiazepinones **157**.



Scheme 46. Asymmetric hydrogenation of benzoxazepines and benzothiazepines **160**.



Scheme 47. Asymmetric hydrogenation of benzoxazines **162**.

With regard to the reduction of heteroaromatic compounds, asymmetric hydrogenation constitutes an efficient strategy to access directly to optically active and partially reduced products of quinolines, quinoxalines and, to a lesser extent, indoles and pyridine derivatives. Enantioselective hydrogenation of heteroaromatic compounds may suffer from the following difficulties:

- 1) The high stability of aromatic compounds usually requires harsh conditions (temperature and pressure), thereby adversely affecting enantioselection.²⁵⁹
- 2) Catalyst deactivation and poisoning by nitrogen- and sulfur-containing heteroaromatic compounds.^{260b,c}

Despite the challenges cited above, many groups have been, and still are, actively pursuing new catalytic systems for challenging heteroaromatic compounds.²⁶⁰ Whilst the iridium-mediated asymmetric hydrogenation²⁶¹ of quinolines and quinoxalines has been widely explored, other heteroaromatic compounds such as isoquinolines,²⁶² pyridines,²⁶³ indoles,²⁶¹ pyrroles,²⁶¹ benzofurans,²⁶⁴ oxazoles²⁶⁵ and imidazoles²⁶¹ have been much less explored, and in some occasions the catalytic systems do not involve the use of iridium complexes. Furthermore, for some types of heteroaromatic compounds, substrate activation is required (this topic will be further discussed in section 2.1.2).

²⁵⁹ Bird, C. W. *Tetrahedron* **1992**, *48*, 335.

²⁶⁰ For recent reviews on the field, see references 247e, 247f, 247k and 247i and 248 and the following ones: (a) Glorius, F. *Org. Biomol. Chem.* **2005**, *3*, 4171. (b) Zhou, Y.-G. *Acc. Chem. Res.* **2007**, *40*, 1357. (c) Wang, D.-S.; Chen, Q.-A.; Lu, S.-M.; Zhou, Y.-G. *Chem. Rev.* **2012**, *112*, 2557.

²⁶¹ For each substrate class, see reference 260, the references cited therein and additionally the references indicated for each particular case.

²⁶² For recent hydrogenations of isoquinolines, see: (a) Shi, L.; Ye, Z.-S.; Cao, L.-L.; Guo, R.-N.; Hu, Y.; Zhou, Y.-G. *Angew. Chem., Int. Ed.* **2012**, *51*, 8286. (b) Iimuro, A.; Yamaji, K.; Kandula, S.; Nagano, T.; Kita, Y.; Mashima, K. *Angew. Chem., Int. Ed.* **2013**, *52*, 2046.

²⁶³ For recent hydrogenations of pyridines, see: (a) Ye, Z.-S.; Chen, M.-W.; Chen, Q.-A.; Shi, L.; Duan, Y.; Zhou, Y.-G. *Angew. Chem., Int. Ed.* **2012**, *51*, 10181.

²⁶⁴ For recent hydrogenations of benzofurans, see: (a) Ortega, N.; Urban, S.; Beiring, B.; Glorius, F. *Angew. Chem., Int. Ed.* **2012**, *51*, 1710.

²⁶⁵ For recent hydrogenations of oxazoles, see: (a) Kuwano, R.; Kameyama, N.; Ikeda, R. *J. Am. Chem. Soc.* **2011**, *133*, 7312.

2.1.2 Importance of Chiral Amines and N-Containing Heterocycles

For decades, chiral amines and *N*-containing structures have been important targets in the synthesis of natural products²⁶⁶ and in the preparation of intermediates of many biologically and physiologically active compounds.²⁶⁷ Simple amines, but specifically *N*-containing heterocyclic compounds, are ubiquitous in biology, and therefore are a mainstay in life, biotechnological and materials science research.²⁶⁸

As a representative example, substituted tetrahydroquinolines (THQ) have attracted considerable attention from organic and medicinal chemists, primarily because they display a wide range of biological activities.^{269, 270} In addition, this bicyclic ring system is present in a number of important natural products (see Figure 44), as exemplified by the antibiotic antiviral virantmycin (**164**),²⁷¹ the NMDA antagonist agent L-689,560 (**165**),²⁷² the naturally

²⁶⁶ *Heterocycles in Natural Product Synthesis*; Majumdar, K. C., Chattopadhyay, S. K., Eds.; Wiley-VCH: Weinheim, 2011.

²⁶⁷ See, for a general overview: (a) Michael, J. P. *Nat. Prod. Rep.* **1997**, *14*, 605. (b) Daly, J. W. *J. Nat. Prod.* **1998**, *61*, 162. (c) O'Hagan, D. *Nat. Prod. Rep.* **2000**, *17*, 435. (d) Daly, J. W.; Spande, T. F.; Garraffo, H. M. *J. Nat. Prod.* **2005**, *68*, 1556. (e) Michael, J. P. *Nat. Prod. Rep.* **2005**, *22*, 603.

²⁶⁸ See, for example: (a) *Pharmaceutical Substances*; Kleemann, A., Engel, J., Kutscher, B., Reichert, D., Eds.; Thieme: Stuttgart, New York, 2001. (b) Roy, B.; De, N.; Majumdar, K. C. *Chem.-Eur. J.* **2012**, *18*, 14560. (c) Yook, K. S.; Lee, J. Y. *Adv. Mater.* **2012**, *24*, 3169.

²⁶⁹ See reference 268a and the following: (a) Leeson, P. D.; Carling, R. W.; Moore, K. W.; Moseley, A. M.; Smith, J. D.; Stevenson, G.; Chan, T.; Baker, R.; Foster, A. C.; et, a. *J. Med. Chem.* **1992**, *35*, 1954. (b) Nagata, R.; Tanno, N.; Kodo, T.; Ae, N.; Yamaguchi, H.; Nishimura, T.; Antoku, F.; Tatsuno, T.; Kato, T.; et, a. *J. Med. Chem.* **1994**, *37*, 3956. (c) Kouznetsov, V.; Palma, A.; Ewert, C.; Varlamov, A. *J. Heterocycl. Chem.* **1998**, *35*, 761.

²⁷⁰ (a) Katritzky, A. R.; Rachwal, S.; Rachwal, B. *Tetrahedron* **1996**, *52*, 15031. (b) Sridharan, V.; Suryavanshi, P. A.; Menendez, J. C. *Chem. Rev.* **2011**, *111*, 7157.

²⁷¹ Omura, S.; Nakagawa, A. *Tetrahedron Lett.* **1981**, *22*, 2199.

²⁷² Leeson, P. D.; Iversen, L. L. *J. Med. Chem.* **1994**, *37*, 4053.

occurring THQ alkaloid galipinine (**166**),²⁷³ angustureine (**168**)²⁷⁴ and cuspareine (**169**),^{273b} or the antibacterial agent flumequine (**167**).²⁷⁵

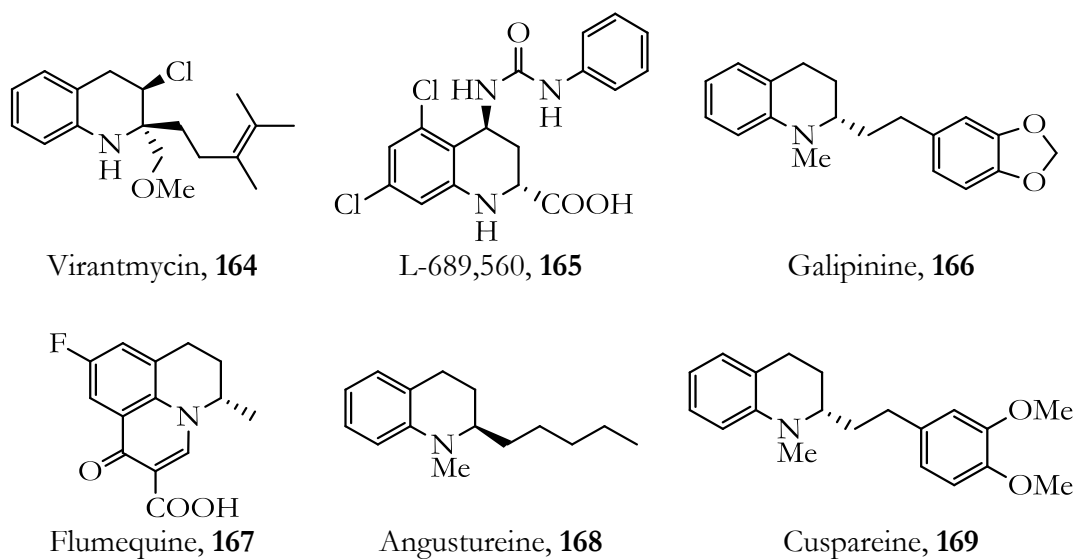
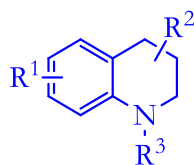


Figure 44. Some relevant chiral tetrahydroquinoline derivatives.

Also, the derivatives of tetrahydroisoquinoline (THIQ),²⁷⁶ have received a lot of attention since many chiral derivatives of THIQs are biologically active, or constitute the core backbone of several APIs.

Some representative examples of these important molecules are depicted in Figure 45, such as the anesthetic agent **170**²⁷⁷ and the urinary

²⁷³ (a) Rakotoson, J. H.; Fabre, N.; Jacquemond-Collet, I.; Hannedouche, S.; Fouraste, I.; Moulis, C. *Planta Med.* **1998**, *64*, 762. (b) Houghton, P. J.; Woldemariam, T. Z.; Watanabe, Y.; Yates, M. *Planta Med.* **1999**, *65*, 250.

²⁷⁴ Jacquemond-Collet, I.; Hannedouche, S.; Fabre, N.; Fouraste, I.; Moulis, C. *Phytochemistry* **1999**, *51*, 1167.

²⁷⁵ Balint, J.; Egri, G.; Fogassy, E.; Bocskei, Z.; Simon, K.; Gajary, A.; Friesz, A. *Tetrahedron: Asymmetry* **1999**, *10*, 1079.

²⁷⁶ Kaur, K.; Jain, M.; Reddy, R. P.; Jain, R. *Eur. J. Med. Chem.* **2010**, *45*, 3245.

antispasmodic product solifenacin (**171**).²⁷⁷ 1-Alkyl substituted tetrahydroisoquinoline alkaloids, such as (*S*)-salsolidine (**172**),²⁷⁸ (*S*)-norreticuline (**176**),^{278b} and (*S*)-norlaudanosine (**177**),²⁷⁹ are of great interest to synthetic chemists because they are key intermediates in the synthesis of more complex alkaloids such as (*S*)-xylopinine²⁸⁰ and (–)-morphine.²⁸¹ Other important chiral molecules containing the THIQ substructure deserve mention also: the AMPA receptor antagonist **173**,²⁷⁷ the alkaloids cryptostyline II and III (**174** and **175**, respectively),²⁸² crispine A (**178**),^{247h, 283} which has shown remarkably cytotoxic activity, and the drug candidate for insomnia treatment almorexant (**179**).^{247f}

²⁷⁷ (a) Berhal, F.; Wu, Z.; Zhang, Z.; Ayad, T.; Ratovelomanana-Vidal, V. *Org. Lett.* **2012**, *14*, 3308. (b) Ruzic, M.; Pecavar, A.; Prudic, D.; Kralj, D.; Scriban, C.; Zanotti-Gerosa, A. *Org. Process Res. Dev.* **2012**, *16*, 1293.

²⁷⁸ (a) Battersby, A. R.; Edwards, T. P. *J. Chem. Soc.* **1960**, 1214. (b) Xie, J.-H.; Yan, P.-C.; Zhang, Q.-Q.; Yuan, K.-X.; Zhou, Q.-L. *ACS Catal.* **2012**, *2*, 561.

²⁷⁹ Corrodi, H.; Hardegger, E. *Helv. Chim. Acta* **1956**, *39*, 889.

²⁸⁰ (a) Munchhof, M. J.; Meyers, A. I. *J. Org. Chem.* **1996**, *61*, 4607. (b) Mastranzo, V. M.; Yuste, F.; Ortiz, B.; Sanchez-Obregon, R.; Toscano, R. A.; Garcia, R. J. L. *J. Org. Chem.* **2011**, *76*, 5036.

²⁸¹ (a) Rice, K. C.; Brossi, A. *J. Org. Chem.* **1980**, *45*, 592. (b) Kitamura, M.; Hsiao, Y.; Ohta, M.; Tsukamoto, M.; Ohta, T.; Takaya, H.; Noyori, R. *J. Org. Chem.* **1994**, *59*, 297.

²⁸² (a) Scott, J. D.; Williams, R. M. *Chem. Rev.* **2002**, *102*, 1669. (b) Chang, M.; Li, W.; Zhang, X. *Angew. Chem., Int. Ed.* **2011**, *50*, 10679.

²⁸³ (a) Zhang, Q.; Tu, G.; Zhao, Y.; Cheng, T. *Tetrahedron* **2002**, *58*, 6795. (b) Wu, T. R.; Chong, J. M. *J. Am. Chem. Soc.* **2006**, *128*, 9646. (c) Hou, G.-H.; Xie, J.-H.; Yan, P.-C.; Zhou, Q.-L. *J. Am. Chem. Soc.* **2009**, *131*, 1366.

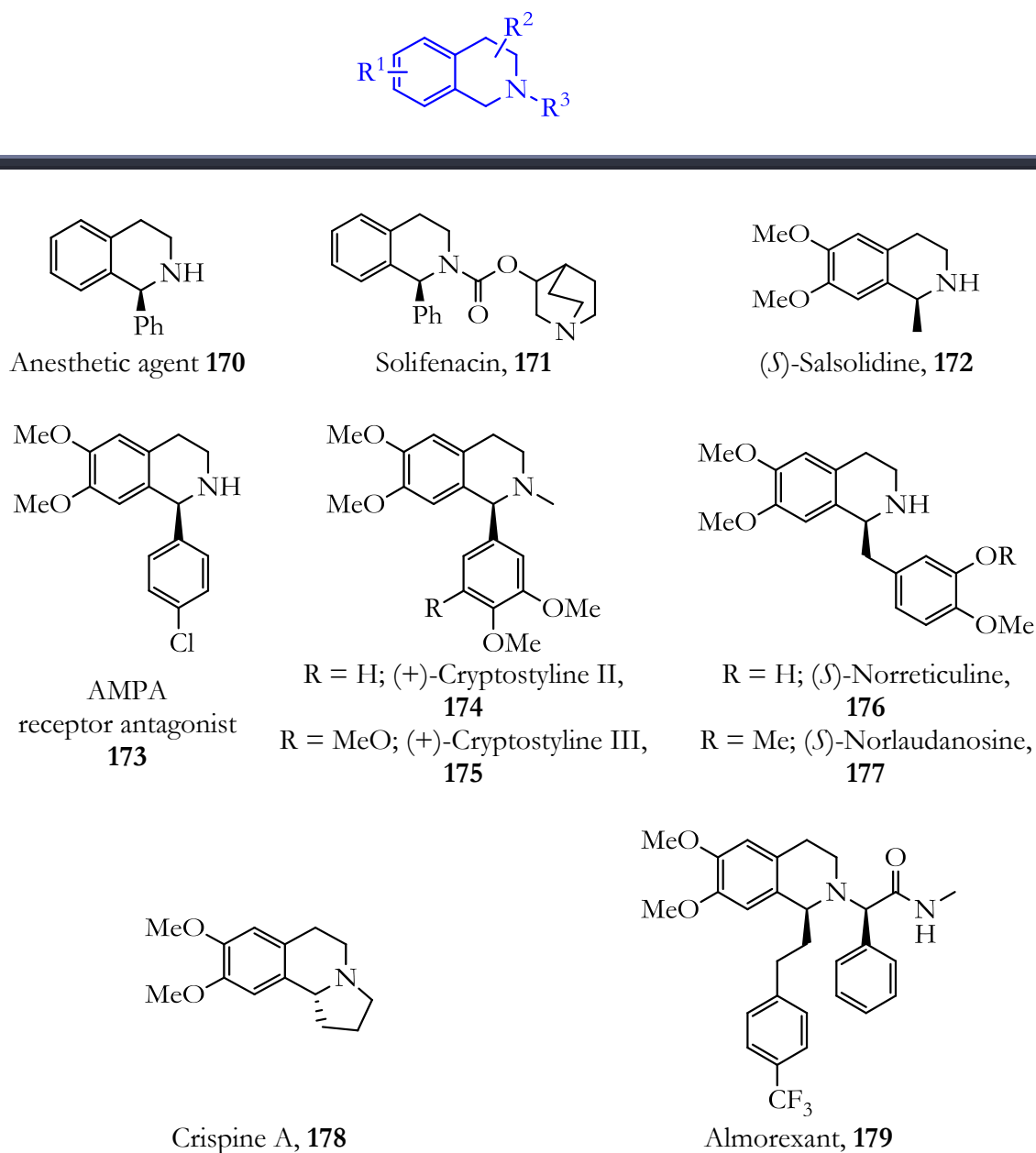


Figure 45. Some relevant chiral tetrahydroisoquinoline derivatives.

Benzodiazepines and benzodiazepinones are other important classes of heterocyclic compounds with interesting biological properties (Figure 46).²⁸⁴

²⁸⁴ (a) *Advances in the Study of Pyrrolo[2,1-*c*][1,4]benzodiazepine Antitumour Antibiotics*, in *Molecular Aspects of Anticancer Drug-DNA Interactions*; Neidle, S., Waring, M. J., Eds.; Macmillan: London, 1993. (b) Horton, D. A.; Bourne, G. T.; Smythe, M. L. *Chem. Rev.* **2003**, *103*, 893. (c) Antonow, D.; Barata, T.; Jenkins, T. C.; Parkinson, G. N.; Howard, P. W.; Thurston, D. E.; Zloh, M. *Biochemistry* **2008**, *47*, 11818. (d) Kumaraswamy, M. N.; Vaidya, V. P.;

Specifically, the pyrrolobenzodiazepinone²⁸⁵ skeleton is present in several naturally occurring antitumor antibiotics,²⁸⁶ such as anthramycin (**180**)^{251a, 286a} and tilivalline (**181**).^{251a, 286b,c} Aptazepine (**182**) is a novel antidepressant agent^{251a, 287} that incorporates the pyrrolobenzodiazepine²⁸⁵ core.

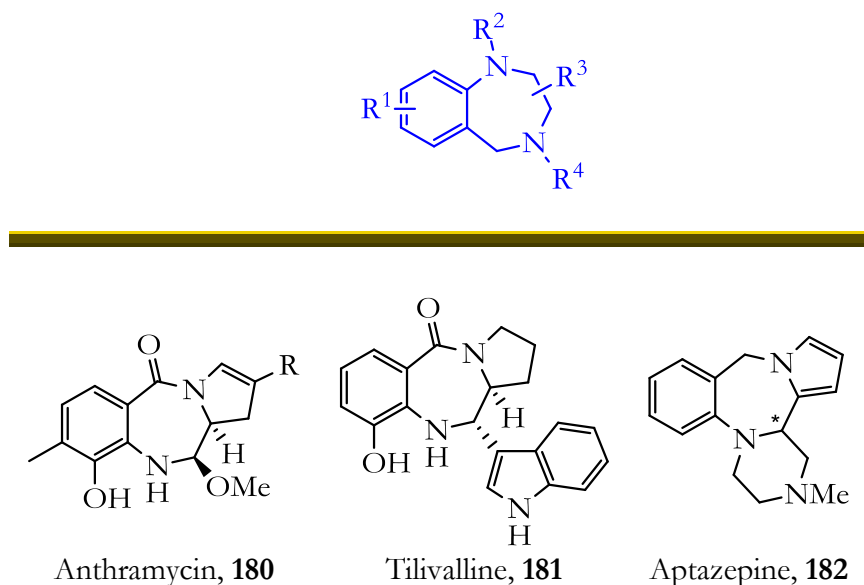
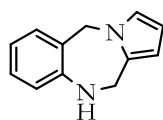


Figure 46. Some relevant chiral benzodiazepinone and benzodiazepine derivatives.

Chandrashekhar, C.; Prathima, M. D. A.; Shivakumar, H.; Mahadevan, K. M. *Int. J. Pharm., Chem. Biol. Sci.* **2013**, *3*, 281.

²⁸⁵ The nomenclature used throughout the text for these heterocyclic compounds correspond to abbreviations that will be used for the sake of simplicity. General structures and systematic and abbreviated names are as follows:



pyrrolobenzodiazepine

(10,11-dihydro-5*H*-benzo[*e*]pyrrolo[1,2-*a*][1,4]diazepine)

²⁸⁶ (a) Komatsu, N.; Kimura, K.; Abe, S.; Kagitani, Y. *J. Antibiot.* **1980**, *33*, 54. (b) Mohr, N.; Budzikiewicz, H. *Tetrahedron* **1982**, *38*, 147. (c) Mori, S.; Aoyama, T.; Shioiri, T. *Tetrahedron Lett.* **1986**, *27*, 6111.

²⁸⁷ (a) Massa, S.; Artico, M.; Mai, A.; Corelli, F.; Botta, M.; Tafi, A.; Pantaleoni, G. C.; Giorgi, R.; Coppolino, M. F. *J. Med. Chem.* **1992**, *35*, 4533. (b) Roszkowski, P.; Maurin, J. K.; Czarnocki, Z. *Synthesis* **2012**, *44*, 241.

The indoline skeleton is another class of ubiquitous scaffold²⁸⁸ found in many naturally occurring alkaloids²⁸⁹ and pharmaceutically active compounds.²⁹⁰ Among the various classes of chiral indolines, 2-substituted indolines have a privileged status due to their presence in many active pharmaceutical ingredients (Figure 47), such as for instance benzastatin E (**183**),^{288, 290c, 291} the angiotensin converting enzyme (ACE) inhibitor pentopril (**184**)^{290c, 292}, which is synthesized from (*S*)-indoline-2-carboxylic acid,²⁹³ and the antihypertensive drugs perindopril (**185**)²⁹⁴ and indolapril (**186**).²⁹⁵

²⁸⁸ See next review and the references cited therein: Liu, D.; Zhao, G.; Xiang, L. *Eur. J. Org. Chem.* **2010**, 3975.

²⁸⁹ (a) Dewick, P. M. *Medicinal Natural Products. A Biosynthetic Approach*, 2nd Ed.; John Wiley and Sons, Ltd: New York, 2002. (b) Gueritte, F.; Fahy, J. *In Anticancer Agents from Natural Products*; Cragg, G. M., Kingston, D. G. I., Newman, D. J., Eds.; CRC Press: Boca Raton, 2005; pp 123–135.

²⁹⁰ (a) Bromidge, S. M.; Duckworth, M.; Forbes, I. T.; Ham, P.; King, F. D.; Thewlis, K. M.; Blaney, F. E.; Naylor, C. B.; Blackburn, T. P.; Kennett, G. A.; Wood, M. D.; Clarke, S. E. *J. Med. Chem.* **1997**, *40*, 3494. (b) Hobson, L. A.; Nugent, W. A.; Anderson, S. R.; Deshmukh, S. S.; Haley, J. J., III; Liu, P.; Magnus, N. A.; Sheeran, P.; Sherbine, J. P.; Stone, B. R. P.; Zhu, J. *Org. Process Res. Dev.* **2007**, *11*, 985. (c) Anas, S.; Kagan, H. B. *Tetrahedron: Asymmetry* **2009**, *20*, 2193. (d) Turnpenny, B. W.; Hyman, K. L.; Chemler, S. R. *Organometallics* **2012**, *31*, 7819. (e) Ni, J.; Wang, H.; Reisman, S. E. *Tetrahedron*, DOI: 10.1016/j.tet.2013.04.003. (f) Ghorai, M. K.; Nanaji, Y. *J. Org. Chem.* **2013**, *78*, 3867.

²⁹¹ (a) Kim, W.-G.; Kim, J.-P.; Koshino, H.; Shin-Ya, K.; Seto, H.; Yoo, I.-D. *Tetrahedron* **1997**, *53*, 4309. (b) Toda, N.; Ori, M.; Takami, K.; Tago, K.; Kogen, H. *Org. Lett.* **2003**, *5*, 269. (c) Ori, M.; Toda, N.; Takami, K.; Tago, K.; Kogen, H. *Tetrahedron* **2005**, *61*, 2075.

²⁹² Gruenfeld, N.; Stanton, J. L.; Yuan, A. M.; Ebetino, F. H.; Browne, L. J.; Gude, C.; Huebner, C. F. *J. Med. Chem.* **1983**, *26*, 1277.

²⁹³ Sato, S.; Watanabe, H.; Asami, M. *Tetrahedron: Asymmetry* **2000**, *11*, 4329.

²⁹⁴ (a) Remko, M.; Bojarska, J.; Jezko, P.; Maniukiewicz, W.; Olczak, A. *J. Mol. Struct.* **2013**, *1036*, 292. (b) Chatragadda, N.; Avula, P. R.; Sunkara, B.; Chandra, B. S. *Am. Chem. Sci. J.* **2012**, *2*, 161. (c) Patel, B. K.; Patel, P. U. *J. Pharm. Sci. Res.* **2013**, *5*, 36.

²⁹⁵ (a) Ryan, M. J.; Boucher, D. M.; Cohen, D. M.; Essenburg, A. D.; Major, T. C.; Mertz, T. E.; Olszewski, B. J.; Randolph, A. E.; Singer, R. M.; Kaplan, H. R. *J. Pharmacol. Exp. Ther.* **1984**, *228*, 312. (b) Blankley, C. J.; Kaltenbronn, J. S.; DeJohn, D. E.; Werner, A.; Bennett, L. R.; Bobowski, G.; Krolls, U.; Johnson, D. R.; Pearlman, W. M. *J. Med. Chem.* **1987**, *30*, 992.

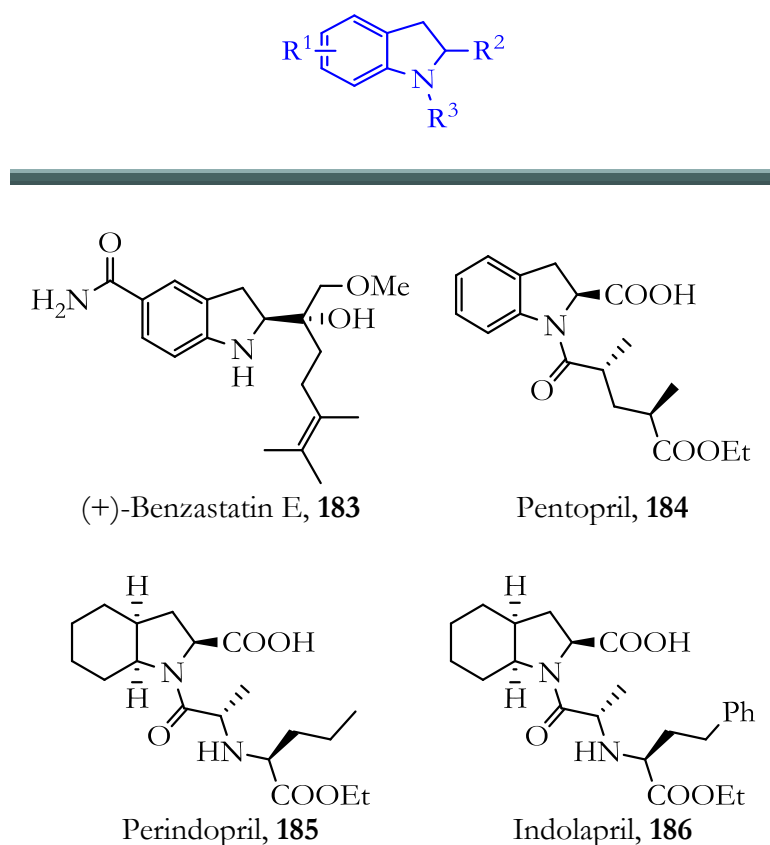


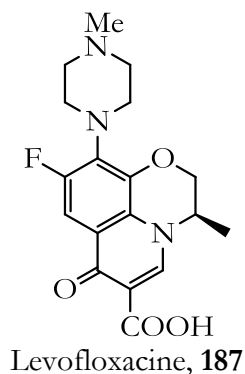
Figure 47. Some relevant chiral indoline derivatives.

Chiral dihydro-2*H*-benzoxazines are valuable building blocks in the synthesis of many pharmaceuticals, such as antidepressants, calcium antagonists, as well as antibacterial, antimicrobial and anti-inflammatory agents.^{268, 296} Several examples of dihydro-2*H*-benzoxazine-containing active pharmaceutical ingredients are depicted in Figure 48 including the potent antibacterial agent levofloxacin (**187**),^{247h, 255b, 297} the cannabinoid CB₁ receptor

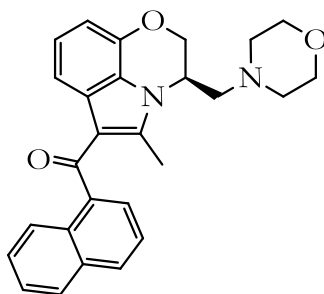
²⁹⁶ (a) *Antibiotics and Antiviral Compounds*; Krohn, K.; Kirst, H. A.; Maag, H., Eds.; VCH: Weinheim, 1993. (b) Achari, B.; Mandal, S. B.; Dutta, P. K.; Chowdhury, C. *Synlett* **2004**, 2449. (c) Ilas, J.; Anderluh, P. S.; Dolenc, M. S.; Kikelj, D. *Tetrahedron* **2005**, *61*, 7325.

²⁹⁷ Atarashi, S.; Yokohama, S.; Yamazaki, K.; Sakano, K.; Imamura, M.; Hayakawa, I. *Chem. Pharm. Bull.* **1987**, *35*, 1896.

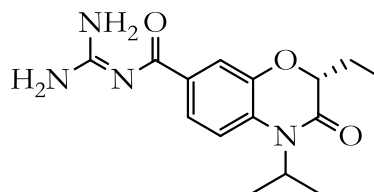
WIN-55,212-2 (**188**),²⁹⁸ the heart disease, myocardial necrosis or arrhythmia agent **189**^{296c} and the azembuja alkaloids like compound **190**.²⁹⁹



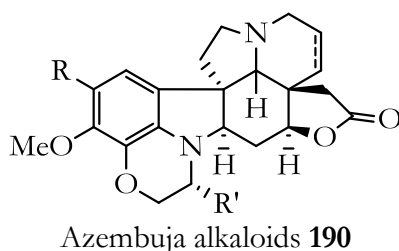
Levofloxacin, **187**



WIN-55,212-2, **188**



Drug for heart disease treatment **189**



Azembuja alkaloids **190**

Figure 48. Some relevant chiral benzoxazine derivatives.

Quinoxalinones are also attractive molecules since they exhibit a wide variety of biological activity, ranging from antidiabetic³⁰⁰ to antiviral properties (in particular against retroviruses such as HIV³⁰¹). Related 3,4-dihydroquinoxalines also possess biological activity as, for example, inhibitors

²⁹⁸ (a) Shim, J.-Y.; Collantes, E. R.; Welsh, W. J.; Subramaniam, B.; Howlett, A. C.; Eissenstat, M. A.; Ward, S. J. *J. Med. Chem.* **1998**, *41*, 4521. (b) McAllister, S. D.; Rizvi, G.; Anavi-Goffer, S.; Hurst, D. P.; Barnett-Norris, J.; Lynch, D. L.; Reggio, P. H.; Abood, M. E. *J. Med. Chem.* **2003**, *46*, 5139.

²⁹⁹ Brown, K. S., Jr.; Djerassi, C. *J. Am. Chem. Soc.* **1964**, *86*, 2451.

³⁰⁰ Gupta, D.; Ghosh, N. N.; Chandra, R. *Bioorg. Med. Chem. Lett.* **2005**, *15*, 1019.

³⁰¹ Roesner, M.; Billhardt-Troughton, U.-M.; Kirsch, R.; Kleim, J.-P.; Meichsner, C.; Riess, G.; Winkler, I., EP708093A1, 1996.

of cholesteryl ester transfer proteins.³⁰² Some of the most relevant chiral structures based on the dihydroquinoxaline or quinoxalinone core are presented in Figure 49, and comprise the reverse transcriptase inhibitor GW420867X (**191**),³⁰³ the anti-HIV agent **192**,^{301, 304} the estrogen receptor **193**,³⁰⁵ the histone inhibitor **194**,³⁰⁶ the anti-arteriosclerosis agent **195**,³⁰⁷ the prostaglandin D2 receptor antagonist **196**,^{307b,308} the B1 receptor antagonists **197**³⁰⁹ and **198**,³¹⁰ the M2 acetylcholine receptor antagonist **199**^{307a,b, 311} and the cholesteryl ester transfer protein (CETP) inhibitors **200**³¹² and **201**.^{304, 302}

³⁰² Jones, Z.; Groneberg, R.; Drew, M.; Eary, C. T., US Patent 20050282812A1, 2005.

³⁰³ Cass, L. M.; Moore, K. H. P.; Dallow, N. S.; Jones, A. E.; Sisson, J. R.; Prince, W. T. *J. Clin. Pharmacol.* **2001**, *41*, 528.

³⁰⁴ Abraham, C. J.; Paull, D. H.; Scerba, M. T.; Grebinski, J. W.; Lectka, T. *J. Am. Chem. Soc.* **2006**, *128*, 13370.

³⁰⁵ Mahaney, P. E.; Webb, M. B.; Ye, F.; Sabatucci, J. P.; Steffan, R. J.; Chadwick, C. C.; Harnish, D. C.; Trybulski, E. J. *Bioorg. Med. Chem.* **2006**, *14*, 3455.

³⁰⁶ Smil, D. V.; Manku, S.; Chantigny, Y. A.; Leit, S.; Wahhab, A.; Yan, T. P.; Fournel, M.; Maroun, C.; Li, Z.; Lemieux, A.-M.; Nicolescu, A.; Rahil, J.; Lefebvre, S.; Panetta, A.; Besterman, J. M.; Deziel, R. *Bioorg. Med. Chem. Lett.* **2009**, *19*, 688.

³⁰⁷ (a) Chang, G.; Didiuk, M. T.; Finneman, J. I.; Garigipati, R. S.; Kelley, R. M.; Perry, D. A.; Ruggeri, R. B.; Bechle, B. M., WO2004085401A1, 2004. (b) Cartigny, D.; Nagano, T.; Ayad, T.; Genet, J.-P.; Ohshima, T.; Mashima, K.; Ratovelomanana-Vidal, V. *Adv. Synth. Catal.* **2010**, *352*, 1886. (c) Cartigny, D.; Berhal, F.; Nagano, T.; Phansavath, P.; Ayad, T.; Genet, J.-P.; Ohshima, T.; Mashima, K.; Ratovelomanana-Vidal, V. *J. Org. Chem.* **2012**, *77*, 4544.

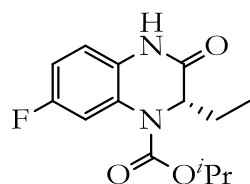
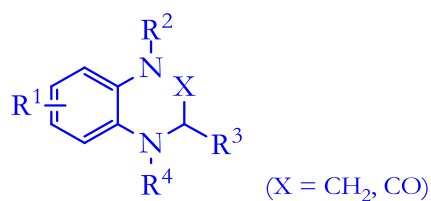
³⁰⁸ Torisu, K.; Kobayashi, K.; Iwahashi, M.; Nakai, Y.; Onoda, T.; Nagase, T.; Sugimoto, I.; Okada, Y.; Matsumoto, R.; Nanbu, F.; Ohuchida, S.; Nakai, H.; Toda, M. *Bioorg. Med. Chem.* **2004**, *12*, 5361.

³⁰⁹ Chen, J. J.; Qian, W.; Biswas, K.; Viswanadhan, V. N.; Askew, B. C.; Hitchcock, S.; Hungate, R. W.; Arik, L.; Johnson, E. *Bioorg. Med. Chem. Lett.* **2008**, *18*, 4477.

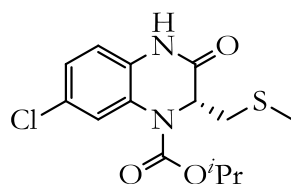
³¹⁰ (a) Su, D.-S.; Markowitz, M. K.; DiPardo, R. M.; Murphy, K. L.; Harrell, C. M.; O'Malley, S. S.; Ransom, R. W.; Chang, R. S. L.; Ha, S.; Hess, F. J.; Pettibone, D. J.; Mason, G. S.; Boyce, S.; Freidinger, R. M.; Bock, M. G. *J. Am. Chem. Soc.* **2003**, *125*, 7516. (b) Morissette, G.; Fortin, J.-P.; Otis, S.; Bouthillier, J.; Marceau, F. *J. Pharmacol. Exp. Ther.* **2004**, *311*, 1121.

³¹¹ Kuhl, A.; Kolkhof, P.; Telan, L.; Peters, J.-G.; Lustig, K.; Kast, R.; Muentner, K.; Stasch, J.-P.; Tinel, H., WO2005028451A1, 2005.

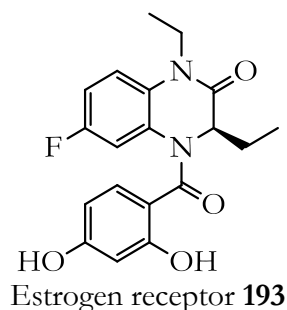
³¹² Eary, C. T.; Jones Zachary, S.; Groneberg Robert, D.; Burgess Laurence, E.; Mareska David, A.; Drew Mark, D.; Blake James, F.; Laird Ellen, R.; Balachari, D.; O'Sullivan, M.; Allen, A.; Marsh, V. *Bioorg. Med. Chem. Lett.* **2007**, *17*, 2608.



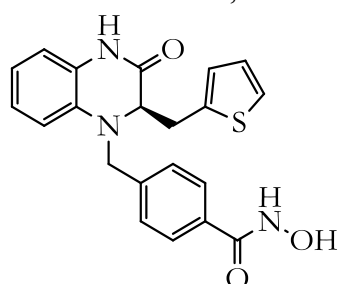
GW420867X, **191**



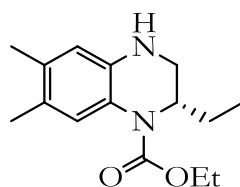
Anti-HIV agent **192**



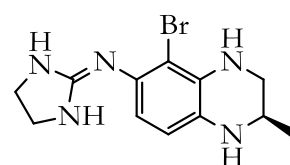
Estrogen receptor **193**



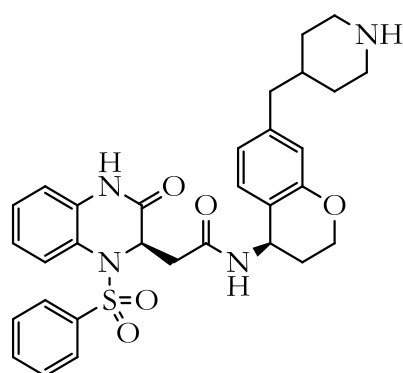
Histone inhibitor **194**



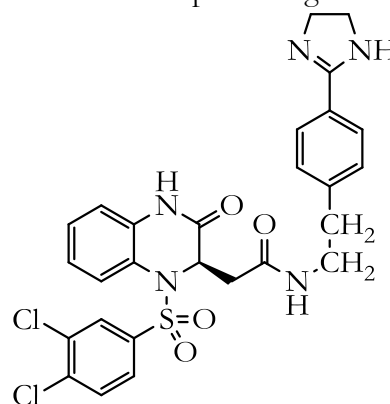
Anti-arteriosclerosis agent **195**



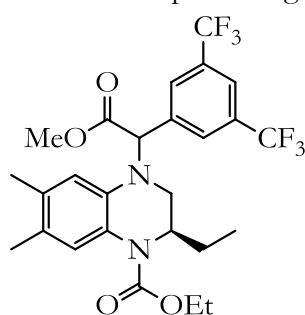
Prostaglandin D2
receptor antagonist **196**



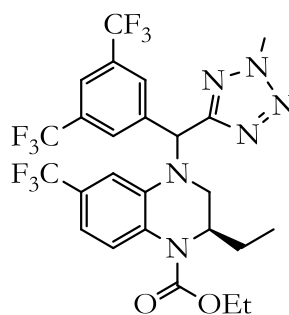
B1 Receptor antagonist **197**



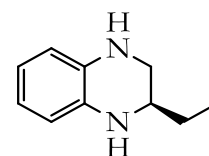
B1 Receptor antagonist **198**



M2 Acetylcholine receptor antagonist
199



CETP Inhibitor **200**



CETP Inhibitor **201**

Figure 49. Some relevant chiral quinoxaline and quinoxalinone derivatives.

Asymmetric reduction of C=N-containing functional groups from unsaturated precursors has played a key role in the preparation of the previously mentioned heterocycles in enantiopure or enantioenriched form.^{247,260} Therefore, iridium-mediated asymmetric hydrogenation of unsaturated heterocycles such as quinolines, quinoxalines, benzoxazines, quinoxalinones and so on, provides a convenient and efficient route to synthesize their (partially) reduced analogs in an enantioselective way.

2.1.3 Strategies for Catalyst and Substrate Activation: the Role of Additives

Hydrogenation of prochiral heterocyclic and heteroaromatic compounds is a much less explored field than the hydrogenation of alkenes, ketones and acyclic imines. In many cases, successful hydrogenation of C=N-containing compounds requires developing particular activation strategies for asymmetric hydrogenation of these substrates. Inherent difficulties that need to be addressed for a highly selective hydrogenation include the following:

- 1) The high stability of aromatic compounds usually requires harsh conditions to break the aromaticity, thereby adversely affecting enantioselection.²⁵⁹
- 2) Deactivation or poisoning of chiral catalysts by *N*- (or *S*-) containing compounds may occur.^{260b,c, 313, 247j}
- 3) The absence of a secondary coordinating group in simple aromatic compounds, in contrast to functionalized alkenes, facilitates a higher number of orientation possibilities of the substrate around the metal center and this may account for the difficulty in achieving high enantioselectivities.

As it was clear that aromaticity would disfavor hydrogenation of heteroaromatics, the first of such compounds to be asymmetrically³¹⁴ reduced were benzo-fused compounds, in which the heteroatom-containing ring is more prone to reduction than their monocyclic analog. This statement can be confirmed by comparing, for instance, the aromaticity index for pyridine and quinoline (compare entries 2 and 4 in Table 16). In accordance with these

³¹³ *Iridium Catalysis, Topics in Organometallic Chemistry*; Andersson, P. G., Ed.; Springer-Verlag: Berlin, 2011.

³¹⁴ For recent and comprehensive reviews on AH of aromatic compounds, see reference 260.

observations, a great deal of examples of highly enantioselective partial hydrogenation of bicyclic (hetero)aromatic compounds have been published in the literature, whilst reports on highly enantioselective hydrogenation methods of monocyclic (hetero)aromatics are less abundant.

Moreover, the higher the number of heteroatoms in a ring, the lower its aromatic character and consequently, the lower the hydrogenation energy becomes. Crabtree *et al.* illustrated this concept by predicting the values of enthalpy of dehydrogenation for benzene, piperidine and piperazine at the DFT level (see Figure 50).³¹⁵ Dehydrogenation reactions are highly endothermic but Crabtree's calculations showed that the presence of one or more nitrogen atoms lowered the unfavorable enthalpy of the reaction.

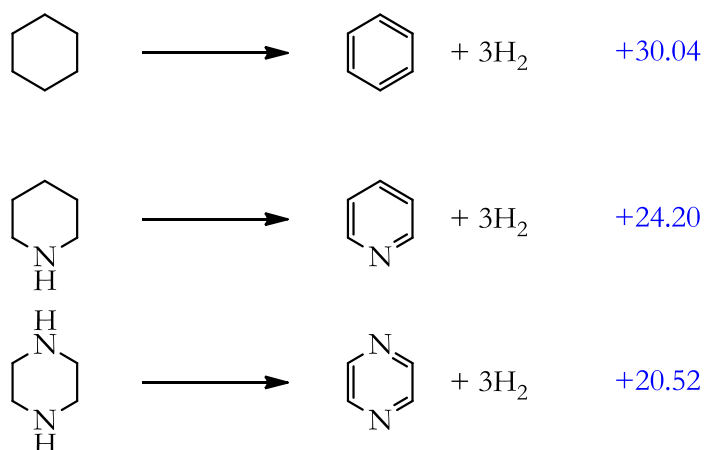
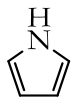
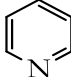
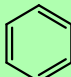
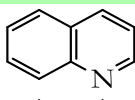
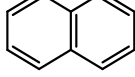
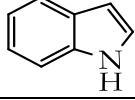


Figure 50. Computed enthalpy of dehydrogenation for some single-ring aromatic compounds (kcal mol⁻¹).

Lastly, the introduction of substituents close to the heteroatoms may lead to weaker binding between the heteroatom and metal center due to steric reasons. Potential poisoning and deactivation effects may thus be reduced.

³¹⁵ Moores, A.; Poyatos, M.; Luo, Y.; Crabtree, R. H. *New J. Chem.* **2006**, *30*, 1675.

Table 16. Unified aromaticity indices (I_A) for a range of selected arenes.²⁵⁹

Entry	Compound	Structure	I_A
1	Pyrrole		85
2	Pyridine		86
3	Benzene		100
4	Quinoline		134
5	Naphthalene		142
6	Indole		146

Substrate activation or catalyst activation (or dual activation when both are combined) have been widely used in iridium-mediated hydrogenations. The mechanisms of action of several additives in hydrogenation (*i.e.* modification of the oxidation state of the metal center, switching on more favored reaction pathways, etc.) are understood and have recently become an active field of research.²⁴⁷ⁱ As an example, it is worth recalling at this stage that iodine is one of the most commonly used additives in iridium(I) chemistry. It has been observed that iodine oxidatively adds to the iridium center, thus promoting a change in its oxidation state. The resulting iridium(III) complexes are more reactive towards hydrogen activation and the overall hydrogenation process is favored.³¹⁶

³¹⁶ It has been reported that iodine increased the reactivity of iridium-mediated asymmetric hydrogenation of imines, presumably *via* transformation of the initial Ir(I) complex to a more catalytically active Ir(III) catalyst, see: (a) Ng Cheong Chan, Y.; Osborn, J. A. *J. Am. Chem. Soc.* **1990**, *112*, 9400. (b) Xiao, D.; Zhang, X. *Angew. Chem., Int. Ed.* **2001**, *40*, 3425. (c) Dorta, R.; Broggini, D.; Stoop, R.; Rueegger, H.; Spindler, F.; Togni, A. *Chem.-Eur. J.* **2004**, *10*, 267. (d) Hou, G.-H.; Xie, J.-H.; Wang, L.-X.; Zhou, Q.-L. *J. Am. Chem. Soc.* **2006**, *128*, 11774.

With regard to substrate activation, certain types of C=N-containing derivatives have also been activated by transforming them into more reactive isomers or derivatives. In some cases, additives can break the aromaticity of the substrate, as in the case of *N*-unprotected indole derivatives.^{260c}

Incorporation of a secondary coordination group into the substrate to assist binding has also been used.^{260b,c} For instance, *N*-containing heterocycles have been transformed in the corresponding chloroformates, with an overall increase in the hydrogenation ease.³¹⁷ The introduction of this activating group on the heteroatom facilitated coordination to the catalyst and additionally prevented catalyst deactivation. Another example belonging to this strategy has been reported by Charette *et al.*, who transformed pyridine derivatives into *N*-benzoyliminopyridinium ylides, which were further hydrogenated in high conversion.³¹⁸

In the latter cases, the addition of the activator involves additional synthetic steps arising from the introduction and removal of the activating group; thus, strategies that do not require further steps or can be achieved by *in situ* modification of the substrate are highly desirable.

Combinations of Brønsted³¹⁹ or Lewis acids (*e.g.* AgSbF₆)³²⁰, as activators, with a transition metal catalyst have been efficiently applied to the AH of imines.³²¹ Activation by the addition of Brønsted acids appears to be a practical way of activation in this chemistry,^{247i,322} given the easy availability of Brønsted acids and the easy deprotonation of the hydrogenated product by

³¹⁷ Lu, S.-M.; Wang, Y.-Q.; Han, X.-W.; Zhou, Y.-G. *Angew. Chem., Int. Ed.* **2006**, *45*, 2260.

³¹⁸ Legault, C. Y.; Charette, A. B. *J. Am. Chem. Soc.* **2005**, *127*, 8966.

³¹⁹ Shao, Z.; Zhang, H. *Chem. Soc. Rev.* **2009**, *38*, 2745.

³²⁰ (a) Li, C.; Xiao, J. *J. Am. Chem. Soc.* **2008**, *130*, 13208. (b) Shirai, S.-y.; Nara, H.; Kayaki, Y.; Ikariya, T. *Organometallics* **2009**, *28*, 802.

³²¹ (a) Li, C.; Wang, C.; Villa-Marcos, B.; Xiao, J. *J. Am. Chem. Soc.* **2008**, *130*, 14450. (b) Li, C.; Villa-Marcos, B.; Xiao, J. *J. Am. Chem. Soc.* **2009**, *131*, 6967. (c) Zhou, S.; Fleischer, S.; Junge, K.; Beller, M. *Angew. Chem., Int. Ed.* **2011**, *50*, 5120.

³²² Akiyama, T. *Chem. Rev.* **2007**, *107*, 5744.

simple workup conditions. Specifically, Ohshima, Ratovelomanana-Vidal, Mashima and co-workers hydrogenated quinolinium halides, which after a simple basic workup of the hydrogenation product, were easily released the desired tetrahydroquinolines.³²³

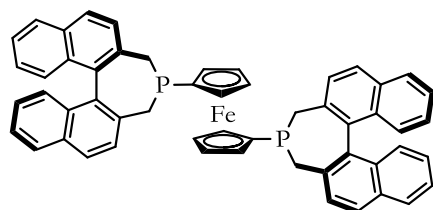
³²³ Tadaoka, H.; Cartigny, D.; Nagano, T.; Gosavi, T.; Ayad, T.; Genêt, J.-P.; Ohshima, T.; Ratovelomanana-Vidal, V.; Mashima, K. *Chem.-Eur. J.* **2009**, *15*, 9990.

2.1.4 Mechanistic Proposals

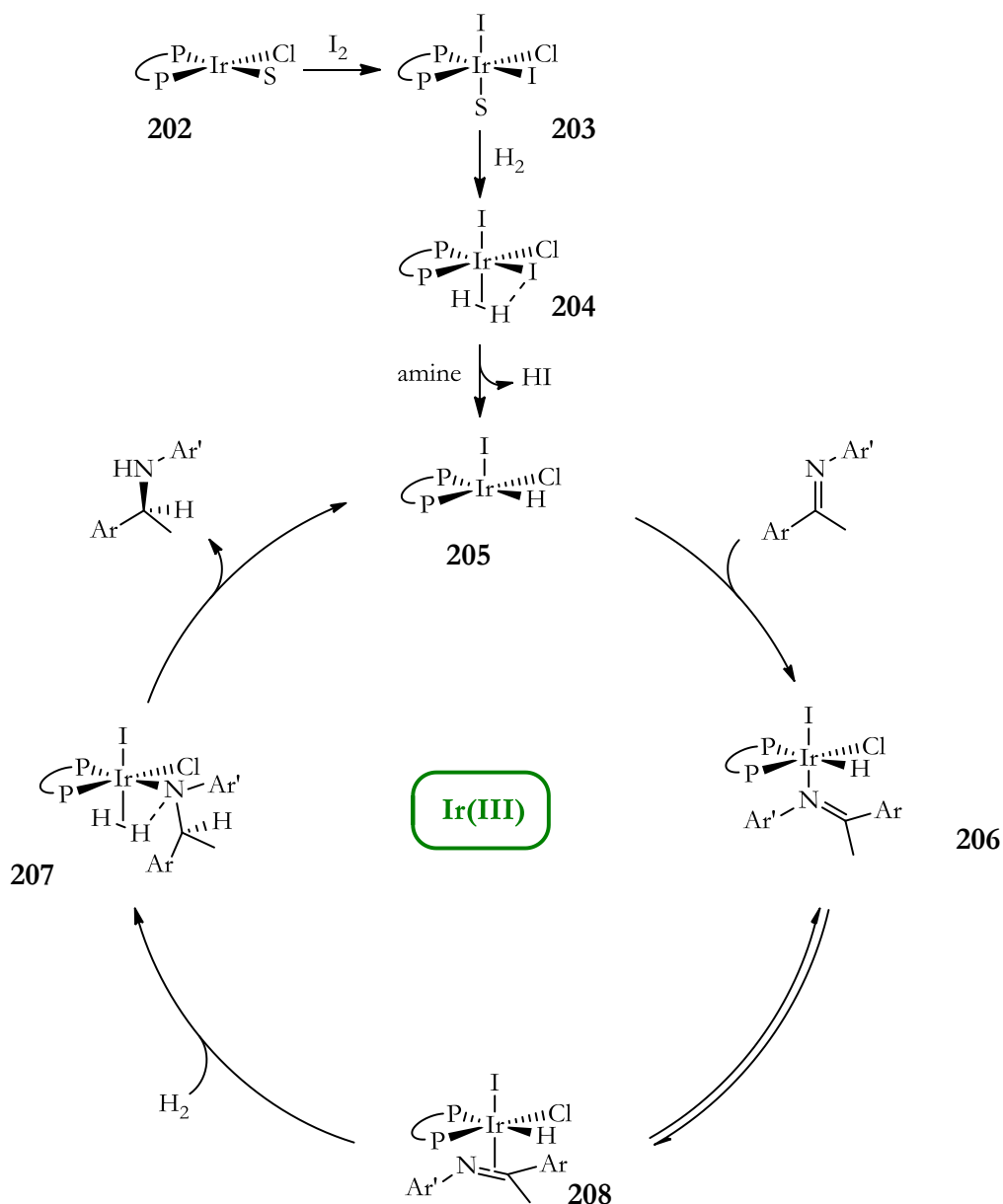
Although the mechanisms for iridium-mediated asymmetric hydrogenation have been less studied than their rhodium counterparts, some sound proposals have been made for the hydrogenation of C=N double bonds, mainly for the hydrogenation of imines, quinolines and isoquinolines, as detailed in the following.

Zhang and co-workers proposed a mechanism for the Ir-f-binaphane-catalyzed³²⁴ asymmetric hydrogenation of imines^{316b} in the presence of I₂ as additive. The addition of iodine in this case was required to achieve high enantioselectivities. The authors proposed a catalytic cycle based on the Ir(III) monohydrido complex **205** (Scheme 48). The first step in the catalyst activation process consists of the oxidative addition of I₂ to the initial Ir(I) complex **202** to give **203**. Coordination of molecular dihydrogen (**204**) followed by base mediated elimination of hydrogen iodide leads to the Ir(III)–H catalyst **205**. The asymmetric hydrogenation process starts with coordination of the imine, in an equilibrating η^1 - η^2 fashion (**206-208**), followed by migratory insertion of the η^2 -C=N group into the Ir-H bond and dihydrogen coordination to give (**207**). The stereogenic carbon is thus created and subsequent H₂ heterolytic cleavage regenerates the Ir(III) catalyst **205**.

324



(R,R)-f-binaphane



Scheme 48. Proposed mechanism for the Ir-f-binaphane-catalysed hydrogenation of imines (S = substrate or solvent).

Several other different mechanisms have been proposed in the literature for various achiral iridium catalysts. Studies from Herrera *et al.* (for $[\text{Ir}(\text{cod})(\text{PPh}_3)_2]^+$ catalyst),³²⁵ Eisenstein *et al.* (for $[\text{Ir}(\text{Cp})(\kappa^2\text{-CO}_3)]$ catalyst),³²⁶

³²⁵ Herrera, V.; Munoz, B.; Landaeta, V.; Canudas, N. *J. Mol. Catal. A: Chem.* **2001**, *174*, 141.

³²⁶ Balcells, D.; Nova, A.; Clot, E.; Gnanamgari, D.; Crabtree, R. H.; Eisenstein, O. *Organometallics* **2008**, *27*, 2529.

Fabrello *et al.* (for general iridium-based *P,P* and *P,N* catalysts)³²⁷ and Oro *et al.* (for $[\text{IrH}_2(\mu_6\text{-C}_6\text{H}_6)(\text{P}^i\text{Pr}_3)]^+$ catalyst³²⁸ and for $[\text{Ir}_2(\mu\text{-H})(\mu\text{-Pz})_2\text{H}_2-(\eta^2\text{-H}_2)(\text{NCMe})(\text{P}^i\text{Pr}_3)_2]^+$ catalyst)³²⁹ have evidenced a wide range of mechanistic possibilities for such a simple transformation. Hopmann *et al.* studied computationally the asymmetric hydrogenation of imines mediated by iridium(I) complexes of chiral phosphinoxazoline³³⁰ ligand ($[\text{Ir}(\text{PHOX})]^+$ complexes).³³¹ They found that all the mechanistic pathways involving imine coordination to the iridium center involved energy barriers 40 to 60 kcal mol⁻¹ higher than those involving unbound C=N groups, and proposed the mechanism depicted in Scheme 49 for the Ir-(PHOX)-mediated imine hydrogenation.

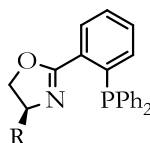
This mechanism initially involves the hydrogenation of cyclooctadiene in complex **209** followed by dihydrogen oxidative addition, which led to isomeric complexes **210** and **211**. Subsequent binding of other ligands (*i.e.* solvent) to **210** or **211** afforded the complex **212**, which are considered the starting point of the catalytic cycle. The reaction proceeds by the displacement of the imine substrate by a H₂ molecule (**213**), followed by proton transfer from an equatorially coordinated H₂ molecule to the nitrogen atom of the unbound imine to give **215**. Subsequent transfer of the hydrido group, located in the *trans* position with respect to the phosphine, to the iminium carbon

³²⁷ Fabrello, A.; Bachelier, A.; Urrutigoity, M.; Kalck, P. *Coord. Chem. Rev.* **2010**, *254*, 273.

³²⁸ Martin, M.; Sola, E.; Tejero, S.; Andres, J. L.; Oro, L. A. *Chem.–Eur. J.* **2006**, *12*, 4043.

³²⁹ Martin, M.; Sola, E.; Tejero, S.; Lopez, J. A.; Oro, L. A. *Chem.–Eur. J.* **2006**, *12*, 4057.

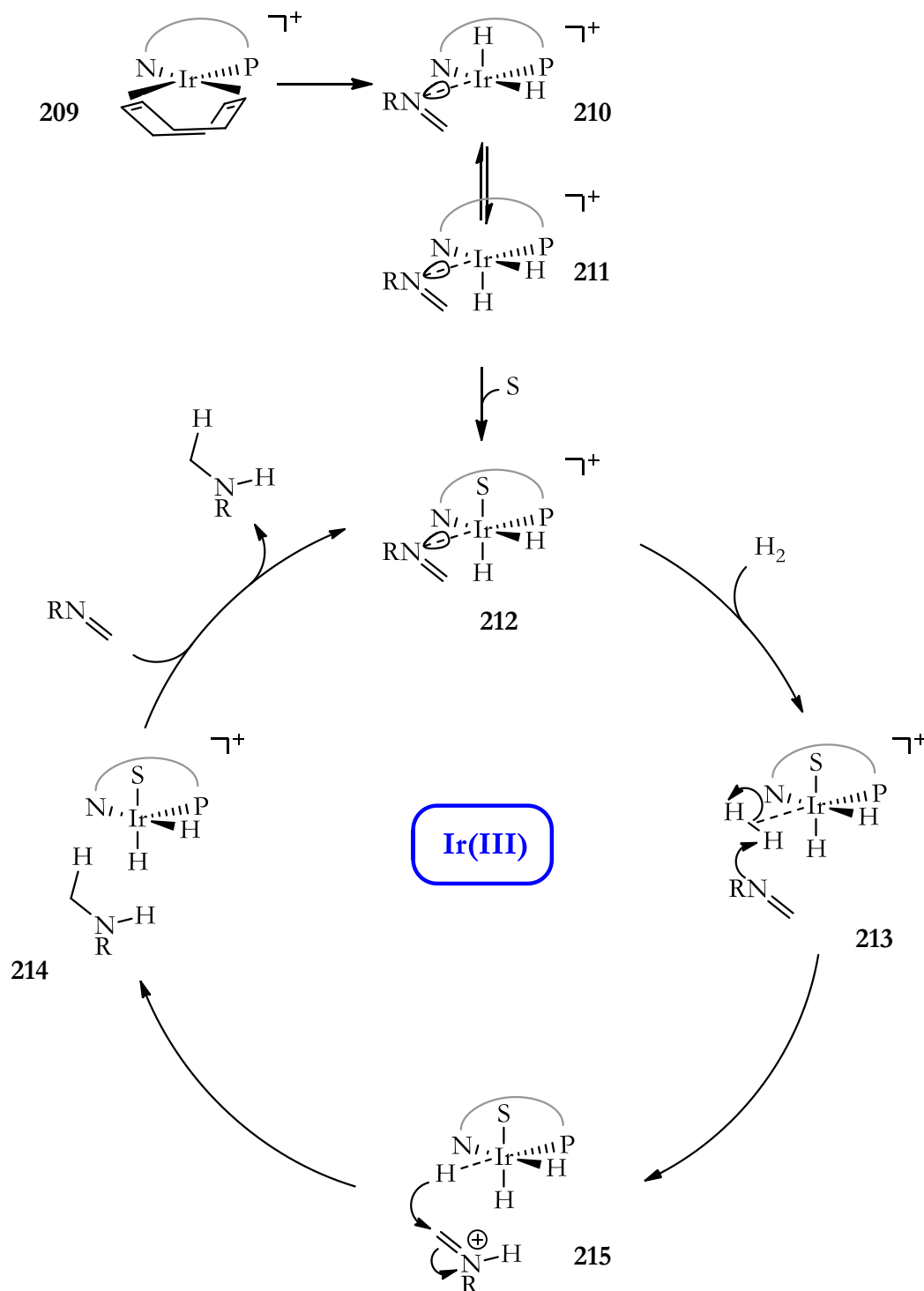
³³⁰



Phosphinoxazoline (PHOX)
Ligands

³³¹ Hopmann, K. H.; Bayer, A. *Organometallics* **2011**, *30*, 2483.

results in the formation of the new C-H bond (**214**). This hydrido group transfer is both the stereo- and rate-determining step. Further coordination of a *N*-containing group to the Ir-center regenerates the catalytic species **212**.



Scheme 49. Outer sphere coordination mechanism for the Ir-(PHOX)-mediated hydrogenation of unfunctionalized imines (S = solvent).

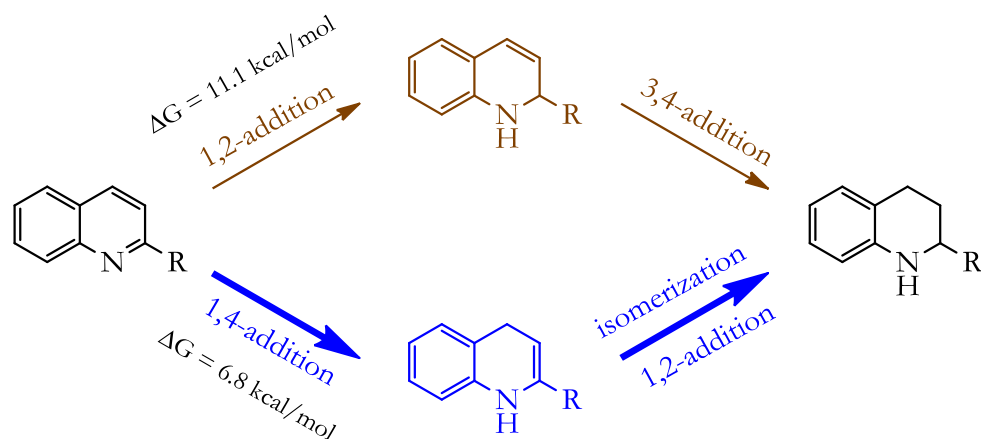
The Hopmann studies with enantiomerically pure $[\text{Ir}(\text{PHOX})]^+$ complexes showed that the free, unbound imine, is able to adopt a tilted orientation that favors the formation of the (*R*)-configured amine. In conclusion, Hopmann *et al.* proposed for the $[\text{Ir}(\text{PHOX})]^+$ -catalyzed hydrogenation of imines an outer sphere coordination mechanism involving stepwise proton and hydride transfers. Due to the absence of substrate-iridium coordination and the flexibility of the unbound imine, the enantioselectivity of this transformation is expected to be more sensitive to the reaction conditions than hydrogenations of bound substrates with the same catalysts.

With respect to the hydrogenation of the heteroaromatic compound quinoline, early mechanistic proposals for this transformation assumed inner sphere coordination of the substrate with Rh-,³³² Ru-³³³ or Ir-based³³⁴ catalysts. In the description of the mechanism proposed by Zhou *et al.*,^{334b} a preferential inner sphere coordination 1,4-addition of dihydrogen, followed by an internal isomerization and dihydrogen 1,2-addition is proposed, instead of a direct 1,2-addition followed by a 3,4-addition route (Scheme 50). Computed thermodynamic values for both routes gave an energetic gap of 4.3 kcal/mol in favor of the 1,4-/1-2-addition route.

³³² (a) Baralt, E.; Smith, S. J.; Hurwitz, J.; Horváth, I. T.; Fish, R. H. *J. Am. Chem. Soc.* **1992**, *114*, 5187. (b) Sanchez-Delgado, R. A.; Rondon, D.; Andriollo, A.; Herrera, V.; Martín, G.; Chaudret, B. *Organometallics* **1993**, *12*, 4291. (c) Bianchini, C.; Barbaro, P.; Macchi, M.; Meli, A.; Vizza, F. *Helv. Chim. Acta* **2001**, *84*, 2895. (d) Bianchini, C.; Meli, A.; Vizza, F. *Eur. J. Inorg. Chem.* **2001**, 43.

³³³ Rosales, M.; Boves, M.; Soscún, H.; Ruetter, F. *J. Mol. Struct. THEOCHEM* **1998**, *433*, 319.

³³⁴ (a) Rosales, M.; Vallejo, R.; Jose Soto, J.; Jhonatan Bastidas, L.; Molina, K.; Baricelli, P. J. *Catal. Lett.* **2010**, *134*, 56. (b) Wang, D.-W.; Wang, X.-B.; Wang, D.-S.; Lu, S.-M.; Zhou, Y.-G.; Li, Y.-X. *J. Org. Chem.* **2009**, *74*, 2780.



Scheme 50. Possible pathways for the hydrogenation of quinolines.

In contrast to the previous mechanistic proposal, and inspired by the outer sphere coordination mechanism proposed by Chan *et al.* for a Ru catalyst,³³⁵ Eisenstein, Crabtree and co-workers performed a combined experimental and theoretical study on the hydrogenation of 2-methylquinoline with achiral iridium complexes incorporating *N*-heterocyclic carbene (NHC) and phosphorus ligands.³³⁶ They proposed a mechanism for the hydrogenation of quinolines, supported by DFT calculations, which showed that the classical inner sphere mechanism (substrate coordination and insertion into a metal-hydride bond) is energetically unfavorable. In their proposed mechanism, a *N*-protonation, 1,4-addition of hydride, 1,4/1,2-isomerization of the C=C bond, *N*-protonation and 1,2-addition sequence in the outer sphere of the metal³³⁷ (Scheme 51) is the energetically favored hydrogenation pathway. The dihydroquinoline isomerization step, that links the first and second H₂ addition cycles, may be favored by protic acid catalysis and is in coexistence with protons delivered by the acidic iridium dihydrogen complex (see Scheme 51

³³⁵ Zhou, H.; Li, Z.; Wang, Z.; Wang, T.; Xu, L.; He, Y.; Fan, Q.-H.; Pan, J.; Gu, L.; Chan, A. S. C. *Angew. Chem., Int. Ed.* **2008**, *47*, 8464.

³³⁶ Dobereiner, G. E.; Nova, A.; Schley, N. D.; Hazari, N.; Miller, S. J.; Eisenstein, O.; Crabtree, R. H. *J. Am. Chem. Soc.* **2011**, *133*, 7547.

³³⁷ Eisenstein, O.; Crabtree, R. H. *New J. Chem.* **2013**, *37*, 21.

for an overall view of the mechanism proposed by Eisenstein, Crabtree and co-workers).

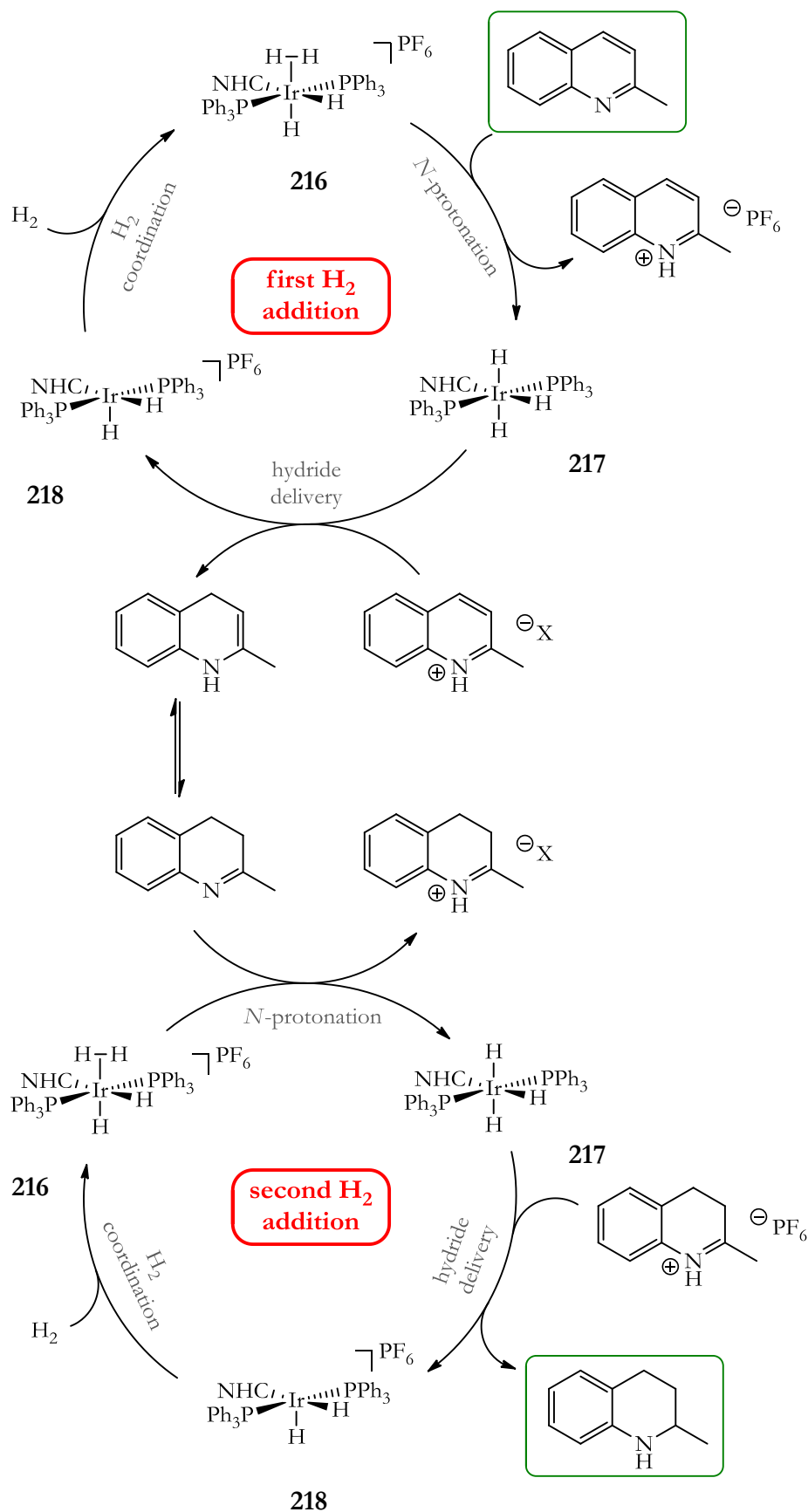
Acid catalysis has been also reported to increase the rate of reaction in several hydrogenations of this type,^{332c, 338} and in these cases the acid is probably involved in the proton transfer step.

Some other mechanisms have been proposed for other substrates, adapted to their binding ability, particular reaction conditions, and their topology and potential tautomeric equilibria. For instance, Mashima, Togni and co-workers³³⁹ have also suggested a metal-ligand bifunctional catalytic mechanism³⁴⁰ in the iridium-mediated hydrogenation of coordinative unhindered substrates (*i.e.* quinoxalines) in the presence of secondary amines as additives.

³³⁸ (a) Mrcic, N.; Lefort, L.; Boogers, J. A. F.; Minnaard, A. J.; Feringa, B. L.; de Vries, J. G. *Adv. Synth. Catal.* **2008**, *350*, 1081. (b) Deport, C.; Buchotte, M.; Abecassis, K.; Tadaoka, H.; Ayad, T.; Ohshima, T.; Genet, J.-P.; Mashima, K.; Ratovelomanana-Vidal, V. *Synlett* **2007**, 2743.

³³⁹ Nagano, T.; Iimuro, A.; Schwenk, R.; Ohshima, T.; Kita, Y.; Togni, A.; Mashima, K. *Chem.-Eur. J.* **2012**, *18*, 11578.

³⁴⁰ (a) Yamakawa, M.; Ito, H.; Noyori, R. *J. Am. Chem. Soc.* **2000**, *122*, 1466. (b) Noyori, R.; Yamakawa, M.; Hashiguchi, S. *J. Org. Chem.* **2001**, *66*, 7931. (c) Ikariya, T.; Murata, K.; Noyori, R. *Org. Biomol. Chem.* **2006**, *4*, 393. (d) Sandoval, C. A.; Ohkuma, T.; Utsumi, N.; Tsutsumi, K.; Murata, K.; Noyori, R. *Chem.-Asian J.* **2006**, *1*, 102. (e) Sandoval, C. A.; Li, Y.; Ding, K.; Noyori, R. *Chem.-Asian J.* **2008**, *3*, 1801.



Scheme 51. Outer sphere coordination mechanism for the $[\text{Ir}(\text{NHC})(\text{PPh}_3)_2]^{3+}$ -mediated hydrogenation of 2-methylquinoline.

2.2 P-OP LIGANDS IN IRIIDIUM-MEDIATED ASYMMETRIC HYDROGENATION

2.2.1 Studies on Iridium-P-OP Coordination

As mentioned in section 1.2.1.3, *P-OP* ligands (phosphine-phosphinites and phosphine-phosphites) contain two phosphorus functionalities which behave as bidentate ligands forming stable complexes with transition metals (Figure 51).

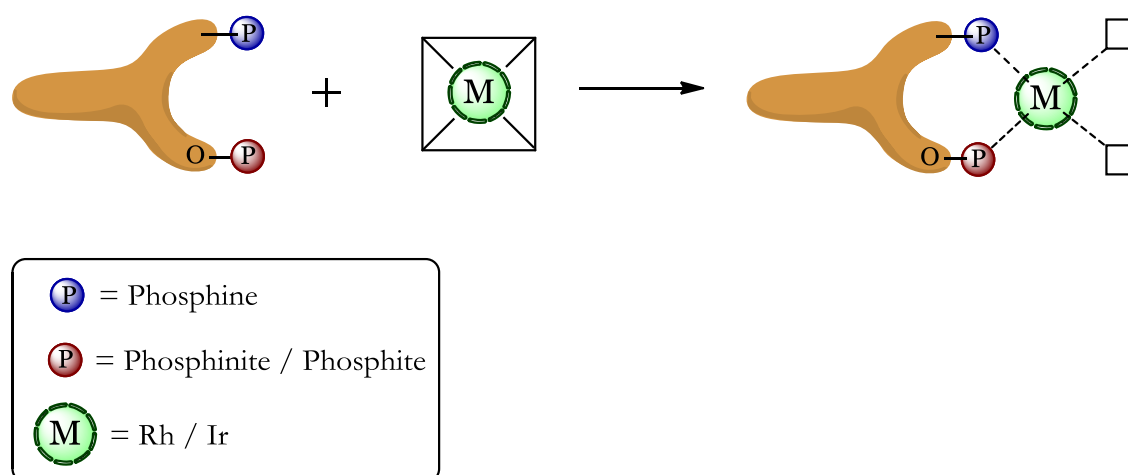


Figure 51. *P-OP* complexation with transition metals.

Following our studies on the chemistry of rhodium complexes derived from *P-OP* ligands, we next examined their coordination behavior with iridium precursors, to form neutral and cationic complexes derived from phosphine-phosphinites and phosphine-phosphites (see Figure 52 and Figure 53).

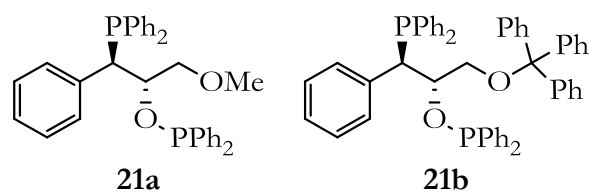


Figure 52. Assayed phosphine-phosphinite ligands.

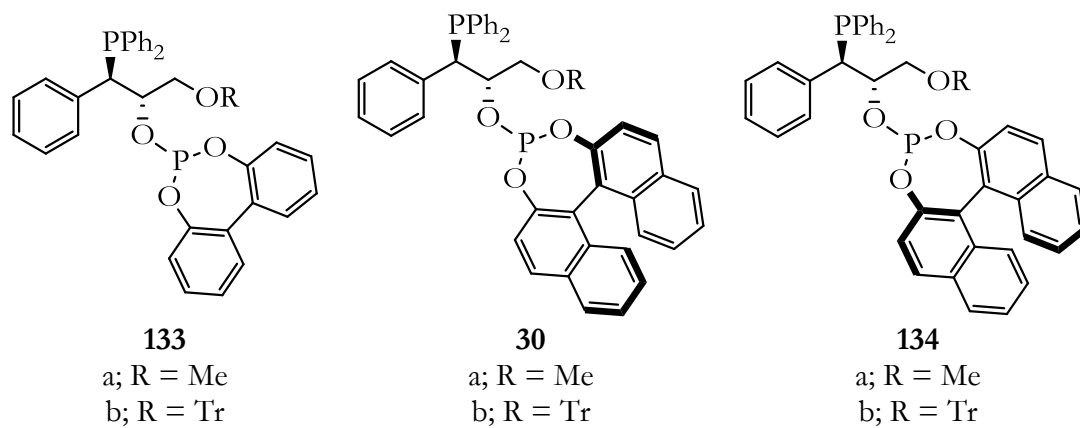


Figure 53. Assayed phosphine-phosphite ligands.

2.2.1.1 IRIIDIUM COMPLEXES FROM PHOSPHINE-PHOSPHINITES

It has been already described in the literature that phosphine-phosphinites form stable chelates with Pt³⁴¹ and Rh³⁴² metal precursors, but to the best of our knowledge, no examples of iridium complexes derived from phosphine-phosphinites have been reported previously. Having obtained phosphine-phosphinites **21**, we decided to study their coordination behavior with different iridium precursors, [$\text{Ir}(\mu\text{-Cl})(\text{cod})\}_2$] and $[\text{Ir}(\text{cod})_2]\text{BArF}$.

Pfaltz *et al.* have reported³⁴³ that iridium complexes incorporating non-coordinating counteranions, like Kobayashi's anion³⁴⁴ (tetrakis(3,5-bis(trifluoromethyl)phenyl)borate, abbreviated as BArF), are more stable toward moisture and less prone to deactivation processes during asymmetric hydrogenation than iridium complexes containing ligands such as chloro.

The benefits of using such anions in homogeneous catalysis include increased solubility of the metal complexes in non-polar organic solvents, and a favoring in ion-pair formation which translates into an increased substrate binding affinity to the metal center.

Neutral $[\text{Ir}(\text{Cl})(\text{cod})(P\text{-}OP)]$ complexes derived from our phosphine-phosphinites were readily formed just by mixing stoichiometric amounts of the iridium precursor [$\text{Ir}(\mu\text{-Cl})(\text{cod})\}_2$] and the corresponding ligand (*Method A*). Complexes **219a,b** (Scheme 52) derived from the methyl-

³⁴¹ Bergamini, P.; Costa, E.; Orpen, A. G.; Pringle, P. G.; Smith, M. B. *Organometallics* **1995**, *14*, 3178.

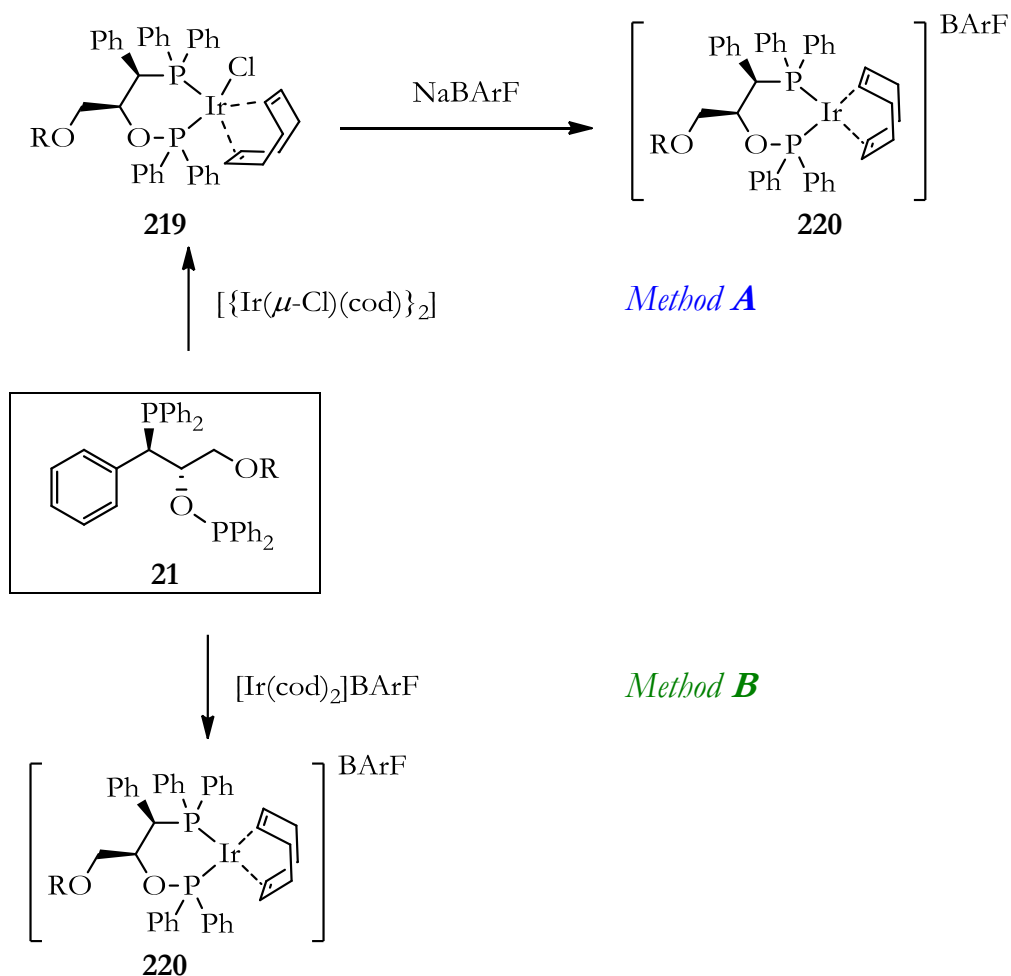
³⁴² (a) Ohe, K.; Morioka, K.; Yonehara, K.; Uemura, S. *Tetrahedron: Asymmetry* **2002**, *13*, 2155. (b) Boyer, N.; Léautey, M.; Jubault, P.; Pannecoucke, X.; Quirion, J.-C. *Tetrahedron: Asymmetry* **2005**, *16*, 2455.

³⁴³ See for example: (a) Lightfoot, A.; Schnider, P.; Pfaltz, A. *Angew. Chem., Int. Ed.* **1998**, *37*, 2897. (b) Pfaltz, A.; Blankenstein, J.; Hilgraf, R.; Hormann, E.; McIntyre, S.; Menges, F.; Schonleber, M.; Smidt, S. P.; Wustenberg, B.; Zimmermann, N. *Adv. Synth. Catal.* **2003**, *345*, 33. (c) Crabtree, R. H. In *Iridium Catalysis*, Top. Organomet. Chem.; Andersson, P. G., Ed.; Springer-Verlag: Berlin, 2011; p 6.

³⁴⁴ Nishida, H.; Takada, N.; Yoshimura, M.; Sonoda, T.; Kobayashi, H. *Bull. Chem. Soc. Jpn.* **1984**, *57*, 2600.

and trityl-substituted ligands **21a** and **21b**, respectively, were quantitatively obtained. Whilst the $[\text{Ir}(\text{Cl})(\text{cod})(\text{P-OP})]$ complexes were stable in solution, attempts to isolate analytically pure samples failed. Their high-resolution ESI mass spectra were in agreement with a mononuclear species. Finally, the $^{31}\text{P}\{^1\text{H}\}$ NMR spectra for **219a,b** showed two doublets arising from the ^{31}P - ^{31}P coupling (for example, for the complex **219a** derived from ligand **21a**: $\delta_{\text{PO}} = 92.0$ ppm, $J = 44.2$ Hz and $\delta_{\text{P}} = 14.0$ ppm, $J = 44.2$ Hz; see Table 18 for the complete $^{31}\text{P}\{^1\text{H}\}$ NMR data).

Most gratifyingly, the chloro ligand in the neutral iridium(I) complexes **219a,b** allowed for chemical manipulation. Further exchange of the chloro ligand by the BArF anion was achieved by simply adding stoichiometric amounts of NaBArF to a solution of iridium complexes **219** in dichloromethane. Precipitation of NaCl in the reaction media indicated that the exchange had occurred. After filtration of the generated salts, followed by chromatographic purification, cationic iridium complexes **220a,b** were obtained as highly pure red solids in good yields of 65% and 90%, for the complexes derived from the methyl- and trityl-substituted ligands **21a** and **21b**, respectively (Scheme 52 and Table 17). The high-resolution ESI mass spectra of cationic iridium complexes **220a,b** were in agreement with the cationic mononuclear species. The ^1H NMR data revealed an unsymmetrical coordination pattern between the ligand backbone and the cod ligand. Finally, the $^{31}\text{P}\{^1\text{H}\}$ NMR spectra for **220a,b** showed two doublets arising from the ^{31}P - ^{31}P couplings (see Table 18 for the complete $^{31}\text{P}\{^1\text{H}\}$ NMR data). All of these results are consistent with the presence of a six-membered chelate ring in these complexes.



Scheme 52. Preparation of iridium complexes derived from phosphine-phosphinite ligands.

The second strategy (*Method B*) consisted in using a phosphine-phosphinite ligand and a cationic iridium(I) precursor ($[\text{Ir}(\text{cod})_2]\text{BArF}$). The complexation reaction was studied in dichloromethane using a slight excess of phosphine-phosphinite ligand **21** with respect to $[\text{Ir}(\text{cod})_2]\text{BArF}$. The reaction proceeded smoothly, although the final reaction mixture contained several unidentified impurities which could not be separated by crystallization. A purification step was necessary (flash chromatography), and complexes **220** were thus isolated in lower yield than that obtained with the previously mentioned stepwise method (complexation with $[\{\text{Ir}(\mu\text{-Cl})(\text{cod})\}_2]$ followed by ligand exchange, *Method A*). Results obtained with both methods are summarized in Table 17.

Table 17. Formation of complexes **220** from phosphine-phosphinite ligands.

Entry	Method	P-OP ligand	Conditions	Product (Yield)
1	A	21a	[{Ir(μ -Cl)(cod)} ₂] + NaBArF	220a (65%)
2	A	21b	[{Ir(μ -Cl)(cod)} ₂] + NaBArF	220b (90%)
3	B	21a	[Ir(cod) ₂]BArF	220a (39%)
4	B	21b	[Ir(cod) ₂]BArF	220b (23%)

Table 18. ³¹P{¹H} NMR data for phosphine-phosphinites **21** and their corresponding iridium complexes **220**.^[a]

Entry	Compound	Phosphinite group		Phosphino group	
		δ (ppm)	J_{P-P} (Hz)	δ (ppm)	J_{P-P} (Hz)
1	21a	116	5.6	-7	5.6
2	220a	103	30.2	12	30.2
3	21b	117	9.6	-9	9.6
4	220b	104	30.2	13	30.2

[a] NMR spectra acquired in CDCl₃ (entries 1, 3) or CD₂Cl₂ (entries 2, 4).

2.2.1.2 IRIIDIUM COMPLEXES FROM PHOSPHINE-PHOSPHITES

Unlike phosphine-phosphinites, several coordination studies involving phosphine-phosphites and different transition metal precursors (Rh,^{345, 346} Pt³⁴⁷ and Ir^{249b}) have been published. For instance, Pizzano *et al.* have demonstrated the formation of chiral iridium chelates with phosphine-phosphite ligands.^{249b}

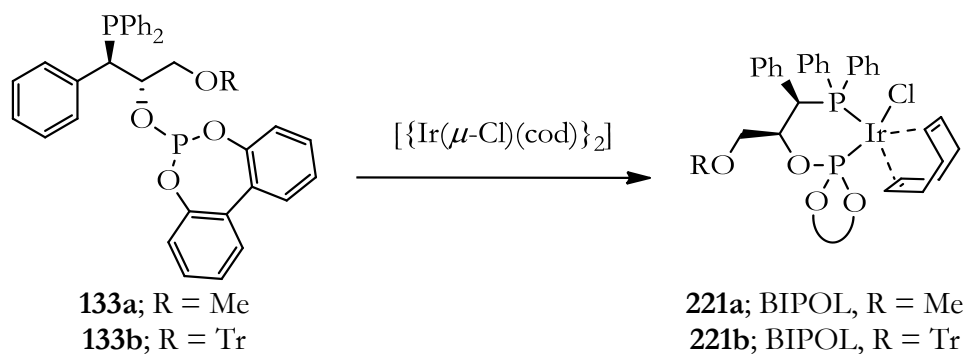
The preparation of neutral [Ir(Cl)(cod)(P-OP)] iridium (I) complexes was achieved in a similar way to that used for phosphine-phosphinite ligands **21** or to that reported by Pizzano *et al.*^{249b} for other phosphine-phosphites. Neutral [Ir(Cl)(cod)(P-OP)] complexes derived from our phosphine-phosphites **133**, **30** and **134** were readily formed by mixing stoichiometric amounts of the iridium precursor [$\{\text{Ir}(\mu\text{-Cl})(\text{cod})\}_2$] and the corresponding ligand in THF as solvent.³⁴⁸ Whilst the [Ir(Cl)(cod)(P-OP)] complexes were stable in solution, attempts to isolate analytically pure samples were unsuccessful. Along these lines and despite many attempts, we were incapable of growing crystals suitable for X-ray analysis. Their high-resolution ESI mass spectra were in agreement with the mononuclear species. The ³¹P{¹H} NMR spectra showed one sharp doublet for the phosphite group and another doublet for the phosphino moiety, arising from the ³¹P-³¹P coupling. Structures of the neutral complexes that were synthesized, compounds **221-223**, are shown in Scheme 53 and Scheme 54.

³⁴⁵ Fernández-Pérez, H.; Donald, S. M. A.; Munslow, I. J.; Benet-Buchholz, J.; Maseras, F.; Vidal-Ferran, A. *Chem.-Eur. J.* **2010**, *16*, 6495.

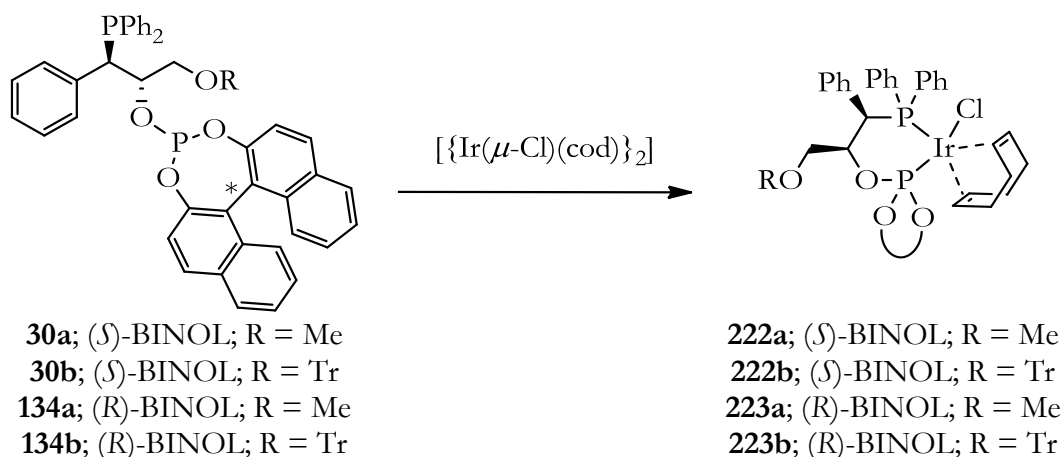
³⁴⁶ (a) Deerenberg, S.; Schrekker, H. S.; van Strijdonck, G. P. F.; Kamer, P. C. J.; van Leeuwen, P. W. N. M.; Fraanje, J.; Goubitz, K. *J. Org. Chem.* **2000**, *65*, 4810. (b) Arena, C. G.; Faraone, F.; Graiff, C.; Tiripicchio, A. *Eur. J. Inorg. Chem.* **2002**, 711. (c) Pàmies, O.; Diéguez, M.; Net, G.; Ruiz, A.; Claver, C. *J. Org. Chem.* **2001**, *66*, 8364.

³⁴⁷ (a) Baker, M. J.; Pringle, P. G. *J. Chem. Soc., Chem. Commun.* **1993**, 314. (b) Hegedüs, C.; Gulyás, H.; Szöllosy, A.; Bakos, J. *Inorg. Chim. Acta* **2009**, *362*, 1650.

³⁴⁸ Although complexation experiments towards neutral complexes derived from phosphine-phosphites were also possible in dichloromethane, the iridium complexes degraded with time under these conditions. This behavior was not observed in THF, thus this solvent was preferred for this chemistry.

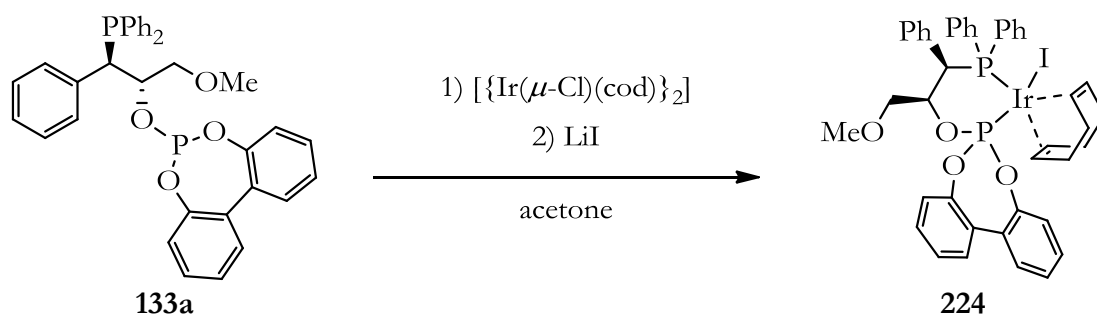


Scheme 53. Neutral Ir(I) complexes derived from ligands **133**.



Scheme 54. Neutral Ir(I) complexes derived from ligands **30** and **134**.

The displacement of the chloro ligand by iodo in $[\text{Ir}(\text{Cl})(\text{cod})(P\text{-}OP)]$ complexes proved to be straightforward. Thereby, $[\text{Ir}(\text{I})(\text{cod})(\mathbf{133a})]$ was cleanly formed by treatment of $[\text{Ir}(\text{Cl})(\text{cod})(P\text{-}OP)]$ and an excess of LiI (50 equiv.) in acetone. In this case, isolation of the iridium complex was possible and **224** crystallized out as a yellow, air stable solid upon layered addition of diethyl ether to their dichloromethane or THF solutions (48% overall yield from the phosphine-phosphinite **133a**, Scheme 55). Furthermore, single crystals of **224** suitable for X-ray diffraction could be grown in a DCM/Et₂O mixture. The $[\text{Ir}(\text{I})(\text{cod})(\mathbf{133a})]$ complex showed the expected atomic connectivity, and with regard to its three-dimensional geometry, the iridium centre had a square pyramidal geometry. Figure 54 shows an ORTEP diagram of this complex, along with selected bond distances and angles.



Scheme 55. Synthesis of $[\text{Ir}(\text{I})(\text{cod})(\mathbf{133a})]$ (**224**), the iodo analog of complex **221a**.

Complex **224** displays a distorted-square-pyramidal coordination geometry, with the iodo ligand located at the apical position. Furthermore, the I-Ir bond is roughly at right angles to both the Ir-P (phosphine) and Ir-P (phosphite) bonds (90.8 and 98.6° , respectively). The angles between the mutually *cis* ligands in the base of the pyramid range from 85.5 to 100.6° . As previously observed by other groups for related complexes,^{249b} the Ir-P (phosphite) distance (2.228 \AA) is appreciably shorter than the Ir-P (phosphine) distance (2.319 \AA). The greater π -acceptor character of the phosphite is also reflected in the Ir-C bond values of **224**, with longer bonds for the olefinic carbons *trans* to phosphine (C(25) and C(26)) than for those *trans* to the phosphite (C(21) and C(22)); mean difference in distance 0.07 \AA .

As mentioned earlier, no crystals suitable for X-Ray analysis could be grown for the related neutral chloro complexes **221-223**. However, there is a very good agreement in the $^{31}\text{P}\{^1\text{H}\}$ NMR spectral data of the complexes $[\text{Ir}(\text{Cl})(\text{cod})(P\text{-}OP)]$ **221-223** and those for $[\text{Ir}(\text{I})(\text{cod})(\mathbf{133a})]$ (see Table 19), which suggests a close structural resemblance between the chloro- and iodo-containing neutral iridium complexes.

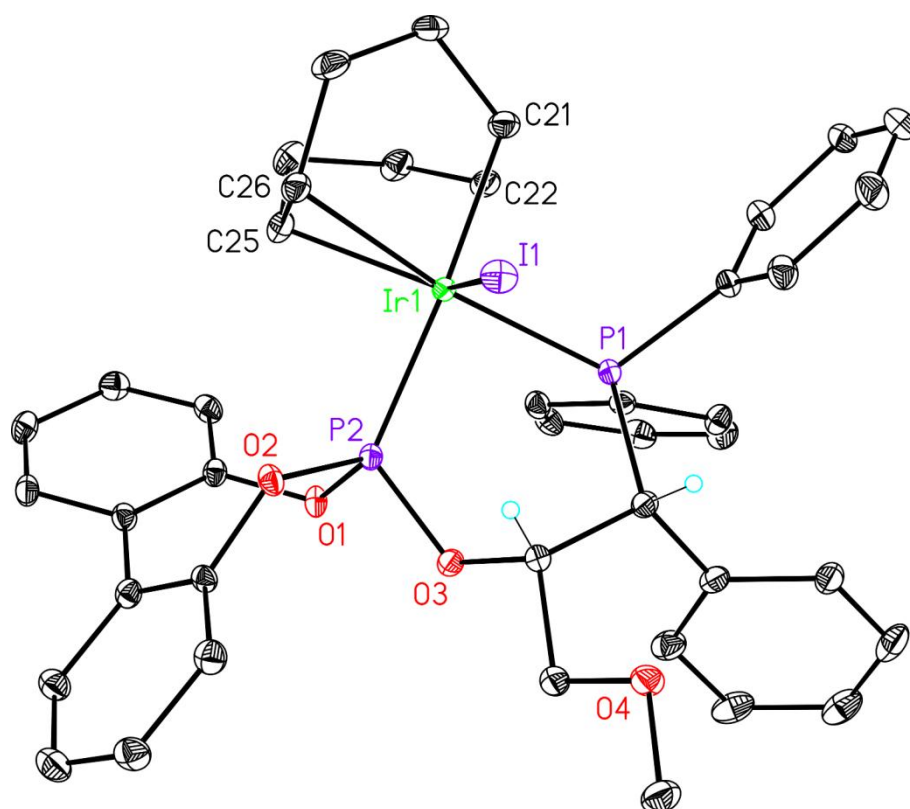


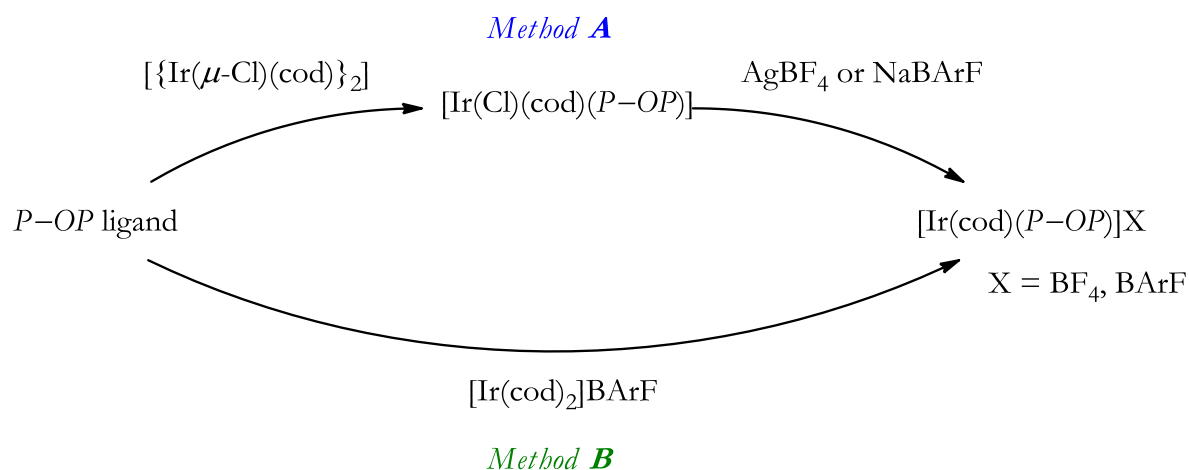
Figure 54. ORTEP view of complex **224**, [Ir(I)(cod)(**133a**)]. H atoms omitted for clarity. Selected bond lengths (Å) and angles (deg): Ir-P(1) = 2.3194(6), Ir-P(2) = 2.2283(7), Ir-C(21) = 2.178(3), Ir-C(22) = 2.168(3), Ir-C(25) = 2.258(3), Ir-C(26) = 2.234(2), Ir-I = 2.8132(3); P(2)-Ir-P(1) = 86.99(2), P(1)-Ir-C(21) = 94.51(7), P(1)-Ir-C(22) = 85.54(7), P(2)-Ir-C(26) = 100.62(8), P(2)-Ir-C(25) = 87.08(8), P(1)-Ir-I = 90.80(2), P(2)-Ir-I = 98.57(2).

Table 19. $^{31}\text{P}\{^1\text{H}\}$ NMR data of $[\text{Ir}(\text{Cl})(\text{cod})(P\text{-}OP)]$ and $[\text{Ir}(\text{I})(\text{cod})(P\text{-}OP)]$ complexes.^[a]

Entry	Complex	Compound	Phosphite group		Phosphino group	
			δ (ppm)	$J_{\text{P-P}}$ (Hz)	δ (ppm)	$J_{\text{P-P}}$ (Hz)
1	-	133a	155.6	10.0	-6.5	10.0
2	$[\text{Ir}(\text{Cl})(\text{cod})(\mathbf{133a})]$	221a	108.0	58.1	13.7	58.1
3	$[\text{Ir}(\text{I})(\text{cod})(\mathbf{133a})]$	224a	105.3	57.9	9.5	57.9
4	-	30a	156.2	11.6	-5.5	11.6
5	$[\text{Ir}(\text{Cl})(\text{cod})(\mathbf{30a})]$	222a	112.4	57.0	15.6	57.0
6	-	134a	156.6	bs	-4.5	bs
7	$[\text{Ir}(\text{Cl})(\text{cod})(\mathbf{134a})]$	223a	107.0	55.6	17.2	55.6

[a] NMR spectra acquired in CDCl_3 (free ligands, entries 1, 3 and 5) or CD_2Cl_2 (neutral iridium complexes).

Cationic complexes from our phosphine-phosphite ligands were attempted by following the methods already employed in the case of phosphine-phosphinites (Scheme 56): *i*) ligand exchange in $[\text{Ir}(\text{Cl})(\text{cod})(P\text{-}OP)]$ (*Method A*), and *ii*) direct complexation with a cationic iridium (I) precursor (*Method B*).



Scheme 56. Preparation of cationic iridium complexes derived from phosphine-phosphite ligands.

When *Method A* was studied, the neutral complex derived from ligand **133a** was subjected to ligand exchange by the less coordinating counteranions BF₄ and BArF, using AgBF₄ or NaBArF as the counteranion source. ³¹P{¹H} NMR analysis showed that, both for the BF₄ and BArF cases, two different iridium complexes were formed. Mono- and bidimensional ³¹P{¹H} NMR analysis (see Figure 55 and Figure 56 for the spectra) revealed that two complexes (labeled as **I** and **II** in the already mentioned figures) were present in *ca.* 1:1 ratio³⁴⁹. Despite many attempts, the separation and subsequent complete characterization of these two iridium complexes was not possible. Interestingly, the same mixture of complexes in *ca.* 1:1 ratio was obtained when *Method B* was followed.

³⁴⁹ Inverse gated decoupled ³¹P{¹H} NMR analysis revealed a ratio between complex I and II equal to 55:45 for the exchange with BF₄ and 59:41 for that with BArF.

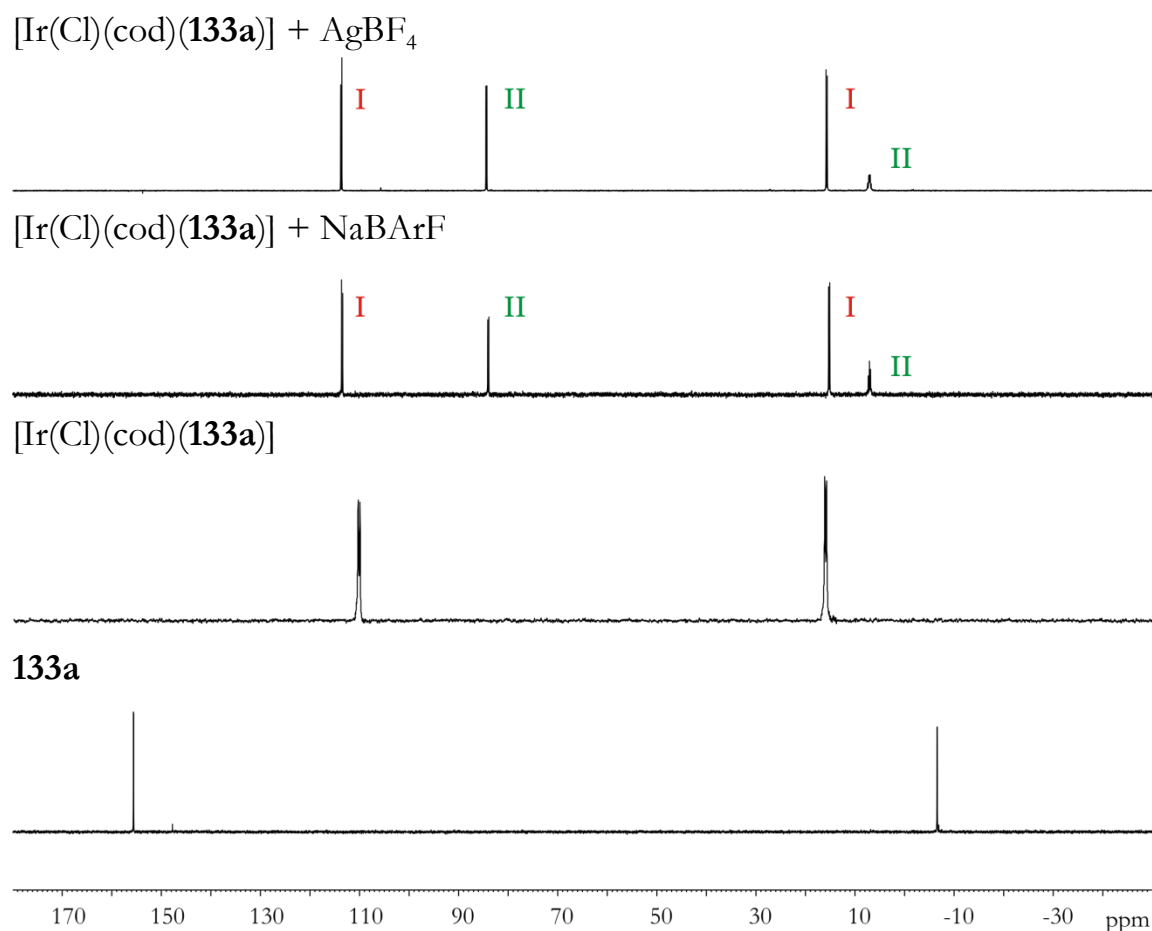


Figure 55. $^{31}\text{P}\{^1\text{H}\}$ NMR spectra of phosphine-phosphite **133a** and their iridium complexes.

NMR analysis of the aforementioned reaction mixtures suggested that species **133a-I** corresponds to the expected $[\text{Ir}(\text{cod})(P\text{-}OP)]\text{BF}_4$ or $[\text{Ir}(\text{cod})(P\text{-}OP)]\text{BArF}$ complex. On the other hand, a detailed analysis of the ^1H NMR and ^{31}P NMR spectra of the crude mixture indicated the presence of a hydride signal at *ca.* $\delta = -8.7$ ppm ($J = 103.4$ Hz), which was also coupled with the phosphino moiety at *ca.* $\delta = 7.1$ ppm in ^{31}P NMR.³⁵⁰ The corresponding cross-peak between the hydride and phosphine signals was also observed by $^{31}\text{P}\text{-}^1\text{H}$ HMBC spectroscopy, which confirmed the presence of a H-Ir-P (phosphino) moiety in the second iridium complex (labeled as **II** in

³⁵⁰ Data from the reaction mixture of $[\text{Ir}(\text{Cl})(\text{cod})(\mathbf{133a})]$ and AgBF_4 .

the already mentioned figures). Therefore, we hypothesize that species **133-II** arises from an intramolecular C-H activation process. Unfortunately, we have not been able to unequivocally prove the structure of these complexes.

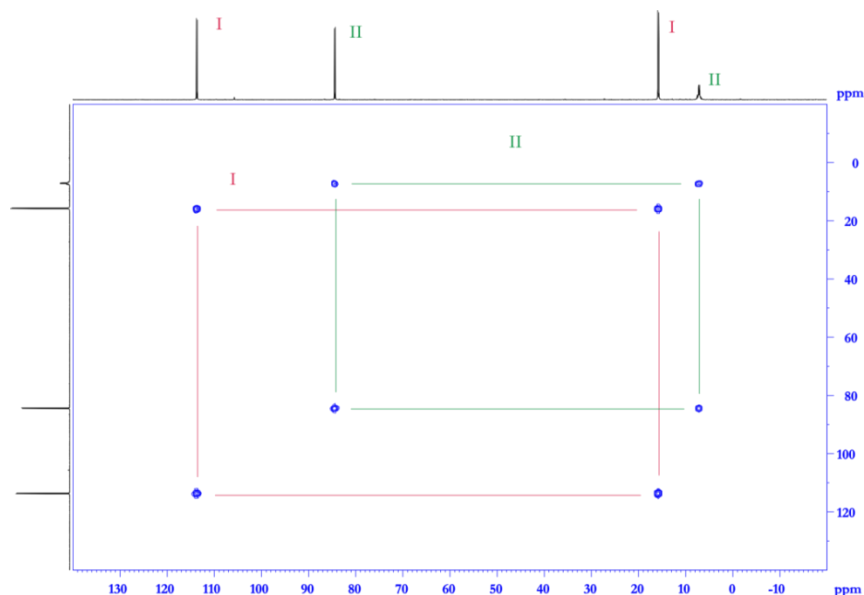
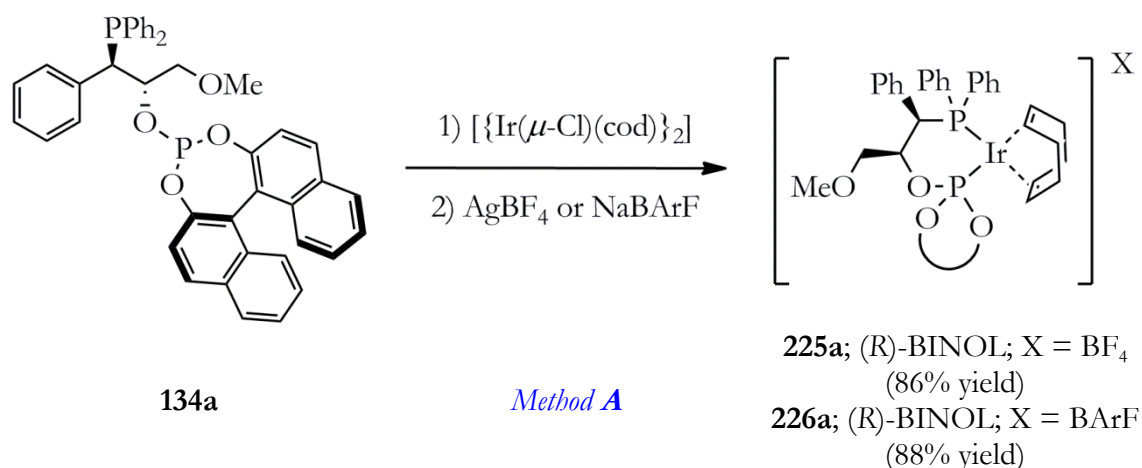


Figure 56. ^{31}P - ^{31}P correlation of the reaction mixture of $[\text{Ir}(\text{Cl})(\text{cod})(\mathbf{133a})]$ and AgBF_4 .

This chemistry was also explored with the neutral iridium complexes containing the configurationally stable phosphine-phosphite ligands derived from (*S*)- and (*R*)-BINOL, **30a** and **134a**, respectively. The same behavior was also observed when $[\text{Ir}(\text{Cl})(\text{cod})(\mathbf{30a})]$ was treated with AgBF_4 or NaBArF following *Method A*: a mixture of the expected $[\text{Ir}(\text{cod})(\mathbf{30a})]\text{BF}_4$ or $[\text{Ir}(\text{cod})(\mathbf{30a})]\text{BArF}$ complexes, along with another iridium complex arising from a C-H activation process was observed (Figure 57) for the ^{31}P NMR spectrum of the reaction mixture obtained with AgBF_4 as the reagent. Most gratifyingly, the expected ligand exchange process took place cleanly over $[\text{Ir}(\text{Cl})(\text{cod})(\mathbf{134a})]$ with AgBF_4 or NaBArF and led quantitatively to the expected cationic iridium complexes $[\text{Ir}(\text{cod})(\mathbf{30a})]\text{BF}_4$, **225a**, or $[\text{Ir}(\text{cod})(\mathbf{30a})]\text{BArF}$, **226a**. Complexes **225a** and **226a** could be isolated from their residual salts (AgCl or NaCl respectively) by filtration and further recrystallization from DCM and Et_2O (or *n*-hexane) in 86% and 88% yield, for

the complexes incorporating BF_4 or BArF moieties, respectively (Scheme 57). Their high-resolution ESI mass spectra were in agreement with the mononuclear species. The $^{31}\text{P}\{^1\text{H}\}$ NMR spectra for **225a** and **226a** showed two sharp doublets from the ^{31}P - ^{31}P couplings (Figure 57) for the ^{31}P NMR spectra of the reaction mixtures obtained with AgBF_4 as the reagent).



Scheme 57. Cationic iridium(I) complexes derived from ligand **134a**.

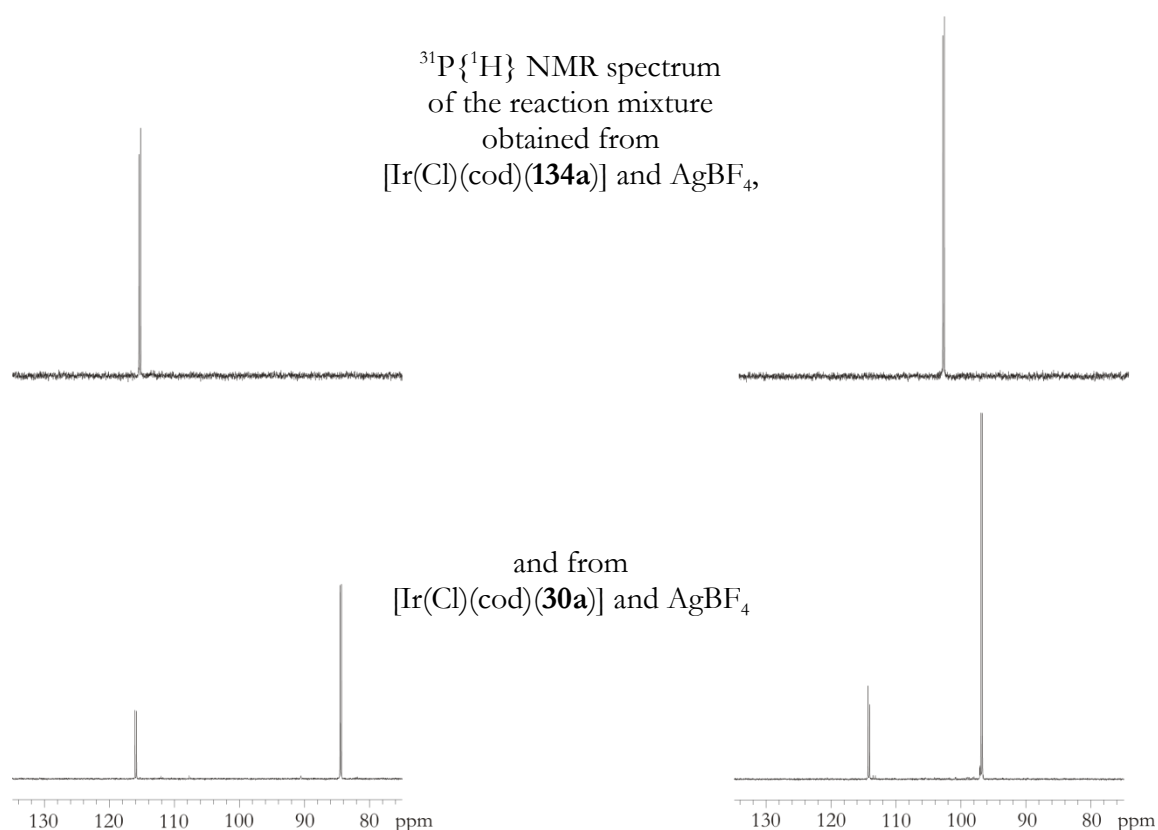


Figure 57. ^{31}P NMR spectra of the reaction mixtures obtained from $[\text{Ir}(\text{Cl})(\text{cod})(\mathbf{30a})]$ and $[\text{Ir}(\text{Cl})(\text{cod})(\mathbf{134a})]$ with AgBF_4 as the reagent.

$^{31}\text{P}\{^1\text{H}\}$ spectral information of all *P-OP* ligands and iridium complexes obtained by ligand exchange from ligands **133a**, **30a** and **134a** have been summarized in Table 20.

Table 20. $^{31}\text{P}\{^1\text{H}\}$ NMR spectral information for cationic iridium complexes obtained by ligand exchange from ligands **133a**, **30a** and **134a**.^[a]

Entry	Complex	Compound	Phosphite group		Phosphino group	
			δ (ppm)	$J_{\text{P-P}}$ (Hz)	δ (ppm)	$J_{\text{P-P}}$ (Hz)
1	-	133a	155.6	10.0	-6.5	10.0
2	$[\text{Ir}(\text{cod})(\mathbf{133a})]\text{BF}_4$		113.7 (84.3) ^[b]	40.3 (36.0) ^[b]	15.6 (7.1) ^[b]	40.3 (36.0) ^[b]
3	$[\text{Ir}(\text{cod})(\mathbf{133a})]\text{BArF}$		113.5 (84.0) ^[b]	40.3 (36.1) ^[b]	15.2 (7.0) ^[b]	40.3 (36.1) ^[b]
4	-	30a	156.2	11.6	-5.5	11.6
5	$[\text{Ir}(\text{cod})(\mathbf{30a})]\text{BF}_4$		115.9 (84.4) ^[b]	40.0 (35.6) ^[b]	24.1 (6.8) ^[b]	40.0 (35.6) ^[b]
6	$[\text{Ir}(\text{cod})(\mathbf{30a})]\text{BArF}$		115.8 (84.1) ^[b]	40.2 (35.7) ^[b]	23.4 (6.8) ^[b]	40.2 (35.7) ^[b]
7	-	134a	156.6	bs	-4.5	bs
8	$[\text{Ir}(\text{cod})(\mathbf{134a})]\text{BF}_4$	225a	115.4	40.6	13.4	40.6
9	$[\text{Ir}(\text{cod})(\mathbf{134a})]\text{BArF}$	226a	112.2	40.4	10.3	40.4

[a] NMR spectra acquired in CDCl_3 (free ligands, entries 1, 4 and 7) or CD_2Cl_2 (cationic iridium complexes, entries 2, 3, 5, 6, 8 and 9).

[b] Data in brackets correspond to the complex arising from a C-H activation process.

Despite many efforts, we have been unable to establish the structure of the iridium complexes that arise from the intramolecular C-H activation process. The value of the coupling constant between the hydrido and phosphino groups ($J = 103.4$ Hz) suggests a *trans*-relative arrangement in the iridium center. With regard to the particular C-H bond that experiences the activation process, either a C-H bond from the cyclooctadiene ligand,³⁵¹ from the binaphthyl group³⁵² or even from a sp^3 hybridized carbon³⁵³ in the ligand backbone may be involved in such a process.

2.2.1.3 $^{31}\text{P}\{^1\text{H}\}$ NMR TITRATIONS OF *P-OP* LIGANDS WITH IRIIDIUM PRECURSORS

Previous complexation studies between our *P-OP* ligands and $[\{\text{Ir}(\mu\text{-Cl})(\text{cod})\}_2]$ involved using stoichiometric amounts of ligand and metal precursor. We also became interested in investigating the outcome of complexation reactions; when different molar ratios of both components were used. These studies were carried out by $^{31}\text{P}\{^1\text{H}\}$ NMR analysis using $[\{\text{Ir}(\mu\text{-Cl})(\text{cod})\}_2]$ and phosphine-phosphite **133b** as the representative ligand. Solutions containing molar ratios of iridium precursor / ligand ranging from 1 : 0.5 to 1 : 2 were prepared and analyzed by $^{31}\text{P}\{^1\text{H}\}$ NMR spectroscopy (see Figure 58).

It has been already discussed that complex $[\text{Ir}(\text{Cl})(\text{cod})(\mathbf{133b})]$ is formed when stoichiometric amounts of ligand and metal precursor are used. The same outcome was obtained with an excess of iridium precursor: two sharp doublets were observed and indicated the formation of the neutral iridium

³⁵¹ Rahaman, S. M. W.; Dinda, S.; Sinha, A.; Bera, J. K. *Organometallics* **2013**, *32*, 192.

³⁵² Liu, W.-B.; Zheng, C.; Zhuo, C.-X.; Dai, L.-X.; You, S.-L. *J. Am. Chem. Soc.* **2012**, *134*, 4812.

³⁵³ (a) Kiener, C. A.; Shu, C.; Incarvito, C.; Hartwig, J. F. *J. Am. Chem. Soc.* **2003**, *125*, 14272.
(b) Madrahimov, S. T.; Markovic, D.; Hartwig, J. F. *J. Am. Chem. Soc.* **2009**, *131*, 7228.

complex $[\text{Ir}(\text{Cl})(\text{cod})(\mathbf{133b})]$ (**221b**) as the only detectable species in solution. Interestingly, when the ligand / iridium ratio was *ca.* 2 or higher, the resulting $^{31}\text{P}\{^1\text{H}\}$ NMR spectrum showed only two sharp triplets (Figure 58 and Figure 60), which were attributed to a new iridium complex, **227**.

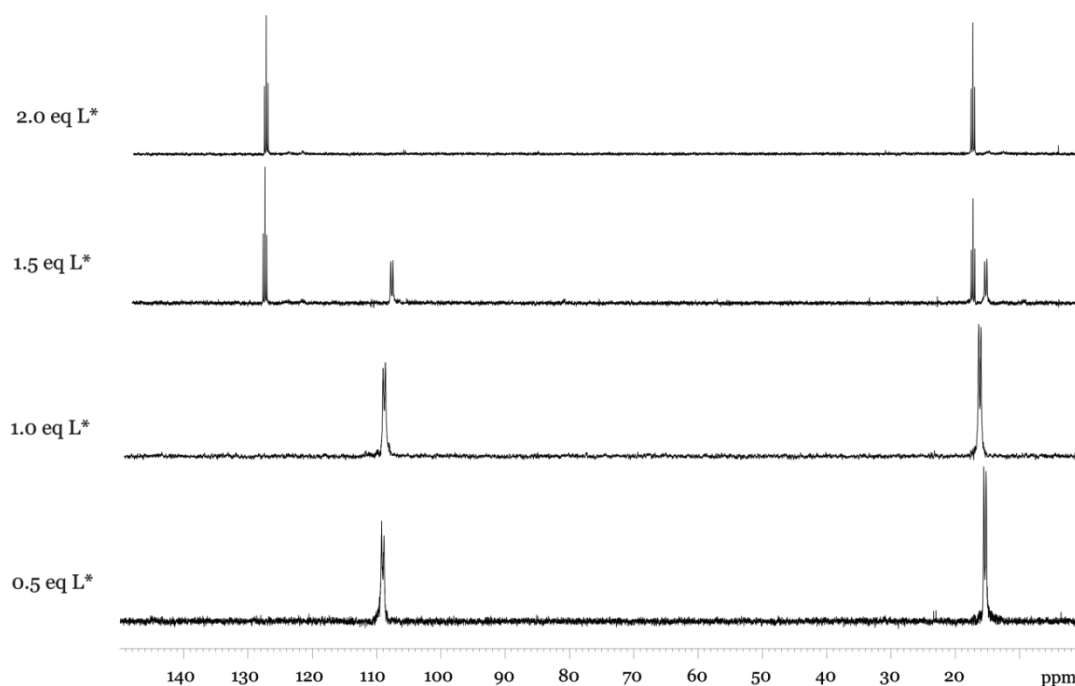


Figure 58. $^{31}\text{P}\{^1\text{H}\}$ NMR titration (400MHz, CD_2Cl_2) of ligand **133b** with $[\{\text{Ir}(\mu\text{-Cl})(\text{cod})\}_2]$ as iridium precursor at different molar ratios.

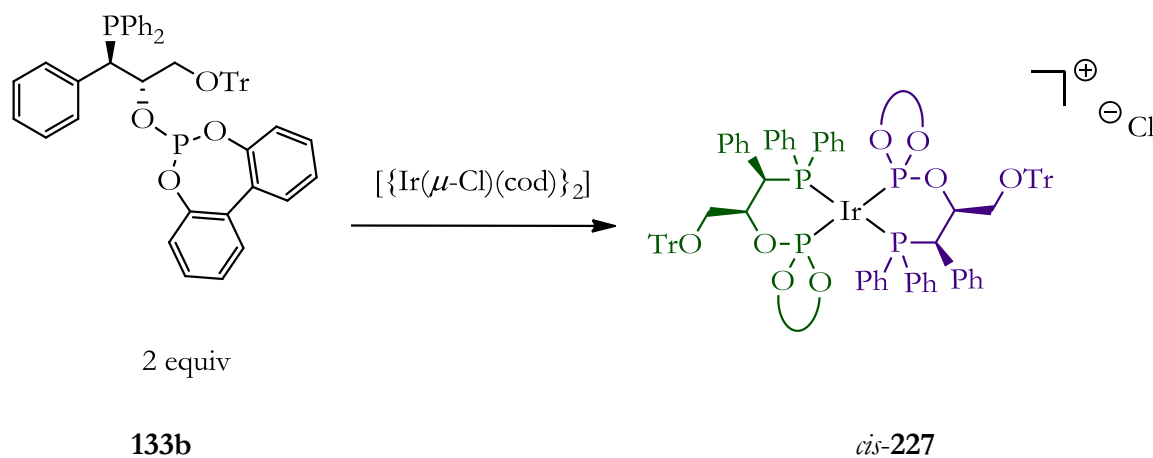
The simplicity of the signals suggested a highly symmetric molecule, such as a 2:1 complex between **133b** and the iridium precursor with a *cis*- or *trans*-arrangement of the phosphino and phosphite groups (see Figure 59 and Scheme 58).³⁵⁴ In the *cis*-complex, the two phosphino and the two phosphite

³⁵⁴ The same type of 2:1 complexes were formed when phosphine-phosphites are combined with $[\text{Rh}(\text{nbd})_2]\text{BF}_4$ in a 2:1 ratio (see the following references). With regard to the *cis*- and *trans*- isomerism for these 2:1 complexes, we follow the nomenclature used by Pizzano *et al.* for their rhodium analogs, in which *cis* means that the phosphine and phosphite groups from two different *P-OP* ligand molecules occupy *cis*-positions (whilst *trans* indicates the contrary). (a) Rubio, M.; Vargas, S.; Suárez, A.; Álvarez, E.; Pizzano, A. *Chem.-Eur. J.* **2007**, *13*, 1821. (b) Doctoral thesis of H. Fernández-Pérez, University Rovira i Virgili, Tarragona, 2009. (c) Farkas, G.; Balogh, S.; Madarasz, J.; Szoellosy, A.; Darvas, F.; Uerge, L.; Gouygou, M.; Bakos, J. *Dalton Trans.* **2012**, *41*, 9493.

moieties are magnetically equivalent, the ^{31}P nuclei in the absence of ^{31}P - ^1H couplings constitute an A_2X_2 spin system, and the signals corresponding to each type of phosphorus groups are observed as triplets by virtue of their coupling with the other two P -nuclei. Spectral data has been summarized in Table 21. There is no evidence for the formation of the corresponding *trans* complex, in which the two phosphino groups and the two phosphite groups are magnetically non-equivalent, even in the absence of ^{31}P - ^1H couplings, and form an $AA'XX'$ spin system in ^{31}P NMR.



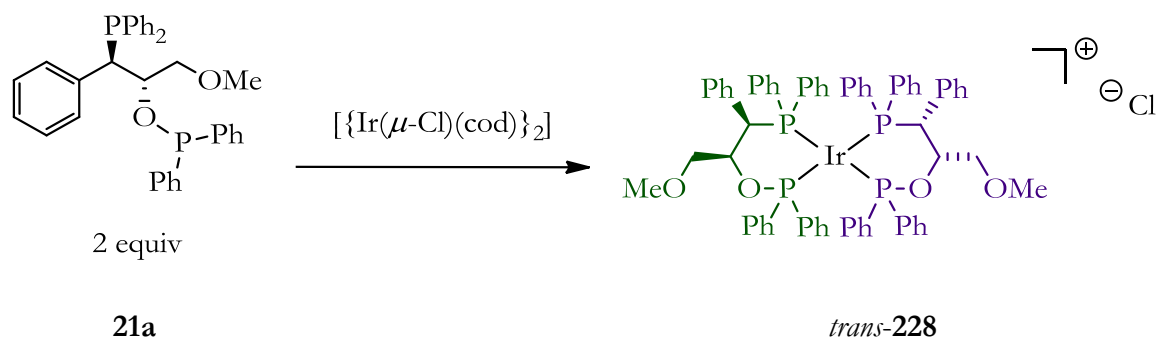
Figure 59. *cis*- and *trans*-Isomerism in iridium bis(chelates) derived from P - OP ligands.



Scheme 58. Formation of the bis(chelate) *cis*-227.

We then studied the complexation behavior of phosphine-phosphinites **21** with $[\{\text{Ir}(\mu\text{-Cl})(\text{cod})\}_2]$ under similar experimental conditions, using **21a** as the representative compound. Unlike phosphine-phosphites, when the iridium to ligand ratio was *ca.* 1:2, the $^{31}\text{P}\{^1\text{H}\}$ NMR showed a complex signal in the characteristic phosphinite region and a broad one in the phosphino region, which sharpened up at $-40\text{ }^\circ\text{C}$ to the same complex signal than that

corresponding to the phosphinite group (Figure 60). The spectrum of the resulting complex **228** constitutes a second order spectrum (see Scheme 59 and Figure 60) and is in agreement with an AA'XX' spin system as the one expected for *trans*-complex **228** (Scheme 59). There was no evidence for the presence of the *cis* derivative.



Scheme 59. Formation of the bis(chelate) *trans*-**228**.

The spectral data of the AA'XX' spin system (³¹P-chemical shifts and ³¹P-³¹P coupling constants) for *trans*-complex **228** could be extracted by fitting the experimental ³¹P{¹H} NMR spectrum to an AA'XX' spin system with gNMR 5.0 (See Figure 61).³⁵⁵ The corresponding results are presented in Table 22.

Table 21. ³¹P{¹H} NMR data for bis(chelate) complexes *cis*-**227** and *trans*-**228**.^[a]

Entry	Compound	Spin system	Phosphite group	Phosphino group
			δ (ppm)	δ (ppm)
1	<i>cis</i> - 227	A ₂ X ₂	129.0	17.5
2	<i>trans</i> - 228	AA'XX'	101.5	8.5

[a] NMR spectra recorded in CD₂Cl₂.

³⁵⁵ gNMR v5.0.6.0 NMR Simulation Program Written by P.H.M. Budzelaar Copyright © 2006 IvorySoft.

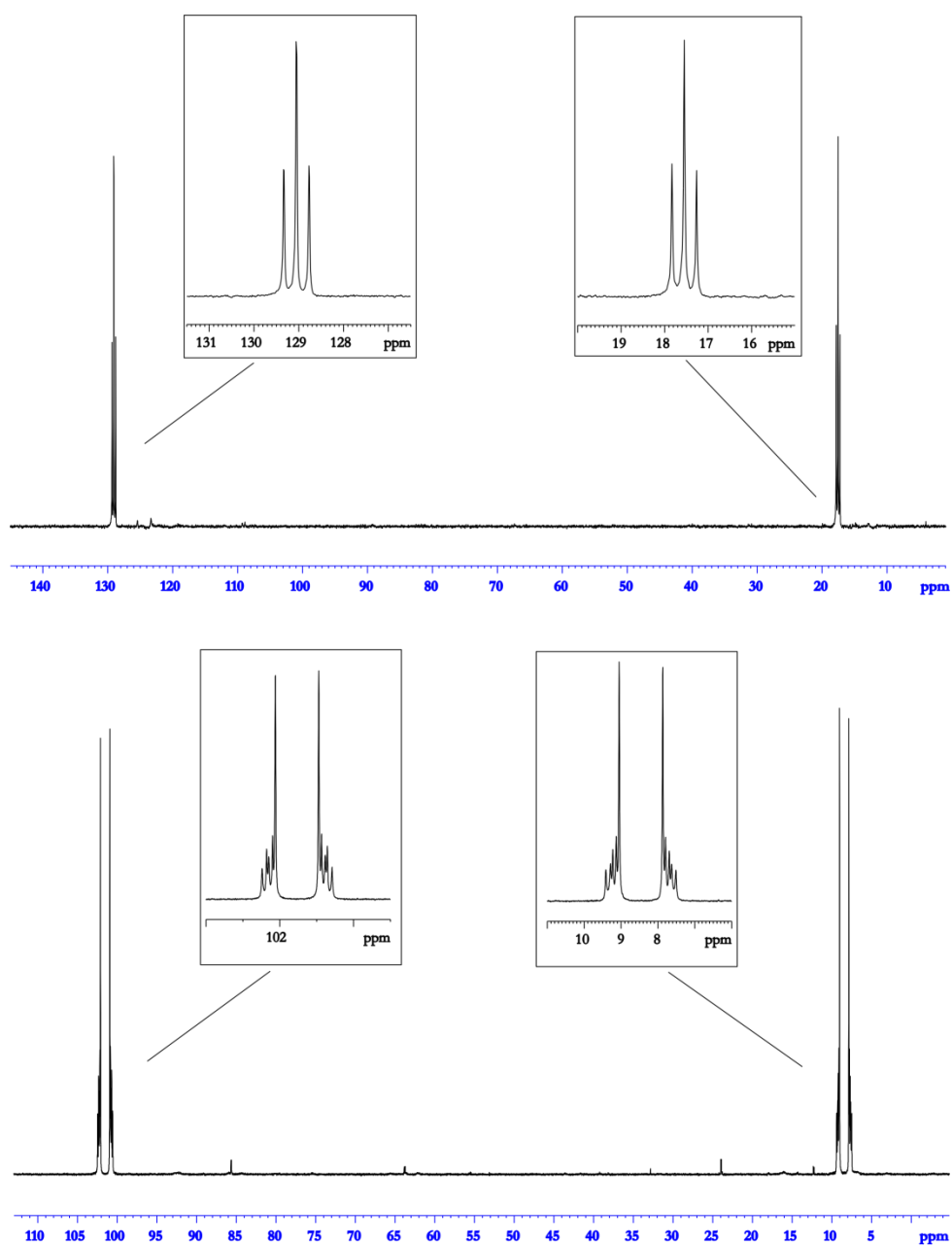


Figure 60. $^{31}\text{P}\{^1\text{H}\}$ NMR spectra (400MHz, CD_2Cl_2) of complexes *cis*-227 (top) and *trans*-228 (bottom; recorded at $-40\text{ }^\circ\text{C}$) at iridium to ligand ratios equal to 1:2.0 and 1:2.2, respectively.

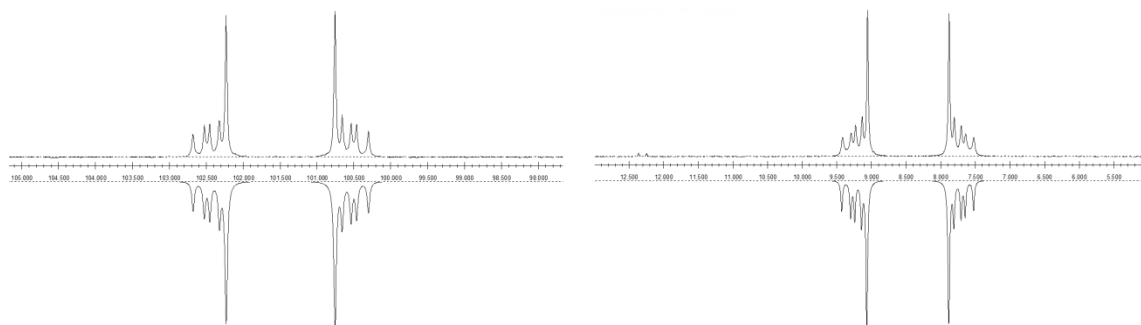


Figure 61. Experimental (top; recorded at $-40\text{ }^{\circ}\text{C}$) and simulated (inverted) $^{31}\text{P}\{^1\text{H}\}$ NMR spectrum for *trans*-**228**.

Table 22. $^{31}\text{P}\{^1\text{H}\}$ NMR spectral data (chemical shifts and coupling constants) for *trans*-**228**.^[a]

Chemical Shift	J_1	J_2	J_3
8.480 $^{31}\text{P}_X$			
8.480 $^{31}\text{P}_{X'}$	34.89 $^{31}\text{P}_X-^{31}\text{P}_{X'}$		
101.522 $^{31}\text{P}_A$	-281.06 $^{31}\text{P}_X-^{31}\text{P}_A$	41.41 $^{31}\text{P}_{X'}-^{31}\text{P}_A$	
101.522 $^{31}\text{P}_{A'}$	41.41 $^{31}\text{P}_X-^{31}\text{P}_{A'}$	-281.06 $^{31}\text{P}_{X'}-^{31}\text{P}_{A'}$	22.81 $^{31}\text{P}_A-^{31}\text{P}_{A'}$

[a] Chemical shift in ppm, coupling constants in Hz, spectrum recorded at $-40\text{ }^{\circ}\text{C}$.

Single crystals of complex *trans*-**228** could be grown in a DCM/Et₂O mixture and its structure was confirmed by X-ray analysis. The complex **228** showed the already discussed atomic connectivity and the iridium centre presented a square planar geometry (see Figure 62 for an ORTEP diagram of *trans*-**228**).

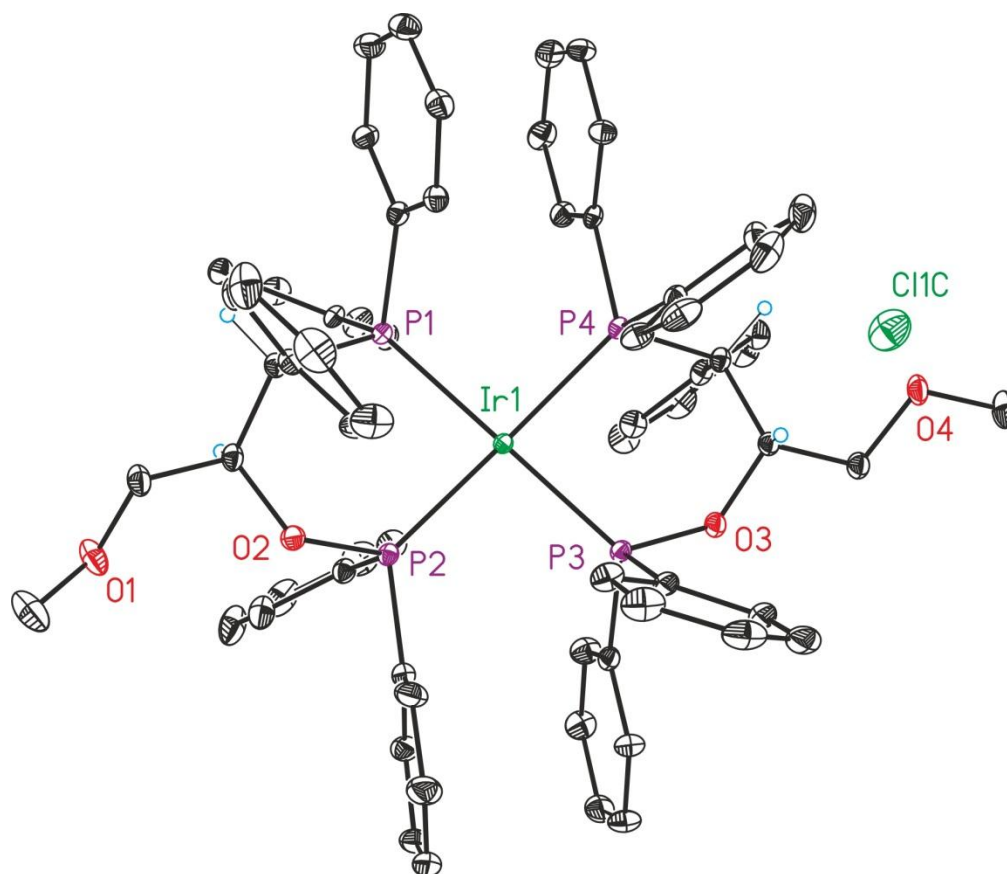


Figure 62. ORTEP view of complex *trans*-228 (H atoms are omitted for clarity).

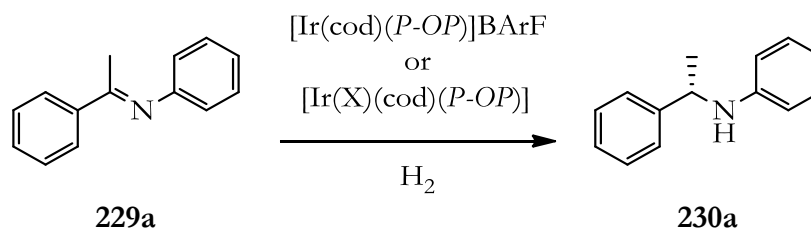
2.2.2 Hydrogenation of N-Containing Structures

Precedents regarding the use of *P-OP* ligands in the Ir-mediated hydrogenation of C=N bonds were very scarce in the literature, as only Pizzano *et al.*^{249, 356} had previously reported the use of cationic iridium(I) complexes derived from enantiomerically pure phosphine-phosphite ligands in the hydrogenation of imines and heteroaromatic derivatives with good enantioselectivities. The next sections detail our efforts towards the asymmetric hydrogenation of acyclic imines (ketimines) and C=N-containing heterocycles (benzoxazines, benzoxazinones, benzothiazinones, quinoxalinones, quinolines, quinoxalines and indoles) using iridium complexes derived from our *P-OP* ligands.

2.2.2.1 HYDROGENATION OF KETIMINES

Our first catalytic studies focused on testing the activity of our phosphine-phosphinite ligands in the Ir-catalyzed asymmetric hydrogenation of ketimines, which were synthesized by simple condensation of the corresponding aniline and carbonyl compounds in toluene in the presence of molecular sieves to scavenge water. Optimization of the hydrogenation conditions were carried out using phosphine-phosphinite complexes **220a** and **220b** and (*E*)-*N*-(phenylethylidene)aniline **229a** as the benchmark substrate (Scheme 60).

³⁵⁶ (a) Vargas, S.; Rubio, M.; Suárez, A.; Pizzano, A. *Tetrahedron Lett.* **2006**, *47*, 615. (b) Rubio, M.; Pizzano, A. *Molecules* **2010**, *15*, 7732.



Scheme 60. Asymmetric hydrogenation of ketimine **229a** catalyzed by $[\text{Ir}(\text{P-OP})]^+$ complexes.

The catalytic activity of both iridium complexes **220a** and **220b** was studied under standard screening conditions for this chemistry (1.0 mol % catalyst, 50 bar H_2) in different solvents. The obtained results are summarized in Table 23.

Table 23. Asymmetric hydrogenation of imine **229a** by iridium complexes **220a** and **220b** in different solvents.^[a]

Entry	Ir complex	Solvent	Conv. [%] ^[b]	ee [%] ^[c] (config.) ^[d]
1	220a	DCM	>99	<i>rac</i>
2	220a	MeOH	71	23 (<i>S</i>)
3	220b	DCM	>99	10 (<i>S</i>)
4	220b	MeOH	56	16 (<i>S</i>)
5	220b	DCE	>99	10 (<i>S</i>)
6	220b	IPA	51	<i>rac</i>
7	220b	THF	>99	10 (<i>S</i>)
8	220b	Toluene	>99	5 (<i>S</i>)

^[a] Reaction conditions: precatalyst / substrate molar ratio = 1.0 : 100, room temperature, 50 bar H_2 , 20 h, 0.2 M in the required solvent, unless otherwise indicated.

^[b] Conversion determined by ^1H NMR.

^[c] Enantiomeric excess determined by HPLC using chiral stationary phases.

^[d] Absolute configuration was assigned by comparison with reported data.

As shown in Table 23, the catalytic activity of both iridium complexes **220a** and **220b** was highly influenced by the solvent. Complete conversions were obtained for chlorinated solvents (see entries 1, 3, 5 in Table 23), THF (entry 7) and toluene (entry 8), whereas the conversion dropped when protic solvents (MeOH or IPA) were used.

Enantiomeric excesses were unfortunately poor in all cases (up to 23% ee with the iridium precatalyst **220a**, Table 23), indicating that our catalysts were not optimal for this transformation.

It has been reported^{316b} that enantioselectivity in iridium-mediated hydrogenation of imines might be enhanced using additives (I₂, several *N*-containing derivatives, etc.). Therefore, we investigated the hydrogenation of substrate **229a** in DCM and MeOH mediated by the iridium complex **220b** (1.0 mol %) using different additives (10 mol %). The results are summarized in Table 24.

The use of additives provided no improvement in terms of conversion or enantioselectivity. It is worth highlighting that the use of I₂ produced a clear drop in the conversion, but more interestingly, a change in the sense of stereoinduction with respect to the reference experiment without any additive (compare entries 1 and 2 and 6 and 7 in Table 24). The origin of the stereoreversed outcome of the reaction with iodine as additive remains to be uncovered, but a change in the catalytic cycle by oxidative addition of I₂ to the metal center^{316b} could account for the observed reversion.

Table 24. Additive effect on the hydrogenation of **229a** in DCM or MeOH as solvent.^[a]

Entry	Solvent	Additive	Conv. [%] ^[b]	ee [%] ^[c] (config.) ^[d]
1	DCM	-	>99%	10 (<i>S</i>)
2	DCM	I ₂	87%	6 (<i>R</i>)
3	DCM	<i>n</i> -Bu ₄ NI	71%	<i>rac</i>
4	DCM	Phthalimide	>99%	10 (<i>S</i>)
5	DCM	Benzylamine	63%	7 (<i>S</i>)
6	MeOH	-	56%	16 (<i>S</i>)
7	MeOH	I ₂	55%	30 (<i>R</i>)
8	MeOH	<i>n</i> -Bu ₄ NI	20%	<i>rac</i>
9	MeOH	Phthalimide	56%	16 (<i>S</i>)
10	MeOH	Benzylamine	4%	n.d.

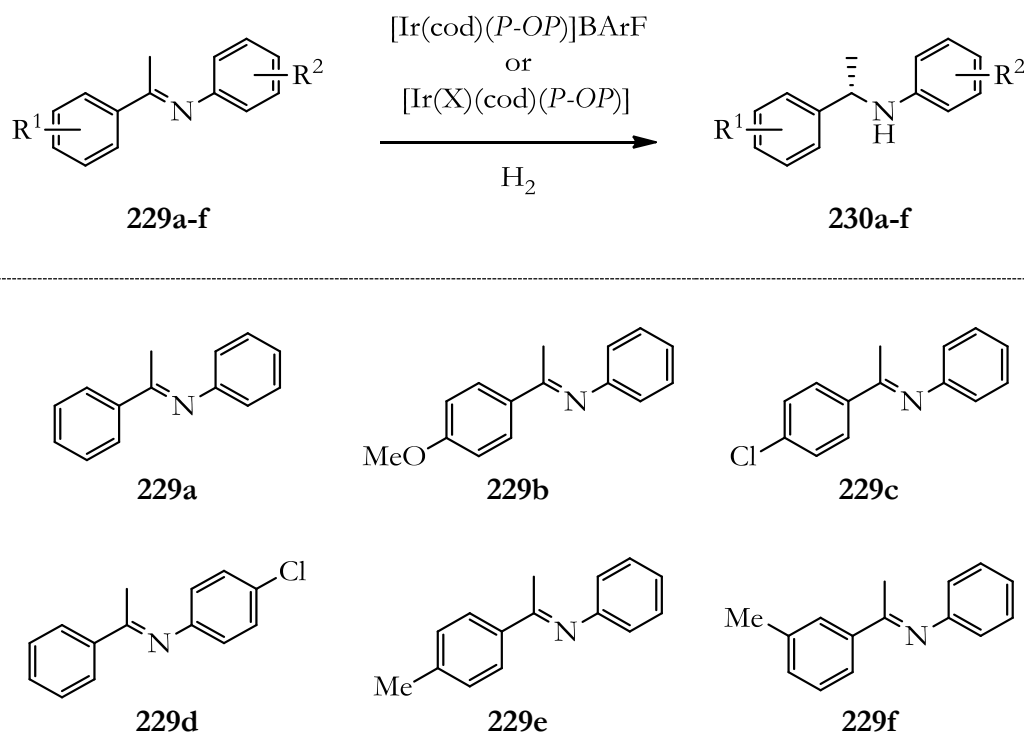
^[a] Reaction conditions: Precatalyst **220b**, 50 bar, r.t., 16h, substrate / catalyst / additive molar ratio = 100 : 1 : 10, unless otherwise indicated.

^[b] Conversion were determined by ¹H NMR.

^[c] Enantiomeric excess determined by HPLC using chiral stationary phases.

^[d] The absolute configurations were determined by comparison with reported data.

We also studied the hydrogenation of a variety of acyclic *N*-aryl imines, **229b-f**, with iridium complexes derived from phosphine-phosphinite **220b** (Scheme 61). The results of these experiments are summarized in Table 25.



Scheme 61. Iridium-mediated asymmetric hydrogenation of ketimines **229b-f** catalyzed by $[\text{Ir}(P\text{-}OP)]^+$ complexes.

As observed in Table 25, the results for the hydrogenations of **229b-f** were analogous to those observed for **229a**:

- i.* DCM was found to provide complete conversions except for substrate **229f**, whereas MeOH decreased the activity of the catalyst as indicated by the lower conversions that are observed.
- ii.* Hydrogenation of substrates **229b-f** proceeded with poor enantioselectivities. The best selectivity was up to 27% ee for substrate **229c** in MeOH using the iridium complex derived from *P-OP* ligand **220b** (entry 4 in Table 25).

Table 25. Substrate scope: Asymmetric hydrogenation of imines **229b-f** using iridium complex **220b**.^[a]

Entry	Substrate	Solvent	Conv. [%] ^[b]	ee [%] ^[c] (config.) ^[d]
1	229b	DCM	>99	<i>rac</i>
2	229b	MeOH	58	20 (<i>S</i>) ^[f]
3	229c	DCM	>99	6 (<i>S</i>) ^[f]
4	229c	MeOH	21	27 (<i>S</i>) ^[f]
5	229d	DCM	>99	2 (<i>S</i>)
6	229d	MeOH	21	9 (<i>S</i>)
7	229e	DCM	>99	2 (<i>S</i>)
8	229e	MeOH	77	25 (<i>S</i>)
9	229f	DCM	6	5 (<i>S</i>)
10	229f	MeOH	3	<i>rac</i>

^[a] Reaction conditions: Precatalyst **220b** ([Ir(cod)(**21b**)]BArF), 50 bar, r.t., 16 h, substrate / catalyst molar ratio = 100 : 1, unless otherwise indicated.

^[b] Conversion determined by ¹H NMR.

^[c] Enantiomeric excess determined by HPLC using chiral stationary phases.

^[d] Absolute configuration was assigned by comparison with reported data.

^[f] Absolute configuration was tentatively assigned by analogy based on the stereochemical outcome for analogous substrates.

The last catalytic studies on the hydrogenation of imines that we performed involved using the neutral iridium complexes of phosphine-phosphite ligands **133a**, **30a** and **134a**, as well as their iodo analog [Ir(I)(cod)(**133a**)] (**224**). Neutral iridium complexes [Ir(Cl)(cod)(*P-OP*)] were prepared *in situ* by mixing [$\{\text{Ir}(\mu\text{-Cl})(\text{cod})\}_2$] as iridium precursor with 1.1 molar equivalents of the corresponding ligand **133a**, **30a** or **134a**, under inert atmosphere in DCM as solvent. Iridium complex [Ir(I)(cod)(**133a**)] was prepared by halogen exchange as previously indicated (Section 2.2.1.2).

Hydrogenation of model imine **229a** was performed at room temperature under 50 bar of H₂. The results are summarized in Table 26.

The catalytic activity of the neutral iridium complexes derived from phosphine-phosphites was found to be high, as all of them provided complete conversion within 20 h. The use of the iodo-analog **224** as precatalyst gave comparable results to those obtained with iridium complexes bearing the chloro ligand (compare entries 1 and 2 in Table 26). On the other hand, enantioselectivities were slightly better with ligands **30a** and **134a** featuring configurationally stable biaryl moieties at the phosphite group. The neutral complex bearing ligand **30a**, based on the (*S*)-BINOL-derived phosphite moiety, afforded the highest enantiomeric excess (up to 39% e.e., entry 3 in Table 26). Interestingly, ligands **30a** and **134a** provided opposite configurations for the hydrogenated product **230a** (compare entries 3 and 4 in Table 26) indicating that the stereodiscrimination process is predominantly controlled by the binaphthyl group of the ligand.

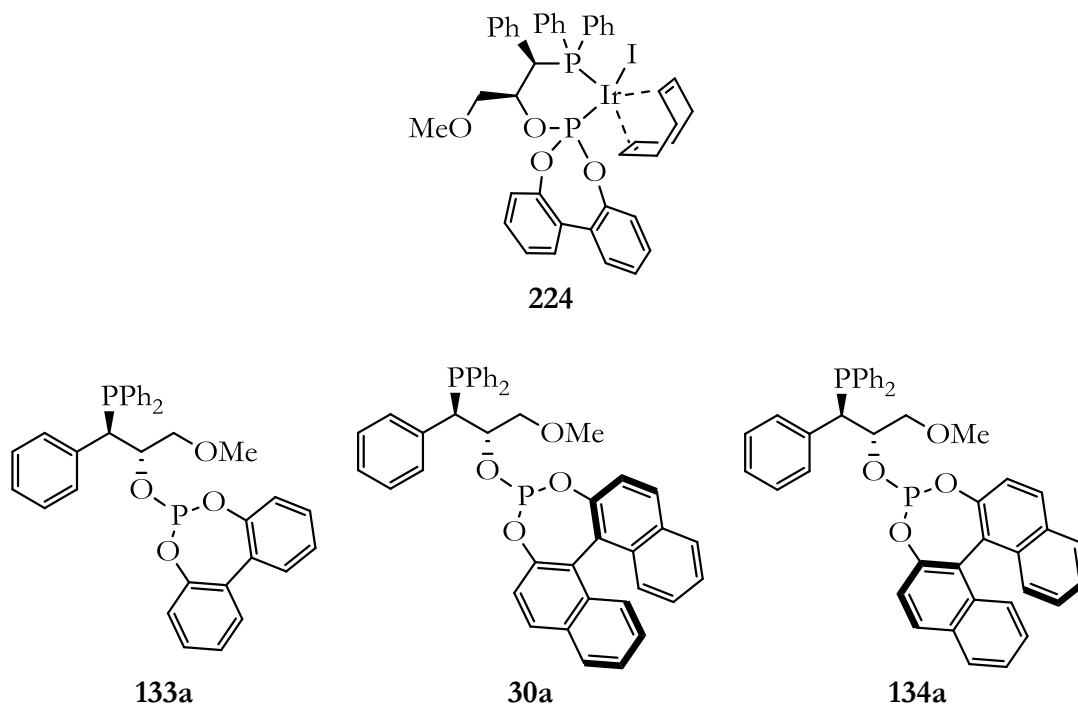


Table 26. Asymmetric hydrogenation of **229a** with the complexes derived from phosphine-phosphite ligands **133a**, **30a** and **134a**.^[a]

Entry	Precatalyst	Conv. [%] ^[b]	ee [%] ^[c] (config.) ^[d]
1	[Ir(Cl)(cod)(133a)]	>99	19 (R)
2	[Ir(I)(cod)(133a)] ^[e]	>99	21 (R)
3	[Ir(Cl)(cod)(30a)]	>99	39 (R)
4	[Ir(Cl)(cod)(134a)]	>99	29 (S)

^[a] Reaction conditions: $[\{\text{Ir}(\mu\text{-Cl})(\text{cod})\}_2] / P\text{-}OP$ ligand / substrate molar ratio = 1.0 : 2.2 : 100, room temperature, 50 bar H_2 , 20 h, 0.2 M in DCM, unless otherwise indicated.

^[b] Conversion determined by ^1H NMR.

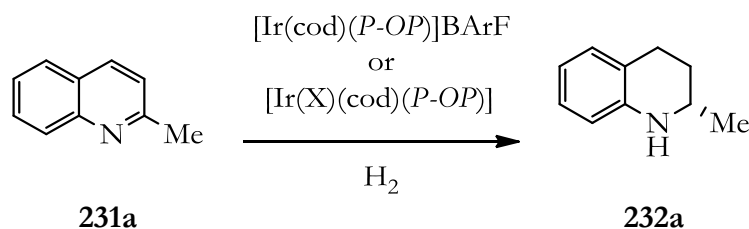
^[c] Enantiomeric excess determined by HPLC using chiral stationary phases.

^[d] Absolute configuration was assigned by comparison with reported data.

^[e] Precatalyst **224**, preformed, 2.0 mol % catalyst loading.

2.2.2.2 HYDROGENATION OF QUINOLINES AND QUINOXALINES

As indicated in the introductory section of this chapter (section 2.1.2), chiral tetrahydroquinoline (THQ) and tetrahydroquinoxaline scaffolds are found in a myriad of biologically active compounds. The high conversions found in the hydrogenation of ketimines encouraged us to explore the asymmetric hydrogenation towards these interesting classes of substrates using the iridium complexes of our *P-OP* ligands. Most of the studied quinolines **231** were commercially available and those not available were prepared by alkylation of the methyl group in 2-methylquinoline with an alkylating agent using *n*-BuLi following described procedures.³⁵⁷ Optimization of the hydrogenation conditions were carried out using phosphine-phosphite ligands **30a** and 2-methylquinoline **231a** as a benchmark substrate (Scheme 62).



Scheme 62. Iridium-mediated asymmetric hydrogenation of 2-methylquinoline catalyzed by [Ir(*P-OP*)]⁺ complexes.

The catalytic activity of the neutral iridium complex derived of **30a** was studied under standard screening conditions for this chemistry (1.0 mol % catalyst, 50 bar H₂) in different solvents. The obtained results are summarized in Table 27. Whilst the best results in terms of conversion were obtained in

³⁵⁷ Qian, B.; Guo, S.; Shao, J.; Zhu, Q.; Yang, L.; Xia, C.; Huang, H. *J. Am. Chem. Soc.* **2010**, *132*, 3650.

THF (entry 4 in Table 27), toluene provided the highest enantioselectivity (compare entries 3 and 4 in Table 27).

Table 27. Initial solvent test in the asymmetric hydrogenation of model quinoline **231a** using $[\text{Ir}(\text{Cl})(\text{cod})(\mathbf{30a})]$ as precatalyst.^[a]

Entry	Solvent	Conv. [%] ^[b]	ee [%] ^[c] (config.) ^[d]
1	DCM	6	46 (R)
2	MeOH	57	14 (R)
3	Toluene	19	68 (R)
4	THF	69	62 (R)

^[a] Reaction conditions: $[\{\text{Ir}(\mu\text{-Cl})(\text{cod})\}_2]$ / *P-OP* ligand / substrate molar ratio = 0.5 : 1.1 : 100, room temperature, 80 bar H₂, 20 h, 0.2 M, unless otherwise indicated.

^[b] Conversion determined by ¹H NMR.

^[c] Enantiomeric excess determined by HPLC using chiral stationary phases.

^[d] Absolute configuration was assigned by comparison with reported data.

Having found toluene and THF to be the best solvents for this transformation using $[\text{Ir}(\text{Cl})(\text{cod})(\mathbf{30a})]$ as precatalyst, we also assessed the catalytic activity of other iridium complexes in the hydrogenation of benchmark substrate **231a** in toluene and tetrahydrofuran. The results are summarized in Table 28.

Although almost all the iridium complexes tested, namely $[\text{Ir}(\text{Cl})(\text{cod})(\mathbf{133a})]$, $[\text{Ir}(\text{Cl})(\text{cod})(\mathbf{133b})]$, $[\text{Ir}(\text{Cl})(\text{cod})(\mathbf{30a})]$, $[\text{Ir}(\text{Cl})(\text{cod})(\mathbf{30b})]$, $[\text{Ir}(\text{Cl})(\text{cod})(\mathbf{134a})]$, $[\text{Ir}(\text{Cl})(\text{cod})(\mathbf{134b})]$ and $[\text{Ir}(\text{cod})(\mathbf{21a})]\text{BArF}$, gave good conversions in the hydrogenation of **231a**, the enantioselectivities varied greatly. The iridium precatalysts that contained the phosphites derived from (*S*)- and (*R*)-BINOL and a methyl group at the R-oxy position (**30a** and **134a**, respectively), as well as those featuring the same phosphite moieties and a trityloxy substituent (**30b** and **134b**), gave high enantioselectivities in the

reduction of the heteroaromatic compound **231a** in THF (62-83% ee; see entries 6, 8, 10 and 12 in Table 28). Furthermore, better enantioselectivities were obtained for the same precatalysts in toluene than in THF (compare entries 6, 8, 10 and 12 with 7, 9, 11 and 13 in Table 28), although at the expense of lower conversions.

Table 28. Asymmetric hydrogenation of 2-methylquinoline **231a** mediated by iridium complexes of *P-OP* ligands.^[a]

Entry	Precatalyst	Solvent	Conv. [%] ^[b]	ee [%] ^[c] (config.) ^[d]
1	[Ir(cod)(21a)]BArF ^[e]	THF	17	15 (R)
2	[Ir(Cl)(cod)(133a)]	THF	64	<i>rac</i>
3	[Ir(Cl)(cod)(133a)]	Toluene	21	11 (<i>S</i>)
4	[Ir(I)(cod)(133a)] ^[e]	THF	>99	6 (<i>S</i>)
5	[Ir(I)(cod)(133a)] ^[e]	Toluene	65	17 (<i>S</i>)
6	[Ir(Cl)(cod)(30a)]	THF	69	62 (R)
7	[Ir(Cl)(cod)(30a)]	Toluene	19	68 (R)
8	[Ir(Cl)(cod)(30b)]	THF	75	70 (R)
9	[Ir(Cl)(cod)(30b)]	Toluene	44	76 (R)
10	[Ir(Cl)(cod)(134a)]	THF	87	83 (<i>S</i>)
11	[Ir(Cl)(cod)(134a)]	Toluene	53	86 (<i>S</i>)
12	[Ir(Cl)(cod)(134b)]	THF	64	79 (<i>S</i>)
13	[Ir(Cl)(cod)(134b)]	Toluene	16	90 (<i>S</i>)

^[a] Reaction conditions: *In situ* formed precatalyst, [$\{\text{Ir}(\mu\text{-Cl})(\text{cod})\}_2$] / *P-OP* ligand / substrate molar ratio = 0.5 : 1.1 : 100, room temperature, 80 bar H₂, 20 h, 0.2 M, unless otherwise indicated.

^[b] Conversion determined by ¹H NMR.

^[c] Enantiomeric excess determined by HPLC using chiral stationary phases.

^[d] Absolute configuration was assigned by comparison with reported data.

^[e] Preformed.

Finally, we did not observe any clear relationship between enantioselectivity and the size of the ligand's R-oxy group. In the iridium-catalyzed hydrogenation of 2-methylquinoline, enantioselectivity dropped slightly in THF as the size of the substituent at the R-oxy position increased in the (*R*)-BINOL-derived ligand **134** (ee decrease from 83% ee to 79% ee; entries 10 and 12 in Table 28). In contrast, the enantioselectivity increased, in THF or toluene, when changing from methyl to trityl in the (*S*)-BINOL-derived ligands **30a,b** (compare entry 6 with 8 and entry 7 with 9 in Table 28). Interestingly, the binaphthyl moiety strongly influences the stereochemical outcome of the reaction: an opposite configuration of product **232a** is obtained with (*S*)-BINOL- and (*R*)-BINOL-derived containing ligands (**30a,b** and **134a,b**, respectively).

As mentioned earlier, several authors have reported that additives^{247i, 339, 358} can improve catalytic activity. Iodine has played a key role in many iridium-based catalytic systems used in this transformation,^{325, 334b, 338a, 359} and indeed in general for the hydrogenation of other heteroaromatic compounds.^{260b,c, 360} Zhou *et al.* proposed a mechanism for the hydrogenation reaction in the presence of I₂ which involves an oxidative addition of Ir(I) to Ir(III).^{334b} We also became interested in studying the effect on the enantioselectivity produced by other additives, most of which are protic acids.²⁴⁷ⁱ

³⁵⁸ Vogl, E. M.; Groger, H.; Shibasaki, M. *Angew. Chem., Int. Ed.* **1999**, *38*, 1570.

³⁵⁹ (a) Keay, J. D. In *Comprehensive Organic Synthesis*; Trost, B. M., Fleming, I., Eds.; Pergamon: Oxford, 1991; Vol. 8, pp 579-601. (b) Wang, D.-W.; Zeng, W.; Zhou, Y.-G. *Tetrahedron: Asymmetry* **2007**, *18*, 1103. (c) Lu, S.-M.; Bolm, C. *Adv. Synth. Catal.* **2008**, *350*, 1101. (d) Wang, X.-B.; Zhou, Y.-G. *J. Org. Chem.* **2008**, *73*, 5640. (e) Tang, W.-J.; Tan, J.; Xu, L.-J.; Lam, K.-H.; Fan, Q.-H.; Chan, A. S. C. *Adv. Synth. Catal.* **2010**, *352*, 1055.

³⁶⁰ (a) Qui, L.; Kwong, F. Y.; Wu, J.; Lam, W. H.; Chan, S.; Yu, W.-Y.; Li, Y.-M.; Gou, R.; Zhou, Z.; Chan, A. S. C. *J. Am. Chem. Soc.* **2006**, *128*, 5955. (b) Tang, W.; Xu, L.; Fan, Q.-H.; Wang, J.; Fan, B.; Zhou, Z.; Lam, K.-h.; Chan, A. S. C. *Angew. Chem., Int. Ed.* **2009**, *48*, 9135.

Table 29. Effect of additives on the Ir-catalyzed asymmetric hydrogenation of quinoline **231a**.^[a]

Entry	Ligand	Additive	Conv. [%] ^[b]	ee [%] ^[c] (config.) ^[d]
1	30a	-	69	62 (R)
2	30a	NBS	83	11 (R)
3	30a	I ₂	>99	7 (R)
4	30a	MeOH	48	64 (R)
5	134a	-	87	83 (S)
6	134a	HCl	>99	84 (S)
7	134a	TsOH	88	81 (S)
8	134a	TFA	67	85 (S)
9	134a	TfOH	82	81 (S)
10	134a	(+)-CSA	62	83 (S)
11	134a	(-)-CSA	74	82 (S)
12	134a	I ₂	>99	18 (S)

^[a] Reaction conditions: *In situ* formed precatalyst, [$\{\text{Ir}(\mu\text{-Cl})(\text{cod})\}_2$] / *P-OP* ligand / additive / substrate molar ratio = 0.5 : 1.1 : 10 : 100, room temperature, 80 bar H₂, 20 h, 0.2 M in THF, unless otherwise indicated.

^[b] Conversion determined by ¹H NMR.

^[c] Enantiomeric excess determined by HPLC using chiral stationary phases.

^[d] Absolute configuration was assigned by comparison with reported data.

In these studies aimed at assessing the effect of the additives in the reduction of **231a** catalyzed by an iridium complex of ligands **30a** or **134a**, we used 10 mol % (relative to **231a**) of NBS,^{361a} iodine,^{361b} methanol, TFA,^{361c} *p*-

³⁶¹ For details on some specific additives, see: (a) References 334c, 339 and 359c for NBS. (b) Wang, W. B.; Lu, S. M.; Yang, P. Y.; Han, X. W.; Zhou, Y. G. *J. Am. Chem. Soc.* **2003**, *125*, 10536., for iodine. (c) Li, Z.-W.; Wang, T.-L.; He, Y.-M.; Wang, Z.-J.; Fan, Q.-H.; Pan, J.; Xu, L.-J. *Org. Lett.* **2008**, *10*, 5265., for TFA and *p*-toluenesulfonic and triflic acids. (d)

toluenesulfonic acid (TsOH),^{361c} triflic acid (TfOH)^{361c} or enantiomerically pure camphorsulfonic acid ((+)- or (-)-CSA).^{361d} Iodine provided a significant increase in the hydrogenation conversion for both catalytic systems derived from ligands **30a** and **134a**, although enantioselectivity dramatically dropped in both cases (entries 3 and 12 in Table 29). With regard to NBS, TFA, MeOH, TsOH, TfOH, and CSA as additives, none of them provided any noticeable improvement; neither in conversion nor in enantioselectivity (see Table 29).

The use of ammonium or quinolinium chloride as an additive has been reported by Feringa *et al.*^{338a} and Zhou *et al.*,³⁶² as well as by Mashima *et al.*³²³ who reported the hydrogenation of quinoline hydrochlorides mediated by Ir catalysts.

Prompted by these results, we also studied the effect of quinolinium chloride as an additive in the hydrogenation reactions mediated by the iridium complexes derived from ligand **134a**, which provided higher enantioselectivities than the ones mediated by those derived from **30a**. We chose adding anhydrous HCl to generate *in situ* the corresponding quinolinium chloride. Remarkably, addition of 10 mol % of anhydrous HCl afforded complete conversion in the hydrogenation of **231a** in THF with iridium complexes derived from ligands that incorporate the (*R*)-BINOL-derived fragment (compare entry 5 and 6 in Table 29). A summary on the effects of all the additives in the conversion and the enantioselectivity for the catalytic systems derived from ligands **30a** and **134a** is also depicted in Figure 63 and Figure 64.

Wang, D.-S.; Chen, Q.-A.; Li, W.; Yu, C.-B.; Zhou, Y.-G.; Zhang, X. *J. Am. Chem. Soc.* **2010**, *132*, 8909.

³⁶² Wang, D.-S.; Zhou, Y.-G. *Tetrahedron Lett.* **2010**, *51*, 3014.

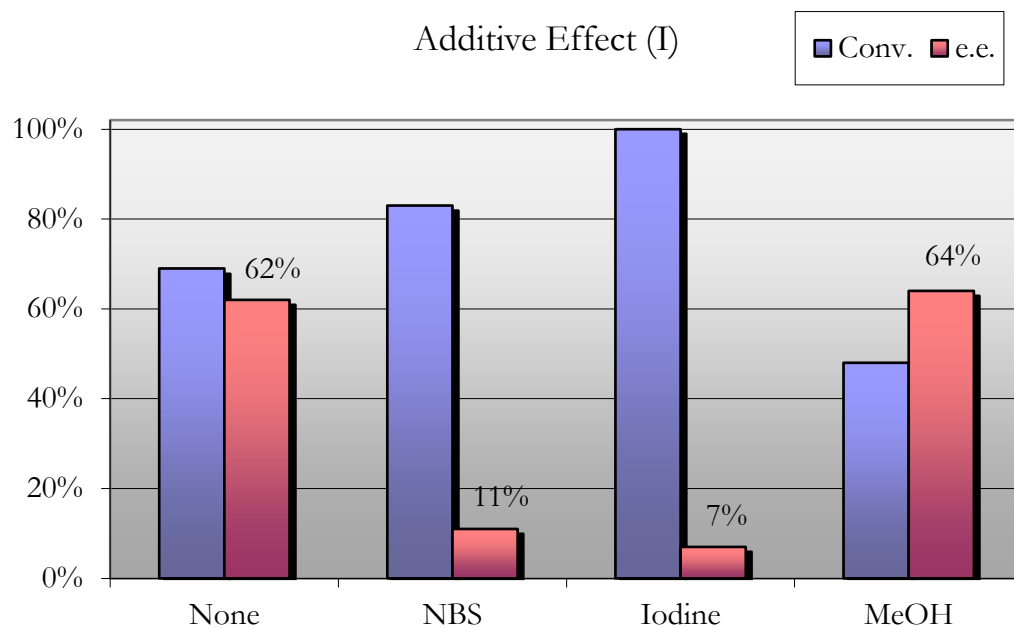


Figure 63. Effect of the additives on the asymmetric hydrogenation of **231a** mediated by $[\text{Ir}(\text{Cl})(\text{cod})(\mathbf{30a})]$.

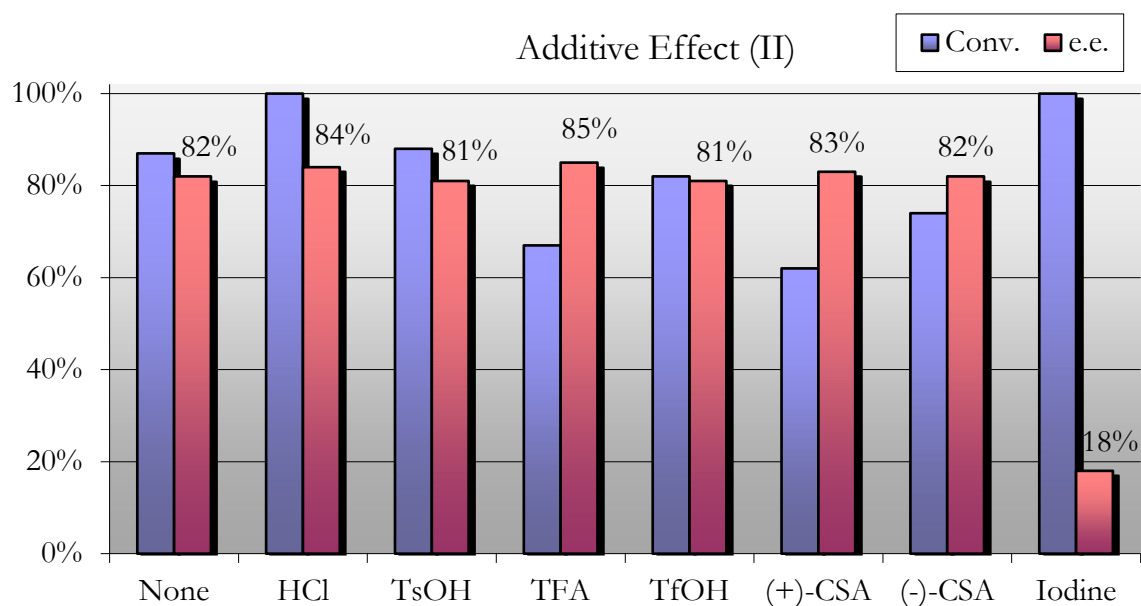


Figure 64. Effect of the additives on the asymmetric hydrogenation of **231a** mediated by $[\text{Ir}(\text{Cl})(\text{cod})(\mathbf{134a})]$.

Having observed the beneficial effects in the conversion and enantioselectivity of the *in situ* generated quinolinium chloride by addition of HCl (10 mol %), we further studied the effect on the hydrogenation of the amount of additive in the asymmetric hydrogenation of **231a** under standard conditions with the best performing solvents (*i.e.* THF and toluene). As observed in Table 30, the optimum amount of additive was found to be 10 mol %, as higher amounts of additive did not bring any benefit, neither in terms of conversion, nor in the level of enantioselectivity. Furthermore, a significant increase in the enantioselectivity was observed in toluene (up to 90%, see entry 7 in Table 30).

Table 30. Effect of the additive amount in the Ir-mediated asymmetric hydrogenation of **231a**.^[a]

Entry	Additive loading (HCl)	Solvent	Conv. [%] ^[b]	ee [%] ^[c] (config.) ^[d]
1	0%	THF	87	83 (S)
2	5%	THF	>99	85 (S)
3	10%	THF	>99	85 (S)
4	20%	THF	>99	84 (S)
5	0%	Toluene	53	86 (S)
6	5%	Toluene	57	90 (S)
7	10%	Toluene	63	90 (S)
8	20%	Toluene	63	90 (S)

^[a] Reaction conditions: *In situ* formed precatalyst, [$\{\text{Ir}(\mu\text{-Cl})(\text{cod})\}_2$] / ligand **134a** / substrate molar ratio = 0.5 : 1.1 : 100, variable amounts of anh. HCl with respect to substrate, room temperature, 80 bar H₂, 20 h, 0.2 M, unless otherwise indicated.

^[b] Conversion determined by ¹H NMR.

^[c] Enantiomeric excess determined by HPLC using chiral stationary phases.

^[d] Absolute configuration was assigned by comparison with reported data.

The effects of hydrogen pressure on the outcome of the hydrogenation reaction of 2-methylquinoline **231a** mediated by $[\text{Ir}(\text{Cl})(\text{cod})(\mathbf{134a})]$ were also studied. Almost no variation in the enantiomeric excess was observed when the reaction was carried out at a reduced pressure of 40 bar of H_2 gas. On the contrary, the catalytic activity slightly decreased, especially when toluene was used as solvent (entries 3 and 4 in Table 31).

Table 31. Hydrogenation of **231a** at reduced H_2 pressure (40 bar) *vs.* standard pressure in catalytic assays for this chemistry (80 bar).^[a]

Entry	Solvent	Additive	Conv. [%] ^[b]		ee [%] ^[c] (config.) ^[d]	
			40 bar H_2	80 bar H_2	40 bar H_2	80 bar H_2
1	THF	-	82	87	83 (<i>S</i>)	82 (<i>S</i>)
2	THF	HCl	>99	>99	84 (<i>S</i>)	85 (<i>S</i>)
3	Toluene	-	21	53	86 (<i>S</i>)	86 (<i>S</i>)
4	Toluene	HCl	52	63	89 (<i>S</i>)	90 (<i>S</i>)

^[a] Reaction conditions: *In situ* formed precatalyst, $[\{\text{Ir}(\mu\text{-Cl})(\text{cod})\}_2]$ / ligand **134a** / additive / substrate molar ratio = 0.5 : 1.1 : 10 : 100, room temperature, 20 h, 0.2 M, unless otherwise indicated.

^[b] Conversion determined by ^1H NMR.

^[c] Enantiomeric excess determined by HPLC using chiral stationary phases.

^[d] Absolute configuration was assigned by comparison with reported data.

The effects of temperature on the performance of our iridium precatalyst derived from ligand **134a** in the hydrogenation of **231a** were also assessed. The results of hydrogenation experiments with temperatures ranging from 0 to 60 °C are summarized in Table 32. The observed trends in the conversion and enantioselectivity of the hydrogenation of **231a** in THF and toluene are graphically represented in Figure 65.

Table 32. Effect of the temperature in the asymmetric hydrogenation of **231a** by $[\text{Ir}(\text{Cl})(\text{cod})(\mathbf{134a})]$.^[a]

Entry	Temperature (°C)	Solvent	Conv. [%] ^[b]	ee [%] ^[c] (config.) ^[d]
1	0	THF	11	83 (<i>S</i>)
2	22	THF	>99	84 (<i>S</i>)
3	31	THF	>99	82 (<i>S</i>)
4	40	THF	>99	82 (<i>S</i>)
5	60	THF	>99	60 (<i>S</i>)
6	22	Toluene	63	90 (<i>S</i>)
7	31	Toluene	86	89 (<i>S</i>)
8	40	Toluene	>99	88 (<i>S</i>)

^[a] Reaction conditions: *In situ* formed precatalyst, $[\{\text{Ir}(\mu\text{-Cl})(\text{cod})\}_2]$ / ligand **134a** / anh. HCl / substrate molar ratio = 0.5 : 1.1 : 10 : 100, 80 bar H₂, 20 h, 0.2 M, unless otherwise indicated.

^[b] Conversion determined by ¹H NMR.

^[c] Enantiomeric excess determined by HPLC using chiral stationary phases.

^[d] Absolute configuration was assigned by comparison with reported data.

We sought to further increase the enantioselectivity by reducing the temperature, but this strategy turned out to be ineffective, as it led to dramatically lower conversion (entry 1 in Table 32). At temperatures higher than room temperature conversion increased, however, a decrease in enantioselectivity was also observed. It can be seen in Figure 65 that the best results (in terms of both conversion and enantioselectivity) were obtained for temperatures ranging from 20 to 40 °C.

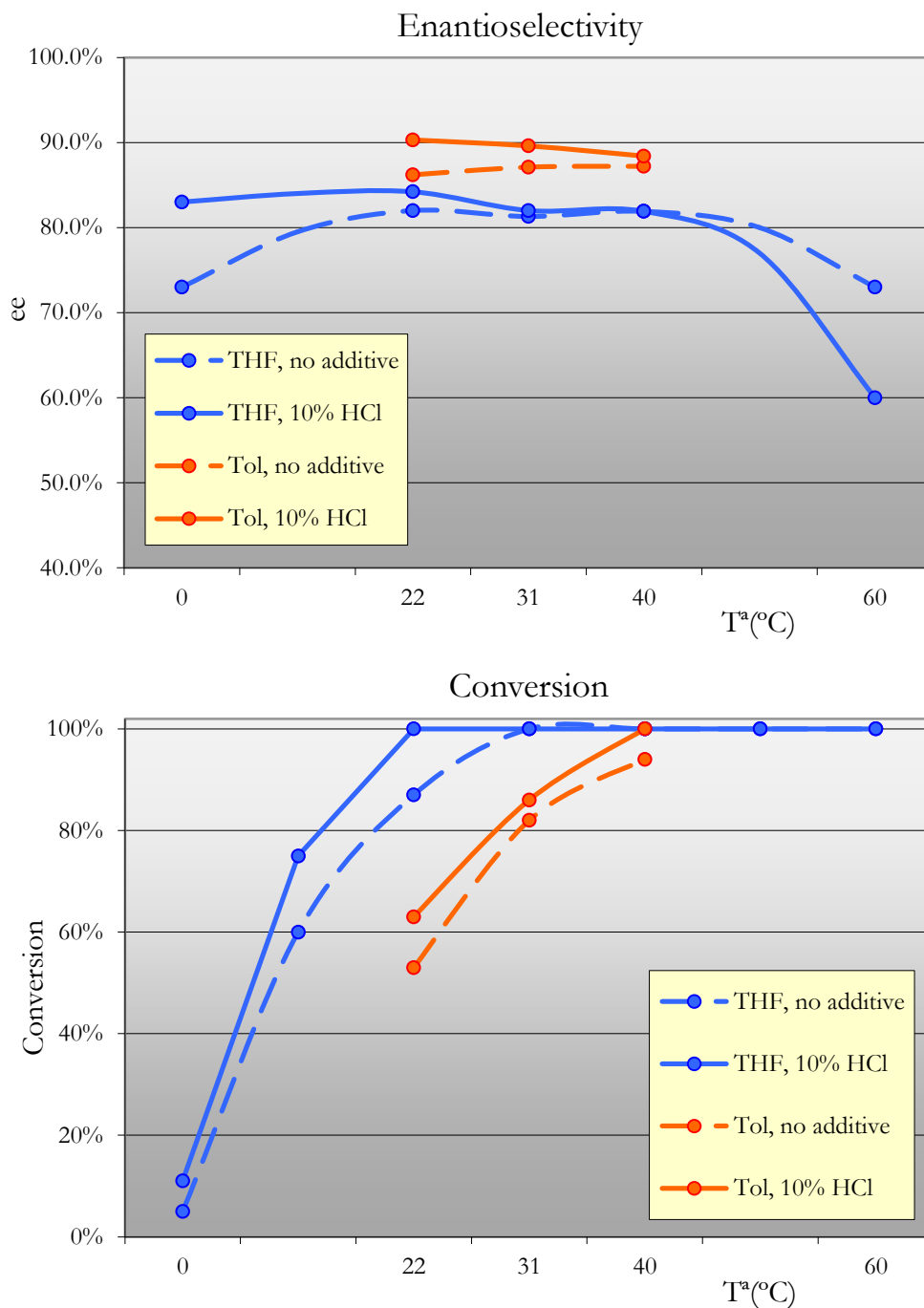


Figure 65. Temperature effect on enantioselectivity (top) and conversion (bottom) in the asymmetric hydrogenation of **231a**.

We then explored the effect of different substrate to catalyst (S/C) ratios in the asymmetric hydrogenation of **231a**. The results of these experiments are summarized in Table 33, and plotted in Figure 66 to aid comparison.

Table 33. Catalyst loading screening in asymmetric hydrogenation of **231a**.^[a]

Entry	S/C ratio	Solvent	Conv. [%] ^[b]	ee [%] ^[c] (config.) ^[d]
1	100	THF	>99	82 (S)
2	200	THF	>99	81 (S)
3	500	THF	>99	82 (S)
4	1,000	THF	87	85 (S)
5	100	Toluene	>99	88 (S)
6	200	Toluene	90	89 (S)
7	500	Toluene	47	90 (S)
8	1,000	Toluene	25	89 (S)

^[a] Reaction conditions: *In situ* formed precatalyst, $[\{\text{Ir}(\mu\text{-Cl})(\text{cod})\}_2]$ / ligand **134a** (10 mol % excess), anh. HCl / substrate molar ratio = 10 : 100, 40 °C, 80 bar H₂, 20 h, 0.2 M, unless otherwise indicated.

^[b] Conversion determined by ¹H NMR.

^[c] Enantiomeric excess determined by HPLC using chiral stationary phases.

^[d] Absolute configuration was assigned by comparison with reported data.

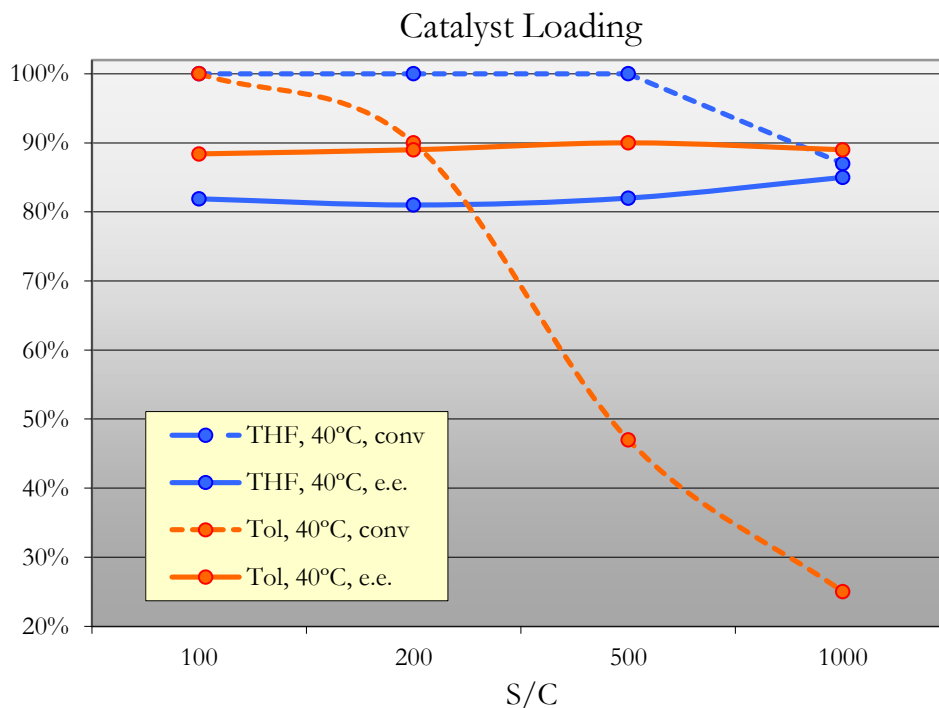


Figure 66. Catalyst loading effects in the hydrogenation of **231a**.

Using THF as solvent, a substrate to catalyst ratio as low as 500 could be used with almost no changes to activity or enantioselectivity (entry 3 in Table 33). However, the activity started to decrease at S/C = 1,000 or higher (entry 4 in Table 33). On the other hand, using toluene as solvent, a detrimental effect on catalytic activity was observed at S/C higher to 200, whereas the enantioselectivity remained unmodified (entries 5 – 8 in Table 33).

As the final step in the optimization process, and in order to evaluate if the reaction temperature could be decreased from 40 °C, we investigated the hydrogenation of **231a** using the already mentioned catalyst in the optimization studies. Hydrogenations were performed with the standard reaction conditions, but extending the reaction time (65 hours, unless otherwise stated). The results of this study have been summarized in Table 34.

Table 34. Asymmetric hydrogenation results at room temperature.^[a]

Entry	Additive	Solvent	Conv. [%] ^[b]	ee [%] ^[c] (config.) ^[d]
1	-	THF	>99	85 (<i>S</i>)
2	HCl	THF	>99	85 (<i>S</i>)
3	-	Toluene	92	89 (<i>S</i>)
4	HCl	Toluene	>99	91 (<i>S</i>)
5 ^[e]	HCl	Toluene	85	93 (<i>S</i>)

^[a] Reaction conditions: *In situ* formed precatalyst, [$\{\text{Ir}(\mu\text{-Cl})(\text{cod})\}_2$] / ligand **134a** / anh. HCl / substrate molar ratio = 0.5 : 1.1 : 10 : 100, 80 bar H₂, room temperature, 65 h, 0.2 M, unless otherwise indicated.

^[b] Conversion determined by ¹H NMR.

^[c] Enantiomeric excess determined by HPLC using chiral stationary phases.

^[d] Absolute configuration was assigned by comparison with reported data.

^[e] Ligand **134b** was used in this case.

Using an extended reaction time of 65 h, and even with toluene as solvent, we observed complete conversion and enantioselectivities of up to 91% ee (entry 4 in Table 34) in the hydrogenation of **231a** using the iridium complex derived from the usual phosphine-phosphite **134a**. The iridium complex derived from the more sterically demanding ligand **134b**, which in addition to containing the (*R*)-BINOL-derived phosphite group incorporates a trityloxy group, also enabled the efficient hydrogenation of quinoline **231a**. Slightly higher enantioselectivities were obtained for ligand **134b** in toluene (93% ee vs 91% ee; entries 4 and 5 in Table 34), although conversion was not complete using the latter ligand. Thus, we chose ligand **134a** for further catalytic studies on the asymmetric hydrogenation of an array of structurally diverse quinolines **231a-i** (Figure 67) under the optimized hydrogenation conditions (1.0 mol % precatalyst, toluene, 10 mol % anh. HCl, 80 bar of H₂ and 65 h of reaction time). These results are summarized in Table 35.

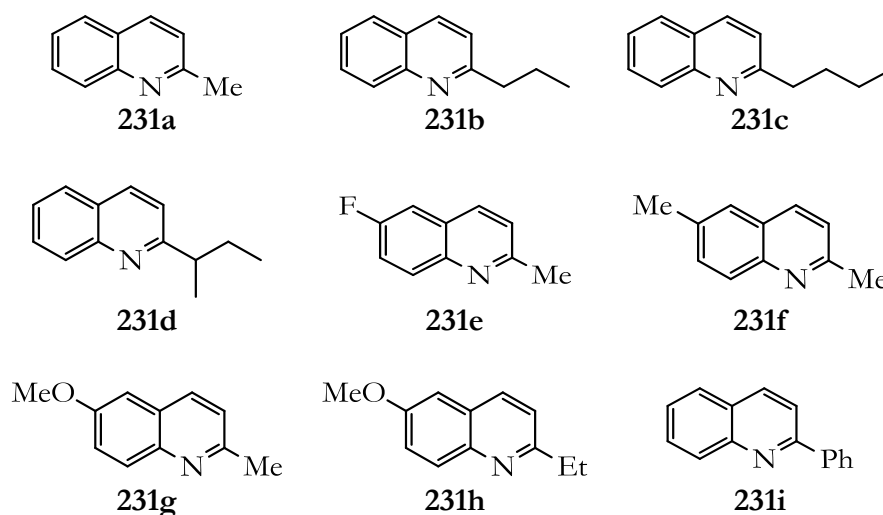


Figure 67. Structural diversity of the quinoline ring in the catalytic hydrogenation study.

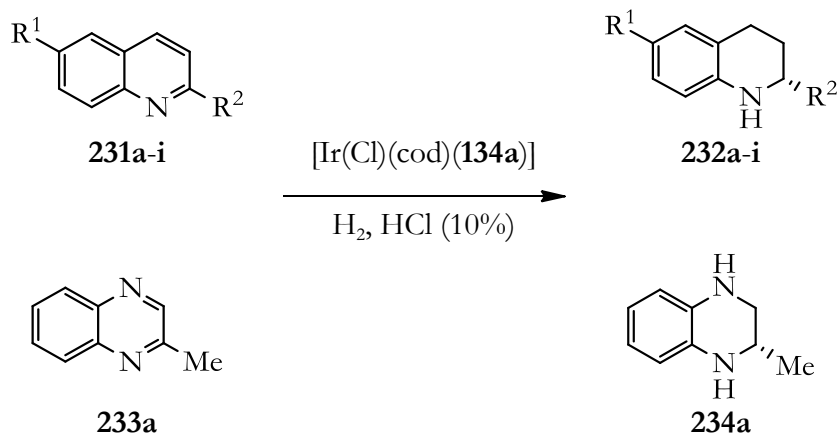


Table 35. Substrate scope of asymmetric hydrogenation of quinolines **231a-i** and quinoxaline **233a**.^[a]

Entry	Substrate	Substituents	Conv. [%] ^[b]	ee [%] ^[c] (config.) ^[d]
1	231a	R ¹ = H; R ² = Me	>99	91 (<i>S</i>)
2	231b	R ¹ = H; R ² = <i>n</i> -Pr	98	71 (<i>S</i>)
3	231c	R ¹ = H; R ² = <i>n</i> -Bu	99	85 (<i>S</i>)
4	231d	R ¹ = H; R ² = <i>i</i> -Bu	>99	88 (<i>R</i>) ^[e]
5	231e	R ¹ = F; R ² = Me	92	88 (<i>S</i>)
6	231f	R ¹ = Me; R ² = Me	74	92 (<i>S</i>)
7	231g	R ¹ = MeO; R ² = Me	38	89 (<i>S</i>)
8	231h	R ¹ = MeO; R ² = Et	23	87 (<i>S</i>) ^[e]
9	231i	R ¹ = H; R ² = Ph	>99	84 (<i>R</i>)
10	233a ^[f]	-	97	70 (<i>R</i>)

^[a] Reaction conditions: *In situ* formed precatalyst, [$\{\text{Ir}(\mu\text{-Cl})(\text{cod})\}_2$] / ligand **134a** / anh. HCl / substrate molar ratio = 0.5 : 1.1 : 10 : 100, 80 bar H₂, room temperature, 65 h, 0.2 M in toluene, unless otherwise indicated.

^[b] Conversion determined by ¹H NMR.

^[c] Enantiomeric excess determined by HPLC using chiral stationary phases.

^[d] Absolute configuration was assigned by comparison with reported data.

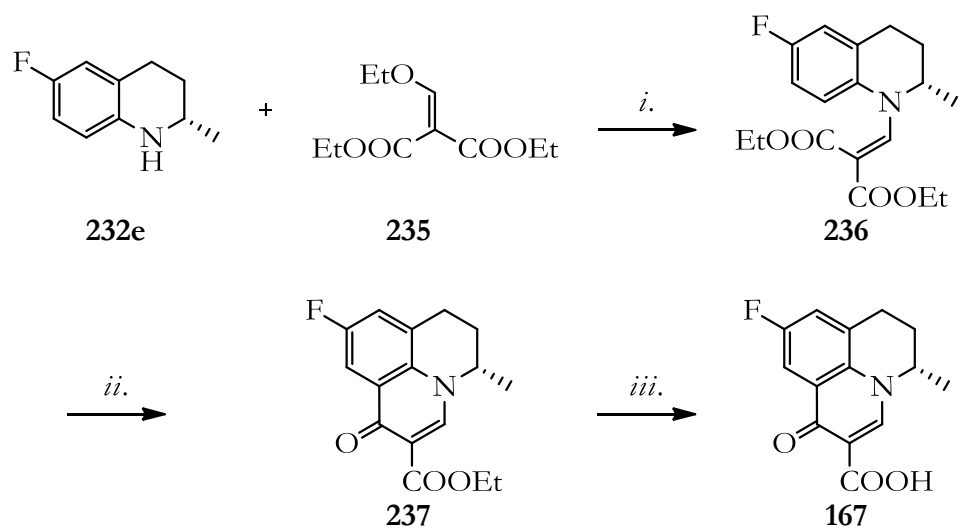
^[e] Absolute configuration was tentatively assigned by analogy based on the stereochemical outcome for analogous substrates.

^[f] Iridium complex containing ligand **30a** was used as precatalyst in this case.

We also explored the hydrogenation of quinoxaline **233a**, a structural analog of quinoline **231a**, to study the applicability of our catalytic system in this new class of heterocycles. The hydrogenation of quinoxaline **233a** (entry 10 in Table 35) was performed with the iridium complex derived from **30a** instead of **134a**, as preliminary experiments showed that ligand **30a** provided higher enantioselectivities.

The chain length of the R² group barely influenced the catalytic activity, since enantioselectivities remained high for R² = Me, *n*-Bu, *i*-Bu (91%, 85%, and 88% ee, respectively; entries 1, 3, and 4 in Table 35) and good for R² = *n*-Pr (71% ee, entry 2 in Table 35). Replacing the alkyl R² group with a phenyl substituent did not affect the catalytic activity, and the enantioselectivity remained high (84% ee; entry 9 in Table 35). Regardless of the electronic nature of the substituent R¹, substrates were hydrogenated with high enantioselectivity (88- 92% ee; entries 5-7 in Table 35), although conversion decreased dramatically in the case where R¹ is an electron-donating group (**231g,h**, R¹ = MeO; entries 7 and 8 in Table 35). In contrast, these complexes failed to give high enantioselectivity in the reduction of quinoxaline **233a** (entry 10 in Table 35).

Remarkably, the fluorosubstituted 1,2,3,4-tetrahydroquinoline **232e** was obtained in high conversion and enantioselectivity (entry 5 in Table 35). Our synthetic methodology constitutes an interesting access to this tetrahydroquinoline, which is a key building block in the preparation of the antibacterial agent flumequine (Scheme 63).²⁷⁵



i. 110-115 °C

ii. Polyphosphoric acid (PPA), 100-110 °C, toluene

iii. H₂O/H⁺

Scheme 63. Synthetic route towards (*S*)-flumequine (**167**) from compound **232e**.²⁷⁵

2.2.2.3 HYDROGENATION OF UNPROTECTED INDOLES

Chiral indolines represent an interesting class of organic molecules, as the indoline core can be found in many biologically active compounds (see, for instance, Figure 47 in section 2.1.2).^{289, 290} In order to obtain these compounds in enantiomerically pure or enantioenriched form, many efficient synthetic methodologies have been developed.^{363, 364} However, direct asymmetric reduction of indoles to obtain chiral indolines, despite its apparent simplicity and feasibility, has not been widely explored.

Seminal reports with moderate results in this field have been reported by Kuwano, Ito and co-workers for the ruthenium- or rhodium-mediated hydrogenation of *N*-protected indoles,³⁶⁵ by Feringa *et al.*³⁶⁶ and by Pfaltz *et al.*³⁶⁷ for rhodium- and iridium-mediated hydrogenation of the same type of compounds. A relevant advance in this field has been reported recently by Zhou, Zhang and co-workers, in the palladium-mediated asymmetric hydrogenation of unprotected indoles.^{361d} Their strategy includes the use of a Brønsted acid as activator (enantiomerically pure camphorsulfonic acid, amongst others), which breaks indole aromaticity by protonation/isomerization of the C=C double bond and formation of an

³⁶³ See the following selected synthetic methods: (a) Arp, F. O.; Fu, G. C. *J. Am. Chem. Soc.* **2006**, *128*, 14264. (b) Hou, X. L.; Zheng, B. H. *Org. Lett.* **2009**, *11*, 1789. (c) Xiao, Y.-C.; Wang, C.; Yao, Y.; Sun, J.; Chen, Y.-C. *Angew. Chem., Int. Ed.* **2011**, *50*, 10661. (d) Ghorai, M. K.; Nanaji, Y. *J. Org. Chem.* **2013**, *78*, 3867. (e) Yang, Q.-Q.; Wang, Q.; An, J.; Chen, J.-R.; Lu, L.-Q.; Xiao, W.-J. *Chem.-Eur. J.* **2013**, DOI: 10.1002/chem.201300988.

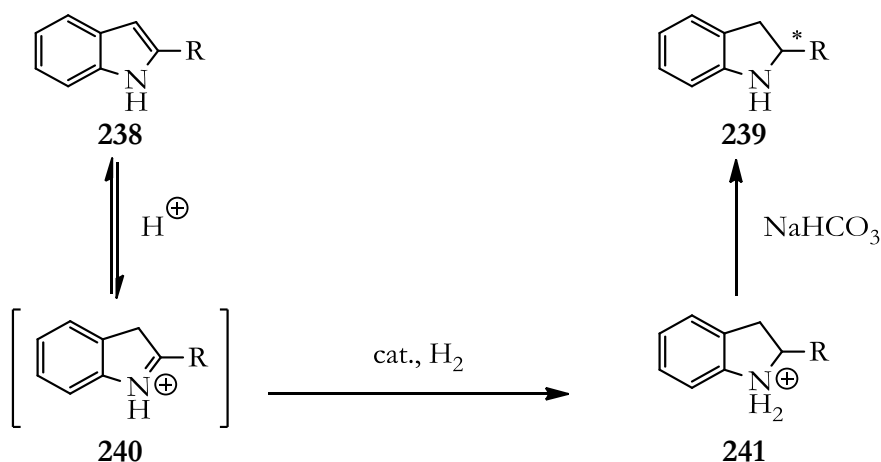
³⁶⁴ For synthetic routes to indolines, see ref 246c and the references cited therein.

³⁶⁵ (a) Kuwano, R.; Sato, K.; Kurokawa, T.; Karube, D.; Ito, Y. *J. Am. Chem. Soc.* **2000**, *122*, 7614. (b) Kuwano, R.; Kaneda, K.; Ito, T.; Sato, K.; Kurokawa, T.; Ito, Y. *Org. Lett.* **2004**, *6*, 2213. (c) Kuwano, R.; Kashiwabara, M.; Sato, K.; Ito, T.; Kaneda, K.; Ito, Y. *Tetrahedron: Asymmetry* **2006**, *17*, 521. (d) Kuwano, R.; Kashiwabara, M. *Org. Lett.* **2006**, *8*, 2653.

³⁶⁶ Mrcic, N.; Jerphagnon, T.; Minnaard, A. J.; Feringa, B. L.; de Vries, J. G. *Tetrahedron: Asymmetry* **2010**, *21*, 7.

³⁶⁷ Baeza, A.; Pfaltz, A. *Chem.-Eur. J.* **2010**, *16*, 2036.

iminium derivative **240**.³⁶⁸ In this process, a new C=N double bond is formed, which can be straightforwardly hydrogenated (Scheme 64).



Scheme 64. Hydrogenation of unprotected indoles by Brønsted acid activation.

Since Zhang and co-workers' seminal work,^{361d} several more reports on Pd-mediated asymmetric hydrogenation of 2-substituted and 2,3-substituted indoles have been published,³⁶⁹ however, reports on the asymmetric hydrogenation of unprotected indoles mediated by iridium complexes are scarce.³⁷⁰ Thus, we became interested in developing an iridium catalytic system derived from our *P-OP* complexes for the hydrogenation of unprotected indoles (Scheme 65). 2-Substituted indoles to be tested in asymmetric hydrogenation were purchased or synthesized following reported procedures.^{361d}

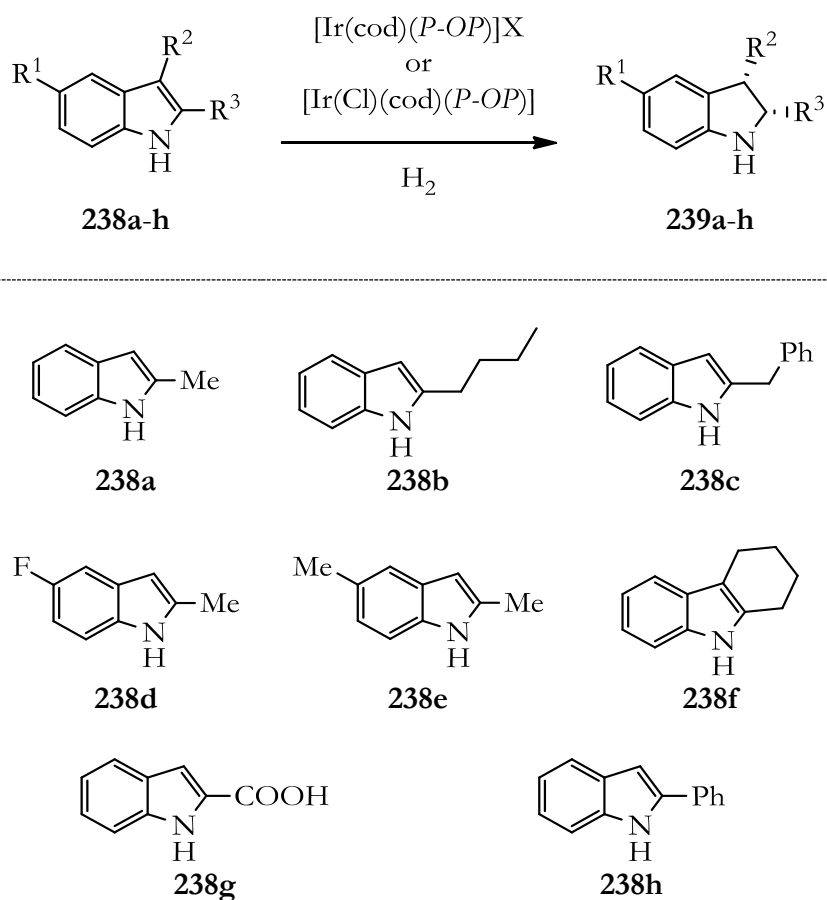
As the starting point of these catalytic studies, we employed the neutral complexes derived from phosphine-phosphite ligands bearing a BINOL-

³⁶⁸ Chen, C.-B.; Wang, X.-F.; Cao, Y.-J.; Cheng, H.-G.; Xiao, W.-J. *J. Org. Chem.* **2009**, *74*, 3532.

³⁶⁹ (a) Wang, D.-S.; Tang, J.; Zhou, Y.-G.; Chen, M.-W.; Yu, C.-B.; Duan, Y.; Jiang, G.-F. *Chem. Sci.* **2011**, *2*, 803. (b) Duan, Y.; Chen, M.-W.; Ye, Z.-S.; Wang, D.-S.; Chen, Q.-A.; Zhou, Y.-G. *Chem.-Eur. J.* **2011**, *17*, 7193. (c) Duan, Y.; Chen, M.-W.; Chen, Q.-A.; Yu, C.-B.; Zhou, Y.-G. *Org. Biomol. Chem.* **2012**, *10*, 1235.

³⁷⁰ Kluwer, A. M.; Detz, R. J.; Abiri, Z.; van der Burg, A. M.; Reek, J. N. H. *Adv. Synth. Catal.* **2012**, *354*, 89.

derived moiety (ligands **30a** and **134a**), as well the cationic complex **225** (derived from (*R*)-BINOL-derived ligand **134a**). Reactions were performed with indole **238a** as a model substrate under standard screening conditions for asymmetric hydrogenation and in the presence of one equivalent of *p*-toluenesulfonic acid (TsOH) to mediate the protonation and double bond isomerization in the indolic derivative **238a**, but in the absence of other additives. The results of this catalytic study are summarized in Table 36.



Scheme 65. Iridium-mediated asymmetric hydrogenation of unprotected indoles catalyzed by $[\text{Ir}(\text{P-OP})]^+$ complexes.

The addition of 1 equiv. of TsOH becomes crucial for achieving a good activity profile (compare entries 1 and 2 in Table 36), thus confirming that the reaction proceeds by hydrogenation of a C=N double bond instead of direct hydrogenation of the C=C double bond in the indole derivative. Ligand **134a** (comprising a (*R*)-BINOL-derived moiety) provided the highest

enantioselectivity (compare entries 2 and 3 in Table 36). On the contrary, the cationic complex $[\text{Ir}(\text{cod})(\mathbf{134a})]\text{BF}_4$ led to poor conversion and low enantioselectivity, regardless of the additive employed (compare entries 1 and 2 with 4 and 5 respectively in Table 36).

Table 36. Asymmetric hydrogenation of indole **238a** mediated by iridium complexes derived from *P-OP* ligands.^[a]

Entry	Precatalyst	Additive	Conv. [%] ^[b]	ee [%] ^[c] (config.) ^[d]
1	$[\text{Ir}(\text{Cl})(\text{cod})(\mathbf{134a})]$	-	11	n. d.
2	$[\text{Ir}(\text{Cl})(\text{cod})(\mathbf{134a})]$	TsOH	69	88 (<i>S</i>)
3	$[\text{Ir}(\text{Cl})(\text{cod})(\mathbf{30a})]$	TsOH	69	78 (<i>R</i>)
4	$[\text{Ir}(\text{cod})(\mathbf{134a})]\text{BF}_4$ ^[e]	-	5	n. d.
5	$[\text{Ir}(\text{cod})(\mathbf{134a})]\text{BF}_4$ ^[e]	TsOH	21	44 (<i>R</i>)

^[a] Reaction conditions: *In situ* formed precatalyst, $[\{\text{Ir}(\mu\text{-Cl})(\text{cod})\}_2] / P\text{-OP}$ ligand / TsOH / substrate molar ratio = 0.5 : 1.1 : 100 : 100, 80 bar H₂, room temperature, 20 h, 0.2 M in THF, unless otherwise indicated.

^[b] Conversion determined by ¹H NMR after basic workup.

^[c] Enantiomeric excess determined by HPLC using chiral stationary phases after basic workup.

^[d] Absolute configuration was assigned by comparison with reported data.

^[e] Compound **225a**, preformed.

Having confirmed that TsOH is crucial for high catalytic activity in the hydrogenation of indole **238a**, we studied the minimum required amount of TsOH to achieve high conversion (see Table 37 for a summary of the results). We inferred from these studies that at least one equivalent of acid is required to achieve the optimal conversion (see entry 5 in Table 37), while catalytic amounts of acid lower than one equivalent led to lower conversions.

In order to determine whether *p*-toluenesulfonic acid was the best possible reagent to mediate the double bond isomerization in indole **238a**, we

tested a broad range of analogous reagents. The results of the experiments are summarized in Table 38.

Table 37. Studies on the effect of the TsOH amount in the hydrogenation of indole **238a**.^[a]

Entry	Additive	Loading	Conv. [%] ^[b]	ee [%] ^[c] (config.) ^[d]
1	-	-	11	n. d.
2	TsOH	10%	22	90 (<i>S</i>)
3	TsOH	40%	42	90 (<i>S</i>)
4	TsOH	80%	65	88 (<i>S</i>)
5	TsOH	100%	69	88 (<i>S</i>)

^[a] Reaction conditions: *In situ* formed precatalyst, $[\{\text{Ir}(\mu\text{-Cl})(\text{cod})\}_2] / P\text{-}OP$ ligand / substrate molar ratio = 0.5 : 1.1 : 100, variable additive loading, 80 bar H₂, room temperature, 20 h, 0.2 M in THF, unless otherwise indicated.

^[b] Conversion determined by ¹H NMR after basic workup.

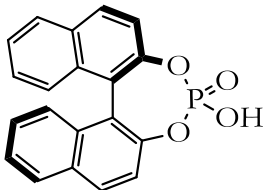
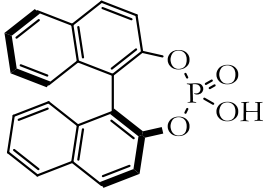
^[c] Enantiomeric excess determined by HPLC using chiral stationary phases after basic workup.

^[d] Absolute configuration was assigned by comparison with reported data.

While enantioselectivities were high regardless of the additive used, conversions varied greatly. Low conversions were achieved when carboxylic acids were used (see entries 1 and 2 in Table 38), moderated conversions were observed with chiral phosphoric acids (see entries 3-5 in Table 38) and high conversions were found with sulfonic acids (see entries 6-10 in Table 38). The observed trend in catalytic activity has been summarized in Figure 68. Disappointingly, enantioselectivities remained unaffected for all the studied additives, as we had expected some level of cooperativity in stereoinduction arising from the ligand and enantiomerically pure additives (compare entries 4 and 5 and entries 8-10 in Table 38). Due to the inability of the chiral counteranion in biasing the stereochemical outcome of the reaction, racemic camphorsulfonic acid (*rac*-CSA) was chosen as the optimal additive, as it simultaneously provided the highest conversion and enantioselectivity (entry

10 in Table 38). Amounts of *rac*-CSA higher than one equivalent did not further improve the conversion (compare entries 10 and 11 in Table 38).

Table 38. Effects of additives in the Ir-catalyzed asymmetric hydrogenation of **238a**.^[a]

Entry	Additive [1.0 equiv.]	Conv. [%] ^[b]	ee [%] ^[c] (config.) ^[d]
1	Benzoic acid	17	90 (<i>S</i>)
2	Trifluoroacetic acid (TFA)	23	90 (<i>S</i>)
3	Diphenylphosphoric acid (DPP)	49	90 (<i>S</i>)
4	 (R)-BNP	55	89 (<i>S</i>)
5	 (S)-BNP	57	89 (<i>S</i>)
6	<i>p</i> -Toluenesulfonic acid (TsOH)	69	88 (<i>S</i>)
7	Methanesulfonic acid (MsOH)	81	88 (<i>S</i>)
8	D-(+)-Camphorsulfonic acid (D-CSA)	80	90 (<i>S</i>)
9	L-(-)-Camphorsulfonic acid (L-CSA)	81	90 (<i>S</i>)
10	<i>rac</i> -Camphorsulfonic acid (CSA)	83	90 (<i>S</i>)
11	<i>rac</i> -Camphorsulfonic acid (CSA) ^[e]	85	89 (<i>S</i>)

^[a] Reaction conditions: *In situ* formed precatalyst, $[\{\text{Ir}(\mu\text{-Cl})(\text{cod})\}_2] / \mathbf{134a} / \text{additive} / \text{substrate molar ratio} = 0.5 : 1.1 : 100 : 100$, 80 bar H_2 , room temperature, 20 h, 0.2 M in THF, unless otherwise indicated.

^[b] Conversion determined by ^1H NMR after basic workup.

^[c] Enantiomeric excess determined by HPLC using chiral stationary phases after basic workup.

^[d] Absolute configuration was assigned by comparison with reported data.

^[e] 1.25 equivalents of acid were used.

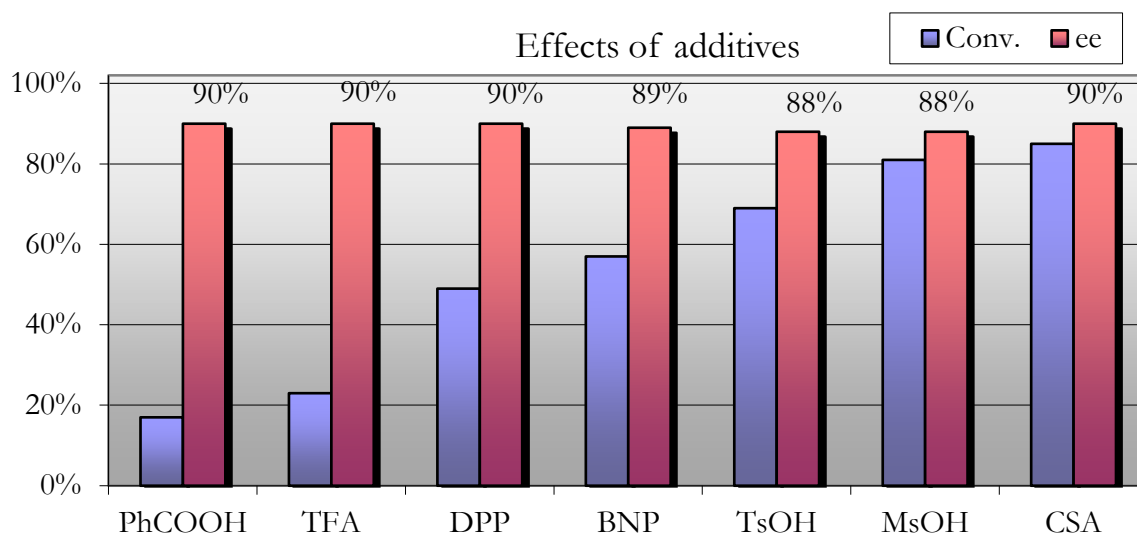


Figure 68. Effects of additives in the asymmetric hydrogenation of **238a** with the iridium complex derived from ligand **134a**.

Other parameters in the reaction conditions, such as temperature, catalyst amount and reaction time, were also optimized in order to develop more efficient hydrogenation conditions, but all the attempts were unsuccessful (Table 39). The asymmetric hydrogenation of **238a** did not prove to be very sensitive to such variations, as conversion and enantioselectivity did not vary significantly.

Table 39. Effect of temperature, reaction time and catalyst loading for the Ir-catalyzed asymmetric hydrogenation of indole **238a**.^[a]

Entry	Reaction conditions	Conv. [%] ^[b]	ee [%] ^[c] (config.) ^[d]
1	0 °C, 40 h, 1.0 mol % cat	83	91 (<i>S</i>)
2	0 °C, 40 h, 2.0 mol % cat	86	91 (<i>S</i>)
3	rt, 40 h, 1.0 mol % cat	86	90 (<i>S</i>)
4	45 °C, 20 h, 1.0 mol % cat	92	87 (<i>S</i>)

^[a] Reaction conditions: *In situ* formed precatalyst, $[\{\text{Ir}(\mu\text{-Cl})(\text{cod})\}_2] / \mathbf{134a} / \text{CSA} / \text{substrate molar ratio} = 0.5 : 1.1 : 100 : 100$, 80 bar H_2 , 0.2 M in THF, unless otherwise indicated.

^[b] Conversion determined by $^1\text{H NMR}$ after basic workup.

^[c] Enantiomeric excess determined by HPLC using chiral stationary phases after basic workup.

^[d] Absolute configuration was assigned by comparison with reported data.

The enantioselectivity increased slightly when the reaction was run at 0 °C, but conversion remained practically unaltered. Analogously, an increase in the catalyst loading up to 2.0 mol % did not bring any significant benefit (see entries 1 and 2 in Table 39). Whilst an extended reaction time did not entail an enhancement in conversion, an increase in the reaction temperature did (45 °C), at the expense of a reduced enantioselectivity (see entries 3 and 4 in Table 39).

As transformations that involve acid-base reactions are generally highly solvent dependent, we studied the effects of different solvents in the conversion and enantioselectivity of the asymmetric hydrogenation of indole **238a**. These experiments are summarized in Table 40.

Table 40. Study of the effects of different solvents on the asymmetric hydrogenation of indole **238a** using the iridium complex derived from ligand **134a**.^[a]

Entry	Solvent	Conv. [%] ^[b]	ee [%] ^[c] (config.) ^[d]
1	THF	83	90 (<i>S</i>)
2	DCM	99	82 (<i>S</i>)
3	IPA	91	86 (<i>S</i>)
4	MeOH	81	70 (<i>S</i>)
5	2-Methyltetrahydrofuran (MeTHF)	92	91 (<i>S</i>)
6	EtOAc	94	86 (<i>S</i>)
7	Dimethyl carbonate (DMC)	>99	84 (<i>S</i>)
8	2-methyl-2-butanol (2M2B)	84	86 (<i>S</i>)
9	Diisopropyl ether (DIPE)	64	83 (<i>S</i>)
10	Dimethoxyethane (DME)	91	88 (<i>S</i>)
11	AcOH ^[e]	26	73 (<i>S</i>)
12	AcOH	52	48 (<i>S</i>)
13	TFA ^[e]	4	72 (<i>S</i>)
14	TFA	3	89 (<i>S</i>)

^[a] Reaction conditions: *In situ* formed precatalyst, $[\{\text{Ir}(\mu\text{-Cl})(\text{cod})\}_2] / \mathbf{134a} / \text{CSA} / \text{substrate molar ratio} = 0.5 : 1.1 : 100 : 100$, 80 bar H_2 , room temperature, 20 h, 0.2 M in the stated solvent, unless otherwise indicated.

^[b] Conversion determined by ^1H NMR after basic workup.

^[c] Enantiomeric excess determined by HPLC using chiral stationary phases after basic workup.

^[d] Absolute configuration was assigned by comparison with reported data.

^[e] No CSA was added as additive.

The hydrogenation reaction was highly solvent dependent and proceeded with high levels of conversion (> 90%) when DCM, IPA, MeTHF, EtOAc, DMC or DME were used as solvents, particularly MeTHF. Additionally a very slight increase in enantioselectivity was observed for MeTHF in comparison with THF (1% increase in the ee), although its magnitude lies in the range of experimental error. Acidic solvents, such as acetic or trifluoroacetic acid, were also tested, but low or very low conversions were found (see entries 11-14 in Table 40) most probably as a result of degradation of the iridium catalyst.

With the optimized hydrogenation conditions for the model indole **238a** known, we expanded the catalytic study to a set of differently 2- and 5-substituted indoles **238a-e** and **238g,h** as well to the carbazole **238f**. The results of this study are summarized in Table 41.

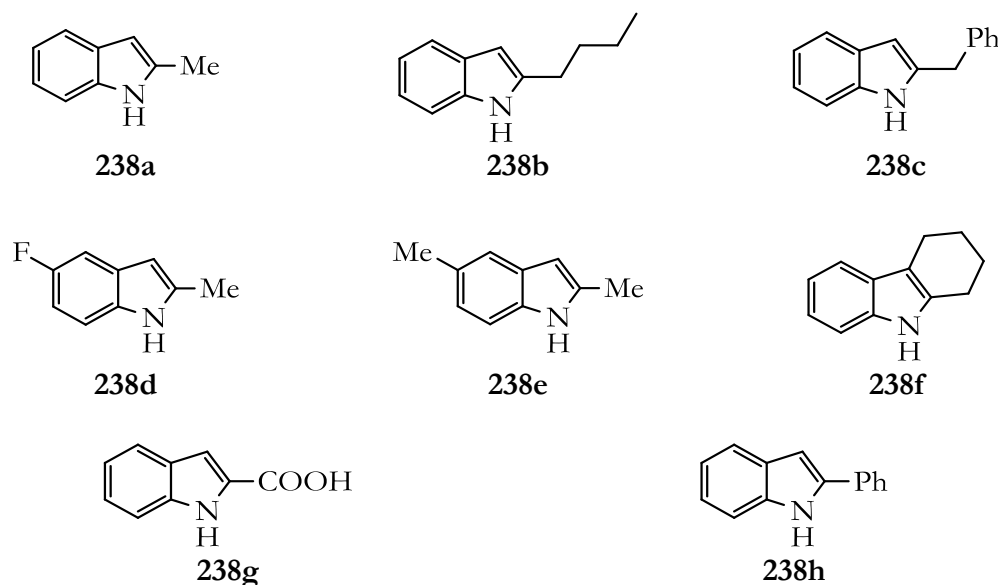


Figure 69. Structural diversity of the indole scaffold in the catalytic hydrogenation study.

The chain length of the R³ group barely influenced the catalytic activity, since enantioselectivities remained high for R³ = Me and *n*-Bu (91% in both cases; see entries 1 and 2 in Table 41). Hydrogenation conversion of indole **238c** with a benzyl substituent at the R³ position was moderate and

enantioselectivity remained high (91% ee), whilst the hydrogenation of the phenyl- and carboxy- substituted analogs **238g** and **238h**, respectively, did not take place (compare entry 3 with entries 7 and 8 in Table 41). Substrates were hydrogenated with high ee regardless of the electronic nature of the substituent R¹ (90% ee; entries 4 and 5 in Table 41), although conversion decreased in the case where R¹ was an electron-withdrawing group (**238d**; R¹ = F; entry 5 in Table 41). The carbazole derivative **238f** was also hydrogenated with moderate conversion and high enantioselectivity (entry 6 in Table 41).

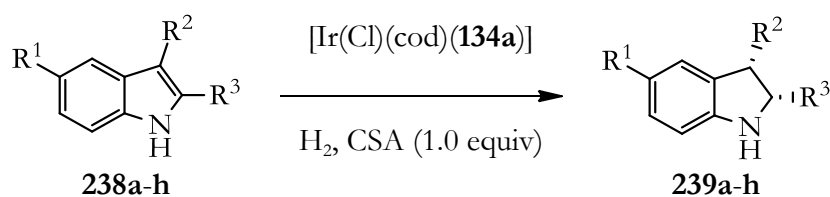


Table 41. Asymmetric hydrogenation of indoles **238a-h** with CSA as additive.^[a]

Entry	Substrate	Substituents	Conv. [%] ^[b]	ee [%] ^[c] (config.) ^[d]
1	238a	R ¹ = H; R ² = H; R ³ = Me	92	91 (<i>S</i>)
2	238b	R ¹ = H; R ² = H; R ³ = <i>n</i> -Bu	85	91 (<i>S</i>)
3	238c	R ¹ = H; R ² = H; R ³ = Bn	67	91 (<i>S</i>)
4	238d	R ¹ = F; R ² = H; R ³ = Me	55	90 (<i>S</i>)
5	238e	R ¹ = Me; R ² = H; R ³ = Me	94	90 (<i>S</i>)
6	238f	R ¹ = H; R ² , R ³ = -(CH ₂) ₄ -	80	91 (<i>S</i>)
7	238g	R ¹ = H; R ² = H; R ³ = COOH	0	n. d.
8	238h	R ¹ = H; R ² = H; R ³ = Ph	0	n. d.

^[a] Reaction conditions: *In situ* formed precatalyst, [$\{\text{Ir}(\mu\text{-Cl})(\text{cod})\}_2$] / **134a** / CSA / substrate molar ratio = 0.5 : 1.1 : 100 : 100, 80 bar H₂, room temperature, 20 h, 0.2 M in MeTHF.

^[b] Conversion determined by ¹H NMR after basic workup.

^[c] Enantiomeric excess determined by HPLC using chiral stationary phases after basic workup.

^[d] Absolute configuration was assigned by comparison with reported data.

It is worth recalling at this point that one equivalent of an additive (camphorsulfonic acid, CSA, in the optimized case) is required. Thus, we envisaged using a polymer-supported equivalent of CSA in order to facilitate recovery once the hydrogenation reaction had finished. Examples of polymer-supported acids are numerous, as exchange resins with sulfonic acids as functional groups are commercially available (*e.g.* AmberlystTM, AmberliteTM or DowexTM type resins). We performed catalytic studies on model substrate **238a** using one equivalent of various acidic resins³⁷¹ as additives under the standard hydrogenation screening conditions (80 bar H₂, THF, rt). We decided to extend the reaction time to ensure the correct diffusion of the reagents through the mesoporous structure of the resins. These results are summarized in Table 42.

Table 42. Acid cation exchange resins as additives in the hydrogenation of model indole **238a**.^[a]

Entry	Acid cation exchange resin	Conv. [%] ^[b]	ee [%] ^[c] (config.) ^[d]
1	Amberlyst 15 Dry	23	90 (<i>S</i>)
2	Amberlite IRN77	3	n. d.
3	DOWEX 50WX8	37	90 (<i>S</i>)

^[a] Reaction conditions: *In situ* formed precatalyst, [$\text{Ir}(\mu\text{-Cl})(\text{cod})_2$] / **134a** / acidic resin / substrate molar ratio = 0.5 : 1.1 : 100 : 100, 80 bar H₂, room temperature, 65 h, 0.2 M in THF.

^[b] Conversion determined by ¹H NMR after basic workup.

^[c] Enantiomeric excess determined by HPLC using chiral stationary phases after basic workup.

^[d] Absolute configuration was assigned by comparison with reported data.

³⁷¹ All the resins used were previously dried and titrated to determine the concentration of acidic groups (equiv./weight of resin).

From the tested resins, DOWEX 50WX8 gave the best results with 90% ee, although conversion was lower than that obtained for CSA (83% conv. with CSA in entry 10, Table 38; 37% conv. in entry 3, Table 42). In order to increase the conversion, we ran another series of experiments in different solvents at increased temperatures (Table 43).

Table 43. Hydrogenation of the model indole **238a** with DOWEX 50WX8 as additive.^[a]

Entry	Solvent	Reaction conditions	Conv. [%] ^[b]	ee [%] ^[c] (config.) ^[d]
1	THF	45 °C, 40 h	68	85 (<i>S</i>)
2	THF / DCM (10% vol)	45 °C, 40 h	72	86 (<i>S</i>)
3	MeTHF	45 °C, 40 h	66	87 (<i>S</i>)
4	MeTHF / DCM (10% vol)	45 °C, 40 h	72	87 (<i>S</i>)
5	MeTHF / DCM (10% vol)	45 °C, 48 h	87	87 (<i>S</i>)

^[a] Reaction conditions: *In situ* formed precatalyst, $[\{\text{Ir}(\mu\text{-Cl})(\text{cod})\}_2]$ / **134a** / DOWEX 50WX8 / substrate molar ratio = 0.5:1.1:100:100, 80 bar H₂, 45 °C, 0.2 M, unless otherwise indicated.

^[b] Conversion determined by ¹H NMR after basic workup.

^[c] Enantiomeric excess determined by HPLC using chiral stationary phases after basic workup.

^[d] Absolute configuration was assigned by comparison with reported data.

An increase in the reaction temperature to 45 °C led to a decrease in the enantioselectivity from 90% to 85% ee (compare entry 3 in Table 42 with entry 1 in Table 43), although conversion increased drastically from 37% to 68%. The use of MeTHF as solvent gave slightly better enantioselectivity (compare entries 1 and 3 in Table 43), and a mixture of MeTHF / DCM (10% vol) finally allowed the conversion to increase to comparable values with those observed in the case of CSA as additive (see entry 5 in Table 43).

With the optimized reaction conditions for the use of the supported additive DOWEX 50WX8 known, we studied the asymmetric hydrogenation of the already studied array of differently substituted indoles using supported sulphonic acid as additives (Table 41). The results of these studies with DOWEX 50WX8 have been summarized in Table 44.

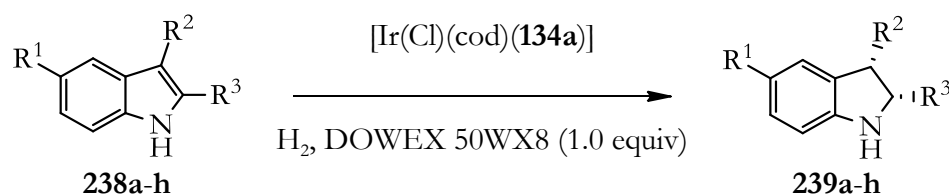


Table 44. Asymmetric hydrogenation of indoles **238** with DOWEX 50WX8 as additive.^[a]

Entry	Substrate	Substituents	Conv. [%] ^[b]	ee [%] ^[c] (config.) ^[d]
1	238a	R ¹ = H; R ² = H; R ³ = Me	87	87 (S)
2	238b	R ¹ = H; R ² = H; R ³ = <i>n</i> -Bu	84	88 (S)
3	238c	R ¹ = H; R ² = H; R ³ = Bn	83	84 (S)
4	238d	R ¹ = F; R ² = H; R ³ = Me	69	85 (S)
5	238e	R ¹ = Me; R ² = H; R ³ = Me	80	86 (S)
6	238f	R ¹ = H; R ² , R ³ = -(CH ₂) ₄ -	26	89 (S)
7	238g	R ¹ = H; R ² = H; R ³ = COOH	0	n. d.
8	238h	R ¹ = H; R ² = H; R ³ = Ph	0	n. d.

^[a] Reaction conditions: *In situ* formed precatalyst, [$\{\text{Ir}(\mu\text{-Cl})(\text{cod})\}_2$]/ **134a** / DOWEX 50WX8 / substrate molar ratio = 0.5:1.1:100:100, 80 bar H₂, 45 °C, 48 h, 0.2 M in MeTHF/DCM (10% vol).

^[b] Conversion determined by ¹H NMR after basic workup.

^[c] Enantiomeric excess determined by HPLC using chiral stationary phases after basic workup.

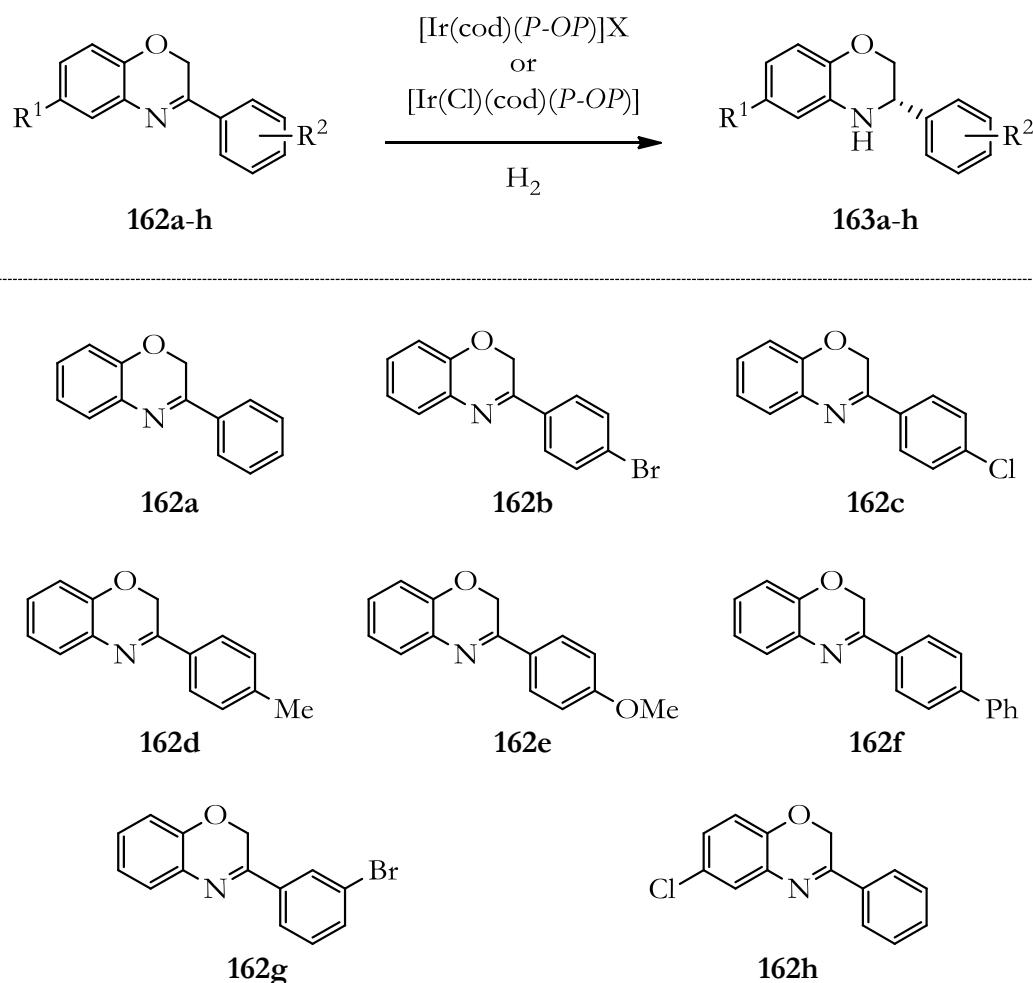
^[d] Absolute configuration was assigned by comparison with reported data.

The enantioselectivities remained high regardless of the steric or electronic nature of the substituents at the R¹ and R³ position (84-89% ee, see entries 1-6 in Table 44). In contrast, conversion was adversely affected by electron-withdrawing groups in the indole backbone (**238d**, R¹ = F, 69% conv., entry 4 in Table 44), which was also observed for this substrate under homogeneous hydrogenation conditions (entry 5 in Table 41). Asymmetric hydrogenation of the sterically congested carbazole **238f** took place also with low conversion (26%, entry 6 in Table 44). The catalytic system was not able to hydrogenate indoles **238g** and **238h**, bearing a phenyl or a carboxylic acid group, respectively, at the R³ position (see entries 7 and 8 in Table 44).

2.2.2.4 HYDROGENATION OF BENZOXAZINES

The reduction of 2*H*-benzo[*b*][1,4]oxazines has been successfully achieved by organocatalytic methods,²⁵⁵ and by relay-catalyzed organocatalytic reduction,²⁵⁷ but only limited success has been reported in the case of the standard asymmetric hydrogenation of the benzoxazines **162**.²⁵³ For this reason we synthesized a range of differently substituted 2-aryl-2*H*-benzo[*b*][1,4]oxazines and tested their enantioselective hydrogenation with our [Ir(*P-OP*)]⁺ catalysts (Scheme 66). 2-Aryl-2*H*-benzo[*b*][1,4]oxazines were easily synthesized by condensation of the appropriate 2-aminophenol and 2-bromoacetophenone derivatives in a basic biphasic medium (K₂CO₃ in a DCM/H₂O mixture) under phase transfer catalyst.³⁷²

³⁷² Similar procedure to the one reported in: Jubinsky, P. T.; Short, M. K.; Ghanem, M.; Das, B. C. *Bioorg. Med. Chem. Lett.* **2011**, *21*, 3479.



Scheme 66. Iridium-mediated asymmetric hydrogenation of benzoxazines **162** catalyzed by $[\text{Ir}(\text{P-OP})]^+$ complexes.

Benzoxazine **162a** was selected as the model substrate for the optimization of the reaction conditions. Initial catalyst screening studies were conducted aimed at identifying the optimal phosphine-phosphite ligand to be used in this transformation, as well as to find out the adequate nature of the iridium complex (*i.e.* neutral or cationic complexes). On the other hand, we were also interested in studying the effect of additives in the outcome of the reaction. The results of these initial catalytic studies have been summarized in Table 45.

Table 45. Asymmetric hydrogenation of benzoxazine **162a** mediated by iridium complexes of *P-OP* ligands.^[a]

Entry	Precatalyst	Additive	Conv. [%] ^[b]	ee [%] ^[c] (config.) ^[d]
1	[Ir(Cl)(cod)(30a)]	-	>99	67 (R)
2	[Ir(Cl)(cod)(134a)]	-	>99	94 (S)
3	[Ir(cod)(134a)]BF ₄ ^[e]	-	>99	6 (S)
4	[Ir(cod)(134a)]BArF ^[e]	-	>99	2 (S)
5	[Ir(Cl)(cod)(134a)]	HCl	>99	90 (S)
6	[Ir(Cl)(cod)(134a)]	HCl ^[f]	99	78 (S)
7	[Ir(Cl)(cod)(134a)]	(S)-BNP	>99	93 (S)
8	[Ir(Cl)(cod)(134a)]	(R)-BNP	>99	94 (S)
9	[Ir(Cl)(cod)(134a)]	CSA	>99	89 (S)

^[a] Reaction conditions: *In situ* formed precatalyst, [$\{\text{Ir}(\mu\text{-Cl})(\text{cod})\}_2$]/ *P-OP* ligand / additive / substrate molar ratio = 0.5:1.1:10:100, 80 bar H₂, room temperature, 20 h, 0.2 M in THF, unless otherwise indicated.

^[b] Conversion determined by ¹H NMR.

^[c] Enantiomeric excess determined by HPLC using chiral stationary phases.

^[d] Absolute configuration was assigned by comparison with reported data.

^[e] Preformed precatalyst.

^[f] 1 equiv. of acid.

Iridium complexes derived from ligand **134a** mediated the hydrogenation of benzoxazine **162a** with complete conversion and 94% ee (entry 2 in Table 45). In contrast, the catalytic system derived from ligand **30a** mediated the formation of opposite enantiomer of compound **163a** with lower enantioselectivity (compare entries 1 and 2 in Table 45), thus indicating that the direction of stereodiscrimination is predominantly controlled by the phosphite group. On the other hand, cationic complexes led to complete

conversion, but with practically no enantioselectivity (compare entries 1 and 2 with 3 and 4 respectively in Table 45).

The use of an array of achiral and chiral additives in this transformation did not bring any benefit: whilst additives did not affect conversion, their use slightly reduced the enantioselectivity of the transformation (compare entry 2 with 5-9 in Table 45).

Table 46. Pressure and catalyst loading effects in the asymmetric hydrogenation of benzoxazine **162a** mediated by the iridium complex derived from **134a**.^[a]

Entry	Reaction conditions	Conv. [%] ^[b]	ee [%] ^[c] (config.) ^[d]
1	40 bar H ₂ , 1.0 mol % cat. loading	>99	95 (<i>S</i>)
2	40 bar H ₂ , 0.5 mol % cat. loading	>99	95 (<i>S</i>)
3	40 bar H ₂ , 0.2 mol % cat. loading	>99	92 (<i>S</i>)
4	40 bar H ₂ , 0.1 mol % cat. loading	>99	88 (<i>S</i>)

^[a] Reaction conditions: *In situ* formed precatalyst, [$\{\text{Ir}(\mu\text{-Cl})(\text{cod})\}_2$]/ *P-OP* ligand = 0.5:1.1, 40 bar H₂, room temperature, 20 h, 0.2 M in THF, unless otherwise indicated.

^[b] Conversion determined by ¹H NMR.

^[c] Enantiomeric excess determined by HPLC using chiral stationary phases.

^[d] Absolute configuration was assigned by comparison with reported data.

Due to the excellent results obtained under standard screening conditions (1 mol % of catalyst, 80 bar H₂, room temperature, 20 h, 0.2 M in THF), we investigated whether the amount of catalyst and pressure could be reduced (Table 46). Conversion remained unaltered at 40 bar of H₂ and the substrate to catalyst ratio could be increased up to 1,000:1. Enantioselectivities remained excellent, although for substrate to catalyst ratios higher than 500:1, enantioselectivity decreased (compare entries 1-3 with entry 4 in Table 46).

In order to test the solvent dependence of this catalytic system, we ran a set of hydrogenations under the previously determined conditions (40 bar H₂, 0.5 mol % catalyst) in several solvents (Table 47)

Full conversion was achieved in all cases regardless of the solvent used, but some differences were observed in enantioselectivity. Ee values remained high with most of the solvents (>90%, see entries 1-3, 6, 7 and 9 in Table 47), but the use of chlorinated (DCM) and protic solvents (IPA or 2M2B) decreased the enantioselectivity (see entries 4, 5 and 8 in Table 47). THF remained as the solvent of choice, affording an excellent value of 95% ee (entry 1 in Table 47) in the reduction of **162a**.

Table 47. Effect of the solvent in the asymmetric hydrogenation of model benzoxazine **162a** using the iridium complex derived from ligand **134a**.^[a]

Entry	Solvent	Conv. [%] ^[b]	ee [%] ^[c] (config.) ^[d]
1	THF	>99	95 (S)
2	MeTHF	>99	93 (S)
3	Toluene	>99	90 (S)
4	IPA	>99	64 (S)
5	DCM	>99	86 (S)
6	EtOAc	>99	91 (S)
7	DMC	>99	90 (S)
8	2M2B	>99	62 (S)
9	DME	>99	92 (S)

^[a] Reaction conditions: *In situ* formed precatalyst, [$\text{Ir}(\mu\text{-Cl})(\text{cod})_2$] / **134a** / substrate molar ratio = 0.25 : 0.55 : 100, 40 bar H₂, room temperature, 20 h, 0.2 M in the stated solvent.

^[b] Conversion determined by ¹H NMR.

^[c] Enantiomeric excess determined by HPLC using chiral stationary phases.

^[d] Absolute configuration was assigned by comparison with reported data.

Once the optimal hydrogenation conditions for **162a** had been established, the hydrogenation of the remaining benzoxazines **162b-h** was studied. These results are summarized in Table 48. The catalyst efficiently mediated the asymmetric hydrogenation of the substrates **162b-h**, with high conversions and enantioselectivities (91% to 95% ee). Enantioselectivities were high and ranged from 91% to 95% ee (see Table 48) regardless of the position and the electronic nature of the substituents at the phenyl R² substituent, or replacing the R¹ group with chlorine.

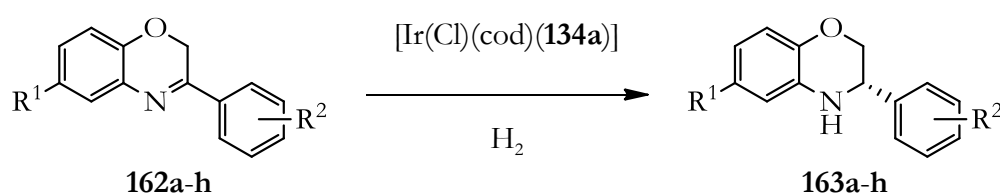


Table 48. Asymmetric hydrogenation of an array of benzoxazines **162**.^[a]

Entry	Substrate	Substituents	Conv. [%] ^[b]	ee [%] ^[c] (config.) ^[d]
1	162a	R ¹ = H; R ² = H	>99	95 (S)
2	162b	R ¹ = H; R ² = <i>p</i> -Br	>99	92 (S)
3	162c	R ¹ = H; R ² = <i>p</i> -Cl	>99	91 (S) ^[f]
4	162d	R ¹ = H; R ² = <i>p</i> -Me	>99	91 (S)
5	162e	R ¹ = H; R ² = <i>p</i> -MeO	>99	91 (S)
6	162f ^[e]	R ¹ = H; R ² = <i>p</i> -Ph	>99	93 (S)
7	162g	R ¹ = H; R ² = <i>m</i> -Br	>99	91 (S)
8	162h	R ¹ = Cl; R ² = H	>99	91 (S) ^[f]

^[a] Reaction conditions: *In situ* formed precatalyst, [$\{\text{Ir}(\mu\text{-Cl})(\text{cod})\}_2$] / **134a** / substrate molar ratio = 0.25 : 0.55 : 100, 40 bar H₂, room temperature, 20 h, 0.2 M in THF.

^[b] Conversion determined by ¹H NMR. Typical isolated yields after column chromatography were >95%.

^[c] Enantiomeric excess determined by HPLC using chiral stationary phases.

^[d] Absolute configuration was assigned by comparison with reported data.

^[e] 80 bar of H₂ were used instead.

^[f] Absolute configuration was assigned on the basis of an X-Ray structure determination.

The absolute configurations of **163h** and **163c** were determined unambiguously by anomalous dispersion effects (Flack parameters = -0.06(4) and -0.04(2), respectively)³⁷³ and were found to be the (*S*)-configured hydrogenation products (Figure 70). This observation is consistent with the sense of stereoreduction observed for the rest of hydrogenated products **163a,b,d-g**, which were assigned by comparison with reported data (for specific rotation values and elution orders in chromatography on chiral stationary phases, see experimental part for details).

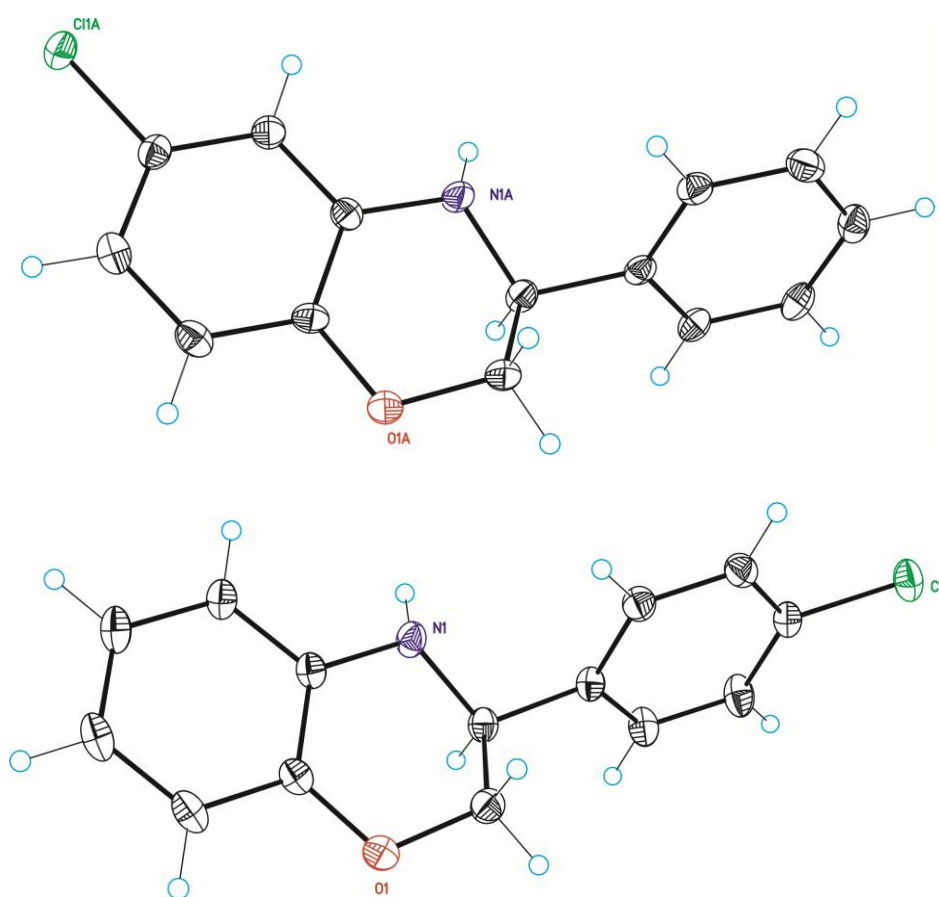
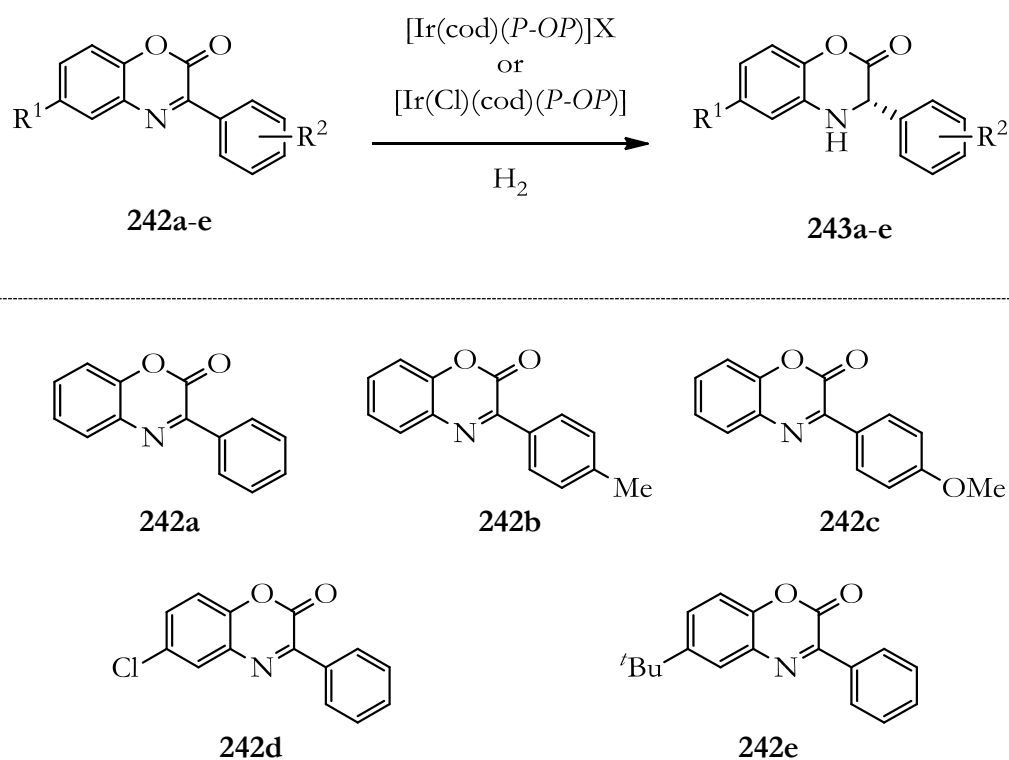


Figure 70. ORTEP view of hydrogenation products **163h** (up) and **163c** (down), showing an *S* absolute configuration of the stereogenic carbon created during hydrogenation.

³⁷³ Flack H. D., *Acta Cryst., Sect. A* **1983**, 876.

2.2.2.5 HYDROGENATION OF BENZOXAZINONES

Once the hydrogenation of 2*H*-benzo[*b*][1,4]oxazines (**162**) was studied, we became interested in the hydrogenation of their structural analogs 2*H*-benzo[*b*][1,4]oxazin-2-ones (**242**). Furthermore, despite a few reports on Brønsted acid catalyzed transfer hydrogenation^{255a} and relay-catalyzed organocatalytic reduction²⁵⁸ of this substrate class that had been published, to the best of this author's knowledge there are no reports of metal-mediated asymmetric hydrogenation of 2*H*-benzo[*b*][1,4]oxazin-2-ones.



Scheme 67. Iridium-mediated asymmetric hydrogenation of benzoxazinones **242** catalyzed by $[\text{Ir}(\text{P-OP})]^+$ complexes.

The required starting materials were straightforwardly synthesized by condensation of aminophenols and α -keto esters.³⁷⁴ Initial hydrogenation

³⁷⁴ Xue, Z.-Y.; Jiang, Y.; Peng, X.-Z.; Yuan, W.-C.; Zhang, X.-M. *Adv. Synth. Catal.* **2010**, *352*, 2132.

studies on these substrates aimed at identifying the optimal chiral iridium catalyst and studying the effect of additives. Benzoxazinone **242a** was chosen as the model substrate for the optimization of the reaction conditions. The results from these initial screening experiments have been collected and summarized in Table 49.

Table 49. Asymmetric hydrogenation of benzoxazinone **242a** mediated by iridium complexes of *P-OP* ligands.^[a]

Entry	Precatalyst	Additive	Conv. [%] ^[b]	ee [%] ^[c] (config.) ^[d]
1	[Ir(Cl)(cod)(30a)]	-	94	78 (<i>R</i>)
2	[Ir(Cl)(cod)(134a)]	-	71	96 (<i>S</i>)
3	[Ir(cod)(134a)]BF ₄ ^[e]	-	4	34 (<i>S</i>)
4	[Ir(cod)(134a)]BArF ^[e]	-	54	51 (<i>S</i>)
5	[Ir(Cl)(cod)(134a)]	HCl	>99	93 (<i>S</i>)
6	[Ir(Cl)(cod)(134a)]	HCl ^[f]	97	91 (<i>S</i>)
7	[Ir(Cl)(cod)(134a)]	(<i>S</i>)-BNP	96	95 (<i>S</i>)
8	[Ir(Cl)(cod)(134a)]	(<i>R</i>)-BNP	81	94 (<i>S</i>)
9	[Ir(Cl)(cod)(134a)]	CSA	>99	94 (<i>S</i>)

^[a] Reaction conditions: *In situ* formed precatalyst, [$\{\text{Ir}(\mu\text{-Cl})(\text{cod})\}_2$] / *P-OP* ligand / additive / substrate molar ratio = 0.5 : 1.1 : 10 : 100, 80 bar H₂, room temperature, 20 h, 0.2 M in THF.

^[b] Conversion determined by ¹H NMR.

^[c] Enantiomeric excess determined by HPLC using chiral stationary phases.

^[d] Absolute configuration was assigned by comparison with reported data.

^[e] Preformed.

^[f] 1 equiv. of acid.

Although none of the tested precatalysts led to complete conversion in the hydrogenation of **242a**, neutral iridium complexes derived from ligand

134a exhibited excellent enantioselectivity (compare entries 1 and 2 in Table 49 which exemplify the catalytic behavior of the two neutral iridium complexes incorporating the (*S*)- and (*R*)-BINOL fragment in the phosphite group). On the other hand, cationic complexes led to much lower conversion values and from low to moderate enantioselectivities (compare entry 2 with entries 3 and 4 in Table 49). The addition of catalytic amounts of additives (10 mol % with respect to substrate) in the hydrogenation of **242a** provided higher conversion at the expense of a slight reduction in enantioselectivity (compare entry 2 with entries 5-9 in Table 49). The additive that better fulfilled the requirements of atom economy and simplicity was HCl (entry 5 in Table 49).

The optimal hydrogenation pressure and catalyst amounts in the hydrogenation of substrate **242a** were also investigated. These experiments are shown in Table 50.

Table 50. Effects of pressure and catalyst amounts in the asymmetric hydrogenation of benzoxazinone **242a** mediated by iridium complex derived from **134a**.^[a]

Entry	Additive (10 mol %)	Reaction conditions	Conv. [%] ^[b]	ee [%] ^[c] (config.) ^[d]
1	-	80 bar H ₂ , 1.0 mol % cat. loading	71	96 (<i>S</i>)
2	HCl	80 bar H ₂ , 1.0 mol % cat. loading	>99	93 (<i>S</i>)
3	-	80 bar H ₂ , 2.0 mol % cat. loading	>99	95 (<i>S</i>)
4	-	40 bar H ₂ , 1.0 mol % cat. loading	65	96 (<i>S</i>)
5	HCl	40 bar H ₂ , 1.0 mol % cat. loading	>99	88 (<i>S</i>)

^[a] Reaction conditions: *In situ* formed precatalyst, [$\{\text{Ir}(\mu\text{-Cl})(\text{cod})\}_2$] / **134a** = 0.5 : 1.1, additive / substrate molar ratio = 10 : 100, room temperature, 20 h, 0.2 M in THF, unless otherwise indicated.

^[b] Conversion determined by ¹H NMR.

^[c] Enantiomeric excess determined by HPLC using chiral stationary phases.

^[d] Absolute configuration was assigned by comparison with reported data.

Whereas benzoxazinone **242a** was hydrogenated with lower conversion under reduced pressure (40 instead of 80 bar H₂, compare entries 1 and 4 in Table 50), the addition of 10 mol % of HCl led to complete conversion, although enantioselectivity was severely affected (see entries 4 and 5 in Table 50). To address these issues, the use of a catalyst loading of 2.0 mol % enabled the complete hydrogenation of **242a** with maximum enantioselectivity without the necessity of using HCl as additive (compare entries 2 and 3 in Table 50).

The high dependence of the outcome of hydrogenation reactions of related substrates with the solvent prompted us to perform a study in order to determine the optimal solvent for the hydrogenation of **242a**. The results were summarized in Table 50.

Table 51. Solvent effects in the asymmetric hydrogenation of model benzoxazinone **242a** using the iridium complex derived from ligand **134a**.^[a]

Entry	Solvent	Conv. [%] ^[b]	ee [%] ^[c] (config.) ^[d]
1	THF	>99	93 (<i>S</i>)
2	MeTHF	>99	93 (<i>S</i>)
3	Toluene	>99	85 (<i>S</i>)
4	IPA	- ^[d]	-
5	DCM	>99	82 (<i>S</i>)
6	EtOAc	>99	83 (<i>S</i>)
7	DCM	>99	81 (<i>S</i>)
8	DME	>99	84 (<i>S</i>)

^[a] Reaction conditions: *In situ* formed precatalyst, $[\{\text{Ir}(\mu\text{-Cl})(\text{cod})\}_2] / \mathbf{134a} / \text{HCl} / \text{substrate}$ molar ratio = 0.5 : 1.1 : 10 : 100, 80 bar H₂, room temperature, 20 h, 0.2 M in the stated solvent, unless otherwise indicated.

^[b] Conversion determined by ¹H NMR.

^[c] Enantiomeric excess determined by HPLC using chiral stationary phases.

^[d] Decomposition products.

All of the tested solvents led to complete conversion. In the case of IPA, a mixture of decomposition products was found. Both THF and MeTHF afforded the highest enantioselectivity (93%, see entries 1 and 2 in Table 51), while the rest of the tested solvents led to lower enantioselectivities, (81-85% ee, see entries 3 and 5-8 in Table 51).

Once the catalytic system had been optimized, the hydrogenation of an array of diversely substituted benzoxazinones **242b-e** was studied using two alternative reaction conditions: 1.0 mol % catalyst amount and 10 mol % of HCl as additive or higher catalyst amounts (2.0 mol %) without additive. The complete set of results are summarized in Table 52.

Although the hydrogenation of the model substrate **242a** proceeded with full conversion under the optimized reaction conditions, only partial hydrogenation of the remaining benzoxazinones **242b-e** was observed. In almost all cases, enantioselectivities achieved with 2.0 mol % of catalyst in the absence of additive were higher than those achieved with 1.0 mol % of catalyst and HCl as additive. The enantioselectivities obtained with all of the studied compounds were very high (from 89% to 99% ee for the products **243b-e** with 2.0 mol % catalyst loading).

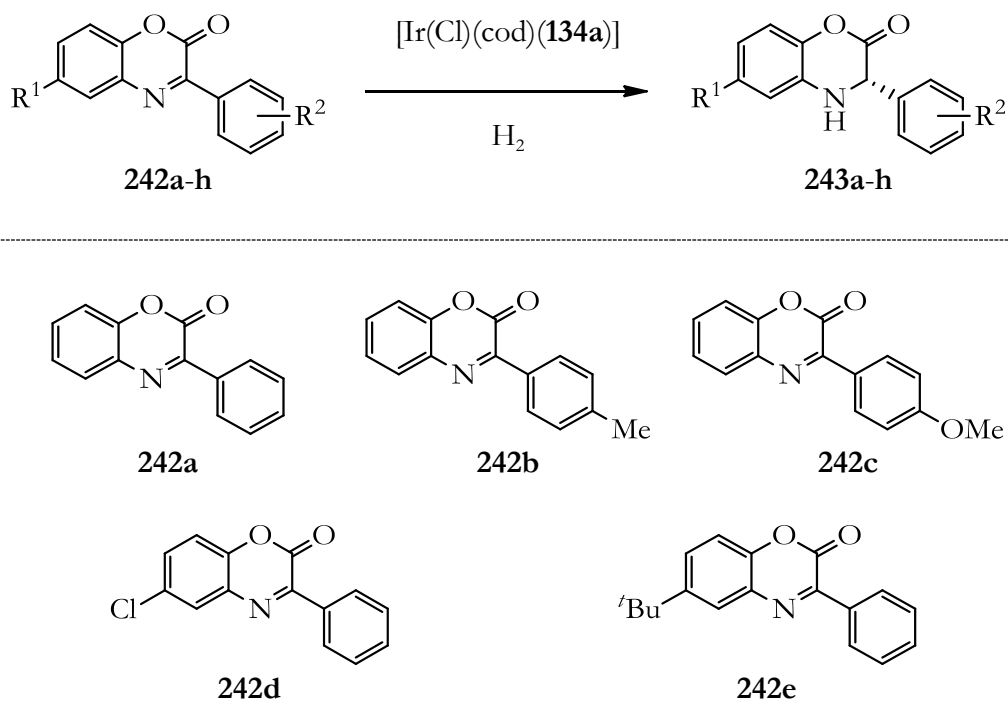


Table 52. Asymmetric hydrogenation of benzoxazinones **242a-e**.^[a]

Entry	Substrate	1.0 mol % cat., HCl		2.0 mol % cat.	
		Conv. [%] ^[b]	ee [%] ^[c] (config.) ^[d]	Conv. [%] ^[b]	ee [%] ^[c] (config.) ^[d]
1	242a	>99	93 (<i>S</i>)	>99	95 (<i>S</i>)
2	242b	85	94 (<i>S</i>)	>99	97 (<i>S</i>)
3	242c	86	96 (<i>S</i>)	51 ^[e]	99 (<i>S</i>)
4	242d	81	91 (<i>S</i>)	62 ^[e]	89 (<i>S</i>)
5	242e	57	91 (<i>S</i>)	49 ^[e]	94 (<i>S</i>)

^[a] Reaction conditions: *In situ* formed precatalyst, $[\{\text{Ir}(\mu\text{-Cl})(\text{cod})\}_2] / \mathbf{134a} = 0.5 : 1.1$, additive (if required) / substrate molar ratio = 10 : 100, 80 bar H_2 , room temperature, 20 h, 0.2 M in THF.

^[b] Conversion determined by ^1H NMR.

^[c] Enantiomeric excess determined by HPLC using chiral stationary phases.

^[d] Absolute configuration was assigned by comparison with reported data.

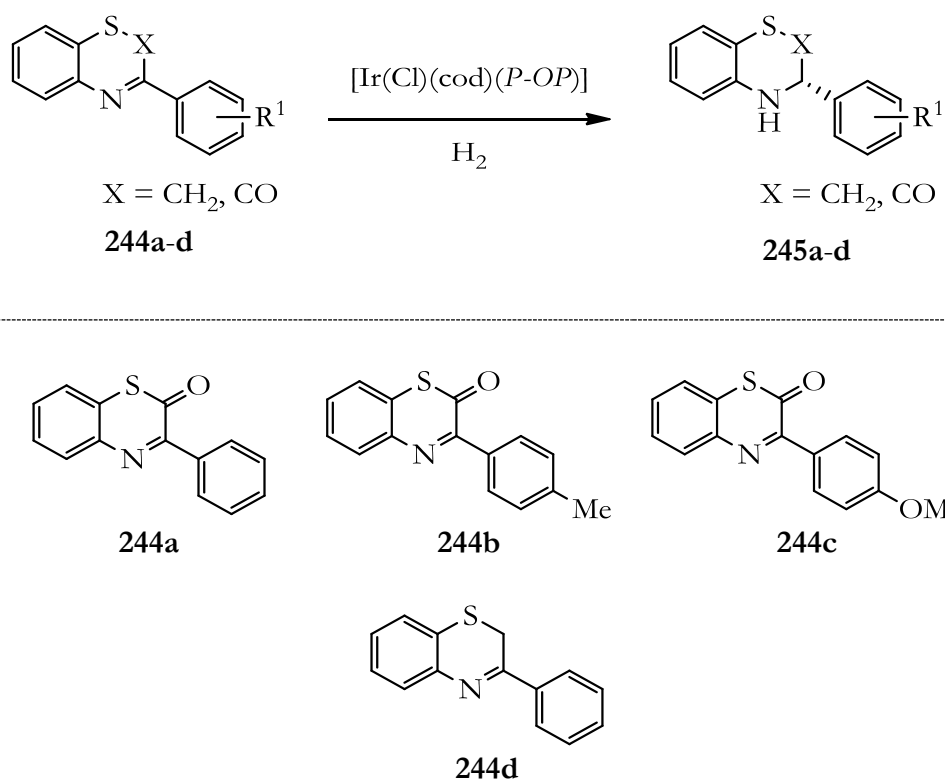
^[e] Isolated yields: **243c**, 45%; **243d**, 54% and **243e**, 42%.

2.2.2.6 HYDROGENATION OF BENZOTHIAZINONES

Metal-catalyzed hydrogenation of sulfur-containing substrates is a challenging process since sulfur compounds are known poisoning agents of metal catalysts, irreversibly binding to them and thus deactivating the catalyst.^{260b,c, 313} Within our exploration of heterocyclic substrates, we considered that the structural thio-analogs of benzoxazines **162** and benzoxazinones **242** were interesting substrates to be asymmetrically hydrogenated with the catalytic systems derived from our *P-OP* ligands. As showed in section 2.1.2, these heterocycles have a diversity of applications, and chiral structures derived from them are highly interesting. Additionally, to the best of the author's knowledge, there were no reports on the asymmetric hydrogenation of these sulfur-containing heterocycles.

Synthetic protocols for preparing substrates **244a-d** were straightforward and involved condensation of aminothiophenols with α -keto esters followed by oxidation to benzothiazinones.³⁷⁵ Hydrogenation studies were performed using the highest performing iridium complex in analogous heterocyclic systems ($[\text{Ir}(\text{Cl})(\text{cod})(\mathbf{134a})]$) aimed at identifying the optimal hydrogenation conditions. Benzothiazinone **244a** and benzothiazine **244d** were chosen as the model substrates for these studies. The results are summarized in Table 53.

³⁷⁵ Sabatini, S.; Kaatz, G. W.; Rossolini, G. M.; Brandini, D.; Fravolini, A. *J. Med. Chem.* **2008**, *51*, 4321.



Scheme 68. Iridium-mediated asymmetric hydrogenation of benzothiazinones **244a-c** and benzothiazine **244d** catalyzed by [Ir(*P-OP*)]⁺ complexes.

The hydrogenation of benzothiazine **244d** required higher H₂ pressures and catalyst loadings to achieve full conversion than those required for its oxo-substituted counterpart. Moderate enantioselectivities were observed and the use of HCl as additive led to even lower enantioselectivities (compare entries 2 and 3 in Table 53). Hydrogenation of benzothiazinone **244a** in the presence of HCl led to full conversion without a detrimental effect on the enantioselectivity (compare entries 4 and 5 in Table 53). As an alternative to the use of HCl as additive, an increase in the amount of catalyst up to 2 mol % provided the same degrees of conversion and enantioselectivity (compare entries 5 and 6 in Table 53).

Table 53. Optimization experiments in the asymmetric hydrogenation of benzothiazinone **244a** and benzothiazine **244d** mediated by iridium complex derived from **134a**.^[a]

Entry	Substrate	Additive (10 mol %)	Reaction conditions	Conv. [%] ^[b]	ee [%] ^[c] (config.) ^[d]
1	244d	-	40 bar H ₂ , 0.5 mol % cat. loading	70	72 (<i>S</i>)
2	244d	-	80 bar H ₂ , 1.0 mol % cat. loading	>99	70 (<i>S</i>)
3	244d	HCl	80 bar H ₂ , 1.0 mol % cat. loading	>99	62 (<i>S</i>)
4	244a	-	80 bar H ₂ , 1.0 mol % cat. loading	77	94 (<i>S</i>)
5	244a	HCl	80 bar H ₂ , 1.0 mol % cat. loading	>99	94 (<i>S</i>)
6	244a	-	80 bar H ₂ , 2.0 mol % cat. loading	>99	94 (<i>S</i>)

^[a] Reaction conditions: *In situ* formed precatalyst, [$\text{Ir}(\mu\text{-Cl})(\text{cod})_2$] / **134a** = 0.5 : 1.1, additive / substrate molar ratio = 10 : 100 if required, room temperature, 20 h, 0.2 M in THF, unless otherwise indicated.

^[b] Conversion determined by ¹H NMR.

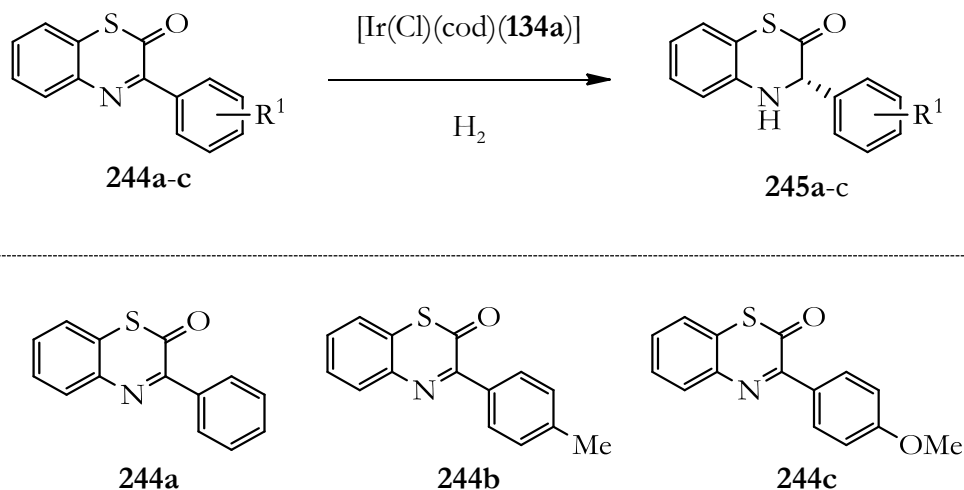
^[c] Enantiomeric excess determined by HPLC using chiral stationary phases.

^[d] Absolute configuration was tentatively assigned by analogy based on the stereochemical outcome for analogous substrates.

With the optimized hydrogenation conditions for these known thioderivatives, we further studied the asymmetric hydrogenation of the benzothiazinones **244a-c**. The results are summarized in Table 54.

Benzothiazinones **244a-c** were efficiently hydrogenated with full conversion using two different reaction conditions: 1.0 mol % catalyst and 10 mol % HCl or 2.0 mol % catalyst with no additive. Gratifyingly, substrates **244b-c** were both hydrogenated with very high enantioselectivity regardless of

the substituents at R¹. Higher degrees of enantioselectivity were observed in the absence of additive (up to 96% ee; see entries 2 and 3 in Table 54).



Scheme 69. Iridium-mediated asymmetric hydrogenation of benzothiazinones **244a-c** catalyzed by $[\text{Ir}(P\text{-}OP)]^+$ complexes.

Table 54. Asymmetric hydrogenation of benzothiazinones **244a-c**.^[a]

Entry	Substrate	1.0 mol % cat, HCl		2.0 mol % cat	
		Conv. [%] ^[b]	ee [%] ^[c] (config.) ^[d]	Conv. [%] ^[b]	ee [%] ^[c] (config.) ^[d]
1	244a	>99	94 (<i>S</i>)	>99	94 (<i>S</i>)
2	244b	>99	91 (<i>S</i>)	>99	95 (<i>S</i>)
3	244c	>99	92 (<i>S</i>)	>99	96 (<i>S</i>)

^[a] Reaction conditions: *In situ* formed precatalyst, $[\{\text{Ir}(\mu\text{-Cl})(\text{cod})\}_2] / \mathbf{134a} = 0.5 : 1.1$, additive (if required) / substrate molar ratio = 10 : 100, 80 bar H₂, room temperature, 20 h, 0.2 M in THF, unless otherwise indicated.

^[b] Conversion determined by ¹H NMR. Typical isolated yields after column chromatography were >95%.

^[c] Enantiomeric excess determined by HPLC using chiral stationary phases.

^[d] Absolute configuration was tentatively assigned by analogy based on the stereochemical outcome for analogous substrates.

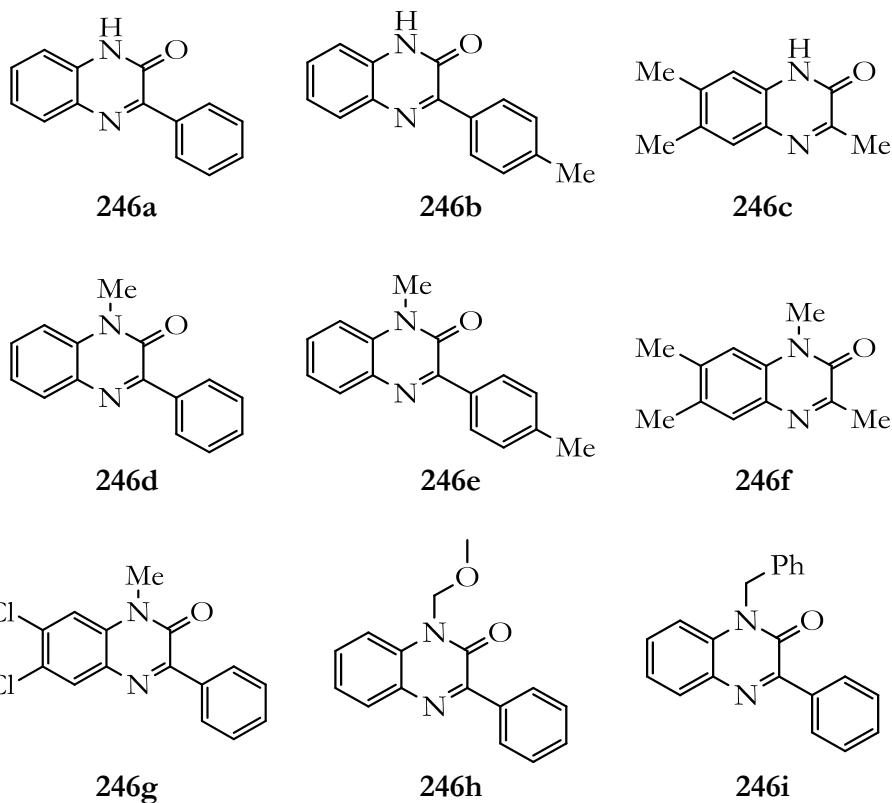
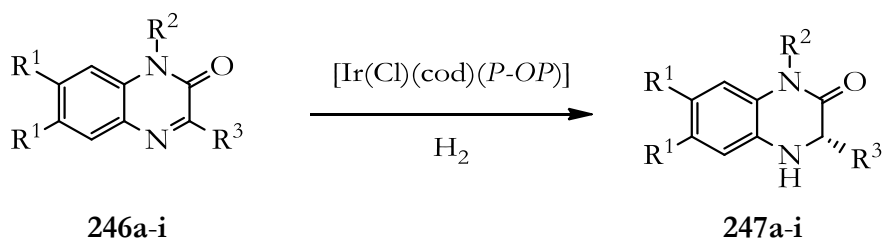
2.2.2.7 HYDROGENATION OF QUINOXALINONES

Quinoxalinones and their enantiomerically pure reduced analogs are found in many biologically active molecules and other key synthetic intermediates. Especially relevant compounds for the pharmacological industry, some of which are accessible by enantioselective reduction of their corresponding quinoxalinones, were presented in section 2.1.2.

Despite the great importance of this class of compound, very few examples of asymmetric reductions of quinoxalinones were found in the literature. To date, only two articles have appeared dealing with the asymmetric reduction of quinoxalinones. Rueping *et al.*²⁵⁶ reported the asymmetric transfer hydrogenation of a series of unprotected quinoxalinones, whereas Zhang *et al.*³⁷⁴ reported the hydrosilylation of a set of alkylated quinoxalinones. A general and direct asymmetric hydrogenation method of these compounds would be highly desirable and we became interested in studying this chemistry on an array of diversely substituted *N*-unprotected and *N*-alkylated quinoxalinones using the iridium complexes derived from our phosphine-phosphites ligands as catalysts.

Efficient synthetic protocols for the preparation of quinoxalinones **246** were known and involved condensation of dianilines with α -keto esters to obtain unprotected quinoxalinones,³⁷⁶ followed by *N*-alkylation if required.³⁷⁴

³⁷⁶ Murthy, S. N.; Madhav, B.; Nageswar, Y. V. D. *Helv. Chim. Acta* **2010**, *93*, 1216.



Scheme 70. Iridium-mediated asymmetric hydrogenation of quinoxalinones **246** catalyzed by $[\text{Ir}(\text{P-OP})]^+$ complexes.

Initial studies were conducted aimed at developing the optimal hydrogenation conditions for these substrates and *N*-unprotected quinoxalinone **246a** and *N*-alkylated quinoxalinone **246d** were chosen as the model substrates. These results are summarized in Table 55.

Table 55. Asymmetric hydrogenation of quinoxalinones **246a** and **246d** mediated by iridium complexes of *P-OP* ligands.^[a]

Entry	Substrate	Precatalyst	Conv. [%] ^[b]	ee [%] ^[c] (config.) ^[d]
1	246a	[Ir(Cl)(cod)(30a)]	98	99 (<i>R</i>)
2	246a	[Ir(Cl)(cod)(134a)]	95	99 (<i>S</i>)
3	246d	[Ir(Cl)(cod)(30a)]	97	99 (<i>R</i>) ^[e]
4	246d	[Ir(Cl)(cod)(134a)]	96	99 (<i>S</i>) ^[e]

^[a] Reaction conditions: *In situ* formed precatalyst, [$\{\text{Ir}(\mu\text{-Cl})(\text{cod})\}_2$] / *P-OP* ligand / substrate molar ratio = 0.5 : 1.1 : 100, 80 bar H₂, room temperature, 20 h, 0.2 M in THF.

^[b] Conversion determined by ¹H NMR.

^[c] Enantiomeric excess determined by HPLC using chiral stationary phases.

^[d] Absolute configuration was assigned by comparison with reported data.

^[e] Absolute configuration was tentatively assigned by analogy based on the stereochemical outcome for analogous substrates.

Almost complete conversion was found in all the cases tested, and although both ligands led to excellent enantioselectivities (99% ee) but with opposed senses of stereodiscrimination in the hydrogenation of the two model substrates **246a** and **246d** (compare entries 1 and 2, and 3 and 4 in Table 55), we chose ligand **134a** for subsequent optimization experiments. With these excellent results in hand, we then explored hydrogenation reactions using lower catalyst loadings at reduced pressures (40 bar of H₂) to determine the efficiency of our catalyst. These experiments were collected in Table 56.

Quinoxalinones **246a** and **246d** were hydrogenated very efficiently at lower pressures and substrate to catalyst ratios as high as 1,000:1 with no loss in enantioselectivity (see Table 56).

Table 56. Determination of the optimal catalyst loading in the asymmetric hydrogenation of quinoxalinones **246a** and **246d** mediated by the iridium complex of **134a**.^[a]

Entry	Substrate	Catalyst loading [%]	Conv. [%] ^[b]	ee [%] ^[c] (config.) ^[d]
1	246a	1.0	99	99 (<i>S</i>)
2	246a	0.1	98	99 (<i>S</i>)
3	246a	0.05	82	99 (<i>S</i>)
4	246d	1.0	98	99 (<i>S</i>) ^[e]
5	246d	0.05	96	99 (<i>S</i>) ^[e]

^[a] Reaction conditions: *In situ* formed precatalyst, [$\{\text{Ir}(\mu\text{-Cl})(\text{cod})\}_2$] / **134a** = 0.5 : 1.1, 40 bar H₂, room temperature, 20 h, 0.2 M in THF, unless otherwise indicated.

^[b] Conversion determined by ¹H NMR.

^[c] Enantiomeric excess determined by HPLC using chiral stationary phases.

^[d] Absolute configuration was assigned by comparison with reported data.

^[e] Absolute configuration was tentatively assigned by analogy based on the stereochemical outcome for analogous substrates.

As perfect enantioselectivities were achieved with THF as solvent, no studies aimed at identifying better alternatives were performed. The rest of quinoxalinones **246** were subjected to hydrogenation using a 0.5 mol % catalyst amount and no further optimization studies were performed. The complete set of experiments is shown in Table 57.

The quinoxalinones **246a-i** were all hydrogenated very efficiently, with conversions ranging from 89% to >99% and enantioselectivities from 90% to 99% ee (Table 57). Quinoxalinones with an alkyl substituent in the α -position to the imine nitrogen required slightly harsher conditions to achieve high conversions (see entries 3, 4 and 7 in Table 57), while higher enantioselectivities were consistently observed for the quinoxalinones with an aryl substituent at R² (see entries 1, 2, 5, 6, 8-10 in Table 57). Interestingly, the catalytic system tolerates diverse substitution patterns at the N1 position of the quinoxalinones: either no protection group (**246a**, entry 1 in Table 57) or a

wide variety of protecting groups, including the Me (**246d**, entry 5 in Table 57), MOM (**246h**, entry 9 in Table 57) and Bn (**246i**, entry 10 in Table 57) groups.

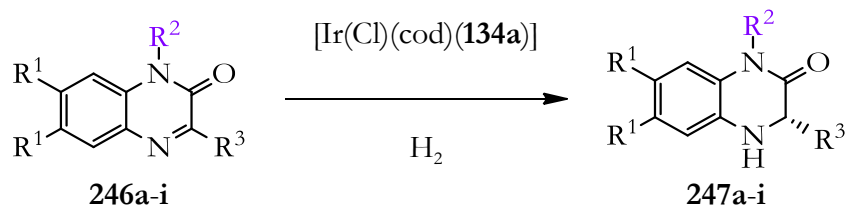


Table 57. Asymmetric hydrogenation of quinoxalinones **246** mediated by the iridium complex of **134a**.^[a]

Entry	Substrate	Substituents	Conv. [%] ^[b]	ee [%] ^[c] (config.) ^[d]
1	246a	R ¹ = H; R ² = H; R ³ = Ph	99	99 (<i>S</i>)
2	246b	R ¹ = H; R ² = H; R ³ = <i>p</i> -Me-C ₆ H ₄	96 ^[f]	99 (<i>S</i>) ^[e]
3	246c	R ¹ = Me; R ² = H; R ³ = Me	78	89 (<i>S</i>) ^[e]
4	246c ^{[g][h]}	R ¹ = Me; R ² = H; R ³ = Me	>99	90 (<i>S</i>) ^[e]
5	246d	R ¹ = H; R ² = Me; R ³ = Ph	98	99 (<i>S</i>) ^[e]
6	246e	R ¹ = H; R ² = Me; R ³ = <i>p</i> -Me-C ₆ H ₄	89 ^[f]	99 (<i>S</i>) ^[e]
7	246f ^[h]	R ¹ = Me; R ² = Me; R ³ = Me	>99	90 (<i>S</i>) ^[e]
8	246g	R ¹ = Cl; R ² = Me; R ³ = Ph	96	99 (<i>S</i>) ^[e]
9	246h	R ¹ = H; R ² = MOM; R ³ = Ph	96	99 (<i>S</i>) ^[e]
10	246i	R ¹ = H; R ² = Bn; R ³ = Ph	94	99 (<i>S</i>) ^[e]

^[a] Reaction conditions: *In situ* formed precatalyst, [$\{\text{Ir}(\mu\text{-Cl})(\text{cod})\}_2$] / **134a** = 0.5 : 1.1, 40 bar H₂, room temperature, 20 h, 0.2 M in THF.

^[b] Conversion determined by ¹H NMR.

^[c] Enantiomeric excess determined by HPLC using chiral stationary phases.

^[d] Absolute configuration was assigned by comparison with reported data.

^[e] Absolute configuration was tentatively assigned by analogy based on the stereochemical outcome for analogous substrates.

^[f] Isolated yield: for **246b**, 92%; for **246e**, 85%.

^[g] 2.0 mol % catalyst loading was used.

^[h] 80 bar H₂ was used.

2.2.3 Deuteration and Mechanistic Studies of the Hydrogenation of Heterocycles

The literature includes only a few experimental or theoretical mechanistic studies of the hydrogenation of heteroaromatic compounds (mainly, of quinolines).^{332a, b, d, 334b, 336} As has been discussed in Section 2.1.4, most of the early studies on iridium-mediated hydrogenations suggested mechanistic pathways involving inner sphere coordination of the substrate to the metal center.^{332a, b, d, 334b} Outer sphere coordination mechanistic pathways have been lately suggested by Crabtree, Eisenstein and co-workers^{336, 337} to operate along the hydrogenation of 2-methylquinoline mediated by iridium complexes containing phosphines and *N*-heterocyclic carbenes (NHC) as ligands. These authors also suggest that quinoline hydrogenation catalysts derived from $[\{\text{Ir}(\mu\text{-Cl})(\text{cod})\}_2]$ and bidentate phosphorus ligands could function by an outer sphere coordination mechanism. The considerable steric bulk of the enantiomerically pure bidentate phosphorus ligands, coupled with the steric demand of the hindered substrates typically used (such as 2-methylquinoline) could make inner sphere substrate coordination unfavorable. Crabtree's and Eisenstein's theoretical study could not locate a concerted outer sphere coordination mechanism for their *NHC,P,P*-iridium complex, where a proton from the dihydrogen ligand and the hydride are simultaneously transferred to the C=N bond. Instead, stepwise proton and hydride delivery³⁷⁷ was found to be the most energetically favored process.

A schematic representation of these two mechanistic alternatives (inner *versus* outer sphere coordination) in the reduction of the C=N bond leading to the generation of the stereogenic carbon alpha to nitrogen in C=N-containing heterocycles has been represented in Figure 71.

³⁷⁷ See the seminal work of Oro *et al.*, ref 328, who first proposed this concept and used it for designing catalysts for the hydrogenation of C=N double bonds.

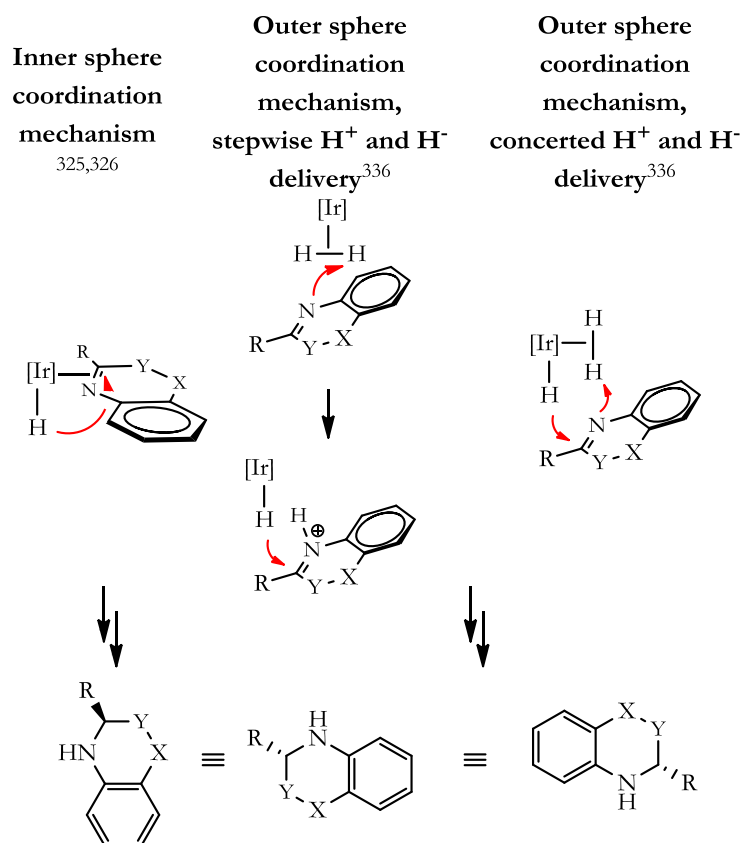
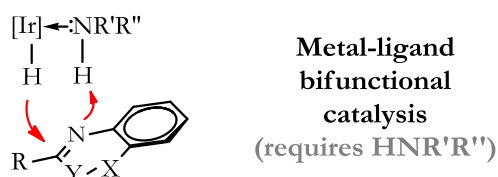


Figure 71. Schematic representation of the mechanistic possibilities in the hydrogenation of the C=N bond that generates a stereogenic carbon alpha to nitrogen in C=N-containing heterocycles (the red arrows just intend to give a sense of approach of the H groups to their final positions).

With regard to the dichotomy on the mechanism that operates in the hydrogenation of the studied C=N-containing heterocycles using the iridium complexes derived from our *P-OP* ligands (inner *versus* outer sphere reaction mechanism³⁷⁸), combined computational and experimental studies aiming at the elucidation of the most likely mechanism will be started in the near future.

³⁷⁸ A metal-ligand bifunctional catalytic hydrogenation (see below for a schematic representation and ref 339) seems to be quite unlikely to operate for quinolines, benzoxazines, benzoxazinones, benzothiazinones and quinoxalinones, as we have not used any secondary amine as additive and coordination of our hindered hydrogenation products to the metal center doesn't seem to be favored.



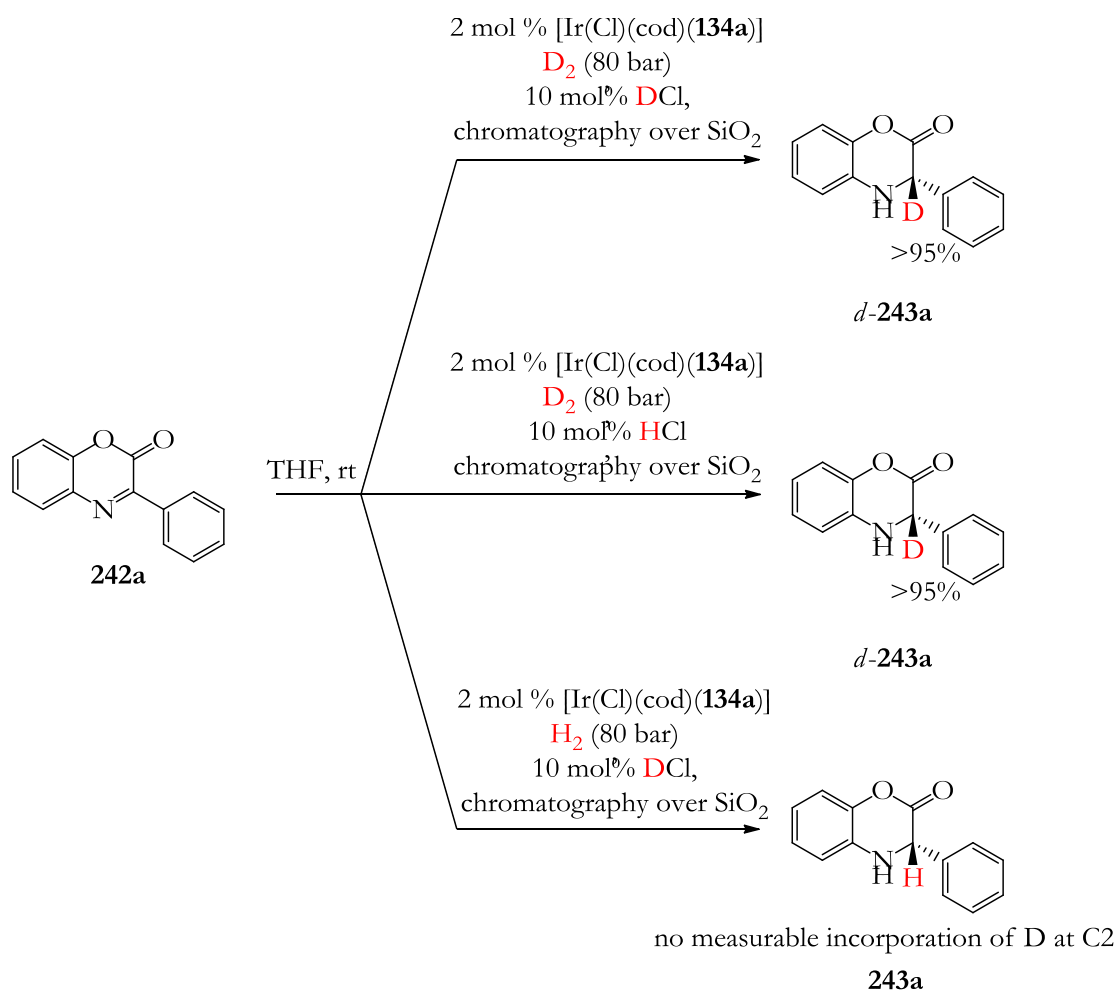
However, it should be recalled at this point that the basic steps in the hydrogenation of the studied C=N-containing heterocycles are the same for both possibilities:

- A 1,2-reduction for benzoxazines (X-Y = O-CH₂), benzoxazinones (X-Y = O-CO), benzothiazinones (X-Y = S-CO) and quinoxalinones (X-Y = NR-CO).
- A 1,4-reduction, followed by tautomerization to the C=N tautomer and 1,2-reduction for quinolines (X-Y = CH-CH).

To gain deeper insight into the aforementioned hydrogenation steps, a series of labeling experiments using H₂/10 mol % of DCl, D₂/10 mol % of HCl and D₂/10 mol % of DCl were performed for one representative example of the first type of substrates involving a 1,2-reduction (benzoxazinone **242a**) and for 2-methylquinoline **231a** with a more complex hydrogenation scenario.

Benzoxazinone **242a** reacted as expected with the labeled reagents. When D₂ was used, full incorporation of deuterium at C2 was observed (see Scheme 71, the H-atoms marked in red indicate the deuterium-labeled positions).³⁷⁹ Conversely, no observable incorporation of deuterium was observed when H₂/10 mol % of DCl was used.

³⁷⁹ Deuterium-hydrogen exchange took place at the nitrogen, either during the chromatographic purification or during spectroscopic analysis, and *N*-deuterated compounds were not observed.



Scheme 71. Deuterium labeling experiments on the asymmetric hydrogenation of benzoxazinone **242a**.³⁸⁰

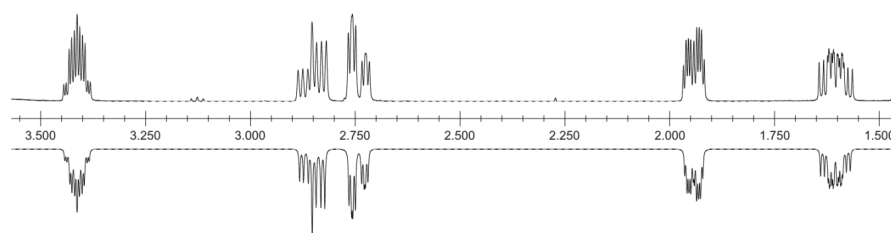
Hydrogenation of 2-methylquinoline (**231a**) with the labeled reagents afforded a complex mixture of isotopic isomers incorporating deuterium atoms at C2, C3 and C4, as well at the methyl carbon of the quinoline. With the aim of being able to fully interpret the complex reaction mixtures of isotopic isomers present, the chemical shifts and coupling constants of all protons in the aliphatic region of 2-methyl-1,2,3,4-tetrahydroquinoline **232a**

³⁸⁰ Degrees of deuterium incorporation at C2 are indicated in each case and based on the integration of 1H NMR signals, except for those marked with the symbol “&” that have been roughly calculated by relative integration of the CH_3 and CH_2D signals in the ^{13}C -NMR spectra (Inverse Gated Decoupling (IGD) ^{13}C NMR spectroscopy).

(H_a-H_e and the methyl group) were measured with selective decoupling ¹H NMR experiments and by fitting the experimental ¹H spectrum to the expected spin system with gNMR 5.0.³⁵⁵ Experimental and simulated spectra together with the ¹H-chemical shifts and coupling constants for the spin system comprising H_a-H_e and the methyl group in 2-methyl-1,2,3,4-tetrahydroquinoline **232a** have been summarized in footnote 381.

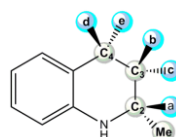
381

Window 1: 1H Axis = ppm Scale = 41.55 Hz/cm

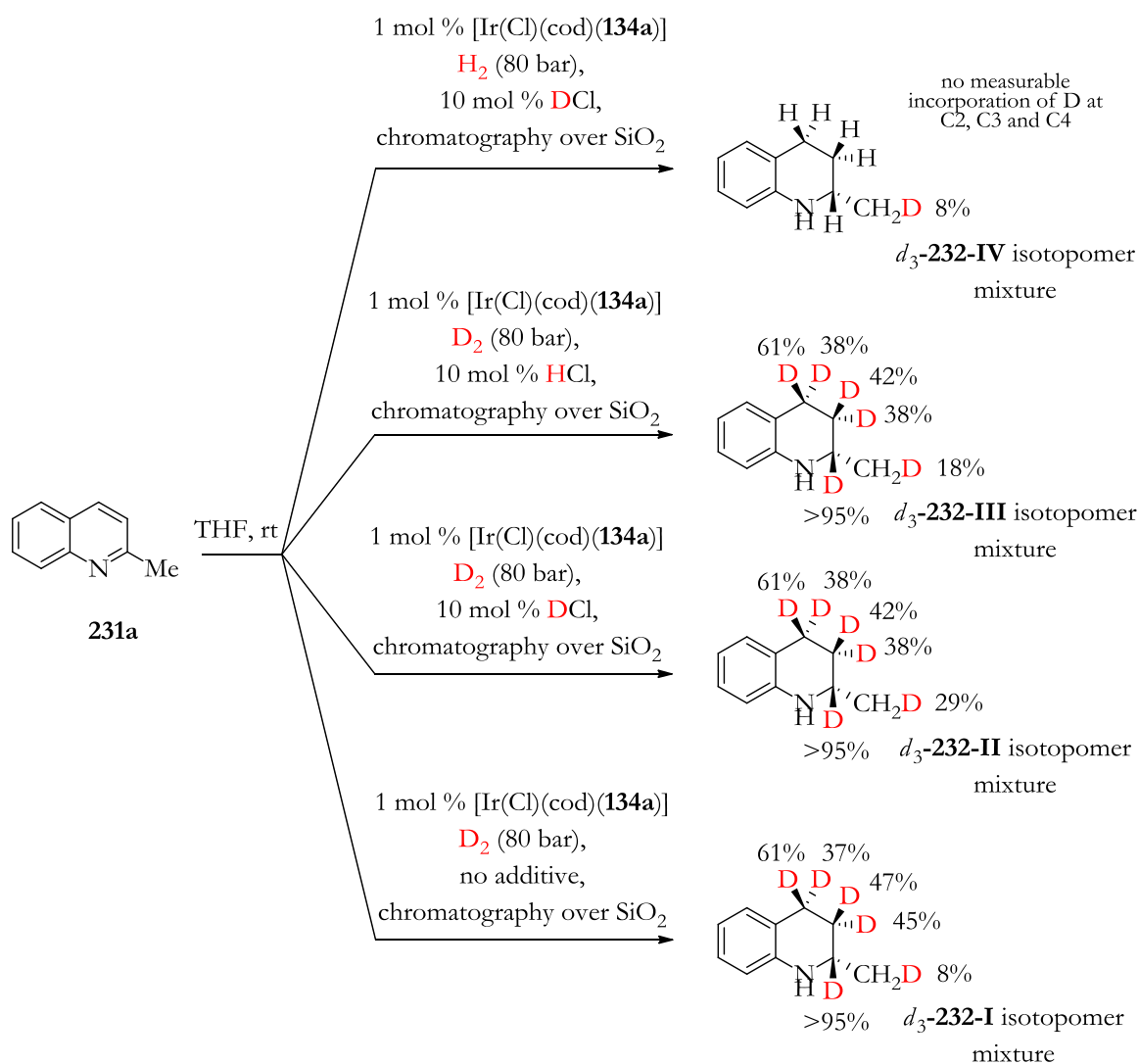


Experimental (top) and simulated (inverted) ¹H NMR spectra of the aliphatic region of 2-methyl-1,2,3,4-tetrahydroquinoline **232a**.

Chemical Shift	<i>J</i> ₁	<i>J</i> ₂	<i>J</i> ₃	<i>J</i> ₄	<i>J</i> ₅	<i>J</i> ₆
3,7 N						
3,413 H _a	0,00 N-H _a					
1,942 H _b	0,00 N-H _b	2,40 H _a -H _b				
1,605 H _c	0,00 N-H _c	8,90 H _a -H _c	-11,50 H _b -H _c			
2,85 H _d	0,00 N-H _d	0,40 H _a -H _d	4,70 H _b -H _d	10,50 H _c -H _d		
2,744 H _e	0,00 N-H _e	0,50 H _a -H _e	3,00 H _b -H _e	4,50 H _c -H _e	-15,00 H _d -H _e	
1,223 Me	0,00 N-M _e	5,90 H _a -M _e	0,00 H _b -M _e	0,00 H _c -M _e	0,00 H _d -M _e	0,00 H _e -M _e



After this preliminary analysis of the ^1H NMR spectrum of the aliphatic region of 2-methyl-1,2,3,4-tetrahydroquinoline **232a**, we could determine the degree of incorporation of deuterium at C2, C3, C4 and the methyl group in **232a** under the different reaction conditions (see Scheme 72; the H-atoms marked in red indicate the deuterium-labeled positions).³⁷⁹



Scheme 72. Deuterium labeling experiments on the asymmetric hydrogenation of 2-methylquinoline **231a**. (Degree of deuterium incorporation at C2 are indicated in each case and based on the integration of ^1H NMR signals, except for those marked with the symbol “&” that have been roughly calculated by relative integration of the CH_3 and CH_2D signals in the ^{13}C NMR spectra (Inverse Gated Decoupling (IGD) ^{13}C NMR spectroscopy).

When D₂ was used, full incorporation of deuterium at C2 was observed in the reduced product in all cases. Variable degrees of deuterium incorporation at C3, C4 and at the methyl group were obtained, depending on the labeling conditions. Surprisingly, when 10 mol % of DCl was used, a *ca.* 8% degree of deuterium incorporation at the methyl group was observed in the absence of D₂ (deuteriation at the methyl group can be clearly seen in the ¹³C NMR traces shown in Figure 72).

Furthermore, a detailed analysis of the structure of deuteriated derivatives of **232a** revealed that, whilst deuterium is incorporated at C3 with no facial preference, deuteride is delivered with moderate stereoselectivity to C4 (*ca.* 2:1 incorporation ratio in favor of the pro-(*S*) position in C4 in the deuteriated derivatives of **232a**, on the basis of ¹H NMR integration).

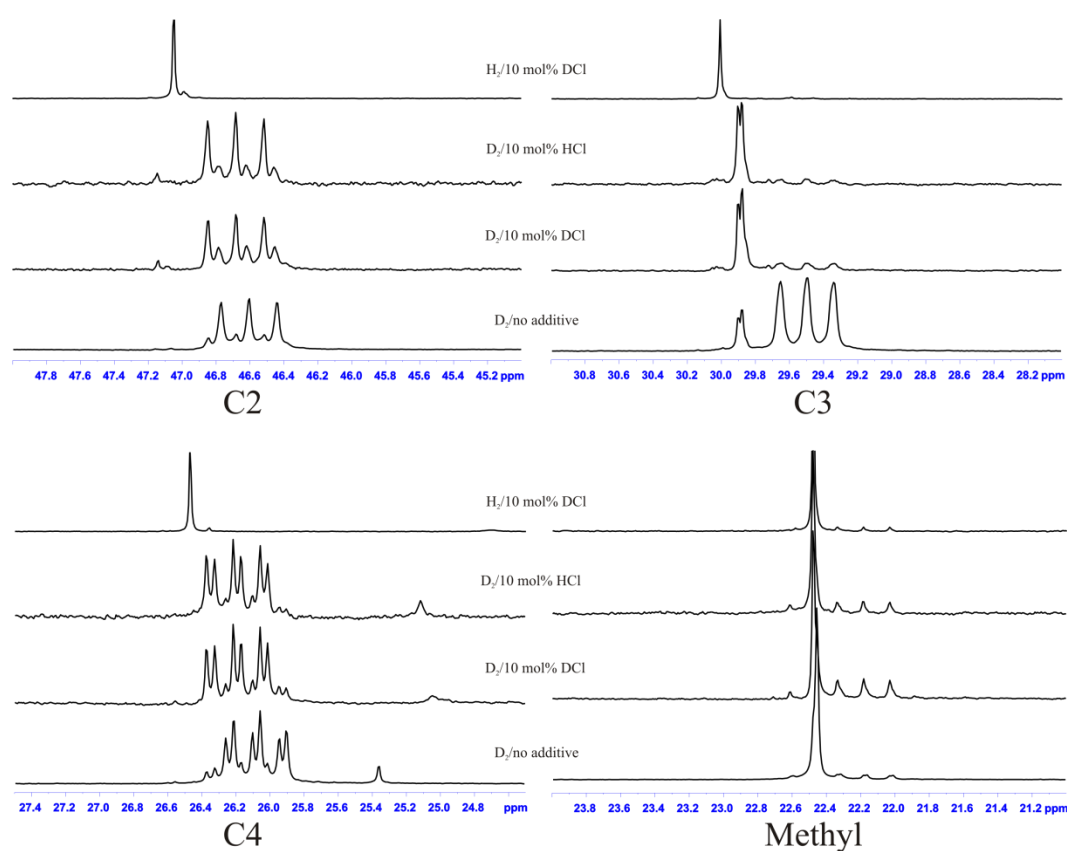
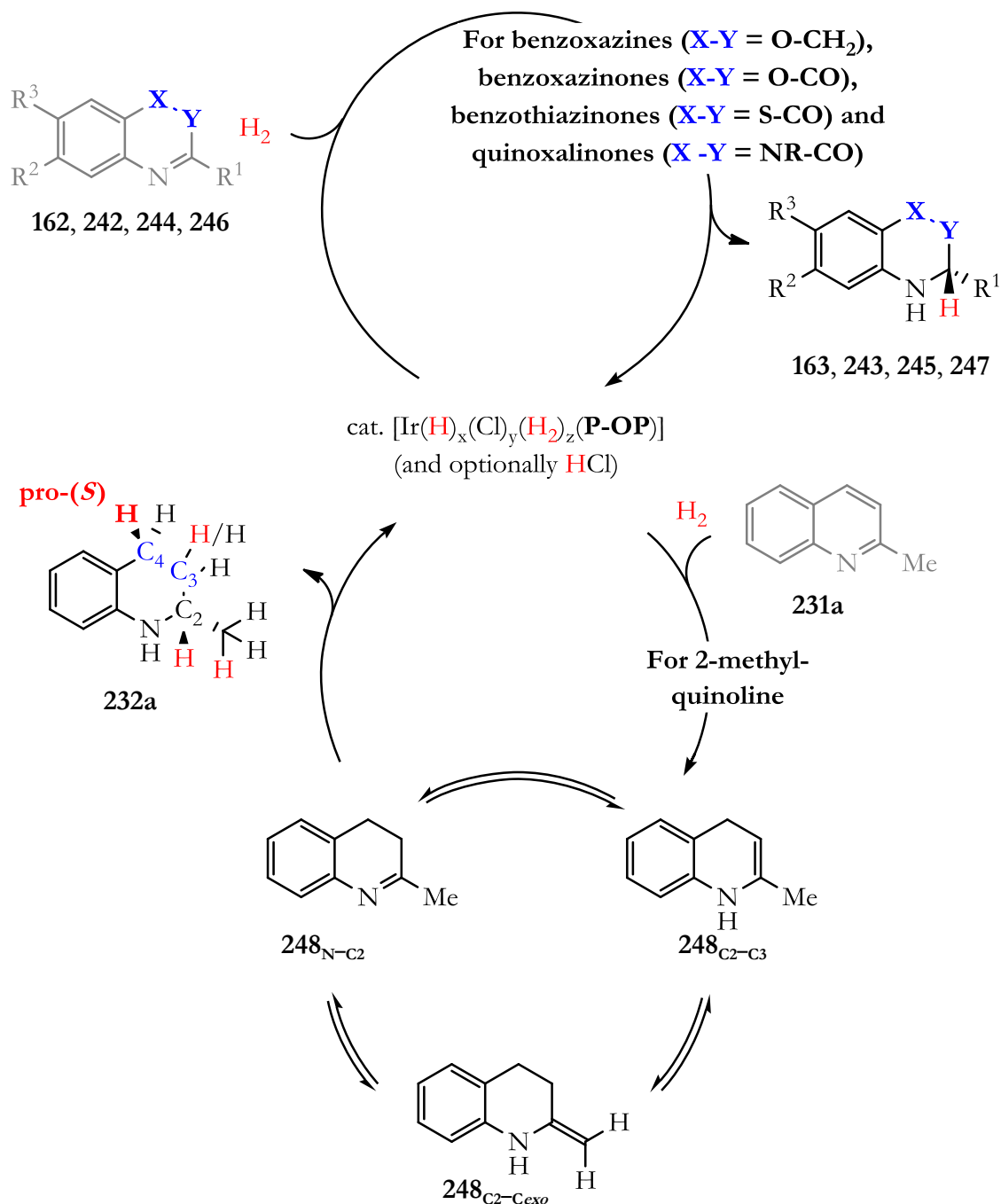


Figure 72. ¹³C NMR signals of C2, C3, C4, C_{Methyl} of d₃-**232I-IV** derived from deuterium labeling experiments.

Overall, several labeling studies on the asymmetric reduction of analogous heterocycles have been published to date,^{255d, 262b, 382} but our findings display several important unreported issues in this chemistry. Firstly, deuteration at the methyl group indicates that dihydroquinoline **248**_{C2-C_{exo}} (see Scheme 73) is formed. Thus, we have identified a complex scenario, in which this dihydroquinoline isomer also participates in the equilibria prior to the addition of the second H₂ molecule. Secondly, our findings suggest that the stereoselectivity of hydrogen incorporation at C4 would be compatible with asymmetric induction at this carbon during hydrogenation, in the event of being substituted. On the contrary, our labeling studies revealed that hydrogen incorporation at C3 proceeds with almost no facial selectivity in the hydrogenation of a tautomerizable quinoline derivatives such as **231a**.

A summary of the results of the labeling studies on the hydrogenation of the studied C=N-containing heterocyclic systems is illustrated in Scheme 73.

³⁸² Yan, P.-C.; Xie, J.-H.; Hou, G.-H.; Wang, L.-X.; Zhou, Q.-L. *Adv. Synth. Catal.* **2009**, *351*, 3243.



Scheme 73. Possible pathways for the hydrogenation of C=N-containing heterocycles.

Future combined experimental and computational studies on the hydrogenation of tautomerizable and non-tautomerizable C=N-containing heterocycles using the iridium complexes derived from our *P-OP* ligands will

hopefully uncover the key factors that govern the most relevant stereodirecting effects in our catalytic system:

- Structure of the catalytic complex
- Inner *versus* outer sphere substrate coordination mechanism
- Substrate's reactive tautomer during hydride delivery
- Rate- and stereodetermining step in the hydrogenation
- Stabilizing and de-stabilizing interactions in the key intermediates and transition states along the reaction coordinate

We are convinced that these future studies will also help us in identifying modifications of the catalytic system (understood as the combination of ligand, metal and additives) that may lead to increased activity and stereoselectivity in the hydrogenation.

At the current stage of the investigations (and based on the findings of other leading groups in the field,^{332a, b, d, 334b, 336, 337} the hydrogenation experimental results, and our previous knowledge on the stereoelectronic features that control stereoselectivity in the rhodium-mediated hydrogenation of alkenes with *P-OP* ligands³⁴⁵), we can only provide *a rough preliminary model for rationalizing the stereochemical outcome of the hydrogenation* reactions of the studied C=N-containing heterocycles, by means of simple quadrant diagram analysis (Figure 73).

Simple quadrant analysis provides a simplified view of the hydrogenation process. Assuming a coordination of the hydrido ligand in an apical position of the metal center (as observed in other iridium-based hydrogenation catalytic cycles^{316b, 336}) and an outer sphere substrate coordination mechanism, placement of the protonated C=N containing derivative in the lower left quadrant with the C=NH⁺ group close to the [Ir]-H bond and the aromatic ring stacked on the binaphthyl ring of the (*R*)-BINOL-derived group, may be

favored by formation of noncovalent attractive interactions between aromatic rings (π - π stacking interactions). Furthermore, several cation-dipole and hydrogen-bonding interactions involving the $C=NH^+$ group may also contribute to this orientation of the heterocyclic system. Delivery of a hydrido group from the side of the metal to the $C=NH^+$ group provides hydrogenation products with the experimentally observed configuration (see Figure 73 and Figure 74).

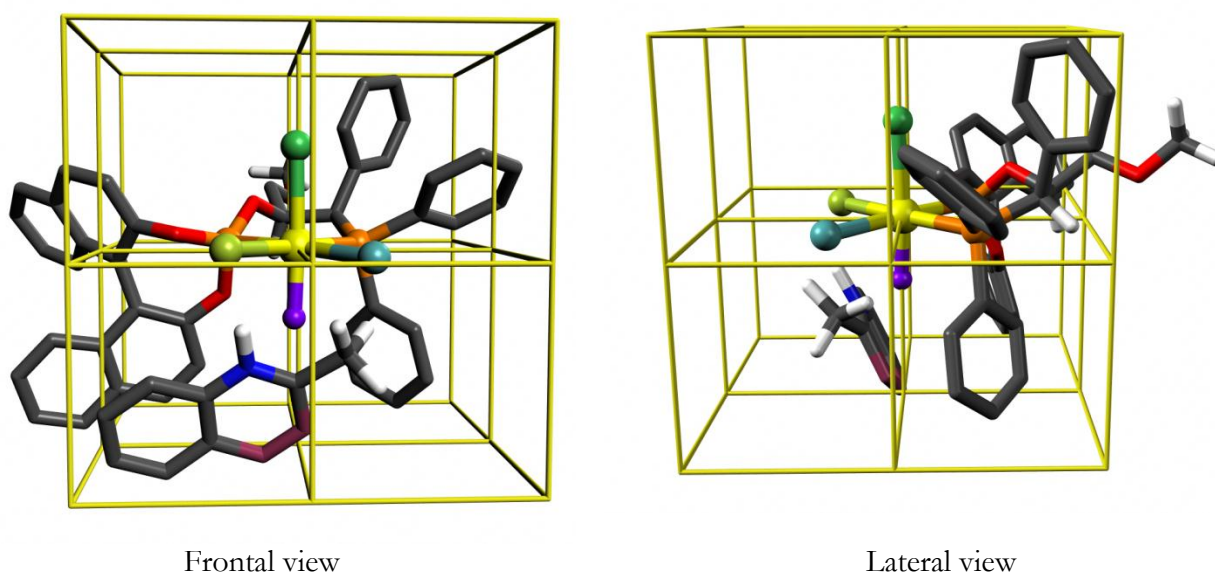


Figure 73. CAChe minimized 3D structure of the outer sphere substrate-catalyst complex previous to hydride delivery to C_α . (Color key: yellow = iridium; orange = phosphorus; red = oxygen; purple = hydrido ligand; maroon = CH_2 / CO / O / S / N , as defined for each substrate class; white = hydrogen; lime, green and turquoise = coordination vacant)

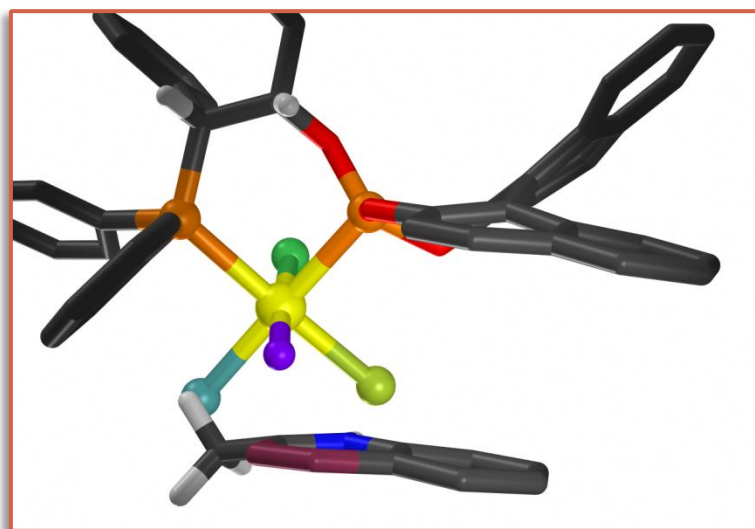


Figure 74. Bottom view and magnification of the outer sphere substrate-catalyst complex.

2.3 EXPERIMENTAL SECTION

2.3.1 General Remarks

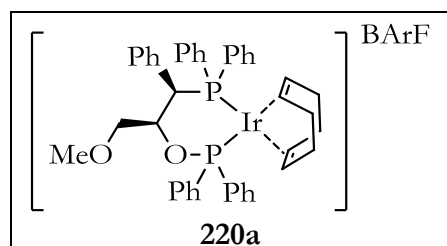
All syntheses were carried out on chemicals as purchased from commercial sources unless otherwise stated. All manipulations and reactions were run under inert atmosphere using anhydrous solvents, in either a Braun glove box or with standard Schlenk-type techniques. Glassware was dried under vacuum and heated with a hot air gun before use. All solvents were dried by using a Solvent Purification System (SPS). Silica gel 60 (230–400 mesh) was used for column chromatography. NMR spectra were recorded in CDCl_3 unless otherwise cited, on a Bruker Avance 400 MHz or 500 MHz Ultrashield spectrometers. ^1H NMR and ^{13}C NMR chemical shifts are quoted in ppm relative to residual solvent peaks, whereas $^{31}\text{P}\{^1\text{H}\}$ NMR chemical shifts are quoted in ppm relative to 85% phosphoric acid in water. $^{11}\text{B}\{^1\text{H}\}$ NMR chemical shifts are quoted in ppm relative to $\text{BF}_3\cdot\text{OEt}_2$ in CDCl_3 . $^{19}\text{F}\{^1\text{H}\}$ NMR chemical shifts are quoted in ppm relative to $\text{BF}_3\cdot\text{OEt}_2$ in CDCl_3 . Integrable $^{13}\text{C}\{^1\text{H}\}$ NMR spectra were recorded using IGD (Inverse Gated Decoupling) pulse sequence. High resolution mass spectra (HRMS) were recorded by using ESI or APCI ionization methods in positive mode. Optical rotations were measured on a Jasco P-1030 polarimeter. Melting points were measured in open capillaries on a Büchi B-540 instrument and are uncorrected. Enantiomeric excesses were determined by GC or HPLC on using chiral stationary phases. GC analyses were performed on an Agilent 6890N chromatograph equipped with a FID detector. HPLC analyses were performed on an Agilent 1200 Series chromatograph equipped with a diode array UV detector.

Crystal structure determination was carried out using a Bruker-Nonius diffractometer equipped with APPEX 2 4K CCD area detector, a FR591 rotating anode with Mo_{K α} radiation, Montel mirrors as monochromator and a Kryoflex low temperature device (T = 100K). Fullsphere data was collected using omega and phi scans. Apex2 V. 1.0-22 (Bruker-Nonius 2004) for the data reduction and SADABS V. 2.10 (2003) for the absorption correction. Crystal structure was achieved using direct methods as implemented in SHELXTL Version 6.10 (Sheldrick, Universität Göttingen (Germany), 2000). Least-squares refinement on F² using all measured intensities was carried out using the program SHELXTL Version 6.10 (Sheldrick, Universität Göttingen (Germany), 2000). All non-hydrogen atoms were refined including anisotropic displacement parameters.

2.3.2 General Synthetic Procedures for the Preparation of Iridium Complexes

2.3.2.1 CATIONIC IRIIDIUM COMPLEXES DERIVED FROM PHOSPHINE-PHOSPHINITE LIGANDS

$[\{\text{Ir}(\mu\text{-Cl})(\text{cod})\}_2]$ was dissolved in CH_2Cl_2 (1.0 mL) and a solution of the corresponding *P-OP* ligand in CH_2Cl_2 (2.0 mL) was added. After 10 min, NaBARF was added and the resulting mixture was stirred at room temperature for 30 min. After filtration of the formed salts through a 0.2 μm filter, the resulting filtrate was purified by flash chromatography on SiO_2 (hexanes/ CH_2Cl_2 1:1) to give the corresponding cationic complexes $[\text{Ir}(\text{cod})(\text{P-OP})]\text{BARF}$ as red powders.



$[\text{Ir}(\text{cod})(\mathbf{21a})]\text{BARF}$ (**220a**). The reaction between $[\{\text{Ir}(\mu\text{-Cl})(\text{cod})\}_2]$ and **21a** was carried out following the general procedure starting from **21a** (9 mg, 0.018 mmol) and $[\{\text{Ir}(\mu\text{-Cl})(\text{cod})\}_2]$ (6 mg, 0.009 mmol). $^{31}\text{P}\{^1\text{H}\}$

NMR (162 MHz, CD_2Cl_2) δ 92.0 (d, $J = 44.2$ Hz, P-O), 14.0 (d, $J = 44.2$ Hz, P-C) (see Figure 75). The resulting iridium complex was not further purified and allowed to react with NaBARF (16 mg, 0.018 mmol) following the general procedure. Complex **220a** was obtained as an intense red solid (19 mg, 65% yield). $[\alpha]_{\text{D}}^{28} = -43.4$ ($c = 1.40$, CH_2Cl_2); ^1H NMR (400 MHz, CD_2Cl_2) δ 7.89-7.12 (m, 35H), 6.55-6.50 (m, 2H), 4.98-4.96 (m, 1H), 4.61-4.59 (m, 1H), 4.55 (d, $J = 16.0$ Hz, 1H), 4.23-4.12 (m, 2H), 4.04-4.02 (m, 1H), 3.29-3.20 (m, 5H), 2.56-2.41 (m, 4H), 2.32-2.27 (m, 2H), 2.14-2.09 (m, 2H); DEPTQ 135 (100 MHz, CD_2Cl_2) δ 161.7 (q, $J = 49.5$ Hz, C), 135.8 (CH), 135.7 (CH), 134.8 (CH), 134.1 (C), 133.45 (C), 133.39 (CH), 133.25 (CH), 133.22 (CH), 133.19 (CH), 132.82 (CH), 132.80 (CH), 132.5 (C), 132.3 (CH), 132.2 (CH), 132.0 (C), 131.9 (CH), 131.8 (CH), 131.38 (CH), 131.35 (CH), 129.7 (CH), 129.62 (CH), 129.58 (CH), 129.5 (CH), 129.43 (C), 129.36 (CH), 129.26 (CH), 129.1 (C), 129.03 (C), 129.00 (C), 128.97 (C), 128.9 (C), 128.8 (CH), 128.72 (CH), 128.69 (C), 128.66 (C), 128.4 (CH), 128.3 (CH), 124.6 (q, $J = 270.8$ Hz, C), 117.5-117.4 (m, CH), 95.0 (d, $J = 13.0$ Hz, CH), 92.9 (d, $J = 9.2$ Hz, CH), 92.7 (d, $J = 9.5$ Hz, CH), 83.6 (d, $J =$

10.7 Hz, CH), 73.8 (dd, $J = 3.6$ Hz, $J = 3.6$ Hz, CH), 72.2 (dd, $J = 8.9$ Hz, $J = 8.9$ Hz, CH₂), 58.8 (CH₃), 41.4 (d, $J = 35.8$ Hz, CH), 32.4 (CH₂), 31.9 (CH₂), 30.0 (CH₂), 29.4 (CH₂); ³¹P{¹H} NMR (162 MHz, CD₂Cl₂) δ 102.9 (d, $J = 30.5$ Hz, P-O), 12.0 (d, $J = 30.5$ Hz, P-C); ¹¹B{¹H} NMR (128 MHz, CD₂Cl₂) δ -6.7; ¹⁹F{¹H} NMR (376 MHz, CD₂Cl₂) δ -62.9; HRMS (ESI⁺) calcd for C₄₂H₄₄O₂P₂¹⁹¹Ir [(M-BArF)⁺] 833.2423, found 833.2396.

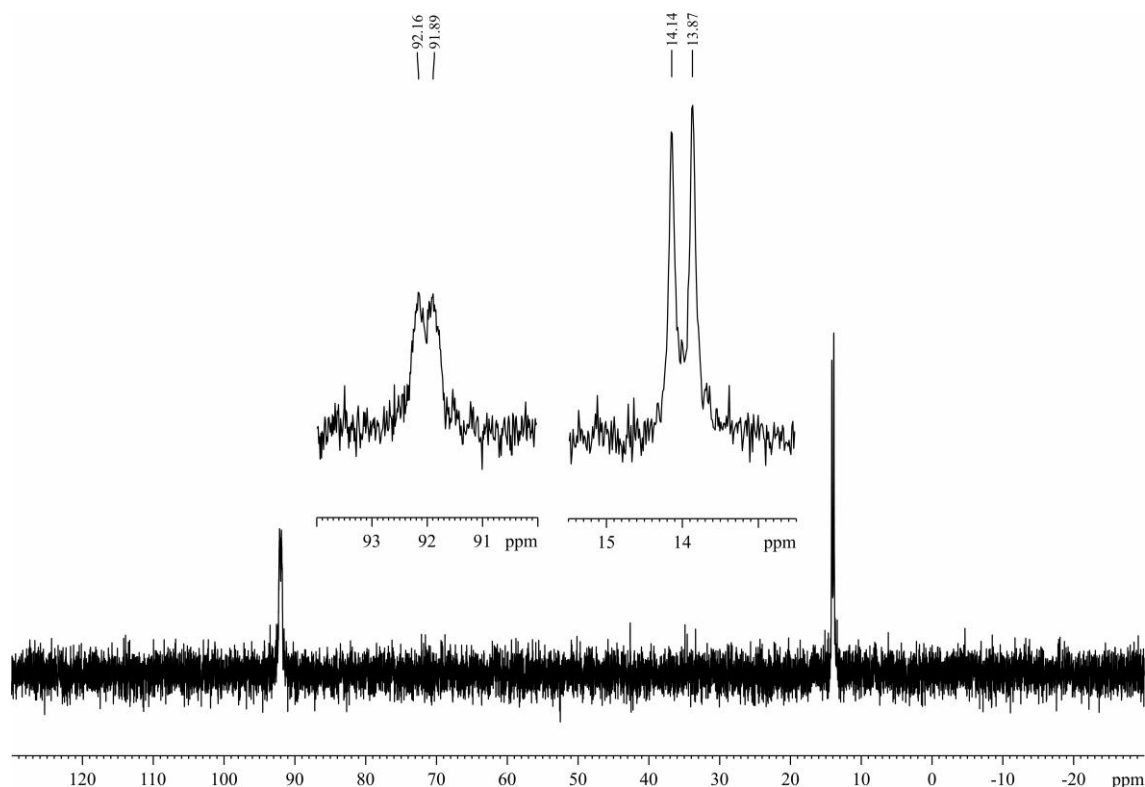
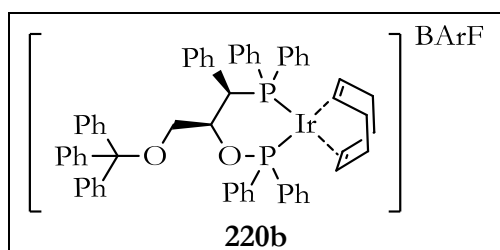


Figure 75. ³¹P{¹H} NMR spectrum of the *in situ* formed neutral iridium complex.



[Ir(cod)(**21b**)]BArF (**220b**). The reaction between [$\text{Ir}(\mu\text{-Cl})(\text{cod})\text{]}_2$] and **21b** was carried out following the general procedure starting from **21b** (14 mg, 0.018 mmol) and [$\text{Ir}(\mu\text{-Cl})(\text{cod})\text{]}_2$] (6 mg, 0.009 mmol). ³¹P{¹H} NMR (162 MHz, CD₂Cl₂) δ

91.1 (bs, P-O), 13.2 (d, $J = 44.4$ Hz, P-C) (see Figure 76). The resulting iridium complex was not further purified and allowed to react with NaBArF (16 mg, 0.018 mmol) following the general procedure. Complex **220b** was obtained as an intense red solid (31 mg, 90% yield). $[\alpha]_D^{28} = -32.2$ ($c = 1.63$, CH₂Cl₂); ¹H NMR (400 MHz, CD₂Cl₂) δ 8.01-7.97 (m, 2H), 7.81-7.63 (m, 12H), 7.63-7.15 (m, 36H), 6.65-6.61 (m, 2H), 5.05 (bs, 1H), 4.72 (d, $J = 15.8$

Hz, 1H), 4.59 (bs, 1H), 4.28-4.20 (m, 1H), 4.07 (bs, 2H), 3.22-3.18 (m, 1H), 2.90 (dd, $J = 9.0$ Hz, $J = 9.0$ Hz, 1H), 2.60-2.39 (m, 4H), 2.32-2.28 (m, 2H), 2.13-2.08 (m, 2H); DEPTQ 135 (100 MHz, CD_2Cl_2) δ 161.8 (q, $J = 49.8$ Hz, C), 143.1 (C), 136.1 (CH), 136.0 (CH), 134.8 (CH), 133.8 (C), 133.25 (CH), 133.23 (CH), 133.15 (CH), 133.1 (C), 133.0 (CH), 132.94 (CH), 132.92 (CH), 132.5 (C), 132.4 (CH), 132.3 (CH), 132.00 (C), 131.97 (C), 131.90 (CH), 131.88 (CH), 131.44 (CH), 131.42 (CH), 130.0 (C), 129.8 (CH), 129.7 (CH), 129.6 (CH), 129.5 (CH), 129.4 (C), 129.3 (CH), 129.09 (C), 129.06 (C), 129.04 (C), 129.01 (C), 128.79 (CH), 128.75 (C), 128.72 (C), 128.68 (CH), 128.61 (CH), 128.55 (CH), 128.4 (CH), 128.2 (CH), 128.0 (CH), 127.9 (CH), 127.4 (CH), 124.6 (q, $J = 272.0$ Hz, C), 117.6-117.4 (m, CH), 95.3 (d, $J = 13.0$ Hz, CH), 93.2 (d, $J = 9.1$ Hz, CH), 93.0 (d, $J = 9.3$ Hz, CH), 87.7 (C), 83.5 (d, $J = 11.0$ Hz, CH), 74.6 (dd, $J = 3.5$ Hz, $J = 3.5$ Hz, CH), 63.3 (dd, $J = 8.9$ Hz, $J = 8.9$ Hz, CH_2), 42.3 (d, $J = 35.8$ Hz, CH), 32.6 (CH_2), 32.1 (CH_2), 29.8 (CH_2), 29.1 (CH_2); $^{31}\text{P}\{^1\text{H}\}$ NMR (162 MHz, CD_2Cl_2) δ 103.6 (d, $J = 30.0$ Hz, P-O), 12.6 (d, $J = 30.0$ Hz, P-C); $^{11}\text{B}\{^1\text{H}\}$ NMR (128 MHz, CD_2Cl_2) δ -6.7; $^{19}\text{F}\{^1\text{H}\}$ NMR (376 MHz, CD_2Cl_2) δ -62.9; HRMS (ESI $^+$) calcd for $\text{C}_{60}\text{H}_{56}\text{O}_2\text{P}_2^{193}\text{Ir} [(\text{M}-\text{BArF})^+]$ 1063.3385, found 1063.3408.

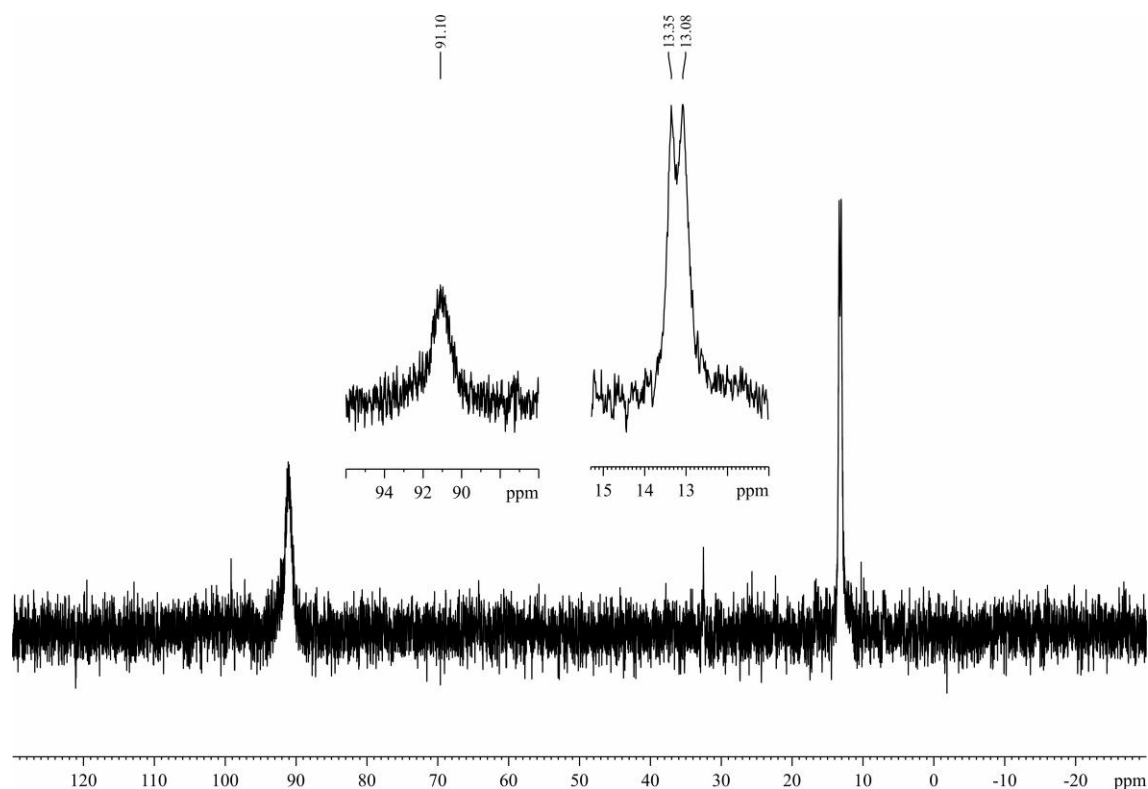
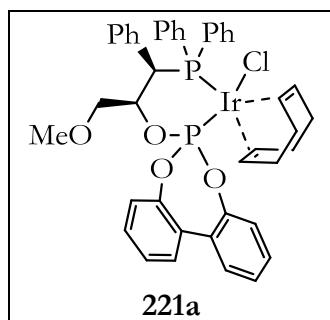


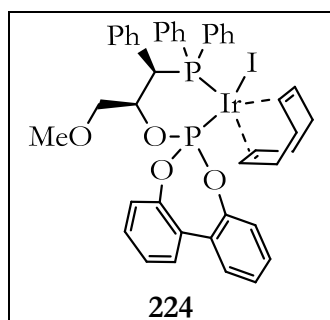
Figure 76. $^{31}\text{P}\{^1\text{H}\}$ NMR spectrum of the in situ formed complex.

2.3.2.2 NEUTRAL IRIIDIUM COMPLEXES DERIVED FROM PHOSPHINE-PHOSPHITE LIGANDS

Method A. *In situ* preparation of the complexes: $[\{\text{Ir}(\mu\text{-Cl})(\text{cod})\}_2]$ was dissolved in THF- d_8 (300 μL) and a solution of the corresponding *P-OP* ligand in THF- d_8 (300 μL) was added. After 15 min stirring, the reaction mixture was *in situ* analyzed to characterize iridium complexes $[\text{Ir}(\text{Cl})(\text{cod})(\text{P-OP})]$.



$[\text{Ir}(\text{Cl})(\text{cod})(\mathbf{133a})]$ (**221a**). Iridium complex **221a** was prepared following the general procedure (method A), starting from **133a** (17.5 mg, 0.0310 mmol) and $[\{\text{Ir}(\mu\text{-Cl})(\text{cod})\}_2]$ (10.4 mg, 0.0155 mmol). ^1H NMR (400 MHz, THF- d_8) δ 7.80-7.20 (m, 18H), 7.10-6.90 (m, 6H), 4.53 (dd, $J = 13.3$ Hz, $J = 3.9$ Hz, 1H), 3.88-3.85 (m, 2H), 3.33-3.11 (m, 7H), 2.86-2.76 (m, 2H), 2.44-2.39 (m, 2H), 1.80-1.72 (m, 2H), 1.37-1.33 (m, 2H); $^{13}\text{C}\{^1\text{H}\}$ NMR (100 MHz, THF- d_8) δ 150.5 (C), 150.4 (C), 150.2 (C), 150.0 (C), 138.0 (CH), 137.9 (CH), 135.82 (C), 135.76 (C), 133.24 (CH), 133.17 (CH), 130.41 (CH), 130.39 (CH), 130.3 (CH), 130.2 (CH), 130.0 (C), 129.9 (C), 129.73 (CH), 129.71 (CH), 129.6 (C), 129.5 (CH), 129.4 (CH), 128.8 (CH), 128.6 (C), 128.0 (C), 127.4 (CH), 127.2 (CH), 127.1 (CH), 126.6 (CH), 126.53 (CH), 126.50 (CH), 125.4 (CH), 125.0 (CH), 123.4 (CH), 121.34 (CH), 121.31 (CH), 76.6 (CH), 73.6 (d, $J = 7.8$ Hz, CH_2), 73.1 (CH), 70.3 (CH), 57.7 (CH_3), 45.8 (d, $J = 30.5$ Hz, CH), 37.4 (CH_2), 27.6 (CH_2); $^{31}\text{P}\{^1\text{H}\}$ NMR (162 MHz, THF- d_8) δ 108.0 (d, $J = 58.1$ Hz, P-O), 13.7 (d, $J = 58.1$ Hz, P-C); HRMS (ESI $^+$) calcd for $\text{C}_{42}\text{H}_{42}\text{O}_4\text{P}_2^{191}\text{Ir} [(\text{M}-\text{Cl})^+]$ 863.2148, found 863.2164.



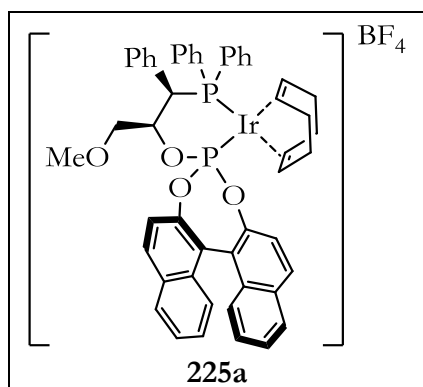
Method B. Preparation of the neutral iodo complex $[\text{Ir}(\text{I})(\text{cod})(\mathbf{133a})]$ (224**).** $[\{\text{Ir}(\mu\text{-Cl})(\text{cod})\}_2]$ (11.4 mg, 0.0170 mmol) was dissolved in CH_2Cl_2 (1.0 mL) and a solution of the corresponding *P-OP* ligand **133** (19.2 mg, 0.0340 mmol) in CH_2Cl_2 (2.0 mL) was added. After 15 min, the solvent was evaporated to dryness and the residue dissolved in dry acetone (2.0 mL). This solution was then transferred to a sealed tube, which contained an acetone

solution (4.0 mL) of LiI (0.227 g, 1.70 mmol). The reaction mixture was stirred at reflux for 24 h while a yellow solid was precipitated. The solid was filtered, washed with dry acetone (3 x 2.0 mL) and dried *in vacuo*. The solid was dissolved in CH₂Cl₂ and precipitated by slow addition of hexanes, producing the corresponding neutral iridium complexes **224** as a yellow powder (16.3 mg, 48% yield). $[\alpha]_D^{28} = -385.4$ (*c* 0.26, CH₂Cl₂); ¹H NMR (400 MHz, CD₂Cl₂) δ 7.79 (bs, 2H), 7.66-7.54 (m, 5H), 7.48-7.33 (m, 9H), 7.23-7.20 (m, 2H), 7.05-6.56 (m, 6H), 4.41 (dd, *J* = 12.6 Hz, *J* = 4.4 Hz, 1H), 4.02 (bs, 1H), 3.31 (ddd, *J* = 10.7 Hz, *J* = 7.0 Hz, *J* = 1.8 Hz, 1H), 3.20 (s, 3H), 3.13 (ddd, *J* = 10.7 Hz, *J* = 5.1 Hz, *J* = 2.0 Hz, 1H), 2.80 (bs, 2H), 2.53-2.48 (m, 2H), 2.09-2.01 (m, 2H), 1.64-1.58 (m, 2H); DEPTQ 135 (100 MHz, CD₂Cl₂) δ 150.6 (C), 150.5 (C), 149.7 (C), 149.6 (C), 137.6 (CH), 133.3 (CH), 133.2 (CH), 130.54 (CH), 130.51 (CH), 130.46 (CH), 130.22 (CH), 130.20 (CH), 129.8 (CH), 129.7 (C), 129.6 (CH), 129.4 (C), 129.2 (CH), 129.0 (C), 128.4 (C), 127.6 (CH), 127.2 (CH), 127.1 (CH), 126.8 (CH), 126.7 (CH), 126.6 (CH), 125.6 (CH), 125.5 (CH), 123.1 (CH), 121.4 (CH), 121.3 (CH), 79.0 (bs, CH), 73.4 (dd, *J* = 7.5 Hz, *J* = 7.5 Hz, CH₂), 58.6 (CH₃), 45.9 (d, *J* = 29.6 Hz, CH), 29.1 (CH₂); ³¹P{¹H} NMR (162 MHz, CD₂Cl₂) δ 105.3 (d, *J* = 57.9 Hz, P-O), 9.5 (d, *J* = 57.9 Hz, P-C); HRMS (ESI⁺) calcd for C₄₂H₄₂O₄P₂¹⁹³Ir [(M-I)⁺] 865.2188, found 865.2219.

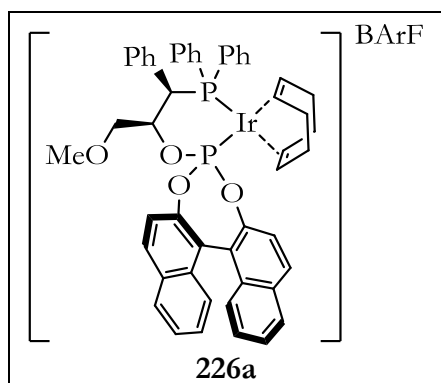
2.3.2.3 CATIONIC IRIIDIUM COMPLEXES DERIVED FROM PHOSPHINE-PHOSPHITE LIGANDS

Cationic complexes [Ir(cod)(**134a**)]BF₄ (**225a**) and [Ir(cod)(**134a**)]BArF (**226a**) were synthesized as follows:

[{Ir(μ -Cl)(cod)}₂] (0.5 equivalent) was dissolved in CH₂Cl₂ (2.0 mL) and a solution of the corresponding *P-OP* ligand (1.0 equivalent) in CH₂Cl₂ (1.0 mL) was added. After 10 min of stirring, AgBF₄ or NaBArF (1.0 equivalent) was added and the resulting mixture was stirred at room temperature for 60 min. After filtration of the formed salts through a 0.2 μ m filter, the resulting filtrate was evaporated. The residue was dissolved in a small amount of DCM and precipitated by slow addition of diethyl ether (BF₄ derivative) or hexane (BArF derivative). Mother liquor was extracted with a syringe and the resulting solid was dried *in vacuo* to give the corresponding cationic complex as red powder.



$[\text{Ir}(\text{cod})(\mathbf{134a})]\text{BF}_4$ (**225a**). The reaction between $[\{\text{Ir}(\mu\text{-Cl})(\text{cod})\}_2]$ and **134a** was carried out following the general procedure starting from **134a** (58.3 mg, 0.0877 mmol), $[\{\text{Ir}(\mu\text{-Cl})(\text{cod})\}_2]$ (29.5 mg, 0.0439 mmol) and AgBF_4 (17.1 mg, 0.0877 mmol). Complex was obtained as an intense red solid (79.7 mg, 86% yield). $[\alpha]_{\text{D}}^{25} = -8.3$ (c 0.5, CH_2Cl_2); ^1H NMR (500 MHz, CD_2Cl_2) δ 8.30-7.12 (m, 25H), 6.54-6.46 (m, 2H), 5.46-5.38 (m, 1H), 5.15-5.06 (m, 1H), 4.55-4.42 (m, 2H), 4.53-4.51 (m, 1H), 3.88-3.79 (m, 1H), 3.03-2.99 (m, 1H), 2.98 (s, 3H), 2.88-2.80 (m, 1H), 2.42-2.30 (m, 4H), 2.24-2.05 (m, 3H), 2.03-1.92 (m, 1H); $^{13}\text{C}\{^1\text{H}\}$ NMR (125 MHz, CD_2Cl_2) δ 147.1 (d, $J = 12.5$ Hz, C), 146.2 (d, $J = 7.6$ Hz, C), 136.1 (d, $J = 11.9$ Hz, CH), 133.8 (d, $J = 2.4$ Hz, CH), 132.6 (C), 132.4 (C), 132.3 (d, $J = 8.7$ Hz, C), 132.1 (C), 131.8 (C), 131.7 (CH), 131.7 (d, $J = 2.4$ Hz, CH), 131.5 (C), 131.4 (CH), 130.8 (CH), 130.2 (d, $J = 10.9$ Hz, CH), 129.9 (C), 129.5 (C), 129.4 (CH), 129.3 (d, $J = 1.7$ Hz, CH), 128.8 (CH), 128.6 (d, $J = 10.0$ Hz, CH), 128.5 (CH), 127.3 (CH), 127.1 (CH), 127.0 (CH), 126.5 (CH), 126.4 (CH), 126.1 (C), 126.0 (CH), 122.9 (d, $J = 2.6$ Hz, C), 121.5 (d, $J = 2.6$ Hz, C), 120.8 (CH), 120.0 (d, $J = 2.4$ Hz, CH), 102.8 (d, $J = 15.0$ Hz, CH), 100.3 (d, $J = 14.1$ Hz, CH), 91.5 (d, $J = 9.2$ Hz, CH), 87.1 (d, $J = 10.1$ Hz, CH), 74.8 (dd, $J = 3.2$ Hz, $J = 3.2$ Hz, CH), 70.9 (dd, $J = 8.4$ Hz, $J = 8.4$ Hz, CH_2), 58.7 (CH_3), 42.5 (d, $J = 36.4$ Hz, CH), 32.0 (d, $J = 2.3$ Hz, CH_2), 31.0 (CH_2), 30.9 (CH_2), 29.6 (CH_2); $^{31}\text{P}\{^1\text{H}\}$ NMR (202 MHz, CD_2Cl_2) δ 115.4 (d, $J = 40.6$ Hz, P-O), 13.4 (d, $J = 40.6$ Hz, P-C); $^{11}\text{B}\{^1\text{H}\}$ NMR (160 MHz, CD_2Cl_2) δ -1.2; $^{19}\text{F}\{^1\text{H}\}$ NMR (471 MHz, CD_2Cl_2) δ -153.4; HRMS (ESI⁺) calcd for $\text{C}_{50}\text{H}_{46}\text{O}_4\text{P}_2^{191}\text{Ir}[(\text{M}-\text{BF}_4)^+]$ 963.2472, found 963.2453.

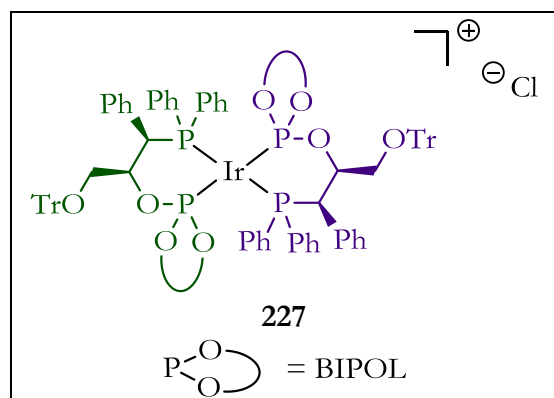


$[\text{Ir}(\text{cod})(\mathbf{134a})]\text{BArF}$ (**226a**). The reaction between $[\{\text{Ir}(\mu\text{-Cl})(\text{cod})\}_2]$ and **134a** was carried out following the general procedure starting from **134a** (67.9 mg, 0.1020 mmol), $[\{\text{Ir}(\mu\text{-Cl})(\text{cod})\}_2]$ (34.3 mg, 0.0511 mmol) and NaBArF (90.5 mg, 0.1020 mmol). Complex was obtained as an intense red solid (140.4 mg, 88% yield). $[\alpha]_{\text{D}}^{25} = -22.4$ ($c = 0.50$, CH_2Cl_2); ^1H NMR (500 MHz, CD_2Cl_2) δ 8.30-7.10 (m, 37H), 6.54-6.46 (m, 2H), 5.50-5.41 (m, 1H), 5.14-5.04 (m, 1H),

4.56-4.44 (m, 2H), 4.54-4.52 (m, 1H), 3.91-3.82 (m, 1H), 3.04-2.97 (m, 1H), 3.00 (s, 3H), 2.90-2.83 (m, 1H), 2.42-2.28 (m, 4H), 2.24-2.03 (m, 3H), 2.01-1.90 (m, 1H); $^{13}\text{C}\{^1\text{H}\}$ NMR (125 MHz, CD_2Cl_2) δ 161.7 (q, $J = 49.8$ Hz, C), 147.1 (d, $J = 12.5$ Hz, C), 146.0 (d, $J = 8.2$ Hz, C), 136.1 (d, $J = 12.5$ Hz, CH), 134.8 (CH), 133.8 (d, $J = 1.8$ Hz, CH), 132.7 (C), 132.3 (d, $J = 8.2$ Hz, CH), 132.1 (C), 131.3 (C), 131.2 (d, $J = 2.4$ Hz, CH), 131.4 (C), 131.2 (CH), 130.9 (CH), 130.1 (d, $J = 11.0$ Hz, CH), 130.0 (C), 129.5 (C), 129.4 (CH), 129.3 (d, $J = 1.5$ Hz, CH), 128.9 (ddd, $J = 31.5$ Hz, $J = 5.7$ Hz, $J = 2.8$ Hz, C), 128.7 (CH), 128.6 (d, $J = 10.0$ Hz, CH), 128.5 (CH), 127.4 (CH), 127.1 (CH), 127.0 (CH), 126.5 (CH), 126.4 (CH), 126.0 (CH), 124.5 (q, $J = 272.5$ Hz, C), 123.0 (d, $J = 2.0$ Hz, C), 121.5 (d, $J = 2.8$ Hz, C), 120.7 (CH), 119.8 (d, $J = 2.0$ Hz, CH), 117.0 (m, CH), 102.8 (d, $J = 15.1$ Hz, CH), 99.9 (d, $J = 14.0$ Hz, CH), 91.6 (d, $J = 8.9$ Hz, CH), 87.0 (d, $J = 9.7$ Hz, CH), 74.8 (dd, $J = 3.2$ Hz, $J = 3.2$ Hz, CH), 70.3 (dd, $J = 8.5$ Hz, $J = 8.5$ Hz, C), 58.6 (CH_3), 42.6 (d, $J = 36.0$ Hz, CH), 31.9 (CH_2), 31.0 (CH_2), 30.9 (CH_2), 29.5 (CH_2); $^{31}\text{P}\{^1\text{H}\}$ NMR (202 MHz, CD_2Cl_2) δ 112.2 (d, $J = 40.4$ Hz, P-O), 10.3 (d, $J = 40.4$ Hz, P-C); $^{11}\text{B}\{^1\text{H}\}$ NMR (128 MHz, CD_2Cl_2) δ -6.6; $^{19}\text{F}\{^1\text{H}\}$ NMR (376 MHz, CD_2Cl_2) δ -62.9; HRMS (ESI⁺) calcd for $\text{C}_{50}\text{H}_{46}\text{O}_4\text{P}_2^{191}\text{Ir}$ [(M-BArF)⁺] 963.2472, found 963.2457.

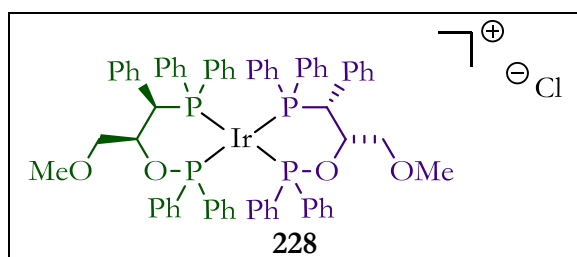
2.3.2.4 IRIIDIUM COMPLEXES **227** AND **228**

To a solution of $[\text{Ir}(\mu\text{-Cl})(\text{cod})]_2$ (0.5 equiv) in DCM was added a solution of the corresponding P-OP ligand (2.0 equiv) and stirred at room temperature for 16h. The resulting filtrate was evaporated *in vacuo* to yield the desired iridium complexes **227** and **228** as orange powders.



$[\text{Ir}(\text{Cl})(\mathbf{133b})_2]$ (**227**). Iridium complex **227** was prepared following the general procedure starting from **133b** (31.60 mg, 0.03986 mmol) and $[\{\text{Ir}(\mu\text{-Cl})(\text{cod})\}_2]$ (6.37 mg, 0.00949 mmol). It was obtained as an intense orange solid (32.0 mg, 85% yield); ^1H NMR (400 MHz, CD_2Cl_2): δ 7.95-6.90 (m, 76H), 5.84 (d,

$J = 8.4$ Hz, 2H), 4.35 (bs, 2H), 4.30-4.22 (m, 2H), 2.97 (dd, $J = 10.4$ Hz, $J = 7.3$ Hz, 2H), 2.87 (dd, $J = 10.4$ Hz, $J = 5.5$ Hz, 2H); $^{13}\text{C}\{^1\text{H}\}$ NMR (100 MHz, CD_2Cl_2): δ 148.8 (C), 148.2 (C), 143.1 (C), 132.7 (CH), 132.5 (CH), 132.4 (C), 131.3 (CH), 130.4 (CH), 130.0 (CH), 129.7 (CH), 129.6 (C), 129.32 (CH), 129.30 (CH), 129.2 (CH), 128.6 (CH), 128.5 (C), 128.3 (CH), 128.1 (CH), 127.6 (CH), 127.3 (CH), 127.0 (CH), 126.8 (CH), 126.4 (CH), 122.3 (CH), 121.6 (CH), 87.4 (C), 76.2 (CH), 63.8 (CH_2), 43.0 (d, $J = 16.6$ Hz, CH); $^{31}\text{P}\{^1\text{H}\}$ NMR (162 MHz, CD_2Cl_2): δ 129.0 (t, $J = 45.5$ Hz, P-O), 17.5 (t, $J = 45.5$ Hz, P-C); MS (ESI⁺) calcd for $\text{C}_{104}\text{H}_{84}\text{O}_8\text{P}_4^{191}\text{Ir} [(\text{M}-\text{Cl})^+]$ 1777.47, found 1777.50.



$[\text{Ir}(\text{Cl})(\mathbf{21a})_2]$ (**228**). Iridium complex **228** was prepared following the general procedure starting from **21a** (50.11 mg, 0.0937 mmol) and $[\{\text{Ir}(\mu\text{-Cl})(\text{cod})\}_2]$ (14.98 g, 0.0223 mmol). It was obtained as an intense orange

solid (58.5 g, 90% yield); ^1H NMR (500 MHz, CD_2Cl_2): δ 8.30-7.90 (m, 10H), 7.80-6.60 (m, 36H), 6.35-6.15 (m, 4H), 4.10-4.00 (m, 2H), 3.83-3.56 (m, 2H), 3.04 (s, 6H), 3.08-2.93 (m, 4H); $^{13}\text{C}\{^1\text{H}\}$ NMR (100 MHz, CD_2Cl_2): δ 137.4 (CH), 137.2 (CH), 133.7 (C), 133.1 (d, $J = 19.8$ Hz, C), 132.6 (CH), 132.1 (CH), 131.0 (d, $J = 9.3$ Hz, CH), 130.4 (d, $J = 10.9$ Hz, CH), 129.9 (CH), 128.5 (CH), 128.2 (d, $J = 10.9$ Hz, CH), 128.0 (d, $J = 10.2$ Hz, CH), 127.9 (d, $J = 8.3$ Hz, CH), 127.8 (d, $J = 5.2$ Hz, CH), 127.1 (d, $J = 4.8$ Hz, CH), 127.0 (d, $J = 4.8$ Hz, CH), 73.8 (CH_2), 73.0 (d, $J = 4.2$ Hz, C), 58.6 (CH_3), 42.6 (d, $J = 32.5$ Hz, CH); $^{31}\text{P}\{^1\text{H}\}$ NMR (162 MHz, CD_2Cl_2): δ 102.8-100.2 (m, P-O), 10.5-6.5 (m, P-C). HRMS (ESI⁺) calcd for $\text{C}_{68}\text{H}_{64}\text{O}_4\text{P}_4^{191}\text{Ir} [(\text{M}-\text{Cl})^+]$ 1259.3361, found 1259.3414.

2.3.3 Preparation and Characterization of Substrates

2-methylquinoline (**231a**), 6-fluoro-2-methylquinoline (**231e**), 2,6-dimethylquinoline (**231f**), 6-methoxy-2-methylquinoline (**231g**), 2-phenylquinoline (**231i**), 2-methylquinoxaline (**233a**), 2-methyl-1*H*-indole (**238a**), 5-fluoro-2-methyl-1*H*-indole (**238d**), 2,5-dimethyl-1*H*-indole (**238e**), 2,3,4,9-tetrahydro-1*H*-carbazole (**238f**), 1*H*-indole-2-carboxylic acid (**238g**) and 2-phenyl-1*H*-indole (**238h**) are all commercially available substrates which were used as received.

(*E*)-*N*-(1-phenylethylidene)aniline³⁸³ (**229a**), (*E*)-*N*-(1-(4-methoxyphenyl)ethylidene)aniline³⁸⁴ (**229b**), (*E*)-*N*-(1-(4-chlorophenyl)ethylidene)aniline³⁸⁵ (**229c**), (*E*)-4-chloro-*N*-(1-phenylethylidene)aniline³⁸⁴ (**229d**), (*E*)-*N*-(1-(*p*-tolyl)ethylidene)aniline³⁸⁶ (**229e**), (*E*)-*N*-(1-(*o*-tolyl)ethylidene)aniline³⁸⁷ (**229f**) are all known compounds and were synthesized using the following procedure: A parallel reactor Mettler Miniblock was charged with molecular sieves (7 g, 4 Å, rods) previously activated in a microwave oven (500 W, 2 min, followed by cool down *in vacuo*), 12 mL of dry toluene, 10 mmol of 1-phenylethanone derivative and 10 mmol of aniline derivative. The resulting mixture was stirred at 80 °C for 65h. Once the reaction was complete and cooled down, the resulting mixture was filtrated through a celite pad, washed with 5 ml of toluene and evaporated. Resulting brownish oil was purified in a Kugelrohr (150-200°C, 5·10⁻² mbar), affording pale yellow compounds in pure form. Spectroscopic data were in agreement with previously reported in literature.

³⁸³ Schnider, P.; Koch, G.; Pretot, R.; Wang, G.; Bohnen, F. M.; Kruger, C.; Pfaltz, A. *Chem.-Eur. J.* **1997**, *3*, 887.

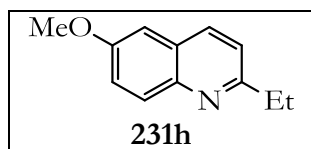
³⁸⁴ Imamoto, T.; Iwadate, N.; Yoshida, K. *Org. Lett.* **2006**, *8*, 2289.

³⁸⁵ Gautier, F.-M.; Jones, S.; Martin, S. J. *Org. Biomol. Chem.* **2009**, *7*, 229.

³⁸⁶ Zhu, S.-F.; Xie, J.-B.; Zhang, Y.-Z.; Li, S.; Zhou, Q.-L. *J. Am. Chem. Soc.* **2006**, *128*, 12886.

³⁸⁷ Hansen, M. C.; Buchwald, S. L. *Org. Lett.* **2000**, *2*, 713.

2-propylquinoline³⁸⁸ (**231b**), 2-butylquinoline³⁸⁹ (**231c**) and 2-isobutylquinoline³⁹⁰ (**231d**) were prepared following reported procedures.³⁵⁷ Spectroscopic data for these compounds were in perfect agreement with the reported ones.



2-ethyl-6-methoxyquinoline (**231h**) Compound **231h** was synthesized following the previous reported³⁵⁷ experimental procedure starting from commercially available **231g**. It was obtained as yellow oil (98% yield). ¹H NMR (400 MHz, CDCl₃) δ 7.97-7.92 (m, 2H), 7.34-7.31 (m, 1H), 7.27-7.24 (m, 1H), 7.04-7.03 (m, 1H), 3.90 (s, 3H), 2.96 (q, *J* = 7.6 Hz, 2H), 1.38 (t, *J* = 7.6 Hz, 3H); DEPTQ 135 (100 MHz, CDCl₃) δ 161.5 (C), 157.2 (C), 143.9 (C), 135.2 (CH), 130.2 (CH), 127.5 (C), 121.8 (CH), 121.0 (CH), 105.2 (CH), 55.5 (CH₃), 32.0 (CH₂), 14.1 (CH₃); HRMS (ESI⁺) calcd for C₁₂H₁₄NO [(M+H)⁺] 188.1075, found 188.1070.

2-butyl-1*H*-indole (**238b**) and 2-benzyl-1*H*-indole (**238c**) were prepared following reported procedures^{361d} and spectroscopic data for these compounds were in perfect agreement with the reported ones.

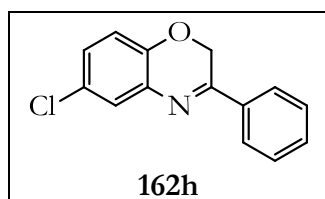
Benzoxazines **162** were synthesized using the following procedure:³⁷² The appropriate 2-aminophenol derivative (4 mmol) and CH₂Cl₂ (80 mL) were added to a 250 mL round bottom flask, then 20% aqueous K₂CO₃ solution (80 mL) and *n*-Bu₄NHSO₄ (136 mg, 0.4 mmol) were added. The adequate 2-bromoacetophenone (4 mmol) was dissolved in 30 mL CH₂Cl₂ and then added slowly to the reaction mixture. Then it was stirred at room temperature for 48 h. The organic layer was washed with water (30 mL) and brine (20 mL), dried over anhydrous MgSO₄. The solvent was removed *in vacuo* and the crude product was purified by flash chromatography (SiO₂) using *n*-hexane/EtOAc mixtures of increasing polarity as the eluent. If required, the isolated product after chromatography was further recrystallized from EtOH to obtain the corresponding benzoxazines.

³⁸⁸ Vieira, P. C.; Kubo, I. *Phytochemistry* **1990**, *29*, 813.

³⁸⁹ O'Byrne, A.; Evans, P. *Tetrahedron* **2008**, *64*, 8067.

³⁹⁰ Lewis, J. C.; Bergman, R. G.; Ellman, J. A. *J. Am. Chem. Soc.* **2007**, *129*, 5332.

3-phenyl-2*H*-benzo[*b*][1,4]oxazine³⁹¹ (**162a**), 3-(4-bromophenyl)-2*H*-benzo[*b*][1,4]oxazine³⁹¹ (**162b**), 3-(4-chlorophenyl)-2*H*-benzo[*b*][1,4]oxazine³⁹² (**162c**), 3-(*p*-tolyl)-2*H*-benzo[*b*][1,4]oxazine³⁹¹ (**162d**), 3-(4-methoxyphenyl)-2*H*-benzo[*b*][1,4]oxazine³⁹¹ (**162e**), 3-([1,1'-biphenyl]-4-yl)-2*H*-benzo[*b*][1,4]oxazine³⁹³ (**162f**) and 3-(3-bromophenyl)-2*H*-benzo[*b*][1,4]oxazine (**162g**) are known compounds and their physical and spectroscopic data were in agreement with the reported ones.



6-chloro-3-phenyl-2*H*-benzo[*b*][1,4]oxazine (**162h**): Pale brown solid, M.p. = 96-99 °C, 63% yield, IR absorption (neat) ν 1608, 1561, 1478, 1446; ¹H NMR (500 MHz, CDCl₃) δ 7.97-7.88, (m, 2H) 7.55-7.45 (m, 3H), 7.42 (d, *J* = 2.6 Hz, 1H), 7.10 (dd, *J* = 8.6 Hz, *J* = 2.6 Hz, 1H), 6.84 (d, *J* = 8.6 Hz, 1H), 5.06 (s, 2H); ¹³C{¹H} NMR (125 MHz, CDCl₃) δ 159.8 (C), 145.0 (C), 135.0 (C), 134.6 (C), 131.6 (CH), 128.8 (CH), 128.2 (CH), 127.5 (CH), 126.9 (C), 126.6 (CH), 116.6 (CH), 63.0 (CH₂); HRMS (ESI⁺) calcd for C₁₄H₁₁ClNO [(M+H)⁺] 244.0524, found 244.0522.

Benzoxazinones **242** were synthesized using the following procedure:³⁷⁴ The appropriate 2-aminophenol derivative (6.0 mmol) and the corresponding α -ketoester³⁹⁴ (6.6 mmol) were dissolved in 50 mL of dry ethanol and the resulting mixture was refluxed for 24 h. Then the solution was cooled to rt and the solvent was removed *in vacuo*. The crude product was purified by flash chromatography (SiO₂) using hexane/EtOAc mixtures of increasing polarity as the eluent. If required, the isolated product after chromatography was further recrystallized from EtOH to obtain the corresponding benzoxazinones.

3-phenyl-2*H*-benzo[*b*][1,4]oxazin-2-one³⁹⁵ (**242a**), 3-(*p*-tolyl)-2*H*-benzo[*b*][1,4]oxazin-2-one^{258a} (**242b**), 3-(4-methoxyphenyl)-2*H*-benzo[*b*][1,4]oxazin-2-one^{258a} (**242c**), 6-chloro-3-

³⁹¹ Jiang, Y.; Liu, L.-X.; Yuan, W.-C.; Zhang, X.-M. *Synlett* **2012**, 23, 1797.

³⁹² Shridhar, D. R.; Sastry, C. V. R.; Bansal, O. P.; Rao, P. P. *Synthesis* **1981**, 912.

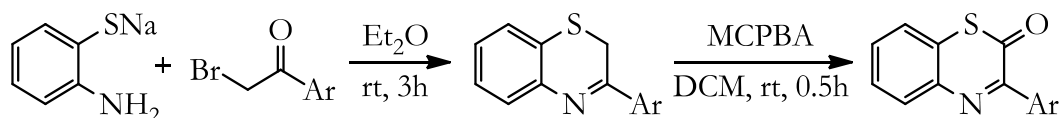
³⁹³ Ding, C.-j.; Wang, Y.; Zhang, W.-w.; Liu, L.; Liang, Y.-j.; Dong, D.-w. *Chem. Res. Chin. Univ.* **2009**, 25, 174.

³⁹⁴ Meng, Q.; Sun, Y.; Ratovelomanana-Vidal, V.; Genet, J. P.; Zhang, Z. *J. Org. Chem.* **2008**, 73, 3842.

³⁹⁵ Miyabe, H.; Yamaoka, Y.; Takemoto, Y. *J. Org. Chem.* **2006**, 71, 2099.

phenyl-2*H*-benzo[*b*][1,4]oxazin-2-one^{258a} (**242d**) and 6-(*tert*-butyl)-3-phenyl-2*H*-benzo[*b*][1,4]oxazin-2-one^{258a} (**242e**) are known compounds and their physical and spectroscopic data were in agreement with the reported ones.

Benzothiazin-2-ones **244** were prepared in a two-step synthesis through their corresponding benzothiazines as follow:³⁷⁵



A solution of NaOMe (504 mg, 9.33 mmol) in anhydrous MeOH (7 mL) was placed in a Schlenk tube. *o*-Aminobenzenethiol (1.192 g, 1.02 mL, 9.33 mmol) was added to the previous solution and the resulting mixture was allowed to stir at rt for 1h to form the sodium *o*-aminobenzenethiolate. Solvent was then evaporated *in vacuo* and dry Et₂O (8 mL) was subsequently added. A solution of the corresponding 2-bromo-1-arylethanone (6.22 mmol) in Et₂O (7 mL) was drop wise added to the previous suspension. The reaction mixture was stirred at room temperature until TLC analysis indicated that there was no unreacted 2-bromo-1-phenylethanone (ca 3h). NaBr was filtered off and the organic solvent was removed under reduced pressure to obtain a yellow residue that was purified by flash chromatography (SiO₂) using hexane/EtOAc mixtures of increasing polarity as the eluent to give the corresponding benzothiazines, which were further oxidized to the desired benzothiazin-2-ones.

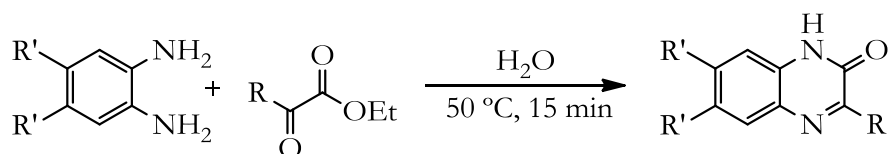
To synthesize 3-aryl-2*H*-benzo[*b*][1,4]thiazin-2-ones **244**, solid MCPBA (*m*-chloroperbenzoic acid, 662 mg, 2.96 mmol) was added to a solution of the previously prepared 2*H*-1,4-benzothiazine derivative (0.985 mmol) in CH₂Cl₂ (25 mL) and the mixture was stirred for 30 min at room temperature. The mixture was then poured in water (25 mL), neutralized with NaHCO₃, and extracted with CH₂Cl₂ (3 × 50 mL). The organic extracts were dried over MgSO₄. The solvent was removed under reduced pressure to obtain a dark residue, which was purified by flash chromatography (SiO₂) using CH₂Cl₂ as the eluent to give the desired 2*H*-1,4-benzothiazin-2-ones **244a-c** as yellow solids.

3-phenyl-2*H*-benzo[*b*][1,4]thiazin-2-one³⁹⁶ (**244a**), 3-(4-methoxyphenyl)-2*H*-benzo[*b*][1,4]thiazin-2-one³⁷⁵ (**244c**) and 3-phenyl-2*H*-benzo[*b*][1,4]thiazine³⁹⁷ (**244d**) are known compounds and their physical and spectroscopic data were in agreement with the reported ones.



3-(*p*-tolyl)-2*H*-benzo[*b*][1,4]thiazin-2-one (**244b**): Yellow solid, M.p. = 114-116 °C, 31% yield, IR absorption (neat) ν 1655, 1631, 1589, 1563; ^1H NMR (400 MHz, CDCl_3) δ 8.04-7.98 (m, 2H), 7.97-7.93 (m, 1H), 7.53-7.43 (m, 2H), 7.41-7.36 (m, 1H), 7.31-7.25 (m, 2H), 2.42 (s, 3H); $^{13}\text{C}\{^1\text{H}\}$ NMR (100 MHz, CDCl_3) δ 178.5 (C), 152.2 (C), 141.1 (C), 136.6 (C), 133.2 (CH), 132.2 (C), 129.8 (CH), 129.3 (CH), 129.0 (CH), 128.7 (C), 127.7 (CH), 125.4 (CH), 21.5 (CH_3); HRMS (ESI⁺) calcd for $\text{C}_{15}\text{H}_{11}\text{N}_2\text{OS}$ [(M+Na)⁺] 276.0454, found 276.0455.

Unprotected 3-substituted quinoxalin-2(1*H*)-ones **246a-c** were prepared by a Hinsberg reaction as follows:³⁷⁶

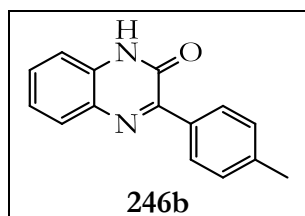


The corresponding benzene-1,2-diamine derivative (15.0 mmol) was dissolved in H_2O (45 mL) at 50 °C, and the corresponding α -keto ester (15.0 mmol) was added to the previous solution. After a short period of time (ca 15 min.), product precipitated from H_2O . The crude product was filtered and dissolved in hot EtOH (5 mL/mmol). The resulting supersaturated solution was allowed to cool down to rt and was further cooled in the refrigerator. The solid precipitate was filtered, dried, and analyzed.

³⁹⁶ Hori, M.; Kataoka, T.; Shimizu, H.; Imai, Y. *Chem. Pharm. Bull.* **1979**, 27, 1982.

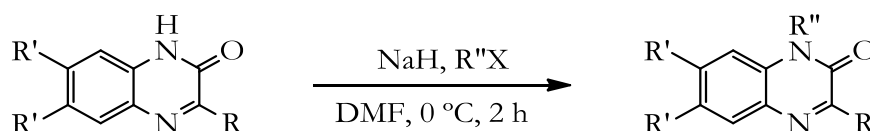
³⁹⁷ Wilhelm, M.; Schmidt, P. J. *Heterocycl. Chem.* **1969**, 6, 635.

3-phenylquinoxalin-2(1*H*)-one³⁷⁶ (**246a**) and 3,6,7-trimethylquinoxalin-2(1*H*)-one³⁹⁸ (**246c**) are known compounds and their physical and spectroscopic data were in agreement with the reported ones.



3-(*p*-tolyl)quinoxalin-2(1*H*)-one (**246b**): Pale yellow solid, M.p. = 230-232 °C, 39% yield, IR absorption (neat) ν 2889, 1668, 1595; ¹H NMR (500 MHz, CDCl₃) δ 8.37-8.32 (m, 2H), 7.96-7.91 (m, 1H), 7.53-7.48 (m, 1H), 7.39-7.27 (m, 4H), 2.45 (s, 3H); ¹³C{¹H} NMR (125 MHz, CDCl₃) δ 156.0 (C), 154.4 (C), 140.9 (C), 133.2 (C), 132.8 (C), 131.0 (C), 130.1 (CH), 129.6 (CH), 129.5 (CH), 129.0 (CH), 124.3 (CH), 115.0 (CH), 21.6 (CH₃); HRMS (ESI⁺) calcd for C₁₅H₁₂N₂NaO [(M+Na)⁺] 259.0842, found 259.0842.

N-Alkylated 3-substituted quinoxalin-2(1*H*)-ones **246d-i** were prepared using the following general procedure:³⁷⁴

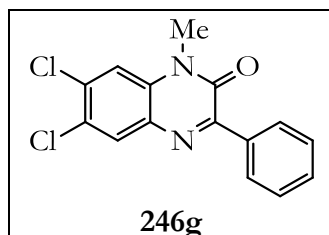


The desired unprotected quinoxalinone (2.0 mmol) was dissolved in dry DMF (15 mL) and the solution was cooled to 0 °C. NaH (6.0 mmol, 240 mg @ 60% dispersion in mineral oil) was then added and the reaction mixture allowed to stir until no more H₂ evolved. The selected electrophile (methyl iodide, bromomethyl methyl ether or bromomethylbenzene, 6.0 mmol) was then added. The mixture was stirred at 0 °C for another 2 h, and then quenched with glacial acetic acid (16 mmol, 0.92 mL). The reaction mixture was poured into H₂O (60 mL) and extracted with EtOAc (3×40 mL). The organic layer was washed with saturated NaHCO₃ (2×15 mL) and brine (1×15 mL) and then dried over MgSO₄. The solvent was removed *in vacuo* to give a solid that was purified by flash

³⁹⁸ Li, X.; Wang, D.; Wu, J.; Xu, W. *Heterocycles* **2005**, *65*, 2741.

chromatography (SiO₂) using hexane/EtOAc mixtures of increasing polarity as the eluent to give the corresponding *N*-alkylated 3-substituted quinoxalin-2(1*H*)-one.

N-alkylated-3-Substituted quinoxalin-2(1*H*)-ones **246d**, **246e**, **246f**, **246h** and **246i** are known compounds³⁷⁴ and their physical and spectroscopic data were in agreement with the reported ones.



6,7-dichloro-1-methyl-3-phenylquinoxalin-2(1*H*)-one (**246g**):

Pale brown solid, M.p. = 186-189 °C, 88% yield, IR absorption (neat) ν 3093, 3060, 2923, 1650, 1594, 1560; ¹H NMR (500 MHz, CDCl₃) δ 8.33-8.27 (m, 2H), 8.00 (s, 1H), 7.54-7.45 (m, 3H), 7.40

(s, 1H), 3.70 (s, 3H); ¹³C{¹H} NMR (125 MHz, CDCl₃) δ 155.1 (C), 154.1 (C), 135.4 (C), 134.3 (C), 132.7 (C), 132.1 (C), 131.1 (CH), 130.9 (CH), 129.6 (CH), 128.2 (CH), 127.5 (C), 115.0 (CH), 29.5 (CH₃); HRMS (ESI⁺) calcd for C₁₅H₁₀Cl₂N₂NaO [(M+Na)⁺] 327.0062, found 327.0068.

2.3.4 General Procedure for the Ir-Mediated Asymmetric Hydrogenation

Method A. *In situ* preparation of the catalyst: A solution of the required amount of iridium precursor ($[\{\text{Ir}(\mu\text{-Cl})(\text{cod})\}_2]$) (0.005 mmol) and the *P-OP* ligand (0.011 mmol) in the corresponding dry and deoxygenated solvent (5.0 mL) was loaded into an autoclave under N_2 atmosphere, in which the required amounts of substrate (1 mmol) and additives (if necessary) were placed beforehand. In all cases the molar concentration of the substrate in the reaction medium was adjusted to a final 0.20 M concentration.

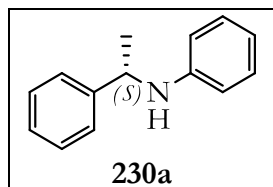
The autoclave was purged three times with H_2 (at a pressure not higher than the selected one) and finally, the autoclave was pressurized with H_2 to the desired pressure. The reaction mixture was stirred at the desired temperature for the stated reaction time. The autoclave was subsequently depressurized, the reaction mixture passed through a short pad of SiO_2 and further eluted with EtOAc (2 x 1 mL). The resulting solution was evaporated *in vacuo*. In reactions that require a basic workup (*i. e.* those ones which imply the addition of 1 equivalent of a Brønsted acid), after carefully releasing the hydrogen, the resulting mixture was concentrated under vacuum and dissolved in saturated aqueous NaHCO_3 (4 mL). After stirring for 10 min, the mixture was extracted with CH_2Cl_2 (2x4 mL), dried over MgSO_4 and then passed through a short pad of SiO_2 and evaporated *in vacuo*. The conversion was determined by ^1H NMR and enantioselectivities were determined by HPLC analysis on chiral stationary phases.

Method B. Pre-formed catalyst: A solution of the required amount of $[\text{Ir}(\text{cod})(\text{P-OP})]\text{BArF}$ or $[\text{Ir}(\text{cod})(\text{P-OP})]\text{BF}_4$ in the corresponding dry and deoxygenated solvent (5.0 mL) was loaded into an autoclave under N_2 atmosphere, in which the required amounts of substrate (1 mmol) and additives (if necessary) were placed beforehand. In all cases the molar concentration of the substrate in the reaction medium was adjusted to a final 0.20 M concentration.

The autoclave was purged three times with H_2 (at a pressure not higher than the selected one) and finally, the autoclave was pressurized with H_2 to the desired pressure. The reaction mixture was stirred at the desired temperature for the stated reaction time. The autoclave

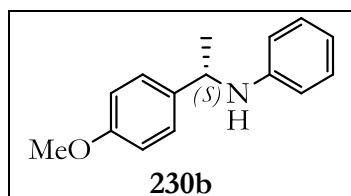
was subsequently depressurized, the reaction mixture passed through a short pad of SiO₂ and further eluted with EtOAc (2 x 1 mL). The resulting solution was evaporated *in vacuo*. In reactions that require a basic workup (*i. e.* those ones which imply the addition of 1 equivalent of a Brønsted acid), after carefully releasing the hydrogen, the resulting mixture was concentrated under vacuum and dissolved in saturated aqueous NaHCO₃ (4 mL). After stirring for 10 min, the mixture was extracted with CH₂Cl₂ (2×4 mL), dried over MgSO₄ and then passed through a short pad of SiO₂ and evaporated *in vacuo*. The conversion was determined by ¹H NMR and enantioselectivities were determined by HPLC analysis on chiral stationary phases.

2.3.5 Characterization of Hydrogenation Products and Determination of the Enantiomeric Excesses

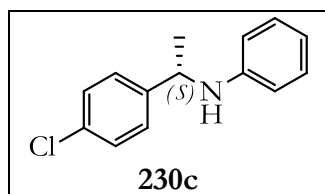


22.0 min.

(*S*)-*N*-(1-phenylethyl)aniline (**230a**): Known compound,³⁸⁴ HPLC conditions: Daicel Chiralcel[®] OD-H (25 cm x 0.46 cm), 98:2 *n*-hexane/2-propanol, 0.50 mL/min, 254 nm, $t_R(S) = 17.7$ min, $t_R(R) =$

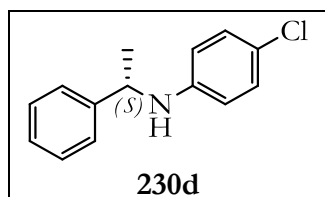


(*S*)-*N*-(1-(4-methoxyphenyl)ethyl)aniline (**230b**): Known compound,³⁹⁹ HPLC conditions: Daicel Chiralcel[®] OD-H (25 cm x 0.46 cm), 99:1 *n*-hexane/2-propanol, 0.50 mL/min, 254 nm, $t_R(S) = 33.6$ min, $t_R(R) = 36.7$ min.



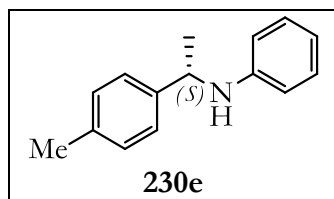
$t_R(S) = 23.4$ min, $t_R(R) = 28.1$ min.

(*S*)-*N*-(1-(4-chlorophenyl)ethyl)aniline (**230c**): Known compound,^{249b} HPLC conditions: Daicel Chiralcel[®] OD-H (25 cm x 0.46 cm), 97:3 *n*-hexane/2-propanol, 0.50 mL/min, 254 nm,

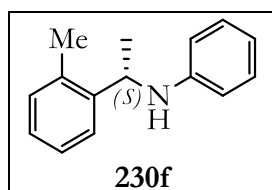


(*S*)-4-chloro-*N*-(1-phenylethyl)aniline (**230d**): Known compound,³⁸⁴ HPLC conditions: Daicel Chiralcel[®] OD-H (25 cm x 0.46 cm), 97:3 *n*-hexane/2-propanol, 0.50 mL/min, 254 nm, $t_R(S) = 17.5$ min, $t_R(R) = 22.3$ min.

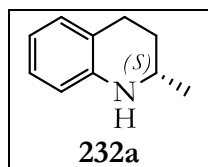
³⁹⁹ Trifonova, A.; Diesen, J. S.; Chapman, C. J.; Andersson, P. G. *Org. Lett.* **2004**, *6*, 3825.



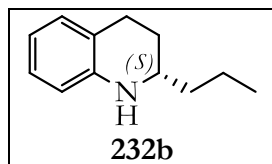
(*S*)-*N*-(1-(*p*-tolyl)ethyl)aniline (**230e**): Known compound,³⁸⁶
HPLC conditions: Daicel Chiralcel[®] OD-H (25 cm x 0.46 cm),
99:1 *n*-hexane/2-propanol, 0.50 mL/min, 254 nm, $t_R(S)$ = 18.2
min, $t_R(R)$ = 20.8 min.



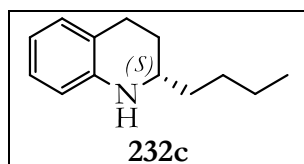
(*S*)-*N*-(1-(*o*-tolyl)ethyl)aniline (**230f**): Known compound,³⁹⁹ HPLC
conditions: Daicel Chiralcel[®] OD-H (25 cm x 0.46 cm), 99:1 *n*-
hexane/2-propanol, 0.50 mL/min, 254 nm, $t_R(S)$ = 19.5 min, $t_R(R)$ =
20.5 min.



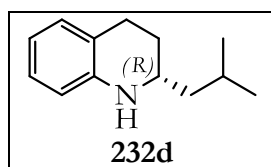
(*S*)-2-methyl-1,2,3,4-tetrahydroquinoline (**232a**): Known compound,^{361b}
HPLC conditions: Daicel Chiralcel[®] OJ-H (25 cm x 0.46 cm), 95:5 *n*-
hexane/2-propanol, 0.50 mL/min, 254 nm, $t_R(S)$ = 22.6 min, $t_R(R)$ = 25.2
min.



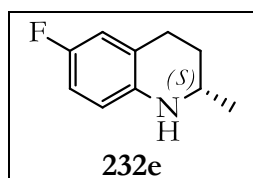
(*S*)-2-propyl-1,2,3,4-tetrahydroquinoline (**232b**): Known
compound,^{361b} HPLC conditions: Daicel Chiralcel[®] OJ-H (25 cm x
0.46 cm), 95:5 *n*-hexane/2-propanol, 0.50 mL/min, 254 nm, $t_R(S)$ =
16.5 min, $t_R(R)$ = 20.7 min.



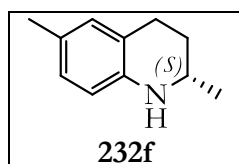
(*S*)-2-butyl-1,2,3,4-tetrahydroquinoline (**232c**): Known
compound,^{361b} HPLC conditions: Daicel Chiralcel[®] OJ-H (25 cm x
0.46 cm), 95:5 *n*-hexane/2-propanol, 0.50 mL/min, 254 nm, $t_R(S)$ =
12.9 min, $t_R(R)$ = 14.9 min.



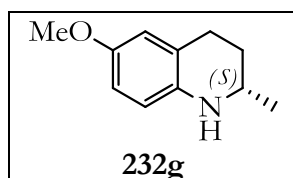
(*R*)-2-isobutyl-1,2,3,4-tetrahydroquinoline (**232d**): Known compound,^{338a} HPLC conditions: Daicel Chiralcel[®] OJ-H (25 cm x 0.46 cm), 95:5 *n*-hexane/2-propanol, 0.50 mL/min, 254 nm, $t_R(S)$ = 13.4 min, $t_R(R)$ = 17.6 min.



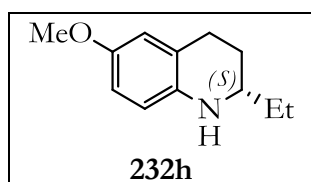
(*S*)-6-fluoro-2-methyl-1,2,3,4-tetrahydroquinoline (**232e**): Known compound,^{361b} HPLC conditions: Daicel Chiralcel[®] OJ-H (25 cm x 0.46 cm), 94:6 *n*-hexane/2-propanol, 0.50 mL/min, 254 nm, $t_R(S)$ = 8.6 min, $t_R(R)$ = 9.0 min.



(*S*)-2,6-dimethyl-1,2,3,4-tetrahydroquinoline (**232f**): Known compound,^{361b} HPLC conditions: Daicel Chiralcel[®] OJ-H (25 cm x 0.46 cm), 90:10 *n*-hexane/2-propanol, 0.50 mL/min, 254 nm, $t_R(S)$ = 24.3 min, $t_R(R)$ = 30.9 min.

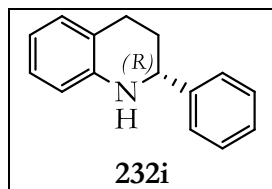


(*S*)-6-methoxy-2-methyl-1,2,3,4-tetrahydroquinoline (**232g**): Known compound,^{361b} HPLC conditions: Daicel Chiralcel[®] OJ-H (25 cm x 0.46 cm), 90:10 *n*-hexane/2-propanol, 0.50 mL/min, 254 nm, $t_R(S)$ = 34.9 min, $t_R(R)$ = 44.7 min.

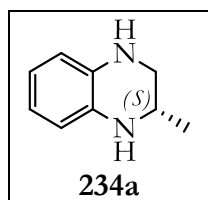


(*S*)-2-ethyl-6-methoxy-1,2,3,4-tetrahydroquinoline (**232h**): White solid, 87% ee, $[\alpha]_D^{27} = -32.1$ (*c* 0.19, CHCl₃); ¹H NMR (400 MHz, CDCl₃) δ 6.62-6.58 (m, 2H), 6.47 (d, *J* = 8.4 Hz, 1H), 3.74 (s, 3H), 3.34 (bs, 1H), 3.14-3.08 (m, 1H), 2.88-2.69 (m, 2H), 2.01-1.94 (m, 1H), 1.64-1.50 (m, 3H), 1.00 (t, *J* = 7.5 Hz, 3H); DEPTQ 135 (100 MHz, CDCl₃) δ 151.8 (C), 138.8 (C), 122.8 (C), 115.3 (CH), 114.6 (CH), 112.9 (CH), 55.8 (CH₃), 53.4 (CH), 29.3 (CH₂), 27.8 (CH₂), 26.8 (CH₂), 10.1 (CH₃); HRMS (ESI⁺) calcd for C₁₂H₁₈NO [(M+H)⁺] 192.1388, found 192.1387;

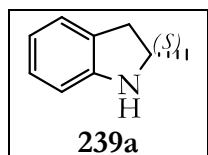
HPLC conditions: Daicel Chiralcel[®] OJ-H (25 cm x 0.46 cm), 90:10 *n*-hexane/2-propanol, 0.50 mL/min, 254 nm, $t_R(-) = 30.4$ min, $t_R(+) = 36.7$ min.



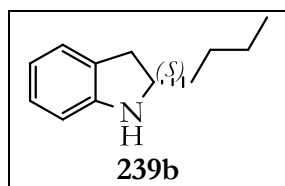
(*R*)-2-phenyl-1,2,3,4-tetrahydroquinoline (**232i**): Known compound,³²³ HPLC conditions: Daicel Chiralcel[®] OJ-H (25 cm x 0.46 cm), 90:10 *n*-hexane/2-propanol, 1.00 mL/min, 254 nm, $t_R(S) = 9.9$ min, $t_R(R) = 13.3$ min.



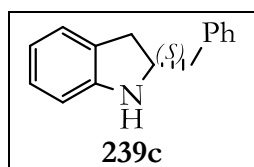
(*S*)-2-methyl-1,2,3,4-tetrahydroquinoxaline (**234a**): Known compound,^{360b} HPLC conditions: Daicel Chiralcel[®] OD-H (25 cm x 0.46 cm), 90:10:0.1 *n*-hexane/2-propanol/ NH_4Et_2 , 0.50 mL/min, 254 nm, $t_R(R) = 13.3$ min, $t_R(S) = 15.6$ min.



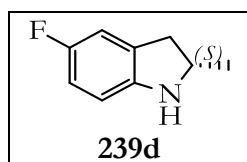
(*S*)-2-methylindoline (**239a**): Known compound,^{361d} HPLC conditions: Daicel Chiralcel[®] OD-H (25 cm x 0.46 cm), 97:3 *n*-hexane/2-propanol, 0.80 mL/min, 254 nm, $t_R(R) = 11.3$ min, $t_R(S) = 13.1$ min.



(*S*)-2-butylindoline (**239b**): Known compound,^{361d} HPLC conditions: Daicel Chiralcel[®] OD-H (25 cm x 0.46 cm), 99:1 *n*-hexane/2-propanol, 1.00 mL/min, 254 nm, $t_R(R) = 8.9$ min, $t_R(S) = 13.2$ min.

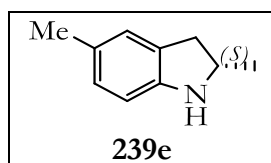


(*S*)-2-benzylindoline (**239c**): Known compound,^{361d} HPLC conditions: Daicel Chiralcel[®] OD-H (25 cm x 0.46 cm), 99:1 *n*-hexane/2-propanol, 1.00 mL/min, 254 nm, $t_R(R) = 16.7$ min, $t_R(S) = 19.5$ min.



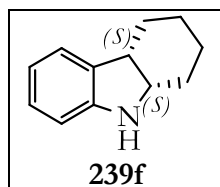
min.

(*S*)-5-fluoro-2-methylindoline (**239d**): Known compound,^{361d} HPLC conditions: Daicel Chiralcel[®] OD-H (25 cm x 0.46 cm), 99:1 *n*-hexane/2-propanol, 1.00 mL/min, 254 nm, $t_R(R)$ = 9.5 min, $t_R(S)$ = 14.5

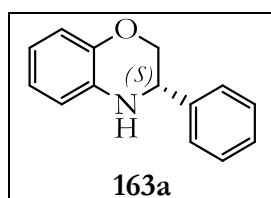


11.7 min.

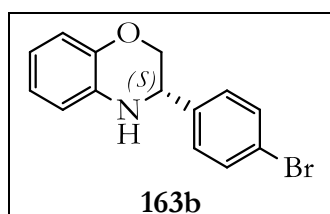
(*S*)-2,5-dimethylindoline (**239e**): Known compound,^{361d} HPLC conditions: Daicel Chiralcel[®] OD-H (25 cm x 0.46 cm), 99:1 *n*-hexane/2-propanol, 1.00 mL/min, 254 nm, $t_R(R)$ = 9.4 min, $t_R(S)$ =



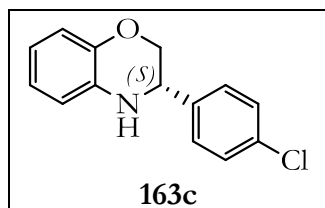
(4*aS*,9*aS*)-2,3,4,4*a*,9,9*a*-hexahydro-1*H*-carbazole (**239f**): Known compound,^{361d} 91% ee, $[\alpha]_D^{25}$ = -22.7 (*c* 1.20, CHCl₃) [lit.:^{361d} $[\alpha]_D^{23}$ = +23.4 (*c* 1.20, CHCl₃) for the 4*aR*,9*aR* enantiomer, 91% ee], HPLC conditions: Daicel Chiralcel[®] IC (25 cm x 0.46 cm), 99:1 *n*-hexane/2-propanol, 1.00 mL/min, 254 nm, $t_R(+)$ = 6.2 min, $t_R(-)$ = 10.2 min.



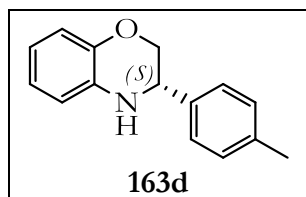
(*S*)-3-phenyl-3,4-dihydro-2*H*-benzo[*b*][1,4]oxazine (**163a**): Known compound,^{253a} 95% ee, $[\alpha]_D^{25}$ = +109.5 (*c* 1.08, CHCl₃) [lit.:^{253a} $[\alpha]_D^{RT}$ = +102.0 (*c* 1.08, CHCl₃) for 88% ee], HPLC conditions: Daicel Chiralcel[®] OD-H (25 cm x 0.46 cm), 80:20 *n*-hexane/2-propanol, 0.6 mL/min, 254 nm, $t_R(R)$ = 16.6 min, $t_R(S)$ = 22.9 min.



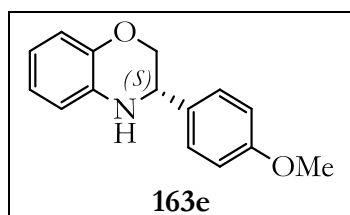
(*S*)-3-(4-bromophenyl)-3,4-dihydro-2*H*-benzo[*b*][1,4]-oxazine (**163b**): Known compound,^{253a} 92% ee, $[\alpha]_D^{25}$ = +91.2 (*c* 1.03, CHCl₃) [lit.:^{253a} $[\alpha]_D^{RT}$ = +89.5 (*c* 1.03, CHCl₃) for 89% ee], HPLC conditions: Daicel Chiralcel[®] OD-H (25 cm x 0.46 cm), 70:30 *n*-hexane/2-propanol, 0.7 mL/min, 254 nm, $t_R(R)$ = 13.8 min, $t_R(S)$ = 27.2 min.



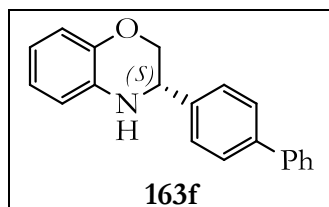
(*S*)-3-(4-chlorophenyl)-3,4-dihydro-2*H*-benzo[*b*][1,4]-oxazine (**163c**): Known compound,^{253a} 91% ee, $[\alpha]_{\text{D}}^{25} = +58.8$ (c 0.70, CHCl₃) [lit.:^{253a} $[\alpha]_{\text{D}}^{\text{RT}} = +59.1$ (c 0.70, CHCl₃) for 90% ee], HPLC conditions: Daicel Chiralcel[®] OD-H (25 cm x 0.46 cm), 70:30 *n*-hexane/2-propanol, 0.7 mL/min, 254 nm, $t_{\text{R}}(\text{R}) = 14.7$ min, $t_{\text{R}}(\text{S}) = 27.8$ min.



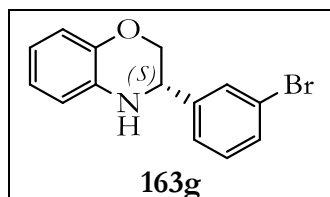
(*S*)-3-(*p*-tolyl)-3,4-dihydro-2*H*-benzo[*b*][1,4]oxazine (**163d**): Known compound,^{253a} 91% ee, $[\alpha]_{\text{D}}^{25} = +68.1$ (c 0.92, CHCl₃) [lit.:^{253a} $[\alpha]_{\text{D}}^{\text{RT}} = +66.8$ (c 0.92, CHCl₃) for 86% ee], HPLC conditions: Daicel Chiralcel[®] OD-H (25 cm x 0.46 cm), 70:30 *n*-hexane/2-propanol, 0.6 mL/min, 254 nm, $t_{\text{R}}(\text{R}) = 11.7$ min, $t_{\text{R}}(\text{S}) = 21.5$ min.



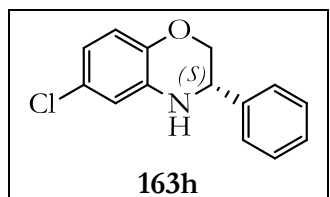
(*S*)-3-(4-methoxyphenyl)-3,4-dihydro-2*H*-benzo[*b*]-[1,4]oxazine (**163e**): Known compound,^{255a} 91% ee, $[\alpha]_{\text{D}}^{25} = +53.2$ (c 1.00, CHCl₃) [lit.:^{255a} $[\alpha]_{\text{D}}^{\text{RT}} = -55.5$ (c 1.00, CHCl₃) for 98% ee of the (R)-enantiomer], HPLC conditions: Daicel Chiralcel[®] OD-H (25 cm x 0.46 cm), 80:20 *n*-hexane/2-propanol, 0.7 mL/min, 254 nm, $t_{\text{R}}(\text{R}) = 10.0$ min, $t_{\text{R}}(\text{S}) = 16.7$ min.



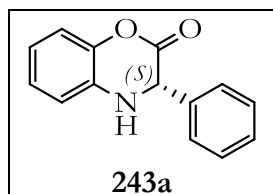
(*S*)-3-([1,1'-biphenyl]-4-yl)-3,4-dihydro-2*H*-benzo[*b*]-[1,4]oxazine (**163f**): Known compound,^{253a} 93% ee, $[\alpha]_{\text{D}}^{25} = +51.3$ (c 1.04, CHCl₃) [lit.:^{253a} $[\alpha]_{\text{D}}^{\text{RT}} = +44.8$ (c 1.04, CHCl₃) for 86% ee], HPLC conditions: Daicel Chiralcel[®] OD-H (25 cm x 0.46 cm), 70:30 *n*-hexane/2-propanol, 0.7 mL/min, 254 nm, $t_{\text{R}}(\text{R}) = 21.9$ min, $t_{\text{R}}(\text{S}) = 31.9$ min.



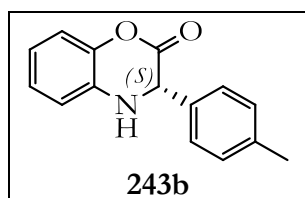
(*S*)-3-(3-bromophenyl)-3,4-dihydro-2*H*-benzo[*b*][1,4]-oxazine (**163g**): Known compound,^{253a} 91% ee, $[\alpha]_{\text{D}}^{25} = +92.2$ (c 1.16, CHCl₃) [lit.:^{253a} $[\alpha]_{\text{D}}^{\text{RT}} = +84.3$ (c 1.16, CHCl₃) for 88% ee], HPLC conditions: Daicel Chiralcel[®] OD-H (25 cm x 0.46 cm), 70:30 *n*-hexane/2-propanol, 0.7 mL/min, 254 nm, $t_{\text{R}}(\text{R}) = 13.4$ min, $t_{\text{R}}(\text{S}) = 20.4$ min.



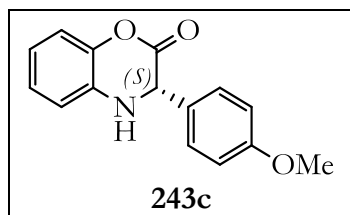
(*S*)-6-chloro-3-phenyl-3,4-dihydro-2*H*-benzo[*b*][1,4]-oxazine (**163h**): Unknown compound, 91% ee, $[\alpha]_{\text{D}}^{25} = +52.6$ (c 1.00, CHCl₃); IR absorption (neat) ν 3378, 3360, 1608, 1495, 1452; ¹H NMR (500 MHz, CDCl₃) δ 7.43-7.33 (m, 5H), 6.78-6.73 (m, 1H), 6.67-6.61 (m, 2H), 4.49 (dd, $J = 8.4$ Hz, $J = 3.0$ Hz, 1H), 4.28 (dd, $J = 10.7$ Hz, $J = 3.0$ Hz, 1H), 4.07 (bs, 1H), 3.96 (dd, $J = 10.7$ Hz, $J = 8.4$ Hz, 1H); ¹³C{¹H} NMR (125 MHz, CDCl₃) δ 142.1 (C), 138.6 (C), 134.8 (C), 128.9 (CH), 128.5 (CH), 127.1 (CH), 126.1 (C), 118.4 (CH), 117.4 (CH), 114.7 (CH), 70.8 (CH₂), 54.0 (CH); HRMS (ESI⁺) calcd for C₁₄H₁₃ClNO [(M+H)⁺] 246.0680, found 246.0685; HPLC conditions: Daicel Chiralcel[®] OD-H (25 cm x 0.46 cm), 80:20 *n*-hexane/2-propanol, 1.0 mL/min, 254 nm, $t_{\text{R}}(\text{R}) = 17.0$ min, $t_{\text{R}}(\text{S}) = 20.1$ min.



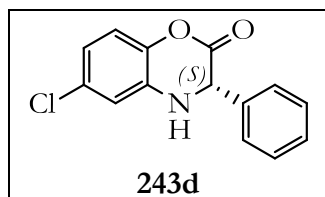
(*S*)-3-phenyl-3,4-dihydro-2*H*-benzo[*b*][1,4]oxazin-2-one (**243a**): Known compound,^{258a} 95% ee, $[\alpha]_{\text{D}}^{25} = +97.5$ (c 0.84, CHCl₃) [lit.:^{258a} $[\alpha]_{\text{D}}^{20} = +98.6$ (c 0.84, CHCl₃) for 98% ee], HPLC conditions: Daicel Chiralcel[®] OD-H (25 cm x 0.46 cm), 80:20 *n*-hexane/2-propanol, 0.6 mL/min, 216 nm, $t_{\text{R}}(\text{R}) = 18.6$ min, $t_{\text{R}}(\text{S}) = 24.6$ min.



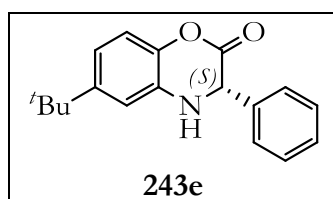
(*S*)-3-(*p*-tolyl)-3,4-dihydro-2*H*-benzo[*b*][1,4]oxazin-2-one (**243b**): Known compound,^{258a} 97% ee, $[\alpha]_{\text{D}}^{25} = +92.0$ (c 0.92, CHCl₃) [lit.:^{258a} $[\alpha]_{\text{D}}^{20} = +92.2$ (c 0.92, CHCl₃) for 99% ee], HPLC conditions: Daicel Chiralcel[®] OD-H (25 cm x 0.46 cm), 70:30 *n*-hexane/2-propanol, 0.7 mL/min, 230 nm, $t_{\text{R}}(\text{R}) = 10.3$ min, $t_{\text{R}}(\text{S}) = 26.8$ min.



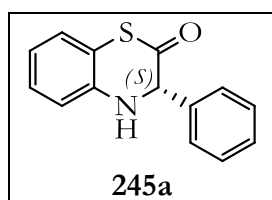
(*S*)-3-(4-methoxyphenyl)-3,4-dihydro-2*H*-benzo[*b*]-[1,4]oxazin-2-one (**243c**): Known compound,^{258a} 99% ee, $[\alpha]_{\text{D}}^{25} = +55.3$ (c 0.98, CHCl₃) [lit.:^{258a} $[\alpha]_{\text{D}}^{20} = +53.2$ (c 0.98, CHCl₃) for 98% ee], HPLC conditions: Daicel Chiralcel[®] OD-H (25 cm x 0.46 cm), 70:30 *n*-hexane/2-propanol, 0.7 mL/min, 230 nm, $t_{\text{R}}(\text{R}) = 12.6$ min, $t_{\text{R}}(\text{S}) = 28.2$ min.



(*S*)-6-chloro-3-phenyl-3,4-dihydro-2*H*-benzo[*b*][1,4]-oxazin-2-one (**243d**): Known compound,^{258a} 89% ee, $[\alpha]_{\text{D}}^{25} = +118.7$ (c 0.84, CHCl₃) [lit.:^{258a} $[\alpha]_{\text{D}}^{20} = +125.2$ (c 0.84, CHCl₃) for 98% ee], HPLC conditions: Daicel Chiralcel[®] OD-H (25 cm x 0.46 cm), 70:30 *n*-hexane/2-propanol, 0.7 mL/min, 230 nm, $t_{\text{R}}(\text{R}) = 11.1$ min, $t_{\text{R}}(\text{S}) = 14.9$ min.

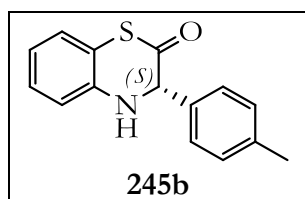


(*S*)-6-(*tert*-butyl)-3-phenyl-3,4-dihydro-2*H*-benzo[*b*]-[1,4]oxazin-2-one (**243e**): Known compound,^{258a} 94% ee, $[\alpha]_{\text{D}}^{25} = +98.8$ (c 0.76, CHCl₃) [lit.:^{258a} $[\alpha]_{\text{D}}^{20} = +100.7$ (c 0.76, CHCl₃) for 98% ee], HPLC conditions: Daicel Chiralcel[®] OD-H (25 cm x 0.46 cm), 70:30 *n*-hexane/2-propanol, 0.7 mL/min, 230 nm, $t_{\text{R}}(\text{R}) = 8.3$ min, $t_{\text{R}}(\text{S}) = 10.9$ min.

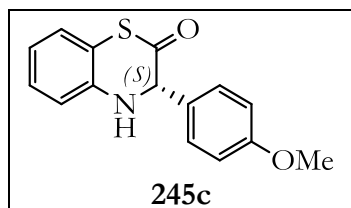


(*S*)-3-phenyl-3,4-dihydro-2*H*-benzo[*b*][1,4]thiazin-2-one (**245a**): Known compound,⁴⁰⁰ 94% ee, $[\alpha]_{\text{D}}^{25} = +102.3$ (c 0.70, CHCl₃), HPLC conditions: Daicel Chiralcel[®] OD-H (25 cm x 0.46 cm), 80:20 *n*-hexane/2-propanol, 0.6 mL/min, 216 nm, $t_{\text{R}}(\text{R}) = 14.8$ min, $t_{\text{R}}(\text{S}) = 18.6$ min.

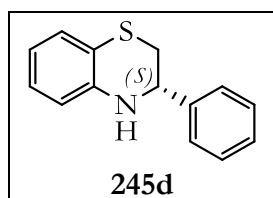
⁴⁰⁰ Ghailane, T.; Saadouni, M.; Boukhris, S.; Habbadi, N.; Hassikou, A.; Kerbal, A.; Garrigues, B.; Souizi, A. *Heterocycles* **2011**, *83*, 357.



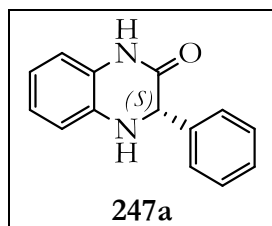
(*S*)-3-(*p*-tolyl)-3,4-dihydro-2*H*-benzo[*b*][1,4]thiazin-2-one (**245b**): Known compound,⁴⁰⁰ 95% ee, $[\alpha]_{\text{D}}^{25} = +112.1$ (*c* 0.70, CHCl₃), HPLC conditions: Daicel Chiralcel[®] OD-H (25 cm x 0.46 cm), 80:20 *n*-hexane/2-propanol, 0.6 mL/min, 220 nm, $t_{\text{R}}(\text{R}) = 13.1$ min, $t_{\text{R}}(\text{S}) = 20.3$ min.



(*S*)-3-(4-methoxyphenyl)-3,4-dihydro-2*H*-benzo[*b*]-[1,4]thiazin-2-one (**245c**): Unknown compound, 96% ee, $[\alpha]_{\text{D}}^{25} = +131.4$ (*c* 0.70, CHCl₃); IR absorption (neat) ν 3341, 1660, 1247, 1036; ¹H NMR (400 MHz, CDCl₃) δ 7.29-7.22 (m, 2H), 7.19-7.11 (m, 2H), 6.97-6.91 (m, 1H), 6.91-6.82 (m, 3H), 4.79 (s, 1H), 4.44 (bs, 1H), 3.79 (s, 3H); ¹³C{¹H} NMR (125 MHz, CDCl₃) δ 197.6 (C), 160.0 (C), 141.5 (C), 129.1 (CH), 128.2 (C), 127.7 (CH), 127.0 (CH), 121.2 (CH), 118.0 (C), 116.8 (CH), 114.4 (CH), 65.9 (CH), 55.3 (CH₃); HRMS (ESI⁺) calcd for C₁₅H₁₃NNaO₂S [(M+Na)⁺] 294.0559, found 294.0562; HPLC conditions: Daicel Chiralcel[®] OD-H (25 cm x 0.46 cm), 80:20 *n*-hexane/2-propanol, 0.6 mL/min, 220 nm, $t_{\text{R}}(\text{R}) = 17.6$ min, $t_{\text{R}}(\text{S}) = 29.2$ min.

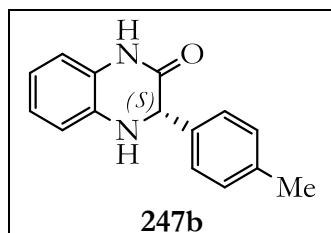


(*S*)-3-phenyl-3,4-dihydro-2*H*-benzo[*b*][1,4]thiazine (**245d**): Unknown compound, 70% ee, $[\alpha]_{\text{D}}^{25} = +24.7$ (*c* 0.70, CHCl₃); IR absorption (neat) ν 3399, 1590, 1478; ¹H NMR (500 MHz, CDCl₃) δ 7.43-7.31 (m, 5H), 7.10-7.05 (m, 1H), 6.97-6.91 (m, 1H), 6.71-6.65 (m, 1H), 6.56-6.51 (m, 1H), 4.68 (dd, *J* = 8.8 Hz, *J* = 2.7 Hz, 1H), 4.13 (bs, 1H), 3.18 (dd, *J* = 12.5 Hz, *J* = 8.8 Hz, 1H), 3.01 (dd, *J* = 12.5 Hz, *J* = 2.7 Hz, 1H); ¹³C{¹H} NMR (125 MHz, CDCl₃) δ 142.9 (C), 142.2 (C), 128.9 (CH), 128.3 (CH), 127.5 (CH), 126.7 (CH), 125.6 (CH), 118.4 (CH), 115.5 (C), 115.4 (CH), 56.2 (CH), 33.2 (CH₂); HRMS (ESI⁺) calcd for C₁₄H₁₃NNaOS [(M+Na+O)⁺] 266.0610, found 266.0613; Anal. Calcd for C₁₄H₁₃NS: C, 73.97; H, 5.76; N, 6.16; S, 14.11. Found: C, 73.26; H, 5.81; N, 6.09; S, 13.28; HPLC conditions: Daicel Chiralcel[®] OD-H (25 cm x 0.46 cm), 85:15 *n*-hexane/2-propanol, 0.3 mL/min, 230 nm, $t_{\text{R}}(\text{R}) = 47.5$ min, $t_{\text{R}}(\text{S}) = 50.2$ min.

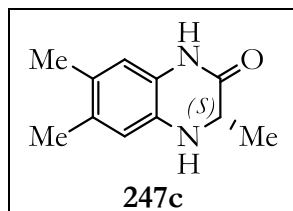


23.3 min.

(*S*)-3-phenyl-3,4-dihydroquinoxalin-2(1*H*)-one (**247a**): Known compound,²⁵⁶ 99% ee, $[\alpha]_{\text{D}}^{25} = +107.9$ (c 1.00, CHCl_3), HPLC conditions: Daicel Chiralcel[®] OD-H (25 cm x 0.46 cm), 80:20 *n*-hexane/2-propanol, 1.0 mL/min, 230 nm, $t_{\text{R}}(\text{S}) = 15.2$ min, $t_{\text{R}}(\text{R}) =$

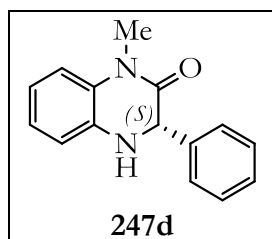


(*S*)-3-(*p*-tolyl)-3,4-dihydroquinoxalin-2(1*H*)-one (**247b**): Unknown compound, 99% ee, $[\alpha]_{\text{D}}^{25} = +81.2$ (c 1.00, CHCl_3); IR absorption (neat) ν 3307, 1673; ^1H NMR (500 MHz, CDCl_3) δ 8.98 (bs, 1H), 7.32-7.27 (m, 2H), 7.16-7.11 (m, 2H), 6.93-6.87 (m, 1H), 6.76-6.65 (m, 3H), 5.02 (d, $J = 1.5$ Hz, 1H), 4.27 (bs, 1H), 2.32 (s, 3H); $^{13}\text{C}\{^1\text{H}\}$ NMR (125 MHz, CDCl_3) δ 167.4 (C), 138.3 (C), 136.2 (C), 133.0 (C), 129.5 (CH), 127.0 (CH), 124.8 (C), 124.0 (CH), 119.3 (CH), 115.6 (CH), 113.7 (CH), 60.5 (CH), 21.2 (CH_3); HRMS (ESI⁺) calcd for $\text{C}_{15}\text{H}_{14}\text{N}_2\text{NaO}$ $[(\text{M}+\text{Na})^+]$ 261.0998, found 261.1001; HPLC conditions: Daicel Chiralcel[®] OD-H (25 cm x 0.46 cm), 80:20 *n*-hexane/2-propanol, 1.0 mL/min, 230 nm, $t_{\text{R}}(+)$ = 19.2 min, $t_{\text{R}}(-)$ = 21.3 min.



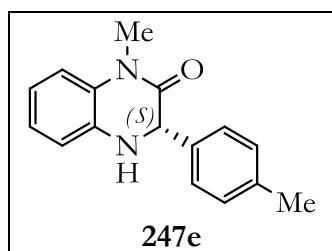
11.3 min.

(*S*)-3,6,7-trimethyl-3,4-dihydroquinoxalin-2(1*H*)-one (**247c**): Known compound,³⁹⁸ 90% ee, $[\alpha]_{\text{D}}^{25} = +40.8$ (c 0.50, CHCl_3), HPLC conditions: Daicel Chiralcel[®] OD-H (25 cm x 0.46 cm), 80:20 *n*-hexane/2-propanol, 1.0 mL/min, 230 nm, $t_{\text{R}}(+)$ = 8.9 min, $t_{\text{R}}(-)$ =



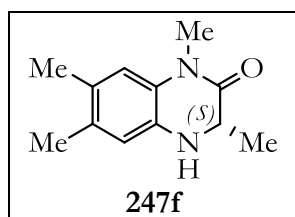
mL/min, 230 nm, $t_{\text{R}}(+)$ = 12.7 min, $t_{\text{R}}(-)$ = 16.3 min.

(*S*)-1-methyl-3-phenyl-3,4-dihydroquinoxalin-2(1*H*)-one (**247d**): Known compound,³⁷⁴ 99% ee, $[\alpha]_{\text{D}}^{25} = +161.5$ (c 0.40, CHCl_3) [lit.:³⁷⁴ $[\alpha]_{\text{D}}^{20} = +153.0$ (c 0.40, CHCl_3) for 92% ee], HPLC conditions: Daicel Chiralcel[®] AD-H (25 cm x 0.46 cm), 80:20 *n*-hexane/2-propanol, 1.0



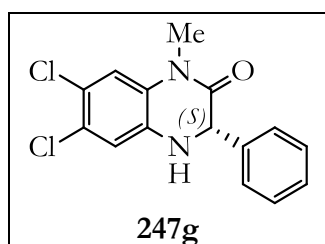
= 16.6 min.

(*S*)-1-methyl-3-(*p*-tolyl)-3,4-dihydroquinoxalin-2(*1H*)-one (**247e**): Known compound,³⁷⁴ 99% ee, $[\alpha]_{\text{D}}^{25} = +111.8$ (c 0.40, CHCl_3) [lit.:³⁷⁴ $[\alpha]_{\text{D}}^{20} = +106.2$ (c 0.40, CHCl_3) for 89% ee], HPLC conditions: Daicel Chiralcel[®] AD-H (25 cm x 0.46 cm), 80:20 *n*-hexane/2-propanol, 1.0 mL/min, 230 nm, $t_{\text{R}}(+)$ = 12.5 min, $t_{\text{R}}(-)$



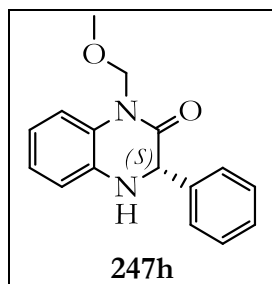
$t_{\text{R}}(+)$ = 8.0 min, $t_{\text{R}}(-)$ = 10.8 min.

(*S*)-1,3,6,7-tetramethyl-3,4-dihydroquinoxalin-2(*1H*)-one (**247f**): Unknown compound, 90% ee, $[\alpha]_{\text{D}}^{25} = +46.2$ (c 0.60, CHCl_3); IR absorption (neat) ν 2920, 1641, 1617, 1465; ^1H NMR (500 MHz, CDCl_3) δ 6.69 (s, 1H), 6.50 (s, 1H), 3.89 (dq, $J = 6.6$ Hz, $J = 1.1$ Hz, 1H), 3.69 (bs, 1H), 3.33 (s, 3H), 2.21 (s, 3H), 2.17 (s, 3H), 1.41 (d, $J = 6.6$ Hz, 3H); $^{13}\text{C}\{^1\text{H}\}$ NMR (100 MHz, CDCl_3) δ 168.4 (C), 132.7 (C), 131.4 (C), 127.6 (C), 127.1 (C), 116.0 (CH), 115.8 (CH), 52.5 (CH), 29.0 (CH_3), 19.3 (CH_3), 19.1 (CH_3), 17.8 (CH_3); HRMS (ESI⁺) calcd for $\text{C}_{12}\text{H}_{16}\text{N}_2\text{NaO}$ [(M+Na)⁺] 227.1155, found 227.1157; HPLC conditions: Daicel Chiralcel[®] AD-H (25 cm x 0.46 cm), 85:15 *n*-hexane/2-propanol, 1.0 mL/min, 230 nm,

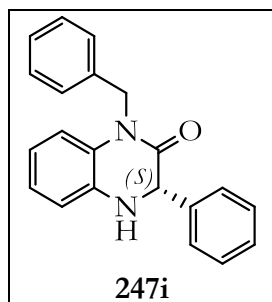


= 36.6 min, $t_{\text{R}}(-)$ = 38.8 min.

(*S*)-6,7-dichloro-1-methyl-3-phenyl-3,4-dihydro-quinoxalin-2(*1H*)-one (**247g**): Unknown compound, 99% ee, $[\alpha]_{\text{D}}^{25} = +242.8$ (c 0.50, CHCl_3); IR absorption (neat) ν 3325, 1658, 1504; ^1H NMR (500 MHz, CDCl_3) δ 7.45-7.20 (m, 5H), 6.96 (s, 1H), 6.80 (s, 1H), 5.04 (s, 1H), 4.50 (bs, 1H), 3.34 (s, 3H); $^{13}\text{C}\{^1\text{H}\}$ NMR (125 MHz, CDCl_3) δ 165.3 (C), 138.5 (C), 134.0 (C), 128.9 (CH), 128.6 (CH), 127.9 (C), 126.8 (C), 126.7 (CH), 122.0 (C), 116.2 (CH), 114.7 (CH), 60.4 (CH), 29.4 (CH_3); HRMS (ESI⁺) calcd for $\text{C}_{15}\text{H}_{12}\text{Cl}_2\text{N}_2\text{NaO}$ [(M+Na)⁺] 329.0219, found 329.0217; HPLC conditions: Daicel Chiralcel[®] AD-H (25 cm x 0.46 cm), 95:5 *n*-hexane/2-propanol, 1.0 mL/min, 230 nm, $t_{\text{R}}(+)$



(*S*)-1-(methoxymethyl)-3-phenyl-3,4-dihydroquinoxalin-2(*1H*)-one (**247h**): Known compound,³⁷⁴ 99% ee, $[\alpha]_{\text{D}}^{25} = +78.1$ (*c* 0.40, CHCl₃) [lit.:³⁷⁴ $[\alpha]_{\text{D}}^{20} = +74.2$ (*c* 0.40, CHCl₃) for 91% ee], HPLC conditions: Daicel Chiralcel[®] AD-H (25 cm x 0.46 cm), 80:20 *n*-hexane/2-propanol, 1.0 mL/min, 230 nm, $t_{\text{R}}(+)$ = 10.8 min, $t_{\text{R}}(-)$ = 14.7 min.



(*S*)-1-benzyl-3-phenyl-3,4-dihydroquinoxalin-2(*1H*)-one (**247i**): Known compound,³⁷⁴ 99% ee, $[\alpha]_{\text{D}}^{25} = +86.4$ (*c* 0.20, CHCl₃) [lit.:³⁷⁴ $[\alpha]_{\text{D}}^{20} = +79.0$ (*c* 0.20, CHCl₃) for 91% ee], HPLC conditions: Daicel Chiralcel[®] AD-H (25 cm x 0.46 cm), 80:20 *n*-hexane/2-propanol, 1.0 mL/min, 230 nm, $t_{\text{R}}(+)$ = 21.6 min, $t_{\text{R}}(-)$ = 23.8 min.

2.3.6 Deuterium Labeling Experiments

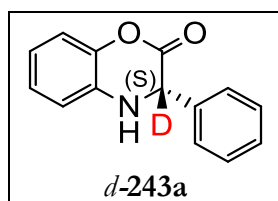
To elucidate the ongoing processes mediated by complexes $[\text{Ir}(\text{Cl})(\text{cod})(\mathbf{134a})]$, a series of labeling experiments were performed in which 2-methylquinoline **231a** and 3-phenyl-2H-benzo[*b*][1,4]oxazin-2-one (**242a**) were hydrogenated using various combinations of D_2 or H_2 as reducing agents, and DCl or HCl as additives. These are two representative examples of substrates in which addition of a protic acid as additive provided an improvement in catalytic activity in their asymmetric hydrogenation, with an increase in ee for the hydrogenation product of 2-methylquinoline **231a**, but a slight decrease in ee for that of **242a**.

A solution of the required amount of iridium precursor $[\{\text{Ir}(\mu\text{-Cl})(\text{cod})\}_2]$ and *P-OP* ligand **134a** in THF or toluene was loaded into an autoclave under N_2 atmosphere, in which the required amounts of substrate 2-methylquinoline **231a** or **242a** ($[\{\text{Ir}(\mu\text{-Cl})(\text{cod})\}_2]/\mathbf{134a}$ /substrate molar ratio = 0.5:1.1:100 or 0.25:0.55:100 for precatalyst levels of 1 or 0.5 mol %, respectively), and additives (1M anhydrous DCl or HCl solution in Et_2O , 10 mol % with respect to substrate) were placed beforehand. In all cases the molar concentration of the substrate in the reaction medium was adjusted to a final volume of 0.75 mL and a final 0.20 M concentration. The autoclave was purged three times with D_2 (at a pressure not higher than the selected one) and finally, the autoclave was pressurized with D_2 to the desired pressure. The reaction mixture was stirred at rt for 20 h. The autoclave was subsequently depressurized, the reaction mixture passed through a short pad of SiO_2 and was further eluted with EtOAc (2 x 1 mL). The resulting solution was evaporated *in vacuo* and crude material was analyzed by ^1H NMR, ^{13}C NMR and MS (APCI $^+$).

DEUTERIUM LABELING STUDIES ON **242a**

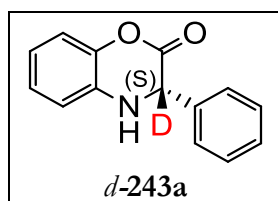
Hydrogenation or deuteration of **242a** was carried out following the procedure indicated above (0.5 mol % of catalyst, 10 mol % of DCl or HCl as additives, rt, 80 bar, 0.2 M solution of substrate in THF, 20 h) using $\text{D}_2/10$ mol % DCl, $\text{D}_2/10$ mol % HCl, and $\text{H}_2/10$ mol % DCl as labeling reagents. We observed full incorporation of deuterium at C2 when

D₂ was used (>95%, no signals attributable to the H-substituted derivative were observed by ¹H NMR) and no observable incorporation of deuterium when H₂/10 mol % DCl was utilized (see Scheme 74 and Figure 77a-d and Figure 78a-d). Deuterium-hydrogen exchange took place at nitrogen either during the chromatographic purification or during NMR or HRMS (ESI⁺) measurements, and *N*-deuterated compounds *d*-**243a** or **243a** were not observed.



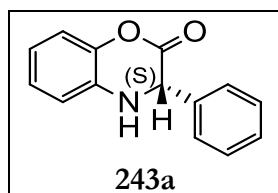
Deuteration product of 242a using D₂/10 mol % DCl (*d*-243a):

¹H NMR (500 MHz, CDCl₃) δ 7.50-7.30 (m, 5H), 7.10-7.00 (m, 2H), 6.90-6.84 (m, 1H), 6.84-6.75 (m, 1H), 4.30 (bs, 1H); ¹³C{¹H} NMR (125 MHz, CDCl₃) δ 165.2 (C), 140.9 (C), 136.4 (C), 132.3 (C), 129.0 (CH), 127.4 (CH), 125.2 (CH), 120.4 (CH), 117.0 (CH), 114.9 (CH), 58.9 (t, *J* = 20.1 Hz, C); MS (APCI⁺) calcd for C₁₄H₁₁DNO₂ [(M+H)⁺] 227.1, found 227.1.



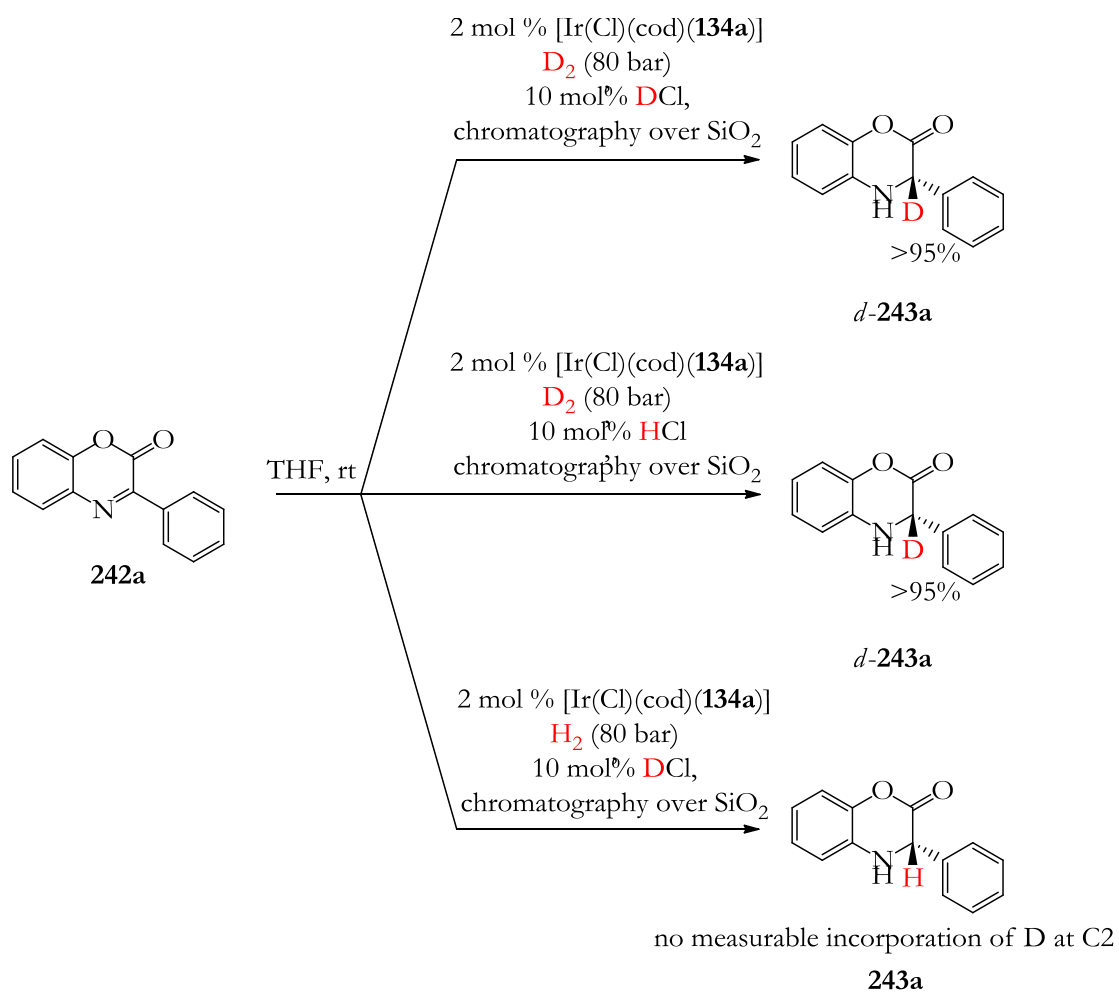
Deuteration product of 242a using D₂/10 mol % HCl (*d*-243a):

¹H NMR (500 MHz, CDCl₃) δ 7.50-7.30 (m, 5H), 7.10-7.00 (m, 2H), 6.90-6.84 (m, 1H), 6.84-6.75 (m, 1H), 4.30 (bs, 1H); ¹³C{¹H} NMR (125 MHz, CDCl₃) δ 165.2 (C), 140.9 (C), 136.4 (C), 132.3 (C), 129.0 (CH), 127.4 (CH), 125.2 (CH), 120.4 (CH), 117.0 (CH), 114.9 (CH), 58.9 (t, *J* = 20.1 Hz, C); MS (APCI⁺) calcd for C₁₄H₁₁DNO₂ [(M+H)⁺] 227.1, found 227.1.

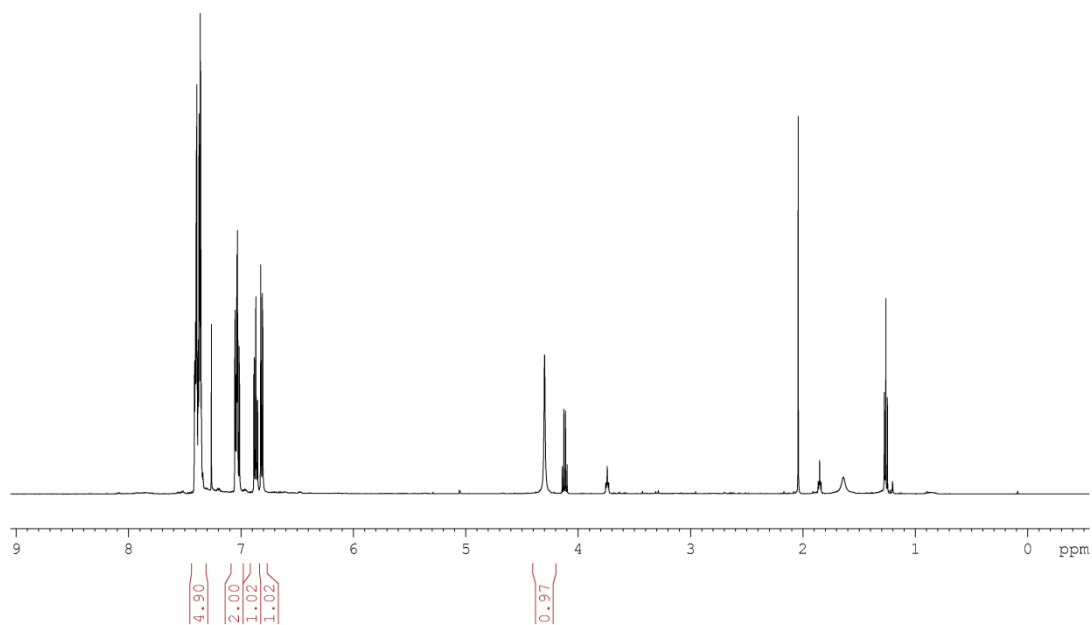


Hydrogenation product of 242a using H₂/10 mol % DCl (243a**):**

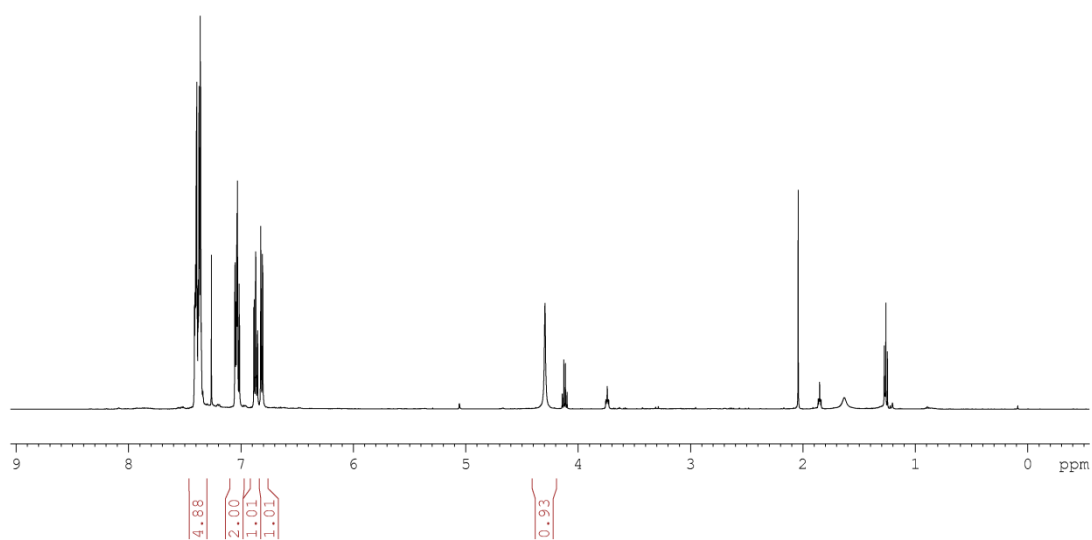
¹H NMR, ¹³C{¹H} NMR and MS (APCI⁺) data were in agreement with those reported for the hydrogenation product using H₂ (Section 2.3.5).



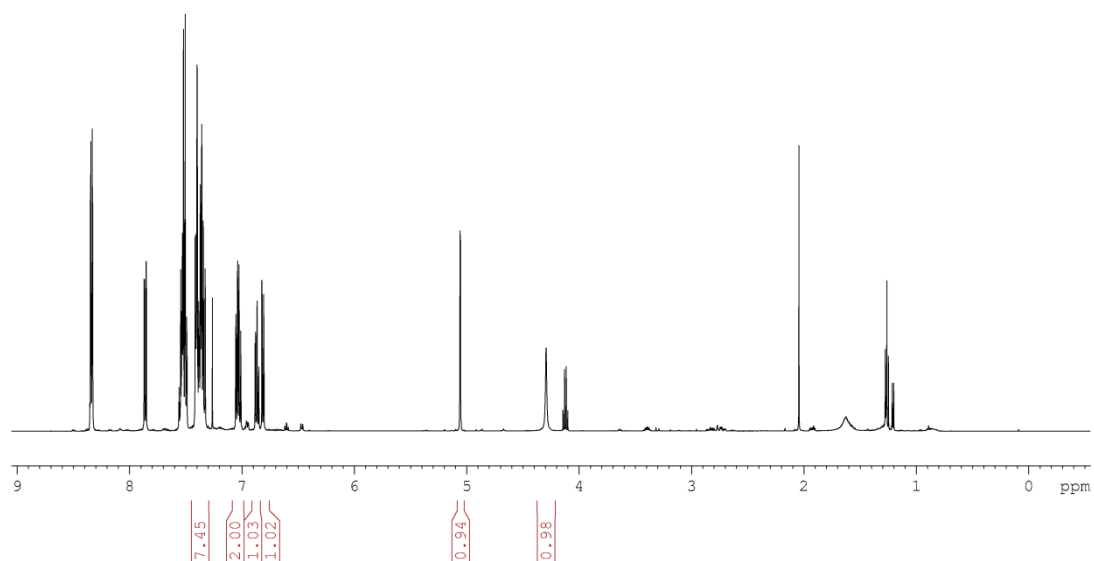
Scheme 74. Deuterium labeling experiments on the asymmetric hydrogenation of benzoxazinone **242a**.³⁸⁰



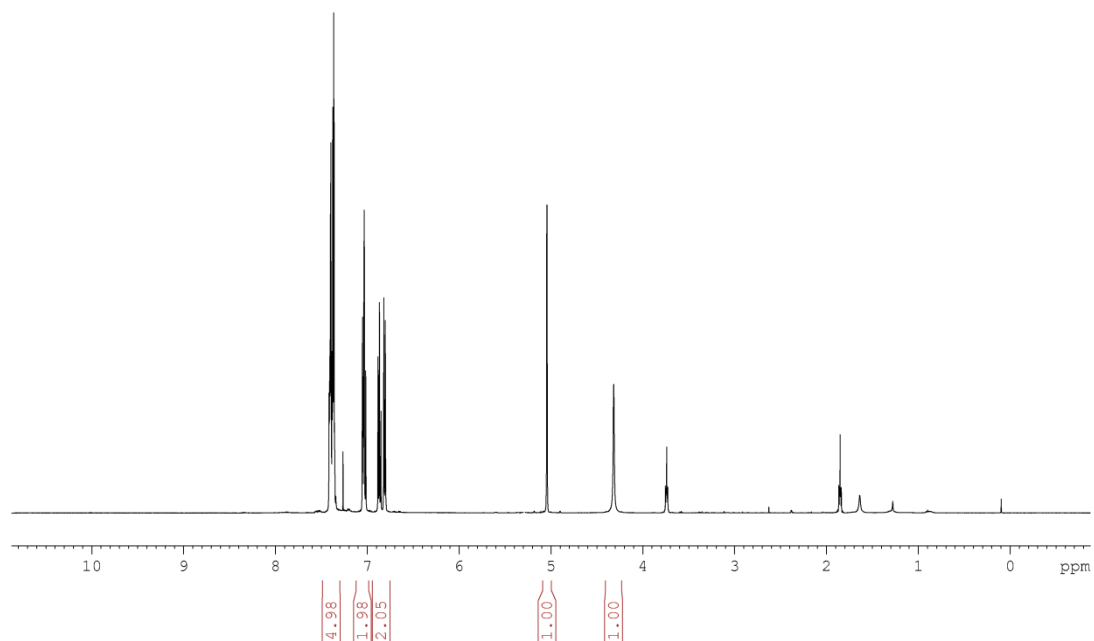
a) ^1H NMR - $\text{D}_2\text{O}/10 \text{ mol } \%$ DCl,



b) ^1H NMR - $\text{D}_2\text{O}/10 \text{ mol } \%$ HCl,

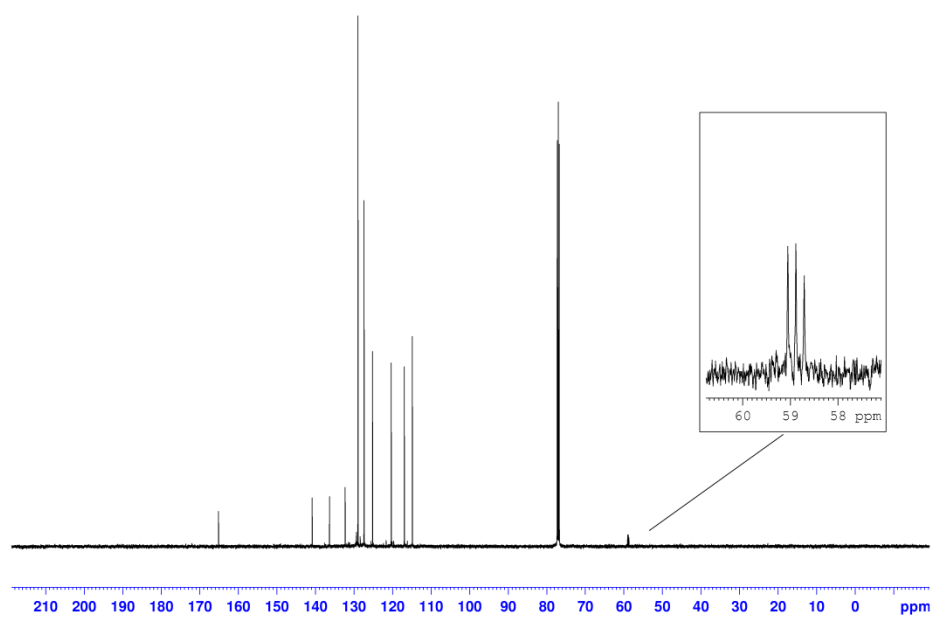


c) ^1H NMR - $\text{H}_2/10$ mol % DCl

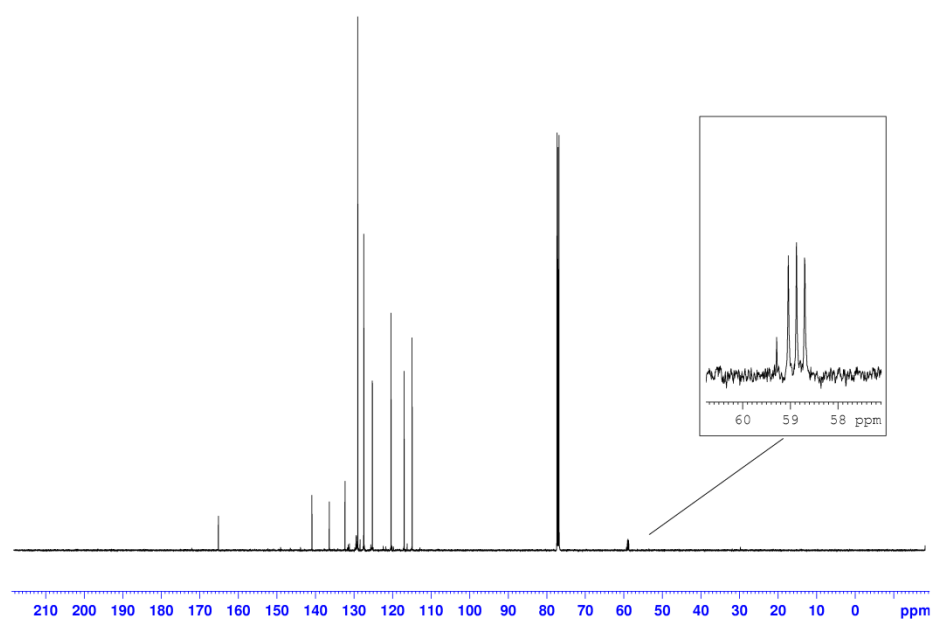


d) ^1H NMR - H_2

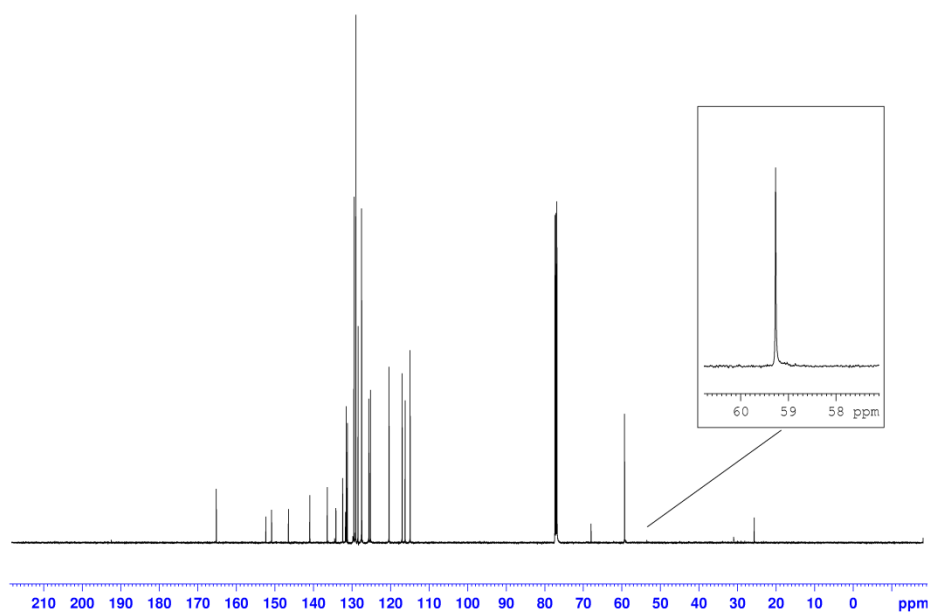
Figure 77a-d. ^1H NMR spectra of 3-phenyl-2H-benzo[*b*][1,4]oxazin-2-one **243a** derived from deuterium labeling experiments.



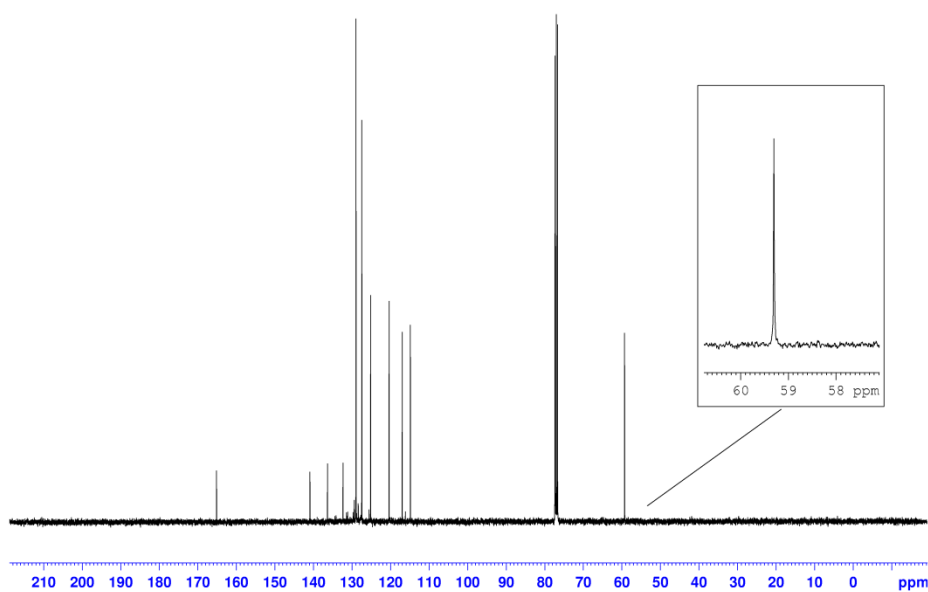
a) $^{13}\text{C}\{^1\text{H}\}$ NMR - $\text{D}_2/10 \text{ mol } \% \text{ DCl}$,



b) $^{13}\text{C}\{^1\text{H}\}$ NMR - $\text{D}_2/10 \text{ mol } \% \text{ HCl}$,



c) $^{13}\text{C}\{^1\text{H}\}$ NMR - $\text{H}_2/10 \text{ mol } \%$ DCl



d) $^{13}\text{C}\{^1\text{H}\}$ NMR - H_2

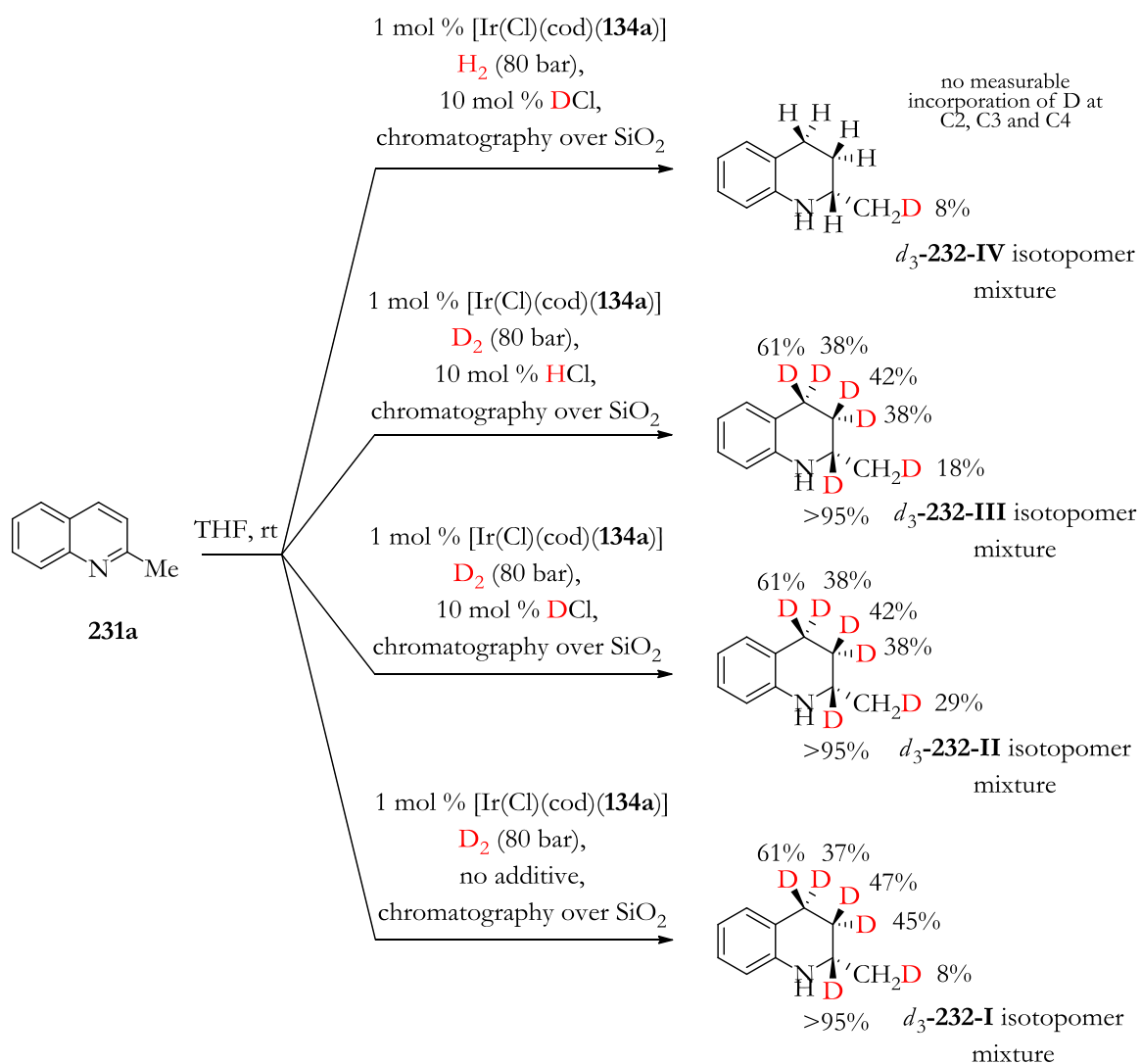
Figure 78 a-d. ^{13}C NMR spectra of 3-phenyl-2*H*-benzo[*b*][1,4]oxazin-2-one **243a** derived from deuterium labeling experiments.

DEUTERIUM LABELING STUDIES ON 2-METHYLQUINOLINE **231a**

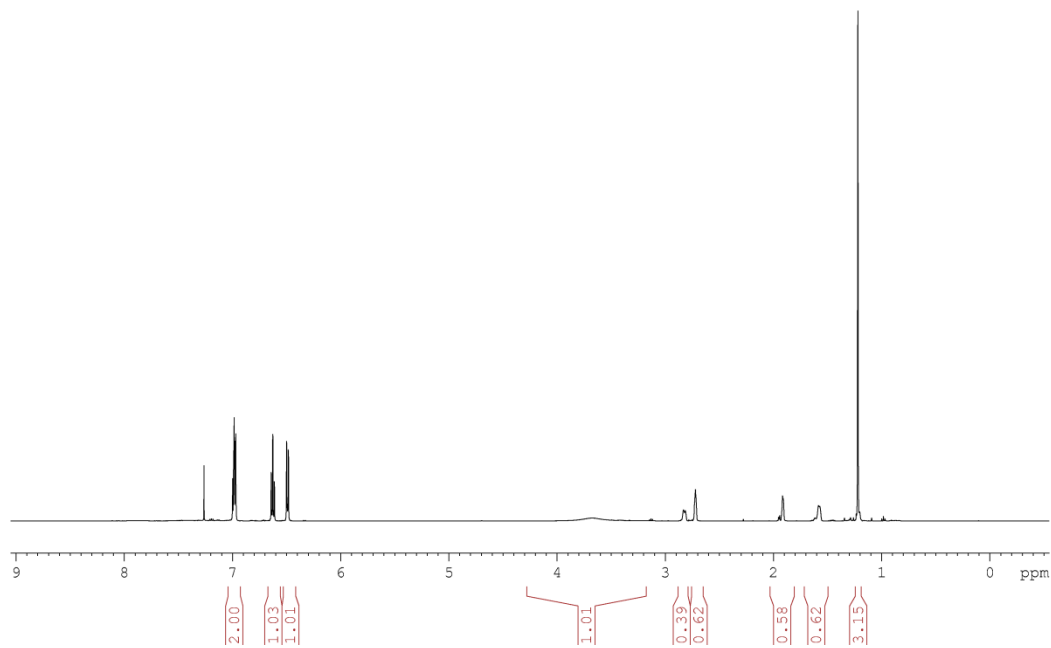
Hydrogenation or deuteration of 2-methylquinoline **231a** was carried out following the aforementioned procedure (1 mol % of catalyst, 10 mol % of DCl or HCl as additives, rt, 80 bar, 0.2 M solution of substrate in THF, 20 h) using D₂/10 mol % DCl, D₂/10 mol % HCl, and H₂/10 mol % DCl and D₂/no additive as labeling reagents.⁴⁰¹

Mixtures of several isotopomers were observed using D₂/10 mol % DCl, D₂/10 mol % HCl, H₂/10 mol % DCl and D₂/no additive. Full incorporation of deuterium at C2 was observed in **232a** in all cases when D₂ was used (>95%, no signals attributable to the H-substituted derivative were observed by ¹H NMR). No incorporation of deuterium at the aromatic carbons was observed (¹H and ¹³C NMR analysis) under all assayed labeling conditions. Variable degrees of deuterium incorporation at C3, C4 and the methyl group in **232a** were observed depending on the labeling conditions. Deuterium-hydrogen exchange took place at nitrogen either during the chromatographic purification or during NMR or MS (APCI⁺) measurements and *N*-deuterated compounds *d*₃-**232a** were not observed. See Scheme 75 and Figure 79a-d for the degrees of incorporation of D at the different carbons in **232a** under all assayed reaction conditions. Figure 80 show the ¹³C NMR signals for C2, C3, C4 and C_{Methyl} for all assayed labeling conditions.

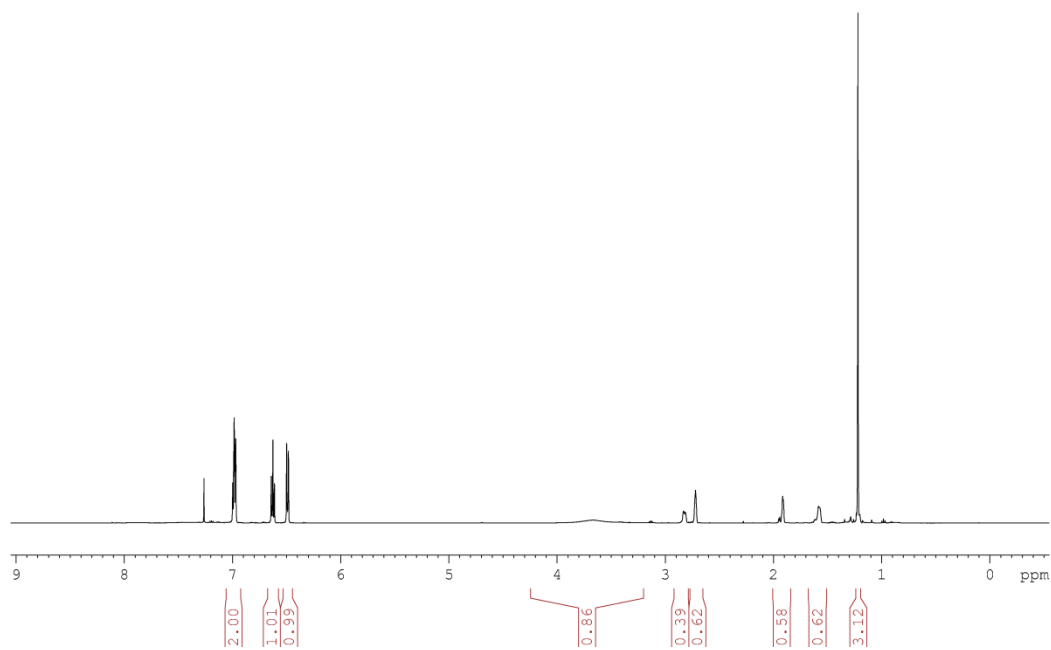
⁴⁰¹ Experiment with D₂/no additive was extended to 65h in order to achieve full conversion.



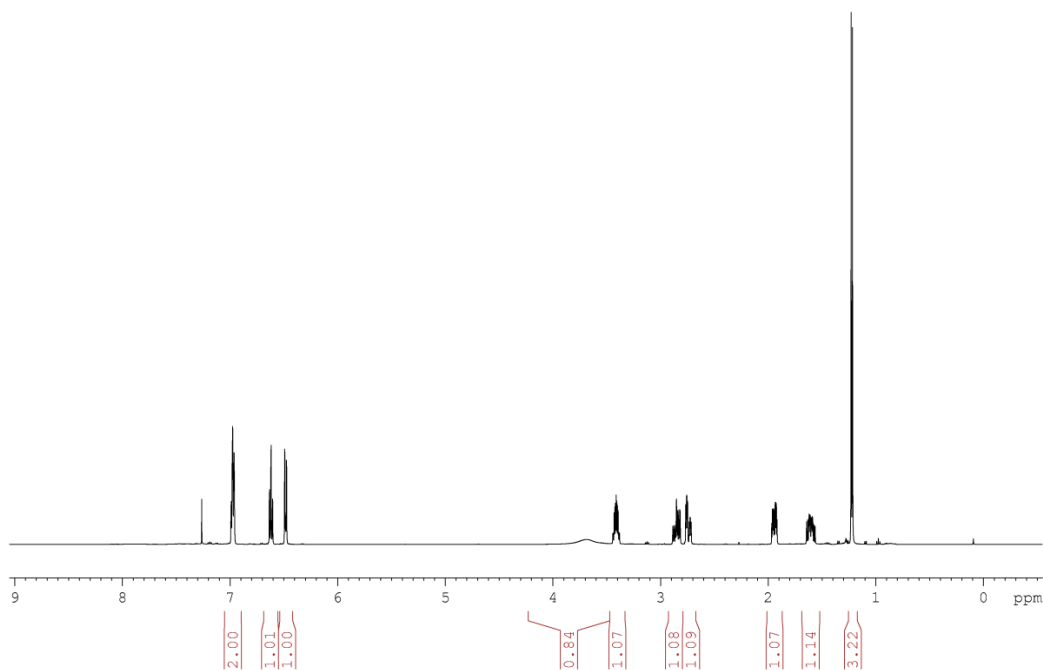
Scheme 75. Deuterium labeling experiments on the asymmetric hydrogenation of 2-methylquinoline **231a**.³⁸⁰



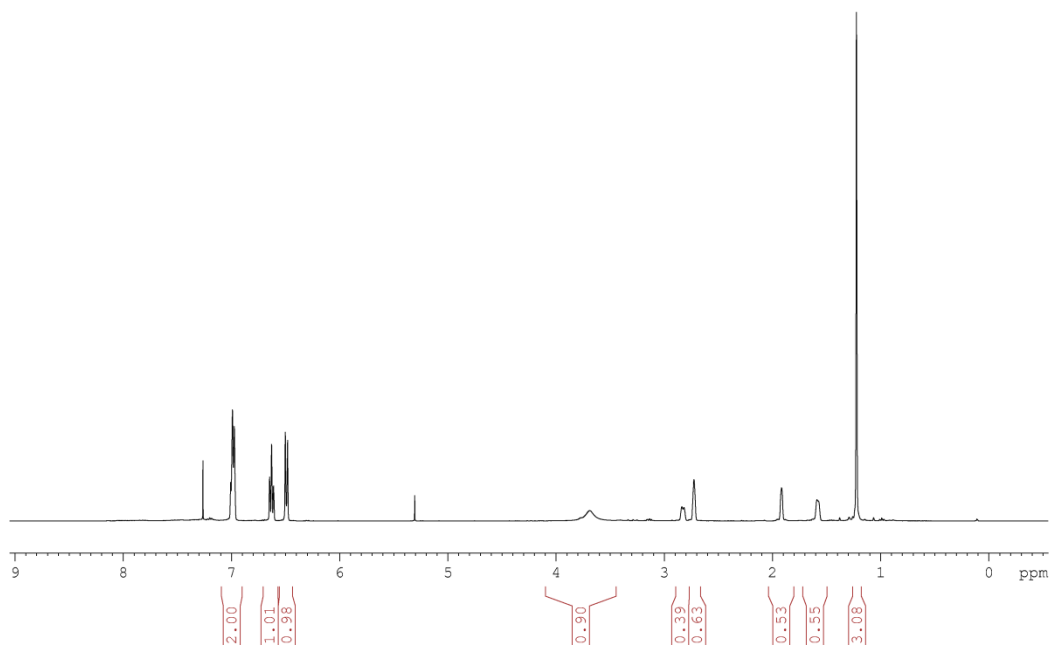
a) ¹H NMR - D₂/10 mol % DCl,



b) ¹H NMR - D₂/10 mol % HCl,



c) ^1H NMR - $\text{H}_2/10 \text{ mol } \% \text{ DCl}$



d) ^1H NMR - $\text{D}_2/\text{no additive}$

Figure 79 a-d. ^1H NMR spectra of d_3 -232I-IV derived from deuterium labeling experiments.

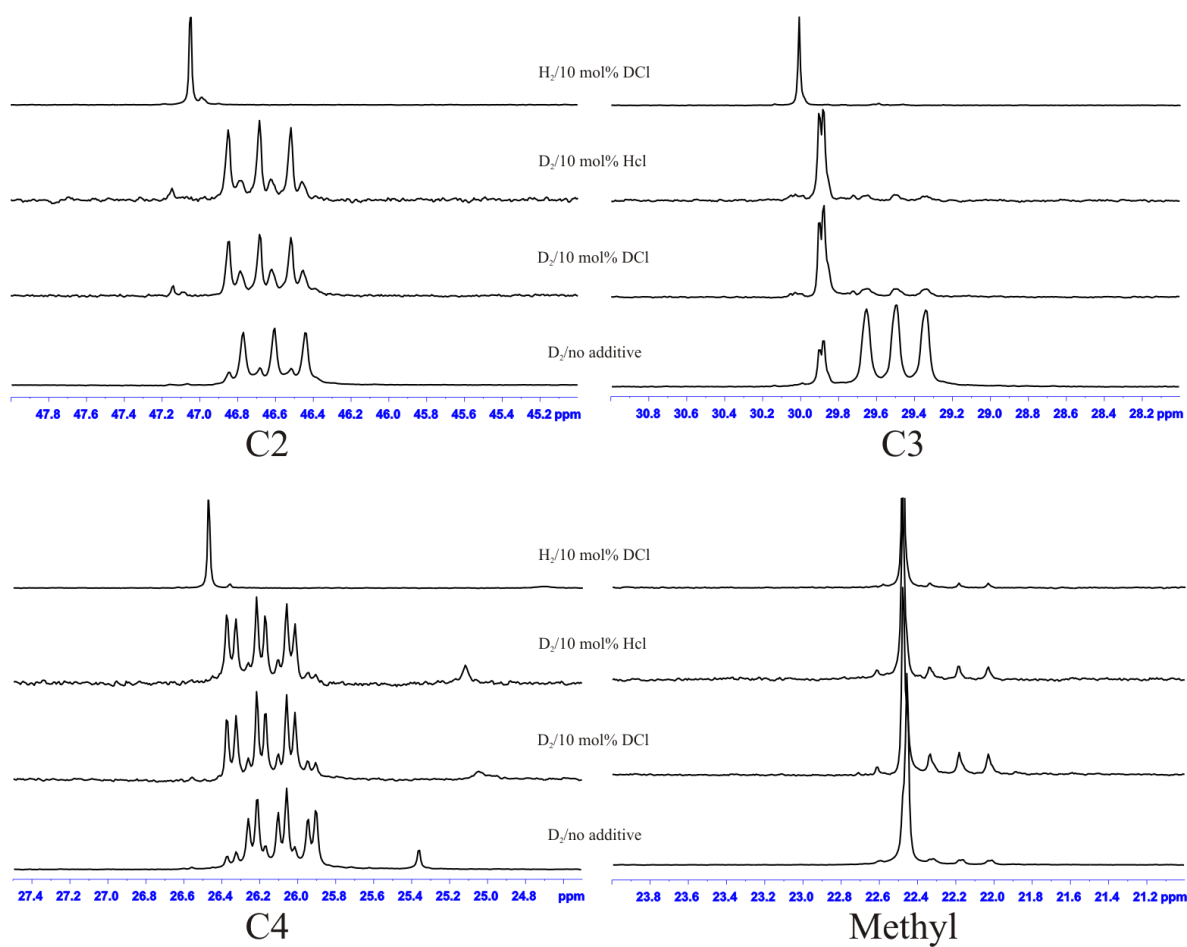
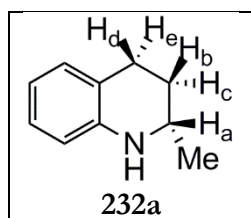


Figure 80. ^{13}C NMR signals of C2, C3, C4, C_{Methyl} of d_3 -**232I-IV** derived from deuterium labeling experiments.

Spectroscopic data of the isotopomer mixtures derived from 2-methylquinoline using D_2 /no additive (mixture d_3 -**232-I**), D_2 /10 mol % DCl (mixture d_3 -**232-II**), D_2 /10 mol % HCl (mixture d_3 -**232-III**), and H_2 /10 mol % DCl (mixture d_3 -**232-IV**):



^1H NMR spectra of 2-methyl-1,2,3,4-tetrahydroquinoline **232a** was recorded (500 MHz, CDCl_3). Simulation of the spectra was performed using gNMR 5.0 (See Figure 81),⁴⁰² which allowed determining ^1H chemical shifts and coupling constants for the spin system comprising H_a - H_e and the methyl group. Spectral data is presented in Table 58. Selective decoupling ^1H NMR experiments confirmed the coupling constant values summarized in Table 58.

⁴⁰² gNMR v5.0.6.0 NMR Simulation Program Written by P.H.M. Budzelaar Copyright © 2006 IvorySoft.

Window 1: 1H Axis = ppm Scale = 41.55 Hz/cm

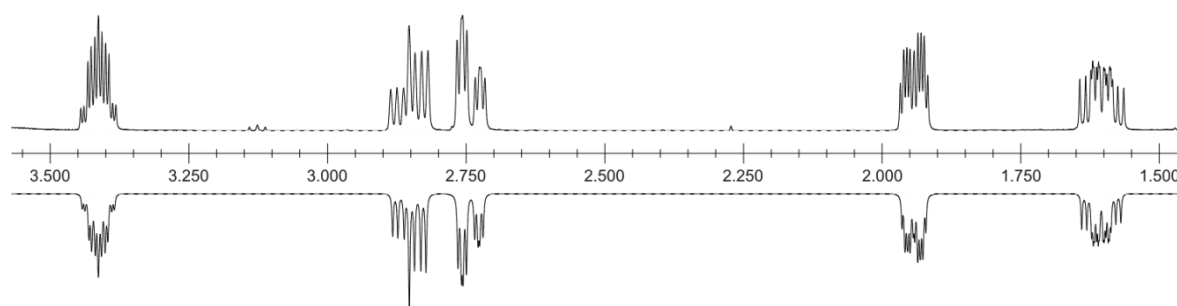
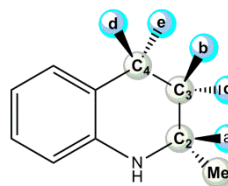


Figure 81. Experimental (top) and simulated (inverted) ^1H NMR spectrum of the aliphatic region of 2-methyl-1,2,3,4-tetrahydroquinoline **232a**.

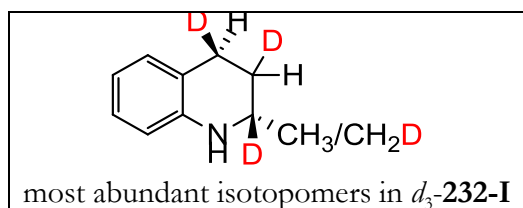
Table 58. Spectral data (chemical shifts and coupling constants) used for the simulation of the aliphatic region of the ^1H NMR spectrum of 2-methyl-1,2,3,4-tetrahydroquinoline **232a**.

Chemical Shift	J1	J2	J3	J4	J5	J6
3,7 N						
3,413 H_a	0,00 N- H_a					
1,942 H_b	0,00 N- H_b	2,40 H_a - H_b				
1,605 H_c	0,00 N- H_c	8,90 H_a - H_c	-11,50 H_b - H_c			
2,85 H_d	0,00 N- H_d	0,40 H_a - H_d	4,70 H_b - H_d	10,50 H_c - H_d		
2,744 H_e	0,00 N- H_e	0,50 H_a - H_e	3,00 H_b - H_e	4,50 H_c - H_e	-15,00 H_d - H_e	
1,223 Me	0,00 N-Me	5,90 H_a -Me	0,00 H_b -Me	0,00 H_c -Me	0,00 H_d -Me	0,00 H_e -Me



Isotopomer mixture d_3 -232-I (obtained using D_2 and no additive).

^{13}C NMR analysis of the signal corresponding to C4 revealed four groups of signals roughly in a 1:1:5:5 ratio.⁴⁰³ Three groups of signals were observed for C3: two groups of signals for two CH_2 groups and one group of signals for a CHD moiety roughly in a 1:11 ratio,⁴⁰⁵ respectively. Full incorporation of deuterium at C2 was observed and two groups of signals for two CD moieties roughly in a 1:5 ratio,⁴⁰³ respectively, were identified (See Figure 80). Two groups of signals for one CH_3 and one CH_2D moieties roughly in a 11:1 ratio,⁴⁰⁵ respectively, were observed. Such deuteration degree at the methyl group is associated with compatible intensities of the C3 signals associated with a CH_2 group (see Figure 80 for an expansion of the C4, C3, C2 and the methyl group signals). Accidental chemical shift equivalence of the different isotopomers in the d_3 -232-I mixture made it not possible to fully assign the structure of all the components



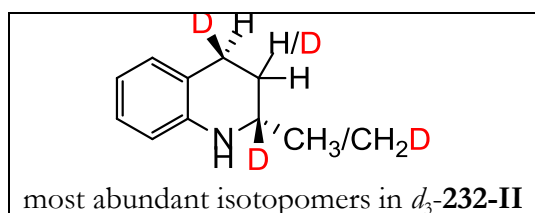
Deuteration products using D_2 / no additive

(isotopomer mixture d_3 -232-I): 1H NMR (500 MHz, $CDCl_3$) δ 7.05-6.95 (m, 2H), 6.70-6.60 (m, 1H), 6.55-6.45 (m, 1H), 3.67 (bs, 1H), 2.90-2.75

(m, 0.39H), 2.75-2.65 (m, 0.63H), 2.00-1.80 (m, 0.53H), 1.70-1.50 (m, 0.55H), 1.22 (s, 3H); $^{13}C\{^1H\}$ NMR (125 MHz, $CDCl_3$) δ 144.8 (C), 129.3 (CH), 126.7 (CH), 121.1 (C), 117.0 (CH), 114.0 (CH), 46.7 (t, $J = 20.7$ Hz, C2), 46.6 (t, $J = 20.7$ Hz, C2), 29.9 (2 x CH_2 , C3), 29.5 (t, $J = 19.9$ Hz, C3), 26.2 (t, $J = 19.7$ Hz, C4), 26.2 (t, $J = 19.7$ Hz, C4), 26.1 (t, $J = 19.7$ Hz, C4), 26.1 (t, $J = 19.7$ Hz, C4), 22.5 (CH_3), 22.2 (t, $J = 19.2$ Hz, CH_2D); MS (APCI⁺) calcd for $C_{10}H_{11}D_3N$ [(M+H)⁺] 151.1, found 151.1.

Isotopomer mixture d_3 -232-II (obtained using D_2 and 10 mol % DCl)

^{13}C NMR analysis of the signal corresponding to C4 revealed four groups of signals roughly in a 3:3:1:1 ratio.⁴⁰³ Three groups of signals were observed for C3: two groups of signals for two CH_2 groups and one group of signals for a CHD moiety roughly in a 3:1 ratio,⁴⁰³ respectively. Full incorporation of deuterium at C2 was observed and two groups of signals for two CD moieties roughly in a 5:3 ratio,⁴⁰³ respectively, were identified (See Figure 80). Two groups of signals for one CH_3 and one CH_2D moiety roughly in a 3:1 ratio,⁴⁰³ respectively, were observed. Such a high deuteration degree at the methyl group is associated with compatible intensities of the C3 signals associated with a CH_2 group (see Figure 80 for an expansion of the C4, C3, C2 and the methyl group signals). Accidental chemical shift equivalence of the different isotopomers in the d_3 -232-II mixture made it not possible to fully assign the structure of all the components.



Deuteration products 232 using D_2 / 10 mol

% DCl (isotopomer mixture d_3 -232-II): 1H

NMR (500 MHz, $CDCl_3$) δ 7.05-6.95 (m, 2H),
6.70-6.60 (m, 1H), 6.55-6.45 (m, 1H), 3.69 (bs,

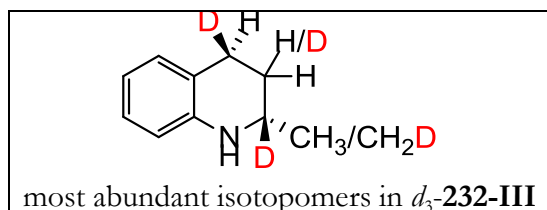
1H), 2.90-2.75 (m, 0.39H), 2.75-2.65 (m, 0.62H), 2.00-1.80 (m, 0.58H), 1.70-1.50 (m, 0.62H), 1.22 (s, 3H); $^{13}C\{^1H\}$ NMR (125 MHz, $CDCl_3$) δ 144.8 (C), 129.3 (CH), 126.7 (CH), 121.1 (C), 117.0 (CH), 114.0 (CH), 46.7 (t, $J = 20.7$ Hz, C2), 46.6 (t, $J = 20.7$ Hz, C2), 29.9 (2 x CH_2 , C3), 29.5 (t, $J = 19.9$ Hz, C3), 26.2 (t, $J = 19.7$ Hz, C4), 26.2 (t, $J = 19.7$ Hz, C4), 26.1 (t, $J = 19.7$ Hz, C4), 26.1 (t, $J = 19.7$ Hz, C4), 22.5 (CH_3), 22.2 (t, $J = 19.2$ Hz, CH_2D); MS (APCI⁺) calcd for $C_{10}H_{11}D_3N$ [(M+H)⁺] 151.1, found 151.1.

⁴⁰³ Relative intensities refer to the group of signals appearing from higher to lower chemical shifts. These relative intensities were calculated by integration of the signals in ^{13}C NMR spectra recorded using an Inverse Gated Decoupling (IGD) pulse sequence. Consequently, they should be regarded as rough estimates.

Isotopomer mixture d_3 -2-III (obtained using D_2 and 10 mol % HCl)

^{13}C -NMR analysis of the signal corresponding to C4 revealed four groups of signals roughly in a 6:6:1:1 ratio.⁴⁰³ Three groups of signals were observed for C3: two groups of signals for two CH_2 groups and one group of signals for a CHD moiety roughly in a 5:1 ratio,⁴⁰⁵ respectively. Full incorporation of deuterium at C2 was observed and two groups of signals for two CD moieties roughly in a 3:1 ratio,⁴⁰³ respectively, were identified (See Figure 80). Two groups of signals for one CH_3 and one CH_2D moiety roughly in a 5:1 ratio,⁴⁰⁵ respectively, were observed. Such a high deuteration degree at the methyl group is associated with compatible intensities of the C3 signals associated with a CH_2 group (see Figure 80 for an expansion of the C4, C3, C2 and the methyl group signals).

Accidental chemical shift equivalence of the different isotopomers in the d_3 -232-III mixture made it not possible to fully assign the structure of all the components.



Deuteration products 2 using D_2 / 10 mol %

HCl (isotopomer mixture d_3 -2-III): 1H NMR

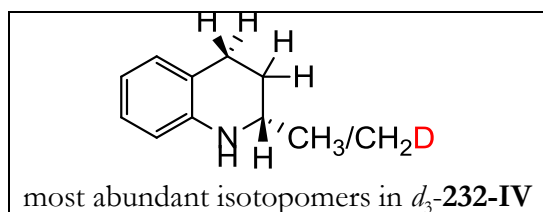
(500 MHz, $CDCl_3$) δ 7.05-6.95 (m, 2H), 6.70-6.60 (m, 1H), 6.55-6.45 (m, 1H), 3.67 (bs, 1H),

2.90-2.75 (m, 0.39H), 2.75-2.65 (m, 0.62H), 2.00-1.80 (m, 0.58H), 1.70-1.50 (m, 0.62H), 1.22 (s, 3H); $^{13}C\{^1H\}$ NMR (125 MHz, $CDCl_3$) δ 144.8 (C), 129.3 (CH), 126.7 (CH), 121.1 (C), 117.0 (CH), 114.0 (CH), 46.7 (t, $J = 20.7$ Hz, C2), 46.6 (t, $J = 20.7$ Hz, C2), 29.9 (2 x CH_2 , C3), 29.5 (t, $J = 19.9$ Hz, C3), 26.2 (t, $J = 19.7$ Hz, C4), 26.2 (t, $J = 19.7$ Hz, C4), 26.1 (t, $J = 19.7$ Hz, C4), 26.1 (t, $J = 19.7$ Hz, C4), 22.5 (CH_3), 22.2 (t, $J = 19.2$ Hz, CH_2D); MS (APCI⁺) calcd for $C_{10}H_{11}D_3N$ [(M+H)⁺] 151.1, found 151.1.

Isotopomer mixture d_3 -232-IV (obtained using H_2 and 10 mol % DCI)

^{13}C -NMR analysis of the signals corresponding to C2, C3 and C4 revealed no deuterium incorporation on these positions, or non-quantifiable (See Figure 80). Two groups of signals for one CH_3 and one CH_2D moieties roughly in a 11:1 ratio,⁴⁰⁵ respectively, were observed (See Figure 80 for an expansion of the C4, C3, C2 and the methyl group signals).

Accidental chemical shift equivalence of the different isotopomers in the d_3 -232IV mixture made it not possible to fully assign the structure of all the components. Major isotopomers present in the sample could be assigned to both depicted structures with CH_3/CH_2D in the methyl position.



Deuteration products 232 using D_2 / 10 mol % HCl (isotopomer mixture d_3 -232-IV): 1H NMR (500 MHz, $CDCl_3$) δ 7.05-6.95 (m, 2H), 6.70-6.60 (m, 1H), 6.55-6.45 (m, 1H), 3.69 (bs, 1H), 3.50-3.35 (m, 1H), 2.90-2.75 (m, 1H), 2.75-2.65 (m, 1H), 2.00-1.80 (m, 1H), 1.70-1.50 (m, 1H), 1.22 (d, 3H, $J = 6.4$ Hz); $^{13}C\{^1H\}$ NMR (125 MHz, $CDCl_3$) δ 144.8 (C), 129.3 (CH), 126.7 (CH), 121.1 (C), 117.0 (CH), 114.0 (CH), 47.2 (C2), 30.1 (C3), 26.6 (C4), 22.6 (CH_3), 22.3 (t, $J = 19.2$ Hz, CH_2D); MS (APCI⁺) calcd for $C_{10}H_{13}DN$ [(M+H)⁺] 149.1, found 149.1.

CONCLUSIONS

Concluding remarks of the thesis

UNIVERSITAT ROVIRA I VIRGILI
HIGHLY MODULAR P -OP LIGANDS FOR RHODIUM- AND IRIIDIUM-MEDIATED ASYMMETRIC HYDROGENATIONS
José Luis Núñez Rico
DL: T.994-2013

CONCLUSIONS

1. We have expanded the existing *P-OP* ligand library to two new ligands, which are closely related to the previous best performing ligand. The newly prepared ligands incorporate a sterically congested group (a trityloxy moiety) at the CH₂OR position. *P-OP* ligands of the two enantiomeric series have been prepared. The synthetic route towards the phosphine phosphite ligands has been optimized by developing a one-pot deprotection-phosphorylation sequence that allows further scale-up of the process and increases efficiency.
2. We have assessed the catalytic performance of our [Rh(*P-OP*)]⁺ complexes by determining the turnover number and turnover frequency parameters in the asymmetric hydrogenation of model substrates of four different types of functionalized alkenes. The hydrogenation rates observed with the four model substrates follow the same trend, independently of the R-oxy group of the ligand: methyl 2-acetamidoacrylate > dimethyl itaconate > 1-phenylvinyl acetate > *N*-(1-phenylvinyl)acetamide. The R-oxy group of the ligand (methoxy or triphenylmethoxy) influences enantioselectivity and catalytic activity. Greater steric bulk around the metal center correlated to greater (or similar) enantioselectivity, but also to slower hydrogenation. The rhodium complex of one of best performing ligands efficiently mediates the hydrogenation with a catalyst to substrate ratio as high as 10,000:1 in the asymmetric hydrogenation of dimethyl itaconate. The same ligand mediated the hydrogenation of methyl 2-acetamidoacrylate with a TOF number at 50% conversion higher than 49,000 h⁻¹.

3. We have evaluated the substrate scope of the reaction by testing an array of thirty-three diversely substituted alkenes, comprising ten β -substituted α -(acylamino)acrylates, five α -substituted enamides, eleven α -substituted enol esters and seven itaconate derivatives and analogs, all having high conversion rates and high to excellent enantioselectivities.
4. We have applied our $[\text{Rh}(P\text{-}OP)]^+$ complexes to the hydrogenation of fifteen strategically devised substrates, which allowed gaining access to biologically active compounds and to precursors of active pharmaceutical ingredients (API's), such as levetiracetam, lacosamide, rivastigmine and aprepitant, among others.
5. We have studied the complexation of our $P\text{-}OP$ ligands with iridium precursors that could lead to catalytically active neutral and cationic iridium complexes for hydrogenation. Stable and well defined chiral iridium complexes were efficiently generated *in situ* from stoichiometric amounts of $[\{\text{Ir}(\mu\text{-Cl})(\text{cod})\}_2]$ and the corresponding $P\text{-}OP$ ligand.
6. We have investigated the enantioselective hydrogenation of a broad array of prochiral nitrogen-containing substrates, which included imines (six examples) and heterocyclic systems such as benzoxazines (eight examples), benzoxazinones (five examples), benzothiazines and benzothiazinones (four examples), quinoxalinones (nine examples), as well as quinolines and quinoxalines (ten examples) and indoles (8 examples). Some of the substrates required the development of activation strategies for successful hydrogenation, which involved using Brønsted acids as additives. Neutral iridium complexes performed better than their cationic counterparts, and provided higher enantioselectivities.

7. We have performed isotopic labeling experiments on $[\text{Ir}(\text{P}-\text{OP})]^+$ catalyzed hydrogenations that allowed us to gain a deep insight in the hydrogenation reaction pathways that take place. In the case of 2-methylquinoline, these studies elucidated the nature of the tautomerization processes after the first addition of H_2 and revealed a complex scenario, in which the corresponding exocyclic tautomer also participated in the equilibria previous to the addition of the second H_2 molecule. These studies also suggested that the stereoselectivity of hydrogen incorporation at C4 in the case of 2-methylquinoline would be compatible with asymmetric induction at this carbon during hydrogenation, in the event of being substituted.